UNIVERSITY OF NAPLES FEDERICO II
DEPARTMENT OF MATERIALS AND PRODUCTION ENGINEERING

DOCTORATE PROGRAMMES IN CHEMICAL, MATERIALS AND PRODUCTION ENGINEERING

PhD Projects on

Intelligent Technologies and Systems for Production Automation

XIX CYCLE

PhD THESIS

Numerical Simulation of Metal Sheet Plastic Deformation Processes through Finite Element Method

SUPERVISOR
PROF. ROBERTO TETI

PHD CANDIDATE
ARCH. AL AZRAQ SOLIMAN MOHAMMED SULIMAN

CO-SUPERVISOR
PROF. ULF ENGEL

PHD PROGRAMME COORDINATOR
PROF. NINO GRIZZUTI

ACADEMIC YEAR 2005-2006

UNIVERSITÀ DEGLI STUDI DI NAPOLI FEDERICO II
DIPARTIMENTO INGEGNERIA DEI MATERIALI E DELLA PRODUZIONE

DOTTORATO DI RICERCA IN INGEGNERIA CHIMICA,
DEI MATERIALI E DELLA PRODUZIONE

Indirizzo in

Tecnologie e Sistemi Intelligenti per l'Automazione della Produzione

XIX CICLO

TESI DI DOTTORATO

Simulazione Numerica dei Processi di Deformazione Plastica delle Lamiere Attraverso il Metodo degli Elementi Finiti

TUTOR
PROF. ROBERTO TETI

DOTTORANDO
ARCH. AL AZRAQ SOLIMAN
MOHAMMED SULIMAN

CO-TUTOR
PROF. ULF ENGEL

COORDINATORE
PROF. NINO GRIZZUTI

Anno Accademico 2005-2006

NUMERICAL SIMULATION OF METAL SHEET PLASTIC DEFORMATION PROCESSES THROUGH FINITE ELEMENT METHODS

INTRUDUCTION

Preface

One of the important tasks for the 21st century is the maintaining of sound ecology. The reduction of the burden on the environment is an inevitable task assigned to industry. In recent years, it has become one of the most important objective for automobiles to make the reduction in weight of auto bodies compatible with the improvement of crashworthiness, particularly with the aim of reducing CO_2 gas emissions by improving fuel consumption. To satisfy these demands, a new grade of steel, the Advanced High Strength Steel (AHSS), has been developed, pushing the boundaries of what was previously possible with conventional steel grades.

Several new commercialized and near-commercialized advanced high-strength steels (AHSS) that exhibit high strength and enhanced formability are being offered around the world. These steels have the potential to affect cost and weight savings while improving performance.

A major negative consequence of using these new materials is the low formability and the elevated springback proportion due to their high strength values. Springback phenomenon has capital importance in situations where dimensional precision is a vital requirement, as the final measures of the component are altered due to changes in the strains, produced by elastic recovery of the material. Engineers turned to forming simulation in order to closely investigate and try to minimize this problem.

The aim of industrial application of the simulation for drawing processes is to replace the physical tryout by the computer tryout, with the intention of time/cost reduction and quality improvement in the die design/manufacturing cycle.

In the past, a number of analyzing methods have been developed and applied to various forming processes. Some of these methods are the slab method, the slip-line field method, the viscoplasticity method, upper and lower bound techniques and Hills general method. These methods have been useful in qualitatively predicting forming loads, overall geometry changes of the deformed blank and material flow and in determining approximate optimum process conditions.

However, a more accurate determination of the effects of various process parameters in the drawing process has become possible only recently, when the finite element method (FEM) was developed for these analyses.

The FEM codes for sheet metal forming may be classified accordingly to their type of integration: implicit or explicit. Their main solution procedures are the dynamic explicit and the static implicit ones. The principal analysis methods used in sheet metal forming simulation are based on shell, membrane and continuum elements.

In the sheet metal forming process a major factor preventing accurate final part dimensions is springback in the material. Springback is the geometric difference between the part in its fully loaded condition, i.e. conforming to the tooling geometry, and when the part is in its unloaded, free state.

In the automotive sector FEM methods for the metal forming analysis are already used, particularly explicit codes like LS-DYNA (LSTC) and PAMSTAMP (EASY) and implicit codes like AUTOFORM. Explicit solvers can be used to simulate dynamic analysis and allow to evaluate wide deformations (like in the drawing process); implicit solvers are suitable to perform a static analysis (like springback). So, in the metal forming process simulation of car body components, a final implicit static step may be used to obtain a static springback solution, after the tool is removed from the die. In this way springback solution begins from stress and strain state of the forming simulation without numerical dynamic oscillations.

In this project, the new class of steels rapresented by the AHSS grade is described in detail. Its forming methods are also mentioned and explained.
Special attention is given to the springback phenomenon, characterizing it and explaining the several variables that influence its proportion.
In the industrial environment, in order to save time, money and resources, physical tryouts have been replaced by virtual tryouts. The codes and elements normally used in these types of simulation programs, as well as their common approaches, are presented and analysed.

Organisation of the Thesis.

This thesis is organized in Four principal sections as it follows :

Section I

The first section contains the introduction, the analysis and study the type of work materials, the plastic deformation process, the springback phenomenon, the Finite element method, and numerical simulation of plastic deformation process.

Section II

In this section the numerical simulations of two applications using the ANSYS-LS DYNA Software have been performed.

The first application consists of an impact test by steel sphare on an alluminium sheet with the objective of determining the influence of the sheet thickness sheet on the constraints and the displacements, when the plasticization of the sheet happens, when the failure of the sheet happens.

The main objective of the Second application is to achieve a sufficiently good simulation of GLARE behaviour when it suffers an impact using the ANSYS LS DYNA Software. The main application of GLARE is in the aerospace industry where it is used in some parts of the aircraft fuselage. Hence, GLARE needs to be resistant to low velocity impacts: bird strike, baggage and ground handling equipment, runway debris, etc. These tests are time consuming, expensive and difficult to perform, so the ability to simulate these tests is of high importance.

Section III

In this third section the numerical simulations of three applications using the AUTOFORM Software have been performed.

The First application regards the forming simulation of two automobile components (a lateral longeron and a deck lid inner body panel) and was performed using the incremental approach of the AutoForm finite element method code. The results obtained were then analysed under several process parameters.

The Second application regardes a test case realized in *AutoForm 4.04 Incremental* code for a simple profile stamping simulation with angle

variations in the component vertical side walls using two different Advanced High Strength Steel (AHSS) materials. An incremental simulation was performed for a stamping process consisting of three stages: forming, trimming and springback. The most important criteria to evaluate the stamping process success are the following result variables: formability, thinning and springback (material displacement and angular displacement).

The **Third** application regards a test case of stamping simulation of a lateral longeron of a Fiat car. Eleven different profiles with differing angular variations realized with DP600 material were considered.

The study was carried out by taking to account the limits proposed by ELASIS, Fiat research centre, with the objective to improve the accuracy of the springback calculations through the use of the numerical simulation of the complete stamping cycle as well as to develop and verify methods to eliminate the effects of sprigback with particular attention to the application of the new AHSS steel.

Section IV

Finally, many details of the research methods and research results and the corresponding discussions are described in the three publications enclosed.

In the **First** publication the FEM analysis of AHSS car body drawing process and springback has been analyzed.

In the **Second** publication the calcolation of the springback in a profile realized with different material, first in Dp600 after in Trip800.

The determination of the springback difference in the profile, realized with different material, is the principal objective.

In the **Third** publication, the springback phenomenon in eleven different profiles with differing angular variations, realized with DP600 material. The principal objective is the search for the best inclination of the profile for the best forming with the least springback.

Acknowledgements

The present PhD thesis work was carried out with support by the following projects:

- EC FP6 Network of Excellence on Innovative Production Machines and Systems (I*PROMS)

- EC FP6 Network of Excellence on Multi-Material micro Manufacture (4M)

- Campania Region, Centre of Competence on Transportation (CRdC Trasporti)

- ELASIS Project on Numerical Simulation of Sheet Metal Stamping in the Automotive Sector

Section I.A

Materials:
Automotive Steels

Section I.A

Materials: Automotive Steels

*I.A.*1 - Introduction

What is steel?

Steel is an alloy of iron and carbon containing less than 2% carbon and 1% manganese and small amounts of silicon, phosphorus, sulphur and oxygen. Steel is the most important engineering and construction material in the world. It is used in every aspect of our lives, from automotive manufacture to construction products, from steel toecaps for protective footwear to refrigerators and washing machines and from cargo ships to the finest scalpel for hospital surgery.

History

Steel was invented by a British inventor called Henry Bessemer in 1856. He founded the Bessemer Steel Company in Sheffield, England, but up to 1859 the company made a loss. By the time the patent ran out in 1870 he had made more than 1 million pounds sterling. Steel is still produced using technology based upon the Bessemer Process of blowing air through molten pig iron to oxidise the material and separate impurities.

*I.A.*1.1 - Characteristics

Flat rolled steels are versatile materials. They provide strength and stiffness with favourable mass to cost ratios, and they allow high speed fabrication. In addition, they exhibit excellent corrosion resistance when coated, high energy absorption capacity, good fatigue properties, high work hardening rates, aging capability, and excellent paintability, which are required by automotive applications. These characteristics, plus the availability of high strength low alloy (HSLA) and alloy steels in a wide variety of sizes, strength levels, chemical compositions, surface finishes, with and without various organic and inorganic coatings, have made sheet steel the material of choice for the automotive industry.

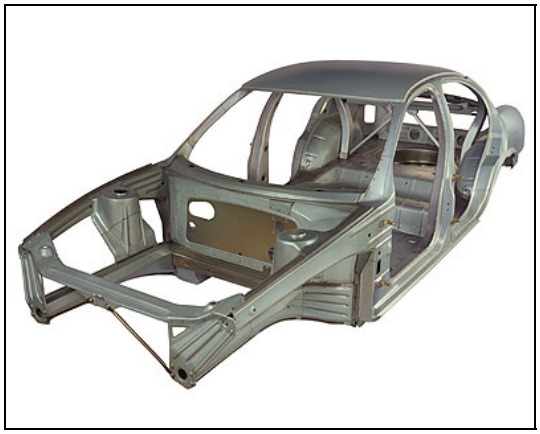

Figure I.A.1 – *An example of sheet stamping utilization in automobile industry.*

User fabrication methods applicable to sheet products include roll, brake and press forming, shearing, slitting, punching, welding, adhesive bonding, etc. Corrosion resistance is attained primarily by the application of coatings, either sacrificial or barrier, to flat rolled steels in continuous zinc or zinc alloy coating operations.

In more recent times, since the international conference on the issues of the global environment in 1997, it has become a necessity more urgent than before to reduce the weight of automobiles along with an inevitable increase in the use of advanced high strength steel (AHSS) or aluminium alloy sheets.

***I.A.*1.2 - Contents of this chapter**

This chapter describes the sheet steel materials available to the automotive industry. Is given special attention to this new type of steel (AHSS) because, nowadays, they are who represent more advantages but, in the other hand, its forming is very difficult.

***I.A.*2 - Steel Making**

Ironmaking - Iron ore, coke and lime are the raw materials fed into the blast furnace to produce liquid iron (often called 'hot metal'). The iron that emerges from the blast furnace contains 4-4.5% carbon and other impurities which make the metal too brittle for most engineering applications.

Steelmaking - The Basic Oxygen Steelmaking (BOS) process takes this liquid iron plus recycled scrap steel, and reduces the carbon content to between 0 and 1.5% by blowing oxygen through the metal in a converter to

produce molten steel. Alternatively, the Electric Arc Furnace (EAF) is used to remelt scrap iron and steel.

Secondary steelmaking - processes are then applied to make fine adjustments to the steel composition, temperature and cleanness.

Casting - The steel is then continuously cast into solid slabs, blooms or billets. Continuous casting has largely replaced traditiona lingot casting.

Primary Forming - Primary forming operations, such as hot rolling are those which are applied to continuous cast slabs, blooms and billets. The main purpose is continuous cast slabs, blooms and billets .

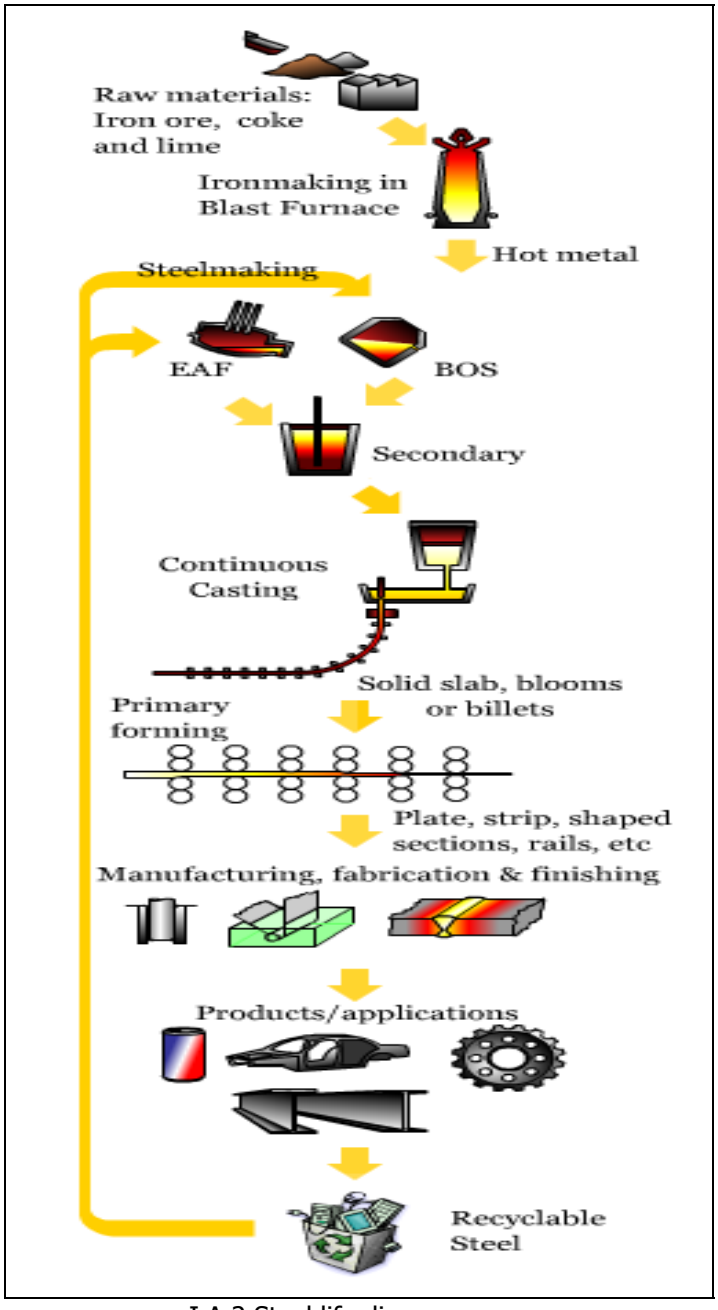

I.A.2 Steel life diagram

Deoxidation Practices

Currently all of the steel for automotive applications is deoxidized. Deoxidization with aluminium is performed during and after pouring of the steel from the BOS into a ladle (secondary steelmaking in Figure 1.2). Other alloying elements can be added to the ladle to produce compositions necessary to attain specified properties in a flat rolled sheet such as higher strength and improved corrosion resistance. Ladle treatments are available to further modify the steel characteristics, such as calcium treatment to reduce

sulphur and modify sulphides, gas stirring to improve uniformity of the alloy additions, or vacuum degassing to lower carbon levels (<0.01%). Additions of titanium and/or columbium in a vacuum degassed heat are used to produce interstitial free (IF) stabilized steels.

Main shape defects after Primary forming operations

Coil Set – Coil set is the most basic and common of all shape defects. It is caused by a length differential from the top to bottom surface of the strip in the lengthwise direction (Figure 1.3). It can come from a previous bending operation or just from coiling the coil in a cold mill, a hot mill, or even on a tension level line.

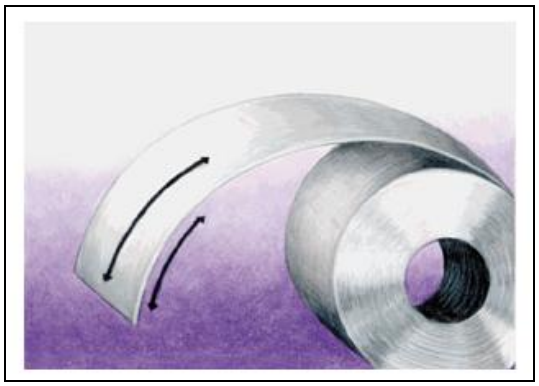

Figure I.A.3 – *Coil set can result from a previous bending operation or from coiling the coil.*

This condition can be corrected by reverse-bending the material, which stretches the short surface and compresses the long surface.To this correction be permanent, the material must be bent past its yield point.

Crossbow – Crossbow is the second most basic of all shape defects. It is also caused by a length differential from the top to the bottom surface of the strip. It is most recognizable in true hot-rolled material with scale that has never been opened.

Like coil set, crossbow is in the direction of the bend, but the bend direction is across the width of the strip (Figure 1.4). Crossbow is related to coil set by Poisson's ratio, which is approximately equal to 0.3 for steel and aluminium

Figure I.A.4 – *Crossbow is in the direction of the end, but the bend direction is across the strip's width.*

When coil set is pulled out, crossbow appears. To remove crossbow, the reverse bend must be made more severe than it would be to remove the same amount of coil set (effectively three times as great as it would be if the strip could be turned 90 degrees and reverse-bent).

Twist – Twisted strip (Figure I.A.5) is caused by a length differential from the inner to outer surfaces of the strip, which simultaneously varies across the width of the strip. It can be caused by a side-to-side temperature differential in the hot strip mill. Twisted strip generally requires more severe bending to correct; like crossbow, it can be corrected by "biting in" deeper at the entry end of the machine.

Figure I.A.5 – *Twisted strip has positive coil set on one side and negative (less positive) coil set on the other.*

Twisted strip has positive coil set on one side and negative (less positive) coil set on the other. This type of defect is readily corrected by the deep mesh of the machine's entry end. This deep mesh turns both edges of the coil to either positive or negative coil set and then gradually reduces the coil to flat as it proceeds out through the tapered mesh of the machine.

*I.A.*3 – Types and Chemistry of Steel

Sheet steels used in the automotive industry are available in the following types:

- Commercial Quality
- Low Carbon – Drawing quality
- IF stabilized – Deep drawing quality
- Dent Resistant
- Bake Hardenable
- Non-Bake Hardenable
- High Strength Low Alloy
- High Strength Solution Strengthened
- **Ultra High Strength**
  - TRIP
  - Dual Phase
  - Complex Phase
  - Martensitic
- Laminated Steels
- Stainless Steels

The low carbon steels are generally less than 0.13% carbon, 0.60% manganese, 0.030% phosphorus, 0.030% sulphur, and greater than 0.02% aluminium. The drawing quality steels have carbon level in the 0.02 to 0.04% range. The Interstitial free (IF) steels are stabilized with Ti, Cb, or Cb + Ti, and are normally ultra low carbon (0.005% max). While most IF steels are produced as drawing quality, solid solution strengthening with P, Mn, and Si can be utilized to produce a higher strength formable steel (with higher n values and r values). (Point I.A.5.3)

Bake hardenable steels utilize carbon in solution to provide an increase in strength during the paint bake cycle due to carbon strain aging. Therefore these steels can be produced in a relatively low strength condition and easily formed into parts. However, after forming and paint baking, a significantly stronger part is produced.

The dent resistant steels contain increased levels of phosphorus (up to 0.10%), and possibly manganese and silicon to low carbon steels and IF steels. The high strength solution strengthened steels contain increased

levels of carbon and manganese with the addition of phosphorous and/or silicon.

The high strength low alloy steels (HSLA) contain the addition of the carbide forming elements Cb, V, or Ti singularly or in combination to a low carbon steel, providing strength through precipitation of fine carbides or carbonitrides of Cb, Ti, and/or V. Microalloying to these grades does reduce the ductility.

Stainless steels are classified into austenitic, martensitic or ferritic steels. The major divisions are the 300 series steels, with nickel stabilized austenite, and the 400 series, which are nickel free but contain 10% or more chromium. Some of these are hardenable by quenching and tempering. The 200 series are special austenitic steels where portions of the nickel are replaced with manganese and nitrogen. The 500 series are low chromium steels (4-6%) but with small additions of molybdenum.

About AHSS chemistry and other properties we will refer with more precision in the next points.

***I.A.*4 – Different Types of Classification**

Automotive steels can be defined in several different ways. The first is by metallurgical designation. Common descriptions include low strength steels (interstitial free and mild steels), conventional high strength steels (carbon manganese, bake hardenable, isotropic, high strength IF, and high transformation induced plasticity, complex phase, and martensitic steels).

The second classification method is based on one of the mechanical properties – strength. High Strength Steels (HSS) are defined as those steels with tensile strengths from 270-700 MPa. Ultra High Strength Steels (UHSS) are defined as steels with tensile strengths greater than 700 MPa.

A third classification method uses another of the mechanical properties – total elongation. As an example, Figure 1.6 compares total elongations (a steel property related to formability) for the different steel types [1]. Note that the tensile strengths of AHSS overlap both the HSS and UHSS range of strengths.

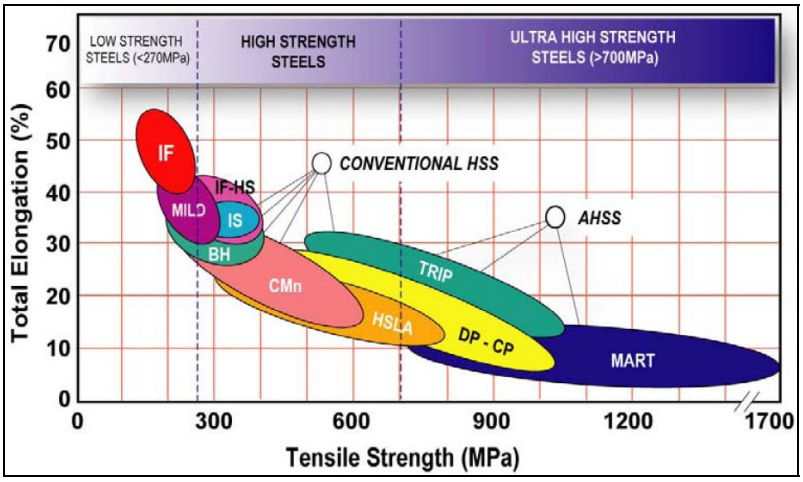

Figure I.A.6 – *Strength-Elongation relationships for low strength, conventional HSS, and AHSS steels.*

*I.A.*5 – Advanced High Strength Steels (AHSS)

New challenges of unprecedented requirements for passenger safety, vehicle performance and fuel economy targets in North America, Europe, and Asia, have forced the automotive industry into advances in material utilization and processing that would have been considered impossible less than a decade ago.

The recent drive towards lightweighting in the transportation industry has led to strong competition between steel and low density metal industries. The steel industry's response to the increasing use of lower density materials, such as aluminium and magnesium, is to develop increasingly higher strength materials while maintaining, or even improving, formability. Thereby making it possible simultaneously to improve the strength characteristics of the parts and reduce the weight through reduction of the steel sheet thickness. In response, the steel industry has recently produced a number of AHSS that are highly formable, yet possess an excellent combination of strength, durability, strain rate sensitivity and strain hardening. These characteristics may enable automotive designers to achieve both weight reduction and improved crash safety.

*I.A.*5.1– AHSS Nomenclature

Classification of AHSS differs from conventional HSS. Since AHSS are relatively new to the Automotive Industry, a consistent nomenclature was not available until the Ultra Light Steel Automotive Body – Advanced Vehicle Concept (ULSAB-AVC) Consortium adopted a standard practice. The practice specifies both yield strength and ultimate tensile strength [2]. In this system, steels are identified as:

XX aaa/bbb where, XX = Type of Steel
aaa = minimum YS in MPa
bbb = minimum UTS in MPa.

The types of steels are defined as:
DP = Dual Phase
CP = Complex Phase
TRIP = Transformation-Induced Plasticity
Mart = Martensitic

For example, DP 500/800 designates dual phase steel with 500 MPa minimum yield strength and 800 MPa minimum ultimate tensile strength.

Table I.A.1 shows some generalized mechanical properties of several advanced high strength steels, which are the grades used in the ULSAB-AVC body structure. The differences between conventional high strength steels and advanced high strength steels arise from the microstructure, which is determined by controlling the cooling rate during processing.

Product	YS (MPa)	UTS (MPa)	Total EL (%)	n-value[a] (5-15%)	r-bar	k-value[b] (MPa)
DP 280/600	280	600	30-34	0.21	1.0	1082
DP 300/500	300	500	30-34	0.16	1.0	762
DP 350/600	350	600	24-30	0.14	1.0	976
DP 400/700	400	700	19-25	0.14	1.0	1028
TRIP 450/800	450	800	26-32	0.24	0.9	1690
DP 500/800	500	800	14-20	0.14	1.0	1303
CP 700/800	700	800	10-15	0.13	1.0	1380
DP 700/1000	700	1000	12-17	0.09	0.9	1521
Mart 950/1200	950	1200	5-7	0.07	0.9	1678
Mart 1250/1520	1250	1520	4-6	0.065	0.9	2021

Where: YS and UTS are minimum values, others are typical values.
Total EL % - Flat sheet.
[a] n-value is calculated in the range of 5 to 15% true strain.
[b] k-value is the magnitude of true stress extrapolated to a true strain of 1.0. It is a material property parameter frequently used by one-step forming simulation codes.

Table I.A.1 – *Typical mechanical properties of AHSS.*

*I.A.*5.2 – Metallurgy of AHSS

The fundamental metallurgy of conventional low and high strength steels is generally well understood by manufacturers and users of steel products. Since the metallurgy and processing of AHSS grades is somewhat novel compared to conventional steels, they will be described here to provide a baseline understanding of how their remarkable mechanical properties evolve from their unique processing and structure.

Dual Phase (DP) Steel

Dual Phase (DP) steels consist of a ferritic matrix containing a hard martensitic second phase in the form of islands. The volume fraction of hard second phases generally increases strength. In some instances, hot rolled steels requiring enhanced capability to resist stretching on a blanked edge (as typically measured by hole expansion capacity) can have a microstructure also containing significant quantities of bainite.

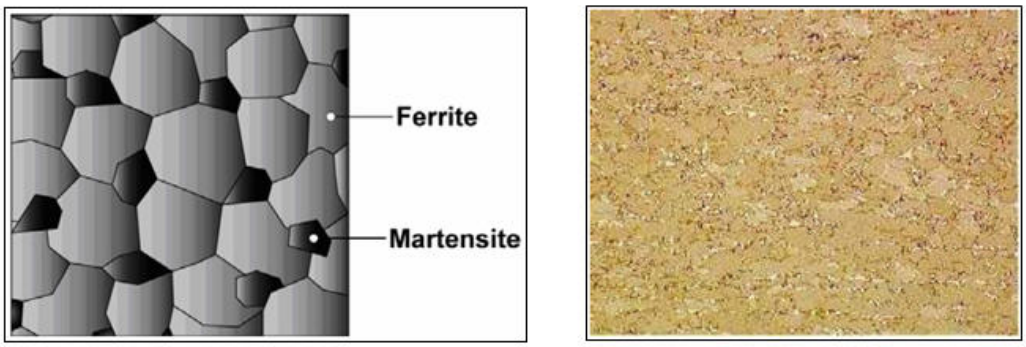

a) *Schematic* ***b)*** *Real*

Figure I.A.7 – *DP Microstructure.*

Figure I.A.7 a) shows a schematic microstructure of DP steel, which contains ferrite plus islands of martensite. The soft ferrite phase is generally continuous, giving to these steels excellent ductility. When these steels deform, strain is concentrated in the lower strength ferrite phase surrounding the islands of martensite, creating the unique high work hardening rate exhibited by their.

The work hardening rate plus excellent elongation give to DP steels a much higher ultimate tensile strength than conventional steels with similar yield strenght. Figure I.A.8 compares the quasi static stress strain behaviour of HSLA steel with a DP steel of similar yield strenght [3]. The DP steel exhibits higher initial work hardening rate, higher ultimate tensile strength, and lower YS/TS ratio than the similar yield strength HSLA.

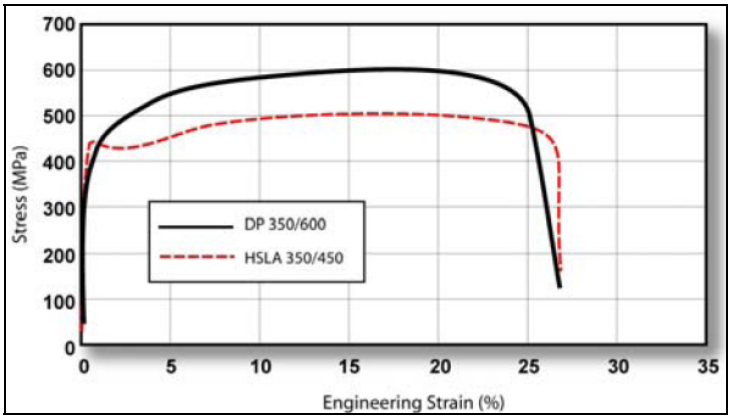

Figure I.A.8 – *Comparison of quasi-static stress-strain behaviour of HSLA 350/450 and DP 350/600 steels.*

DP and other AHSS also have a bake hardening effect that is an important benefit compared to conventional steels. The bake hardening effect is the increase of the yield strength resulting from elevated temperature aging (created by the curing temperature of paint bake ovens) after prestraining (generated by the work hardening due to deformation during stamping or other manufacturing process). The extend of the bake hardening effect in AHSS depends on the specific chemistry and thermal histories of the steels.

In DP steels, carbon enables the formation of martensite at practical cooling rates by increasing the hardenability of the steel. Manganese, chromium, molybdenum, vanadium, and nickel, added individually or in combination, also help increase hardenability. Carbon also strengthens the martensite as a ferrite solute strengthener, as do silicon and phosphorus. These additions are carefully balanced, not only to produce unique mechanical properties, but also to maintain the generally good resistance spot welding capability. However, when welding the highest strength grade (DP 700/1000) to itself, the spot weldability may require adjustments o welding practice.

Transformation-Induced Plasticity (TRIP) Steel

The microstructure of TRIP steels is composed by a minimum of 5% volume of retained austenite embedded in a primary ferrite matrix. Hard phases such as martensite and bainite are also present in varying amounts. A schematic TRIP steel microstructure is shown in Figure I.A.9 a).

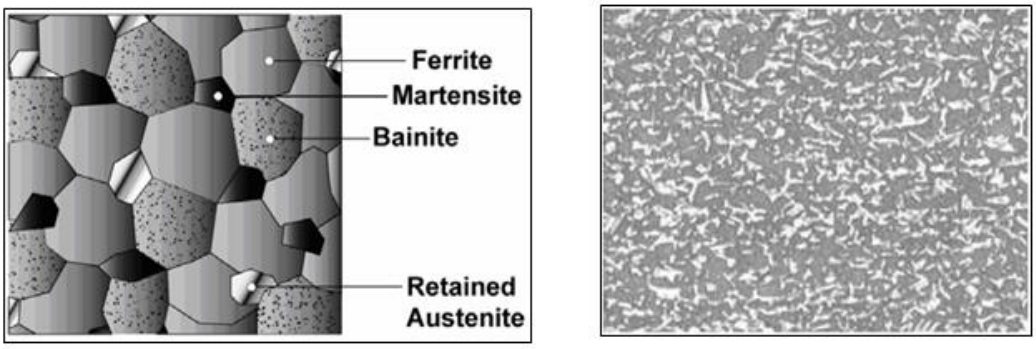

a) *Schematic* ***b)*** *Real*

Figure I.A.6 – *TRIP Microstructure.*

During deformation, the dispersion of hard second phases in soft ferrite creates a high work hardening rate, as observed in the DP steels. However, in TRIP steels the retained austenite also progressively transforms to martensite with increasing the strain, thereby increasing the work hardening rate at higher strain levels. This is illustrated in Figure 1.10, where the stress-strain behaviour of HSLA, DP and TRIP steels of approximately similar yield strength [3]. The TRIP steel has a lower initial work hardening rate than the DP steel, but the hardening rate persists at higher strains while work hardening of the DP starts decreasing, providing a slight advantage in the most severe stretch forming and cup drawing applications.

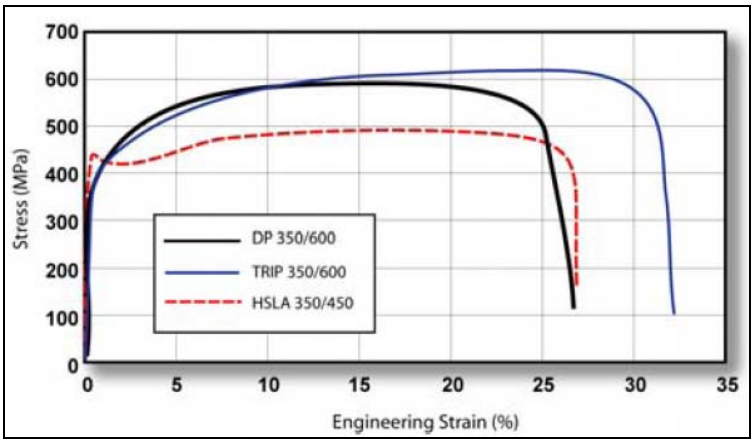

Figure I.A.10 – *Comparison of the quasi-static stress-strain behaviours of HSLA 350/450, DP 350/600 and TRIP 350/600.*

The work hardening rates of TRIP steels are substantially higher than for conventional HSS, providing significant stretch forming and unique cup drawing advantages. This is particularly useful when designers take advantage of the high work hardening rate (and increased bake hardening effect) to design a part utilizing the as formed mechanical properties.

TRIP steels contains higher quantities of carbon than DP steels to decrease the initial martensite temperature till ambient one to form the retained austenite phase. Suppressing the carbide precipitation during bainitic transformation is crucial for TRIP steels. Silicon and aluminium are used to avoid carbide precipitation in the bainite region.

The strain level at which retained austenite begins to be transformed in martensite can be designed by adjusting the carbon content. At lower carbon levels, the retained austenite begins to transform almost immediately upon deformation, increasing the work hardening rate and formability during the stamping process. At higher carbon contents, the retained austenite is more stable and only begins to be transformed at strain levels beyond those produced during forming. At these carbon levels the retained austenite persists into the final part. It transforms to martensite during subsequent deformation, such as a crash event.

TRIP steels can therefore be engineered or tailored to provide excellent formability for manufacturing of complex AHSS parts or to exhibit high work hardening during crash deformation provinding excellent crash energy absorption. The additional alloying requirements of TRIP steels degrade their resistance spot-welding behaviour. This can be addressed somewhat by modification of the welding cycles used (for example, pulsating welding or dilution welding).

Complex Phase (CP) Steel

Complex phase steels typify the transition to steel with very high ultimate tensile strengths. CP steels consists in a very fine microstructure of ferrite and a high volume fraction of hard phases that are further strengthened by fine precipitates. They use many of the same alloy elements found in DP and TRIP steels, but additionally have small quantities of niobium, titanium, and/or vanadium to form fine strengthening precipitates. CP steels display higher yield strengths for equal tensile strength levels of 800 MPa and greater. These steels are mainly characterized by high deformability, high energy absorption, and high residual deformation capacity.

Martensitic (Mart) Steel

To create Martensitic steels, the austenite that exists during hot rolling or annealing is transformed almost entirely to martensite during quenching on the run-out table or in the cooling section of the continuous annealing line. This structure can also be developed with post-forming heat treatment. Martensitic steels provide the highest strengths, up to 1700 MPa ultimate

tensile strength. These steels are often subjected to post quench tempering to improve ductility, and can provide substantial formability even at extremely high strengths.

Carbon is added to martensitic steels to increase hardenability and for strengthening the martensite. The data in Figure I.A.11 illustrates the relationship between carbon content and tensile strength in untempered martensite. Manganese, silicon, chromium, molybdenum, boron, vanadium, and nickel are also used in various combinations to increase their hardenability.

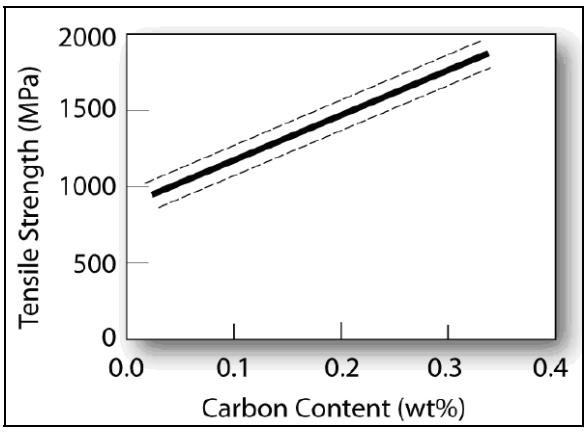

Figure I.A.11 – *Relation of carbon content and tensile strength in untempered martensite.*

*I.A.*5.3 – Mechanical Properties of AHSS

By combining a high number of different microstructures not traditionally found in conventional HSS, a wide range of properties are possible with AHSS. This allows steel companies to tailor the processing to meet the ever more focused application requirements demanded by the automotive industry.

Comparing these AHSS with their conventional HSS counterparts becomes much more difficult. The same minimum tensile strength can be found with a variety of steel types having different yield strengths. One example is TRIP 450/800, DP 500/800, and CP 700/800 steels with the same minimum tensile strength but with different yield strengths and typical total elongations in the range of 29%, 17%, and 13%, respectively. Almost every AHSS steels have their properties determined when are produced. However, the TRIP properties change during deformation when the retained austenite transforms to islands of martensite. The amount and rate of this transformation depends on the type and quantity of deformation, the strain rate, the temperature of the sheet metal, and other conditions unique to specific a part, tool and press.

Yield Strength vs. Total Elongation

A large range of yield strengths are available for the AHSS. Stretching is related to the total elongation obtained in a standard tensile test. Figure I.A.12 shows the general relationship between yield strength and total elongation for AHSS compared to other HSS. [1]

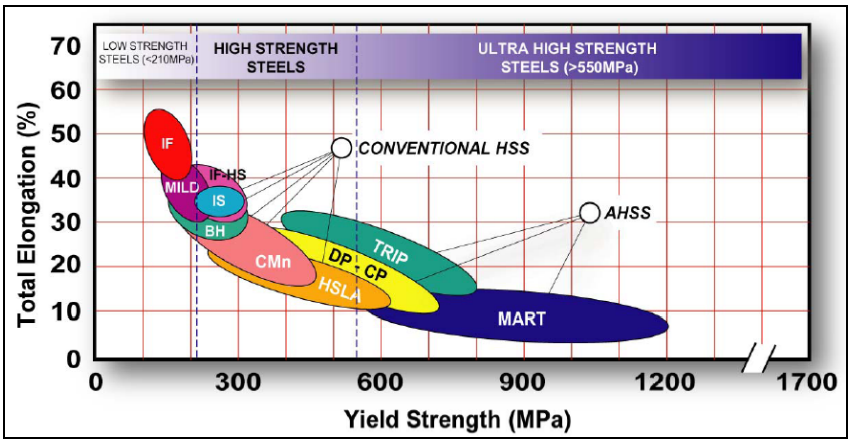

Figure I.A.12 – *Relationship between yield strength and total elongation for various types of steel.*

Note that the families of DP, CP, and TRIP steels generally have higher total elongations than HSLA steels with equal yield strengths.

Most AHSS steels have no yield point elongation (YPE). Some samples of high strength DP grades and TRIP steels may show YPE but the value typically should be less than 1%. These values are in contrast with various HSLA grades, which can have YPE values greater than 5%.

Tensile Strength vs. Total Elongation

The relationship between ultimate tensile strength and total elongation for the various types of steels in Figure I.A.13 is similar that observed in Figure I.A.12.

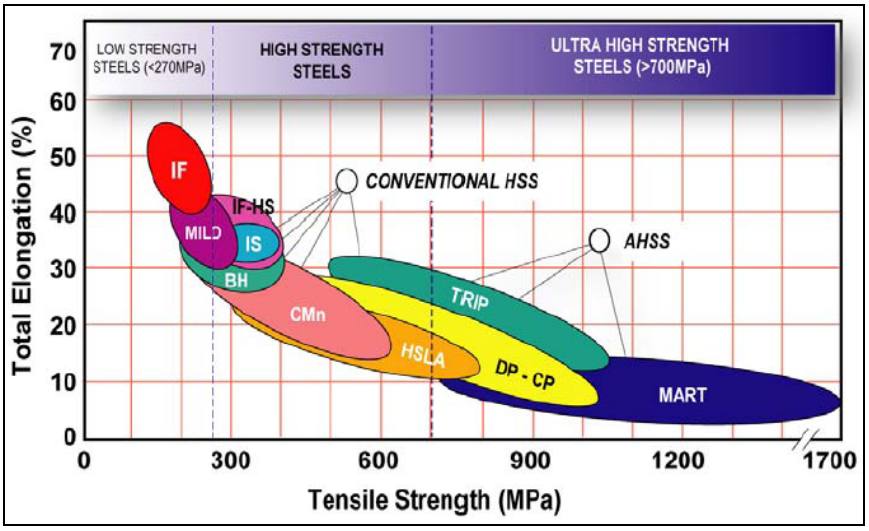

Figure I.A.13 – *Relationship between ultimate tensile strength and total elongation for various types of steel. [1]*

When ordering steel based on tensile strength, the DP, CP, and TRIP steels in general, still have, at equal tensile strengths higher total elongations than HSLA steels.

Work Hardening Exponent (n value)

Stretch forming capability of a material is controlled primarily by the work hardening exponent, *n*, defined by the stress-strain equation:

$$\sigma = K\varepsilon^{n}$$

where σ is the current true stress to continue deformation, K is a constant for the metal under test, ε is the true strain, and n is the work hardening exponent.

The *n* value influences stretch forming in two ways. First, the height of the FLD, defined by FLD_0, is a direct function of the n value [4]. This relationship is shown by the plot in Figure I.A.14, which indicates that the FLD increases with increasing the work hardening exponent. This relationship is valid only for HSS with yield strengths greater than 345 MPa. For steels with yield strengths less than 345 MPa, the level of the FLD has been experimentally shown to be constant. [5]

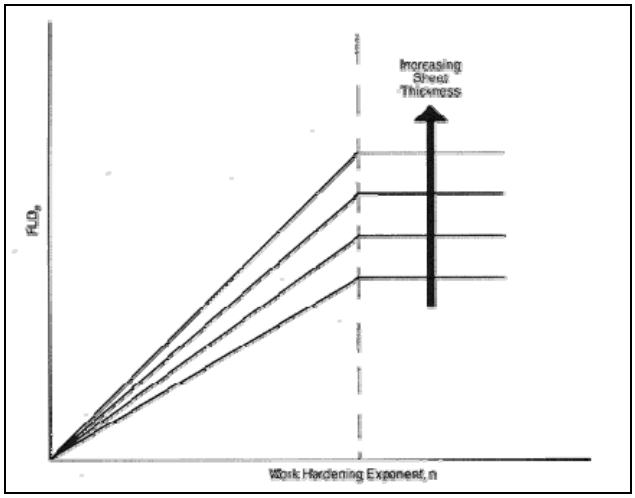

Figure I.A.14 – *Influence of sheet thickness and n value in* $FLD_{O.}$

Second, the n value is one of the factors which determine the uniformity of the strain distribution; the other important factors are lubrication, part/die design, and press adjustments [6]. A high n value means greater work hardening of the metal. This means the metal will more uniformly distribute the strain in the presence of a stress gradient [7].

Unfortunately, the comparison of DP and HSLA n-value requires more than comparing two single values for a given yield strength. The following tensile test data shows why. In one study, HSLA 350/450 has a 0.14 *n* value and the DP 350/600 has the same in a standard test procedure to measure it, over a strain, in a range of 5% to 15%. No differences are reported, which is contrary to increased stretchability gained when using DP steels. On the other hand, a number of different DP steels, showing a wide range of *n* values, were observed for a given strength level.

Unlike the HSLA 350/450 steel that has an approximately constant *n* value over most of its strain range, the DP 350/600 *n* value starts higher and then decreases with strain increasing, as the initial effect of the original martensite islands decreasing. To capture this behaviour, the instantaneous *n* value as function of strain must be determined.

These values for the HSLA 350/450 and DP 350/600 shown in Figure I.A.15 clearly indicate this much higher *n* value for DP steel at strain less than 5%. This fact tends to restrict the onset of strain localization and growth of sharp strain gradients. Minimization of sharp gradients on the length of line also reduces the amount of sheet metal thinning.

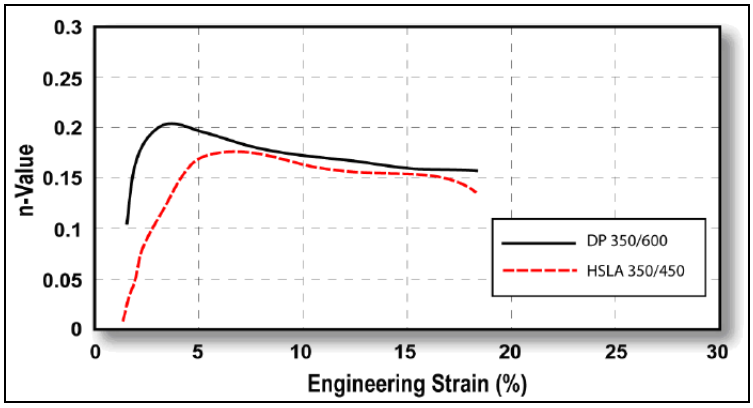

Figure I.A.15 – *Instantaneous n values versus strain for DP 350/600 and HSLA 350/450 steels.[3]*

This reduction on thinning for a channel is presented in Figure I.A.16 [8]. Substitution of DP 350/600 for HSLA 350/450 reduced the maximum thinning from 25% to just over 20%.

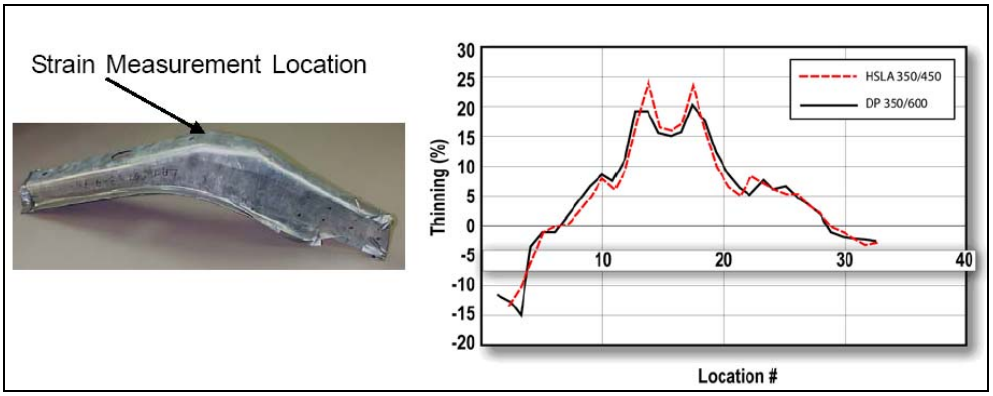

Figure I.A.16 – *Thinning strain distribution for a channel produced with DP and HSLA steels.*

Unlike the DP steels where the increase in *n* value is restricted to the low strain values, the TRIP steels constantly create new islands of martensite while the steel is deformed to higher strain values. These new martensite islands maintain the high value of *n* as shown in Figure I.A.17.

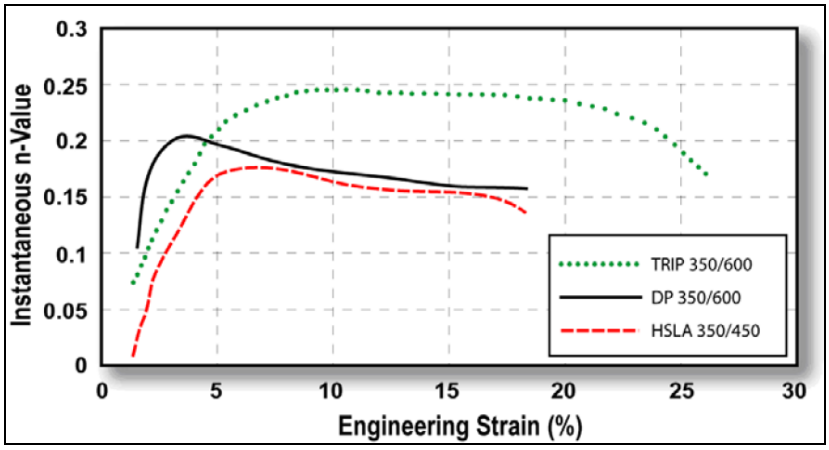

Figure I.A.17 – *Instantaneous n values versus strain for TRIP, DP, and HSLA steels. [3]*

The continued high *n* value of the TRIP steel relative to the HSLA steel contributes to increase the total elongation. The increased *n* value at higher strain levels further restricts strain localization and increases the height of forming limit curve.

Normal Anisotropy Ratio (r value)

The normal anisotropy ratio (r) defines the ability of the metal to deform in the thickness direction relative to deformation in the plane of the sheet. For *r* values greater than one, the sheet metal resists thinning. Values greater than one improve cup drawing, hole expansion, and other forming modes where metal thinning is detrimental.

High-strength steels with UTS greater than 450 MPa and hot-rolled steels have an *r* value approximation one. Therefore, HSS and AHSS at similar yield strengths perform equally in forming modes influenced by the *r* value.

Bake Hardening

Strain aging was measured using a typical value for an automotive paint/bake cycle, consisting of 2% uniaxial pre-strain followed by baking at 170ºC for 30 min. Figure I.A.18 defines the measurement of work hardening (B minus A), unloading to C (for baking), and reloading to yielding at D for measurement of bake hardening (D minus B or E minus B).

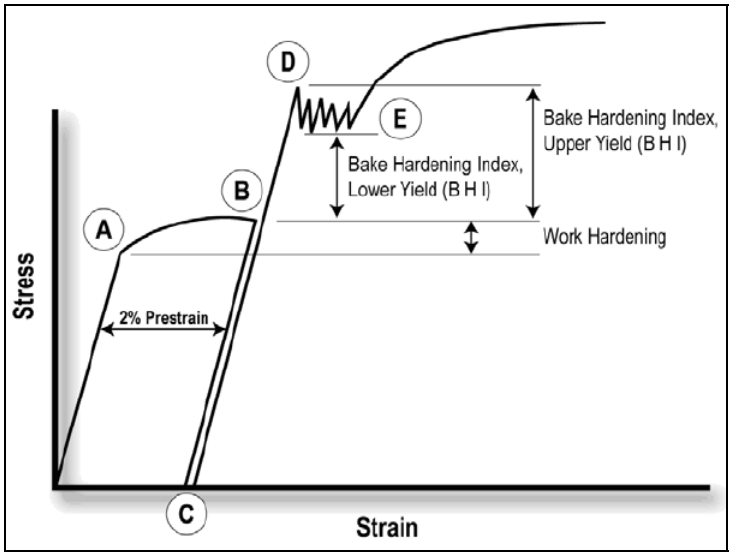

Figure I.A.18 – *Measurement of work hardening index and bake hardening index.*

Figure I.A.19 shows the work hardening and bake hardening increases for prestrained and baked tensile specimen. The HSLA shows little or no bake hardening, while AHSS such as DP and TRIP steels shows large positive bake hardening index. The DP steel also has a significantly higher work hardening than HSLA or TRIP steel due to it higher strain hardening at low strains.

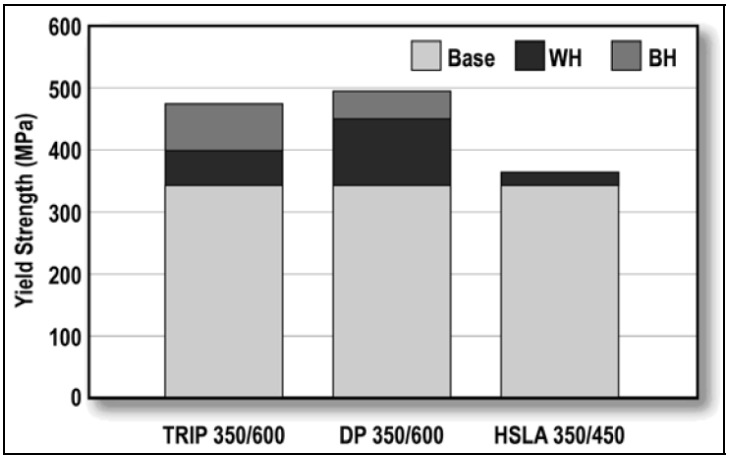

Figure I.A.19 – *Comparison of work hardening (WH) and bake hardening (BH) for TRIP, DP, and HSLA steels. [8] [9]*

*I.A.*5.4 – Structural Steel Performance of AHSS

The superior formability of advanced AHSS, compared with conventional HSS of similar initial yield strengths, give the automotive designer more flexibility to optimize part geometry. This point discusses other component

performance criteria that also affect vehicle performance such as stiffness, strength, durability, and crash energy management.

Stiffness

The stiffness of a component is controlled by material modulus of elasticity (E) and component geometry (including gauge). Since the modulus of elasticity is constant for steel, changing the grade will not influence vehicle stiffness; the designer must modify component geometry. The enhanced formability of AHSS offers greater design flexibility, which will allow a designer to improve component stiffness without increasing mass or sacrificing strength. Reductions in gauge can be offset by changes in geometry or the use of continuous joining techniques such as laser welding or adhesive bonding.

Strength

Component strength is a function of its geometry and yield and/or tensile strength. As noted previously, AHSS offer improvements in design flexibility due increased formability and enhanced work and bake hardening capability. The combination of superior work hardening and excellent bake hardening enhances the final as-manufactured strength of AHSS components.

Crash Management

DP and TRIP steels with ferrite as a major phase show higher energy absorbing property than conventional HSS, particularly after pre-deformation and paint baking treatments. Two key features contribute to this high energy-absorbing property: high work hardening rate and large bake hardening effect.

The relatively high work hardening rate, exhibited by AHSS steels, leads to a higher ultimate tensile strength than the one exhibited by conventional HSS of similar yield strength. This provides for a larger area under the stress-strain curve, indicating greater energy absorption when deformed in a crash event to the same degree as conventional steels. The high work hardening rate also allows for a better strain distribution during crash deformation, providing more stable and predictable axial crush that is crucial for maximizing energy absorption during a front or rear crash event.

The relatively large bake hardening effect also increases the energy absorption of DP and TRIP steels by further increasing the area under the

stress-strain curve. Conventional HSS do not exhibit a strong bake hardening effect and do not benefit from this strengthening mechanism.

Figure I.A.20 illustrates the difference in energy absorption between DP and TRIP steels as a function of their static (traditional tensile test speed) yield strength [10].

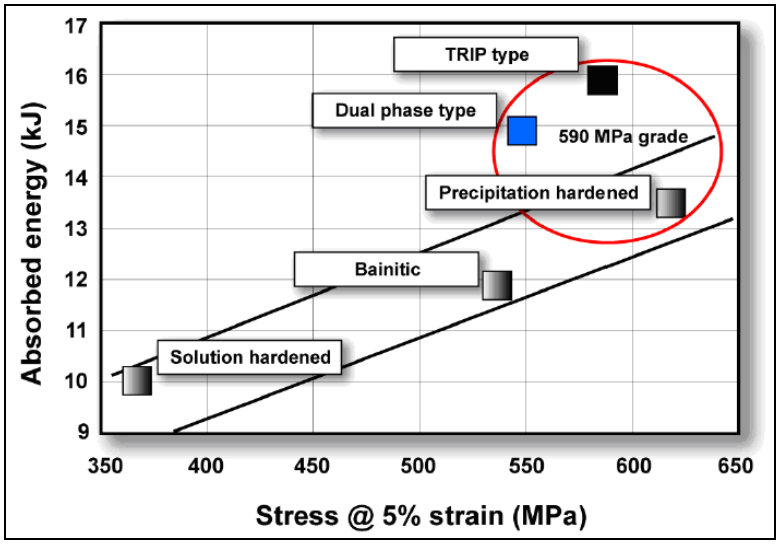

Figure I.A.20 – *Absorbed energy for square tube as function of static yield strength.*

Figure I.A.21 shows the calculated absorbed energy plotted against total elongation for a square tube component. The absorbed energy remains constant for the DP and TRIP steels, but the increase in total elongation allows for formation into complex shapes. For a given critical crash component, the higher elongations of DP and TRIP steels, generally, do not increase energy absorption when compared to conventional HSS. In some applications the DP and TRIP grades could increase energy absorption over that of a conventional HSS if the conventional steel doesn't have sufficient ductility to accommodate the required crash deformation and splits rather than fully completing the crush event. In the latter case, substituting DP or TRIP steel, with sufficient ductility to withstand full crash deformation, will improve energy absorption by restoring stable crush and permitting more material to absorb crash energy.

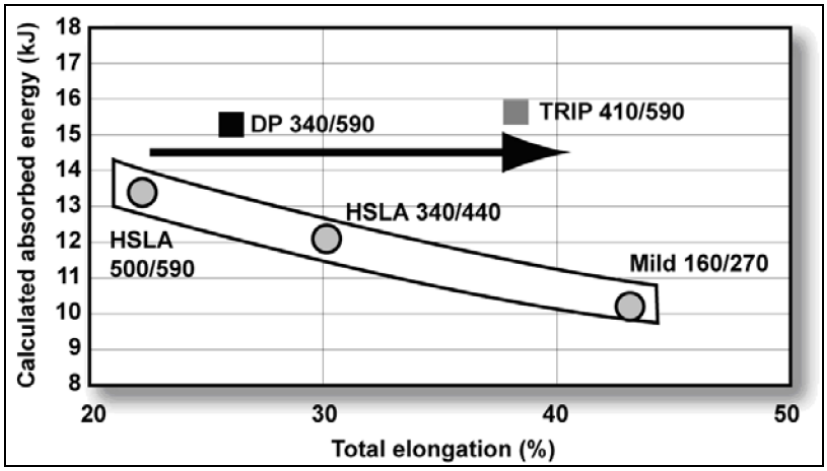

Figure I.A.21 - *Calculated absorbed energy for a square tube as a function of total elongation.[10]*

Fatigue

Fatigue in a structural component involves complex relationships among several factors including geometry, thickness, applied loads and material endurance limit [10].

The fatigue strength of AHSS steels is higher than the one of precipitation-hardened steels or fully bainitic steels with similar yield strength for many metallurgical reasons. For example, in DP steels the dispersed fine martensite particles retard the propagation of fatigue cracks, and in TRIP steels, the transformation of retained austenite can relax the stress field and introduce a compressive stress that can also improve fatigue strength. Figures I.A.22 and I.A.23 illustrate the improvements in fatigue capability.

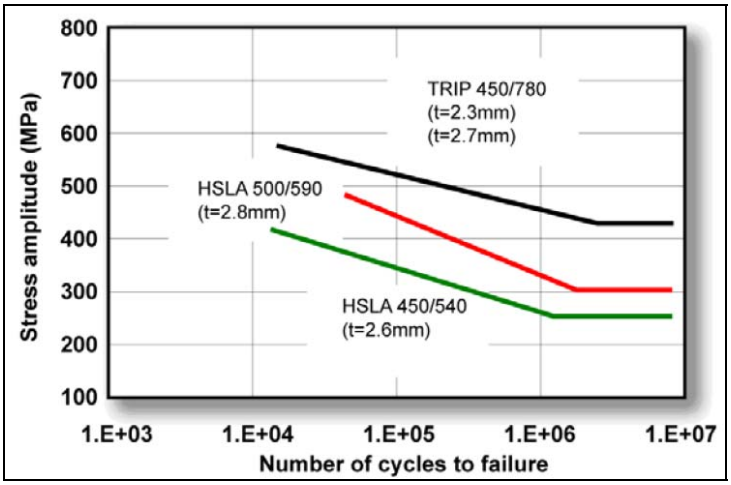

Figure IA.22 - *Fatigue characteristics of TRIP 450/780 steel compared to convention steels. [12]*

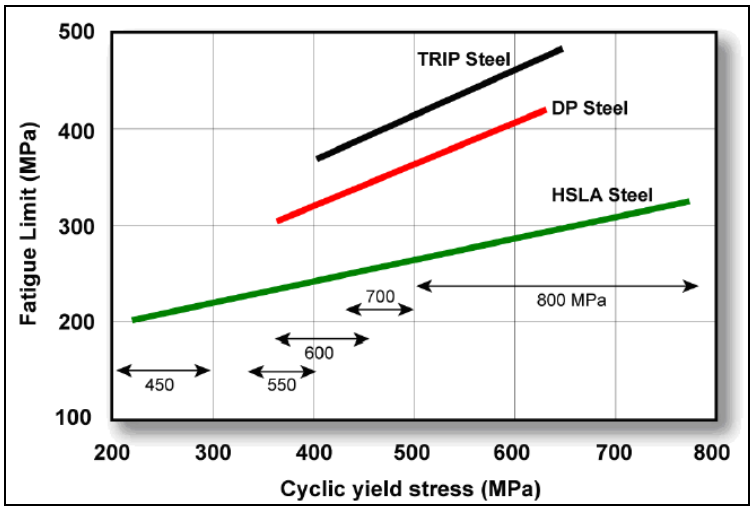

Figure I.A.23 - *Fatigue limit for AHSS compared to conventional steels. [10]*

*I.A.*5.5 - AHSS Processing

All AHSS are produced by controlling the cooling rate from the austenite or austenite plus ferrite phase, either on the runout table of the hot mill (for hot-rolled products) or in the cooling section of the continuous annealing furnace (continuously annealed or hot-dip coated products).

Martensitic steels are produces from the austenite phase by rapid quenching to transform most of the austenite to martensite.

Dual phase ferrite plus martensite steels are produced by controlled cooling from the austenite phase (in hot-rolled products) or from the two-phase ferrite plus austenite phase (for continuously annealed and hot-dip

coated products) to transform some austenite to ferrite before a rapid cooling to transform the remaining austenite to martensite.

TRIP steels typically require the use of an isothermal hold at an intermediate temperature, which produces some bainite. The higher silicon and carbon content of TRIP steels also result in significant volume fractions of retained austenite in the final microstructure.

Complex-phase steels also follow a similar cooling pattern, but here the chemistry is adjusted to produce less retained austenite and form fine precipitates to strengthen the martensite and bainite phases.

*I.A.*6 – Comparative Cost and Mass I.A.6

Many factors affect overall component cost such as corrosion resistance, component life, and subsequent processing operations. Material costs, which can vary widely, are only one factor in the overall cost. A more expensive material that meets performance requirements and requires less processing may generate lower overall cost than a less expensive material.

Table I.A.24 gives approximate comparative cost data for twelve types of steel that can be used to advantage by the automotive designer.

Type	Approximate Relative Cost
Hot Rolled Carbon	0.80
Cold Rolled Carbon	1.00
Bake Hardenable	1.10
Hot Dipped Galvanized	1.12
Aluminized	1.21
Electrogalvanized	1.35
HSLA	1.15
Dual Phase	1.40
Martensitic	1.50
Aluminum Sheet Type 5052	4.8
Austenitic Stainless Type 304	5.7
Ferritic Stainless Type 409	2.6
Martensitic Stainless Type 410	2.8
PH Stainless 17-4	9.0

Table 1.24 - *Approximate relative costs of various sheet steels.*

I.A.7 **Bibligraphy:**

[1] International Iron and Steel Institute, UltraLight Steel Auto Body - Advanced Vehicle Concepts (ULSAB – AVC) Report / AISI Training Session Document (2002).

[2] ULSAB-AVC Consortium, Technical Transfer Dispatch #6, "ULSAB-AVC Body Structure Materials," May, 2001.

[3] A. Konieczny, "Advanced High Strength Steels – Formability," 2003 Great Designs in Steel, American Iron and Steel Institute (February 19, 2003).

[4] American Iron and Steel Institute, Sheet Steel Formability, AISI, Washington, D.C., (1984).

[5] Keeler, S. P. and Brazier, W. G., "Relationship Between Laboratory Material Characterization and Press-Shop Formability," Microalloying 74 – New York, N.Y., (1977), pp. 517-530.

[6] Keeler, S. P., "Sheet Metal Stamping Technology – Need for Fundamental Understanding," Mechanics of Sheet Metal Forming – Material Behaviour And Deformation Analysis, General Motors Research Symposium, Plenum Press, New York, (1978), pp. 3-17.

[7] Heyer, R. H. and Newby, J. R., "Effects of Mechanical Properties on Biaxial Stretchability of Low Carbon Steels," Trans. S'E, 77, (1969), Also S'E Paper No. 680094.

[8] M. Shi, G. Thomas, X. Chen and J. Fekete, "Formability Performance Comparison between Dual Phase and HSLA Steels", Proceedings of 43rd Mechanical Working and Steel Processing, Iron & Steel Society, 39, p.165 (2001).

[9] A. Konieczny, "On the Formability of Automotive TRIP Steels", SAE Technical Paper No. 2003-01-0521 (2003).

[10] M. Takahashi, "Development of High Strength Steels for Automobiles," Nippon Steel Technical Report No. 88 (July 2003).

[11] R. Shaw, B. K. Zuidema, "New High Strength Steels Help Automakers

Reach Future Goals for Safety, Affordability, Fuel Efficiency, and Environmental Responsibility" SAE Paper 2001-01-3041.

[12] M. Takahashi et al, "High Strength Hot-Rolled Steel Sheets for Automobiles", Nippon Steel Technical Report No. 88 (July 2003).

Section I.B

Plastic deformation process

*I.B.*1 – Introduction

Definition

In metal forming, a piece of material is plastically deformed between tools to obtain the desired product applicable in automobiles, domestic appliances, building products, aircraft, food and drink cans and a host of other familiar products. There are two main classes of metal forming, the bulk and the sheet metal forming (the thickness of the piece of material is small compared to the other dimensions). Sheet metal forming (SMF) is a widely used production process: in 2004, 310 million tons of steel sheet and 12 million tons of aluminium sheet was produced worldwide which was approximately 40% of the total steel and aluminium production. Then principal characteristics of sheet metal forming processes are:

(1) The workpiece is a sheet or a part fabricated from a sheet;

(2) The surfaces of the deforming material and of the tools are in contact;

(3) The deformation usually causes significant changes in shape, but not in cross-section (sheet thickness and surface characteristics), of the sheet;

(4) The component of stress state normal to the sheet plane is generally much smaller than the stresses in the sheet plane;

(5) In some cases, the magnitude of permanent plastic and recoverable elastic deformation is comparable, therefore elastic recovery or springback may be significant.

The technical-economic advantages of SMF are that it is a highly efficient process that can be used to produce complex parts. It can produce parts with high degree of dimensional accuracy and increased mechanical properties along with a good surface finish. But the limitation is that the deformation imposed in SMF process is complicated.

History

Forming is an old art, examples of formed jewellery made of gold date back to 3000 BC. The primary objective of metal forming is to produce a desired shape change and therefore in this process, it must be recognised that material properties affect the process, and processing alters the material properties.

The primary stamping press was invented in 1769 by John Pickering (a London toymaker), Richard Ford and John Smith, both of Birmingham (Figure I.B.1). In such time, this invention was extremely importance because increase the speed production of many brass articles and thereby increased this demand.

Figure I.B.1 – *Example of one old stamping machine.*

Interaction between adjacent stages

Historically, the progression of an automotive sheet metal body forming from conception to production has been a segmented series of events. Styling, part design, material selection, dies design, die build, die tryout, and part production have been performed in a sequential manner. Interaction between adjacent stages has been minimal at best. For example, die designers have had little input into the design of the part, and rarely did they interact with the press room tryout staff. The activities of each segment in the sequence have been conducted within its own sphere of work by its own group members. Interaction among the different groups has been very limited.

Nowadays, simultaneous engineering requires that representatives from all units involved in the conception to production sequence become involved together at the earliest possible point in the design. Ideally, the simultaneous engineering concept even brings specialists from material, lubricant and other outside suppliers into the initial design phase, where major design changes can be made most easily in a cost and time effective manner.

Interaction of various functions requires a number of common crossover points for all participants: identical language, understanding of basic sheet metal formability, formability limits, press shop terminology, and a framework for analysis. Only then can diverse participants communicate and understand each other to accomplish the best, low cost design that will have optimum manufacturing feasibility.

Contents of this chapter

This chapter describes some of the most important methods of metal forming (Point *I.B.*2). Since this project deals with the stamping process, this study will be focused on it, describing every stamping processes (Point *I.B.*3.2) with reference to some of main forming defects (Point *I.B.*6.1) and to the principal presses used to transform a simple sheet in a complex part (Point *I.B.*5.1).

*I.B.*2 - Manufacturing Processes

*I.B.*2.1 – Stamping

Stamping is one type of sheet metal forming process, which is widely used in automotive industries. The popularity of stamping is mainly due to its high productivity, relatively low assembly costs and the ability to offer high strength and lightweight products [1].

These process is applied with the intention of manufacturing a product with a desired shape and no failures. The final product shape after stamping is defined by the tools, the blank and the process parameters.

Metal stamping involves forming a piece of metal with a dedicated piece of tooling and stamping the piece through a mechanical press. During the metal stamping operation, the upper die is attached to the ram and the lower die is attached to the stationary bolster. As the press is activated, the ram moves vertically towards the bolster to form the piece of metal over the lower die. Metal stamping presses can perform a diverse range of operations such as blanking, piercing, forming and drawing as well as combinations of these processes.

These operations are done with dedicated tooling also known as hard tooling. This type of tooling is used to make high volume parts of one configuration of part design. (By contrast, soft tooling is used in processes such as CNC turret presses, laser profilers and press brakes). All these operations can be done either at a single die station or multiple die stations — performing a progression of operations, known as a progressive die.

The deformation patterns of the sheet material are influenced by the material properties and the friction conditions. Generally, sheet material behaves anisotropically which means that the material shows a different deformation behaviour in different directions because of the rolling process. An example of anisotropy is the development of ears in cylindrical cup drawing. The friction conditions during forming depend on the lubricant, the presence of coatings on the blank, surface roughness of the tools and the blank, blankholder pressure and process velocity.

Without extensive knowledge of the influences of all these variables on the deep stamping process, it is hardly possible to design the tools adequately and make a proper choice of blank material and lubricant to manufacture a product with the desired shape and performance.

In general, the deformation of sheet materials in the stamping process is classified by four principal types of deformation modes; bending, deep drawing, stretching and flanging.

*I.B.*2.2 – Roll Forming

Cold roll forming is a process whereby a sheet or strip of metal is formed into a uniform cross section by feeding the stock longitudinally through a roll forming mill. The mill consists of a train with pairs of driven roller dies, which progressively form the flat strip until the finished shape is produced. The number of pairs of rolls depends on the type of material being formed, the complexity of the shape being produced, and the design of the particular mill being used (Figure I.B.2). A conventional roll forming mill may have as many as 30 pairs of roller dies mounted on individually driven horizontal shafts. Roll forming is one of the few sheet metal forming processes that is confined to a single primary mode of deformation. Unlike most forming operations that have various combinations of stretching, drawing, bending, bending and straightening, and other forming modes, the roll forming process is nothing more than a carefully designed series of bends. In roll forming, metal thickness is not changed except for a slight thinning at the bend radii.

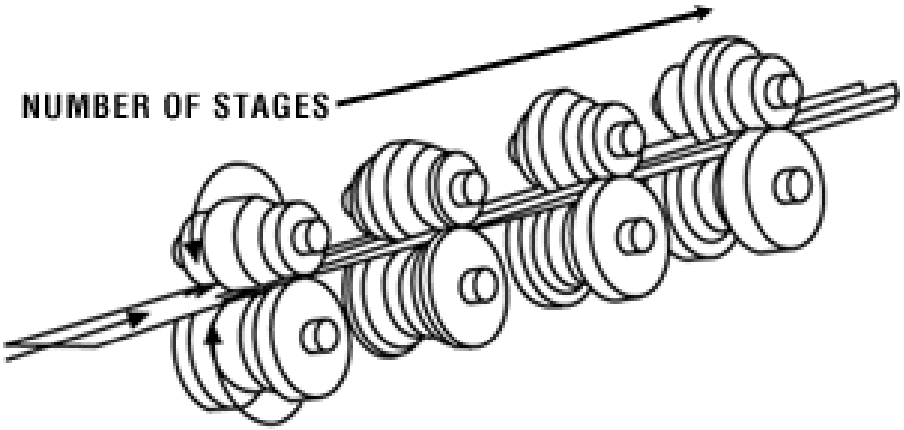

Figure I.B.2 – *Roll Forming process.*

The roll forming process is particularly suited to the production of long lengths of complex shapes held to close tolerances. Large quantities of these parts can be formed with a minimum of handling and manpower. The process can be continuous by coil feeding and exit cutting to length. Entry material can be pre-painted or otherwise coated. Operations such as notching, slotting, punching, embossing and curving can easily be combined with contour roll forming to produce finished parts off the exit end of the roll forming mill. In fact, ultra high-strength steel reinforcing beams, with sweeps up to 50, only need to have the mounting brackets welded to them before shipment to the assembly line.

***I.B.*2.3 - Hydroforming**

There are two types of hydroforming, sheet and tubular. Sheet hydroforming is typically a process where only a female die is constructed and a bladder membrane performs as the punch. High pressure fluid (usually water) forces the bladder against the steel sheet until it takes the shape of the female die. Sheet hydroforming has not been developed to the point it can be effectively utilized by the automotive industry. It remains a process used for low volume, large parts such as those encountered in aircraft and bus sheet metal forming.

In tubular hydroforming, a straight or pre-bent tube is laid into a lower die. The upper and lower dies are then clamped together. Next, conical nozzles are inserted and clamped into each end of the tube. Finally, a fluid (usually water) is forced at a high pressure into the tube until it takes the shape of the die. While tube hydroforming technology has been around for decades, the mass production of automotive parts only became cost effective about 1984.

The benefits of hydroforming are usually found via part consolidation and the elimination of engineered scrap. Box sections, consisting of two hat sections welded together, lend themselves to cost-effective replacement by a single hydroformed part. Punches, mounted in the forming dies, are used to pierce holes during forming, eliminating subsequent machine operations.

The structural integrity of a hydroformed part, made from a single continuous tube, is superior to that of a part made from two or more components. Weight savings of 10 to 20% can be achieved via both reducing gauge and eliminating weld flanges. If flanges are necessary for attachment, they can be created by pinching the tube during the hydroforming process.

High volume tubular hydroformed parts are currently incorporated into automotive components such as axles, exhaust manifolds, suspensions, frames, drive shafts and shock absorbers. While hydroforming technology has not been used to date for bumper systems, it does have potential over the longer term due to the many advantages it offers

***I.B.*2.4 – Hot Forming (**Plannja)

The Plannja hot forming process was developed by Plannja Hard Tech, a division of Plannja Steel, which in turn is a subsidiary of Swedish Steel AB. Plannja Hard Tech uses this process to produce a wide variety of products from automotive door impact beams to lawn mower blades, to bumper reinforcing beams [2].

Developed blanks made from full hard, cold rolled, sheet steel are continuously fed into a gas fired furnace. The blanks are heated to austenitizing temperatures, approximately 900° C, in about 3 to 5 minutes. A set of two or four blanks, depending on their size, is then fed into a hydraulic press. The press cycles down, remaining in that position while the dies quickly cool the formed blanks until the temperature is approximately 38° C, well below the martensite finish temperature. The time required to cool the parts in the dies is approximately 10 seconds per mm of thickness (ex. a set of parts 2 mm thick will take 20 seconds to cool).

The light scale that forms during the hot forming process is removed by shot blasting with chromium shot. This leaves a thin film of chromium and iron on the surface of the part, thus eliminating the need for re-oiling to prevent oxidation and corrosion. If a very high degree of tolerance is required, holes can be machined into the finished part, but due to the ultra high-strength of the material in the finished part, it is best to incorporate the holes into the developed blank. The chemistry of the incoming steel and the cooling rate of the hot forming process are designed to achieve the final mechanical properties of the finished part.

Yield strengths up to 1200 MPa result in high part strength and reduced part weight. The combination of high hardness (up to 48 Rockwell C) and good toughness gives improved wear resistance. The repeatability of

dimensions is very good, even in long production runs. There is no springback, a phenomenon which is common with cold forming processes. Weldability is excellent due to the low carbon content. Formability is also excellent at the 900° C forming temperature. Highly complicated components can be produced in one piece. One disadvantage of the Plannja process is the relatively slow production rate due to the length of time a part must remain in the dies to ensure proper cooling

*I.B.*2.5 - Incremental Forming

This process is used to form sheet metal into complicated shapes without the use of either a male or female die. The process uses a single point tool which plastically deforms sheet metal to give a local micro-deformation. By doing this incrementally, and controlling the tool path with a CNC mill, the plastically deformed points are, in effect, added as the tool moves to give a final shape (Figure I.B.3). The sheet metal is held in place by a blankholder which moves in a vertical plane on four posts. Deformation of the strip can be achieved in one of two ways: either with a supporting, fixed tool about which the single point forming tool moves or by inversion of the process in which the supporting, fixed tool is not used.

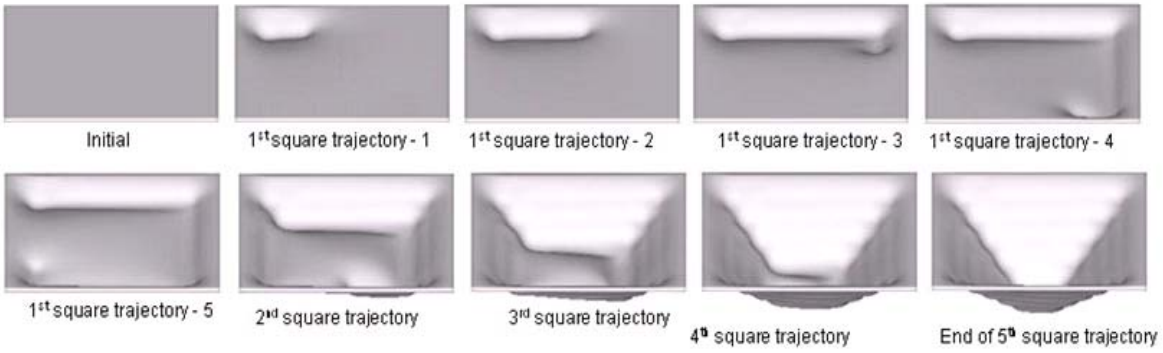

Figure I.B.3 – *Some stages of an Incremental forming process.*

*I.B.*2.6 – Extrusion

In the process of extrusion (Figure I.B.4), a billet is placed into a chamber with a shaped opening (called a die) on one end and a ram on the other. As the ram is forced into the chamber, the workpiece is forced out through the die. The extrudate, a long product (ex. a rod), emerges through the die duplicating its cross sectional shape. The flow lines indicate that a dead metal zone forms in the corner on the exit side of the chamber where the separated ring of a triangular cross section remains stagnant.

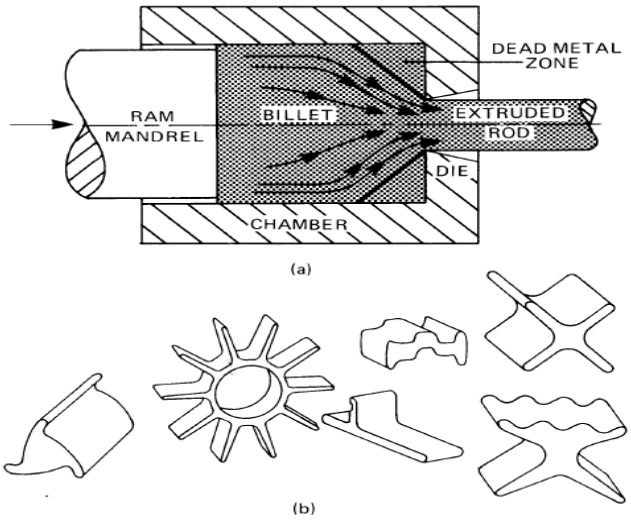

Figure I.B.4 – a) *Extrusion Process,* ***b)*** *Some parts manufactured by extrusion process*

*I.B.*2.7 – Forging

The process of forging is performed on a press or a hammer. Basically, the ingot is placed between two platens that are forced one against each other, squeezing the ingot between them (Figure I.B.5). A variety of shapes can be produced between flat platens by manipulation of the ingot while the platens squeeze and release the workpiece repeatedly. Alternately, the platens may be shaped with a cavity that imparts its shape on the product.

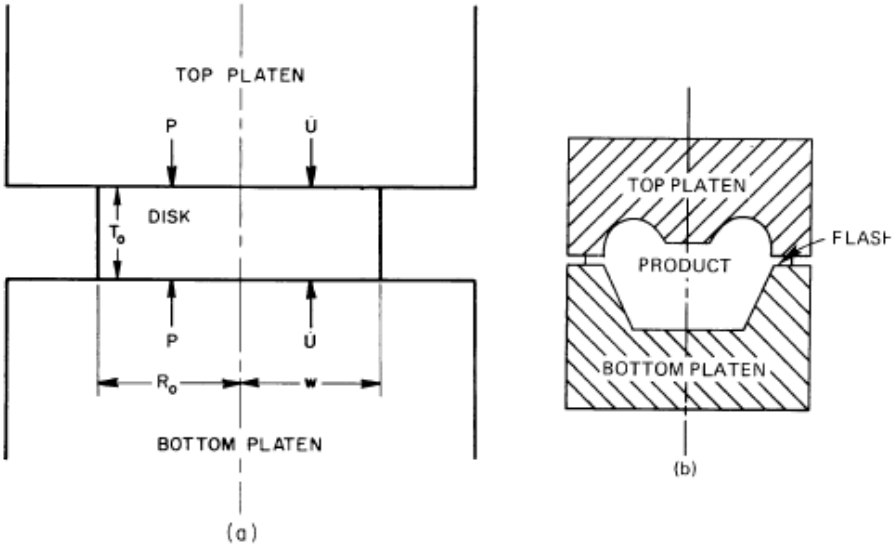

Figure I.B.5 – *Forging process.*

*I.B.*3 – Stamping Process

Stamping operations convert coils of steel received from the steel mill into parts. The parts are rarely used in their as formed condition, they are usually assembled with other stampings or parts by welding, bonding, or mechanical fastening (Figure I.B.6). Subsequent operations are important in that they place constraints on the part design and forming operations. For example, welding may require a weld flange of minimum width that must be buckle free. [3], [4]

Figure I.B.6 – *The assembly of a vehicle in an automotive industry.*

*I.B.*3.1 - A Simple Stamping

Two methods are used to divide a complex part into its component sections. The first method, by the geometry of the part, is generally used by the stylist and part designer. It describes the final geometry and dimensions of the functional part independent of how the geometry was obtained. The second method, by forming operations or forming mode, is used by the die designer to generate the required geometry. It consists of an initial stamping which then usually undergoes a number of additional operations, such as restrike, trim, flange, and punch, before it becomes a finished part. The initial stamping may or may not resemble the final part.

A distinction is made here between a stamping and a part. A stamping is the deformed sheet anywhere in the production cycle, it represents some stage along the production cycle. The initial stamping usually needs to undergo several forming and processing sequences before it becomes a part and leaves the stamping operation. When a stamping becomes a part, it may not yet be suitable to put on the automobile. For example a door panel

needs an inner door part, outer door part, door intrusion beam, locks, hinges, etc (Figure I.B.7). The finished part is the final goal of the stylist and the part designer; intermediate stamping operations are the concern of the die designer.

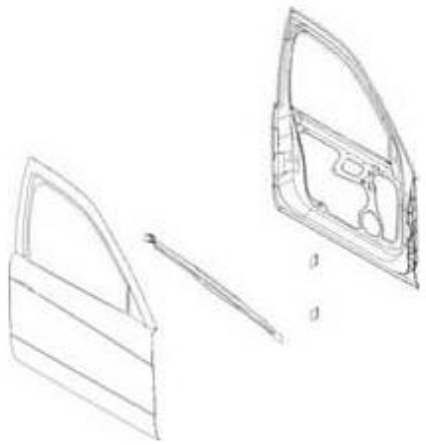

Figure I.B.7– *An inner and an outer door part.*

Figure I.B.8 shows a complex part that represents geometries commonly found in typical automotive body panels. The geometry of the part can be prescribed by specifying the dimensions of the top surface, the side walls, the corners, and the flanges. Added to this overall stamping geometry are sub areas such as embossments, holes, slots, and other functional zones. The part designer thinks in terms of the required geometry to accomplish the required function or the geometry needed to fulfill the styling shape, usually without concern about how the part is to be made

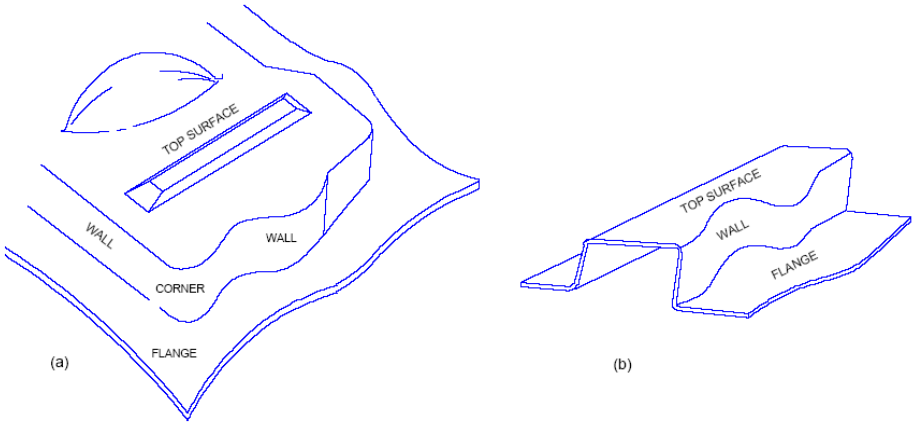

Figure I.B.8 – *Schematic of a part with a combination of geometries.*

The second method of breaking down a complex part is by its forming operations or forming modes. Typical forming operations are listed in Table 2.1 and defined in Point *I.B.3.2 - Description of Forming Modes*. Note that specific geometric shapes can be created by more than one forming operation or mode, as illustrated Figure I.B.8 b). The geometric characteristics are similar to Figure I.B.8 a), but the forming operations are different.

GEOMETRY	FIRST OPERATION	SUBSEQUENT OPERATION
Top Surface	None Stretch Emboss	Restrike Emboss
Corner	Cup Draw	Redraw Ironing
Wall	Bending Bend-and-Straighten Shrink Flange Stretch Flange	Post Stretch
Flange	Draw Bead Contours	Trim and Reflange
Other	Blank	Trim Pierce Punch Extrude

Table I.B.1 – *Relationship between part geometry and forming mode.*

*I.B.*3.2 - Description of Stamping Modes

a) Stretching

In the most common stretching mode, the blank is completely clamped at the die ring or binder by hold down pressure or lock beads (Figure I.B.9 a)). A contoured punch is then pushed through the die opening into the clamped blank. All deformation stretching occurs in the metal that is originally within the die opening. The deformation state is biaxial tension, which results in a thinning of the metal over the entire dome. In the laboratory, stretchability is commonly evaluated by a hemispherical punch.

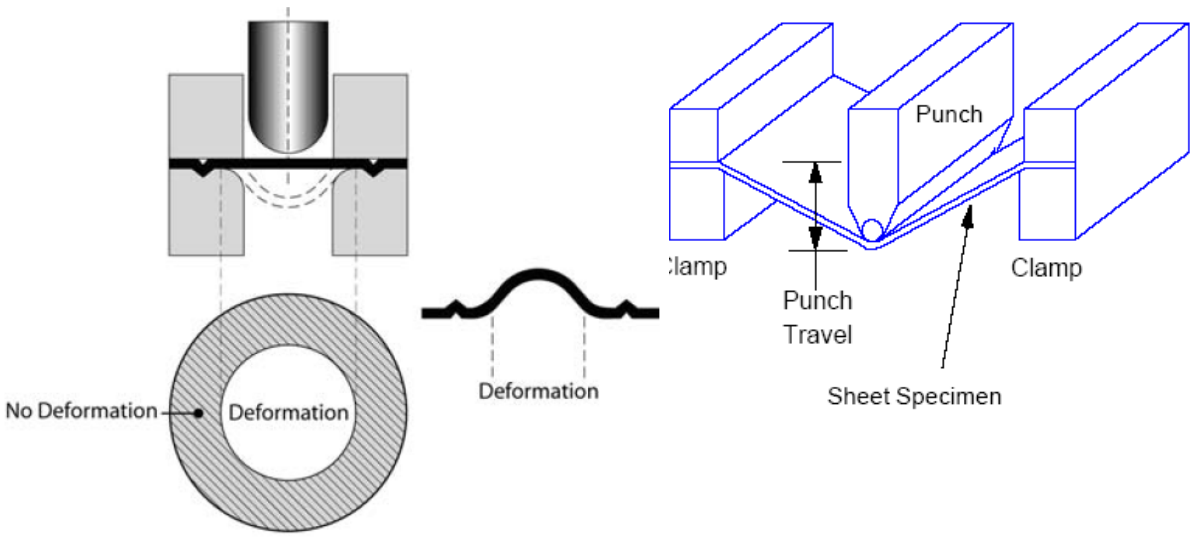

a) *Biaxial* ***b)*** *Plane Strain*

Figure I.B.9 – *Stretch forming in which no deformation is allowed in the flange area and all deformation occurs in the die opening over the punch.*

Plane strain stretching is a special case of stretching (Figure I.B.9 b)), where the punch is very long compared to its width. Again the blank is securely clamped at the ends. Deformation now occurs only across the punch face; no deformation occurs along the punch length. This deformation mode is commonly found in character lines and the edge of stampings.

Limits for stretching are defined by forming limit diagrams, which are briefly described in point *I.B*.5.4. Unfortunately, the distribution of stretch over a punch is very no uniform and varies from point to point, both in major strain and minor strain. This variation is due to punch geometry, lubrication, and many other factors. The most accurate analysis is accomplished during soft tooling tryout.

b) Deep Drawing

When a sheet is pulled into a die cavity, and it must contract to flow into the cavity in areas such as at a corner or in the flange of a circular cup, the sheet is said to be undergoing drawing (Figure I.B.10). Deep drawing generates compressive forces in the flange area being drawn into the die cavity. Negative minor strains are generated. In contrast to failures in stretching, failures in drawing do not normally occur in the flange area where the compression and flow of sheet metal is occurring. Instead, necking and fracture occur in the wall of the stamping near the nose of the punch. Failure occurs here because the force causing the deformation in the flange must be transmitted from the punch through this region. If the force required to deform the flange is too great, it cannot be transmitted by the wall without overloading the wall.

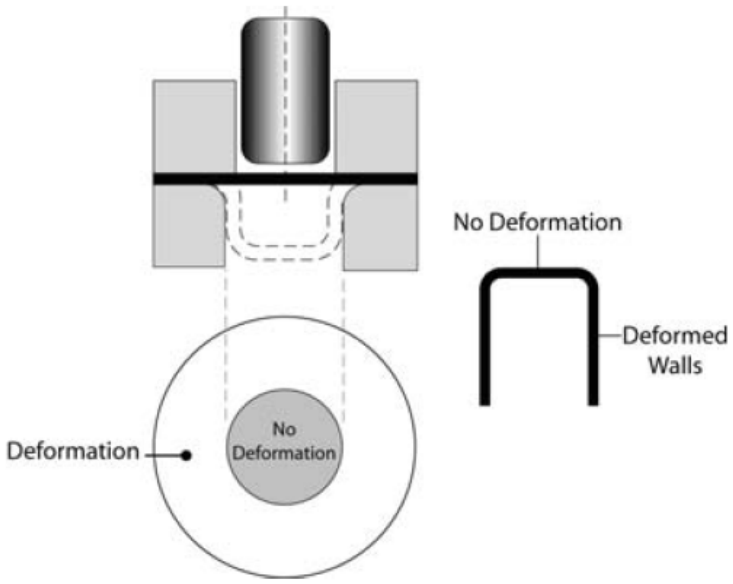

Figure I.B.10 – *Deep (cup) drawing.*

The cup drawing operation is rather well defined compared to the stretch forming operation. The design limits are defined by the Limiting Drawing Ratio (LDR).

$$LDR = \frac{D}{d} \qquad (2.2)$$

Where **D** = diameter of the largest blank that can be successfully drawn into a cup with a diameter **d**.

The LDR is a function of the r value of steel (Figure I.B.11), the thickness of the steel (Figure I.B.12), and the radii of the punch and die (Figure I.B.13).

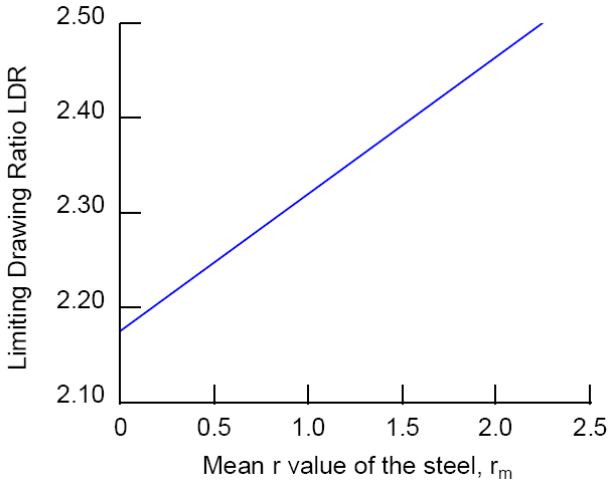

Figure I.B.11 – *The LDR as a function of r.*

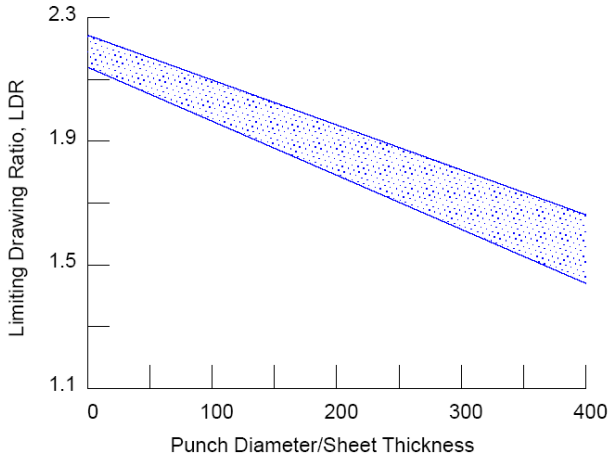

Figure I.B.12 – *The limiting drawing ratio, LDR, decreases as sheet thickness decreases for a given punch diameter*

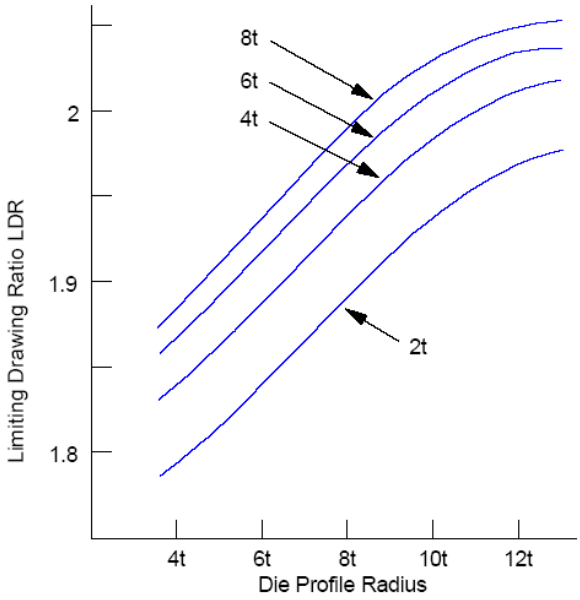

Figure I.B.13 – *The limiting drawing ratio is a function of both the die profile radius and the punch profile radius (t = sheet thickness)*

b.1 - Principles for successful deep drawing

Successful deep drawing depends on many factors. Ignoring even one of them during die design and build can prove disastrous. However, regardless of the many factors involved, the most important element to a successful deep drawing operation is initiating metal flow. The following are key elements affecting metal flow, and each of them should be considered when designing, building, or troubleshooting deep drawing stamping dies:

1. Material type
2. Material thickness
3. N and R values
4. Blank size and shape
5. Part geometry
6. Press speed (ram speed)
7. Draw radii
8. Draw ratio
9. Die surface finish
10. Die temperature
11. Lubricant
12. Draw bead height and shape
13. Binder pressure
14. Binder deflection
15. Standoff height

Because thicker materials are stiffer, they hold together better during deep drawing. Thicker materials also have more volume, so they can stretch longer distances.

The N value, also called the work hardening exponent, describes the ability of a steel to stretch. The R value—the plastic strain ratio—refers to the ability of a material to flow or draw. Blank sizes and shapes that are too large can restrict metal flow, and the geometry of parts affects the ability of metal to flow. Press speeds must allow time for materials to flow.

Die surface finishes and lubricants are important because they can reduce the coefficient of friction, allowing materials to slide through tools more easily. Die temperatures can affect the viscosity of lubricants.

As a controller of metal flow, draw bead height and shape can cause materials to bend and unbend to create restrictive forces going into a tool. Increasing binder pressure exerts more force on a material, creating more restraint on material going into the tool.

The remaining key elements affecting metal flow are examined in more detail in the remainder of this article. To illustrate the principles of metal flow, this article examines two basic draw shapes, round and square. All deformation modes that occur in any given part shape are present in one of these common shapes.

b.1.1 - ***Round Draws***

The draw ratio is among the most important elements to be considered when attempting to deep draw a round cup. The draw ratio is the relationship between the size of the draw post and the size of the blank. The draw ratio must fall within acceptable limits to allow metal to flow.

During forming, a blank is forced into circumferential compression, which creates a resistance to flow. If the resistance is too great, the cup fractures. If the post is too small or too far from the blank edge, the metal stretches and thins to the point of failure. If the post is the appropriate distance from the blank edge, and the die entry radius is acceptable, the metal can flow freely, progressively thickening as it enters the die cavity (Figure I.B.14).

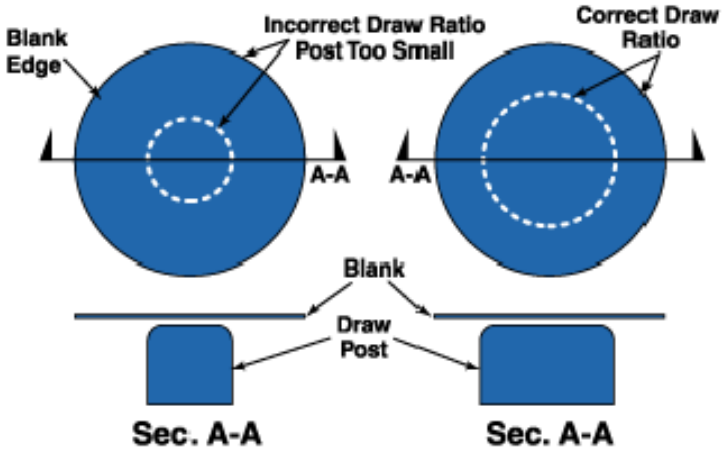

Figure I.B.14 - In the illustration of incorrect draw ratio (L), the too-small post would cause metal to thin to the point of failure, while the correct draw ratio (R) will result in a successfully deep drawn part

When a very tall small-diameter part is being processed, draw reductions likely will be necessary (Table I.B.1). A draw reduction is a process in which a part is first

Thickness of Material in Inches	Percentage of Reduction from Blank to 1st Draw	Percentage of Reduction from 1st Draw to 2nd Draw	Percentage of Reduction from 2nd Draw to 3rd Draw
0.010 - 0.014	27%	18%	17%
0.015 - 0.019	32%	20%	19%
0.020 - 0.024	35%	21%	20%
0.025 - 0.029	39%	22%	21%
0.030 - 0.034	42%	23%	22%
0.035 - 0.039	44%	26%	24%
0.040 - 0.044	46%	28%	25%
0.045 - 0.049	47%	28%	25%
0.050 - 0.054	47%	29%	26%
0.055 - 0.059	48%	29%	26%
0.060 - 0.069	48%	30%	27%
0.070 - 0.125	49%	31%	27%

Table I.B.1 - Reduction percentages for various thicknesses of draw-quality steel.

formed within acceptable draw ratio limits and then is progressively reduced or reshaped to a desired shape and profile.
The most important factor to remember when performing draw reductions is that all of the material necessary to make the final part shape must be present in the first draw. Figure I.B.15 is a reduction chart for the first, second, and third draws with draw-quality steel. Reduction percentages are based on metal thickness and type.

To determine the post diameter and height of the first draw, the total surface area of the finished part must be calculated. (If the part is to be trimmed, allow additional material during this calculation.) The calculated surface area is then converted into a flat blank diameter.

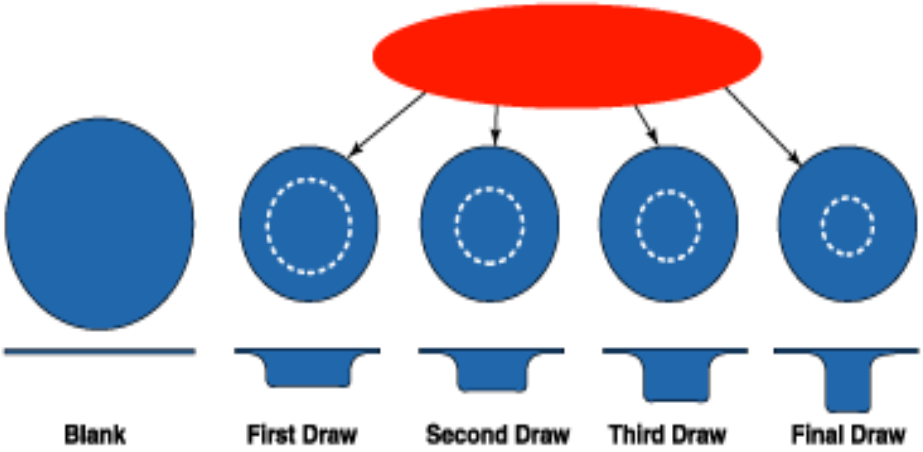

Figure I.B.15 - During draw reductions, the blank diameter should not change after the first draw

The primary step in calculating the first draw post diameter is determining the blank diameter. Multiplying the blank diameter by the percentage given in the chart, and then subtracting the result from the original blank diameter, yields the diameter of the first draw post. It is important to remember that all dimensions are taken through the centerline of the material. The height of the first draw is an area calculation directly related to the amount of material necessary to make the finished part.

b.1.2 - ***Die Entry Radii***

Other important factors for successful deep drawing are the size, accuracy, and surface finish of the die entry radius. Decisions regarding the die entry radius should be based on material type and thickness.
If a die entry radius is too small, material will not flow easily, resulting in stretching and, most likely, fracturing of the cup. If a die entry radius is too large, particularly when deep drawing thin-gauge stock, material begins to wrinkle after it leaves the pinch point between the draw ring surface and the binder. If wrinkling is severe, it may restrict flow when the material is pulled through the die entry radius.
Table I.B.2 provides general guidelines for die entry radii for round draws of draw-quality steel ranging in diameters from about 1.5 to 15 inches.

The die entry must be produced accurately in a fashion that makes it true and complete. It should be hook-free and polished in the direction of flow. High-wear tool steel should be used for die entry radii.

Metal Thickness	Minimum Radius
0.015 - 0.020	0.156
0.020 - 0.030	0.187
0.030 - 0.040	0.218
0.040 - 0.050	0.234
0.050 - 0.060	0.250
0.060 - 0.070	0.281
0.070 - 0.080	0.312
0.080 - 0.090	0.343
0.090 - 0.100	0.375
0.100 - 0.110	0.406
0.110 - 0.120	0.437
0.120 - 0.130	0.468
0.130 - 0.140	0.500

Table I.B.2 **-** Minimum die entry radii are shown in this chart for round draws involving various thicknesses of draw-quality steel

b.1.3 - ***Binder Pressure***

Sufficient binder pressure must be present to control metal flow. If binder pressure is inadequate, the material wrinkles during compression. The wrinkles then cause the binder to further separate from the draw ring surface, and control of the material will be lost. Wrinkles will also be forced to unwrinkle when the material is squeezed between the post and the cavity walls. This can pull metal on the top of the cup and result in fracture.
The problem of too much binder pressure can be overcome by using standoffs. Standoffs maintain a given space between the draw ring surface and the binder, and they should be set at 110 percent of the metal thickness to allow for compressive thickening. If the standoff gap is too small, the material will be pinched tightly between the draw ring and the binder surface, reducing its ability to flow freely. If the standoff gap is too large, the material will wrinkle during circumferential compression.
The recommended binder pressure for round draws of low-carbon draw-quality steel is 600 pounds per lineal inch around the post (draw post diameter x 3.141). For high-strength, low-alloy, and stainless steels, 1,800 pounds of pressure per lineal inch should be used. Other guidelines to remember when the processing draw reductions are:

1. Design open-ended draw cavities for draw depth adjustment.

2. Once the proper draw ratio is achieved, metal will flow and the part can be drawn partially or completely off the binder.
3. After the first draw, the blank diameter should not change.

b.1.4 - ***Square Draws***

Square draws are similar to round draws because they contain four 90-degree profile radii. Because of the radial corner profile, material flowing toward the corners is forced into compression. The straight sections of the square are simply being bent and unbent. Considerably less flow restriction takes place in the straight walls of a square draw than in the corners (Figure I.B.16).

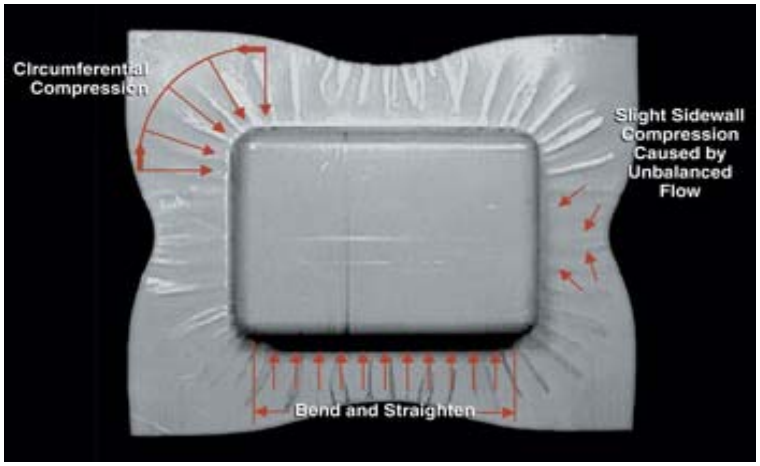

Figure I.B.16 – Flow restriction

Increasing the profile radius of the draw greatly increases the ability to draw deeper in a single operation (Figure I.B.17) because a larger-profile radius reduces compression. Too much compression in a corner restricts metal flow, resulting in fracture.

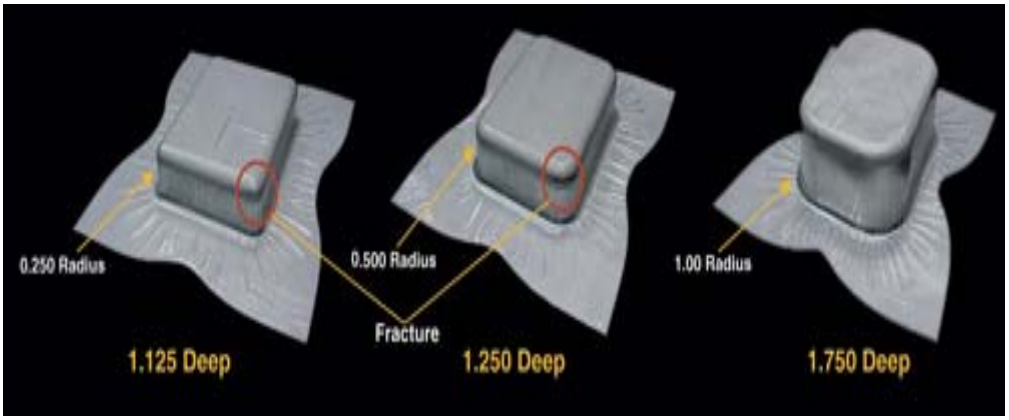

Figure I.B.17 – Ability to draw deepper

Increasing the profile radius and reducing the blank size reduce forming severity. Mitering the corners of the blank also can help to reduce compression.
To help balance metal flow conditions during square draws involving heavy metals, it may be necessary to draw spot the corner areas of the binder or draw ring face with respect to the increasing material thickness. This process allows metal to thicken in corners without being pinched excessively between the draw ring and the binder.
If a proper draw spot is achieved, blank holding force is evenly distributed through the perimeter of the drawn shell. When thin metal is used, draw spotting the corners may cause undesirable wrinkling in the relieved areas. This results primarily from a lack of control of the metal flow and the inability of thin stock to resist wrinkling.
If the square drawn shell is too tall to be drawn in a single operation, it must undergo a draw reduction. As with round draws, all material necessary to make the final part must be present in the first draw. Draw reductions for square shells are achieved by increasing the profile radius to acceptable compression limits and increasing the width and length to obtain the necessary surface area of the finished part.
Other guidelines to follow when drawing square shells include:

1. Use the minimum blank size required to make the part.
2. Use standoffs to control metal flow, not binder pressure.
3. To redraw a square shell, increase the width, length, and profile radius of the first draw to contain the necessary surface area of the final part geometry.

Successful deep drawing is a combination of many important factors. Although designing and building deep draw dies is fast becoming a science, the fundamental metal flow principles should never be ignored, for they are the foundations of a successful deep drawing operation.

c) Bending

Bending is one of the most common methods used to change the shape of sheet metal. Almost all sheet metal forming operations involve bending. V–bend and U-bend are shown in Figure I.B.18 a). In each case a punch forces the metal into a long channel die as both free edges swing upward. The wiping bend or flanging operation, shown in Figure I.B.18 b), varies in that one edge is held securely while the punch wipes or swings the free edge down.

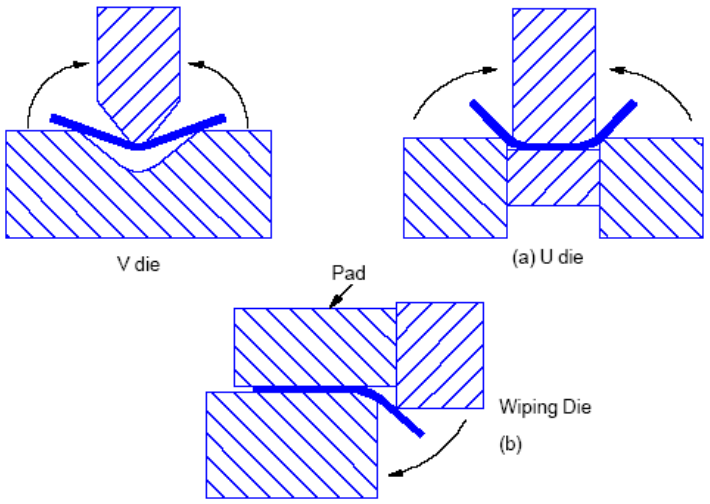

Figure I.B.18 – *Types of bending along a straight bend line.*

All bending operations have several characteristics in common. First, one or more metal edges swing through space. This swing must be calculated to allow for sufficient room in the tooling. Second, the metal bends along a narrow line that acts much like a plastic hinge. Third, metal outside the plastic hinge is unstrained and remains in the as received condition.

Bending is different from other forming modes in that a severe strain gradient is developed from one surface to the other. During bending, the maximum tensile strain occurs on the convex surface of the stamping, while the maximum compressive strain occurs on the concave surface. Somewhere within the sheet metal is a neutral axis, which does not change length. A common design assumption is that the surface area of the bend, and the thickness at the bend, do not change.

The radius of a bend in sheet metal forming is generally specified in terms of thickness of metal being bent. A sheet with a thickness of 0.75 mm bent over a radius of 3 mm would have a *4t* bend. Bends therefore can vary from zero thickness to infinity (no bend) at one location and the bending can change from one location to another, even reversing the direction of the bend.

In designing bends, the best approach is to use a finite element program. Lacking that, there are many standards for bend requirements of materials in general and for specific kinds of materials under special conditions. These should be referenced when selecting a material and it's bending radii.

For automotive stampings the metal thickness of cold rolled steel is generally in the range of 0.5 mm to 1.8 mm. The outer body panels will cover a smaller range from 0.6 mm to 0.9 mm. The bend radii for most of these stampings should be between *3t* and *9t.* Larger radii, up to *25t,* are

used if the design requires a rounded look. Too sharp a bend will cause excessive tearing, especially if there are tensile forces associated with the bend. Sharper bends usually require a restrike operation. Too large a bend radius introduces the possibility of excessive springback and the necessary larger spacing needed between the bend dies can cause loss of control of the metal being bent.

Bends are most frequently made to angles up to 90° by the vertical movement of a punch into a die opening. A hinge die can be used to overbend beyond 90°. Further bending and flattening to form a hem can be accomplished by a subsequent punch action against a backing plate.

d) Flanging

Flanging along a straight line is identical to the bending described above. When the line of bending is changed from straight to curved, another degree of complexity is added to the operation. The metal outside the plastic hinge no longer remains in the as received condition; it experiences either tensile (positive) or compressive (negative) deformation.

Shrink flanging is one form of flanging (Figure I.B.19 a)). As the name implies, the flange length shrinks during forming. Each radial zone (shaded region) is folded 90° along a radial line to form the flange or wall. Since the arc length of the final flange or wall is smaller than the arc length of the element from which it was formed, compression must take place in the circumferential direction. Increasing the flange depth, increase the amount of compression. In addition, the compression is the largest at the top of the flange and is zero at the flange radius. Stretch flanging is the opposite to shrink flanging (Figure I.B.19 b)). Here a tensile stretch is required to generate the increase in line length. Hole expansion is a common example of stretch flanging.

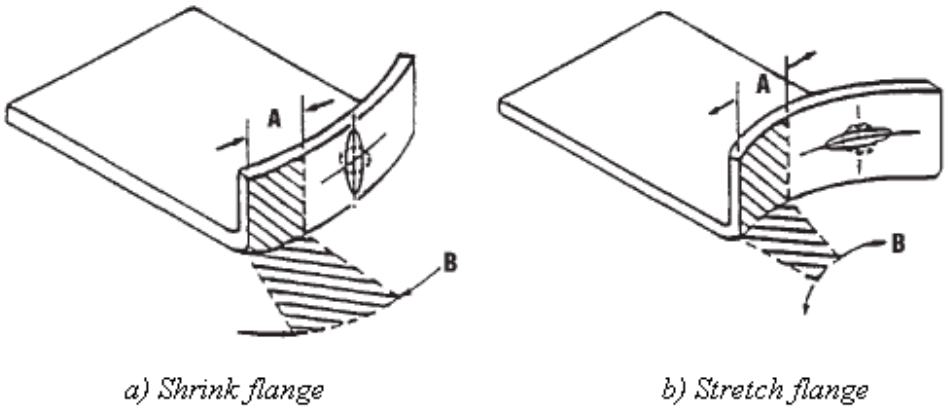

a) Shrink flange *b) Stretch flange*

Figure I.B.19 – *Bending along a curved bend axis*

When bending a flanged inside corner, the corner radius should be at least *14t* and the length of the flange should be at least *4t*. If an outside corner is to be formed with a flange, the minimum radius of the corner should be *5t* and the angle of the corner no sharper than 60°.

In hemmed corners where the metal of the flange is folded back against the sheet, the minimum allowed corner radii are increased to *24t* for an inside and *7t* for an outside corner, again no sharper than 60°.

Flanges and hems are used to straighten the edges of sheet metal parts, give a smooth rounded edge to a part, or to provide hidden joints. They can be either concave or convex but in either case problems of too little metal for an inside flange, or too much metal for an outside flange, must be handled during the bending process. This is accomplished by limiting the width of the flange, cutting notches in the corner flange metal to reduce the amount of metal to be bent and stretched or shrunk, or designing offsets to take up excess metal. Offsets are displacements of a few metal thicknesses, similar to those used to form license plate numbers. For corner flanges, the offsets can be considered designed wrinkles. Edges that must be strengthened further than is possible by hemming are curled.

Shrink flanging tends to generate buckles and loose metal. Careful control of punch/die clearances is required to produce a "clean" flange. In contrast, stretch flanges suffer from edge cracking and tearing if the stretching limits are exceeded. The simplest analysis is to calculate the increase in length of line assuming that the stretch flange is made up of segment (s) of a circle. The elongations for steel are compared to the experimental hole expansion limits shown in Figure I.B.20. These limits are conservative for stretch flanges. Unlike the true hole expansion test where the entire hole perimeter is subjected to the same elongation, the adjacent metal in a stretch flange may be undeformed or may even be in the shrink flanging mode. Thus adjacent areas to the stretch flange may be able to feed metal into the stretch zone and reduce the required elongation.

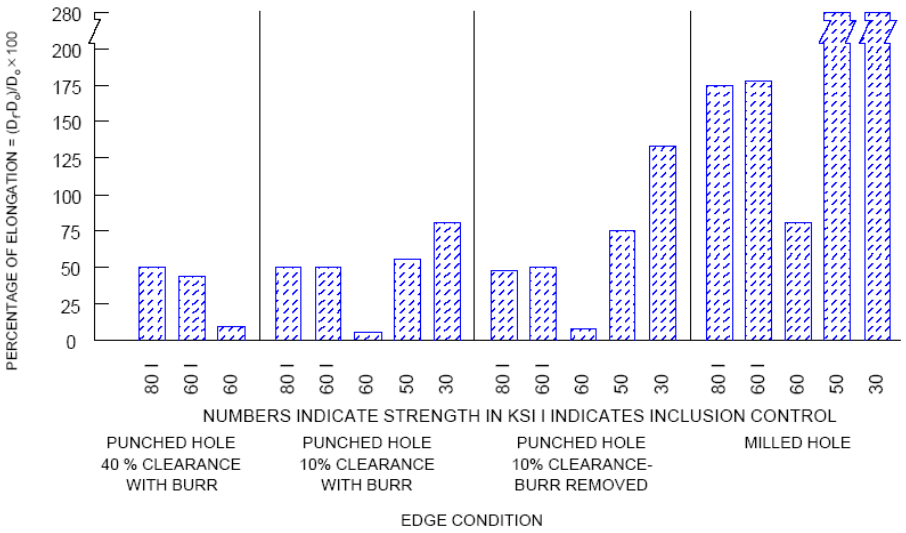

Figure I.B.20 – *Measured percent hole elongations as a function of hole quality and steel grade*

e) Bend-and-Straighten

A bend-and-straighten operation generates a final shape that is identical with that generated by a bending operation (Figure I.B.21). However, the intermediate steps are very different and generate different characteristics in the final product. In the bend-and-straighten operation, the swing of the metal is prevented by the blankholder. The bottom radius is formed around the punch by a bend operation while a simultaneous bend is formed around the die radius.

Thereafter, each additional element in the final wall begins in the flange and is pulled towards the radius zone. Because the die radius line is straight, no compression is created along the radius line. Upon entering the die radius zone, the element is bent to conform to the radius contour. When leaving the radius zone, the element must be unbent or straightened to conform again to the straight wall. Thus, this operation is descriptively called bend-and-straighten.

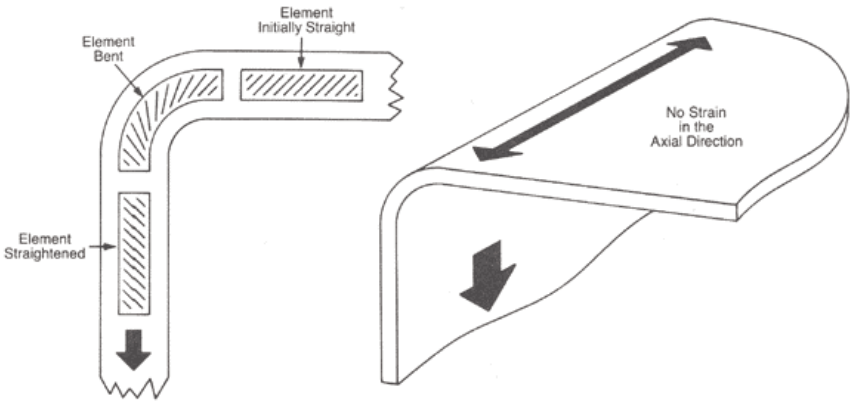

Figure I.B.21 – *Bend and straighten.*

The primary difference between bending and bend-and-straighten is the condition of the final wall. In the bend operation, the final wall is swung into position and remains in the unworked state. During the bend-and-straighten operation, the metal is worked first in one direction (tension or compression depending on the convex or concave side of the bend) and then worked in the reverse direction. This bending and unbending hardens the metal and reduces the residual formability of the material for subsequent stamping operations. Substantial portions of the major panels are formed by the bend-and-straighten mode of deformation.

In the bend-and-straighten mode, metal flows in a straight path from the binder zone into the die radius, over the die radius in the bending operation, and out of the die radius in the straightening operation. Tensile strain is generated on the convex surface during bending and on the concave side during straightening. Because the tension on the concave side follows compression (which work hardens the metal and depletes usable formability), the concave side is more severely affected. Severity of this operation depends on the ratio of the bend radius to the sheet metal thickness. When the die radius is less than *4t,* the operation is too severe. However, when the die radius exceeds *10t*, an unsupported band is created between the die radius and the punch radius. The ideal die radius is *6t* to *8t*.

Any tension created in the binder area can add a stretch component to the pure bend-and-straighten operation. This restraint can be created by additional binder or hold down pressure or by the insertion of "draw beads" into the binder surface. The beads are placed in the bend-and-straighten areas to restrict metal flow into the die cavity, creating an added stretch component.

f) Hole Expansion

Typical limits for hole expansion for steel are given in Figure 2.20 The maximum amount of elongation depends on the quality of the edge of the expanding hole and the stretchability of the steel. The hole expansion capacity of the steel increases with increasing *n* value, total elongation and *r* value (Point I.B.5.3).

g) Cutting

Cutting operations in one plane are classified by the terms shearing, blanking, slitting, piercing, and lancing. Cutting operations in more than one plane are classified by the terms trimming and parting.

- Shearing

Shearing is done by a blade along a straight line. The work metal is placed between a stationary lower blade and a movable upper blade and is severed by bringing the blades together. This method commonly is used to produce rectangular and square blanks (Figure I.B.22). Nondeveloped blanks are generated by shearing.

Figure IB.22 *– Shearing.*

- *Blanking*

Blanking is cutting up a large sheet of stock into smaller pieces suitable for the next operation in stamping, such as drawing and forming. Often this is combined with piercing.

Blanking can be as simple as a cookie cutter type die to produce prototype parts, or high speed dies that run at 1000+ strokes per minute, running coil stock which has been slit to a specified width.

For production parts, the final configuration of the drawn or formed shape needs to be established before the blank die can be built-since the blank size and the slit width size needs to be established precisely.

- *Slitting*

Slitting is cutting lengths (usually coils) of sheet metal into narrower lengths by means of one or more pairs of circular knives. This operation often precedes shearing or blanking and is used to produce exact blank or nesting widths.

- *Piercing*

Piercing is the operation of cutting internal features (holes or slots) in stock. Piercing can also be combined with other operations such as lance and form (to make a small feature such as tab), pierce and extrude (to make an extruded hole). All these operations can be combined with blanking.

Piercing of all the holes is best done together to ensure good hole-to-hole tolerance and part repeatability. However if the material distorts, the method described below can be done.

When there are large numbers of holes, in a tight pitch, there could be distortions, due to the high amount of tension on the upper surface due to stretching and compression on the bottom surface. This causes the material not to lay flat. This can be avoided by staggering the piercing of the holes. Holes are punched in a staggered pattern; then the other holes are punched in the alternate staggered pattern.

Often called perforating, piercing is a metal cutting operation that produces a round, square, or special-shaped hole in flat sheet metal or a formed part. The main difference between piercing and blanking is that in blanking, the slug is used, and in piercing the slug is discarded as scrap. The cutting punch that produces the hole is called the pierce punch, and the hole the punch enters is called the matrix (Figure IB.23).

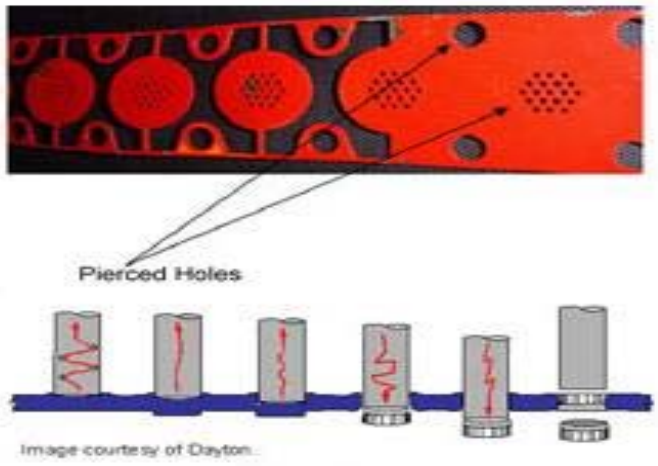

Figure IB.23 – *Piercing.*

- *Lancing*

In lancing, the metal is sliced or slit in an effort to free up metal without separating it from the strip. Lancing often is done in progressive dies to create a part carrier called a flex or stretch web (Figure IB.24).

Figure IB.24 *– Lancing.*

- *Trimming*

Trimming removes unwanted metal from the finished part that was required for some previous stamping operation, such as binder areas, or was

generated by a previous stamping operation, such as the earring zone on the top of a deep drawn cup.

- *Parting*

Parting operations are used to separate two identical or mirror image parts that were formed together (typically for the expediency of making two parts at one time or to balance the draw operation of a no symmetrical part). Parting is also an operation that involves two cut-off operations to produce contoured blanks from strip. Scrap is produced in this parting process.

*I.B.*3.3 – Interaction of Stamping Modes

Forming modes usually interact because most stampings are composed of several distinct areas, each of which is formed by one of the primary forming modes. The two shapes shown Figure I.B.8 are reproduced in Figure I.B.25 with the geometrical designations replaced by the respective forming modes used to generate the geometrical shapes.

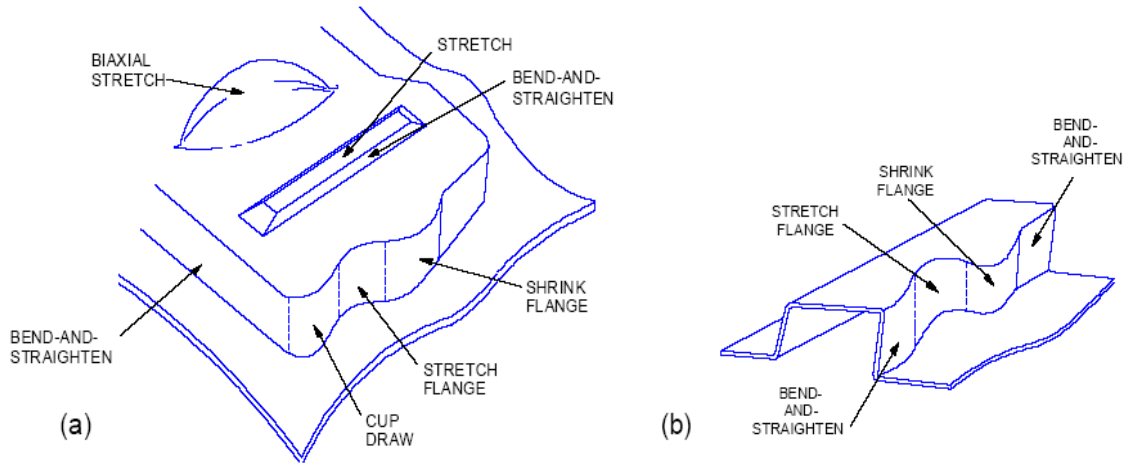

Figure IB.25– *Schematic of a part with composite forming operations*

After the first stamping is formed, a wide option of secondary forming operations is available to change the shape created by each of the initial forming modes. For example, trimming and reverse flanging of the initial flange may present problems.

These forming modes are interactive and are constantly changing in response to a large number of variables. For example, the blank width may be increased to provide an additional flange, after trimming, to meet subsequent welding requirements. The additional flange will restrict metal

flow from the binder (hold down) area and thereby increase the depth of the stamping required by stretching over the punch. This may drive the deformation over the punch into a failure condition. This trend can be reversed by increasing the die radius to allow easier flow of the extended blank into the die cavity. However, if the die radius is now too large for the final part, a restrike operation will be required to sharpen the radius to the required (not desired) dimension.

Unfortunately, an increase or decrease in interface lubricity, with respect to the surface characteristics of the incoming steel, can inadvertently cause the same reaction in the die and cause variations from part to part. Thus, the first task at hand is to understand the forming modes and how they interact to provide the desired part shape, and therefore the required stamping.

*I.B.*3.4 – Sequence of Operations

The production sequence becomes important after the part has been designed and the forming modes selected. This sequence may place additional limits on the forming modes and even on the initial part design. In any case, knowledge of terminology is important to simultaneous engineering.

Initial Blank

The stamping operation begins with a blank, which is created either by shearing or blanking (Figure I.B.26 a)). Shearing is a straight cut across the coil width to form a square or rectangular blank. Blanking creates a blank bounded by a contoured line composed of straight and curved segments. While shearing is easier to perform, it may waste metal.

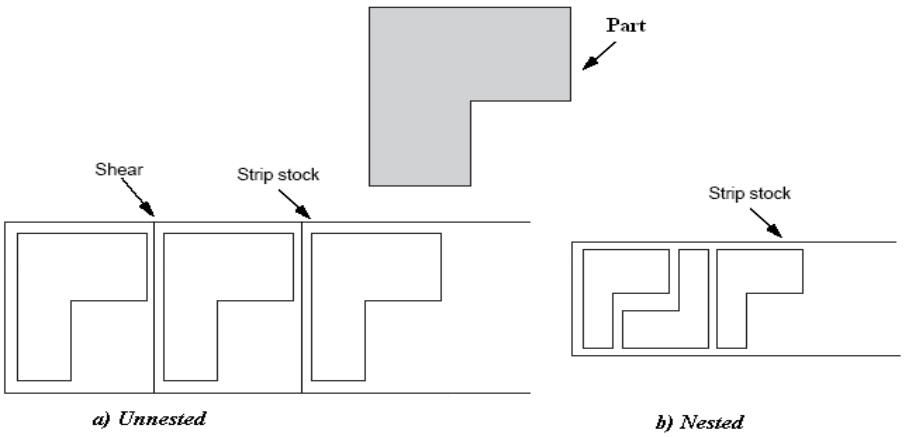

Figure I.B.26 – *Nesting irregular blanks in layout to save material*

Contoured blanks can be nested (Figure I.B.26 b)) to reduce the metal that must be removed as trim. This trim metal is intentionally and unavoidably wasted from the initial blank on every stamping. Sometimes large segments of offal can be reapplied on smaller parts, but careful study of the economics must be made. The costs of steel collection, storage, reapplication, accounting, scheduling, etc. may outweigh the savings generated by the amount of the scrap metal actually used.

Another reason for contouring the blanks by a blanking operation is to match the blank perimeter to the perimeter of the die opening. Matching encourages more uniform metal flow into the die cavity, prevents excessive buckling in the flange, and reduces the drag of extra flange metal behind critical zones. A third reason for contouring the blanks is to create the final flange/part contour in the blank in order to eliminate a trimming operation after forming.

Shearing or blanking operations can be performed in several ways. They may be performed in material receiving, where coils of steel are blanked and the stacks of blanks shipped to the press line. Blanks may be made at the head of the press line as the coil is unwound into a washer, blanker, oiler combination. Blanks may also be created in the die at the start of the forming stroke.

First Stamping

The first stamping operation may be the operation where the majority of the stamping shape is formed, or it may be a preform. A preform is a stage that typically gathers metal into a zone for later use. For example, a dome of metal is created in the centre of the blank while the metal on the edges is unrestrained and free to move (Figure I.B.27). This preform operation allows the necessary length of line to be generated without excessive tension, localized metal thinning over tight radii, and possible breakage. The main forming sequence then follows to generate the major panel shape.

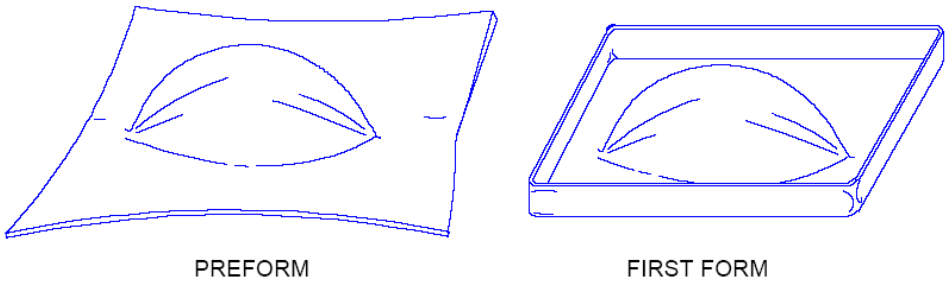

Figure I.B.27 – *Preforming allows metal to flow into critical areas before the surrounding metal is locked.*

If the sequence were reversed, the edges of the stamping would be restrained or even locked. Instead of metal flowing from the binder, the entire length of line would be generated by stretching the limited length of metal. Any number of preform stages may precede the major forming operations; the number is a function of the part requirements and each requires a separate die.

A typical first stamping operation would be:

1. Blank insertion

The blank may be inserted by hand, automatic feed equipment, gravity slide, or many other methods.

2. Blank positioning

This is accomplished by hand, stops, guide pins, index fingers, or other methods.

3. Closing the binder (blankholder)

This action places restraint on the blank to control metal flow into the die cavity and reduce buckling within the flange material. The binder ring may be in a single plane or may be developed in the third dimension. The developed binder preforms the blank closer to the contours of the punch. This helps to eliminate metal being trapped under the punch, avoids pulling metal into the die on sharp radii, encourages uniform metal flow, and balances forces on the punch to avoid skidding of the character line.

4. Punch Action

The punch now moves towards the blank, contacts the blank, and moves the specified distance into the die cavity. The main portion of the forming is accomplished during this segment.

5. Retraction

The punch and blankholder ring retract to create a die opening. The height of the die opening depends on the stroke of the press and the dimensions of the die set; it must be greater than the height of the stamping being withdrawn.

6. Ejection

Various levers, air, spring, arm, and other systems are used to remove the stamping from the die.

7. Transfer

Manual, semi-automatic, or automatic systems are used to transfer the stamping from one die to the next. The next die may be in the same press in

the case of progressive die sets or transfer presses. It may be in the next press in a press line, elsewhere in the plant, or in another plant somewhere across the country.

Subsequent Operations

Many parts are formed in a sequence of forming operations as opposed to a single operation. The primary reason for multiple operations is that the severity of the forming is too great to be accomplished in a single operation. A prime example is the restrike operation (Figure I.B.28). Attempting to stretch metal into a die cavity by stretching over a very sharp radius punch (a) would result in failure. Instead the metal surface area or length of line is generated by stretching over a generous radius punch. A restrike (b) then redistributes the metal into the desired configuration without an additional tensile increase in the length of line.

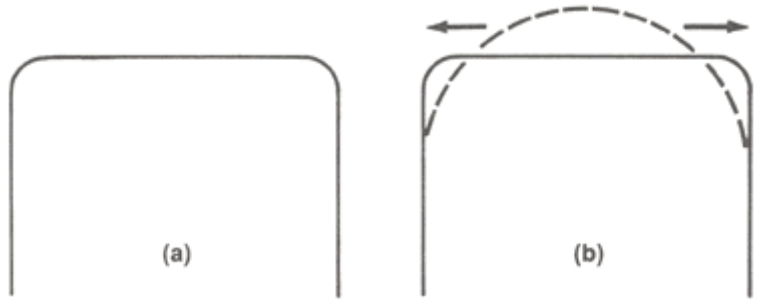

Figure I.B.28 – *Second forming operations are more successful when the length of the line is generated in the first operation over generous radii.*

Another common subsequent forming operation is redrawing. Limits are imposed on the blank diameter which can be drawn into a cup of a given diameter. Should a deeper cup be required, an intermediate diameter cup is drawn first. This cup is then redrawn in one or more subsequent stages to achieve the final diameter and height. In some case the cup is ironed to obtain additional cup height.

This and other subsequent forming operations, like flange, reverse flange, rim, punch, pierce or extrude, are well described in this two textbooks. [5, 6]

Any one of the subsequent operations may be the finish or final operation, depending on the die designer. The only requirement of the finish operation is that the part be finished as it leaves this operation in compliance with the part print. During the production day, numerous stampings are removed from the finish operation, taken to checking fixtures to determine

accuracy to part print, to "green rooms" for visual evaluation of surface quality, and to other part quality audits.

*I.B.*3.5 – Press and Tooling Descriptions

Presses

The press is one of the major components of the forming system. For example, a specific material/lubricant/die combination can produce satisfactory stampings in one press line and be incapable of producing satisfactory stampings in another press line. This is especially true for stampings which lack sufficient “safety margin” and are balanced at the onset of failure. Likewise, the ability to produce quality stampings without loose metal, buckles, waves, low spots, and other surface defects depends on the characteristics of the press in which the stamping is produced. Some presses have very accurate alignment and tight guidance systems. Other presses have loose guidance systems and the punch to die alignment, as well as blankholder reproducibility, changes from one stamping to the next.

Presses are identified by different methods. Some of the more common methods are:

1. *Tonnage*

Typical identifications are 300 ton, 600 ton, 200 ton outer slide/400 ton main ram.

2. *Source of Power*

Occasionally the source of power is manual, either hand or foot powered. Mechanical powered presses, sometimes called toggle presses, store energy in a flywheel, and transfer it to the workpiece by gears, cranks, eccentrics, or levers. Hydraulic cylinders apply the load in hydraulic presses.

There are three main differences between these two types of presses. One of them is the load/stroke characteristics. The hydraulic press has a constant load capacity throughout the entire stroke, whereas the mechanical drive reaches maximum load capacity only at the bottom of the stroke. This becomes more important for pure stretch forming operations which require maximum blank clamping loads to be exerted at ram positions far removed from the bottom dead center and high up on the stroke curve where load capacity is low for mechanical presses.

Another difference is the length of the stroke. A hydraulic press can be set easily at any stroke within the limits of the hydraulic cylinder travel. The ram stroke on the mechanical press is fixed.

A third difference is the speed curves. The hydraulic press can operate either at a constant ram speed or any programmed speed cycle desired. The speed curve of the mechanical press is neither constant nor programmable, but is a fixed sine wave. The speed ranges from zero at the beginning and end of the stroke to maximum speed at the halfway point. This particular speed curve may not be ideal for some critical stampings. However, minimum information on this effect appears in the literature.

3. Number of slides

Presses may be classified as single action, double action or triple action.

Single Action Process: these presses are widely used, especially when surface quality is not a priority requirement. This procedure is based in a single slide (Ram) movement: the punch is stationary, the die moves down in its direction pressing the metal sheet against the blankholder, and then deforms the blank with the punch (Figure I.B.29). Cycle time is reduced by approximately 25% in comparison with the double action presses.

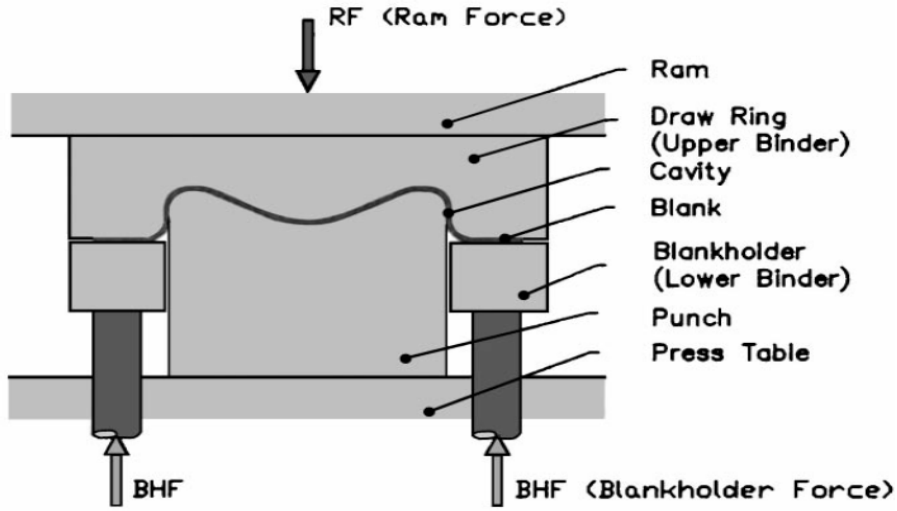

Figure I.B.29 – *Single action Press*

Double action: These presses are usually used to form components with large drawing widths needing large efforts, or uniquely because good surface quality is an important requirement. In this press type, two distinct and successive actions are performed: the blank's blocking and its posterior deformation. The first step is performed through the blankholder descending movement, pressing the blank against the die with a previously defined force factor; the second step is characterised by punch movement towards the die, deforming the blank (Figure I.B.30).

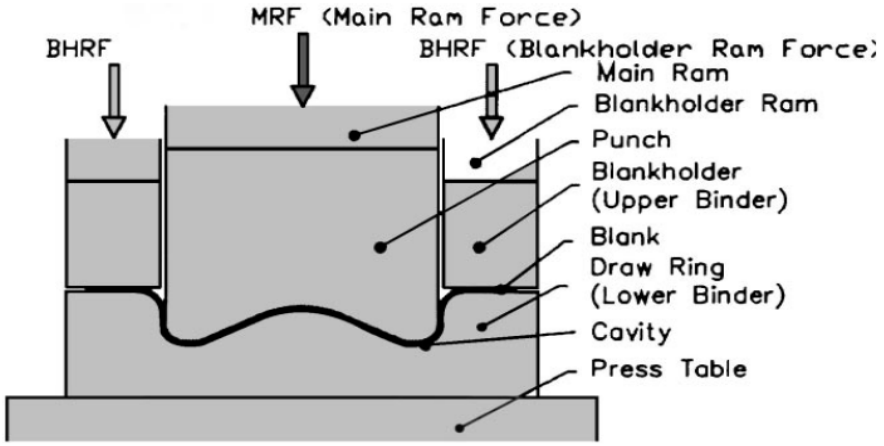

Figure I.B.30 – *Double action press.*

Triple action press: These presses are only applied to manufacture complex stamping parts. They are three moving slides, two slides moving in the same direction and a third lower slide moving upward through the fixed bed in a direction opposite to the blankholder and inner slides. This permits reverse-drawing, forming, or beading operations while both upper actions are dwelling.

4. Type of frame

Mechanical presses are classified as straight side or gap frame.

5. Forming function

Presses are classified as blanking presses, press brakes, draw presses, trim presses, four slide presses, etc.

6. Size of the press opening and press bed

The content of the press line, in terms of total number of presses and the capabilities of each, is essential to the design and manufacturing of a part. Large stamping plants have a fixed number of presses of fixed size and types in each line. The number of dies can be less than the number of presses. However, when the number of dies exceeds the number of presses available, a major problem occurs and off -line operations are required. Thus, the complexity of a given part may be governed by the number and type of dies and the number of operations that can be performed in each die. Simultaneous engineering is advantageous because the characteristics are known for the press line to be used in forming each stamping. The alternative is to design to a uniform set of specifications for all die sets and presses.

Dies

One or more dies is placed within the press opening. Die is a generic term used to denote the entire press tooling used to cut or form sheet metal. The term is also used to denote just the female half of the press tool (Figure I.B.31). The major components of the die are the guidance system, punch, blankholder, drawbeads and female die.

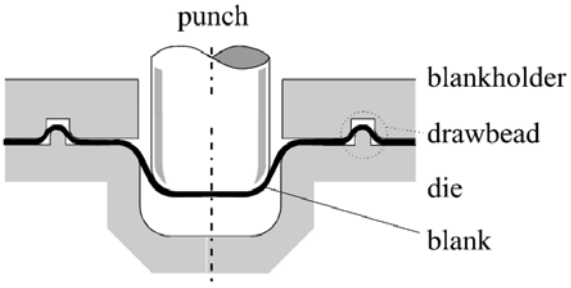

Figure I.B.31 – *Example of the main components of a die.*

Punch – represent the positive shape of the element/part (male) and forces the metal into the die with the intention of deforming the sheet according with it volume.

Die – represent the negative shape of the element/part (female) and, at the end of loading phase, receive the punch with the deformed sheet.

Blankholder – are a double action, one is control the material flow rate into the die cavity and another is to facilitate the extraction of the piece at the end of the stamping process.

Drawbeads – are a local flow control mechanism, provided by protrusions in the blankholder-die region. The material is forced to traverse the drawbead when the punch moves into the die cavity, causing a local restraining of the material flow.

These last two components, which represent the flow control system, have extremely importance in guarantee the quality of a sheet metal stamping part.

Generally, the material flow is only controlled by the blankholder: a restraining force is created by friction between the tools and the blank. However, during the forming stage, the blankholder does not make contact with the entire blank which means that it cannot fully control the material flow. Moreover, when a high restraining force is required, a higher blankholder force must be applied which may cause excessive wear in the tools and galling in the blank [7]. Therefore, a local control mechanism is

desired which restrains the material flow sufficiently at relatively low blankholder pressure. These demands can be fulfilled by drawbeads, which are protrusions on the die surface (Figure I.B.31). A drawbead consists of two components, the bead itself and a matching groove, the contra-bead. The drawbead creates a restraining force by cyclically bending and unbending the sheet as it traverses the drawbead, causing strain hardening and a change in the strain distribution with consequently thinning of the blank. [8, 9, 10, 11]

*I.B.*4 – Lubrication

Lubricants in sheet metal forming have many purposes. Some are applied at the steel mill at the time the steel is produced to prevent rusting; they remain on the steel and become a primary aid to forming. Some are applied in the stamping plant after blanking. Others are contained in blank washers which serve the dual purpose of blank cleaning and lubricant application. Finally, a few may be selectively applied within the press to assist metal flow in a critical area of the stamping.

The list of required lubricant characteristics usually is long. Cleanability, compatibility (with everything from phosphate treatment to adhesives), cost effectiveness, storageability, weldability, toxicity, solubility, and even formability are included.

In terms of formability, lubricants have two primary functions. The first function deals with the control of sheet metal movement. This movement may take place from the binder area into the cavity of the die or may occur over the radius of the punch. The lubricant may encourage metal flow through a low coefficient of friction or restrict metal flow through a high coefficient. The key is a reproducible behaviour which will consistently duplicate exactly the metal flow intended by the die designer.

The second function of a lubricant is prevention of scoring and galling. Here the lubricant must maintain sufficient isolation between the workpiece (sheet metal) and the tool to prevent metal accumulation on the tooling (galling) which eventually leads to metal plowing (scoring). In a similar manner, wear of the tooling must either be avoided or reduced to a tolerable minimum.

Two main types of Lubricants

Historically, extreme-pressure (EP) lubricants have been considered the best approach to achieving high-performance tool protection on the most demanding deep-drawn or heavy-gauge formed parts. Sulphur and chlorinated EP additives blended with straight oil have a long history of improving tool life success.

With the introduction of new-generation metals such as HSS, and stringent environmental and disposal requirements, EP oil's value has diminished. Under the high heat required to form HSS, EP oils lose their performance. They can't provide the physical tool-protecting barrier required for extreme-temperature (ET) applications. ET versions of high-solids polymers (HSP) lubricants do provide the necessary protection.

As metal deformation in the stamping press raises tool and metal temperature, EP oils become thinner, and in some cases flash or burn (Figure I.B.32). The average HSP lubricant has a thin viscosity when applied. However, as the temperature rises, the viscosity becomes thicker and more tenacious. In fact, ET fluids are heat-seeking and will attach to hot metal, creating a friction-reducing film barrier. This protective barrier allows the tool to stretch and form metal without splitting or metal pickup during the most demanding operations, thus controlling friction and metal flow.

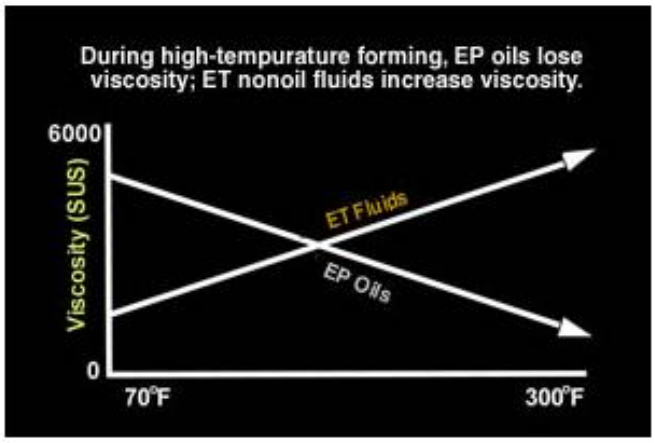

Figure I.B.32 – *Comparison between ET Fluids and EP Oils.*

*I.B.*5 – General Metal Deformation

*I.B.*5.1 – Failure Modes

Sheet metal forming operations are typical mechanical problems characterized by a product with a deviating shape or with failures, usually caused by an incorrect design of the tools and the blank shape or an incorrect choice of material and process parameters. Once such problems are started, they tend to persist and the stiffness of the specific area decreases. Therefore, deformation begins to be localized and eventually proceeds to final collapse or rupture.

A deviating shape is caused by elastic recovery and can be easily

explain. When the level of stress exceeds the yield strength of the material, the deformation is composed of both elastic and plastic deformation. When the sheet of metal is unloaded from the plastic deformation region, the plastic component of deformation is retained and the shape generated by plastic deformation remains. The elastic component attempts to neutralize itself; this reverse of deformation is called springback, and, due it importance, will be studied with precision in *Chapter 3 – Springback.*

The most frequent types of failures (mechanical problems) are wrinkling, necking (and subsequently tearing) and orange peel.

Wrinkling – Wrinkling may occur when the minor stress in the sheet is compressive. Wrinkling of the flange areas can be suppressed by the blankholder. However, wrinkling may also occur in unsupported regions or regions in contact with only one tool. Figure I.B.33 shows the forming of a shell with a conical wall. A compressive hoop stress may arise in the unsupported wall at C if too much material is allowed to be drawn into the cavity. [12]

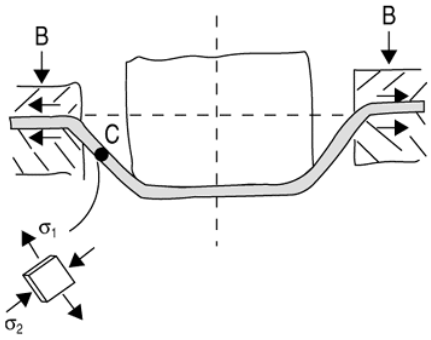

Figure I.B.33 – *Forming of a shell with a conical wall.*

The usual remedy is to increase the blankholder force, B, that increases the radial stress, and strain. The lateral hoop contraction accompanying this radial stretching helps alleviate the hoop compression. How much stretching is required depends on the *r* value of the material, which is the ratio of width-to-thickness strain in the tensile test. Less radial stretching is required with a high *r* value, decreasing the chance of tearing failure. The *r* value of drawing quality steel is typically >1 and that of aluminium sheet <1 so the wrinkling problem is more severe in aluminium. The wrinkling tendency is also affected by elastic modulus, sheet thickness, and tooling so there is no single wrinkling limit for a material, and the inclusion of this line in the general diagram (Figure I.B.34) is not strictly valid.

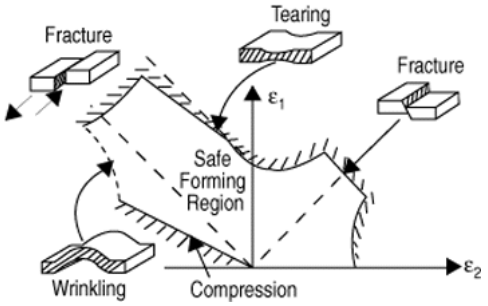

Figure I.B.34 – A schematic plot of the window of safe straining for simple paths the forming-limit diagram

Necking – is a condition of local instability under the influence of large tensile forces. Once necking starts, the deformation becomes non-uniform throughout the part as it is under bucking and wrinkling cases. Deformation is concentrated in a local area, often denominated through-thickness necks. They are characterized by localized line thinning across the surface of the sheet with a width on the scale of the sheet thickness. Through-thickness necks proceed very rapidly towards fracture.

The occurrence of necking or rupture is final and requires the rejection or redesign of the manufacturing process. This does not necessarily imply that the absence of said failure mode give an acceptable process. Normal process and material variations inevitably lead to necking and rupture during production runs.

Orange Peel – It's surface roughness resulting from working metal of large grain size, due to uneven flow or to the appearance of the overly large grains usually the result of annealing at too high a temperature. The surface is similar in texture to an orange peel.

*I.B.*5.2 – Material Formability Parameters

A number of parameters or sheet metal characteristics can be measured and correlated to the capability of the sheet metal to be formed by different forming modes. Unfortunately, different forming modes correlate with different parameters. Therefore, when sheet steel is made, the critical forming mode must be known so that the value of the appropriate forming parameter can be maximized. The parameters of interest to the simultaneous engineering team are work hardening exponent (n), plastic strain ratio (r), strain rate hardening exponent, total elongation, yield strength, and forming limit.

*I.B.*5.3 – Circle Grid Analysis

Circle Grid strain analysis (CGA) is a technique employed during die tryout, and sometimes during production, to analyze and quantify plastic deformation in sheet metal. Analysis of the grids can suggest methods for reducing forming severity [13], making die tryout more of a science and less an art.

A sheet of steel is prepared for CGA by applying a circle grid onto the surface. There are various techniques available for these. Circular grids are normally made in two different ways. They can be made electro-chemically or photo-chemically, both processes having particular advantages and disadvantages, and they are well descripting in *Appendix A.*

Many different grid patterns exist. A typical grid, shown in Figure I.B.35, consists of 2.54 mm diameter circles arranged in rows and columns on 3.18 mm centres, and a 6.35 mm square grid pattern. The etched pattern remains intact while the steel is processed through the forming operations. Plastic deformation in the steel causes the circles to deform into ellipses. The amount of plastic strain at each circle can be observed and quantified by measuring the major and minor diameters of the ellipses. The relatively small size of the circles, and fairly precise measuring procedures give a detailed, quantified pattern of plastic strain in the stamping. [14, 15]

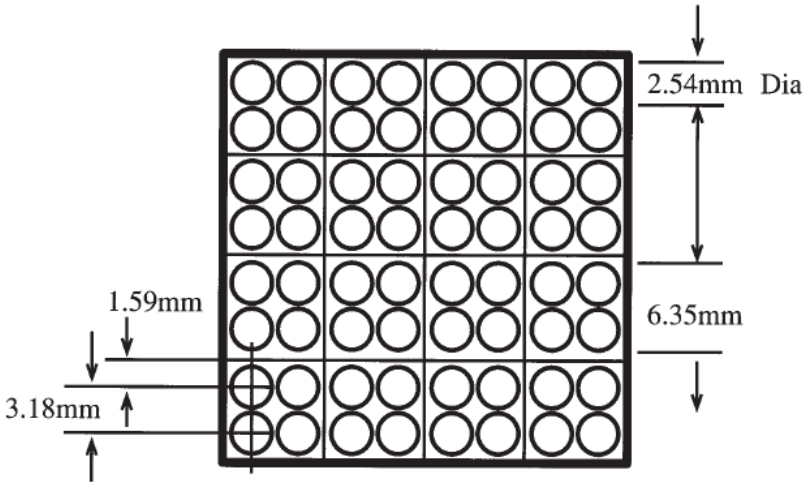

Figure I.B.35 – *Typical circle grid pattern.*

A series of CGA runs is often made through various stages of metal forming. When deep draws are required, the press may be stopped at several increments of punch travel (such as 25%) and the samples compared to track the plastic strain at each location on the part. When stampings are made on progressive dies, samples are made for each stage. This procedure indicates at what stage forming problems occur as well as where the critical locations are on the part.

The orientation of the major axis indicates the direction of major strain. Strain is quantified by comparing the major and minor axes with the original diameter of the circles according to the formula:

$$\% \text{ Strain} = \frac{l_2 - l_1}{l_1} \text{ x } 100$$

(2.1)

Where: **l1** = initial circle diameter
l2 = final major or minor ellipse diameter

The major diameter of the ellipse is always larger than the initial circle diameter, so that major stretch is always positive. The minor diameter may be greater or less; minor stretch may thus be either positive or negative (Figure I.B.36).

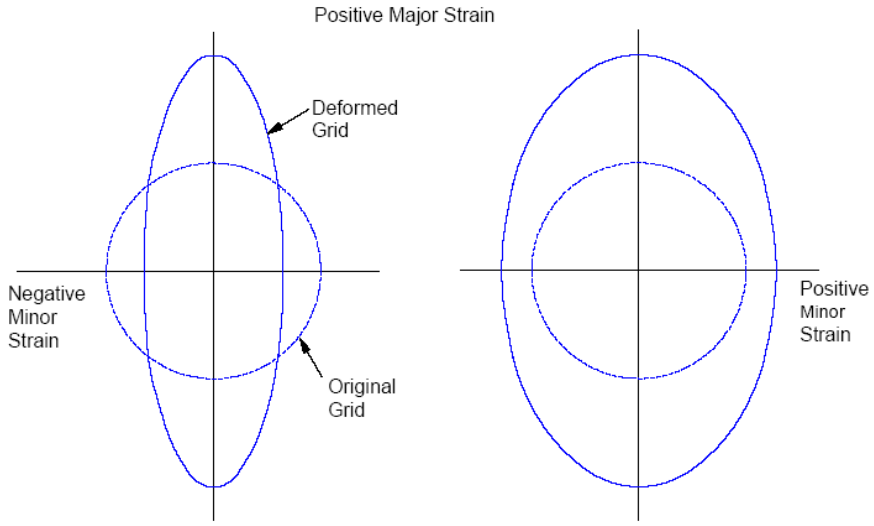

Figure I.B.36– *Representation of strains by etched circles.*

*I.B.*5.4 Forming Limit Diagram

In the past 40 years, the concept of the Forming Limit Diagram (FLD) introduced by Keeler and Backofen [16] and Goodwin [17] has created a significant impact in both academia and industry on how we determine the maximum deformation that a material can withstand during a sheet metal stamping process. In a FLD, the Forming Limit Curve (FLC) represents the maximum major principal strains that can be reached in sheet materials at given minor principal strains prior to the onset of localized necking. Past

engineering practices have shown the advantages of using FLDs in examining the failure potential, which include a good representation of material's stretchability and the easiness when used for trouble shooting.

The FLD is derived from the circle grid analysis to provide information useful to die designers, part designers, and steel suppliers. The percent of major and minor strain, which are computed in the CGA, are plotted on a forming limit diagram such as the one shown in Figure I.B.37, which applies to a low carbon, low strength steel 1 mm thick.

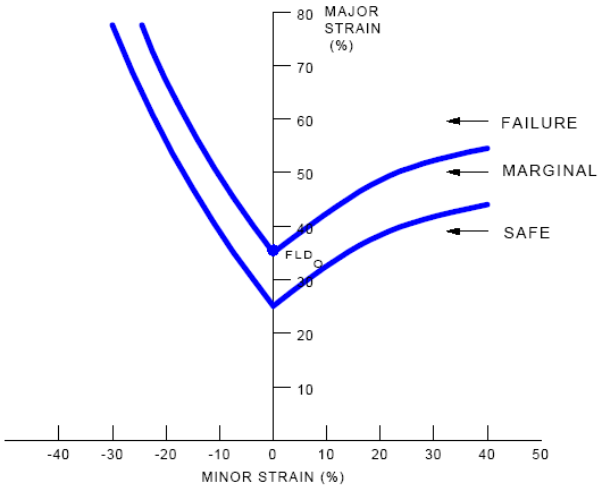

Figure I.B.37 – *Typical forming limit diagram.*

The diagram has a vertical axis for positive major strain and a horizontal axis for positive and negative minor strain. Two parallel curves separated by 10% strain on the vertical scale divide the diagram into three zones. Points on the stamping with large amounts of strain are plotted in relation to the axes. Locations that plot in the upper, or failure zone, will regularly fail by severe necking or tearing. Those in the intermediate, or marginal zone, will experience some failures depending on material and process variables. Those that fall into the lower, or safe zone, should not experience failures. The FLD indicates that the maximum allowable strain, and consequently the maximum length of line that can be generated in any direction, is influenced by the minor strain associated with it. The lowest value of major strain occurs when the minor strain is zero (plane strain). Positive minor strain allows some increase in major strain; negative minor strain allows substantial increase.

When areas of failure or potential failure are indicated, variables are adjusted such as binder pressure, die clearance, lubrication, steel grade or thickness. Best procedure ensures that all points fall safely below the marginal zone so that process changes, such as die wear and variations in die lubricant and sheet stock, will not shift any points into the marginal zone.

All forming limit curves for the grades of steel used in automotive bodies have essentially the same shape. The difference is their vertical position on the diagram, which is determined by the work hardening exponent, *n*, (Point 1.4.3) and thickness of the steel. Figure I.B.38 shows the relationship of *n* value and thickness to the plane strain intercept (FLD0) for low carbon steel. The FLD0 locates the curve on the grid. These characteristics allow the analyst to use one curve for all steel grades just by positioning it correctly on the vertical axis.

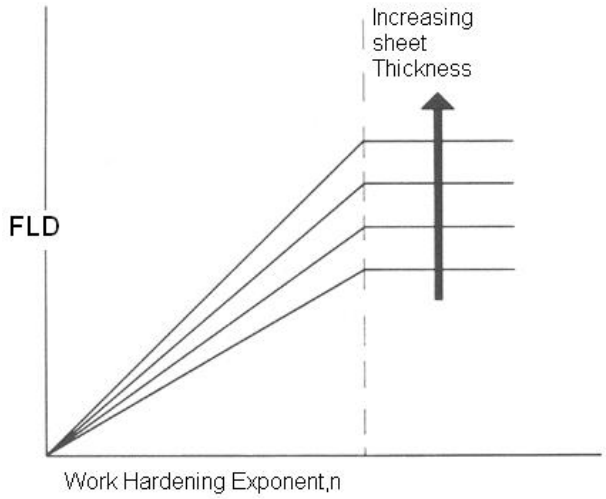

Figure I.B.38 – *Effects of n value and metal thickness on formability of low carbon steel*

The experimental methods for determining FLDs are well established. To clarify how CGA is used to construct FLD, is showed in *Appendix B* the method from stretching over a hemispherical punch. This method was proposed by Erichsen to evaluate the stretchability of the metals, and adapted by Hecker [18] to do a relation between CGA and FLD.

Knowledge of forming limits is important throughout the entire product design to production cycle.

First is the computerized forming process development (virtual die tryout), which requires forming limits for the selected steel type and grade to assess the forming severity (hot spots) for each point on the stamping. Next is the process and tool design stage where specific features of the tooling are established and again computer-validated against forming limits for the specific steel.

Troubleshooting tools for die tryout on the press shop floor utilize forming limits to assess the final severity of the part and to track process improvements. Finally, forming limits are used to track part severity throughout the production life of the part as the tooling undergoes both intentional (engineering) modifications and unintentional (wear) changes.

Two different types of forming limits are presented in this section. The first is the traditional forming limit curves that apply to all modes of sheet metal forming. The second is sheared edge stretching limits that apply strictly to the problem of stretching the cut edge of sheet metal.

*I.B.*6 - Crash Management

DP and TRIP steels with ferrite as a major phase show higher energy absorbing property than conventional HSS, particularly after pre-deformation and paint baking treatments. Two key features contribute to this high energy-absorbing property: high work hardening rate and large bake hardening effect.

The relatively high work hardening rate, exhibited by AHSS steels, leads to a higher ultimate tensile strength than the one exhibited by conventional HSS of similar yield strength. This provides for a larger area under the stress-strain curve, indicating greater energy absorption when deformed in a crash event to the same degree as conventional steels. The high work hardening rate also allows for a better strain distribution during crash deformation, providing more stable and predictable axial crush that is crucial for maximizing energy absorption during a front or rear crash event.

The relatively large bake hardening effect also increases the energy absorption of DP and TRIP steels by further increasing the area under the stress-strain curve. Conventional HSS do not exhibit a strong bake hardening effect and do not benefit from this strengthening mechanism.

Figure I.B.42 illustrates the difference in energy absorption between DP and TRIP steels as a function of their static (traditional tensile test speed) yield strength .

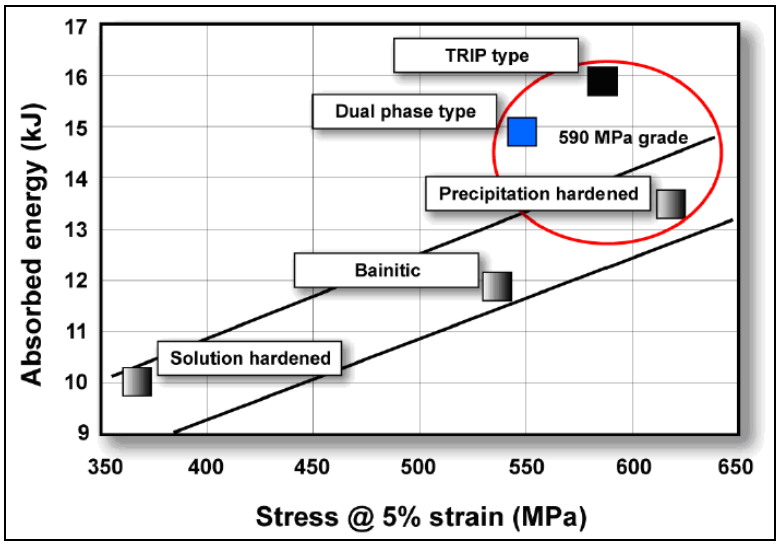

Figure IB..42 – Absorbed energy for square tube as function of static yield strength

Figure I.B.43 shows the calculated absorbed energy plotted against total elongation for a square tube component. The absorbed energy remains constant for the DP and TRIP steels, but the increase in total elongation allows for formation into complex shapes. For a given critical crash component, the higher elongations of DP and TRIP steels, generally, do not increase energy absorption when compared to conventional HSS. In some applications the DP and TRIP grades could increase energy absorption over that of a conventional HSS if the conventional steel doesn't have sufficient ductility to accommodate the required crash deformation and splits rather than fully completing the crush event. In the latter case, substituting DP or TRIP steel, with sufficient ductility to withstand full crash deformation, will improve energy absorption by restoring stable crush and permitting more material to absorb crash energy.

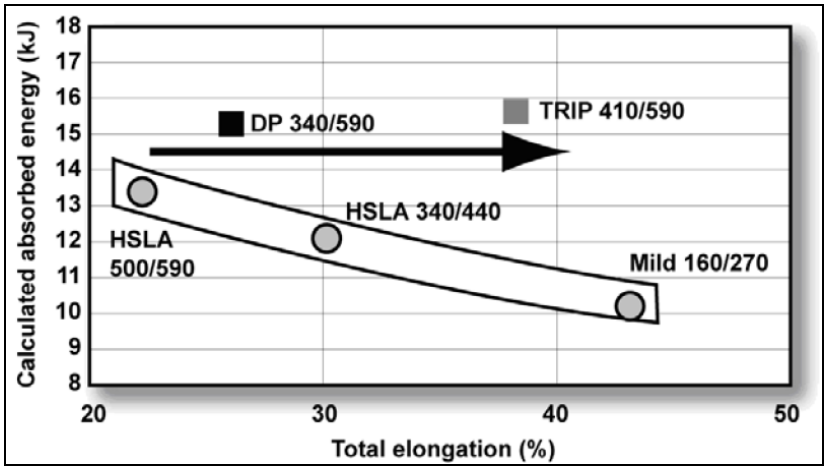

Figure I.B.43 - Calculated absorbed energy for a square tube as a function of total elongation

***I.B.*7 - Fatigue**

Fatigue in a structural component involves complex relationships among several factors including geometry, thickness, applied loads and material endurance limit.

The fatigue strength of AHSS steels is higher than the one of precipitation-hardened steels or fully bainitic steels with similar yield strength for many metallurgical reasons. For example, in DP steels the dispersed fine martensite particles retard the propagation of fatigue cracks, and in TRIP steels, the transformation of retained austenite can relax the stress field and introduce a compressive stress that can also improve fatigue strength. Figures I.B.44 and I.B.45 illustrate the improvements in fatigue capability.

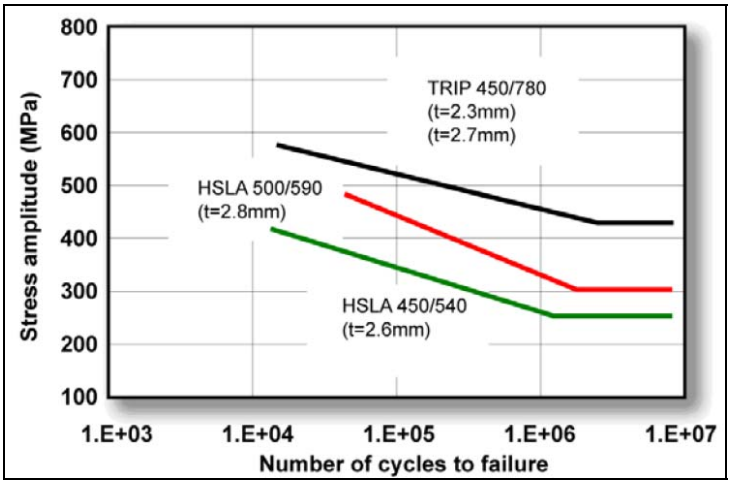

Figure I.B.44 - Fatigue characteristics of TRIP 450/780 steel compared to convention steels

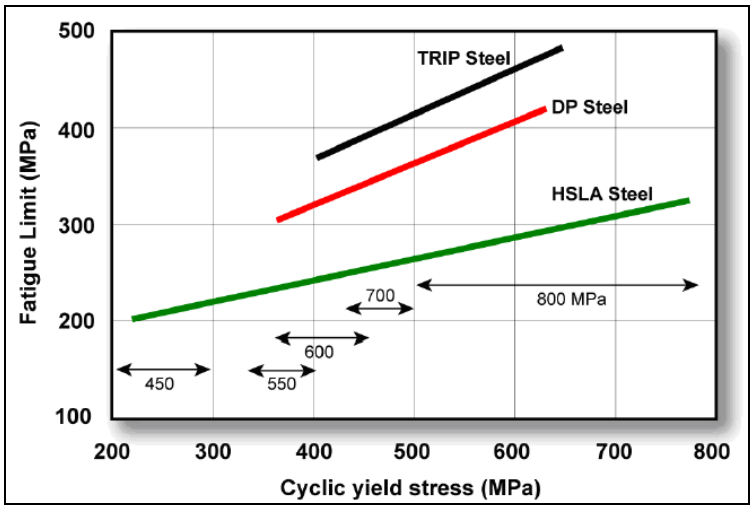

Figure I.B.45 - Fatigue limit for AHSS compared to conventional steels

I.B.8. Bibliography **:**

1) Jian Cao, Brad L Kinsey et al., "Next Generation Stamping Dies-Controllability and Flexibility". Robotics and Computer Integrated Manufacturing, 17, 2001, pp. 49-56
2) High-Strength Steel Bulletin, Edition 9, Auto/Steel Partnership, 2000 Town Center, Suite 320, Southfield, MI 48075-1123.
3) Inter Keeler, S. P., "Understanding Sheet Metal Formability Vol. II", Paper No. 35A, Metal Fabricating Institute, Rockford, IL., (1970).
4) Marciniak, Z., "Assessment of Material Formability," Advanced Technology Of Plasticity, Proceedings of the First International Conference on Technology of Plasticity, Tokyo, (1984), pp. 685-694.
5) Eary, D. F. and Reed, E. A., Techniques of Pressworking Sheet Metal, 2nd Ed., Prentice-Hall, Englewood Cliffs, New Jersey, (1974).
6) Sachs, G., Principles and Methods of Sheet-Metal Fabricating, Reinhold Publishing Corp., N.Y., (1966).
7) Xu S.G., M.L. Bohn, K.J. Weinmann, "Drawbeads in sheet metal stamping - A review", SAE 970986, Sheet Metal Stamping Symposium, Detroit, 1997.
8) Wouters P., G. Montfort, J. Defourny, "Numerical simulation and experimental evaluation of the modifications of material properties in a drawbead", Recent Developments in Sheet Metal Forming Technology, M.J.M. Barata Marques (ed.), Lisbon, p. 389-401, 1994.
9) Carleer B.D., T. Meinders, J. Huétink, "Equivalent drawbead model in finite element simulations", Proceedings of the 3rd International Conference on Numerical Simulations of 3-D Sheet Metal Forming Processes, J.K. Lee et al. (eds.), Dearborn, Michigan, p. 25-31, 1996.
10) Triantafyllidis N., B. Maker, S.K. Samanta, "An analysis of drawbeads in sheet metal forming: part 1 - problem formulation", J. Eng. Mat. Tech., vol. 108, p. 321-327, 1986.
11) Maker B., S.K. Samanta, G. Grab, N. Triantafyllidis, "An analysis of drawbeads in sheet metal forming: part 2 - experimental verification", J. Eng. Mat. Tech., vol. 109, p. 164-170, 1987.
12) J. Havranek, *Sheet Metal Forming and Energy Conservation*(Metals Park, OH: ASM, 1976), pp. 245-263
13) American Iron and Steel Institute, *Sheet Steel Formability*, August 1984, Washington D.C.
14) Keeler, S. P., Circle Grid Analysis (GCA), National Steel Booklet, Livonia, Michigan, (1986).
15) Dinda, S., James, K.F., Keeler, S.P. and Stine, P.A. "How to Use Circle Grid Analysis for Die Tryout", Metals Park, Ohio, American Society for Metals, 1981.
16) Keeler, S. P. and Backofen, W. A. (1964) Plastic instability and fracture

in sheets stretched over rigid punches, ASM Trans. Quart. 56, 25.
17) Goodwin, G. M. (1968) Application of strain analysis to sheet metal forming problems in the press shop. SAE paper No. 680093.
18) Hecker, S. S. " A Simple Forming Limit Curve Technique and Results on Aluminum Alloys," Sheet Metal Forming and Formability, Proceedings of the 7th Biennial Congress of the International Deep Drawing Research Group, Amsterdam (1972) 5.1-5.8.

Section I.C

Springback

Springback

*I.C.*1 – Introduction

Sheet metal forming involves the transformation of a flat sheet of metal into a useful shape. A common problem in this transformation is the distortion in the shape of the stamping that occurs when the deforming load is removed or when the stamping is removed from the tooling. This dimensional change is called springback and results from changes in strain produced by elastic recovery.

Springback is inherent in all sheet metal forming processes. Many factors could affect springback in the process, such as material variations in mechanical properties, sheet thickness, tooling geometry (including the die radius and the gap between the die and the punch), lubricant condition, geometry of the part, etc. In summa, springback results from the interaction of all components of the Forming System. The importance of springback depends on the end application, quality requirements, subsequent processing steps, etc. For example, excessive or variable springback in a channel which is subsequently welded with critical dimensional control is an important processing parameter. On the other hand, springback in the back corner of a floor pan may be relatively unimportant and corrective action may be unnecessary.

Three basic approaches are used to correct for springback. The first, design of the forming process to eliminate the springback through control of the stress-strain patterns generated in the stamping during the forming operation. The second isn't to control the springback but to compensate for the springback in the original design of the tooling – for example overbending – such that the final part will be dimensionally correct. The third is changing a little bit the part design without forget his functionality.

Each of these approaches requires an understanding of the causes of springback and the factors which affect its magnitude. With this knowledge, trial and error attempts at springback correction become more effective. Ideally, a method is required for quantitatively predicting the magnitude and direction of the springback and/or the residual stress distribution after the forming operation is completed.

Springback is one of the most difficult problems in applying high strength steel (HSS) to automotive body parts. Because all of that, the AHSS manufacturing is nowadays a big challenge to the biggest companies (principally in the automotive field), therefore an exhaustive studied is applied to understand the all problematic in stamping this new type of steel.

I.C.2 – Origins of Springback

Springback is the result of elastic recovery of the sheet metal after deformation. This can be easily shown from the stress-strain curve obtained from a tensile specimen (Figure I.C.1). Unloading (by removing all external forces and moments) from plastic deformation zone A would follow line AC to C, where DC is the permanent deformation (plastic) and CB is the recovered deformation (elastic). Although this elastic recovered deformation at a given location is very small, it can cause significant shape change due to its mechanical multiplying effect on other locations when bending deformation and/or curved surfaces are involved. The magnitude of springback is governed by the tooling or component geometry and resultant residual stress distribution through the sheet thickness after forming. Creating a uniformly distributed residual stress across the sheet and through the thickness eliminates the source of mechanical multiplier effects and thus leads to reduced springback problems.

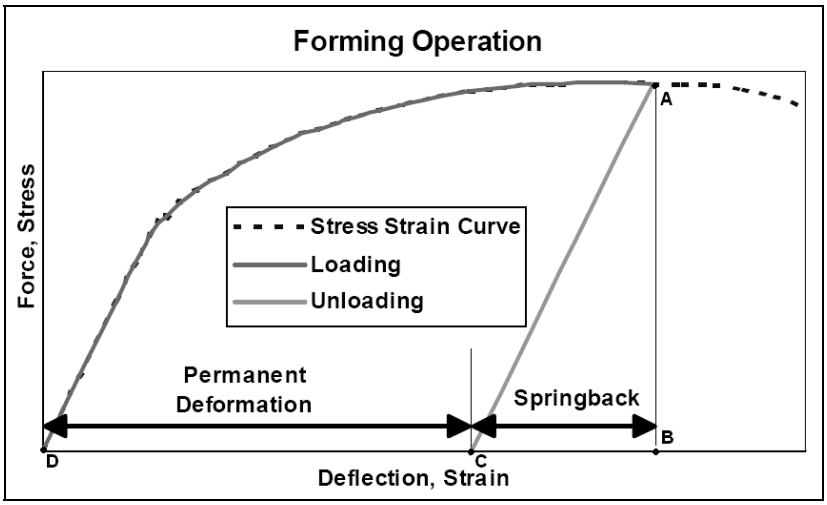

Figure I.C.1 *– Stress and Strain during forming.*

In most sheet metal stampings, the recovery strain is combined with one of several mechanical multiplying factors which tend to greatly magnify the shape change [1]. To illustrate this important phenomenon, bending is used.
In a typical bending operation, the stress distribution through the sheet thickness while still under the forming moment (load) is shown in Figure I.C.2. The inside surface of the bend has a compressive stress, while the outside of the bend has a tensile stress – each of which must recover in the opposite

direction upon unloading. Although the recovery strain is very small, significant shape changes can be generated by the mechanical multiplying effect.

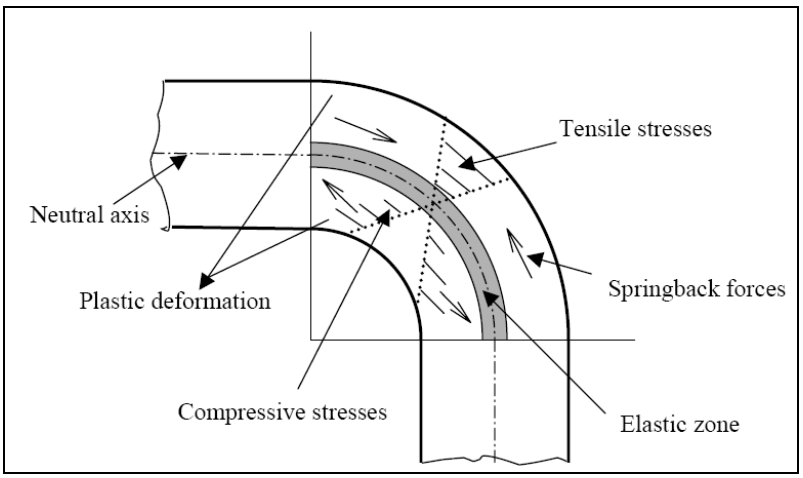

Figure I.C.2 *– Stresses in the sheet during the bending.*

I.C.3 – Variables affecting Springback

There are several variables that influence the amount of springback that is seen in a bend after a stamping process. In this point is specified those that are more important, specifying their contribution on changing the final dimensions of the work piece.

To complement the next sub points is given here the equation I.C.1 which Mike Gedeon [2], after a complex study, propose to calculate the ratio of springback in 90º bending angles.

$$K = \frac{\alpha_{final}}{\alpha_{initial}} = -25.54 \cdot X^3 + 17.91 \cdot X^2 - 5.85 \cdot X + 1.08$$

(I.C.1)

$$\text{where } X = \left(\frac{Yield\ Strength}{Elastic\ Modulus}\right) \cdot \left(\frac{Inside\ Bend\ Radius}{Strip\ Thickness}\right)$$

(I.C.2)

Analysing the next Figure (I.C.3) is concluded conclude that, which bigger is the ratio between $\alpha_{final}/\alpha_{initial}$ (ideally 1), smaller will be the rate of springback because the initial and the final angles are more "equals".

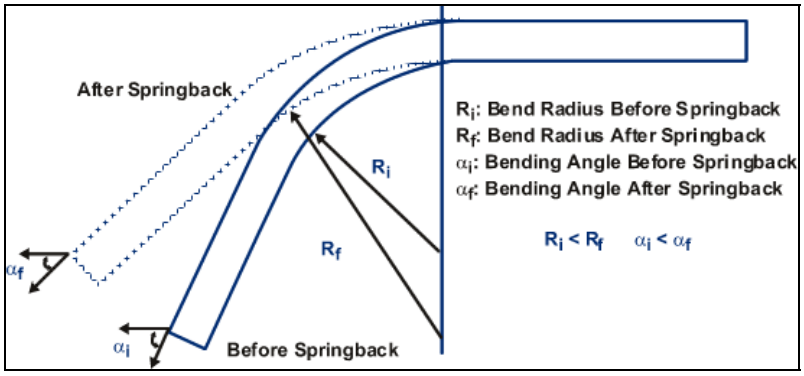

Figure I.C.3 *– Bending angle after and before Springback.*

In such case, and looking for the next figure (Figure I.C.4) respective to the equation above, is verified that, decreasing parameter *X*, increase *K* which imply a smaller ratio of springback.

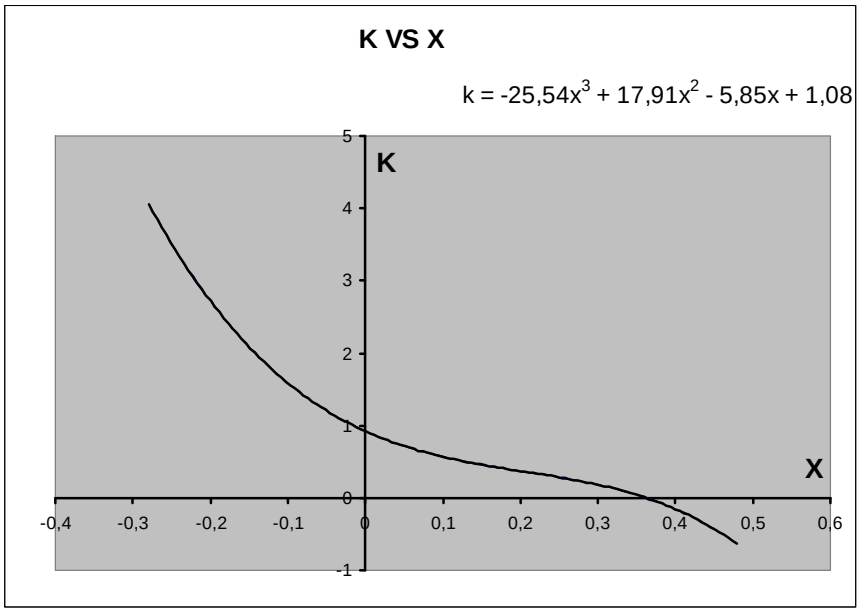

Figure I.C.4 *– Relation between K ($\alpha_{final}/i_{initial}$) and X.*

To conclude: decreasing *X* ☐ increase *K*☐ decrease *Springback*

Increases Springback	Decreases Springback
Lower Modulus	Higher Modulus
Higher Strength	Lower Strength
Thinner Strip	Thicker Strip
Larger Bend Radius	Smaller Bend Radius

Figure I.C.5 *– The most important variables affecting Springback.*

I.C.3.1 **– Material's Characteristics**

a) Mechanical Properties

The selection of the material has a crucial importance in the stamping of each part. A material with higher yield strength will have a greater ratio of elastic to plastic strain, and will exhibit more springback than a material with lower yield strength. On the other hand, a material with a higher elastic modulus will show less springback than a material with a lower elastic modulus.

This fact can be explained by two ways:

- *Analysing the above equation (I.C.1)* – is possible to conclude that, when the yield strength increase and/or the Young's modulus decrease (with other variables constant), the parameter *K* decrease, so the ratio of springback increase;

- *Analysing the Stress/Strains graphic (I.C.6)* – with submit of two different steel samples to a tensile test, and unloading with a uniform load, it's easy to conclude that the elastic recovery is higher in the steel with a high yield strength.

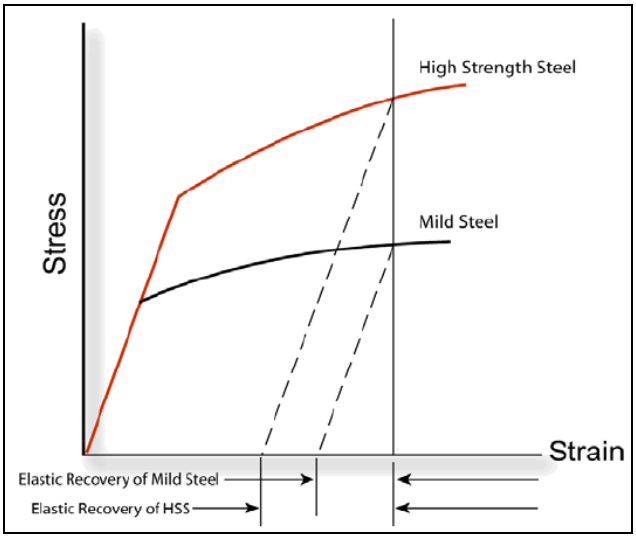

Figure I.C.6 *– Schematic showing amount of springback is proportional to stress.*

Springback is a major difference between HSS and AHSS. For example, the channels shown in Figure I.C.7 were made sequentially in a draw die with a pad on the post.

Figure I.C.7 *– Two channels made sequentially in the same die.*

The strains distributions were very close with almost identical lengths of line. However, the stress distributions were very different because of the steel property differences between DP and HSLA steels.

b) Sheet Thickness

A low value of sheet thickness plays an equal role to that that characterises high bend radius values. Doing one reference to a mono axis model, the deformation caused on a generic fibre that is a *y* distance of neutral axis is equal to y/R (R is the bend radius). The maximum deformation is verified in the outer layer of the sheet, and that will be s/2R. This means that reducing *s* decreasing the deformations and consequently increases the amount of springback.

It's also possible see that in the equation I.C.1, low values of sheet thickness imply higher *X* values, which means, higher Springback.

I.C.3.2 **– Forming Parameters**

a) Inside Bend Radius

The inside bend radius will be, at the end of loading phase, coincident with the punch bend radius. From looking at the equation we see that increasing bend radius (while keeping everything else constant) has the same effect as increasing Yield Strength or decreasing Young's Modulus, which will clearly lead to a greater springback. This makes sense because a bigger initial radius means that the stress in the material due to bending will be lower and therefore the ratio plastic deformation vs. elastic deformation will be smaller which leads to a greater springback.

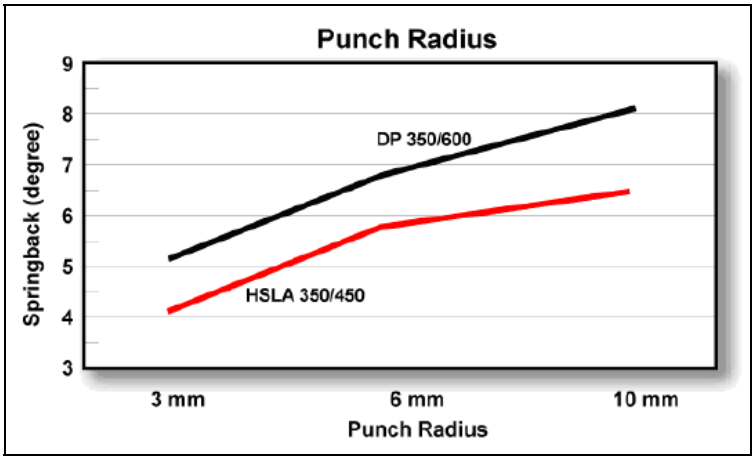

Figure I.C.8 *– Influence of bend (Punch) radius in the Springback angle.*

b) Tool Gap

This one was studied by Nan Song, Dong Qian, Jian Cao and Wing Kam Liu [3], and they concluded, after some experiences, that the springback angle increases as the tool gap increases, like it's possible to see in the figure I.C.9.

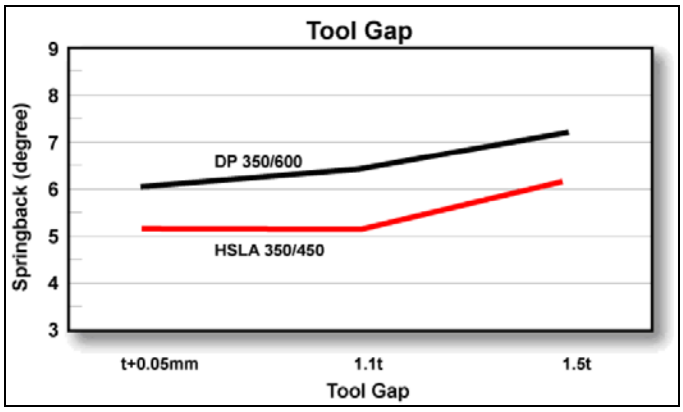

Figure I.C.9 - *Influence of tool gap in the Springback angle. [4]*

c) Die Temperature

This variable only influences the anisotropic materials and was studied by Y. T. Keum and B.Y. Han [5]. With reference an Eq. recommended by Lue [6], they concluded that Springback decreases with an increasing of die temperature. This can be explained by the fact that the strength coefficient is smaller than other material properties like elastic modulus, strain hardening exponent, etc. The next figure shows the difference of springback after a bending test associated with test temperatures from room-temperature and 350ºC.

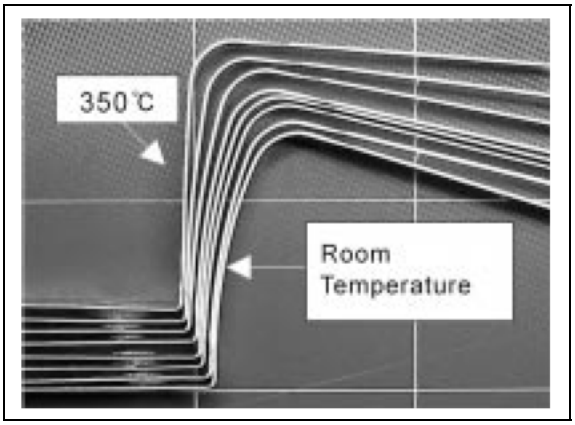

Figure I.C.10 – *Influence of temperature in the Springback angle.*

d) Blankholder Force (Load)

The blankholder force is one of the most important variables in the forming process. Controlling it is the key to some problems like wrinkles, fracture and springback. At this last the BHL is inversely proportional with the ratio of springback, like is shown by the picture I.C.11.

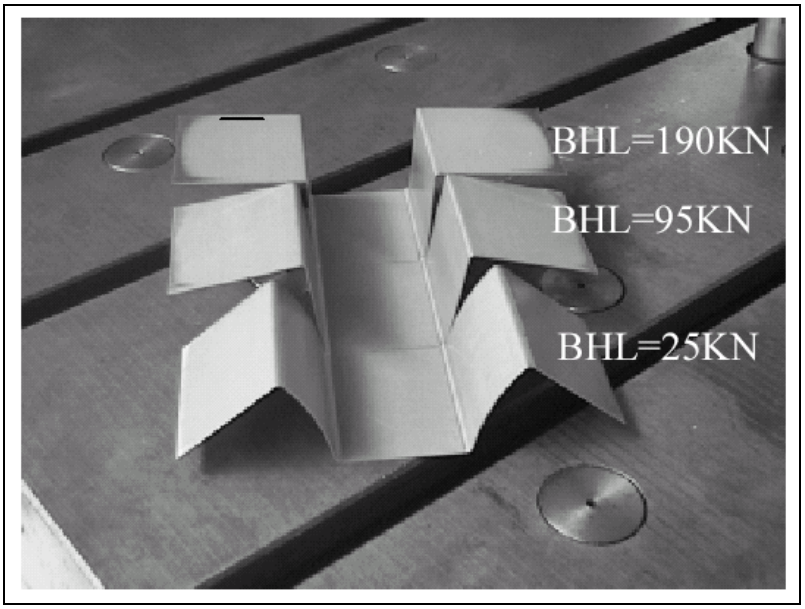

Figure I.C.11 – *Relation between springback and blankholder load.*

Because controlling all of these variables in the manufacturing process is nearly impossible, springback, in turn, cannot be readily controlled. Adding to the difficulty is the fact that springback is a highly nonlinear effect; therefore, simulations and correcting methods are complicated.

I.C.4 **– Types of Springback**

Five modes of springback are commonly found in channels and underbody components – angular change, sidewall curl, twist, global shape change, edge line warping and surface distortion.

In this is search it is focus on the first three type be because they are the most frequent.

Angular change : The angle forming two sides inclosing a bending edge line deviates from the die angle. Figure I.C.12

Sidewall curl : The straight side wall becomes curved. . Figure I.C.13

Twist : The two cross-section rotate differently along their axis. . Figure I.C.14

Edge line warping : The bending edge line deviates in curvature from the edge line of the die. . Figure I.C.15

Global shape change : The desired shape of the die is not achieved when the punch is at bottom. Global shape changes, such as reduced curvature when unloading the panel in the die, are usually corrected by springback compensation measures. The key problem is springback variation during the run of the stamping and during die transition. . Figure I.C.16

Surface distortion : Local buckling occurs on the surface of a body panel after forming. Springback defects develop from local reaction to residual stress patterns within the body of the stamping. Common examples are high and low spots, oil canning, and other local deformations that form to balance total residual stresses to their lowest value. Figure I.C.117

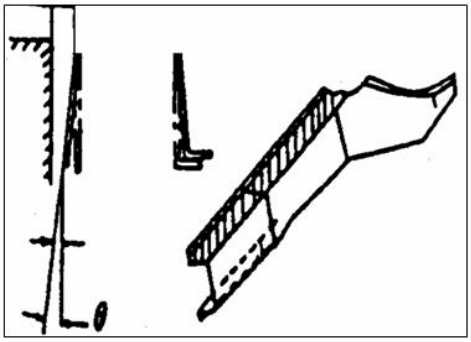

Figure I.C.12 **Angular change**

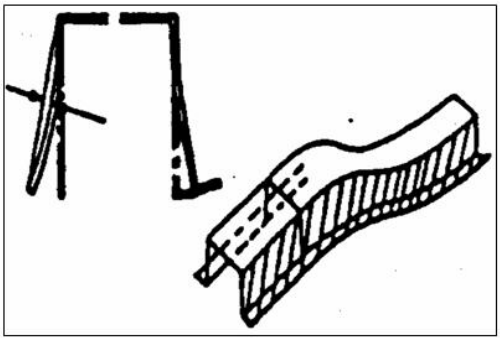

Figure I.C.13 **Sidewall curl**

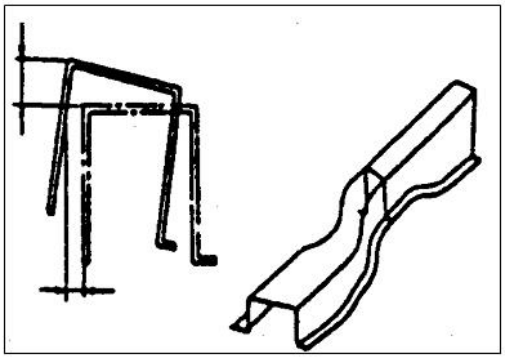

Figure I.C.14 **Twist**

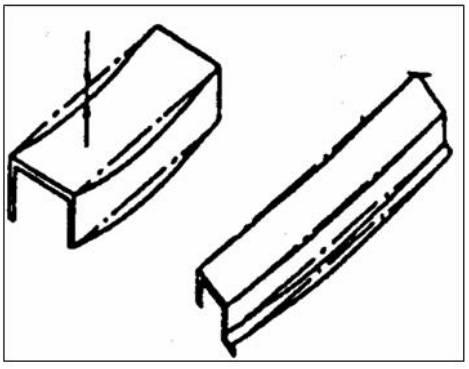

Figure I.C.15 **Edge line warping**

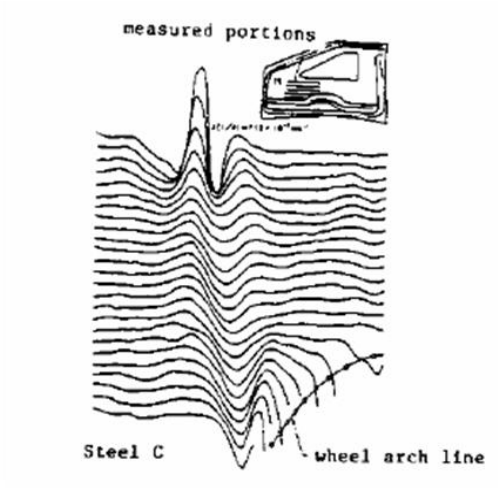

Figure I.C.16 **Global shape change**

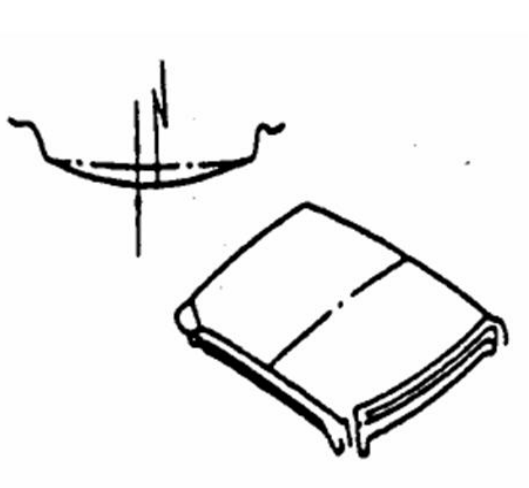

Figure I.C.17/ **Surface distortion**

I.C.4.1 **– Angular Change**

Angular change, is the angle created when the bending edge line (the stamping) deviates from the line of the tool. The springback angle is measured off the punch radius (Figure I.C.18). If there is no sidewall curl, the angle would be constant up the wall of the channel.

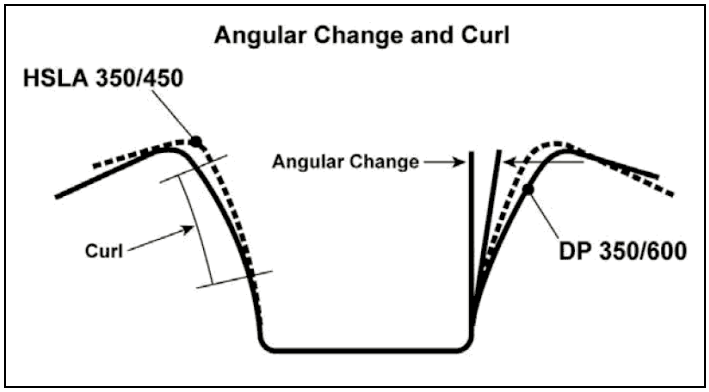

Figure I.C.18 *– Schematic showing difference between angular change and sidewall curl.*

Angular/cross-section change is caused by stress difference in the sheet thickness direction when a sheet metal bends and unbends over a die radius. This stress difference in the sheet thickness direction creates a bending moment at the bending radius after dies are released, which results in the angular change. The key to eliminating or minimizing the angular change is to eliminate or to minimize this bending moment.

I.C.4.2 **– Sidewall Change**

Sidewall curl is the curvature created in the side wall of a channel (Figures I.C.7 and I.C.11). This curvature occurs when a sheet of metal is drawn over a die/punch radius or through a draw bead. The primary cause is uneven stress distribution or stress gradient through the thickness of the sheet metal. This stress is generated during the bending and unbending process. The inside surface initially generates compressive stresses while the outer surface generates tensile stresses.

During the bending and unbending sequence, the deformation histories for both sides of the sheet are unlikely to be identical. This usually manifests itself by flaring the flanges, which is an important area for joining to other parts. The resulting sidewall curl can cause assembly difficulties for rail or channel sections that require tight tolerance of mating faces during assembly. In the worst case, a gap resulting from the sidewall curl can be so large that welding is not possible.

Figure 3.19 illustrates what happens when sheet metal is drawn over the radius (a bending and unbending process). The deformation is side A changes from tension during bending to compression during unbending and the deformation in side B changes from compression to tension during bending and unbending. As the sheet enters the sidewall, side A is in compression and side B is in tension, although both sides may have similar

amounts of strain. Once the punch is removed from the die cavity (unloading), side A tends to elongate and side B to contract due to the elastic recovery.

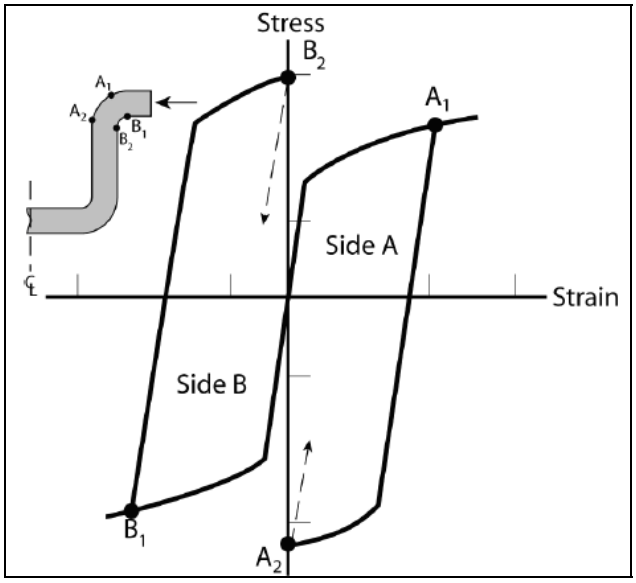

Figure I.C.19 *– Origin and mechanism of sidewall curl*

This difference in elastic recovery in side A and side B is the main source of sidewall curl. The higher the strength of the deformed metal, the greater the magnitude and difference in elastic recovery between sides A and B and the increase in sidewall curl. The strength of deformed metal depends not only on the as-received yield strength, but also on the work hardening capacity. This is one of the key differences between conventional HSS and AHSS. Clearly, the rule for minimizing the sidewall curl is to minimize the stress gradient through the sheet thickness.

Difference between HSS and AHSS

The difference in strain hardening between conventional HSS and AHSS explains how the relationship between angular change and sidewall curl can alter. Figure i.c.20 shows the crossover of the stress – strain curves when the steels are specified by equal tensile strengths. At the lower strain levels usually encountered in angular change at the punch radius, AHSS have a lower level of stress and therefore less springback.

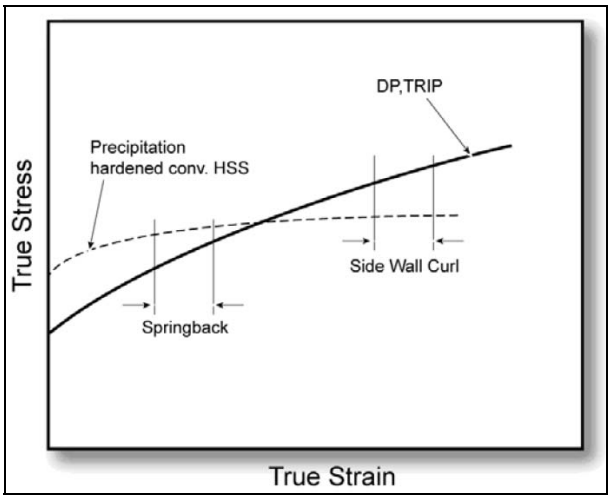

Figure I.C.20 *– Schematic description of the effect of hardening property on shape-fixability. [7]*

This difference for steels of equal tensile strength (but different yield strengths) is shown in Figure i.c.21. Of course, the general trend is increased angular change for increasing steel strength.

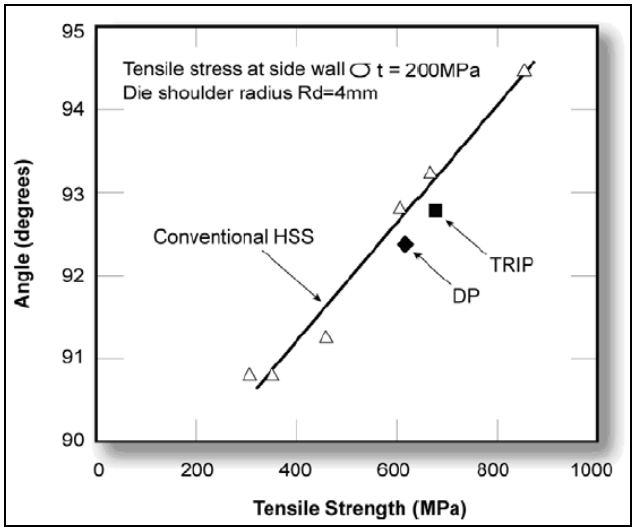

Figure I.C.21 *– The AHSS have less angular change at the punch radius for equal tensile strength steels. [7]*

Sidewall curl is a higher strain event because of the bending and unbending of the steel going over the die radius. For the two stress-strain curves (shown in Figure I.C.13) the AHSS are at a higher stress level with increased elastic stresses. Therefore the sidewall curls is greater for the AHSS (Figure I.C.22).

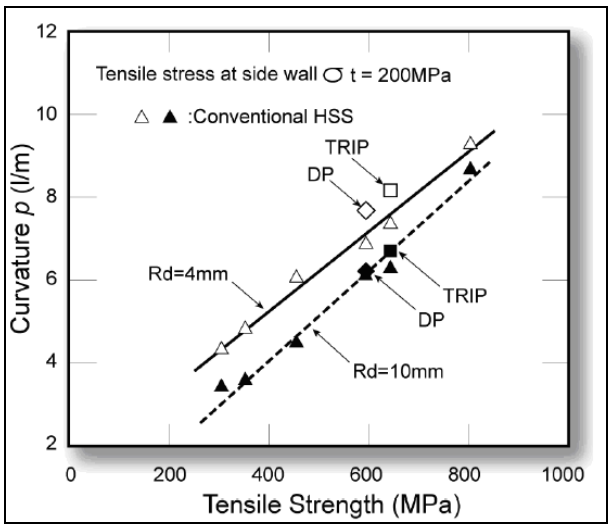

Figure I.C.22 *– The AHSS have greater sidewall curl for equal tensile strength steels. [8]*

Now assume that the comparison is made between a conventional HSS and an AHSS specified at the same yield stress. Figure 3.13 would then show the stress-strain curve for the AHSS is always greater (and sometimes substantially greater) than the curve for HSS. Now the AHSS channel will have greater springback for both angular change and sidewall curl compared to the HSS channel. This result would be similar to the channels shown in Figure I.C.7.

These phenomena are dependant on many factors, such as part geometry, tooling design, process parameter, and material properties, and in some cases they may not even appear. However, the high work-hardening rate of the DP and TRIP steels causes higher increases in the strength of the deformed steel for the same amount of strain. Therefore, any differences in tool build, die and press deflection, location of pressure pins, and other inputs to the stamping can cause varying amounts of springback – even completely symmetrical stampings.

I.C.4.3 **– Twist**

Twist is defined as two cross-sections rotation differently along their axis. Twist is caused by torsion moments in the cross-section of the part. The torsional displacement (twist) develops as a result of unbalanced springback and residual stresses acting in the part to create a force couple which tends

to rotate one end of the part relative to another. As shown in Figure I.C.23, the torsional moment can come from the in-plane residual stresses in the flange, the sidewall, or both.

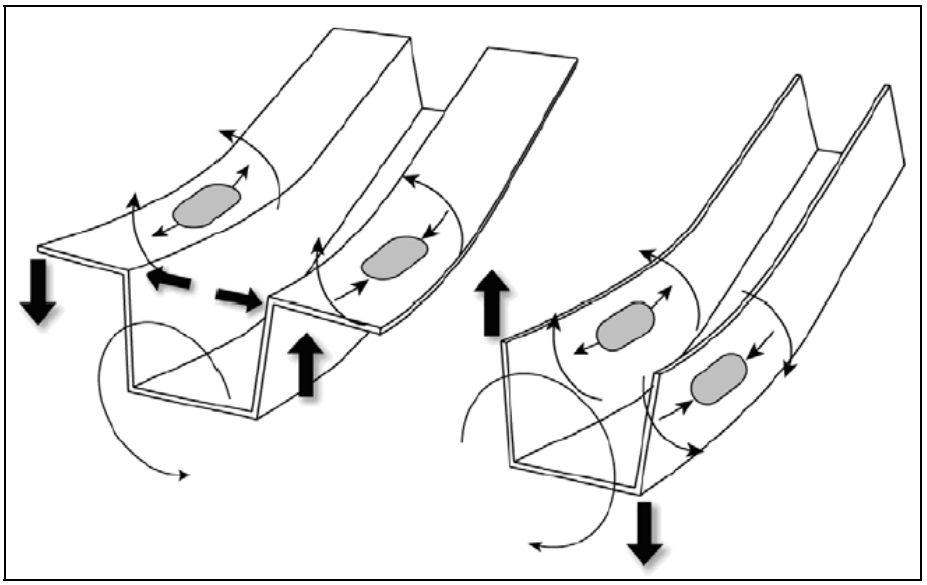

Figure I.C.23 *– Torsion Moment from flange or sidewall residual stress. [9]*

The actual magnitude of twist in a part will be determined by the relationship between unbalanced stresses on the part and stiffness of the part in the direction of the twist. Low torsional stiffness values in long, thin parts are reason high aspect ratio parts have significantly higher tendencies to twist. There is also a lever effect, whereby the same amount of twist will result in a larger displacement in a long part than would be the case in a shorter part with a similar twist angle.

The tendency for parts to twist can be overcome by reducing the imbalance in the residual stresses forming the force couple that creates the torsional movement. Unbalanced forces are more likely in unsymmetrical parts, parts with wide flanges or high sidewalls, and in parts with sudden changes in cross section. Parts with unequal flange lengths or non-symmetric cutouts will be susceptible to twist due to unbalanced springback forces generated by theses non-symmetrical features.

Even in geometrically symmetrical parts, unbalanced forces can be generated if the strain gradients in the parts are non-symmetrical. Some common causes of non-symmetrical strains in symmetrical parts are improper blank placement, uneven lubrication, uneven die polishing, uneven blankholder pressure, misaligned presser, or broken/worn draw beads. These problems will result in uneven material draw in with higher strains and higher

elastic recoveries on one side of the part compared to the other, thereby generating a force couple and inducing twist.

Twist can also be controlled by maximizing the torsional stiffness of the part – by adding ribs or other geometrical stiffeners or by redesigning or combining parts to avoid long, thin sections which will have limited torsional stiffness.

I.C.5 **– Springback Correction for AHSS**

I.C.5.1 **– Part Design**

- Successful application of any material requires close coordination of part design and the manufacturing process.

- Design structural frames (such as rails and crossbars) as open-end channels to permit forming operations rather than draw die processes. AHSS stampings requiring draw operations (closed ends) are limited to a reduced depth of a draw. Less complex, open-ended stamped channels are less limited in depth.

- Designs AHSS channel shaped part depth as consistent as possible to avoid forming distortions.
- Springback computer simulations should be used whenever possible to predict the trend of springback and to test the effectiveness of solutions.
- Design the part and tool in such a way that springback is desensitized to variations in material, gauge, tools and forming processes (a robust system and process) and that the effects of springback are minimized rather than attempt to compensate it.
- Design the punch radius as sharp as formability and product/style allow. Small bend radii (<2t) will decrease the springback angle and variation (Figure I.C.24) [10]. However, stretch bending will be more difficult as yield strength increases. In addition, sharp radii contribute to excessive thinning.
-

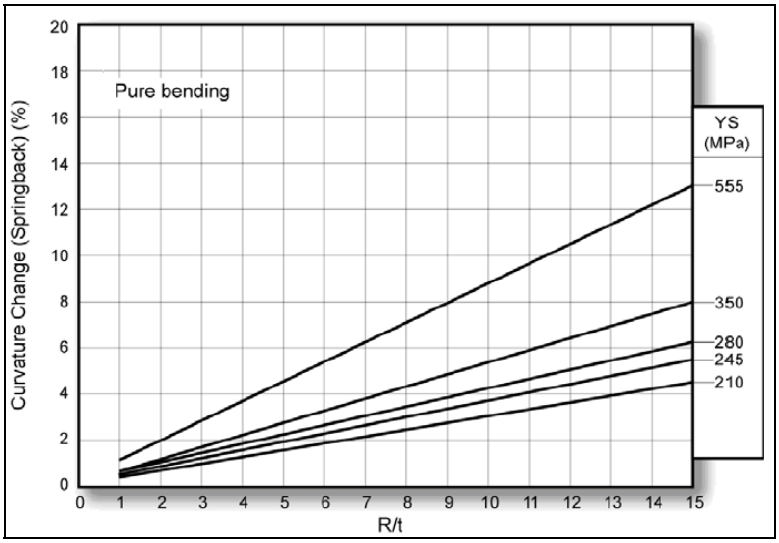

Figure I.C.24 *– Angular changes increased by YS and bend radius to sheet thickness ratio.*

- Design opposing sidewalls of channels as open angles to allow overbend for springback correction dies. Required overbend increases with steel tensile strength. For example, at a given bending radius, Mild steel may need 3 degrees per side but up to 10 degrees per side may be required for the higher strength AHSS grades, such as DP 500/800 and TRIP 450/800.
- All shape transitions should be gradual to avoid distortions, especially in areas of metal compression. Minimize stretch/compression flanges whenever possible.
- Curved parts with unequal length sidewalls in the fore-aft direction will develop torsional twist after forming. The shorter length wall can be under tension from residual forming stresses. Torsional twist is more pronounced with the higher strength steels. The problem can be relieved by adding strategically placed beads or other shapes in the shorter length wall equalize of length of line.

- Cross-section design for longitudinal rails, pillars, and cross members.

The rear longitudinal rail cross-section in sketch *A* of Figure I.C.25 does not allow overbend for springback compensation in the forming die. In addition, the forming will produce severe sidewall curl in AHSS channel-shaped cross sections. These quality issues can be minimized be designing a cross section similar to sketch *B* that allows for overbend during forming. Sidewall curl is also diminished with the cross-sectional design. Typical wall opening angles should be 6 degrees for DP 350/600 and 10 degrees for DP 850/1000. In addition, the cross section in sketch *B* will have the effect of reducing the impact shock load when the draw punch contacts the AHSS sheet. The vertical draw walls shown in sketch *A* require higher binder pressures and higher punch forces to maintain process control.

Inner and outer motor-compartment rails also require an optimized cross-section design for AHSS applications- Sketch *A* in Figure I.C.25 shows a typical rectangular box section through the inner and outer rails. This design will cause many problems for production due to sidewall curl and angular change. The hexagonal section in sketch *B* will reduce sidewall curl and twist problems, while permitting overbend for springback compensation in the stamping dies.

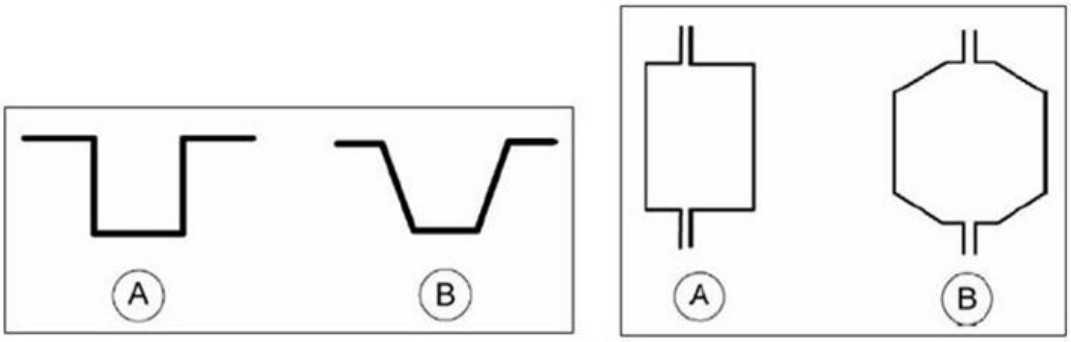

Figure I.C.25 – change rail cross section from A to B reduce Springback problem with AHSS [11]

- ***Draw Beads***

A considerable force is required from a nitrogen-die cushion in a single-acting press to set draw beads in AHSS before drawing begins. The nitrogen-die cushion may be inadequate for optimum pressure and process control. In some cases, binder separation may occur because of insufficient cushion tonnage, resulting in a loss of control for the stamping process.

The high impact load on the cushion may occur several inches up from the bottom of the press stroke. Since the impact point in the stroke is both a higher velocity point and a derated press tonnage, mechanical presses are very susceptible to damage due to these shock loads. Additional flywheel energy is dissipated by the high shock loads, well above bottom dead centre of the stroke.

A double-action press will set the draw beads when the outer slide approaches bottom dead centre where the full tonnage rating is available and the slide velocity is substantially lower. This minimizes any shock loads on die and press and resultant load spikes will be less likely to exceed the rated press capacity.

I.C.5.2 **– Process Design**

a) General Guidelines

- Multiple stage forming processes may be desirable or even required, depending on the part shape. Utilize secondary operations to return a sprung shape back to part datum. Care must be taken though to ensure that any subsequent operation does not exceed the work hardening limit of the worked material. Use multi-stage computerized forming process development to confirm strain and work hardening levels. Try to fold the sheet metal over radius instead drawing or stretching over a radius.

b) Angular Change

- Apply in-plane tension after bending (post-stretch). This can be done by designing a process with bending forming first and stretching later or by locking the binder with movable beads ate the end of the stroke and applying additional stretch (Figure I.C.26). Sidewall curl also can be minimized and made more stable by post-stretch. Note that these post-stretch forming operations normally require significantly higher forming force to be effective since the sidewalls have significant work hardening resulting from the forming operation.

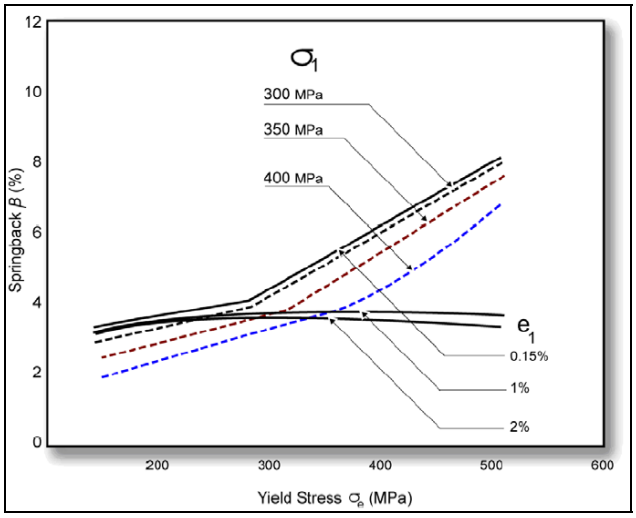

Figure I.C.26 *– A post-stretch greater than 1% eliminates the increase in springback as the yield stress increases. [12]*

- Several springback solutions to reduce angular change and/or sidewall curl are shown in Figure I.C.27. [13]

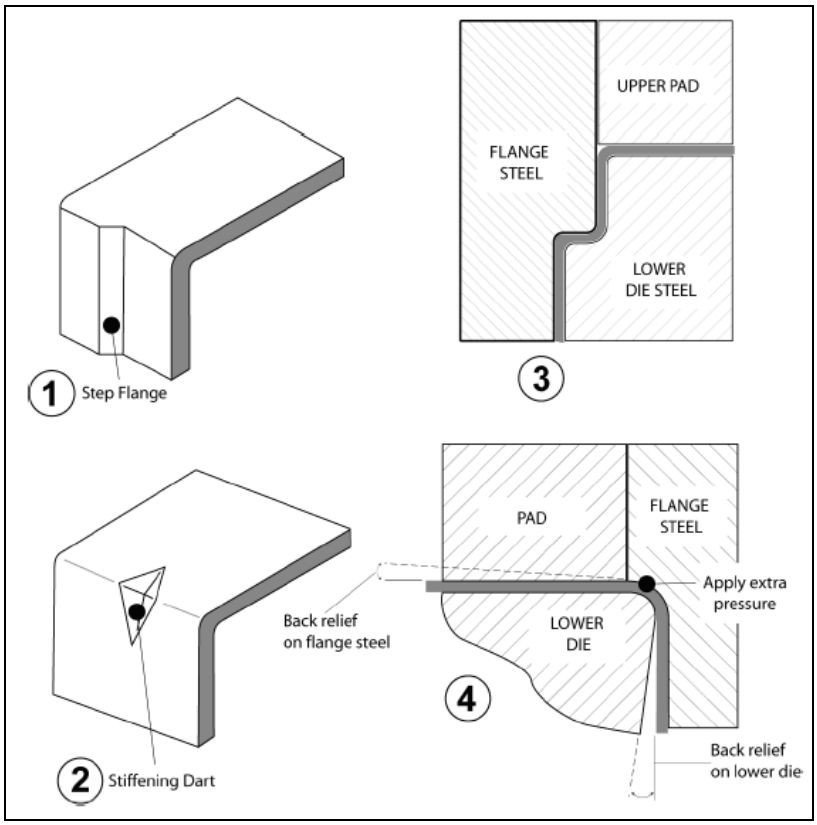

Figure I.C.27 *– Methods to reduce angular springback.*

- If overbend must be incorporated for some parts, use tool/die radii less than the part radius and use back relief for the die/punch.

- Maintain die clearance as tight as allowed by formability and press capability (Figure I.C.28). [9]

-

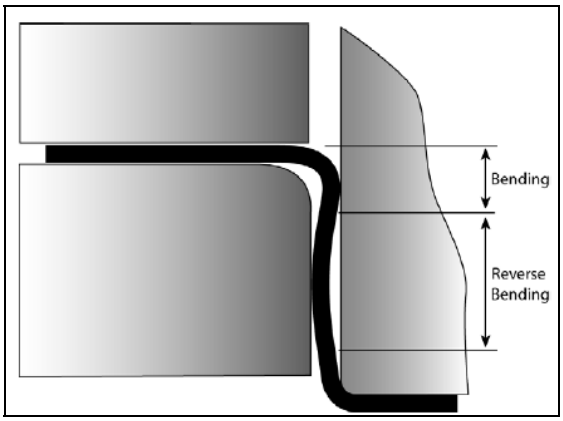

Figure I.C.28 *– Reducing die clearance restricts additional bending and unbending as the sheet metal comes of the die radius to minimize angular change.*

- If necessary, add one or two extra forming steps. For example, use pre-crown in the bottom of channel-type parts in the first step and flatten the crown in the second step to eliminate the springback at sidewall (Figure I.C.29). [14]

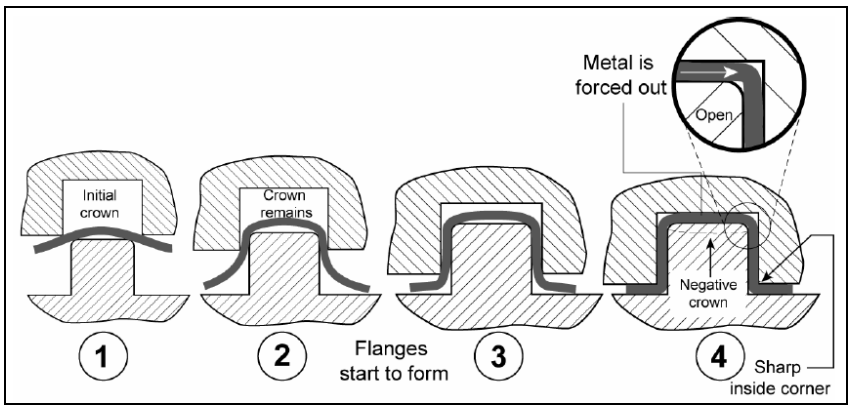

Figure I.C.29 *– Schematic showing how bottom pre-crown can be flattened to correct for angular springback.*

- Use geometry compensation methods to compensate the die, which can be tested with computerized forming process development.

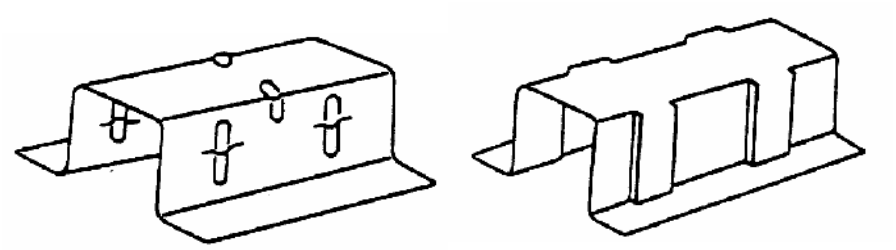

-Examples for "stiffeners" or "darts"

c) Sidewall Curl

Guidelines for Draw Dies and Stretch-Form Dies

- Equalize depth of draw as much as possible
- Stretch-forming produces a stiffer panel with less springback than drawing. Potential depth of the panel is diminished for both processes as the strength of the material increases. Deeper AHSS stampings will require the draw process.
- Binder pressure must be increased for AHSS. For example, DP 350/600 requires a tonnage 2.5 times greater than that required for AKDQ of comparable thickness. Higher binder pressure will reduce panel springback.
- A restrike operation may be required after trimming to ensure dimensional precision. The restrike die should sharpen the radius and provide sidewall stretch (post-stretch) of approximately 2%.
- Maintain a *1.1t* maximum metal clearance in the draw dies.
- Lubrication, upgraded die materials, and stamping process modifications must be considered when drawing AHSS.

Guidelines for Form Dies

- Set-up the die to allow for appropriate overbend on sidewalls.
- Equalize the depth of forming as much as possible.
- Use a post-stretch (explained below) for channel-shaped stamping. For less complex parts, one form die should be sufficient. For more geometrically complex parts, the first die will form the part with open sidewalls. The second die will finish the form in a restrike die with post-stretch of the sidewalls. Part geometry will determine the required forming process.
- Some complex parts will require a form die with upper and lower pressure pads. To avoid upstroke deformation of the part, a delayed return

pressure system must be provided for the lower pad. When a forming die with upper pad is used, sidewall curl is more severe in the vertical flange than in the angular flange.

- Provide higher holding pressure. DP 350/600 requires a force double that needed for mild steel.
- When using form dies, keep a die clearance at approximately *1.3t* to minimize sidewall curl. Die clearance at *1t* is not desirable since the sidewall curl reaches the maximum at this clearance.
- Do not leave open spaces in the die flange steels at the corners of the flanges. Fit the radius on both sides of metal at the flange break. Spank the flange radius at the bottom of the press stroke.
- Bottom the pad and all forming steels at the bottom of the press stroke.

Post-stretch

Several process schemes are used to increase sidewall strain by 1-2% at the end of the stroke. The flange area is locked by a moveable bead, lock step, another die, or some other process to impart the post-stretch. This post-stretch removes the tension to a compressive residual stress gradient through the sheet thickness and generates a nearly constant tensile stress through the sheet thickness. Upon release of the forming force, the length of the sidewall shrinks a very small amount with very little residual sidewall curl. In addition, different strengths of AHSS and HSS have approximately the same amount of residual sidewall curl (Figure I.C.26) that can be removed by modification of tool geometry. The die geometry is shown in the next Figure (I.C.30).

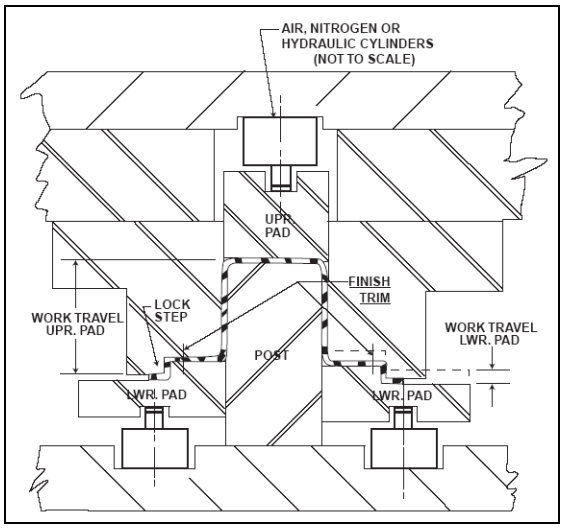

Figure I.C.30 – *An example of a Post-Stretch die.*

However, because of the high strength nature of AHSS, it may be difficult to achieve sufficient stretch to the sidewall by simply increasing the blank holding force. Lock beads may be needed to prevent metal flow into the wall during post-stretching.

Further Die process guidelines for high strength sheet steel stamping die.

In order to properly plan for operations involving HSS, the die process planner must be aware of the potential effects of residual stress and elastic recovery in stamped parts. He must try to foresee those part designs and die processes that would produce distortion in the finished stamping and plan corrective action accordingly. Part areas that will be placed in tension or compression by the forming process will develop residual stresses. Residual stress, elastic recovery and the resultant distortions are caused by a combination of material characteristics, die process and part geometry.

For structural parts, such as rails & crossbars, residual stress may result in a stamping with sidewall curl or springback. Springback is not accurately predictable through forming simulation. It is vital that the die process planner specify those part modifications and die processes which will reduce the springback phenomena resulting from residual stress. Small bend radii are an important part design element for springback reduction. Proper overbend for springback compensation is important for the die process. In addition, a die process that induces 2% or greater stretch in the part will also minimize the problem. See post-stretch form die sketches 5 & 6 on pages 36 & 37.

The die process planner must specify a forming die process that best suits the part geometry and material characteristics while keeping the stamping under control throughout the die operation. Flanges that are in compression during the forming action must be controlled with pressure pads to avoid buckling and overlapped metal.

Form and Flange Dies -

This sketch illustrates the type of die that can be used for mild steel parts with minimal shape
transitions. It is normally not an effective process for high strength materials. All part radii should be small with this process. as shown in figure I.C.31 below.

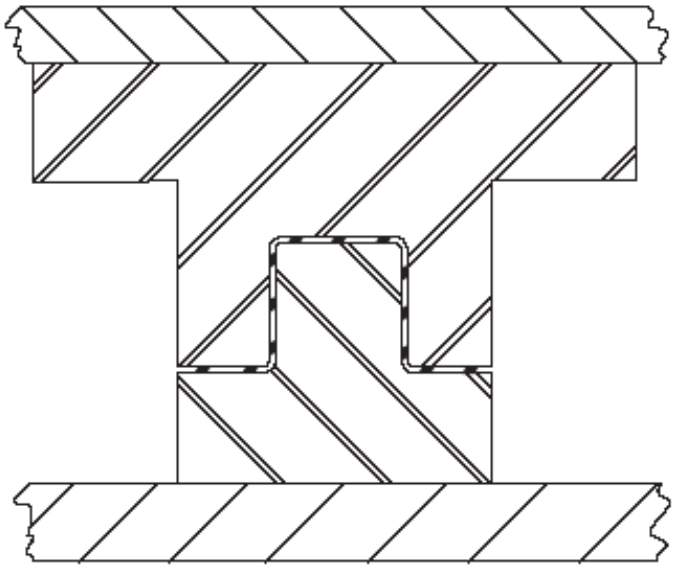

Figure I.C.31 **Solid Form Die**

Parts with contours in the die plan view or elevation will require an upper pressure pad. The holding pressure requirement increases with the material strength and with more complex part geometry. All part radii should be small with this process, as shown in figure I.C.32 below

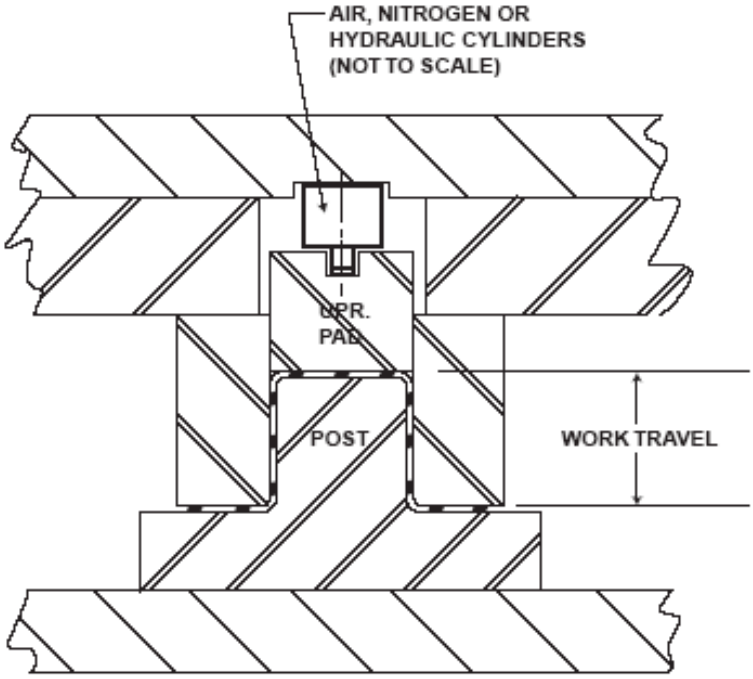

Figure I.C.32 **Solid Form Die**

Contoured parts with compression flanges will require a lower pressure pad to control buckling
in areas of metal compression. Part contours in the plan view or elevation can cause metal compression during the forming process. Buckling due to metal compression increases with higher strength steels. This process is sometimes referred to as a "draw-action" form die. Post radii should be small, but flange radii may need to be slightly larger for higher strength grades when using this process. An oversized radius will increase sidewall curl, as shown in figure I.C.33 below.

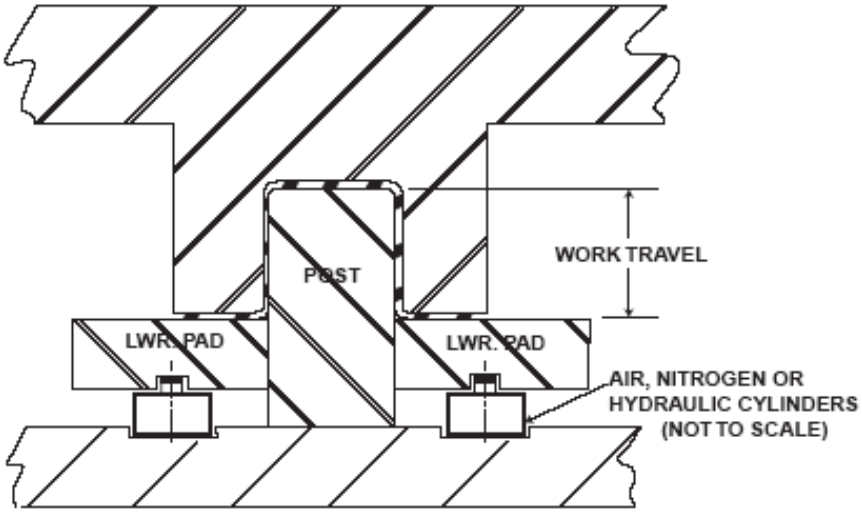

Figure I.C.33 **Form Die-Draw Action (Lower Pad)**

For high strength steel parts with more complex geometry, a die process using upper and lower pads may be required. A lower pad delayed return system must be employed with this two-pad process in order to avoid upstroke deformation of the part. This can be done with hydraulic cylinders, nitrogen cylinders (Delayed Return and Control or DRAC type) or a mechanical pad lock-down device. Post radii should be small to reduce spring back on walls. Flange radii may need to be slightly lager, as shown in figure I.C.34 below.

Opposing upper and lower pressure pad are effective in controlling distortion on channel shaped or "hat section" parts that have more severe shape in the plan view and/or elevation. These part shapes result in compression and stretching of metal during the stamping process which must be controlled in order to produce an acceptable part. This type of die has been avoided in the past due to the opposing pressure pads causing an "upstroke deformation" of the part. In order to use this process, the lower pad must be locked down

during the press upstroke. Nitrogen cylinders are available with delayed return features for this purpose.
A programmable hydraulic cushion system is even more effective.

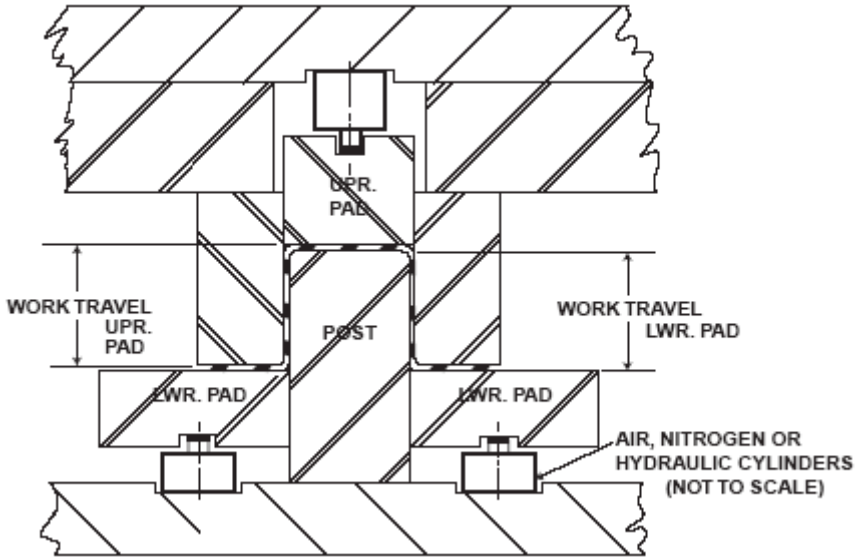

Figure I.C.34 **Form Die-Draw Action (Upper and Lower Pads)**

Post-stretch or "shape set" is a form and flange die process technique whereby the stamping is locked-up and stretched over the die post prior to the press reaching bottom dead center. A lower pressure pad with lock beads is normally designed to engage the sheet metal blank and upper die steels about 6 mm or less from bottom dead center. The resultant stretch in the part is effective in reducing residual stresses and part-to-part variation caused by non-uniform material. A lower pad lock-down device is required to avoid upstroke deformation of the part by the opposing pressure pads. See figure 5 and 6.

This process uses a lower pad with a lock step and high pressure to stretch the part over the die post before the die bottoms. The lower pad has only minimal travel, enough to stretch the part sidewalls at least 2%. This process can be very effective in reducing springback and sidewall curl of HSS stampings that do not have severe compression flanges. A lower pad delayed-return system is also required with this process.
Note: Parts with severe compression of metal on sidewalls or flanges will require a lower restraining pad action for the full depth of the part, as shown in figure I.C.35 below.

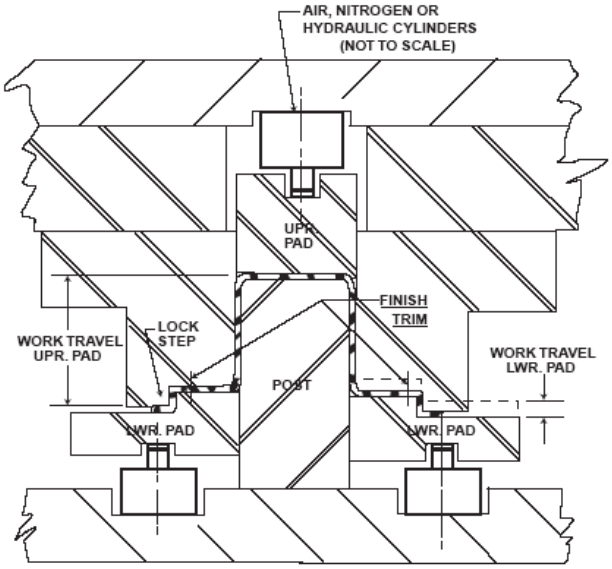

Figure I.C.35 **– Post-Stretch Form Die (Upper and Lower Pads)**

This variation of the post stretch process uses a solid lock step in place of the lower pad-mounted lock step. It also will stretch the part sidewalls. The amount of stretch will be determined by the depth of the lock step. This process is limited to those applications without compression of metal in side walls and flanges, as shown in figure I.C.36 below.

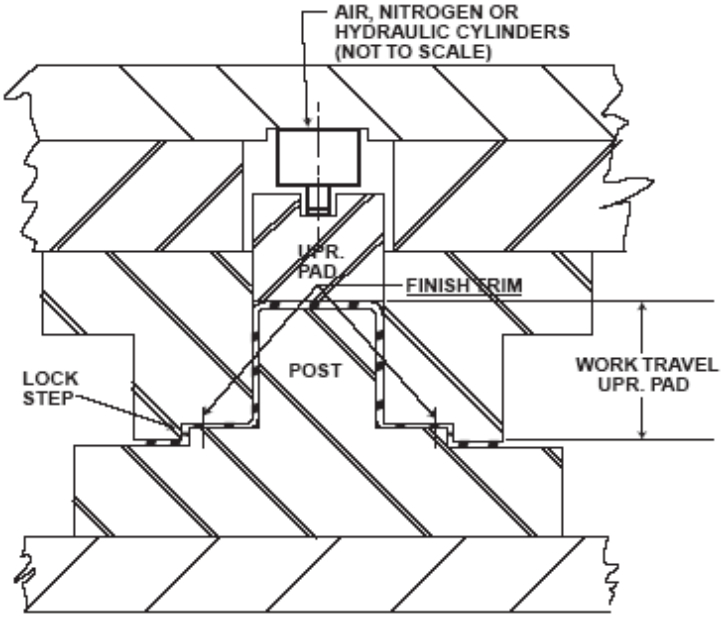

Figure I.C.36 **– Post-Stretch Form Die (Upper Pad)**

Some parts with more severe plan view and elevation contours, and/or unequal length sidewalls, will require draw die operations. The binder pressure can be provided by die-mounted cylinders or a press bed pressure system. This process uses a rough blank and requires a subsequent trim die to remove the binder scrap. For HSS parts of 270 MPa (40 KSI) and higher, an open-end draw die is recommended, as shown in figure I.C.37 below.

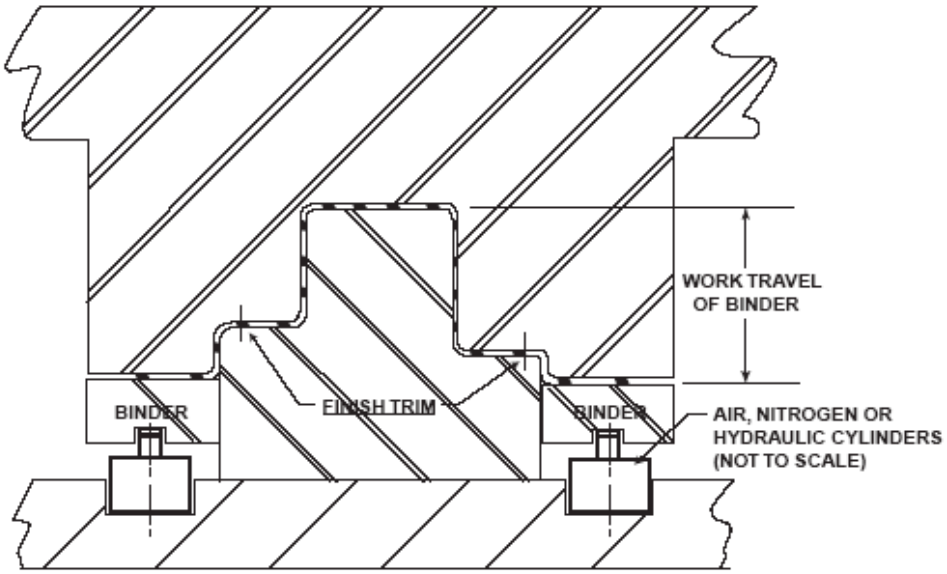

Figure I.C.37 **– Draw-Die Single Action Press (Lower Binder)**

This type of die requires a double action press. It is used primarily for drawn panels with large surface areas, as shown in figure I.C.38 below.

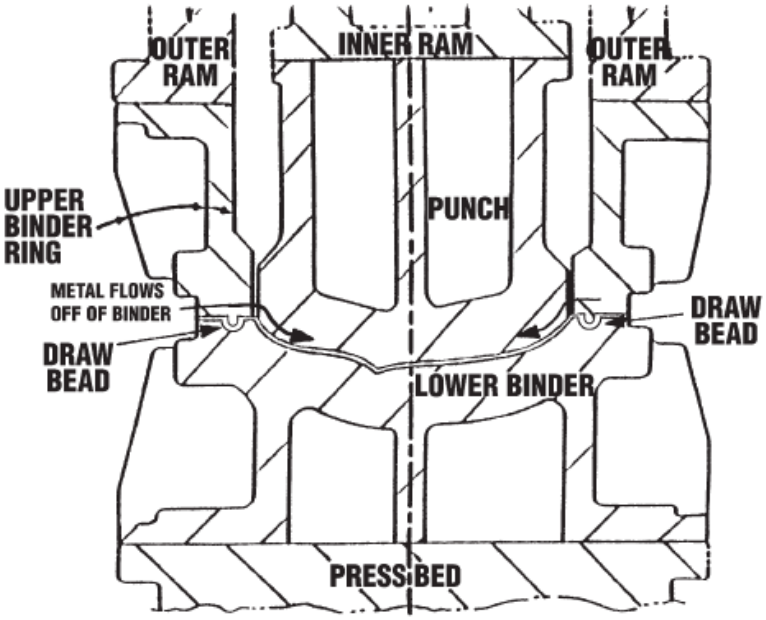

Figure 8I.C.38**– Double Action Draw-Die.**

This type of draw die runs in a single action press. Cycle time is reduced by approximately 25% from the double action press, as shown in figure I.C.39 below.

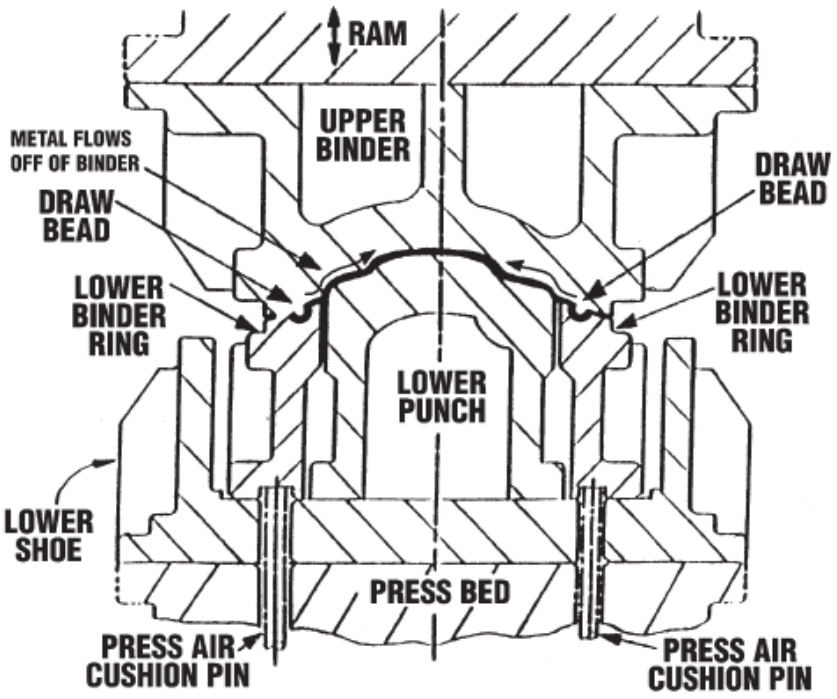

Figure I.C.39**– Air Cushion Draw-Die**

The stretch form die is used to induce bi-axial stretch and work hardening in outer panels. The result is a stiffer panel with better dent resistance. However, panel depth is limited, as shown in figure I.C.40 below.

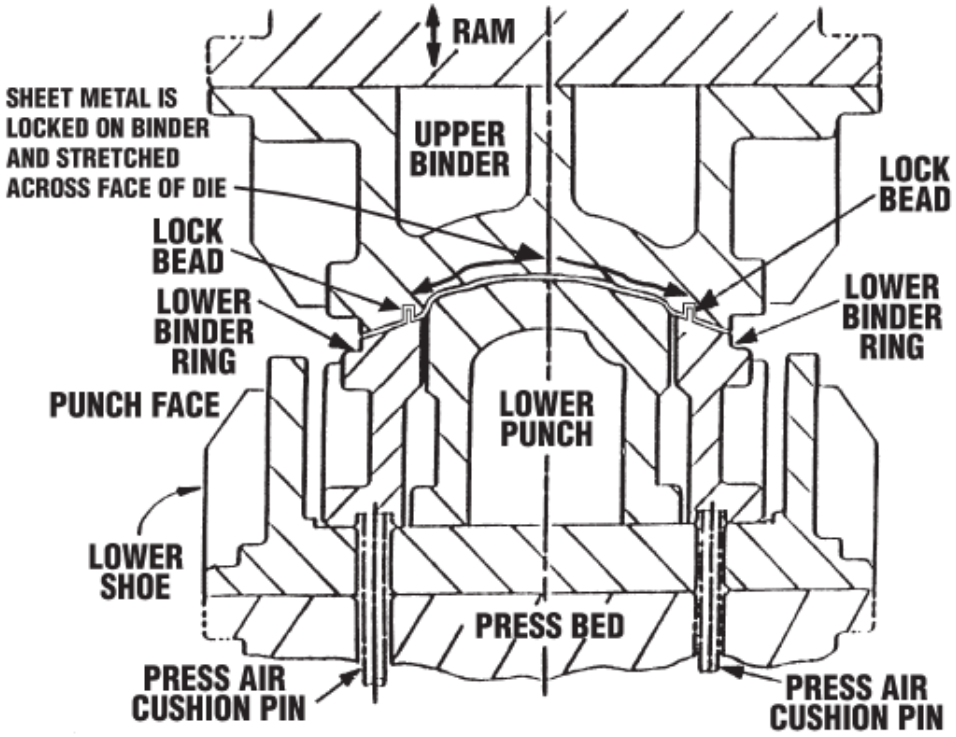

Figure I.C.40 **– Stretch-Form Die**

I.C.6. Bibliography**:**

[1] Gerdeen J. C. and Duncan, J. L., "Springback in Sheet Metal Forming," Report on AISI Project 1201-456, (1986).

[2] Mike Gedeon, *Elastic Springback*, Brush Wellman Engineered Materials.

[3] N. Song, D. Quian, J. Cao and W. K. Liu, "Effective Prediction of Springback in Flanging", Journal of Engineering Materials and Technology, October 2001.

[4] S. Sadagopan and D. Urban, "Formability Characterization of a New Generation of High Strength Steels," American Iron and Steel Institute (March 2003).

[5] Y. T. Keum and B.Y. Han, "Springback of FCC sheet in warm forming", Journal of Ceramic Processing Research. Vol. 3, No. 3, pp. 159-165 (2002).

[6] Daw-Kwei Leu, "A simplified approach for evaluating bendability and springback in plastic bending of anisotropic sheet metals", Journal of Materials Processing Technology (1997) 9-17.

[7] T. Katayama et al, "Effects of Material Properties on Shape-Fixability and Shape Control Techniques in Hat-shaped Forming," Proceedings of the 22nd IDDRG Congress, p.97 (2002).

[8] M. F. Shi, Internal National Steel Corporation report.

[9] K. Yoshida, "Handbook of Ease or Difficulty in Press Forming," Translated by J. Bukacek and edited by S-D Liu (1987).

[10] M. Shi, "Springback and Springback Variation Design Guidelines and Literature Review," National Steel Corporation Internal Report (1994).

[11] J. Noel, HSS Stamping Task Force, Auto/Steel Partnership.

[12] M. Ueda and K. Ueno, "A Study of Springback in the Stretch Bending of

Channels," Journal of Mechanical Working Technology, 5, p.163 (1981).

[13] High Strength Steel (HSS) Stamping Design Manual, Auto/Steel Partnership (2000).

[14] High Strength Steel (HSS) Stamping Design Manual, Auto/Steel Partnership (1997).

Section I.D

Finite element method

Finite Element Analysis

*I.D.*1 – General application of Finite element method

Because of higher requirements on the quality of products and narrow tolerances of measures, optimising, planning and simulating of forming processes becomes more and more important. As the computational power has increased during the last years, numerical methods play an outstanding roll. The most important numerical method is the method of finite elements (FEM). Numerous finite element programmes have been developed which are able to solve linear, non linear, static, dynamic, elastic, plastic, elastic – plastic, steady state, transient, isotherm as well as non isotherm problems, during the last years. In this case we have to differ between "general purpose" and "special purpose" programs.

Today many forming processes are carried out without a previous or accompanied finite element analysis of course. However, if the material flow or the loads of the rolling devices have to be investigated exactly, the numerical simulation is a must, if one does not want to invest too much money and time in practical experiments. Furthermore practical experiments cause a loss of production of a rolling plant, for example. If the material flow and the stresses in the rolling pieces as well as the forming tools are well known, critical forming steps and deformations can be corrected and avoided. [1]

Finite element analysis software enables engineers to perform the following tasks:

- Build computer models or transfer CAD models of structures, products, components, or systems.
- Apply operating loads or other design performance conditions.
- Study physical responses, such as stress levels, temperature distributions, or electromagnetic fields.
- Optimize a design early in the development process to reduce production costs.
- Do prototype testing in environments where it otherwise would be undesirable or impossible (for example, biomedical applications).

The principal applications of the Finite element methodo it consists in:

- Structural Analysis
- Analyzing Thermal Phenomena
- Fluids Analysis
- Electromagnetic Field Analysis.

I.D.2 **- many analyses can be performed With Finite Element Method:**

I.D.2.1 **- Structural analysis**

Structural analysis is probably the most common application of the finite element method. The term *structural* (or *structure*) implies not only civil engineering structures such as bridges and buildings, but also naval, aeronautical, and mechanical structures such as ship hulls, aircraft bodies, and machine housings, as well as mechanical components such as pistons, machine parts, and tools.
The seven types of structural analyses are explained below. The primary unknowns (nodal degrees of freedom) calculated in a structural analysis are *displacements*. Other quantities, such as strains, stresses, and reaction forces, are then derived from the nodal displacements.
Structural analyses are available in Program as the ANSYS Multiphysics, ANSYS Mechanical, ANSYS Structural, and ANSYS Professional programs.
We can perform the following types of structural analyses:
- *Static Analysis*--Used to determine displacements, stresses, etc. under static loading conditions. Both linear and nonlinear static analyses. Nonlinearities can include plasticity, stress stiffening, large deflection, large strain, hyperelasticity, contact surfaces, and creep.
- *Modal Analysis*--Used to calculate the natural frequencies and mode shapes of a structure. Different mode extraction methods are available.
- *Harmonic Analysis*--Used to determine the response of a structure to harmonically time-varying loads.
- *Transient Dynamic Analysis*--Used to determine the response of a structure to arbitrarily time-varying loads. All nonlinearities mentioned under Static Analysis above are allowed.
- *Spectrum Analysis*--An extension of the modal analysis, used to calculate stresses and strains due to a response spectrum.
- *Buckling Analysis*--Used to calculate the buckling loads and determine the buckling mode shape. Both linear buckling and nonlinear buckling analyses are possible.
- *Explicit Dynamic Analysis*--This type of structural analysis is available in program as the ANSYS LS-DYNA.. Explicit dynamic analysis is used to calculate fast solutions for large deformation dynamics and complex contact problems.
- *Implicit static analysis.*
With the static implicit method that equilibrium is checked after each time step and thus will lead to more accurate results. The main drawback of this method however, is that the computation time depends quadratically on the number of d.o.f. if a direct solver is used. Another drawback is that the

stiffness matrix is often ill conditioned which can make the method unstable and detoriates the performance of iterative solvers. [2].

- Structural Static Analysis

A static analysis calculates the effects of *steady* loading conditions on a structure, while ignoring inertia and damping effects, such as those caused by time-varying loads. A static analysis can, however, include *steady* inertia loads (such as gravity and rotational velocity), and time-varying loads that can be approximated as static equivalent loads (such as the static equivalent wind and seismic loads commonly defined in many building codes).
Static analysis is used to determine the displacements, stresses, strains, and forces in structures or components caused by loads that do not induce significant inertia and damping effects. *Steady* loading and response conditions are assumed; that is, the loads and the structure's response are assumed to vary slowly with respect to time. The kinds of loading that can be applied in a static analysis include:

- Externally applied forces and pressures
- Steady-state inertial forces (such as gravity or rotational velocity)
- Imposed (nonzero) displacements
- Temperatures (for thermal strain)
- Fluences (for nuclear swelling)

- Modal Analysis.

Definition of Modal Analysis

You use modal analysis to determine the vibration characteristics (natural frequencies and mode shapes) of a structure or a machine component while it is being designed. It also can be a starting point for another, more detailed, dynamic analysis, such as a transient dynamic analysis, a harmonic response analysis, or a spectrum analysis.

Uses for Modal Analysis

You use modal analysis to determine the natural frequencies and mode shapes of a structure. The natural frequencies and mode shapes are important parameters in the design of a structure for dynamic loading conditions. They are also required if you want to do a spectrum analysis or a mode superposition harmonic or transient analysis.
You can do modal analysis on a prestressed structure, such as a spinning turbine blade. Another useful feature is modal cyclic symmetry, which allows you to review the mode shapes of a cyclically symmetric structure by modeling just a sector of it.

- Harmonic Response Analysis.

Uses for Harmonic Response Analysis.

Harmonic response analysis is a technique used to determine the steady-state response of a linear structure to loads that vary sinusoidally (*harmonically*) with time. The idea is to calculate the structure's response at several frequencies and obtain a graph of some response quantity (usually displacements) versus frequency. "Peak" responses are then identified on the graph and stresses reviewed at those peak frequencies.

This analysis technique calculates only the steady-state, forced vibrations of a structure. The transient vibrations, which occur at the beginning of the excitation, are not accounted for in a harmonic response analysis.Harmonic analysis can also be performed on a prestressed structure, such as a violin string (assuming the harmonic stresses are much smaller than the pretension stress).

Any sustained cyclic *load* will produce a sustained cyclic *response* (a *harmonic* response) in a structural system. *Harmonic response analysis* gives you the ability to predict the sustained dynamic behavior of your structures, thus enabling you to verify whether or not your designs will successfully overcome resonance, fatigue, and other harmful effects of forced vibrations.

- Transient Dynamic Analysis.

Definition of Transient Dynamic Analysis.

Transient dynamic analysis (sometimes called time-history analysis) is a technique used to determine the dynamic response of a structure under the action of any general time-dependent loads. You can use this type of analysis to determine the time-varying displacements, strains, stresses, and forces in a structure as it responds to any combination of static, transient, and harmonic loads. The time scale of the loading is such that the inertia or damping effects are considered to be important. If the inertia and damping effects are not important, you might be able to use a static analysis instead

The basic equation of motion solved by a transient dynamic analysis is

$(M)\{ u''\} + (C)\{u' \} + (K)\{u\} = \{F(t)\}$

where:

(M) = mass matrix

(C) = damping matrix

(K) = stiffness matrix

{u''} = nodal acceleration vector

{u'} = nodal velocity vector

{u} = nodal displacement vector

{F(t)} = load vector

At any given time, *t*, these equations can be thought of as a set of "static" equilibrium equations that also take into account inertia forces ((M){u" }) and damping forces ((C){u' }). The ANSYS program uses the Newmark time integration method to solve these equations at discrete time points. The time increment between successive time points is called the *integration time step*.

- Spectrum Analysis

Definition of Spectrum Analysis

A spectrum analysis is one in which the results of a modal analysis are used with a known *spectrum* to calculate displacements and stresses in the model. It is mainly used in place of a time-history analysis to determine the response of structures to random or time-dependent loading conditions such as earthquakes, wind loads, ocean wave loads, jet engine thrust, rocket motor vibrations, and so on.

What is a Spectrum

- The *spectrum* is a graph of spectral value versus frequency that captures the intensity and frequency content of time-history loads.

Response Spectrum

A *response spectrum* represents the *response* of single-DOF systems to a time-history loading function. It is a graph of response versus frequency, where the response might be displacement, velocity, acceleration, or force.

- Buckling Analysis

Definition of Buckling Analysis

Buckling analysis is a technique used to determine *buckling loads* - critical loads at which a structure becomes unstable - and *buckled mode shapes* - the characteristic shape associated with a structure's buckled response.

Types of Buckling Analyses

Two techniques are available in the FEM, for predicting the buckling load and buckling mode shape of a structure: *nonlinear* buckling analysis, and *eigenvalue* (or linear) buckling analysis. Since these two methods frequently yield quite different results, let's examine the differences between them before discussing the details of their implementation.

Nonlinear Buckling Analysis

Nonlinear buckling analysis is usually the more accurate approach and is therefore recommended for design or evaluation of actual structures. This technique employs a nonlinear static analysis with gradually increasing loads to seek the load level at which your structure becomes unstable. Using the nonlinear technique, your model can include features such as initial imperfections, plastic behavior, gaps, and large-deflection response.

Eigenvalue Buckling Analysis

Eigenvalue buckling analysis predicts the theoretical buckling strength (the bifurcation point) of an ideal linear elastic structure. This method corresponds to the textbook approach to elastic buckling analysis: for instance, an eigenvalue buckling analysis of a column will match the classical Euler solution. However, imperfections and nonlinearities prevent most real-world structures from achieving their theoretical elastic buckling strength. Thus, eigenvalue buckling analysis often yields unconservative results, and should generally not be used in actual day-to-day engineering analyses.

- Gasket Joints Simulation.

Gasket joints are essential components in most structural assemblies. Gaskets as sealing components between structural components are usually very thin and made of many materials, such as steel, rubber and composites. From a mechanics point of view, gaskets act to transfer force between components. The primary deformation of a gasket is usually confined to one direction, namely, through thickness. The stiffness contributions from membrane (in plane) and transverse shear are much smaller in general compared to the through thickness. The stiffness contribution therefore is assumed to be negligible.

A typical example of a gasket joint is in engine assemblies. A thorough understanding of the gasket joint is critical in engine design and operation. This includes an understanding of the behavior of gasket joint components themselves in an engine operation, and the interaction of the gasket joint with other components.

- Contact.

Contact problems are highly nonlinear and require significant computer resources to solve. It is important that you understand the physics of the problem and take the time to set up your model to run as efficiently as possible.

Contact problems present two significant difficulties. First, you generally do not know the regions of contact until you've run the problem. Depending on the loads, material, boundary conditions, and other factors, surfaces can come into and go out of contact with each other in a largely unpredictable and abrupt manner. Second, most contact problems need to account for friction. There are several friction laws and models to choose from, and all are nonlinear. Frictional response can be chaotic, making solution convergence difficult.

In addition to these two difficulties, many contact problems must also address multi-field effects.

- Fracture Mechanics.

Cracks and flaws occur in many structures and components, sometimes leading to disastrous results. The engineering field of fracture mechanics was established to develop a basic understanding of such crack propagation problems.
Fracture mechanics deals with the study of how a crack or flaw in a structure propagates under applied loads. It involves correlating analytical predictions of crack propagation and failure with experimental results. The analytical predictions are made by calculating fracture parameters such as stress intensity factors in the crack region, which you can use to estimate crack growth rate. Typically, the crack length increases with each application of some cyclic load, such as cabin pressurization-depressurization in an airplane. Further, environmental conditions such as temperature or extensive exposure to irradiation can affect the fracture propensity of a given material.

- Composites.

Composite materials have been used in structures for a long time. In recent times composite parts have been used extensively in aircraft structures, automobiles, sporting goods, and many consumer products.
Composite materials are those containing more than one bonded material, each with different structural properties. The main advantage of composite materials is the potential for a high ratio of stiffness to weight. Composites used for typical engineering applications are advanced fiber or laminated composites, such as fiberglass, glass epoxy, graphite epoxy, boron epoxy and Glare.
The finite element method allows you to model composite materials with specialized elements called *layered elements*. Once you build your model using these elements, you can do any structural analysis (including nonlinearities such as large deflection and stress stiffening).

- Fatigue.

Definition of Fatigue

Fatigue is the phenomenon in which a repetitively loaded structure fractures at a load level less than its ultimate static strength. For instance, a steel bar might successfully resist a single static application of a 300 kN tensile load, but might fail after 1,000,000 repetitions of a 200 kN load.
The main factors that contribute to fatigue failures include:

- Number of load cycles experienced
- Range of stress experienced in each load cycle
- Mean stress experienced in each load cycle
- Presence of local stress concentrations

A formal fatigue evaluation accounts for each of these factors as it calculates how "used up" a certain component will become during its anticipated life cycle.

- p-Method Analysis.

The p-method obtains results such as displacements, stresses, or strains to a user-specified degree of accuracy. To calculate these results, the p-method manipulates the polynomial level (p-level) of the finite element shape functions which are used to approximate the real solution.
This feature works by taking a finite element mesh, solving it at a given p-level, increasing the p-level selectively, and then solving the mesh again. After each iteration the results are compared for convergence against a set of convergence criteria. You can specify the convergence criteria to include displacement, rotation, stress or strain at a point (or points) in the model, and global strain energy. The higher the p-level, the better the finite element approximation to the real solution.
In order to capitalize on the p-method functionality, you don't have to work only within the confines of p-generated meshes. The p-method is most efficient when meshes are generated considering that p-elements will be used, but this is not a requirement. Of course, you might want to create and mesh your model using p-elements, but you can also perform a p-method solution using meshes that have been generated with h-elements (generated by ANSYS or your CAD package), if the elements are at least mid-noded. This provides you with the flexibility of taking advantage of the p-method solution option independently of how the mesh was created. The p-method can improve the results for any mesh automatically.

- Beam Analysis and Cross Sections.

Beam elements are used to create a mathematical one-dimensional idealization of a 3-D structure. They offer computationally efficient solutions when compared to solid and shell elements.
What Are Cross Sections?
A cross section defines the geometry of the beam in a plane perpendicular to the beam axial direction. some methods of analysis supplies a library of very commonly-used beam cross section shapes, and permits user-defined cross section shapes.

- Shell Analysis.

Shell elements are used to create a mathematical 2-D idealization of a 3-D structure. They offer computationally efficient solutions for modelling shell structures when compared to solid elements.

I.D.2.2 - **Analyzing Thermal Phenomena**

A *thermal analysis* calculates the temperature distribution and related thermal quantities in a system or component. Typical thermal quantities of interest are:

- The temperature distributions
- The amount of heat lost or gained
- Thermal gradients
- Thermal fluxes.

Thermal simulations play an important role in the design of many engineering applications, including internal combustion engines, turbines, heat exchangers, piping systems, and electronic components. In many cases, engineers follow a thermal analysis with a stress analysis to calculate *thermal stresses* (that is, stresses caused by thermal expansions or contractions).

I.D.2.3 **- Fluids Analysis**

Some type of Fluids Analysis they are listed under:

- Flotran CFD (Computational Fluid Dynamics).

The Flotran analysis CFD (Computational Fluid Dynamics) option to the other software offer you comprehensive tools for analyzing 2-D and 3-D fluid flow fields. Using the Flotran CFD elements, you can achieve solutions for the following:

- Lift and drag on an airfoil
- The flow in supersonic nozzles
- Complex, 3-D flow patterns in a pipe bend

In addition, you can use many features to perform tasks including:

- Calculating the gas pressure and temperature distributions in an engine exhaust manifold
- Studying the thermal stratification and breakup in piping systems
- Using flow mixing studies to evaluate potential for thermal shock
- Doing natural convection analyses to evaluate the thermal performance of chips in electronic enclosures
- Conducting heat exchanger studies involving different fluids separated by solid regions

- Acoustics.

Acoustics is the study of the generation, propagation, absorption, and reflection of sound pressure waves in a fluid medium. Applications for acoustics include the following:

- Sonar - the acoustic counterpart of radar

- Design of concert halls, where an even distribution of sound pressure is desired
- Noise minimization in machine shops
- Noise cancellation in automobiles
- Underwater acoustics
- Design of speakers, speaker housings, acoustic filters, mufflers, and many other similar devices.
- Geophysical exploration

Types of Acoustic Analysis

An acoustic analysis, programs, usually involves modeling the fluid medium and the surrounding structure. Typical quantities of interest are the pressure distribution in the fluid at different frequencies, pressure gradient, particle velocity, the sound pressure level, as well as, scattering, diffraction, transmission, radiation, attenuation, and dispersion of acoustic waves. A *coupled acoustic analysis takes the fluid-structure interaction into account. An uncoupled acoustic analysis models only the fluid and ignores any fluid-structure interaction*.

- Thin Film Analysis.

Thin film is a small gap of fluid between moving surfaces. This thin layer of fluid can alter the structural response of the structure by adding stiffness and/or damping to the system. Movement normal to the gap produces a *squeeze film* effect. Movement tangential to the gap produces a *slide film* effect.

Thin film effects are important in macrostructures, but they are particularly critical in microstructures where the damping and stiffening effects of thin layers of air can significantly affect the behavior of devices used in micro-electromechanical systems (MEMS). Squeeze film effects are important in devices such as accelerometers and micromirrors. Slide film effects are important in devices such as comb drives.

One method for assessing the effect of thin films is to use thin film fluid elements based on the Reynolds number (which is known from lubrication technology and rarified gas physics) to calculate the stiffening and damping effects. These effects can then be added to the overall system model. Separate element types are used to assess squeeze and slide film effects.

I.D.2.4 - **Electromagnetic Field Analysis**

Magnetic analyses, available in the Finite element method programs, calculate the magnetic field in devices such as:

Power generators	Magnetic tape/disk drives
Transformers	Waveguides
Solenoid actuators	Resonant cavities

Electric motors	Connectors
Magnetic imaging systems	Antenna radiation
Video display device sensors	Filters
Cyclotrons	

Typical quantities of interest in a magnetic analysis are:

Magnetic flux density	Power loss
Magnetic field intensity	Flux leakage
Magnetic forces and torques	S-parameters
Impedance	Quality factor
Inductance	Return loss
Eddy currents	Eigenfrequencies

Magnetic fields may exist as a result of an electric current, a permanent magnet, or an applied external field. [3]

what's the Finite Element Method

Most analysis software employs the finite element method (FEM), where the geometry of the component to be deformed is divided or "discretised" into simplified regular shapes called "elements". There is a large range of elements available of varying complexity (or degrees of freedom) that can model different modes of deformation (and temperature fields, electromagnetic fields, etc.) [4].

The aim of industrial application of the FE simulation of stamping processes is to replace the physical tryout by the computer tryout, with the intention of time/cost reduction and quality improvement in the die design/manufacturing cycle [5].

Literature Review

Rapid developments in computer hardware make the finite element analysis of complex deformation responses increasingly applicable. The finite element method is used worldwide to simulate the deep drawing process and has become a reliable numerical simulation technology.

The finite element method is a powerful numerical technique that has been applied in the past years to a wide range of engineering problems. Although much finite element (FE) analysis is used to verify the structural integrity of designs, more recently FEM has been used to model fabrication processes.

When modelling fabrication processes that involve deformation, such as sheet metal forming (SMF), the deformation process must be evaluated in terms of stresses and strain states in the body under deformation including contact issues. The major advantage of this method is its applicability to a wide class of boundary value problems with little restriction on work piece geometry.

For an accurate simulation of a real-life deep drawing process an accurate numerical description of the tools is necessary, as well as an accurate description of material behaviour, contact behaviour and other process variables.

The numerical description of the tools is provided by CAD packages which are generally used by tool designers. The description of material behaviour, contact behaviour and other process variables evolved from rather simple models in the earlier days to more and more sophisticated models nowadays. This evolution is due to the elaborate work of researchers working in the field of metal forming and is shown in authoritative conferences concerning sheet metal forming. Developments have been made in the field of finite element types, mesh adaptivity, material laws, failure criteria, wrinkling and surface defects, springback, contact algorithms, friction, simulation of new processes (for example hydroforming), optimization and process design.

The three basic requirements for the successful commercial application of numerical simulation are [6]: (1) simplicity of application;
(2) accuracy; and
(3) computing efficiency.

The characteristic features of the finite element method are [7]: The domain of the problem is represented by a collection of simple sub domains, called *finite elements.* The collection of finite elements is called *the finite element mesh*. Over each finite element, the physical process is approximated by functions of desired type (polynomials or otherwise), and algebraic equations relating physical quantities at selective points, called *nodes*, of the element are developed.

The use of finite element analysis is beneficial in the design of tooling in sheet metal forming operations because it is more cost effective than trial and error.

The prime objective of an analysis is to assist in the design of the product by:

(1) Predicting the material deformation and

(2) Predicting the forces and stresses necessary to execute the forming operation.

I.D.3 ***Finite Element Codes***

Implicit vs. Explicit Codes

The FEM codes for sheet metal drawing may be classified accordingly to their type of integration (explicit or implicit).

Explicit method solves for equilibrium at time t by direct time integration. This explicit procedure is conditionally stable since iterative procedure is not implemented to reach equilibrium and also Δt is limited by natural time.

Implicit code solves for equilibrium at the every time step $(t+ \Delta t)$. Depending upon the procedure chosen, each iteration requires the formation and solution of the linear system of equations.

The two main solution procedures for the simulation of deep drawing processes are the dynamic explicit and the static implicit procedure.

The **dynamic explicit method** is frequently used in simulations of the deep drawing process, since it reduces the computational time drastically, using a diagonal mass matrix system to solve the equations of motion. For this method, the computational time depends linearly on the number of degrees of freedom (d.o.f.). However, the drawbacks of the explicit method are that small time steps are needed and that equilibrium after each time step cannot be checked, which can result in wrong stress distributions and unrealistic product shapes. Another drawback is that springback calculations are very time consuming.

The advantage of a **static implicit method** is that equilibrium is checked after each time step and thus will lead to more accurate results. The main drawback of this method however, is that the computation time depends quadratically on the number of d.o.f. if a direct solver is used. Another drawback is that the stiffness matrix is often ill conditioned which can make the method unstable and detoriates the performance of iterative solvers. [8].

In sum, explicit codes are favoured for solving large problems although implicit codes yield more accurate results. To intensify the use of implicit codes for solving large problems, the computation time of these codes has to be decreased drastically.

The following table summarizes the differences between implicit and explicit codes.

Implicit	Explicit
Large time increment can be adopted and the equilibrium is rigorously satisfied at the end of the time step	It restricts the time increment to very small size in order to maintain the out of balance force within admissible tolerance
In some cases implicit finite element analysis may develop convergence problems associated with sudden changes on the contact conditions between work piece and tools	The solution procedure is stable even if the deformation dependent contact problem is included in the process
Several equilibrium iterations must be performed for each time step, and for each iteration it is necessary to solve a set of linear equations	It requires fewer computations per time step. Complex geometries may be simulated with many elements that undergo large deformations
They are not well suited to solving the interaction of a large number of nodes with rigid tooling, but they do handle the springback calculation very efficiently	Although explicit codes are well suited to solving large sheet-forming models with large number of deformable elements, calculation of geometry after springback may be difficult
Generally favoured for relatively slow problems with static or slowly varying loads	Generally favoured for fast problems such as impact and explosion

Table 4.1 – *Implicit vs. Explicit codes*

Numerous researches have been done on the use of the finite element code for sheet metal forming simulations. Kamita et al. [9] have developed an elasto-plastic finite element code based on static-explicit FE, which is suitable for plastic instability and also springback problems. This code was used by Sunaga et al [10] to analyze the automotive sheet metal forming process.

Paulsen and Welo [11] analyzed the bending process with an implicit code and reported good agreement between experimental and simulation results.

Clausen et al. [12] compared implicit and explicit simulations, finding that the response differences were almost negligible.

Investigations have shown that explicit method is well suited for solving large sheet forming models, and implicit codes handle the springback calculation very efficiently.

Hence, recently researchers have adopted a new method of coupling the implicit and explicit methods to solve complex sheet metal forming processes would save design effort and production time.

Narasimhan et al. [13] have used ANSYS/LS-DYNA explicit coupled with ANSYS implicit for springback simulation.

Finn et al. [14] combined the commercial codes LS-DYNA3D and NIKE3D for prediction of springback in automotive body panels.

Taylor et al. [15] discussed the numerical solution of sheet-metal forming applications using the ABAQUS general purpose implicit and explicit finite-element modules.

Recently, a method was developed which decreases the computational time of implicit codes by factors, which makes the implicit finite element code competitive with explicit finite element code for large scale problems. This method is based on introducing dynamics contributions into the implicit finite element code.

As a result, a mass matrix is introduced. When this mass matrix is diagonalized and added to the stiffness matrix, the diagonal terms of the system matrix will increase and the matrix will be better conditioned, which makes an effective use of iterative solvers possible. Another advantage of introducing dynamics contributions into an implicit finite element code is that it stabilizes the computation, especially when the problem is under-constrained. For example, when closing a doubly curved blankholder, the sheet only makes contact at two or three points which give rise to stability problems when the simulation is started and no inertia effects are present in the simulation.

The dynamics contributions are successfully implemented for both the plane strain element (only displacement d.o.f.) and shell element (displacement and rotational d.o.f.). Mass is added to the displacement d.o.f.'s via a lumped or consistent mass matrix approach. Besides, mass is added to the rotational d.o.f. via a mass moment of inertia approach. Deep drawing simulations are performed to investigate the performance of the dynamics contributions in combination with iterative solvers. It is concluded that the computation time can be decreased by a factor 5-10.

Summary of Elements Used in Sheet Metal Forming Simulation

FEA of the sheet metal forming problem usually adopts one of three analysis methods based on the membrane, shell and continuum element [16].

The Table 4.2 summarizes the elements used in finite element method for sheet metal forming simulation.

Element	Specialty	Limitation
Membrane	Computational efficiency and better convergence in contact analysis than the shell or continuum element [16]	It does not consider bending effect and has to tolerate inaccuracy in the bending dominant problems
Shell	Can capture the combination of stretching and bending as opposed to membrane elements. Use of shell element gives more number of degrees of freedom to capture accurate stress distribution including in- plane and out-plane deformation	It takes a substantial amount of computational time and computer space for its 3-D calculation with integration in the thickness direction
Continuum	Are used where fully 3-D theory is needed to describe the deformation process. They can handle through-thickness compressive straining whereas shell elements cannot	More elements are needed to describe the shell-type structures, so that a large system of equations must be solved [17]

Table 4.2 – *Elements used in SMF Simulation*

I.D.4 – Sheet Metal Forming Simulation

In the past a number of analyzing methods have been developed and applied to various forming processes. Some of these methods are the slab method, the slip-line field method, the viscoplasticity method, upper and lower bound techniques and Hills general method. These methods have been useful in qualitatively predicting forming loads, overall geometry changes of the deformed blank and material flow and in determining approximate optimum process conditions.

However, a more accurate determination of the effects of various process parameters on the deep drawing process has become possible only recently, when the finite element method was developed for these analyses [18].

Finite element method is generally composed of three basic steps, namely: pre-processing of input data, computational analysis, and post-processing of results.

The description of these terms when simulating sheet metal forming process is [19]:

Pre-processing: it is the creation of a geometric model for the part to be formed, the imposition of the appropriate boundary conditions for the

forming process, the selection of the constitutive equation for plastic deformation, and the selection of material and process variables.

Computational analysis: involves solving appropriate equations to obtain the deformed shape of the part.

Post-processing: Results from numerical simulation runs provide predicted shapes of the panels as well as stress and strain distribution data for the entire surface area of the formed parts. Surface stress and strain data for the deformed shapes are given in the form of colour-coded or contour plots to facilitate the interpretation of results.

Sheet Metal Forming Codes

Table 4.3 summarizes a few commercially available finite element codes that are popularly used for sheet metal forming simulation.

Code	Implicit / Explicit	Specialty	Limitations
Sheet Metal Forming Codes			
AUTOFORM	Implicit	Highly automated	Convergence-Contact elements
ITAS	Explicit	Plastic instability: wrinkling, springback	Difficulty in matrix computation
PAMSTAMP	Explicit	With CAD, model stamping operation can be simulated	Strain in local longitudinal and lateral direction not available
SHEET	Implicit	Simulates the stretch/draw forming operation of plane strain sections	Through thickness stress variations i.e. bending stresses
Generic Codes			
LS-DYNA	Explicit	Can handle complex problems with large deformation, and has no convergence problems	Does not have pre-processor and complex post-processor
ABAQUS	Implicit - Explicit	Problems with large deformation, no	Does not have pre-processor

		convergence problems	
ANSYS	Implicit	Availability to use user material model	There is convergence problem during nonlinear analysis and contact conditions

Table 4.3 – *Commercially Available Finite Element Codes for SMF Simulation*

General purpose finite element codes are not generally suitable for metal forming simulation because they are not optimised for these applications, and often do not include features such as automatic remeshing, robust evolving contact algorithms and a tailored, easy-to-use interface which are essential for practical implementation.

*I.D.*5. Bibliography :

[1] PHILIPP, M., HARRER, O., SCHWENZFEIER, W., WÖDLINGER, R. and FISCHER, CH.: Turn-up and turn-down phenomena in plate rolling. 5th International ESAFORM Conference, Krakow, 2002.

[2] M. Kawka, A. Makinouchi; "Shell-Element Formulation in the Static Explicit FEM Code for the Simulation of Sheet Stamping". Journal of Materials Processing Technology, 50, 1995, pp. 105-115.

[3] Guide of Ansys

[4] Dr Miller B and Bond R. The practical use of simulation in the sheet metal forming industry, 2001.

[5] M. Kawka, A. Makinouchi; "Shell-Element Formulation in the Static Explicit FEM Code for the Simulation of Sheet Stamping". Journal of Materials Processing Technology, 50, 1995, pp. 105-115.

[6] W. Kubli, J. Reissner, "Optimization of Sheet-Metal Forming Process Using the Special-Purpose Program AUTOFORM". Journal of Materials Processing Technology, 50, 1995, pp. 292-305.

[7] J.N. Reddy, An Introduction to Finite Element Method, Mc Graw Hill, Inc., 2nd ed., 1993.

[8] M. Kawka, A. Makinouchi; "Shell-Element Formulation in the Static Explicit FEM Code for the Simulation of Sheet Stamping". Journal of Materials Processing Technology, 50, 1995, pp. 105-115.

[9] Kiyoshi Kamita, Takamichi Arakawa, Hiroshi Fukiharu and Akitake Makinouchi, "Evaluation of Geometrical Defects by Finite Element Simulation in the Sheet Metal Forming Processes," European Congress on Computational Methods in Applied Sciences and Engineering, ECCOMAS, 2000.

[10] Hideyuki Sunaga and Akitake Makinouchi, "Sheet Metal Forming Simulation System for Predicting Failures in Stamping Products," RIKEN review No.14 December 1996, pp. 47-48.

[11] Paulsen F, Welo T., "Applications of Numerical Simulation in the

Bending of Aluminum-Alloy Profiles," Journal of Materials Processing Technology, 58, 1996, pp. 274-85.

[12] Clausen A H, Hopperstad O S, Langseth M., "Stretch Bending Analyses Using Implicit and Explicit FE Codes," Proceedings of the 10th Nordic Seminar on Computational Mechanics, Tallinn, Estonia, 1997.

[13] Narkeeran Narasimhan, Michael Lovell, "Predicting Springback in Sheet Metal Forming: An Explicit to Implicit Sequential Solution Procedure," *Finite Elements in Analysis and Design,* 33, 1999, pp. 29-42.

[14] M J Finn, P C Galbraith, L Wu, J O Hallquist, L Lum, T L Lin, "Use of a Coupled Explicit-Implict Solver for Calculating Spring-Back in Automotive Body Panels," *Journal of Materials Processing Technology,* 50, 1995, pp. 395-409.

[15] L. Taylor, J Cao, A P Karafillis and M C Boyce, "Numerical Simulations of Sheet-Metal Forming," Journal of Materials Processing Technology, 50, 1995, pp. 168-179.

[16] Hoon Huh, Tae Hoon Choi; "Modified Membrane Finite Element Formulation for Sheet Metal Forming Analysis of Planar Anisotropic Materials," International Journal of Mechanical Sciences, 42, 1999, pp. 1623-1643.

[17] M. Kawka, A. Makinouchi; "Shell-Element Formulation in the Static Explicit FEM Code for the Simulation of Sheet Stamping". Journal of Materials Processing Technology, 50, 1995, pp. 105-115.

[18] Schenk O and Hillmann M. Optimal design of metal forming die surfaces with evolution strategies. Journal Computers&Structures, Volume 82, Issues 20-21 , August 2004, Pages 1695-1705.

[19] M Y Demeri and S. C Tang, "Post Processing Analysis in Sheet Metal Forming Simulation," *JOM*, June 1992, pp. 14-16.

Section I.E

Simulation Process of Plastic Deformationw through the FEM

I.E.1 – Introduction

The simulation of the forming process offers substantial rationalization reserves, for example optimizing of component and tool thus also the enhancement of process reliability. The program systems currently in use must be extended in various directions in order to accommodate the growing practical needs. For further improved accuracy, along with the focuses of development discussed here it will be necessary in future also to make allowance for better representation for the elastic properties of the tool. The ultimate consequence of this is that, for complete simulation, the elastic properties of the press or hammer also will be taken into account. The results of this simulation will be constitute the basis for optimizing the stiffness and weight of tools.

In metal forming, process simulation is used to predict metal flow, strain, temperature distribution, stresses, tool forces and potential sources of defects and failures. In some cases, it is even possible to predict product microstructure and properties as well as elastic recovery and residual stresses.

In massive forming, simulation of 2D problems, e.g. axisymmetric and plane or near-plane strain, is truly state of the art. The application for 3D problems is still not widely used in industry because it is not always cost effective and requires considerable engineering and computation time. In sheet forming, however, 3D simulations are extensively used in stamping industry.

The main reasons of process simulation are:

a) reduce time to market
b) reduce cost of tool development
c) predict influence of process parameters
d) reduce productions cost product quality
e) improve product quality
f) better understanding of material behaviour
g) reduce material waste

while the goals of manufacturing using these techniques are.

a) accurately predict the material flow
b) determine the filling of the swage or die
c) accurate assessment of net shape
d) predict if laps or other defects exists
e) determine the stresses, temperatures, and residual stresses in the work piece
f) determine optimal shape or perform

Moreover, using simulation it is possible to:

a) determine material properties such as grain size
b) determine local hardness

c) predict material damage
d) predict phase changes and composition
e) simulate the influence of material selection

As simulation allows to capture behaviour that cannot be readily measured it provides deeper insight into manufacturing process.

The principal steps involved in integrated product and process design for metal forming are schematically illustrated in Figure I.E.1, where there are based on functional requirements, the geometry (shape, size, surface finishes, tolerances) and the material are selected for a part at the design stage. It is well known that the design activity represents only a small portion, 5 to 15 percent, of the total production costs of a part. However, decisions made at the design stage determine the overall manufacturing, maintenance and support costs associated with the specific product.

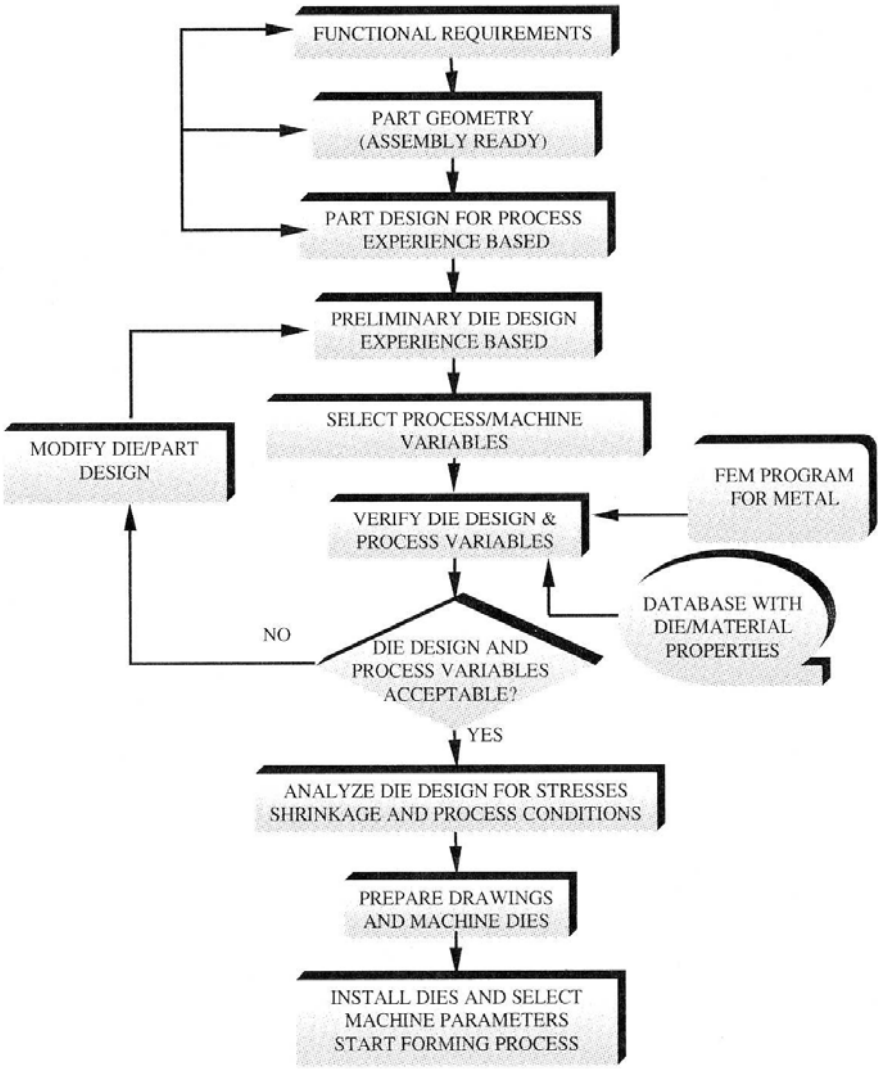

Figure I.E.1 - Product and process design for metal forming

Once the part is designed for a specifics process, the steps outlined in Figure 1 , lead to a rational process design.

The application of computer aided methods in generally forming processes and partly today especially important precision or net shape forming processes involves:

a) the conversion of the assembly-ready part geometry into a formable geometry
b) the preliminary design of tools/dies necessary to perform the operations used for forming the parts
c) the analysis and optimisation of each forming operation and the associated tool design, to reduce process development and trial and error, and
d) manufacturing of tools and dies by CNC milling or by EDM or another similar technology

The ascertaining of process-specific factors in production engineering by means of process simulation serves the efficient manufacture of products of specified properties. Three objectives are emphasised:

a) review of the feasibility of an existing concept for the manufacture of a product
b) assessment of product characteristic
c) enhancement of understanding as to what really goes on in a process for the purpose of optimising the manufacturing technique

To achieve these goals, however, it only makes sense to use process simulation if this is more economical in the long run than experimental repetition of the actual process.

I.E.2 **–Why the new technology for the Stamping**

The automotive industry faces world-wide serious challenges: fierce market competition and strict governmental regulations on environmental protection. The strategy of the automakers to meet these challenges is sometimes called the 3R Strategy:

- Reduction in time-to-market;
- Reduction in development costs to gain competitiveness, and;
- Reduction in the vehicle weight to improve fuel efficiency.

The solutions to achieve this triple goal are essentially based on the implementation of CAD/CAE/CAM technologies in product development and process design.

A very significant component of this endeavour is focused on the reduction of the tooling costs and the lead-time related to the stamping of auto-body panels, even under increasing technological difficulties such as the use of aluminium alloys and high-strength steels, and requirements for higher geometrical accuracy of stamped parts.

To deal with the problems brought about by these trends, which are beyond past experience, numerical methods for sheet forming simulation are becoming more and more important, replacing the physical tryout of stamping dies by a computer tryout.

The success of numerical simulation depends mainly on the advances in forming simulation codes, but progress in other related technologies is also important.

Examples of related technology are:

- the CAD systems that rapidly construct and modify tool surfaces;
- modern mesh generators to, more or less automatically, create FE-meshes on CAD surfaces;
- visualization hardware and software, which enables users to grasp the huge data, and, finally;
- the computer hardware, which makes it possible to perform large scale simulations within reasonable time.

The use of simulation software in metal forming processes has increased significantly in recent years. The rapid development of software technology, together with faster and lower-cost computer hardware, have recently enabled many manufacturing operations to be modelled cost-effectively, that only a few years ago would have been considered impractical.

Using sheet metal forming simulation it is possible to reduce both the development costs of stamping a new part and the production lead time.

Figure I.E.2 represents a simplified summary of the current forming process analysis based on stamping simulation technology.

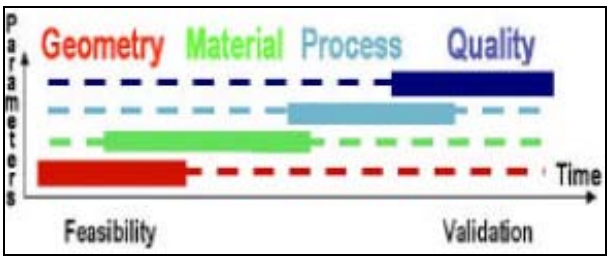

Figure I.E.2 – *Typical stamping simulation process*

One can identify the main parameters that are influencing the stamping process: the part geometry and the die run-off design, the materials selection, the manufacturing hardware and process, and final quality control.

Concurrent engineering, parallel tasking and the optimization of the different tasks using simulation technology lead to a drastic lead time and cost reduction.

Simulation has allowed the reduction of physical testing, as well as the anticipation of costly downstream problems by enabling the application of the upfront approach.

Historical Background

The use of finite element simulation technology for stamping applications is growing rapidly these days, but when looking at the recent history of virtual stamping, one can distinguish several main time periods.

The first period, before 1990, was in fact a pre-industrialization period. In this period, people started using computers to understand how to improve the forming process. At this stage the different attempts were mainly focused on approaches such as expert system and knowledge based methods.

An important breakthrough occurred with the success of forming simulation applying finite element software to stamping related problems as well. By that time, at around 1990, a considerable effort has been made on making the finite element technology accessible enough for industry to use in common complex industrial problems.

Figure I.E.3 illustrates the history track of simulation lead-time for a typical industrial case. It shows that the simulation lead-time for a total analysis (including meshing, set-up, calculation and visualizing the results) of a representative component, in this case a front fender from Mazda, was reduced from 50 days in 1990 to 15 days in 1994.

Today, such a case could be analyzed in less than one week, including the die face generation, the formability analysis and springback. And the tendency is clearly to continue decreasing, with even more accurate results.

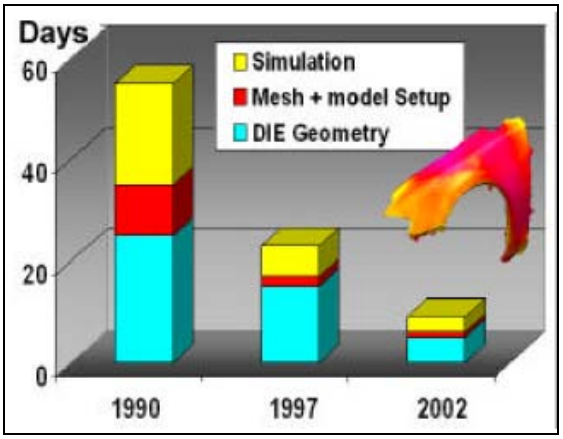

Figure I.E.3 – *Lead-time of a stamping simulation*

This dramatic reduction in the total simulation time came not only from the rapidly improving computer technology, but was more influenced by the introduction of new tools in the finite element world, such as adaptive meshing (1994), automatic discretisation/meshing of CAD models (1995), easier and more standardized input (1996) and the introduction of new implicit algorithms for a rapid and qualitative forming evaluation (1998). In short, one can say that during this period, roughly from 1990 to 2000, the main emphasis for virtual stamping simulation software was focused on formability aspects.

This means that the main usage of stamping simulation software concentrated on strain predictions and in the introduction of stamping related know-how.

However, the user wanted to know if a certain part was feasible. If not where did it fail, where would wrinkling happen, its forming limit curve's aspect, etc.

Over the years, stamping simulation software has helped to reduce the costs and lead-time of various components considerably. Nowadays that's even more evident.

Input data required for simulation

SMF codes such as AutoForm, PamStamp and LS-Dyna demand the same input data. The surface geometry of the component and the metal sheet are input as either VDA or IGES format.

From this part geometry the tool surfaces can be built using special functions in the programs.

Another method is to import complete tool surfaces created in some 3D-CAD program.

In the forming simulation the tools are assumed to be completely rigid compared to the sheet metal. In this case only the surfaces of the tools interacting in the forming process need to be imported.

Required material data are:

-Coefficient of friction. Varies depending on the material or different lubricants.

-Poisson's number

-Specific mass density

-Young's modulus

-Parameters for the strain-hardening curve depending on the material

-Parameters for the material law depending on the material type

-Parameters for the forming limit curve depending on the material

The simulation process

After the simulation model is created (including the different tool components, data for the material and process parameters as binder force, punch velocity, etc.) the forming simulation can be conducted.

The simulation usually contains the following steps:

-Only gravity applied to get the shape or deformation of the metal sheet when it is placed on the binder; very important if a thin sheet is used

-Closing of the binder is the first step of the forming process. The binder is moved towards the die and forces the sheet against the die.

-Drawing, when the punch is moved down in the die and the forming process is simulated.

-Trimming, when scrap is removed from the component.

-Springback, when the tool surfaces are removed and the elastic part of the strains in the component can relax.

Convergence Criteria

The modelling of sheet metal forming processes is one example of highly nonlinear problems where the iterative solution procedure can become very slow or diverge [17].

The non-linearities observed can be categorized as geometrical non-linearities, material non-linearities (due to plastic deformation), friction force reversals and contact mode changes.

In a static finite element code, high mesh resolution can cause convergence problems, especially for large deformable elements . But a

sufficiently fine mesh must be generated so that the fine features are captured.

According to K. C. Ho et al. [18], in order to obtain optimal and reliable convergence, it is essential that the rigid tool surface representation is smooth.

Evaluation criteria

In order to evaluate the possibility of wrinkling, cracking etc. the strains in the formed component are analysed and compared against the forming limit curve, see Figure I.E.4. This curve is extracted from biaxial strain tests, for example via the Erichsen test. The test specimen of the material has been drawn until fracture or diffuse necking.

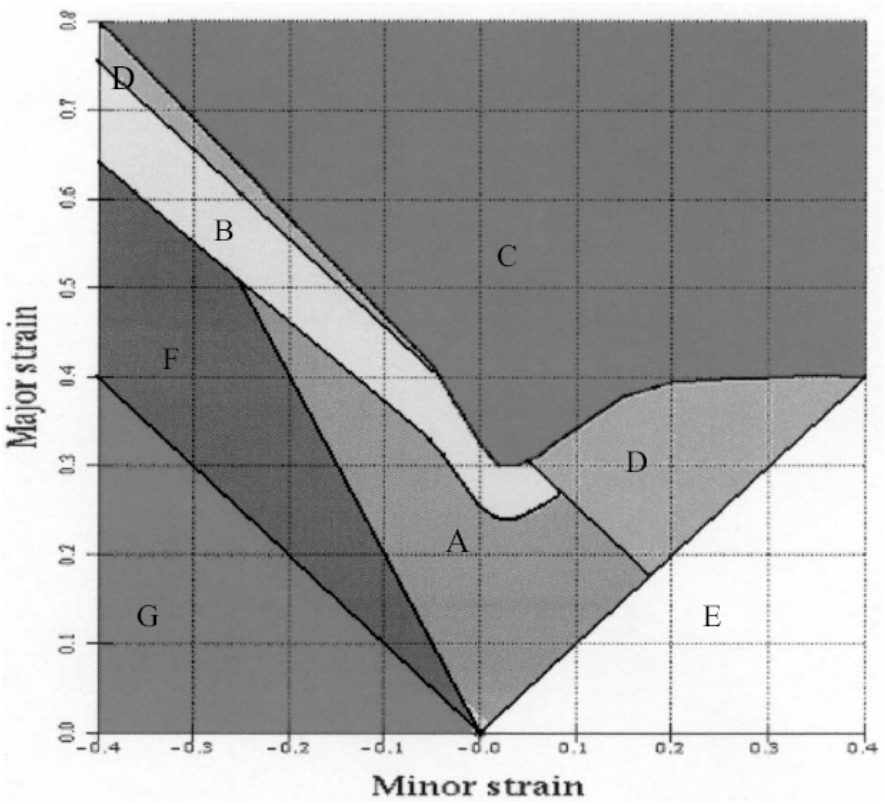

Figure I.E.4 – *Forming limit diagram of major vs. minor strain, distinguishing different domains*

The curve that forms the lower boundary of the area C is the forming limit curve.

The curve describes the level of strain that the actual material can withstand until failure, cracking or wrinkling occurs. Following a rule of thumb experience to assure that the component not will break the strain level should not exceed 80% of the level of the forming limit curve.

The different areas in the diagram are:

A. Recommended! Appropriate use of the forming abilities of the material
B. Danger of rupture or cracking.
C. The material has cracked.
D. Severe thinning.
E. Insufficient plastic strain, risk of springback
F. Tendency to wrinkling.
G. Fully developed wrinkles.

Adaptive Remeshing

Today, industries such as the automotive and aerospace industry require the solution of highly complex problems concerning three-dimensional geometries, non-linear material behaviour, contact conditions and large deformations. Consequently, the numerical simulation of these types of problems is potentially very expensive, even when simplifying assumptions such as membrane kinematics are made.

Despite the high computer power available, it is desired that a computation can be performed overnight. Hence, the computational costs (computation time, time to prepare the initial element mesh and the amount of data to store) must be minimized while still maintaining the desired accuracy.

This goal can be achieved by adaptive remeshing: the initial finite element mesh can be changed in a specific way during the simulation.

Adaptive remeshing has two major advantages. First, the computational costs can be reduced by starting the simulation with a relatively coarse mesh. Remeshing at specific parts in the mesh can take place when these coarse elements are no longer able to accurately describe the geometry or the steep gradients in state variables, and this is usually the case in the final stage of the forming process.

Second, when large deformations develop, the initial mesh can be highly distorted, so that the numerical simulation becomes unstable or crashes. To prevent a high mesh distortion, adaptive remeshing can be applied to enhance the element mesh during simulation.

Globally, the adaptive remeshing procedure can be divided into three phases. First, some measure of the accuracy of the solution is required. This

so-called error estimator will be used to define a remeshing criterion (e.g. an error indicator based on thickness error, an indicator based on a geometric error and a wrinkling risk indicator).

Next a new mesh must be generated which must satisfy specific requirements. The elements to be refined are equally divided into 4 new elements (triangular). No use is made of constraints; the elements at the boundary of the refined area are splitted into two elements.

Finally, a procedure for the transfer of state variables and boundary conditions from the old mesh to the new mesh is programmed.

As a result, the refinement procedure can successfully be applied in simulations of the deep drawing process, significantly decreasing the required CPU-time for an accurate simulation.

Besides, the coupling between a wrinkling risk indicator and the adaptive remeshing procedure can be a powerful tool to simulate wrinkling behaviour during the forming process without an excessive increase in computational time.

I.E.3 – New Requirements in Metal Forming Analysis

Part Geometry

It's obvious that the esthetics of automobile design have evolved dramatically; more classic shapes have given way to futuristic designs that mix sweeping curves and sharp angles. In addition, the unveiling of these new designs has accelerated; what were once just futuristic prototypes must now quickly become production automobiles. Next to that, customers' expectations have reduced the economic life cycle of a car and as such new models have to be introduced more frequently with wider varieties and extended customization.

Materials

With an increased market demand for "green" automobiles (i.e. fuel efficient) and improved safety, manufacturers have had to evaluate and use new materials for structural components, body and trim as well.

Because of these requirements, new aluminium alloys and new grade of steel such as ultra high strength steel have been developed, pushing the boundaries of what was previously possible with conventional steel grades.

A very recent trend in the automotive industry is the use of dual phase and TRIP steels.

In order to closely investigate materials' behaviour, they turn to forming simulations to study its behaviour during the forming process.

The main advantage of using these new materials is that it helps reduce (or control) weight, while increasing safety.

For a component to be manufactured effectively, these new materials require a much greater degree of precision and parameterization to answer the needs of forming simulation. A customizable model that keeps track of part material history and parameters such as strain rate, kinematic hardening, etc, has become a requirement in order to attain the last 10% of accuracy at the stresses level.

A major negative consequence of using these new materials is the absence of knowledge about its behaviour during crash testing.

Recent studies illustrate the impact of the manufacturing process on the components' performance. Since traditional crash simulation did not take part material history into account, simulation has not proved to be good enough to predict accurately the performance in physical testing of critical parts and subassemblies.

However, with a simulation that kept track of part material history (i.e. stress and strain undergone during forming) simulation proved to be much more accurate. Thus, the use of new materials has made it a requirement for stamping simulation today to be able to maintain a part's full history through seamless data transfer.

Manufacturing Process

New hardware, such as the crossbar transfer press, has been created to accelerate production. This new hardware has modified the production process itself, which creates secondary problems such as transferring of blanks, positioning and trimming of blanks and the disposal of scrap material.

Also, in the last decade we observed the successful introduction of several new innovative forming technologies such as hydro-forming, tailored blanks, etc. The aim of these new developments was always to reduce the number of components, while at the same time optimizing the number of forming steps. This was a very good example on how collaborative work led to real success with relatively short lead-time.

Another example of a new requirement for simulation can be seen from the evolution in welding technology, where the increased use of laser welding requires a more sophisticated clamping system and a very low flange tolerance. This technology has a large impact indeed on tolerance control, which translates to springback problems on the part at the forming stage. This evolution in process again illustrates the need for increased precision and tighter control during stamp simulation.

Industrial stamping simulation evolution

A closer look at the total time that is required for formability analysis shows that one can distinguish three main phases in simulation work: **Die design**, **Formability** & **Try-out**, and **Quality** & **Re-work** due to springback problems. The success of the forming try-out lead time and cost reduction results in priority shifting toward the need to reduce the other mentioned tasks. It allows achieving a significant overall process improvement and ensuring more robust design approach in collaborative environment, which today is essential for multinational corporations that work with suppliers and manufacturers all over the world. See figure I.E.5

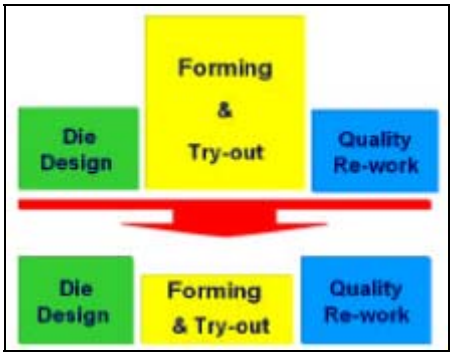

Figure I.E.5 – *Stamp simulation evolution*

The previous paragraphs have raised some examples in the evolution of the forming process: from new designs, to improved materials, to new hardware and advanced processes.

As a consequence, forming simulation has become “incomplete”. The focus has shifted from the initial objective (formability analysis) to global quality control, and integration. Stamp simulations need to adapt to these new requirements. The most important among these are:

- Providing a streamlined scalable environment that encompasses every step in the process from early feasibility to final validation;
- Increased precision through models parameterization to assess new process and new materials and their properties, to accurately predict springback behaviour and surface quality problems;
- Seamless simulation data transfer and management to keep track of part history at every stage in the process in order to check the performance and the robustness of the product and its consistency as well;
- Optimal exploitation of the available computers resources in customizable extended collaborative environment.

These new requirements in sheet metal forming urged the necessity of a new generation of virtual stamping software.

I.E.4 – New Generation of Sheet Metal Forming Programs

The previous point clearly indicated that there is a need for a complete integrated scalable streamlined stamping solution, covering the entire design process from part design through die design and die evaluation, tuning and validation of the process.

Actually, the new solution is the result of years of innovative approach where several industry leaders are involved not only in the validation phase, but already from the early specification phase. An example of this is the Stamping Simulation Development Group, which was initiated in 2000, and represents leaders from the European automotive industry.

First, each company developed their own systems in order to meet their specific needs. However, such original systems have become obsolete. The reason is that the commercial systems have become strong, integrating many functions and achieving user friendliness, while in-house systems have found it difficult to maintain their quality without making further investments, which each individual company could not afford.

Depending on the objective of the simulation work, sheet-forming programs can be subdivided into the following 3 main areas: One Step, Incremental and Die Design programs.

The first two types of forming simulation are used to assess parts manufacturing feasibility, while the third is focused on the design of the tools.

One Step "Inverse" Programs

One-step forming simulation provides designers with an indication of manufacturing feasibility. Here, the analysis does not simulate the complete forming process because it is performed without any tooling boundary condition input. One-step simulation uses only material data and the geometry of a designed part to calculate material strains by mapping back to the flat sheet. Feasibility is determined by comparison with the forming limit of the material.

These programs work in reverse to what is normally expected from a simulation program. The part geometry with or without addendum is 'unfolded' back to the flat blank shape or to a curved blankholder profile. A One Step simulation can be used to assess very quickly whether the part is feasible by predicting material thickness distribution, cracks, wrinkles, plastic strain and minimum blank outline.

Quicker than an Incremental simulation, an entire OneStep analysis will typically take a few minutes even for complex parts, including the import of part geometry from CAD, the automatic filling of holes and the specification of process parameters. Refinements to a basic OneStep simulation can be made by including the restraining effect of the addendum/flange area and

the application of binder force and friction. The addendum can be generated automatically from part and binder surface geometry by specifying punch opening and flange boundary lines. A full tool analysis can also be performed if the CAD geometry is available or has been created in a 'Die Designer' system.

In a typical One Step application, the engineer will begin with only the part geometry and perhaps some idea of the likely punch opening line of the tools and the final outline of the drawn sheet ('the flange boundary').

After inputting this information, to perform the simulation, the program creates a mesh of the entire drawn sheet, including the addendum and flange areas, and fills holes and missing zones in the CAD geometry where necessary. During this stage, the mesh is automatically refined with smaller elements in areas of higher curvature and strain gradients to maximise accuracy. Then, a OneStep program such as *AutoForm-OneStep* 'unfolds' the sheet to predict the minimum blank outline and make a formability assessment of the final part (wrinkles, cracks, thinning etc). Then it is possible to analyse, for example, the final thickness distribution.

Incremental Programs

Incremental forming simulations model the entire forming process. Here, the analysis inputs include the part and the tool geometry, the material properties of the part, the blank size and shape, frictional coefficient, press conditions and the drawbead effects. The outputs show levels and distribution of material strain, failure prediction, thickness profiles and wrinkling tendency.

These programs offer a full process model that simulates the forming stages as accurately as possible in the logical order, from blankholder closing to final flanging. Consequently, incremental simulations are computationally more intensive than the equivalent *One-step* analysis, and require tooling information to be input.

There are two types of incremental code based on either 'implicit' or 'explicit' mathematical formulations.

As a 'virtual tryout' of the production method, an incremental simulation will often be used to simulate the entire stamping process, with capabilities to model the initial deflection of the sheet due to gravity, blankholder closing, first draws and restrikes, sheet repositioning, cutting operations, flanging and springback. Some codes can also simulate hydro-mechanical (fluid forming) processes for sheets and tubes.

Some advantages of simulation for die manufacturing are the minimisation of blank utilisation, allowing binder and die surface sizes to be kept to a minimum, for tool weight reductions; and the determination of

kinematic and force requirements for production planning and press selection.

Development trends in incremental forming simulation

The state-of-the-art in incremental FE-simulation of sheet metal forming incorporates a combined implicit and explicit integration of time. In general, tooling is described as rigid. Material can be described using shell elements, membrane elements or volume elements. With this type of simulation, it is possible to generate first process parameters, which offers the possibility to predict problems prior to parts manufacturing.

Development trends in forming simulation consider new concepts such as elastic die components, segmented blankholder, and springback behaviour of formed parts.

Die Design Tools

When tooling information is required in a OneStep or Incremental analysis, the creation of the tooling geometry using a traditional CAD system is often very time-consuming, and can form a 'bottleneck' when trying to run several simulations quickly to optimise a die design. Consequently, simulation programs now include integrated rapid die geometry creation tools that enable tooling concepts to be designed and evaluated by simulation more quickly.

Developed specifically for automotive die designers, toolmakers and sheet metal stampers, additional surfaces are created for the addendum and blankholder areas of the tools. Moreover, if the die geometry is parametrically linked to the simulation, optimisation programs can automatically modify the tools until the desired process is achieved.

I.E.5 **– Springback Simulation**

The automotive industry places rigid constraints on final shape and dimensional tolerances. Hence springback prediction and compensation is critical in this highly automated environment.

In the past two decades, finite element method has proven to be a powerful tool in simulating sheet metal forming processes. With the increasing demand from the industries to shorten the lead times and with increased usage of lightweight, higher strength materials in manufacturing auto-body panels, the simulation of springback has become essential for proper design of the forming tools.

Springback simulation is difficult and complicated; to obtain useful results requires accurate material and geometric description of the process in the formulation.

The interaction of the workpiece with the tooling needs to be described precisely.

Various approaches were adopted and formulated by researchers in the past years to accurately simulate springback in sheet metal forming processes. Advances in springback simulation to reduce computational time and increase overall efficiency of the process have been tremendous. Studies involving the use of different types of materials models, finite element codes, elements, hardening rules, frictional constraints, etc., are reported in literature [19,20,18,21-25].

Nilsson et al [26] simulated springback in V-die bending for several materials neglecting friction. The true stress-strain curve from a tensile test was used as the material description. They noted a good correlation between simulation and experimental results.

Huang and Leu [27] have used elasto-plastic incremental finite-element computer code based on an updated Lagrangian formulation to simulate the V-die bending process of sheet metal under the plane-strain condition. Isotropic and normal anisotropic material behaviour was considered including nonlinear work hardening.

Huang et al [28] studied springback and springforward phenomena in V-bending process using an elasto-plastic incremental finite element calculation.

Ogawa et al. [29] did a somewhat similar study but used different element mesh sizes and compared their results with experimental predictions.

Lee and Yang [30] evaluated the numerical parameters that influence the springback prediction by using FE analysis of a stamping process.

Song et al [31] have showed that a material property described by the kinematic hardening law provides a better prediction of springback than the isotropic hardening law. Analytical model and FEA results were compared with the experimental results.

Li et al. [32] used a linear hardening model and an elasto-plastic power-exponent hardening model to study the springback in V-free bending. According to their results, the material-hardening mode directly affects the springback simulation accuracy.

Geng et al [33] have also showed that the simulated springback angle depends intimately on both hardening law after the strain reversal and on the plastic anisotropy. They have analyzed a series of draw bend-tests using a new anisotropic hardening model that extends existing mixed kinematic/isotropic and non-linear kinematic formulations.

Li et al. [34] compared the use of solid and shell elements in their springback simulation with 2D and 3D finite element modelling.

*I.E.*6. Bibliography :

16 Y Demeri and S. C Tang, "Post Processing Analysis in Sheet Metal Forming Simulation," *JOM,* June 1992, pp. 14-16.

17 ven K. Esche, Gary L Kinzel, and Taylan Altan, "Issues in Convergence Improvement for Non-Linear Finite Element Programs," International Journal for Numerical Methods in Engineering, 40, 1997, pp. 4577-4594.

18 C Ho, J Lin, and T A Dean, "Integrated Numerical Procedures for Simulating Springback in Creep Forming Using ABAQUS," *ABAQUS UK Users Group Conference,* 2001.

19 . Tan, B. Persson and C. Magnusson, "An Empiric Model for Controlling Springback in V-die Bending of Sheet Metals," Journal of Materials Processing Technology, 34, 1992, pp. 449-455.

20 .C. Chu, "Elastic-Plastic Springback of Sheet Metals Subjected to Complex Plane Strain Bending Histories," *International Journal of Solids and Structures*, 22, no. 10, 1986, pp.1071-1081.

21 orestin, F. Boivin, M. and Silva, C., "Elasto Plastic Formulation Using a Kinematic Hardening Model for Springback Analysis in Sheet Metal Forming," *Journal of Materials Processing Technology,* 56, 1996, pp. 619-630.

22 hang, L C and Lin, Z., "An Analytical Solution to Springback of Sheet Metals Stamped by Rigid Punch and an Elastic Die," Journal of Materials Processing Technology, 63, 1997, pp. 49-

54.

23 radley N. Maker, "Implicit Springback Calculation Using LS-DYNA," 5th International LS-DYNA Users Conference, 21-22, Sept. Southfield, MI, USA, 1998.

24 embit M. Kutt, Jerrell A. Nardiello, Patricia L. Ogilvie et al, "Non-Linear Finit Element Analysis of Springback," *Communications in Numerical Methods in Engineering,* 15, 1999, pp. 33-42.

25 . Micari, A. Forcellese, L. Fratini, F. Gabrielli and N. Alberti, "Springback Evaluation in Fully 3-D Sheet Metal Forming Processes".

26 nnika Nilsson, Lars Melin, Claes Magnusson, "Finite-Element Simulation of VDie Bending: a Comparison with Experimental Results," Journal of Materials Processing Technology, 65, 1997, pp. 52-58.

27 ou-Min Huang and Daw-Kwei Leu, "Effects of Process Variables on V-Die Bending Process of Steel Sheet," International Journal of Mechanical Sciences, 40, no. 7, 1998, pp. 631-650.

28 uang, Y. M., Lu, Y. H and Makinouchi, A., "Elasto-Plastic Finite-Element Analysis of V-Shape Sheet Bending," *Journal of Materials Processing Technology,* 35, 1992, pp. 129-150.

29 gawa, H., Makinouchi, A., Takizawa, H., and Mori, N., "Development of an Elasto-Plastic FE Code for Accurate Prediction of Springback in Sheet Bending Processes and its Validation by Experiments," Advanced Technology of Plasticity 1993 Proceedings of Fourth International Conference on Technology of Plasticity, pp. 1641-1646.

30 ee, S W and Yang, D Y., "An Assessment of Numerical Parameters Influencing Springback in Explicit Finite Element Analysis of Sheet Metal Forming Process," *Journal of Materials Processing Technology,* 80-81, 1998, pp. 60-67.

31 an Song, Dong Qian, Jian Cao, et al., "Effective Models for Prediction of Springback in Flanging," *Transactions of the ASME,* 123, October 2001, pp. 456- 461.

32 uechun Li, Yuying Yang, Yongzhi Wang Jun Bao and Shunping Li, "Effect of the Material-Hardening Mode on the Springback Simulation Accuracy of V-Free Bending," *Journal of Materials Processing Technology,* 123, 2002, pp. 209-211.

33 .T. Keum, K.B Lee, "Sectional Finite Element Analysis of Forming Processes for Aluminum Alloy Sheet Metals," *International Journal of Mechanical Sciences,* 42, 2000, pp. 1911-1933.

34 . P. Li, W.P. Carden and R. H. Wagoner, "Simulation of Springback". International Journal of Mechanical Sciences, 44, 2002, pp.103-122.

Section II.A

The First Test case is the impact of sphere in steel into sheet metal

II.A.1 – FEM Analyses

Considered to the direct methods, the finite element technique further extends the idea of discretization, this time of the very structure or solid under investigation. This allows to broaden the class of problems amenable to solution so as to include those dealing directly with modern technology. On the other hand, a sufficiently fine mesh and/or high order of approximation within elements ensure that the error is kept reasonably small. This technique requires the processing of extensive data and may efficiently be implemented with the help of computers only. . [1]

II.A.1.1 Fundamental Concepts

FEM cuts a structure into several elements (pieces of the structure). Then it reconnects elements at "nodes" as if nodes were pins or drops of glue that hold elements together.
This process results in a set of simultaneous algebraic equations. Figures 1,2,3 below show Fundamental Concept of Finite Element Method. . [2].

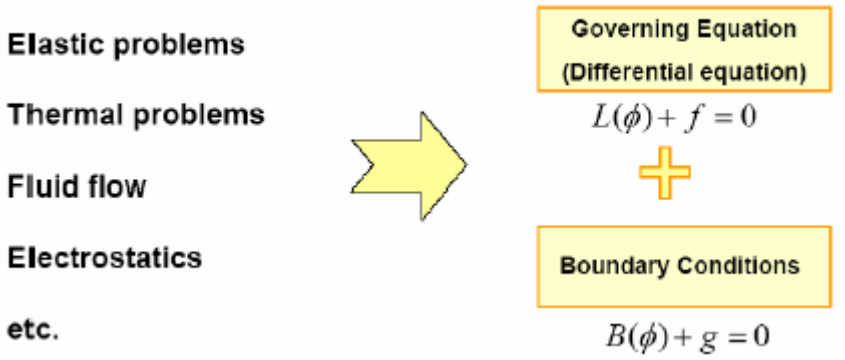

Figure 1. Many engineering phenomena can be expressed by "governing equations" and "boundary conditions". . [2]

Figure 2. FEM Resolution way; FEM approximates problem equations to a set of algebraic equations.
. [2]

Figure 3. Behaviour is the unknown parameter of the problem. . [2]

II.A.1.2 **Methodology**

As it is very difficult to make the algebraic equations for the entire domain, problem
methodology resolutions with Finite Elements Method consists in:
· Divide the domain into a number of small, simple elements. Show figure 4.

· A field quantity is interpolated by a polynomial over an element.
· Adjacent elements share the DOFs at connecting nodes.

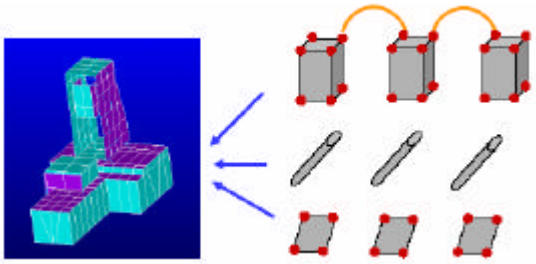

Figure 4. Example. Small piece of structure. [2]

· Obtain the algebraic equations for each element and put all the element equations together.
· Solve the equations, obtaining unknown variables at nodes. [2]

II.A.1.3 **ANSYS LS-DYNA**

ANSYS finite element analysis software enables engineers to perform the following tasks:

- Build computer models or transfer CAD models of structures, products, components, or systems.
- Apply operating loads or other design performance conditions.

- Study physical responses, such as stress levels, temperature distributions, or electromagnetic fields.
- Optimize a design early in the development process to reduce production costs.
- Do prototype testing in environments where it otherwise would be undesirable or impossible (for example, biomedical applications).

The ANSYS program has a comprehensive graphical user interface (GUI) that gives users easy, interactive access to program functions, commands, documentation, and reference material. An intuitive menu system helps users navigate through the ANSYS program. Users can input data using a mouse, a keyboard, or a combination of both. [3]

II.A.1.4 **LS-DYNA**

LS-DYNA is a general-purpose, explicit and implicit finite element program used to
analyze the nonlinear dynamic response of three-dimensional inelastic structures. Its fully automated contact analysis capability and error-checking features have enabled users worldwide to solve successfully many complex crash and forming problems.

ANSYS LS-DYNA supports both 2-D and 3-D explicit elements, and features an
extensive set of single-surface, surface-to-surface and node-to-surface contact as well as
a contact analysis option that automatically creates the contact surfaces. ANSYS LSDYNA also gives optional methods for fast solution processing.
LS-DYNA is used to solve multi-physics problems including solid mechanics, heat
transfer, and fluid dynamics either as separate phenomena or as coupled physics, e.g., thermal stress or fluid structure interaction. [4].

II.A.1.5 **Material Models and Contacts**

LS-DYNA has over one hundred metallic and non-metallic material models: Elastic,
Nonlinear Elastic, Elastoplastic, Foam, Damage, Equations of State, Others.[5].
Over 25 different contact options are available. These options primarily treat contact of:
deformable to deformable bodies, single surface contact in deformable bodies, and

deformable body to rigid body contact. Multiple definitions of contact surfaces are
possible.[5]

A sheet of aluminium alloy bounded on the side, submitted to the impact of a sphere made of steel with an initial velocity.

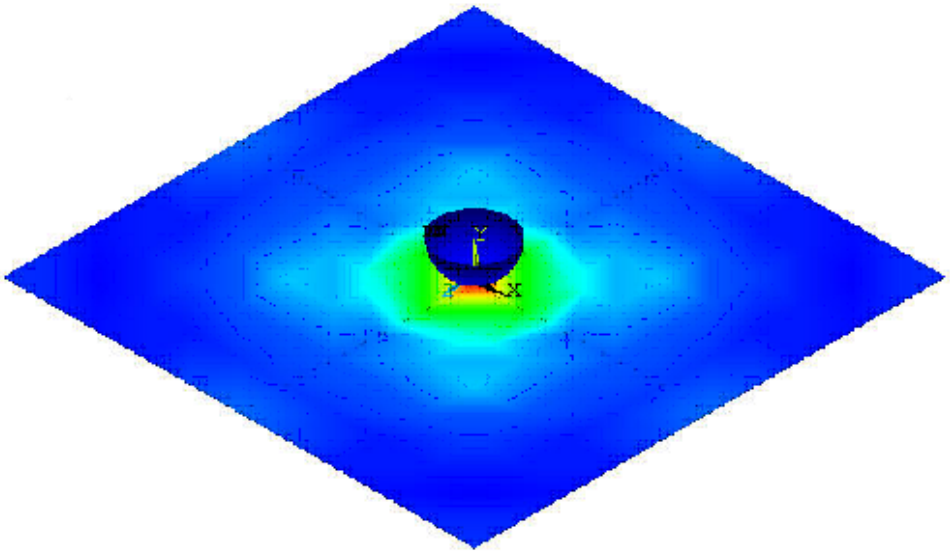

II.A.2 - **CONTEXT**

I have made the dynamic study of a system by Finite Method Analysis with ANSYS version 7.0 . For that, I used the LS-DYNA extension of ANSYS.

The advantage of this software is also to avoid making complicated calculation by hand.

II.A.3 - **DESCRIPTION OF THE PROBLEM**

The problem is about a sheet of aluminium alloy bounded on the side, submitted to the impact of a sphere made of steel with an initial velocity.
This is a square sheet of 10 cm by side. The sphere has a radius of 7,5 mm and is 5 mm above the sheet:

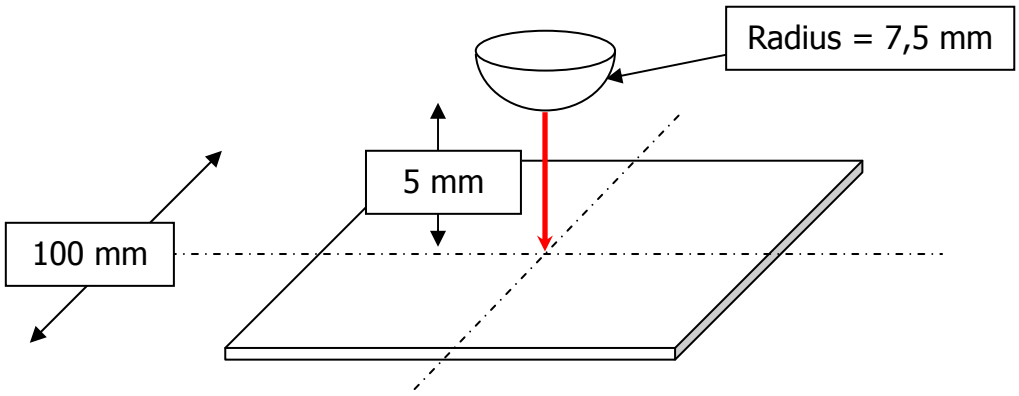

Chosen Materials

I have chosen an aluminium alloy T6 which corresponds to a non-linear material. This material is the kind of material used in the automotive and the aeronautic field. The sphere is made of common steel. Here are the mechanical characteristics of the materials:

Elements	**Materials**	**E (GPa)**	**□Yield (MPa)**	**□break (MPa)**	**□**	**□ (kg.mm^{-3})**
Sheet	Aluminium 6061-T6	68,9	276	310	0.33	2.7*10 $^{-6}$

Sphere	Steel AISI 1005	200	x	x	0.29	7,872 *10 $^{-6}$

II.A.4 - **AIMS OF THE SIMULATION**

This is a double study dealing with the analysis of the maximal constraints and displacement to which the sheet is submitted during the movement. Three questions are risen then:

⇨ ***What is the influence of the thickness of the sheet on the constraints and the displacements?***

⇨ ***When does the plasticization of the sheet happen?***

⇨ ***When does the break of the sheet happen?***

II.A.5 - **PROCEDURE OF THE SIMULATION**

Several sheets have been simulated, with different thicknesses between 0,1 mm and 0,5 mm. [1]

II.A.5.1 - **Simplification of the problem**

We can notice that the problem has 2 plans of symmetry, which enables us to simplify the problem. Thus, we have studied a quarter of a sheet submitted to a quarter of a semi-sphere. Here is a representation of the different geometrical links obtained after simplification:

[1] We will make the simulation with sheets of thickness more or less high if it is more accurate for the interpretation of the results.
We will also increase the velocity of the sphere in order to see the maximal stress and deformation before the break.

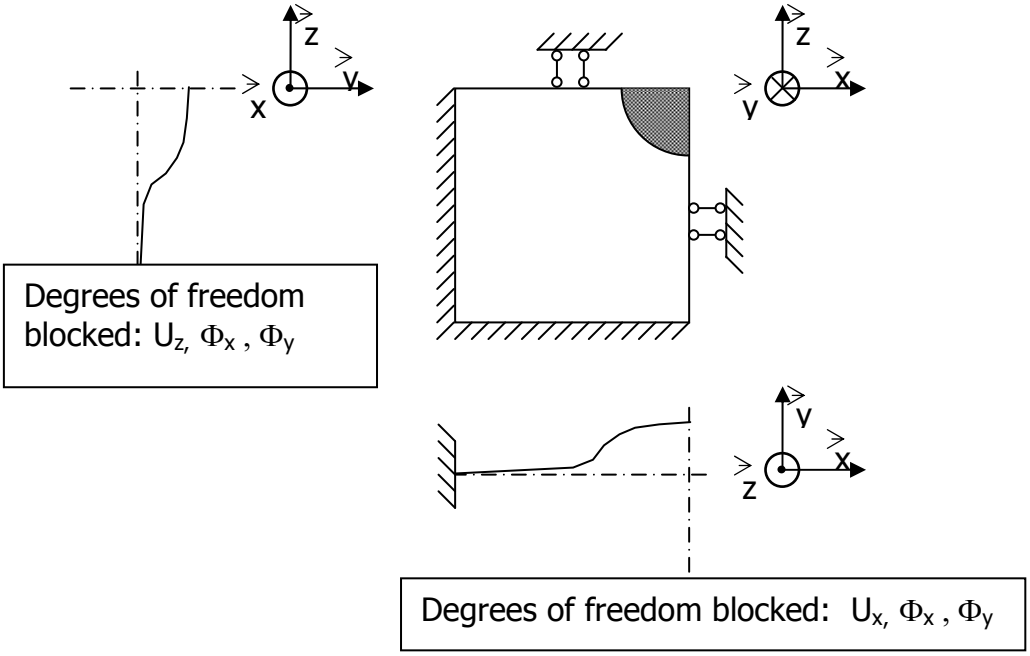

II.A.5.2**- Decreasing of the calculation time**

Given that we had to do several simulations for each thickness, we have chosen to reduce the calculation time of the microprocessor by dividing the sphere in 2 parts and empting it of its volume. Actually, this "shell" has a thickness of 1 mm. Finally, the sheet is submitted to the impact of an « empty » shell in steel:

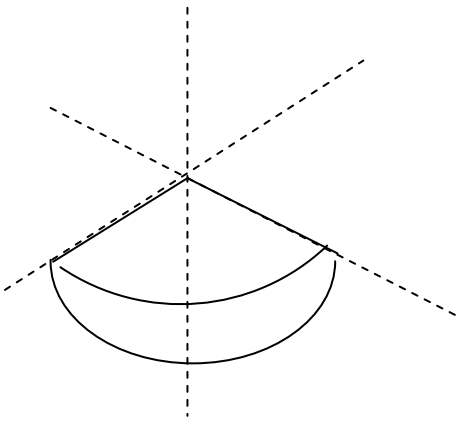

II.A.5.3 - Choice of the element type

Parts	Finite Element type	Number of degrees of freedom of the element	Number of nodes
Sheet	**Solid**	**9**	**8**
Sphere	**Thin Shell**	**12**	**4**

Representation of each type of finite element:

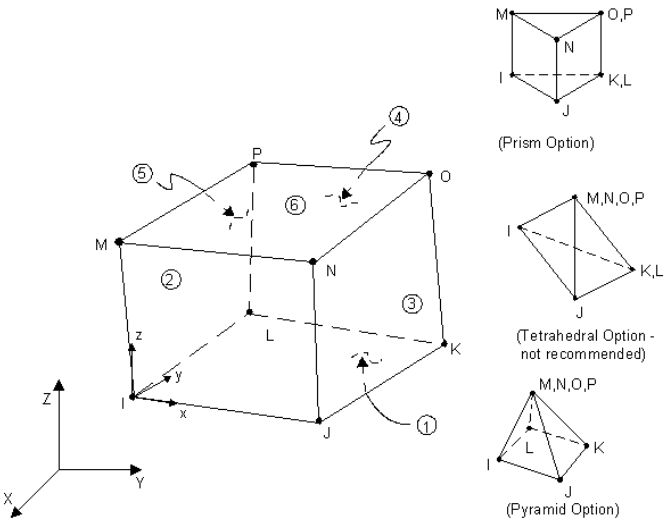

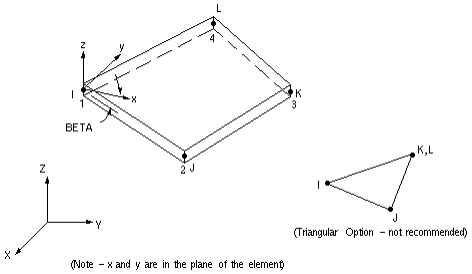

Element type « Solid » *Element type « Thin Shell »*

- Element Name: SOLID164
- Nodes: I, J, K, L, M, N, O, P
- Degrees of Freedom: UX, UY, UZ, VX, VY, VZ, AX, AY, AZ

- Element Name: SHELL163
- Nodes I, J, K, L
- Degrees of Freedom: UX, UY, UZ, VX, VY, VZ, AX, AY, AZ, ROTX, ROTY, ROTZ

II.A.5.4 - Meshing

We have chosen to do an automatic meshing on the surface for the sphere, given its quite complicated shape. On the contrary, we have chosen to do a regular meshing on the volume for the sheet.

II.A.5.5 - Dynamical parameters

II.A.5.5.1 Contact's definition

The definition of this contact was difficult to determinate first, because we didn't know exactly what the shape of the surface of the sphere in contact with the sheet (a point, a surface with a circular or elliptical shape?). We finally decided to try with a single contact between 2 surfaces. Concerning the coefficient of friction or of sliding, we decided to put a medium value between 0 and 1. Indeed it is quite difficult to find the coefficient between a specifically type of aluminium alloy and a steel. The external conditions like the lubrification, the air and other things are to be given and have a lot of influence on these coefficients.

- Single contact between 2 surfaces « Single Surface »
- Static friction coefficient: 0,5
- Dynamical friction coefficient : 0,5
- Sliding coefficient : 0,5

II.A.5.5.2 Initial velocity

At the time t=0, the sphere, with a mass of 2,79 g ([2]), will have a velocity of 500 mm/s. We have chosen a quite slow velocity, so that we can increase it during the next simulations to see for example the influence of the speed on the stresses and the displacement of the sheet.

II.A.5.5.3 Simulation time

We have chosen a simulation time of 0,06 second so that the sphere has the time to leave completely the surface of the sheet. A calculation in the **annexe 3** has enabled us to estimate that the sphere needs about 0,01 second to touch the sheet when its initial velocity is 500 mm/s and about 0,001 second when its initial velocity is 5000 mm/s.

[2] This mass is obtained by a justifying calculus in annexe 2

*II.A.*6 RESULTS

In order to evaluate as well as we can the stresses, we have chosen to consider only the Von Mises equivalent stress. Let's remind us the formula of this stress:

$$\sigma_{eq} = \sqrt{\sigma_x^2 + \sigma_y^2 + \sigma_z^2 - (\sigma_x\sigma_y + \sigma_x\sigma_z + \sigma_y\sigma_z)}$$

σ_x, σ_y, σ_z are the principal values. σ_{eq} must be of course under the yield stress so that the sheet doesn't break.

Sheet of 0,1 mm

Maximal displacement in the centre of the sheet (mm)	**2.502**
Maximal stress (MPa)	**189,399**

Sheet of 0,2 mm

Maximal displacement in the centre of the sheet (mm)	**1,506**
Maximal stress (MPa)	**170,064**

Sheet of 0,3 mm

Maximal displacement in the centre of the sheet (mm)	**1,107**
Maximal stress (MPa)	**133,714**

Sheet of 0,4 mm

Maximal displacement in the centre of the sheet (mm)	**0,912**
Maximal stress (MPa)	**128,067**

Sheet of 0,5 mm

Maximal displacement in the centre of the sheet (mm)	**0,73**
Maximal stress (MPa)	**119,674**

We can see that the maximal Von Mises equivalent stress doesn't come over the Yield stress. Also, we decided to reduce the thickness of the sheet in order to obtain a value of a stress superior than 276 MPa which is the Yield stress of our aluminium. But this research is only theoretical given the physical limit of the sheet. Indeed, the minimum thickness of an industrial sheet is around 0,1 mm.

II.A.*7* Graphics

Appearance of the stresses

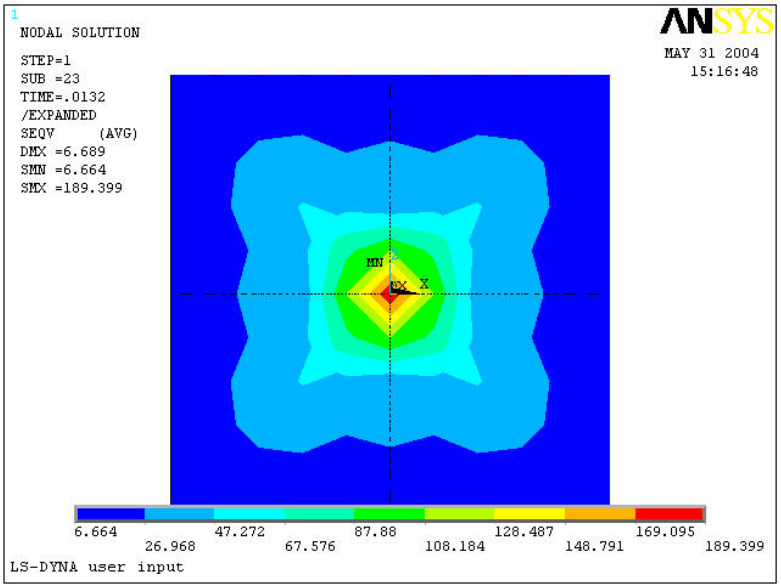

Sheet of 0,1 mm

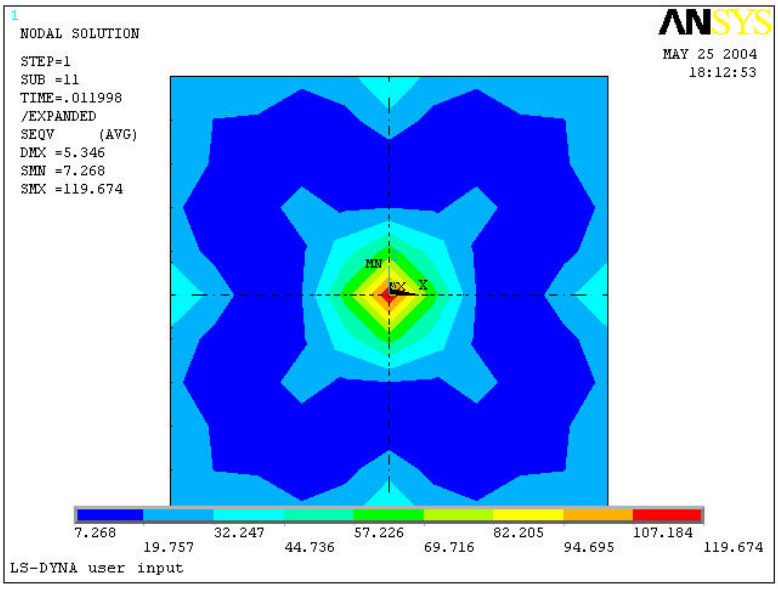

Sheet of 0,5 mm

Comments:

We can see that the maximum Von Mises stress is located in the middle of the sheet. It's much more in the periphery that we find the little values. This is also verifying what we are doing, a test of impact.

This result could be surprising regarding to the classical result of a constant force in the middle of a sheet (or a beam). In this other case, the force imposed is constant and the main stresses are in the periphery.

Appearance of the displacement

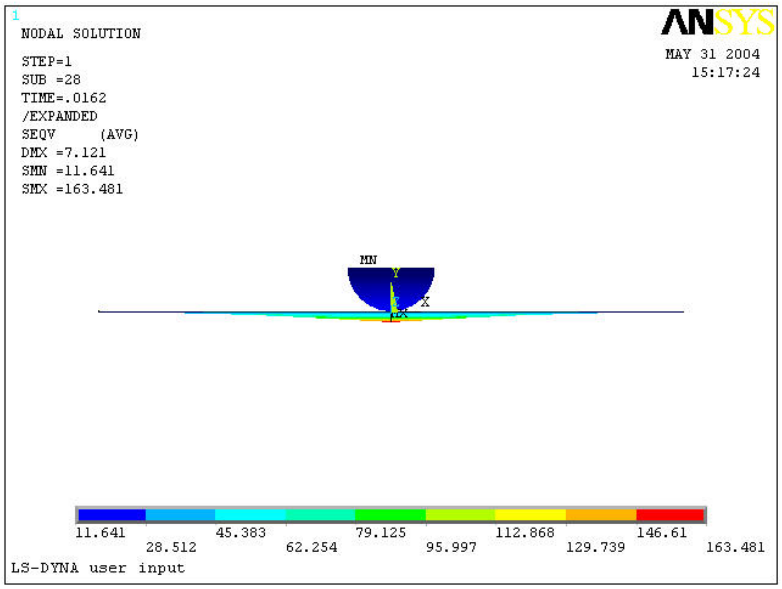

Displacement for a sheet of 0,1 mm

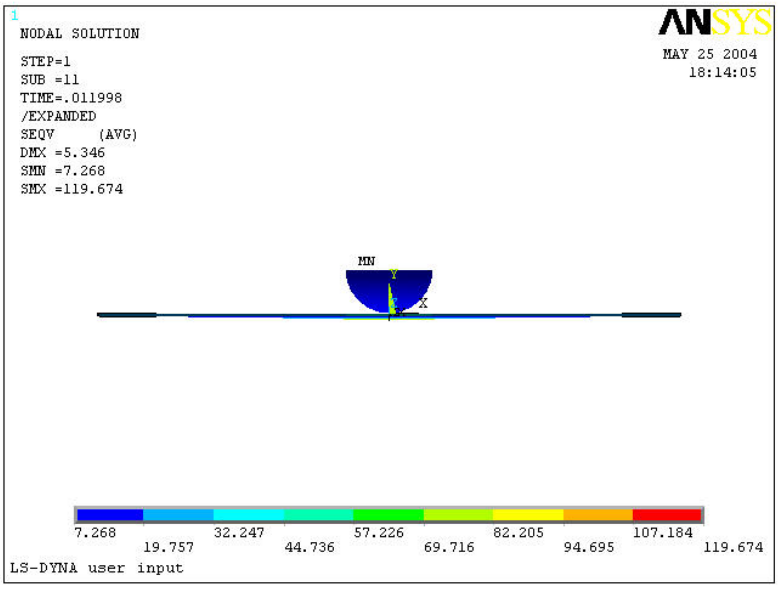

Displacement for a sheet of 0,5 mm

Evolution of the stress of Von Mises in function of the time

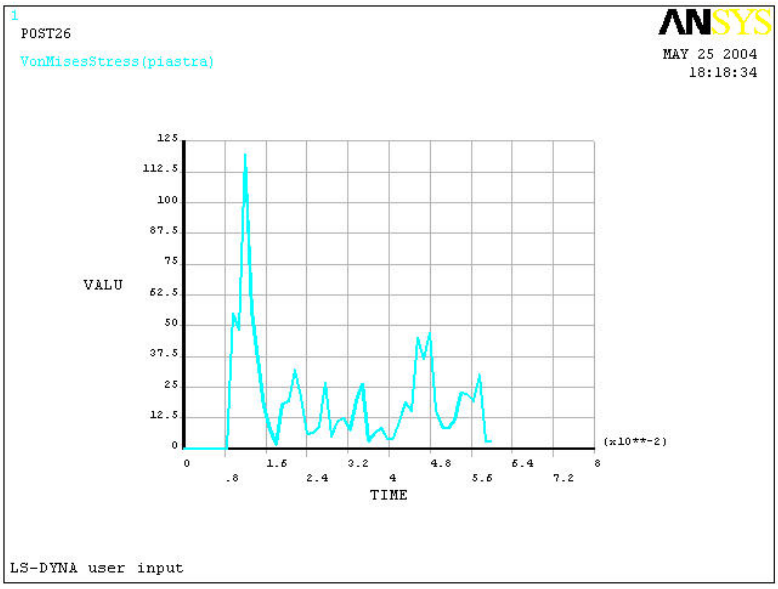

Sheet of 0,5 mm

Comments:

These curves enable us only to say that more the sheet is large and more the stresses are irregular. We can see a phenomenon of vibration of what we will speak further with more reliable curves.

Variation of the displacement in function of the distance to the centre of the sheet

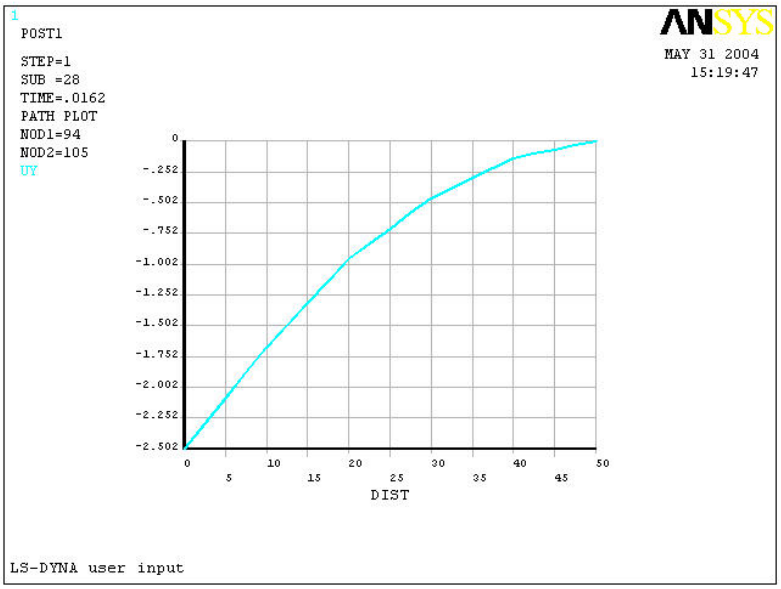

Sheet of 0,1 mm

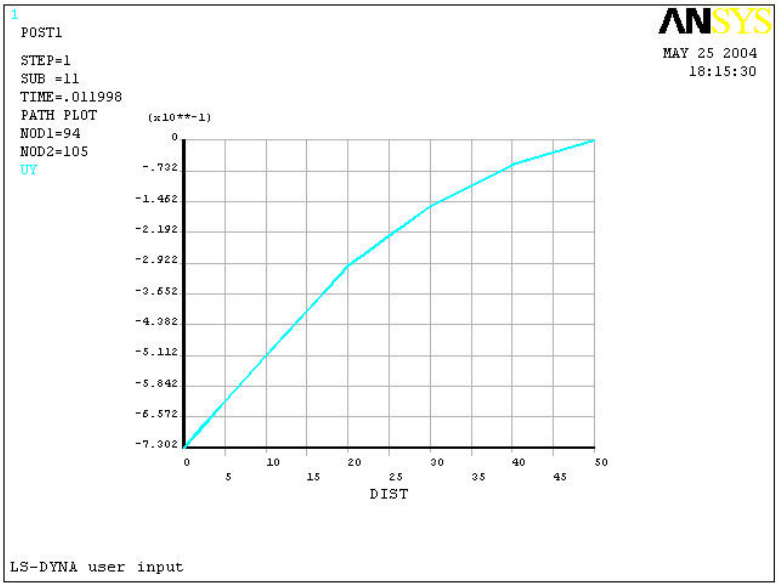

Sheet of 0,5 mm

Comments:

We can just see here that the shape of the sheet at the maximum displacement seems to be quite regular. Also, we can notice that the value of the maximum displacement decreases whereas the thickness of the sheet increases: it goes from about 16 mm for a "sheet" of 0,01 mm to nearly 0,7 mm for a sheet of 0,5 mm.

Variation of the displacement of the sphere and the sheet in function of the time

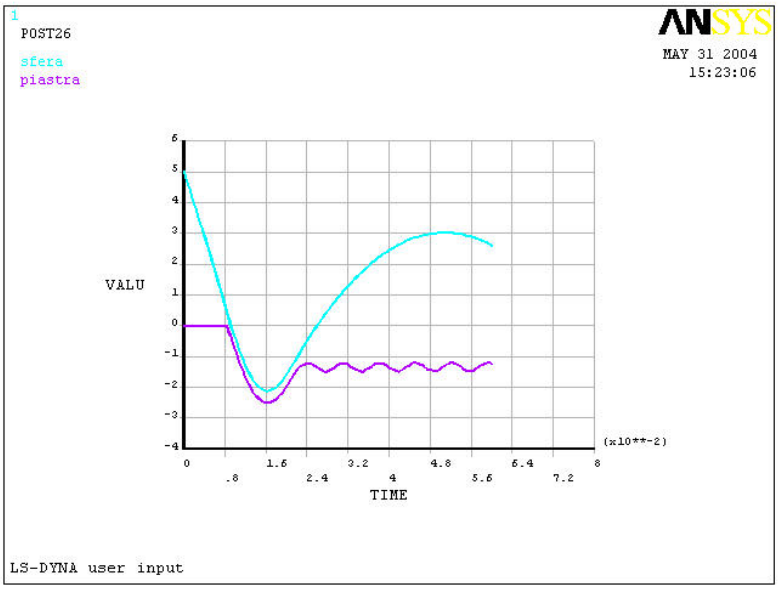

Sheet of 0,1 mm

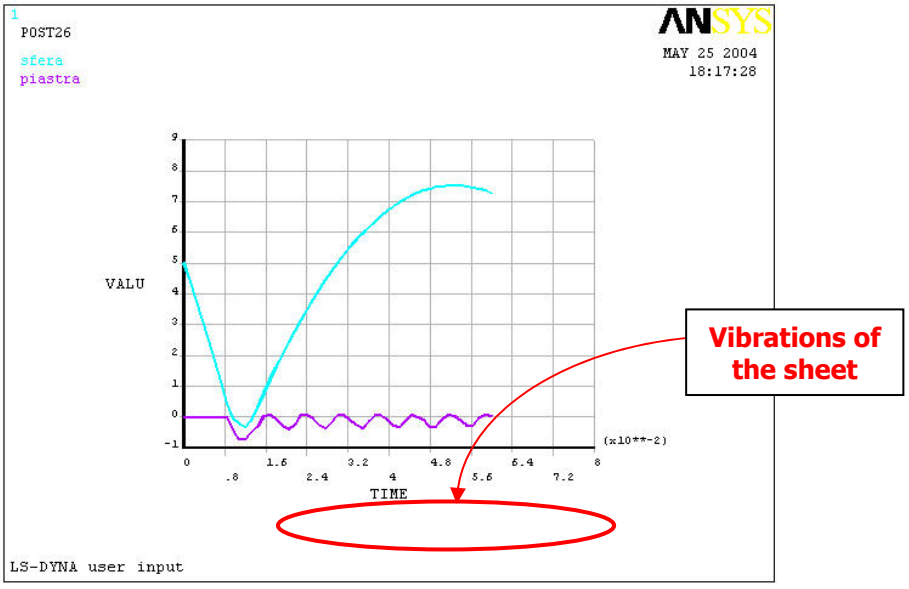

Sheet of 0,5 mm

Comments:

These curves are really interesting to understand what is happening during the movement. Indeed we can see here how the sphere comes in contact with the sheet and how it reacts.

For small thicknesses, the sphere comes literally denting in the sheet until the time where they lose contact with each other. Then we can notice a phenomenon of vibrations of the sheet confirming what we said before. We can by this way see the residual deformation of the sheet by doing the average of these vibrations. Of course, the larger the sheet is and the smaller the residual deformation is.

Concerning the sphere, it is nearly jumping more and more over the sheet with the increase of the thicknesses of the sheets. The sphere is higher at the end of the movement than at the beginning with the sheet of a thickness of 0,5 mm

Synthesis table

NUMBER OF SHEET	THICKNESS (mm)	MAXIMUM DISPLACEMENT (mm)	MAXIMUM STRESS (MPa)
1	0,01	16,073	339,716 (broken)
2	0,05	4,273	256,801
3	0,1	2,502	189,399
4	0,2	1,506	170,064
5	0,3	1,107	133,714
6	0,4	0,912	128,067
7	0,5	0,73	119,674

II.A.8 INTERPRETATIONS- CONCLUSIONS

With these tables, we have obtained curves which seemed to be following a trend. Also we have decided to interpolate these curves to mathematical curves, as we can see on the next graphics.

Variation of the displacement in function of the thickness

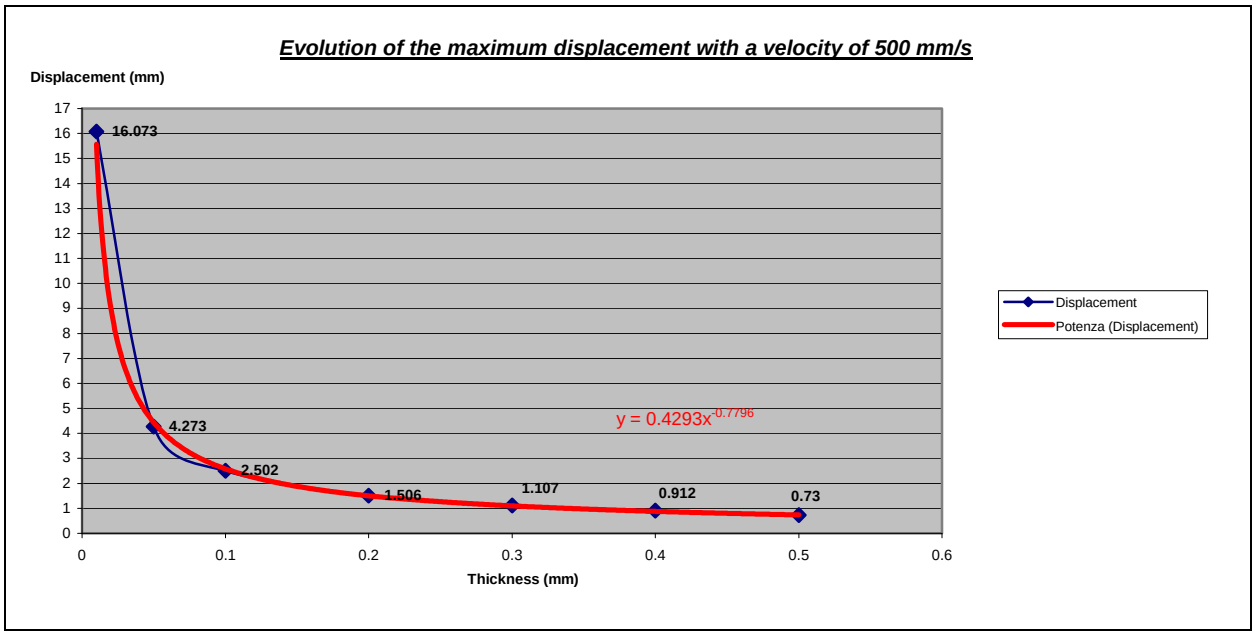

We can see here how huge would be the displacement of the centre of a "sheet" of 0.01 mm.

. ***Variation of the stress of Von Mises in function of the thickness***

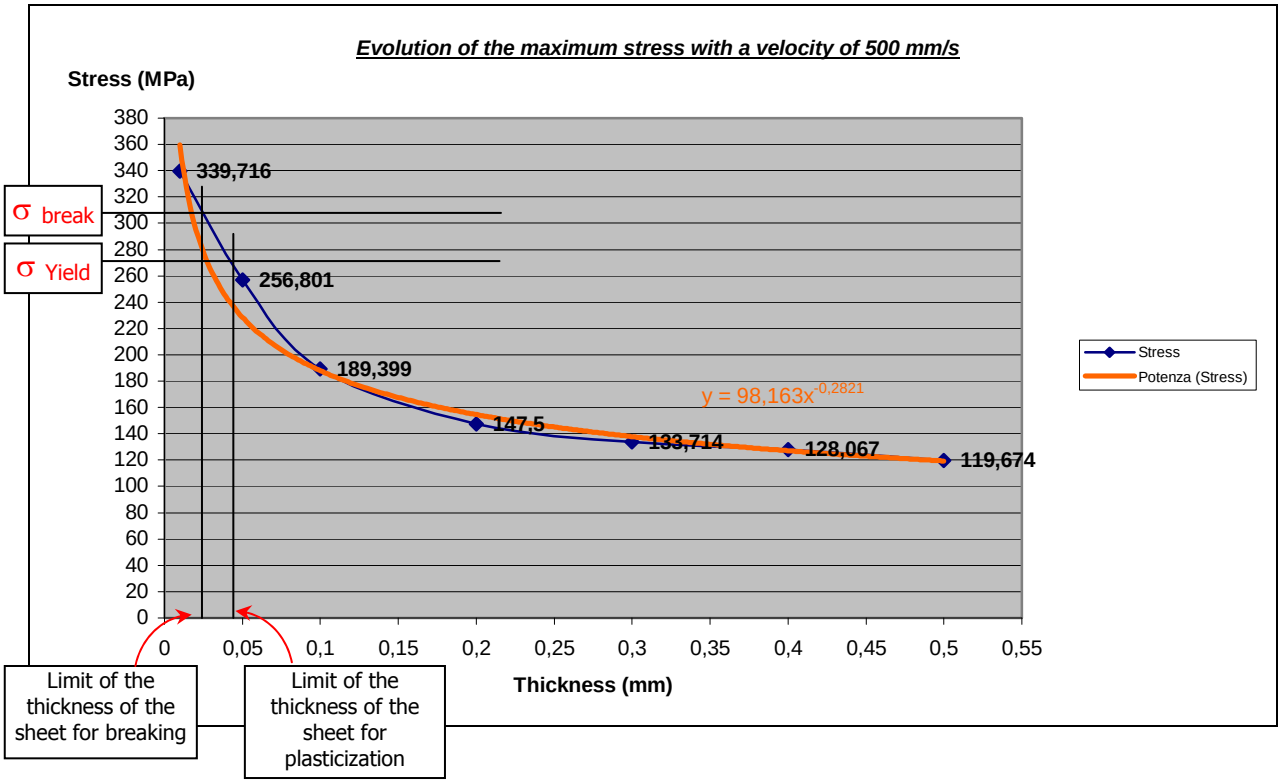

When is there plasticization? When is there breaking?

As we can see, the displacement and the stress of Von Mises decrease as long as we increase the thickness of the sheet. The very little values that we have put for the thickness were just supposed to help us to see for which theoretical thickness the plasticization appears and when the break comes, and respecting the same conditions of simulation. Indeed, thanks to this graphic, we have been able to say that a sheet of 0,035 mm would plasticize and that a sheet of 0,02 mm would break. Nevertheless, these values are practically impossible to obtain by any kind of methods of forming or stamping. For these reasons, we have decided to change one parameter of the simulation which could enable us to see the plasticization and the break of a « real » sheet, which means with a thickness of at least 0,1 mm. Also we have done others simulations by increasing the velocity of the sphere, until the sheet is submitted to a bigger stress than the yield stress (276 MPa) and the break stress (310 MPa). Let's see those results in the following part.

II.A.9 SECOND RESULTS

We have also done three new series of simulation with the velocities

of 1000 mm/s, 2000 mm/s, 5000 mm/s and that for each sheet. The reader will be able to see all the graphics concerning the simulation in the **annexe 4**.
But we put also the one with the velocity of 500 mm/s to be able to compare and to see the interests of this parameters' change.

Velocity of 500 mm/s

Thickness (mm)	Displacement	Stress
0,01	16,073	339,716
0,05	4,273	256,801
0,1	2,502	189,399
0,2	1,506	147,5
0,3	1,107	133,714
0,4	0,912	128,067
0,5	0,73	119,674

We have done the simulation even for the "sheet" of 0,05 mm in order to see if the sheet would break at that speed

Velocity of 1000 mm/s

Thickness (mm)	Displacement	Stress
0,01	x	x
0,05	8,984	296,648
0,1	5,316	264,371
0,2	3,221	225,948
0,3	2,389	191,766
0,4	1,905	182,019
0,5	1,558	172,233

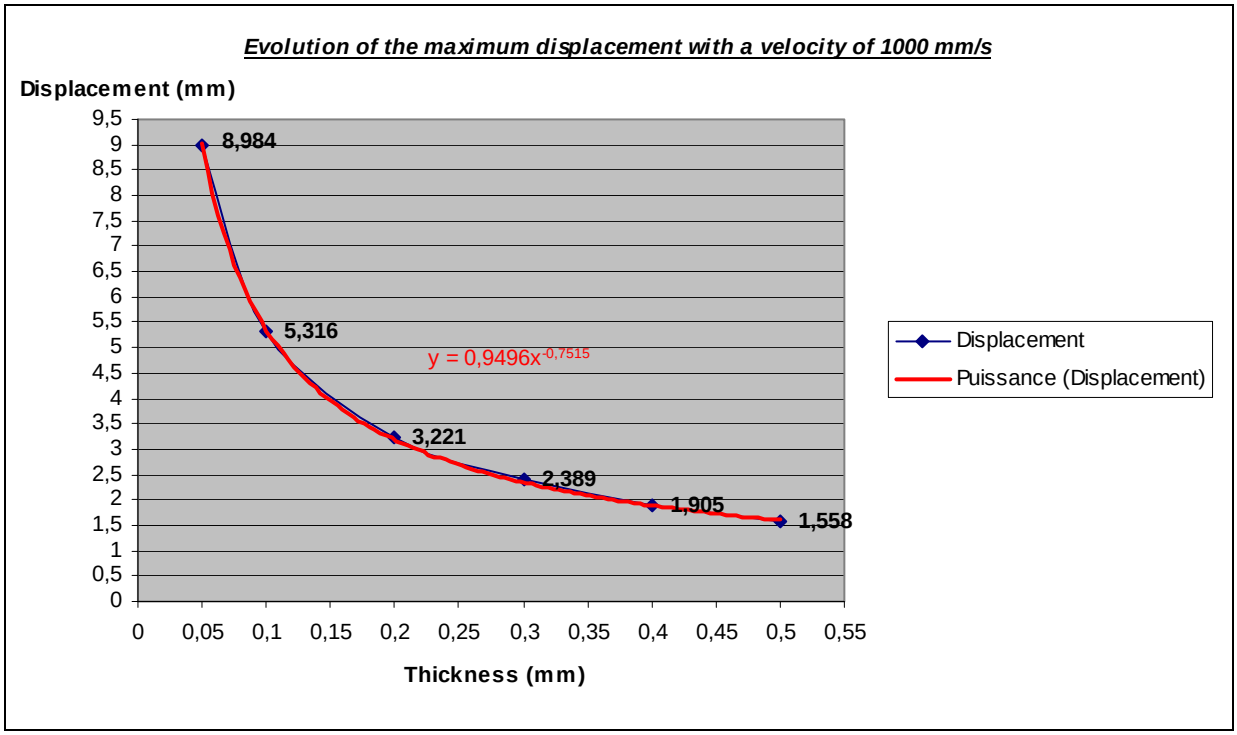
Evolution of the maximum displacement with a velocity of 1000 mm/s
Displacement (mm)
9,5
9
8,5
8
7,5
7
6,5
6
5,5
5
4,5
4
3,5
3
2,5
2
1,5
1
0,5
0
8,984
5,316
3,221
2,389
1,905
1,558
y = 0,9496x-0,7515
0
0,05
0,1
0,15
0,2
0,25
0,3
0,35
0,4
0,45
0,5
0,55
Thickness (mm)
Displacement
Puissance (Displacement)

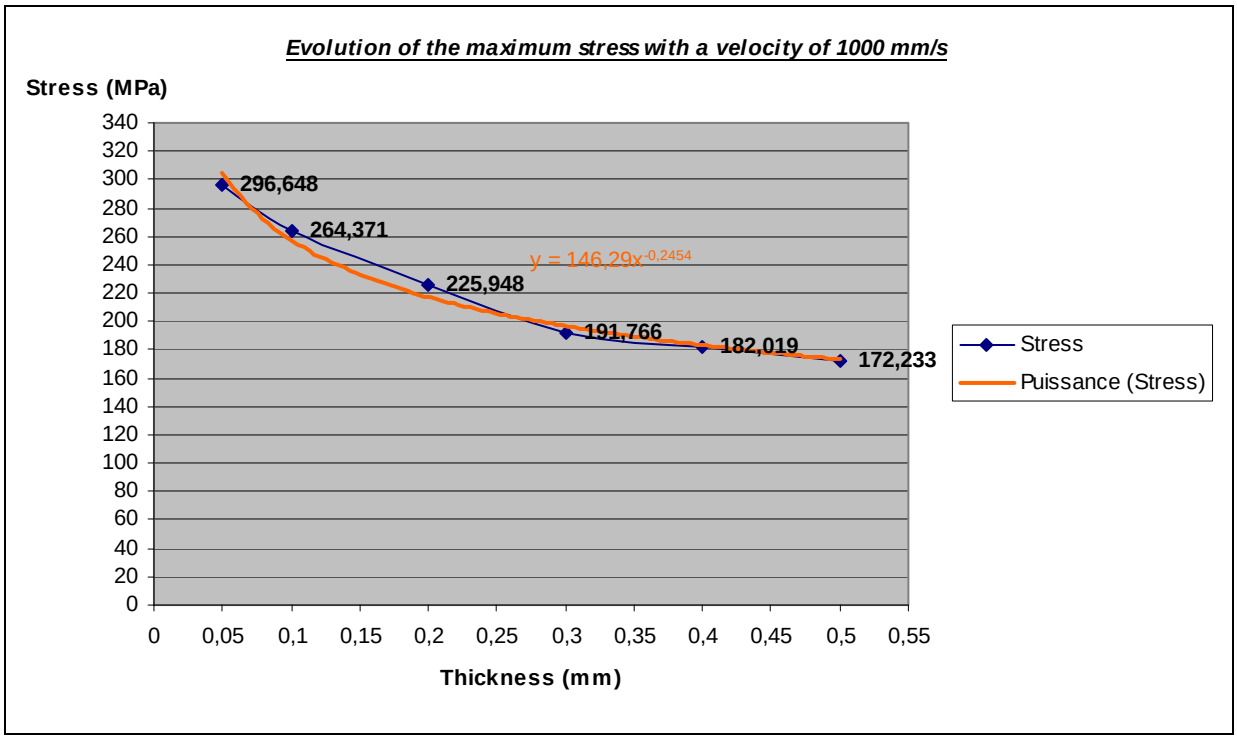
Evolution of the maximum stress with a velocity of 1000 mm/s
Stress (MPa)
340
320
300
280
260
240
220
200
180
160
140
120
100
80
60
40
20
0
296,648
264,371
225,948
191,766
182,019
172,233
y = 146,29x-0,2454
0
0,05
0,1
0,15
0,2
0,25
0,3
0,35
0,4
0,45
0,5
0,55
Thickness (mm)
Stress
Puissance (Stress)

Velocity of 2000 mm/s

Thickness (mm)	Displacement	Stress
0,01	x	x
0,05	x	x
0,1	12,707	316,532
0,2	7,759	283,497
0,3	5,775	263,617
0,4	4,707	248,092
0,5	3,98	230,228

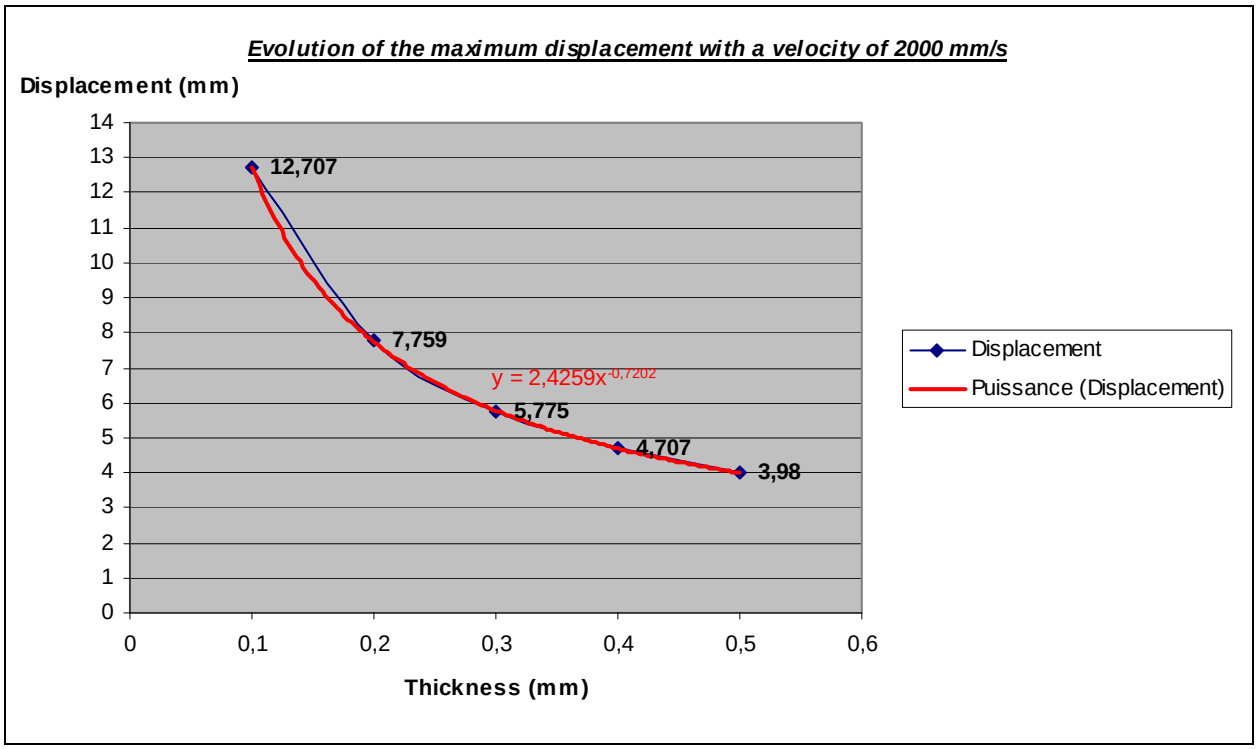

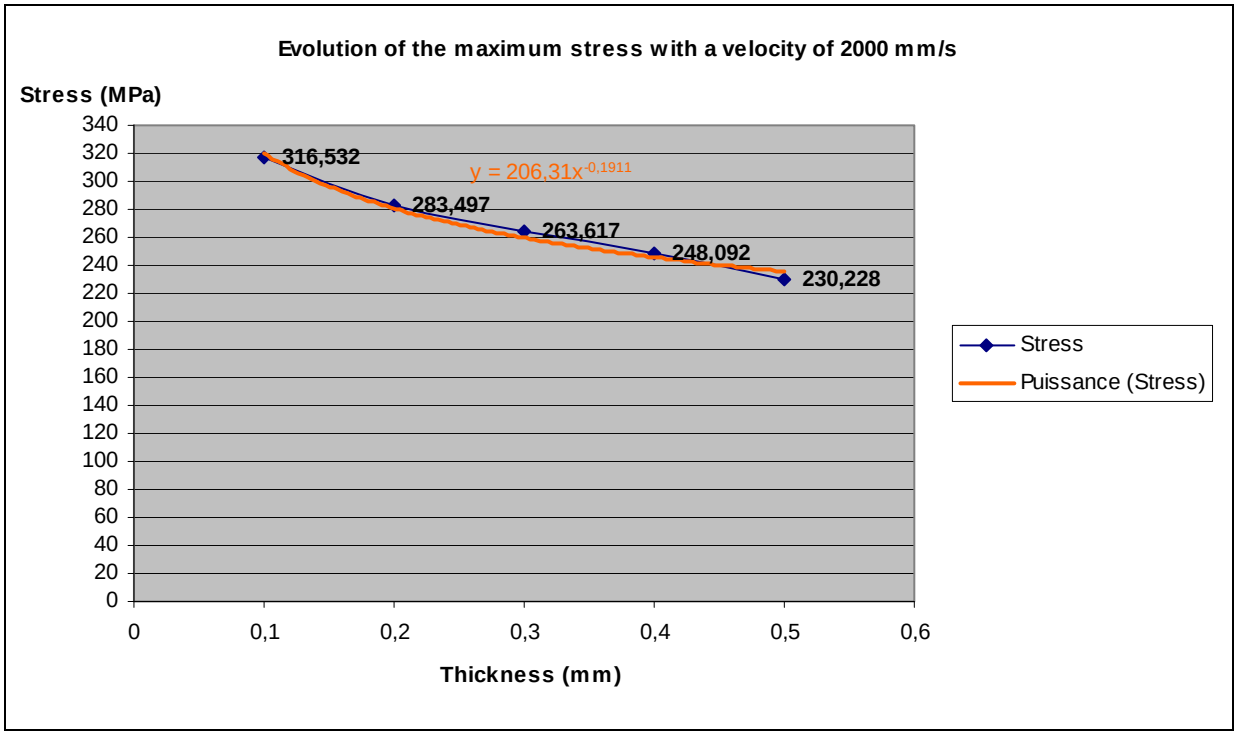

Velocity of 5000 mm/s

Thickness (mm)	Displacement	Stress
0,01	x	x
0,05	x	x
0,1	35,495	463,46
0,2	22,151	364,673
0,3	17,638	332,47
0,4	14,823	308,472
0,5	12,895	306,771

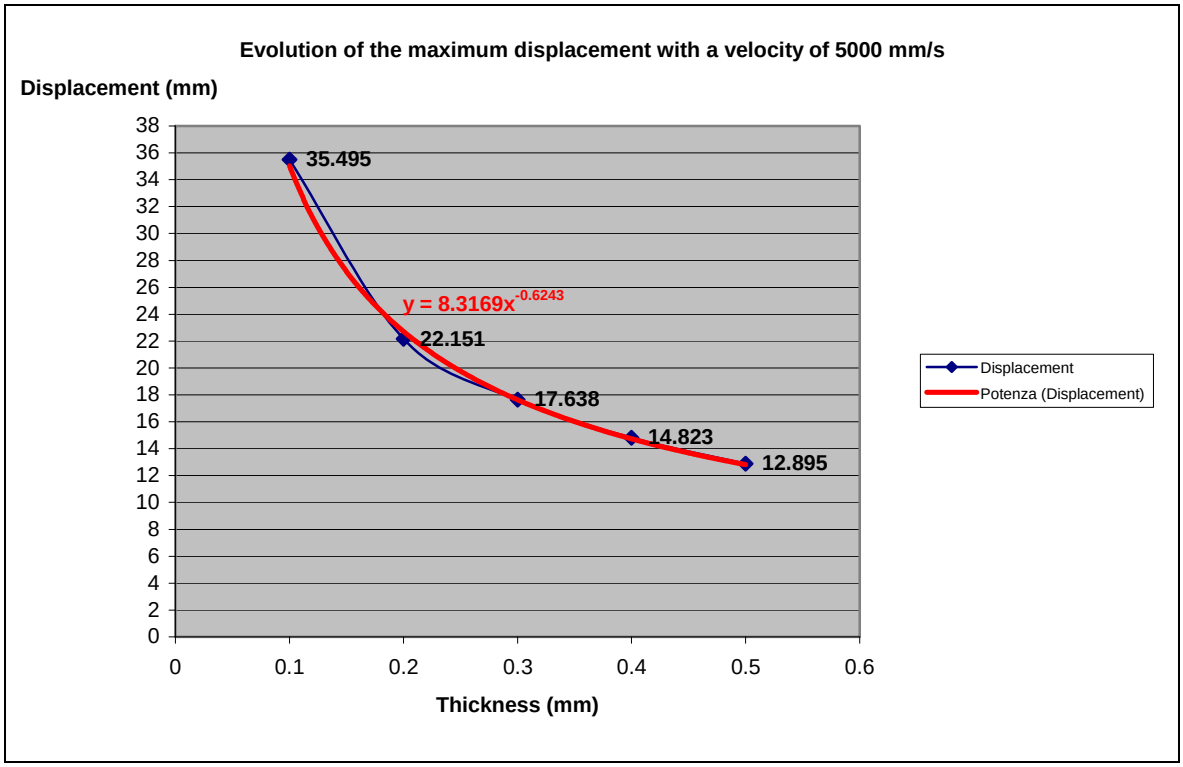
Evolution of the maximum displacement with a velocity of 5000 mm/s
Displacement (mm)
38
36
34
32
30
28
26
24
22
20
18
16
14
12
10
8
6
4
2
0
0
0.1
0.2
0.3
0.4
0.5
0.6
Thickness (mm)
35.495
22.151
17.638
14.823
12.895
y = 8.3169x-0.6243
Displacement
Potenza (Displacement)

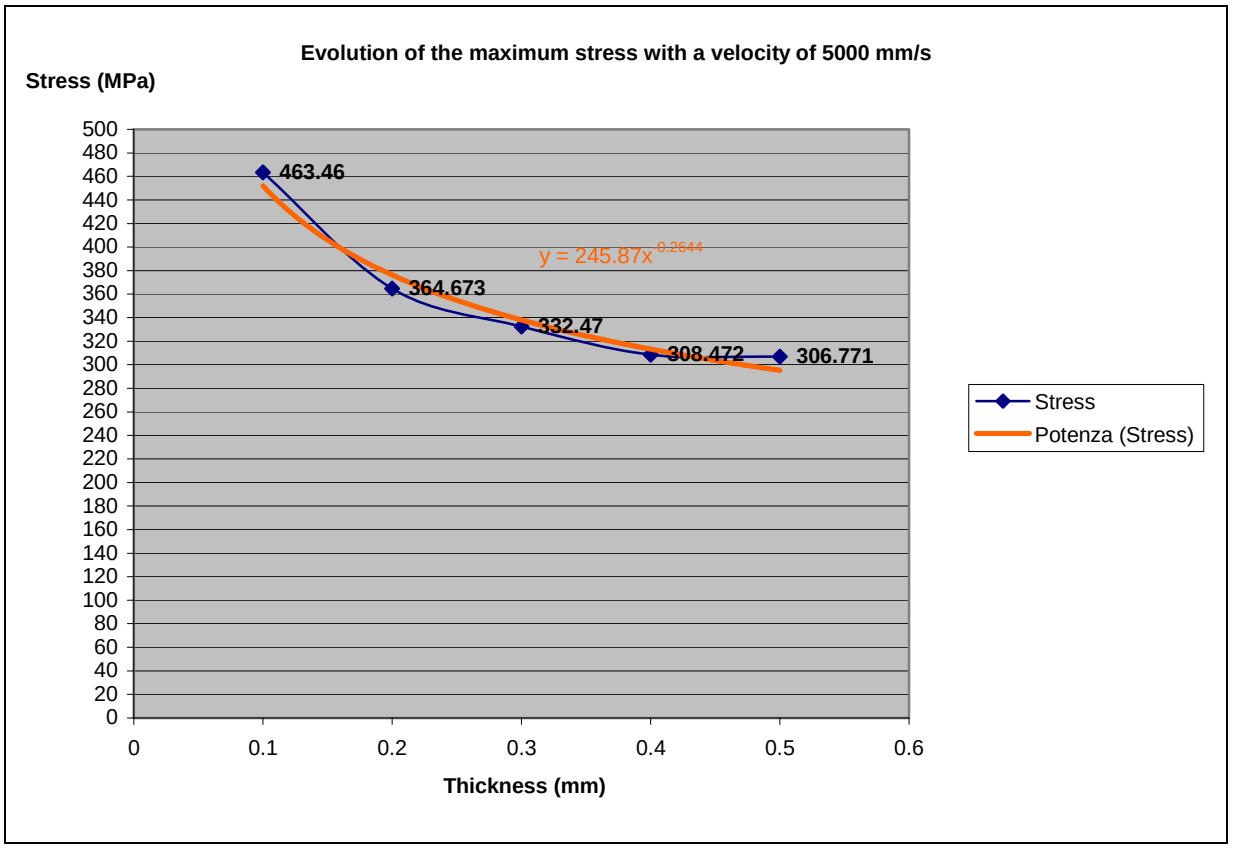
Evolution of the maximum stress with a velocity of 5000 mm/s
Stress (MPa)
500
480
460
440
420
400
380
360
340
320
300
280
260
240
220
200
180
160
140
120
100
80
60
40
20
0
0
0.1
0.2
0.3
0.4
0.5
0.6
Thickness (mm)
463.46
364.673
332.47
308.472
306.771
y = 245.87x-0.2644
Stress
Potenza (Stress)

Comments:

The displacement of the sheet seems to be following a curve with an equation of the type $A/x^{0,7}$, with A a certain coefficient and x the value of the thickness.

The stress of the sheet seems also to be following a curve with an equation of the type $B/x^{0,27}$, with A an other coefficient and x the value of the thickness.

II.A.8.5 Influence of the velocity on the maximum displacement

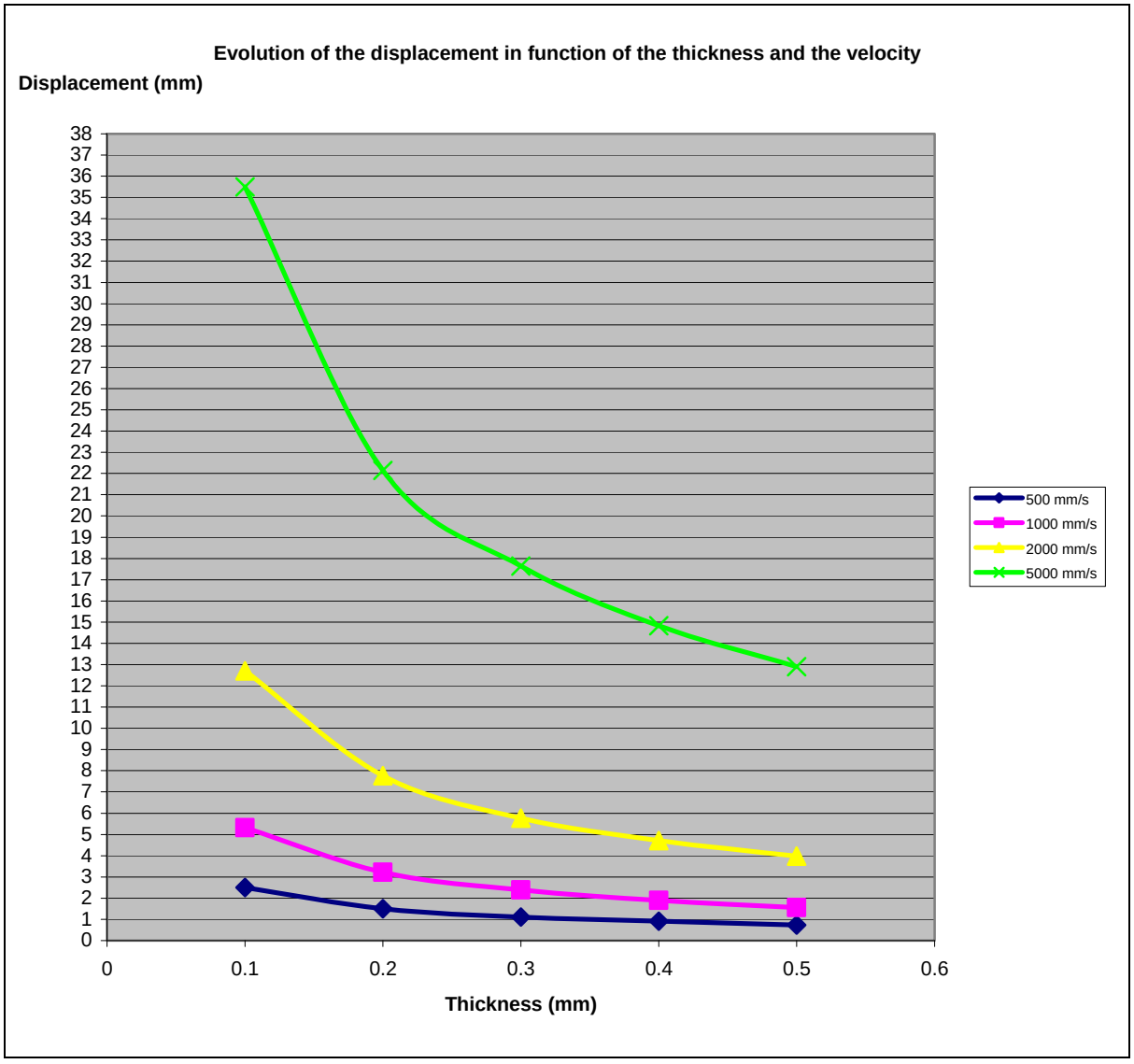

Influence of the velocity on the maximum stress of Von Mises

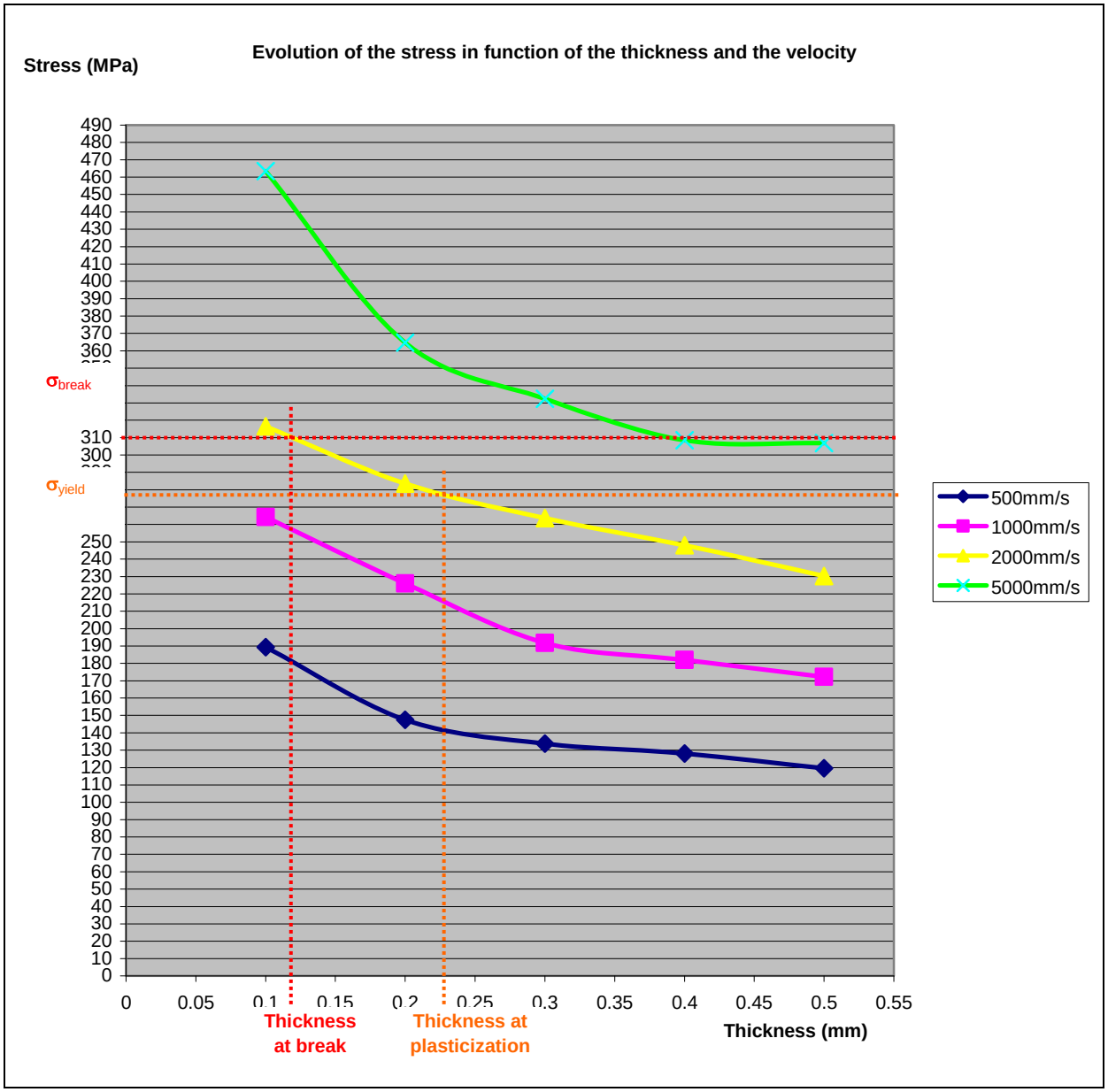

Conclusions

As we can see, when we increase the velocity, the maximum stress of Von Mises increases. It is the same for the maximum displacement. Fortunately, this is not a surprise. But the interesting point is that we know now that the sphere has to have a minimum velocity of 2000 mm/s so that

the sheet breaks. At the speed of 5000 mm/s, the sheet breaks for every thickness except the one of 0,5 mm.

Concerning the plasticization, we know that it does not arrive at a speed of 1000 mm/s. We have the plasticization for a sheet of about 0,225 mm with the speed of 2000 mm/s.

To conclude, we can say that the sheet will not plasticize as long as the speed of the sphere does not overcome 1000 mm/s.
Concerning the break, the velocity of the sphere must not be more than 2000 mm/s.

ANNEXES

ANNEXE 1

Calculation of the energy of the sphere at the impact

We want to know the total energy of the sphere when it hits the sheet, so: at z=0. We have:

$$E = E_P + E_k + U$$

With: E = total energy of the sphere
E_p = potential energy of the sphere
E_k = kinetic energy of the sphere
U = internal energy of the sphere ≈ 0 Joule

Let's take the origin of the energy at z=0. In this case, at z=0, E_p=0 and we have:

$$E = E_k = \frac{1}{2} \cdot m \cdot v^2$$

With: m = mass of the sphere
v = velocity of the sphere

And: $m = \rho \cdot V$
With: ρ = volumic mass of the sphere (=7,872e^{-6} kg/mm^3)
V = volume of the sphere

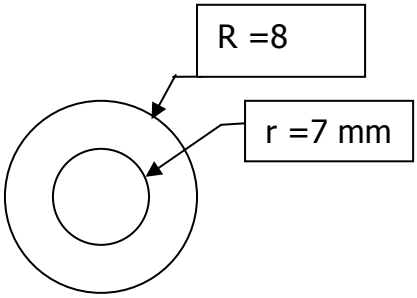

$$V = \frac{4}{3} \cdot \pi \cdot (R^3 - r^3)$$

N.A: V= 707,906 mm^3
m=5,57 g

For half a sphere, we have: m=2,79 g.

Now, let's calculate the velocity of the sphere at the impact for each initial velocity:

$$v = v_0 + a \cdot t = v_0 + g \cdot t$$

- For v_0=500 mm/s, v=590 mm/s
  E = 486 □J
- For v_0=1000 mm/s, v=1047,9 mm/s
  E = 1532 □J
- For v_0=500 mm/s, v=2024,4 mm/s
  E = 5717 □J
- For v_0=500 mm/s, v=5009,8 mm/s
  E = 35012 □J

ANNEXE 2

Calculation of the period of the sphere's fall

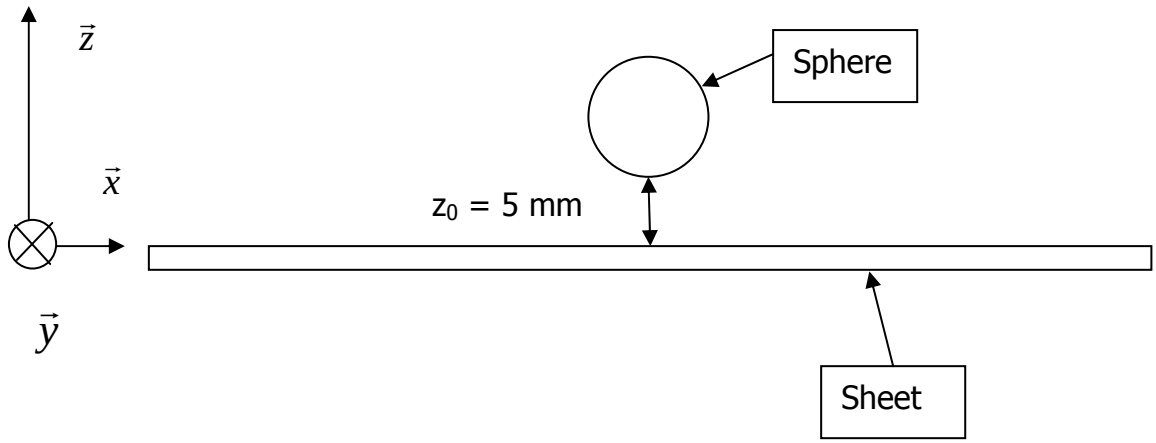

We can apply the basic principle of dynamic to the sphere:

$$\sum \vec{F} = m \cdot \vec{a}$$

With: $\vec{F}$ = all the forces applied to the sphere
m = mass of the sphere
$\vec{a}$ = acceleration of the sphere.

But the sphere is only submitted to its own gravity force. Thus, we can write the following equation, after a projection on the vertical axis:

$$-m \cdot g = m \cdot a$$

With: g = gravity acceleration (= 9,81 m/s^2).

Then, it comes:

$$a = -g$$

After two successive integrations on the time, we can obtain:

$$z = -\frac{1}{2} \cdot g \cdot t^2 - v_0 \cdot t + z_0$$

with : z = position of the lowest point of the sphere on the vertical axis
z_0 = initial position of the lowest point of the sphere on the vertical axis (=0,005 m)
v_0 = initial velocity of the sphere
t = time

We want to know how long the period of the fall is. It is the period between the moments when the sphere is at z_0 and when it is at z=0. So, we have to solve the following equation:

$$-\frac{1}{2} \cdot g \cdot t^2 - v_0 \cdot t + z_0 = 0$$

The two solutions of this equation are:

$$t_1 = \frac{1}{g} \cdot (-v_0 + \sqrt{v_0^2 + 2 \cdot z_0 \cdot g}) \qquad \text{or:} \qquad t_2 = \frac{1}{g} \cdot (-v_0 - \sqrt{v_0^2 + 2 \cdot z_0 \cdot g}) \leq 0$$

As t_2 is negative, this solution is impossible. So, we have:

$$t = \frac{1}{g} \cdot (-v_0 + \sqrt{v_0^2 + 2 \cdot z_0 \cdot g})$$

<u>Numerical applications:</u>

- For v_0=500 mm/s, t=0,009174 s
- For v_0=1000 mm/s, t=0,004883 s
- For v_0=2000 mm/s, t=0,002485 s
- For v_0=5000 mm/s, t=0,000999 s

ANNEXE 3

Graphics for different velocities and thicknesses

At the velocity of 1000 mm/s:

- ***Sheet of 0,1 mm***

Displacement for a sheet in function of the distance

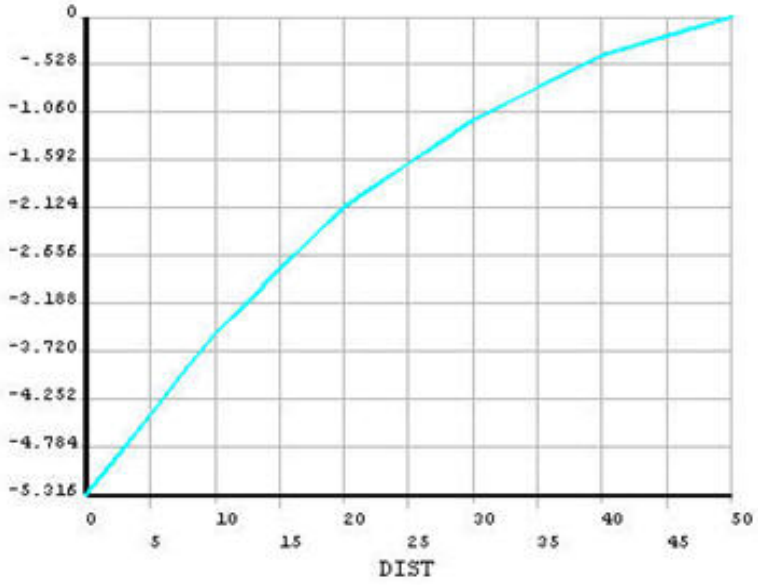

Displacement for a sheet and the ball in function of the time

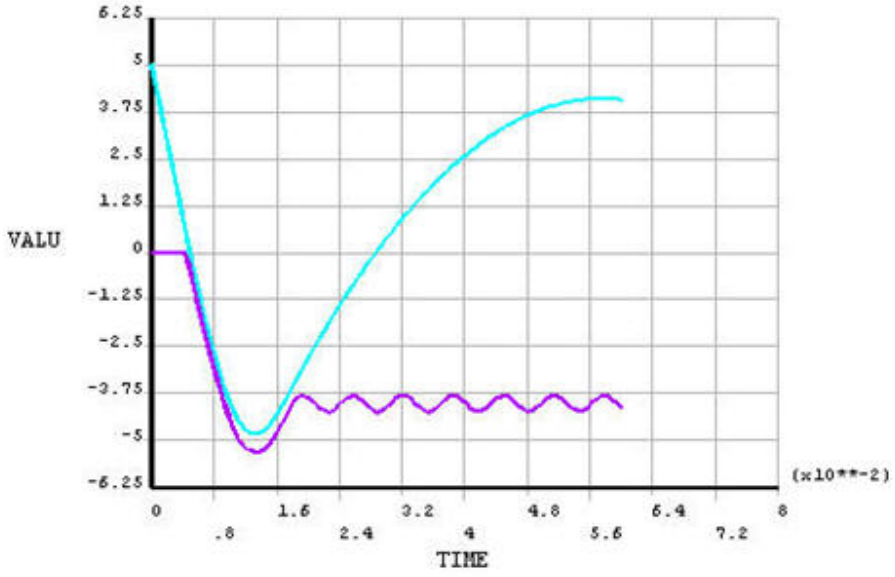

Evolution of the stress of Von Mises for the sheet in function of the time

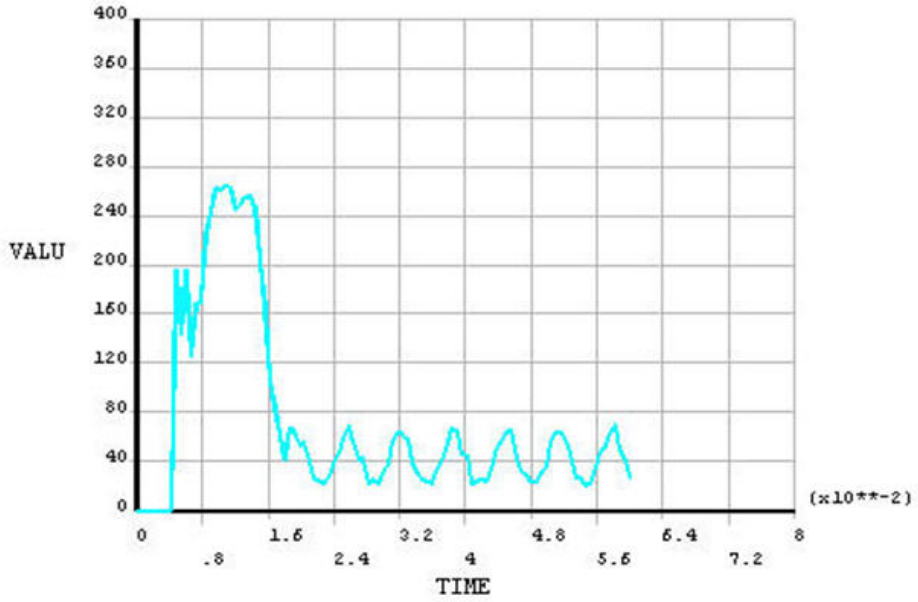

- ***Sheet of 0,5 mm***

Displacement for a sheet in function of the distance

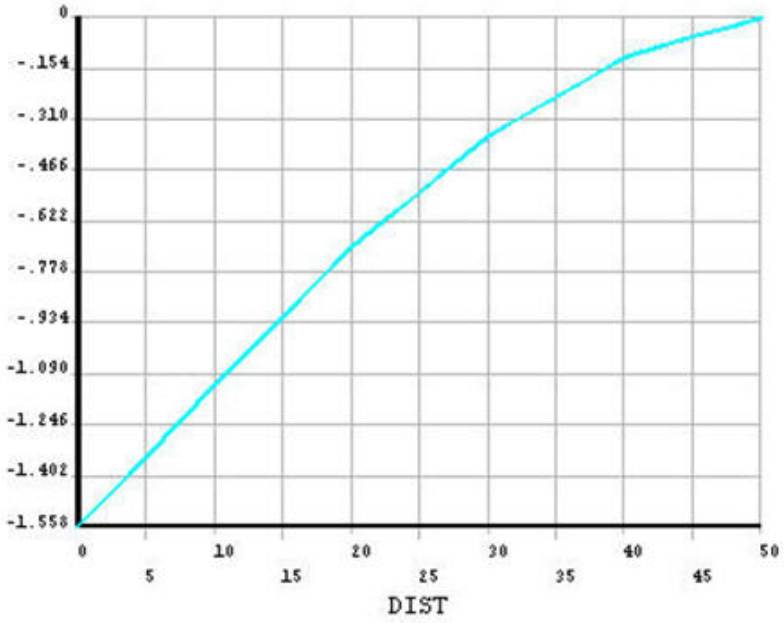

Displacement for a sheet and the ball in function of the time

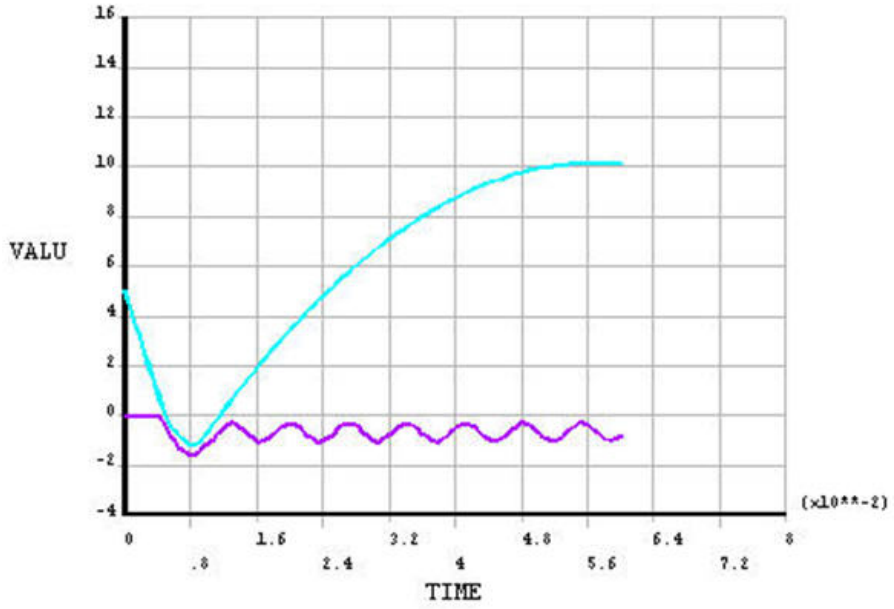

Evolution of the stress of Von Mises for the sheet in function of the time

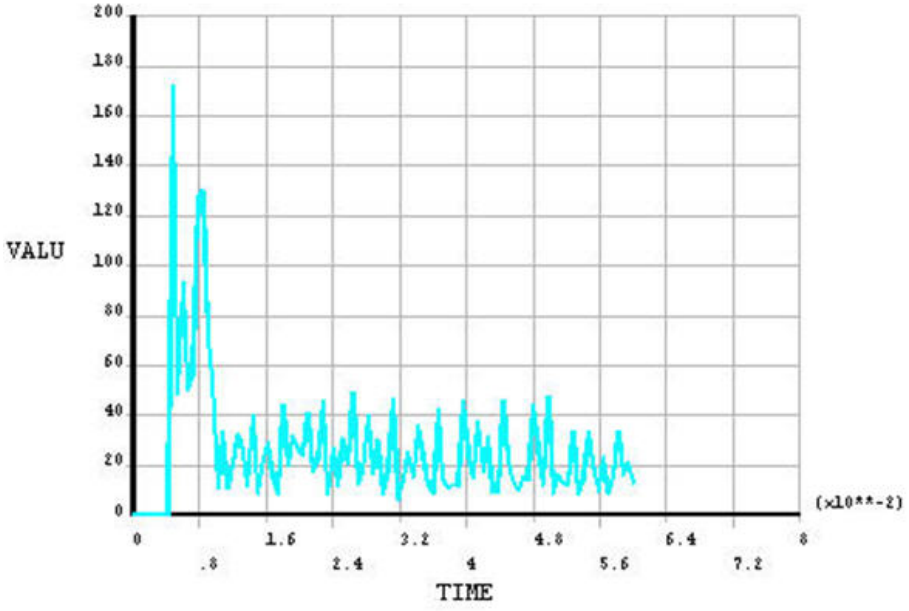

At the velocity of 2000 mm/s

- ***Sheet of 0,1 mm:***

Displacement for a sheet in function of the distance

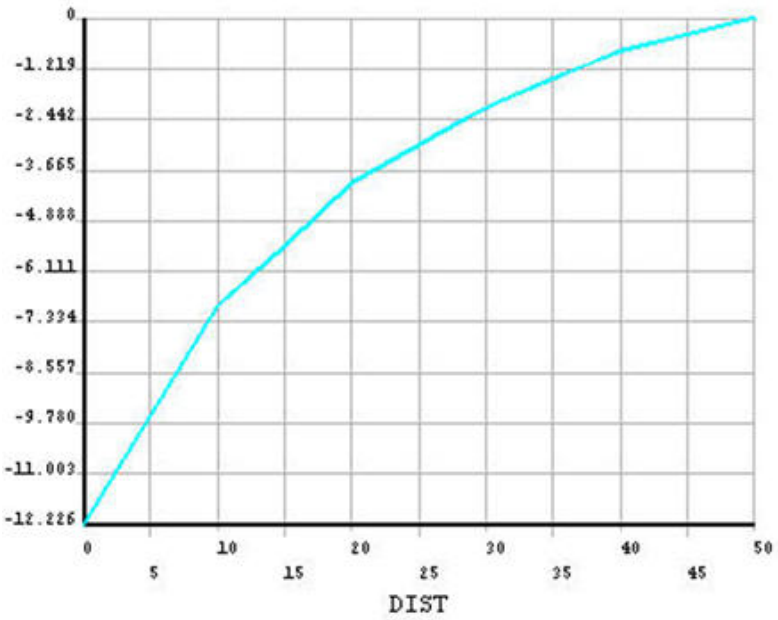

Displacement for a sheet and the ball in function of the time

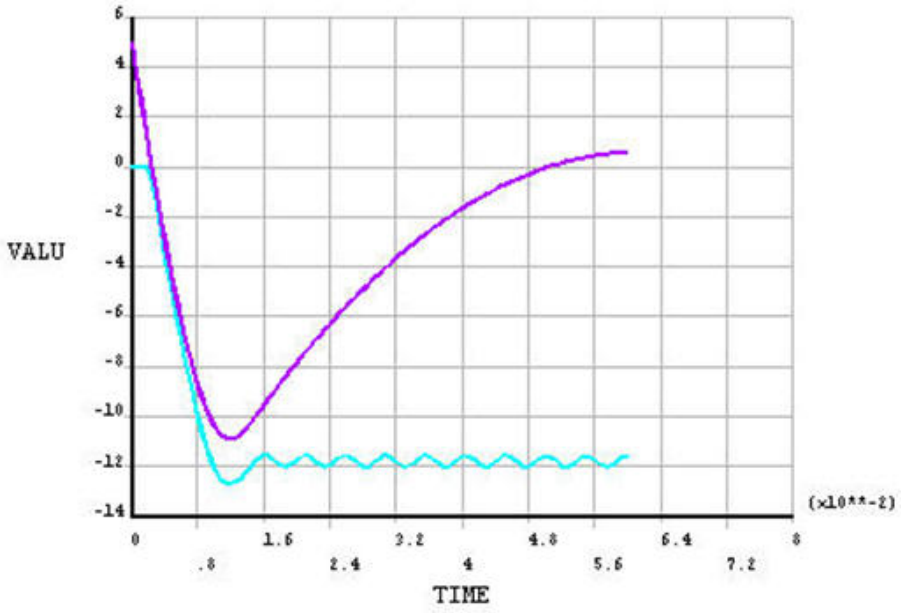

Evolution of the stress of Von Mises for the sheet in function of the time

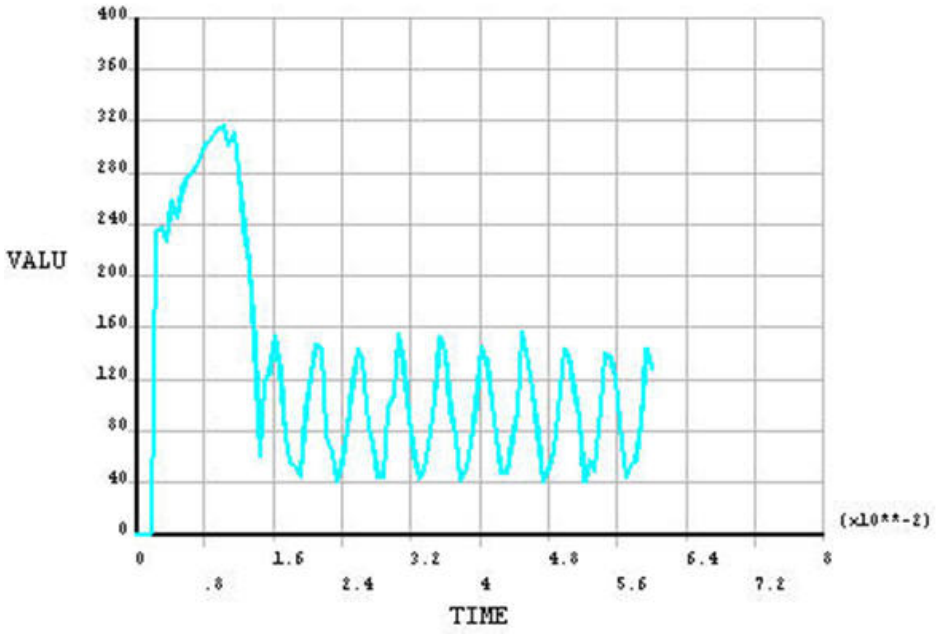

Evolution of the deformation for the sheet in function of the time

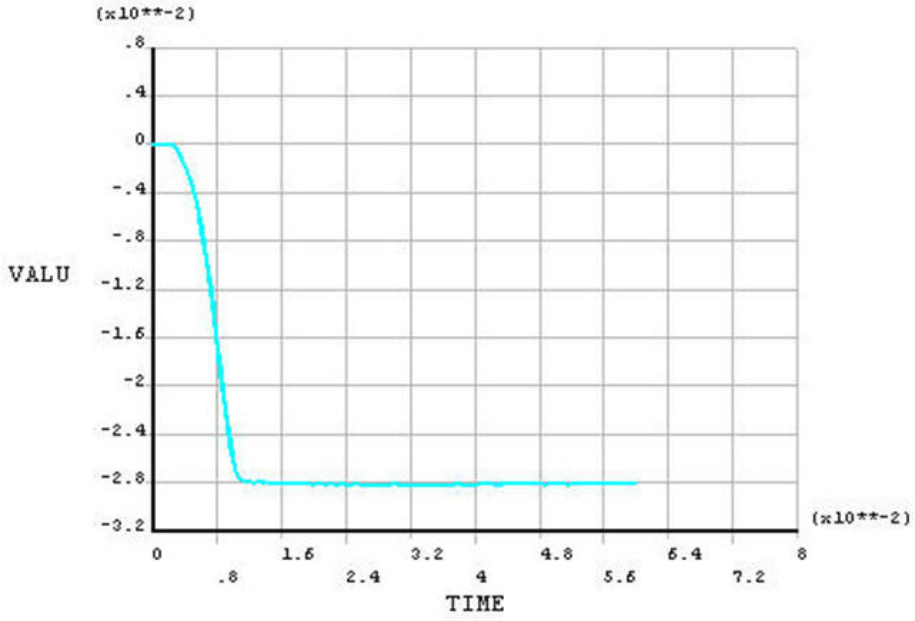

- ***Sheet of 0,5 mm:***

- **Displacement for a sheet in function of the distance**

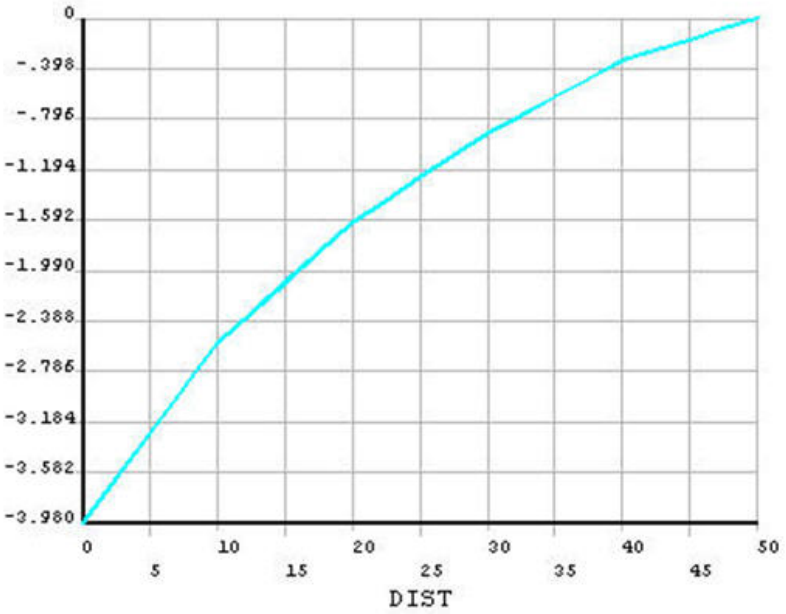

Displacement for a sheet and the ball in function of the time

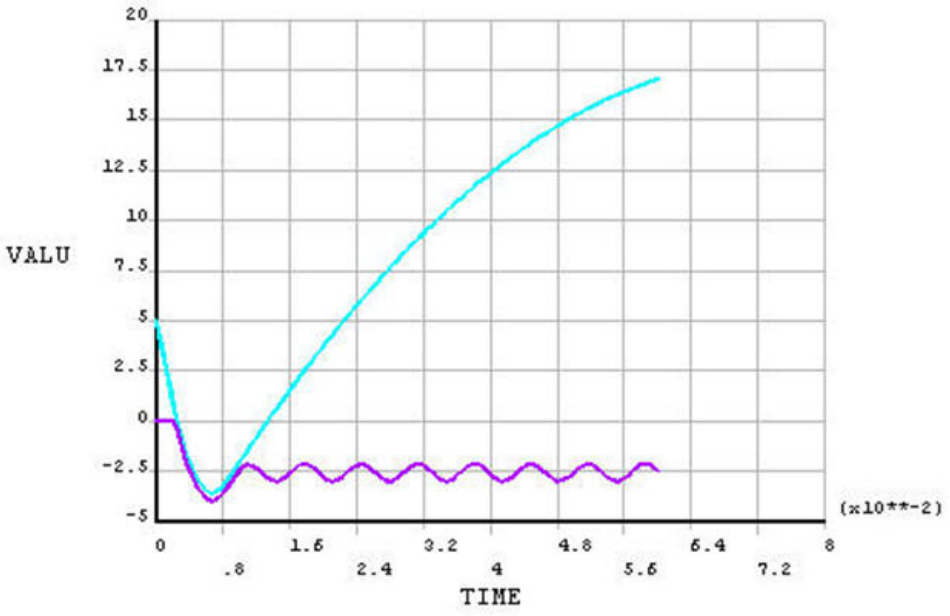

Evolution of the stress of Von Mises for the sheet in function of the time

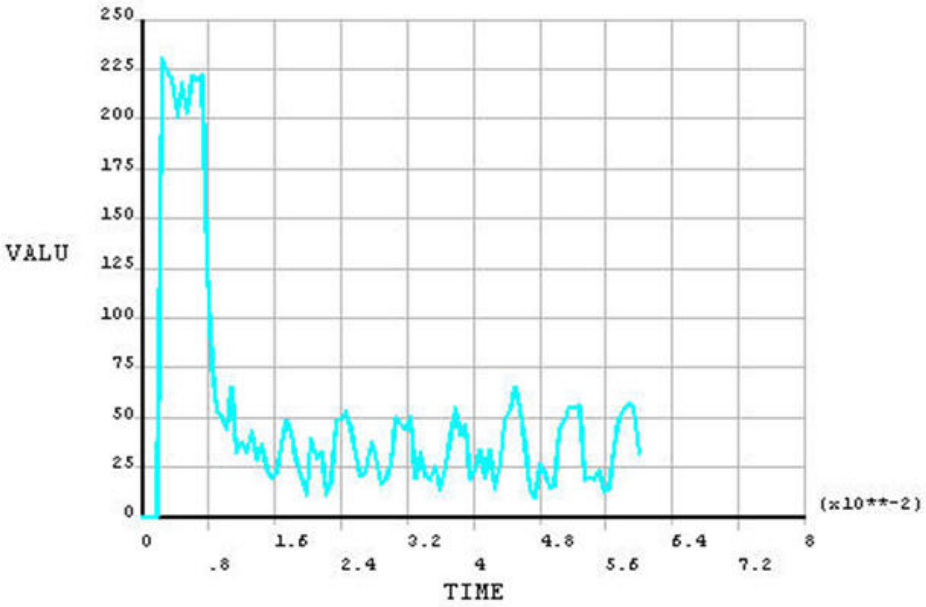

Evolution of the deformation for the sheet in function of the time

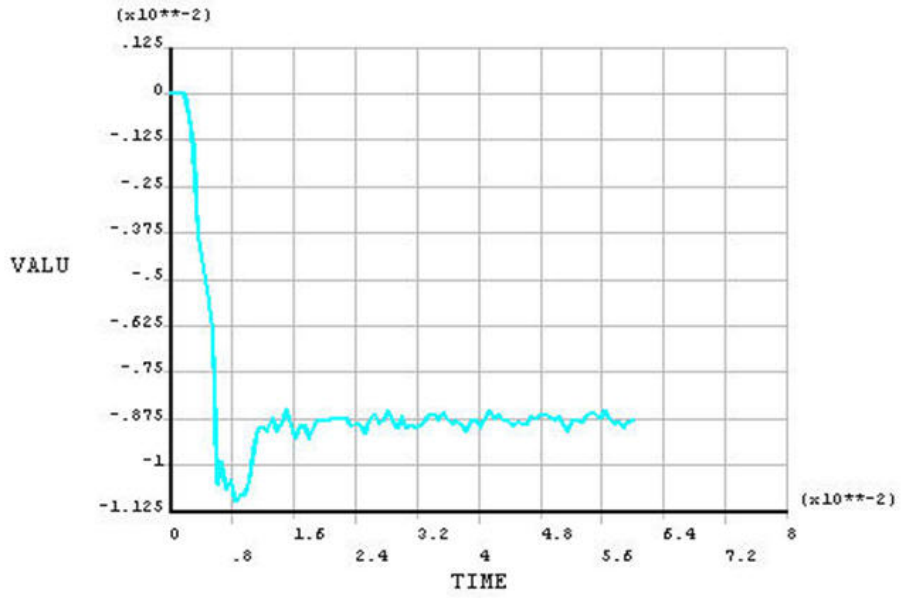

- ***At the velocity of 5000 mm/s:***

➢ ***Sheet of 0,1 mm:***

Displacement for a sheet in function of the distance

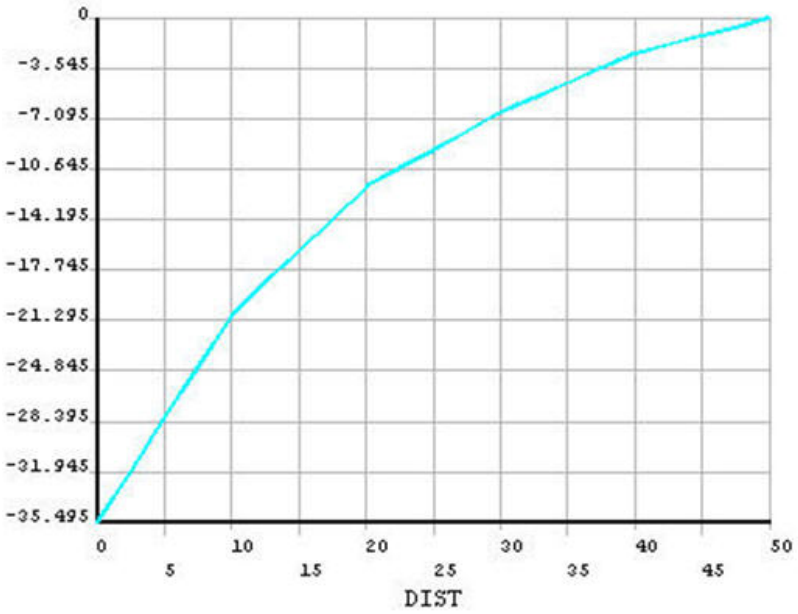

Displacement for a sheet and the ball in function of the time

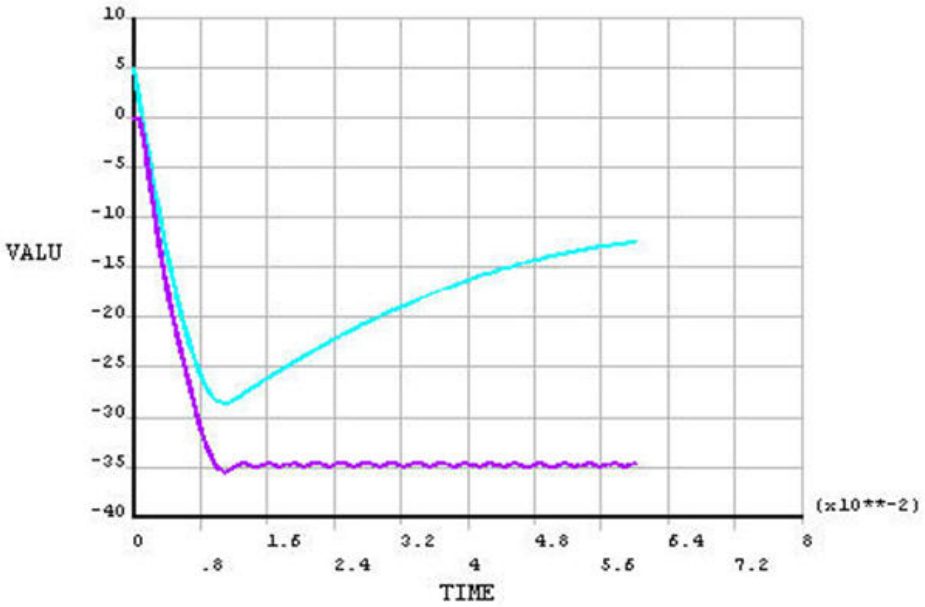

Evolution of the stress of Von Mises for the sheet in function of the time

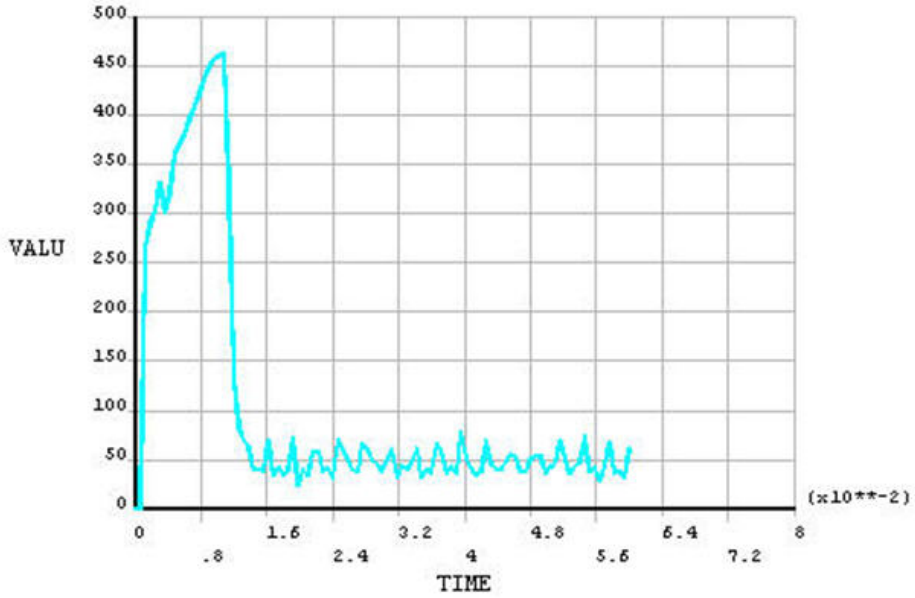

Evolution of the deformation for the sheet in function of the time

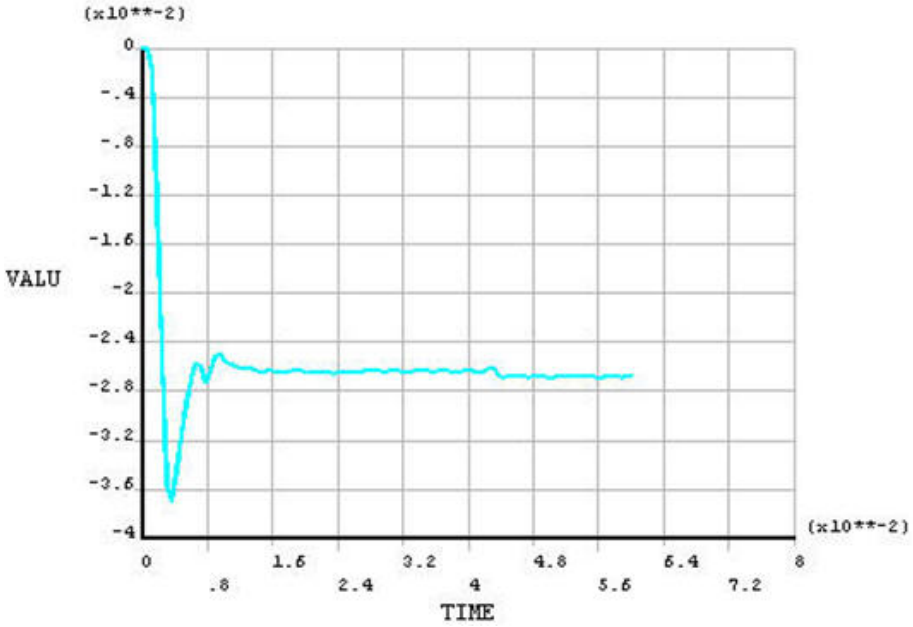

- ***Sheet of 0,5 mm:***

Displacement for a sheet in function of the distance

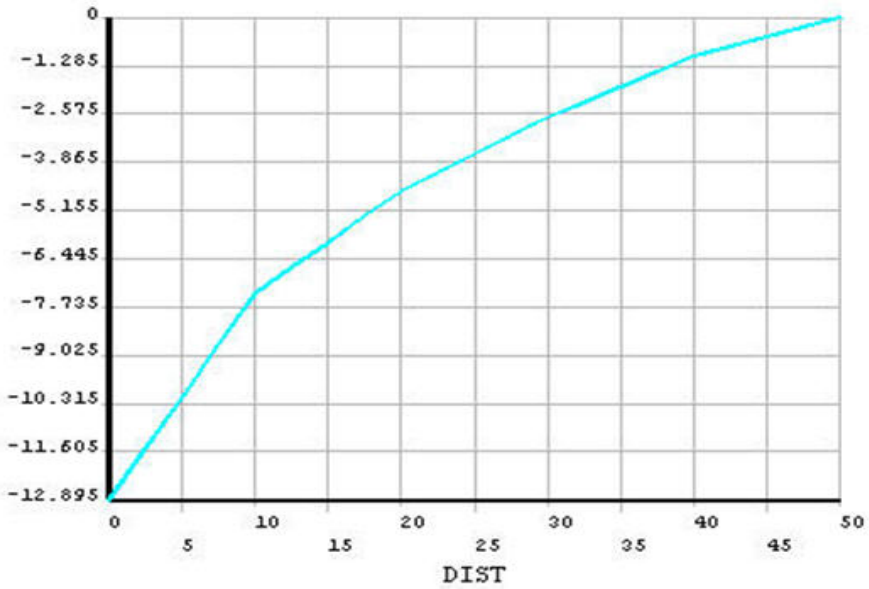

Displacement for a sheet and the ball in function of the time

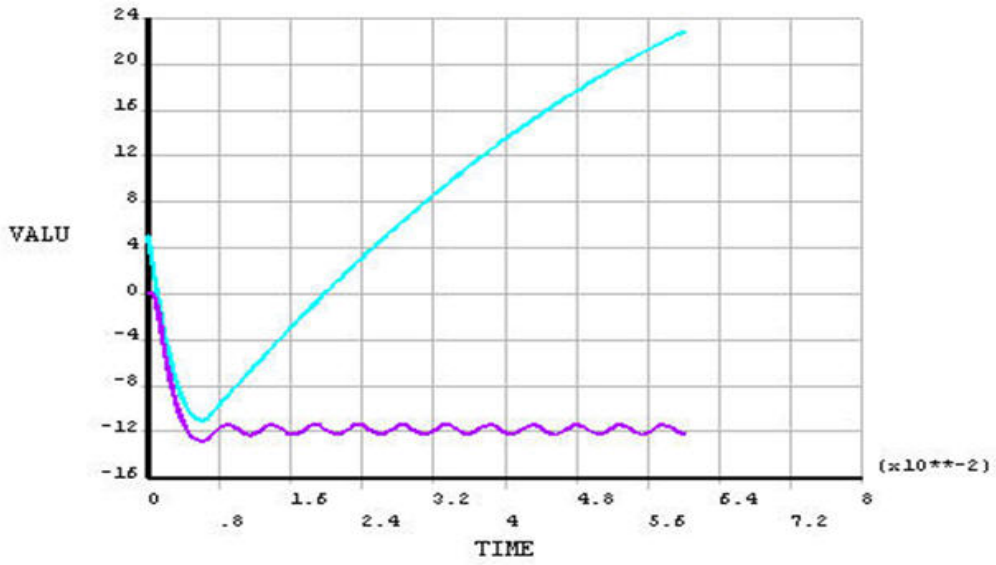

Evolution of the stress of Von Mises for the sheet in function of the time

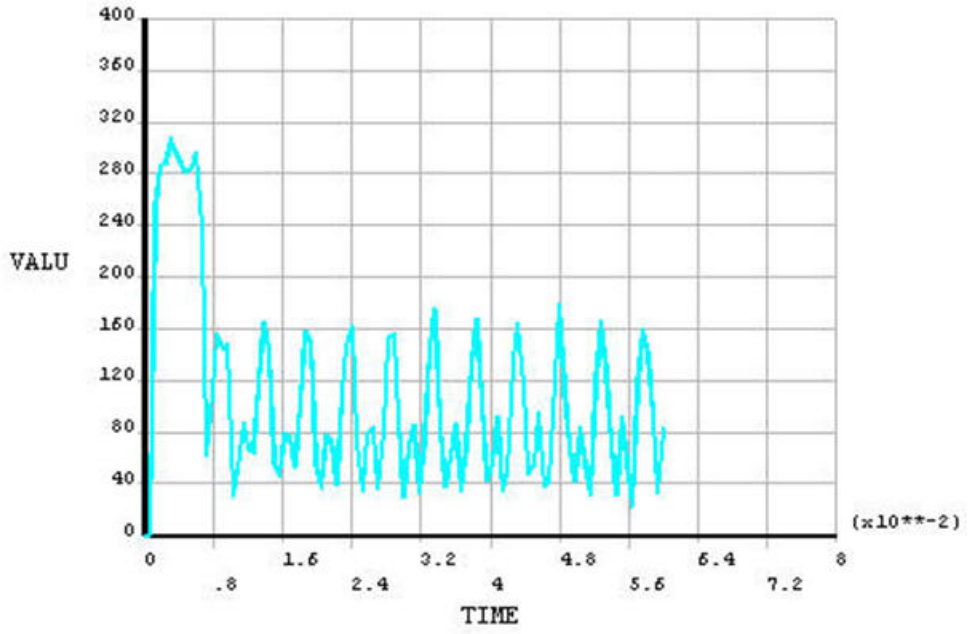

Evolution of the deformation for the sheet in function of the time

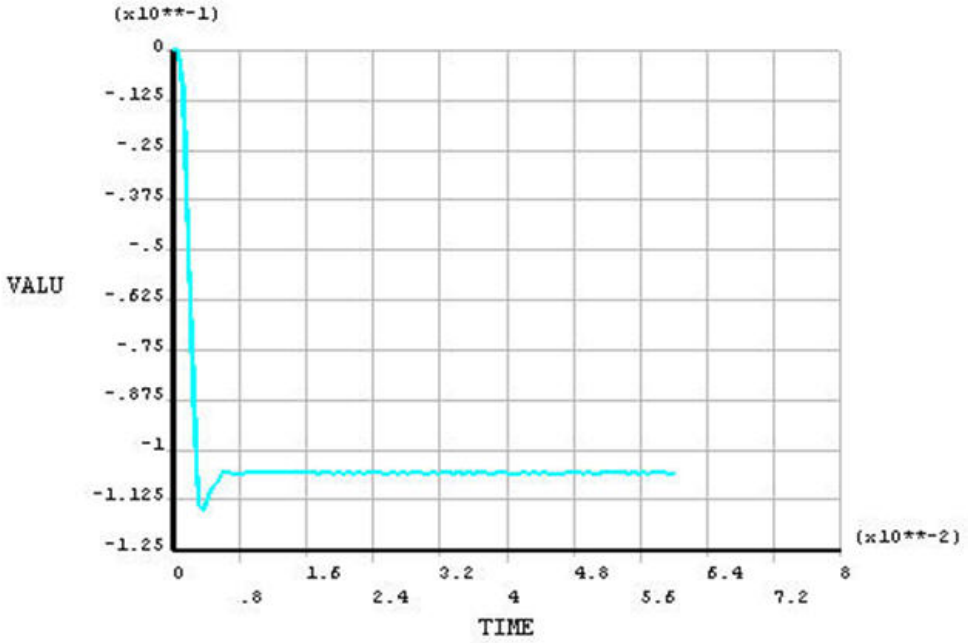

Annexe 4

Evolution of the stress in function of the energy of the sphere

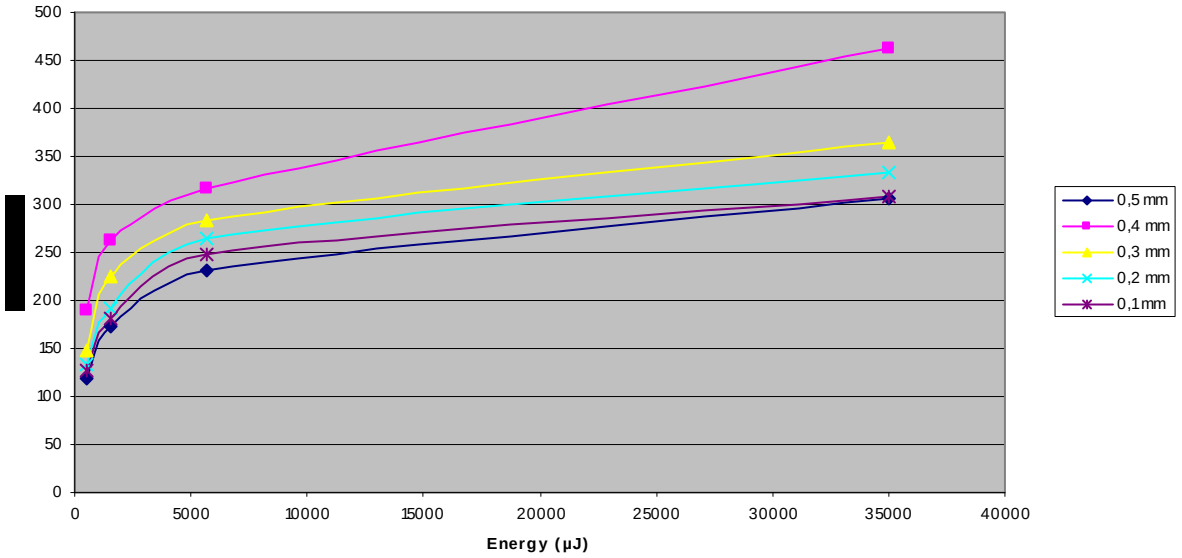

Evolution of the displacement in function of the energy of the sphere

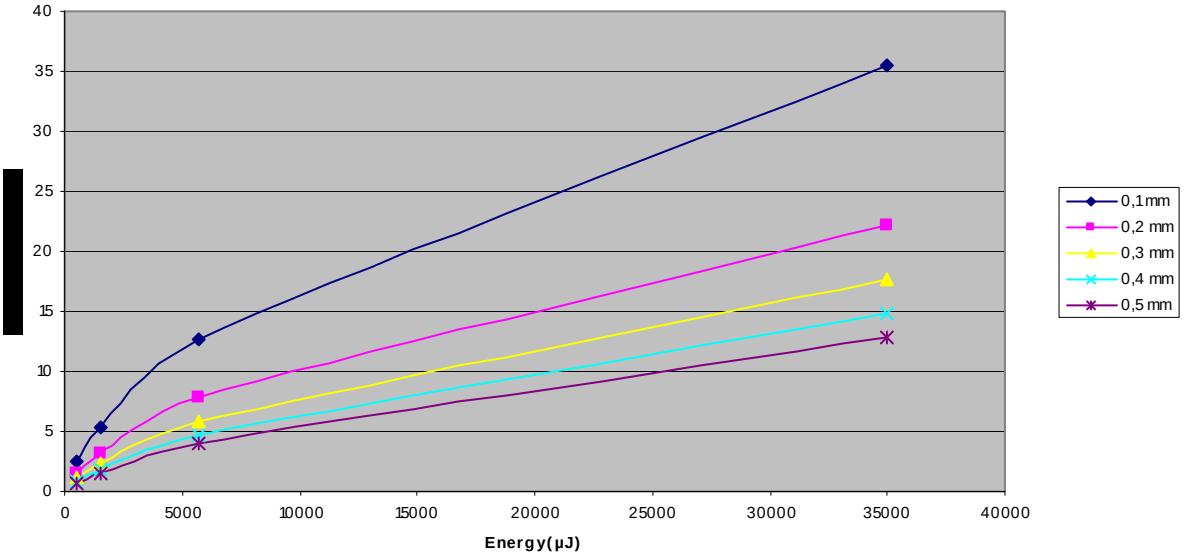

I.A.11. Bibliography :

[1] Beltzer, A.I. 1990. Variational and finite element method: a symbolic computation approach. Berlin.
[2] de Weck, Olivier - Young Kim, Il. January 2004. Finite Element Method, Engineering Design and Rapid Prototyping [read April 22nd 2005] http://ocw.mit.edu/NR/rdonlyres/Aeronautics-and-Astronautics/16-810January--IAP-2004/21C7E953-505B-41C7-8DB7-25A0E5D98B4E/0/l4_cae.pdf
[3] Ansys guide
[4](Getting Started with LS-DYNA 2002: 1-1).
[5] (LS-DYNA Developed by Livermore Software Technology Corp. Material Models: 1)
[5] *www.matweb.com*
[6] *www.goodfellow.com*

Section II.B

The Second test case is sheet of Glare and a sheet of aluminium alloy bounded on the side, submitted to the impact of a sphere made of steel with an initial velocity.

III.B.1 - **INTRODUCTION**

The main objective of this work is to achieve a sufficiently good simulation of GLARE behaviour when it suffers a impact using the ANSYS LS DYNA Software. The main application of GLARE is in the aerospace industry where it is used in some parts of the fuselage of aircraft. Hence, GLARE needs to be resistant to low velocity impacts: bird strike, baggage and ground handling equipment, runway debris, etc. These tests are time consuming, expensive and difficult to perform, so the ability to simulate these tests is of high importance.

III.B.2 - **WHAT IS GLARE ?**

GLARE (GLAss REinforced) is the name of a glass fibre reinforced metal laminate, developed at the TU-Delft. Alternating sheets of thin aluminium foils and high strength glass fibre epoxy prepegs are used as layers for this composite. There are several types of GLARE that differ one from another in the thickness and the number of the layers. Being a very recent material, there is little information about it; GLARE shows excellent properties in fatigue. Hence, Glare is suitable as a material for the pressurized fuselage of commercial aircraft. GLARE has become famous for its application in the new large aircraft, the Airbus A-380 (built to compete with Boeing's 747 "jumbo jet") and will be used in the upper part of its fuselage. GLARE main advantages are[1] :

- Damage tolerance
  - fatigue
  - impact
  - corrosion
- Reduced weight
- Fire resistance

Figure III.B.1: ***Layers of the Glassfibre Reinforced Metal Laminate GLARE***

Figure III.B.2 a: ***Airbus***

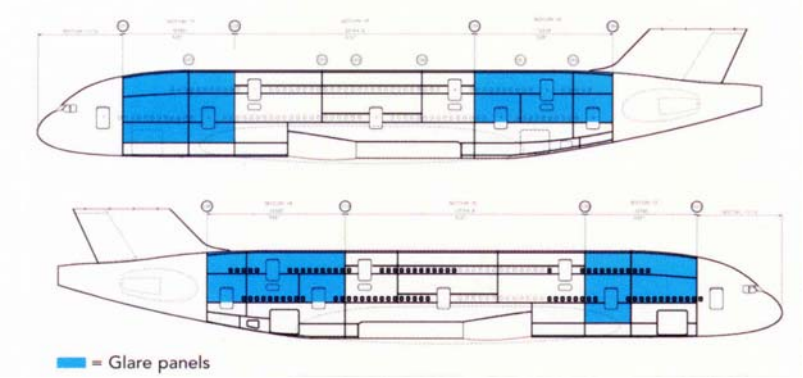

Figure III.B.3: ***Airbus secion***

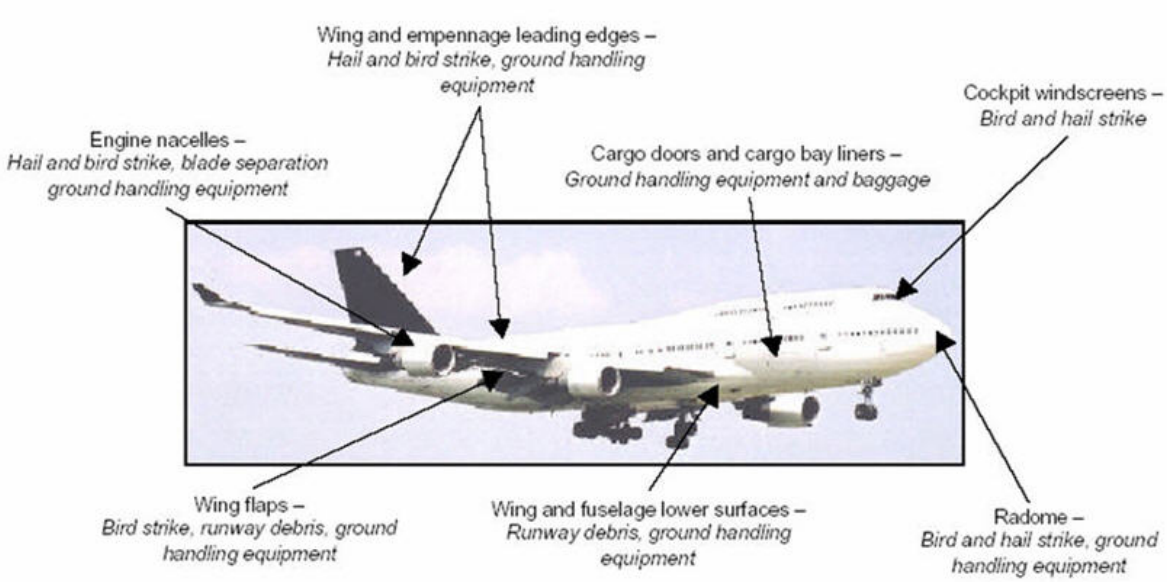

FigureIII.B.4 Impact prones areas on modern transport aircraft

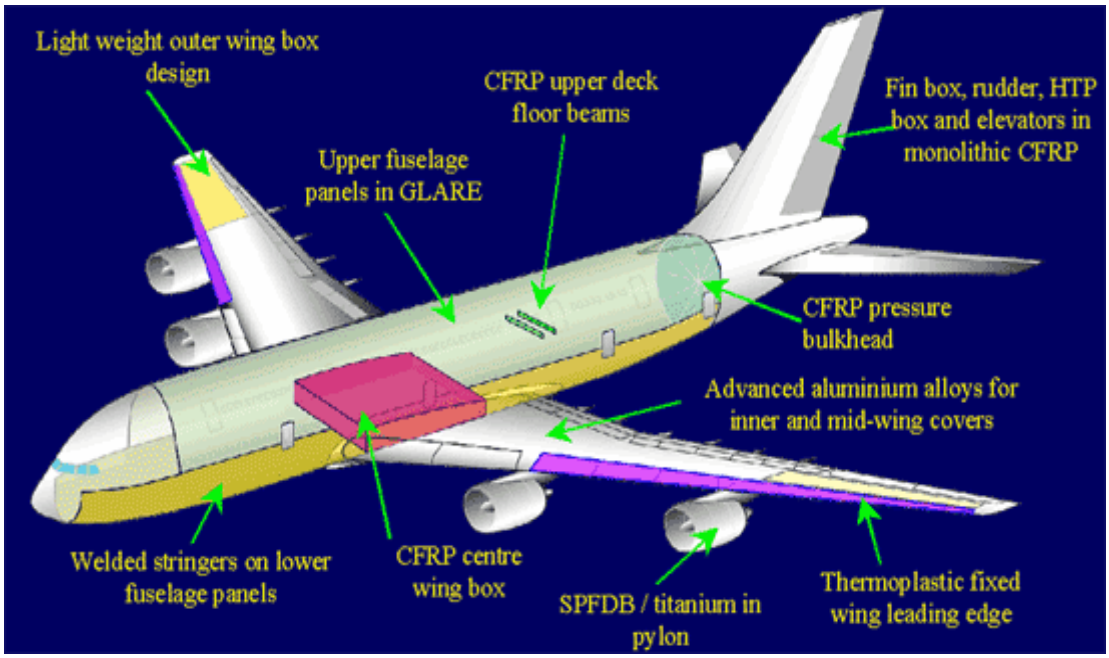

Figure III.B.5**: *Advanced Materials used in aircraft*.**

Legend
CFRP: Carbon Fiber Reinforced Polymer;
HTP: High Tensile Polymer;
SPFDB: Super Plastic Forming and Diffusion Bonding of Titanium and Aluminium;

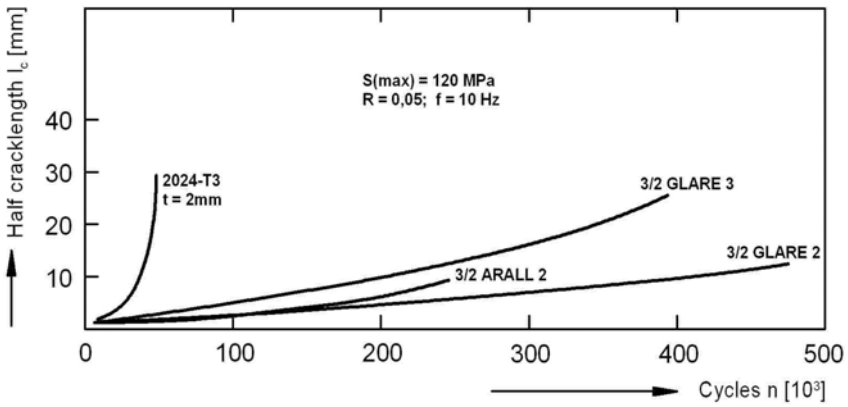

Figure III.B.6: ***Crack Growth behaviour of unidirectional GLARE 2, cross-plied GLARE 3, ARALL 2 and 2024-T3 for a fuselage loading***

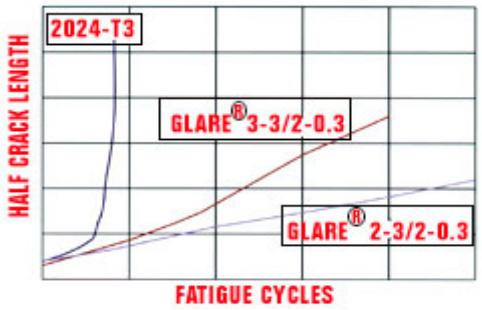

Figure III.B.7: ***Fatigue cracks are less likely to form and take longer to grow in Glare than with solid 2024 aluminium. The Glare layers can be tailored for different characteristics.***

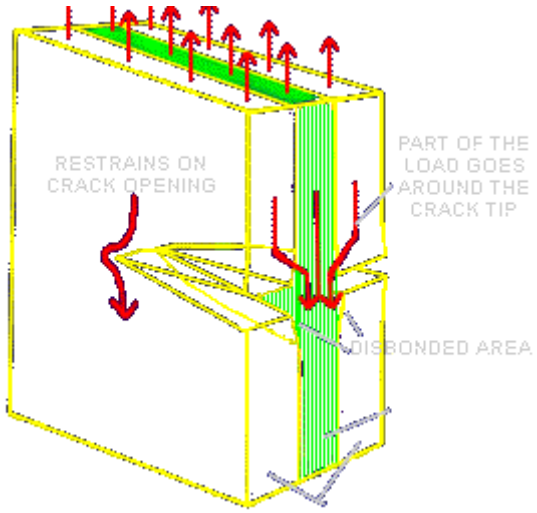

Figure III.B.8: ***Mechanism that Retards Crack Growth.***

FML have a high fatigue resistance, achieved by the intact bridging fibres in the wake of the crack, which restrain crack opening. Controlled delamination in the material enables some crack opening without fibre failure. The laminates can be formed and machined like aluminium alloys and have the high specific strength of composite materials: they combine the best of two worlds. The FML can be stretched after curing in order to reverse the internal stress system in the material. Due to the difference in the thermal expansion coefficients, the as-cured laminate has tensile stresses in the aluminium layers and compressive stresses in the fibre layers. During the stretching operation the aluminium layers deform plastically, while the fibre/epoxy layers remain elastic. Therefore residual stresses are present in the laminate after unloading. After the post-stretching operation the laminates have a favourable compressive (crack closing) stress in the aluminium sheets and a tensile stress in the fibres. Several types and lay-ups are commercially available[1].

FATIGUE OF FIBRE METAL LAMINATES

Fatigue strength is what fibre metal laminates where designed for, and they do excel in it.

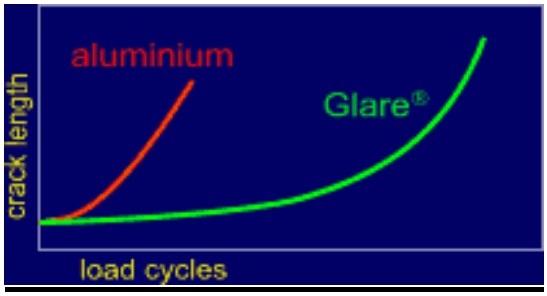

Figure III.B.9: Graphic that shows GLARE'S superiority over aluminium when fatigue resistance is concerned.

FIRE RESISTANCE

Due to the layered build up of GLARE and ARALL remarkable burn-trough properties.

Due to the high melting temperature of the glass fibre (1500 °C) the fibres remained intact, whereas the epoxy burned and formed a carbon layer around the fibres. Delamination of the laminate took place, which caused a very effective insulation as can be seen in the picture.

No flame penetration was observed for Glare after 10 minutes, whereas the 2024-T3 samples showed burn-through within 100 sec at approximately 1150 °C. [1]

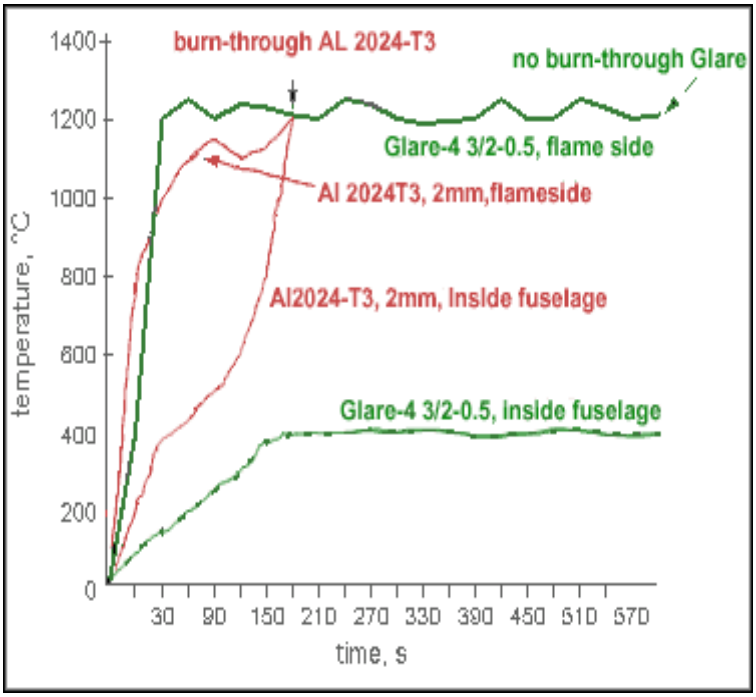

Figure III.B.10: ***Comparison of the Fire resistance properties between Aluminium and GLARE***

III.B.3 - **METHODOLOGY OF THE WORK**

The goal of this work was to find a reasonably good way to perform a simulation on the behaviour of GLARE under a low velocity impact. Easier said than done, modelling GLARE in ANSYS is difficult because of the interaction between layers.

The scarcity of information on GLARE made progression slow and the only available information on it was on the internet and even there everything found was generic, consisting almost exclusively of magazine articles. ANSYS tutorials and a previous thesis gave some guidance but advancing on this was like shooting in the dark. Comparing GLARE to aluminium is very important because GLARE is supposed to substitute aluminium and because the mechanical properties of aluminium are similar to those of GLARE so it is a point of reference. It was decided to simulate GLARE and aluminium and then compare the results.

III.B.4 - **GLARE AND FIBER METAL LAMINATES**

Composite materials have been subject of permanent interest of several industries specialists during the last few decades. The first military composite applications in the aircraft industry were in the thirties and forties and triggered off their commercial use after the Second World War. The use of modern composites enables significant weight reduction in the structures. Composites offer many advantages when compared to alloys, especially high strength and stiffness, excellent fatigue properties and corrosion resistance. On the other side, they have several disadvantages like low fracture toughness and moisture absorption. In addition, inspections can be difficult and maintenance complicated or impossible. These arguments speak for the use of aluminium alloys in primary aircraft structures and they are the main reason why airworthiness authorities did not accept composite materials in a wider scale. [2]

During the last few decades, many scientists aimed their efforts to develop a fatigue resistant material, which would keep low weight and good mechanical properties of aluminium alloys. The most successful in this field was the team of Prof. Schjive at Delft University of Technology, which developed fibre metal laminates (FML) called ARALL (Aramid Reinforced Aluminium Laminates) and GLARE (GLAss REinforced) at the beginning of the eighties. FML are a new group of aerospace materials that join the advantages of aluminium alloys and composites, having high strength and excellent fatigue properties. They are created by stacking thin aluminium sheets (0.2-0.5mm) and prepegs containing aramid or glass fibres. GLARE and ARALL started to be produced commercially by the structural laminates company formed by Alcoa and Akzo at the beginning of the nineties. Both

types of FML were already used as a replacement of aluminium sheets in thin walled structural applications and also tested in thicker lay-ups for lug applications. Selection of different types of laminate components together with the possibility to vary the volume fraction and fibre orientation offers unlimited number of material properties of the resulting product. Large scale investigation at the Delft University of Technology led to the definition of the most appropriate FML configurations that cover a wide range of possible applications. ARALL was used for production of the C17 aft cargo door, GLARE for cargo floor applications on several Boeing 777 airplanes, lower wing panels of the Fokker 27, etc. Several FML test programs are under way at Airbus consortium and GLARE was chosen as the fuselage skin material of the new high capacity plane A3XX, which should enter in the production line as the A380 in 2006.

Studies of carbon fibre use in FML concept were also performed. Laminates called CARE (Carbon REinforced) are not commercially available at this time. Carbon fibres are relatively expensive but thanks to the growing volume production, they became more available and the wide scale of their mechanical properties (strength, stiffness) makes them very attractive. In addition, the application of different alloys in FML concept is being studied e.g. titanium.

There are two types of FML currently available ARALL and GLARE. Their configuration is shown in table xxx. Other types are in phase of development and testing. Especially combinations of aluminium alloys and carbon fibres called CARE seem promising. The use of titanium alloys was also tested.

Table I : Commercially Produced Types of FML [2]

	ARALL 1	ARALL 2	GLARE 1	GLARE 2	GLARE 3	GLARE 4
Alloy Type	**7075-T6**	**2024-T3**	**7075-T6**	**2024-T3**	**2024-T3**	**2024-T3**
Metal Sheet Thickness [mm]	**0.3**	**0.2-0.4**	**0.3**	**0.2-0.4**	**0.2-0.4**	**0.2-0.4**
Type of Fibre	**Aramid**	**Aramid**	**R-glass**	**R-glass**	**R-glass**	**R-glass**
Prepreg Thickness [mm]	**0.22**	**0.22**	**0.25**	**0.25**	**0.25**	**0.375**
Fibre Orientation	**II**	**II**	**II**	**II**	**X(50/50)**	**X(70/30)**

Note:
II: Uniaxial fibre orientation, two prepreg layers [0/0];
X(50/50): Biaxial fibre orientation, two prepreg layers [0/90];
X(70/30): Biaxial fibre orientation, three prepreg layers [0/90/0];

III.B.4.1 **GLARE**

Laminates based on aluminium alloys and glass fibre/epoxy prepegs are currently the most available and cost effective. Thin aluminium alloy sheets (0.2-0.4mm) are used for this type of FML. There are two types of alloys with different mechanical applications. 2024-T3 alloy has very good fatigue resistance and high ductility. 7075-t6 or 7475-T76 have high strength, good fatigue properties and lower ductility. Glass fibres with a relative volume of about 60% in epoxy matrix (3M, AF-163-2) form the optimal prepreg layer of FML. Prepregs are 0.125mm thick. Two prepregs are used together in most cases so the resulting thickness of a prepreg layer in the laminate is of 0.25mm. GLARE 4 presents one exception where three prepregs with a total thickness of 0.375mm are used. [2]

Table II : Mechanical Properties of FML Components

	FIBRE			PREPREG			ALUMINIUM	
	Aramid Twaron HM	Glass R-Glass	Carbon T300	Aramid (50%)	Glass (60%)	Carbon (60%)	2024-T3	7075-T6
R_m [MPa]	2800	4400	3500	1400	2500	2100	455	538
$R_{p0.2}$ [MPa]	-	-	-	-	-	-	359	483
E [GPa]	125	84	230	62.5	51.6	138	72.5	71.1
ε_{ult} [%]	2.3	5.1	1.5	2.3	5.1	1.5	14	8
ρ [Kg/m^3]	1450	2540	1770	1300	1980	1570	2780	2780

Table III: Different Types of Fibre Metal Laminates

grade	Al alloy	pre-preg	orientation	thickness (mm)	post stretch
ARALL 1	7475-T6	aramid-epoxy	unidirectional	0.2 - 0.4	0.4%
ARALL 2	2024-T3	aramid-epoxy	unidirectional	0.3 - 0.4	no
ARALL 3	7475-T76	aramid-epoxy	unidirectional	0.3 - 0.4	0.4%
GLARE 1	7475-T76	glass-epoxy	unidirectional	0.3 - 0.4	yes
GLARE 2	2024-T3	glass-epoxy	unidirectional	0.2 - 0.4	no
GLARE 3	2024-T3	glass-epoxy	0°/90° cross-ply	0.2 - 0.4	no
GLARE 4	2024-T3	glass-epoxy	0°/90°/0° cross-ply	0.2 - 0.5	no
GLARE 5	2024-T3	glass-epoxy	0°/90°/90°/0° cross-ply	0.2 - 0.5	no

Note:

The laminates can be applied in various thicknesses, e.g. a 3/2 lay-up means a laminate with three aluminium layers and two intermediate fibre/epoxy layers: [Al/pre-preg/Al/pre-preg/Al]. The fibre/epoxy layers of a 3/2 lay-up can be multiple cross-plied 0/90 layers or can be unidirectional, e.g.: [Al/0°/90°/Al/0°/90°/Al] is a cross-plied lay-up.

The surface of aluminium sheets is anodized and primed. This surface treatment provides good strength of the bond and good corrosion protection in case of eventual moisture penetration into the adhesive joint. Chromic or phosphoric acid anodizing is used. Aluminium cladding of outer laminate sheets can be used to increase the corrosion resistance. At the end of the curing cycle in a autoclave (at increased temperature and pressure, depending on type of matrix, usually around 120^0C and 0.3-1MPa during 90 minutes) the residual stress in all layers develops. It is caused by different thermal expansion coefficients of aluminium and prepeg. Tensile residual stress remains in aluminium layers and compressive in prepeg layers. This laminate condition is called 'as cured'. The orientation of the residual stress is possible to reverse by plastic deformation of the entire laminate sheet. This procedure called 'post-stretching' is used mostly for laminates based on 7075-T6 and 7475- T76 that do not have such good fatigue properties as those of 2024-T3. Compressive residual stress in aluminium layers significantly improves the fatigue behaviour of the laminate.

GLARE exhibits very good strength, especially in the fibre direction. It has slightly lower stiffness when compared to aluminium. Fatigue life of GLARE specimens is 10X-100X higher than that of aluminium alloys. [2]

Table IV: Mechanical Proprieties of FML

	t_{AL}	t_{pr}	R_m [MPa]	$R_{p0.2}$ [MPa]	E [GPa]	ρ [Kg/m^3]
ARALL1	**0.30**	**0.22**	**897**	**535**	**67.5**	**2160**
ARALL2	**0.30**	**0.22**	**849**	**411**	**68.3**	**2160**
GLARE1	**0.30**	**0.25**	**1494**	**530**	**62.2**	**2420**
GLARE2	**0.20**	**0.25**	**1670**	**416**	**60.9**	**2340**
	0.30	**0.25**	**1449**	**406**	**63.0**	**2420**
	0.40	**0.25**	**1295**	**399**	**64.5**	**2470**
GLARE3	**0.30**	**0.25**	**849**	**382**	**51.3**	**2420**

Note:
All values are for longitudinal direction (L) and laminate thickness t>4 mm.

III.B.4.2 **ARALL**

ARALL laminates are also based on thin aluminium alloy sheets in this case combined with prepegs containing Twaron HM aramid fibres produced by ENKA in a epoxy matrix AF-163-2 that was developed especially for use in ARALL by 3M. prepegs are 0.215mm thick and the relative fibre volume is 50%. Higher fibre volume is not recommended due to the decrease in adhesion between fibres and epoxy matrix and because of the danger of fibre pulling out from the matrix. Another disadvantage of aramid fibres is

the low resistance to compressive deformation. Because of this it is necessary to 'post-stretch' the ARALL laminate sheets after curing, and to reverse the residual stress to tensile in prepreg layers and compressive in aluminium layers.

ARALL laminates are produced only with uniaxially fibres. They exhibit lower strength but higher stiffness when compared to GLARE. Fatigue resistance is the best in the case of asymmetric tensile cycle loading. Thanks to the low density of aramid fibres ARALL is the lightest of the currently produced types of FML.

III.B.4.3 **CARE**

CARE is based on a combination of thin aluminium alloy sheets and carbon fibres prepregs. Application of prepregs containing various carbon fibres from high strength to high modulus types were tested at Delft University of Technology.

The possibility of galvanic corrosion presents a potential problem when combining carbon fibres and aluminium. The fibres in the prepregs are covered by an epoxy matrix, which should represent an isolating layer, but in spite of that, direct contact between fibre and aluminium can occur. Only two ways of preventing the eventual galvanic cell formation were developed and tested so far:

- aluminium sheets covered by very thin (0.02mm) thermoplastic layer based on polyetherimide (PEI)
- thin glass fibre prepreg (0.1mm) isolates the carbon fibre prepreg on both sides

CARE laminates with uniaxially and biaxially oriented fibres were tested. They show similar strength as ARALL laminates. The stiffness of CARE strongly depends on the type of fibres used and can be twice as high when compared to ARALL or GLARE. Fatigue performance might be slightly lowered when PEI coating is used but it still is fully comparable with the fatigue performance of GLARE. Specific weight of CARE varies between values valid for ARALL and GLARE depending on the applied type of carbon fibres and isolating layer. There is no commercial version of CARE currently available.

III.B.4.4 **Titanium CARE or HTCL**

Information about this group of laminates is mentioned only in a few sources and is very brief. Series of tests were performed at Delft University in the beginning of the nineties. The material was named Titanium CARE. This type of FML is also subject of interest by scientists from NASA-Langley research centre where FML research is performed since the middle nineties under the name Hybrid Titanium Composite Laminate (HTCL). The fatigue performance dramatically increased when compared with monolithic titanium according with both sources. For elevated temperature applications (150-400ºC) the use of polymeric matrices (e.g. Poly-Imide (PI) or Poly-Ether-Keton (PEEK)) is necessary. Thermally loaded components of hypersonic aircraft or spaceships will be the potential applications of Ti-CARE or HTCL. [2]

PROBLEM DESCRIPTION

The simulation consists in impacting a Hollow semi-sphere into a square bounded sheet (of aluminium or GLARE).

GEOMETRY

The sphere diameter is of 15mm and the sheet as a surface of 100*100mm^2 with a variable thickness.

The sphere is thrown with a 1000mm.s^{-1} initial velocity 5mm above the sheet and submited to the acceleration of gravity (9.81mm.s^{-2}).

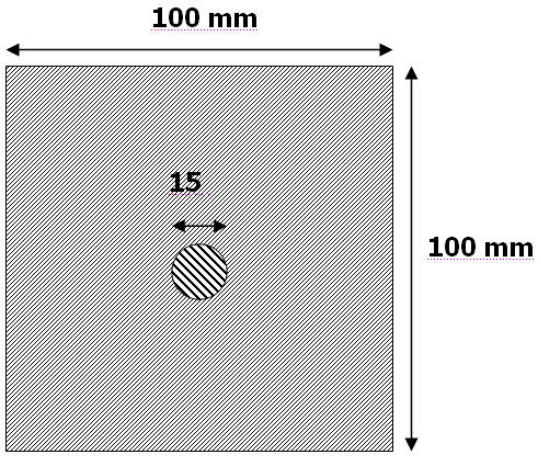

Figure III.B.11: Problem geometry

USED MATERIALS

The chosen materials were 2024-T3 aluminium, construction steel and S2 glass fibre. The aluminium and glass fibre where chosen because the GLARE layers are made of these materials. For the sphere it was used the construction steel. The materials properties are these:

Table V: Material Properties

	Materials	E [Gpa]	σ_{Yield} [MPa]	σ_{max} [MPa]	v	ρ[Kg.mm^{-3}]
Sheet	**Aluminium 2024-T3**	**73.1**	**345**	**483**	**0.33**	**$2.78*10^{-6}$**
	S2 Glass Fiber	**86.9**	**-**	**4890**	**0.23**	**$2.46*10^{-6}$**
Sphere	**Steel AISI 1045**	**205**	**530**	**625**	**0.29**	**$7.85*10^{-6}$**

*III.B.*5 - SIMULATION

*III.B.*5.1 PROBLEM SIMPLIFICATIONS

Due to the double symmetry it is possible to cut the sheet and the sphere in four and reduce the calculation time. To simplify even further the simulation the sphere was made hollow with only 1mm of thickness and divided in two, hence becoming a 1mm thick shell semi-sphere.

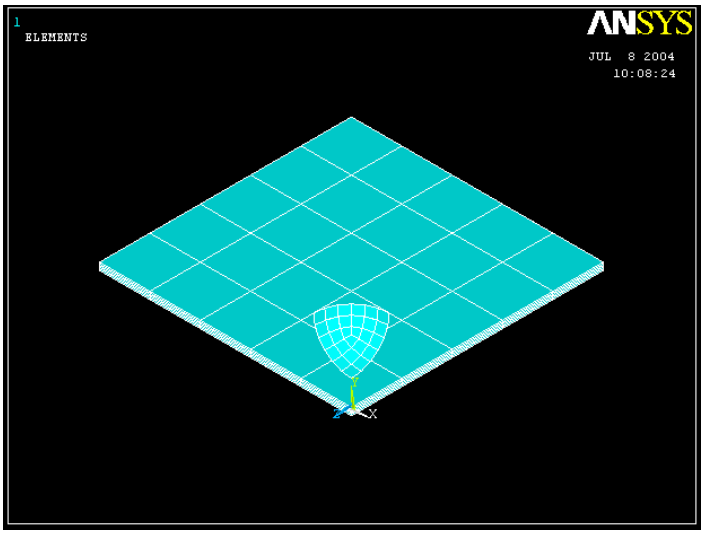

FigureIII.B.12*: **Double symmetry***

III.B.5.2 **ELEMENT TYPE**

For the sphere the THIN SHELL163 element was chosen because it is adequate to the dynamic role and to shell type objects like the semi-sphere.

The SHELL163 element is a four noded element with both bending and membrane capabilities. Both in-plane and normal loads are permitted. The element has twelve degrees of freedom at each node: translations, accelerations, and velocities in the nodal x, y, and z directions and rotations about the nodal x, y, and z-axis. This element is used in explicit dynamics analysis only.

The S/R co-rotational Hughes-Llu element formulation was chosen. The Hughes-Llu element formulation is based on a degenerated continuum formulation. This formulation results in substantially large computational costs, but it is effective when very large deformations are expected.

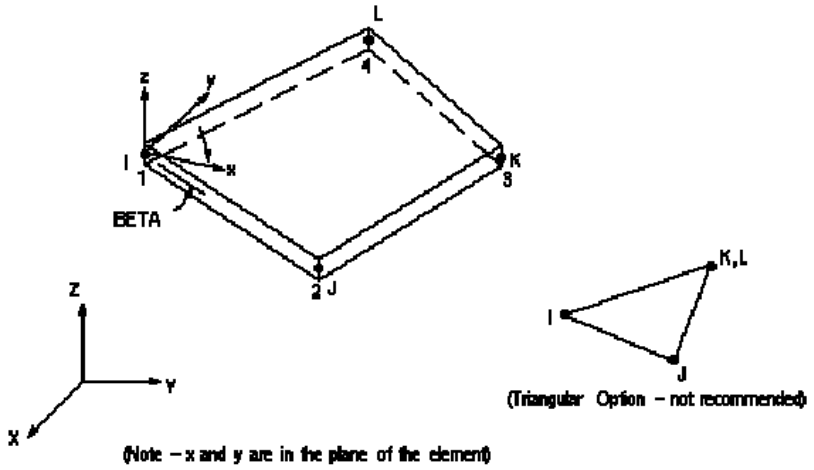

Figure III.B.13***: Shell163 explicit thin structural shell element***

For the sheet it was used the SOLID164 element. SOLID164 is used for the three-dimensional modelling of solid structures. The element is defined by eight nodes having the following degrees of freedom at each node: translations, velocities, and accelerations in the nodal x, y, and z directions. This element is used in explicit dynamic analysis only.

The element formulation chosen was the fully integrated selectively-reduced solid with lagrangian element continuum treatment.

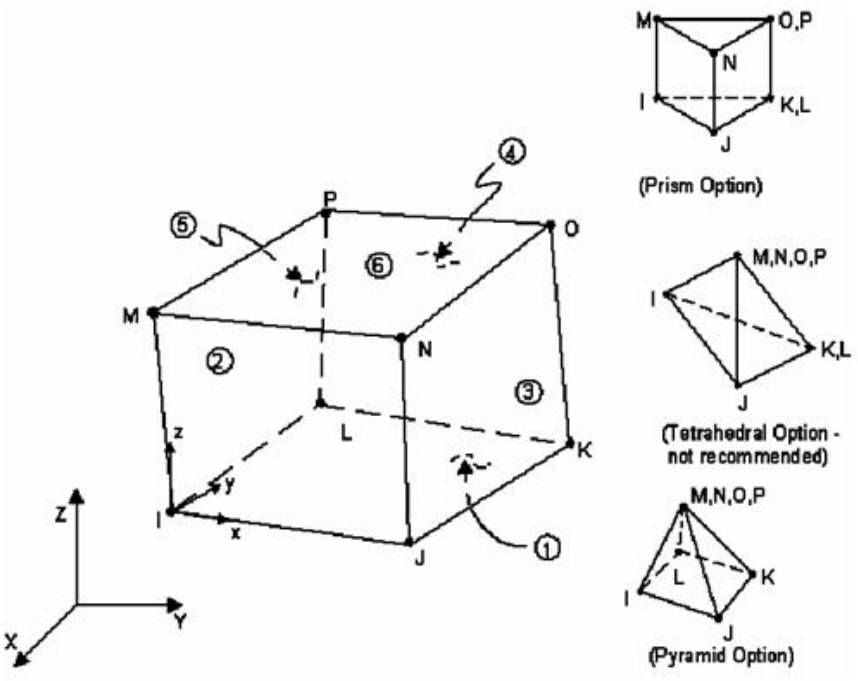

Figure III.B.14***: Solid164 explicit 3-D structural solid element***

III.B.5.3 **MATERIAL MODELS**

The number of material models necessary, depends on whether we are using an aluminium sheet or a Glare's one. In the first case we will use two material models, one for the steel sphere (rigid material) and the other for the aluminium sheet (nonlinear, inelastic, kinematic hardening, bilinear kinematic). In the case of GLARE since it is made of aluminium and glass fibre layers we will need three. Two of those were already mentioned above (steel and aluminium). For the glass fibre we will use the linear elastic isotropic model.

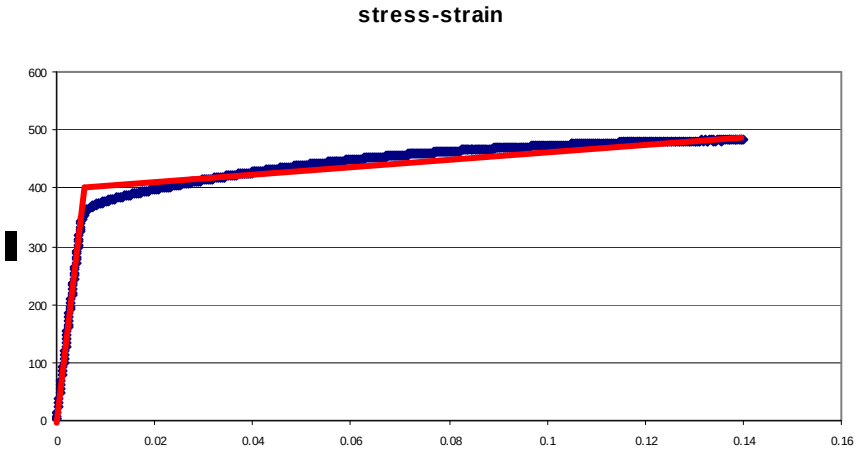

Figure III.B.15: ***Graphic showing the bilinear model of aluminium***

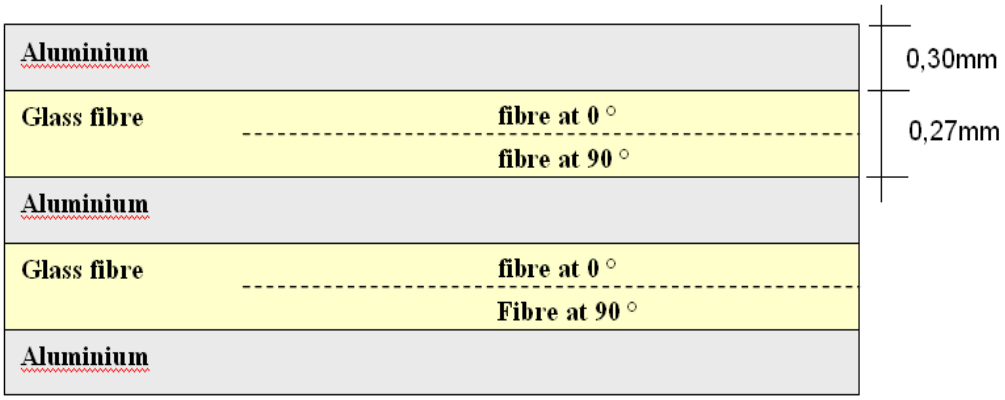

Figure III.B.16*: Representation of the several layers of GLARE*

III.B.5.4 **MESHING**

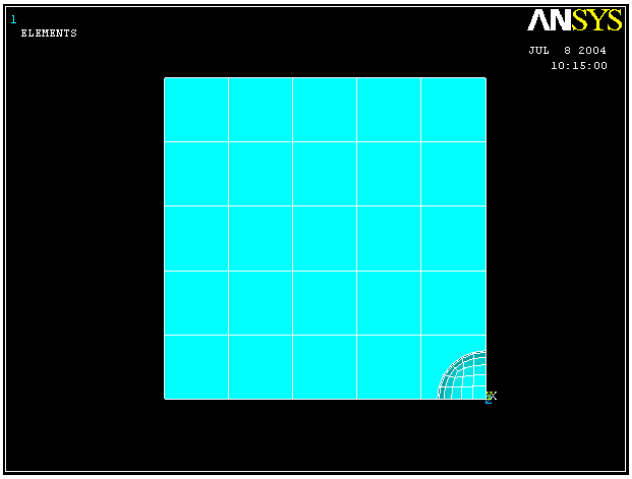

Figure III.B.17***: Image of the meshing done in one simulation***

An automatic meshing was done to the surface of the sphere, due to the not so simple nature of its shape. For the sheet it was decided to use the regular meshing. The element size of the mesh was of 2mm for the sphere and of 10mm for the sheet. In the sheet hexagonal elements were used instead of the quadrate ones used in the sphere. When GLARE was used, every layer had its mesh, this increased the simulation time substantially, and that is why the size of the mesh elements could not be greatly decreased, and therefore the reliability of the simulation was reduced.

III.B.5.5 **CONTACT PARAMETERS**

The contact definition is one of the key parameters to achieve a good simulation, but is also a very difficult parameter to choose, especially in the case of GLARE.

The automatic (ASTS) surface to surface contact type was selected to define the interaction between the sphere and the sheet. For the static and dynamic friction coefficient, due to the difficulty of finding these values they were given the "reasonable" value of 0.5.

In the case of Glare there is an additional contact due to the interaction between layers. With a tolerance within 0.1mm the element layers were merged in the hope that this would be enough.

SOLUTION PARAMETERS

SPHERE VOLUME

$$V = \frac{4}{3} \cdot \pi \cdot (R^3 - r^3)$$

With: R (external radius)=8mm
r (internal radius)=7mm
In this case it is a semi-sphere so: Vssp=V/2= $3.539e^{-7}m^3$

SPHERE MASS

$$m = \rho \cdot V$$

With: m = mass of the sphere
ρ = volumic mass of the sphere (=$7.85e^{-6}kg/mm^3$)
V = volume of the sphere
For a semi-sphere, we have: mssp=m/2=2.778g.

SPHERE ENERGY

The total energy of the sphere when it hits the sheet is at z=0:

$$E = E_P + E_k$$

With: E = total energy of the sphere
E_p = potential energy of the sphere
E_k = kinetic energy of the sphere

But at z=0, E_p=0 so we have:

$$E = E_k = \frac{1}{2} \cdot m \cdot v^2$$

The velocity of the sphere at the impact for each initial velocity:

$$v = v_0 + a \cdot t = v_0 + g \cdot t$$

For v_0=250mm.s^{-1}, t=0,01537s, v=400mm.s^{-1}, E =2.22e^{-4} J

For v_0=500mm.s^{-1}, t=0,00917s, v=590mm.s^{-1}, E =4.83e^{-4} J

For v_0=1000mm.s^{-1}, t=0,00488s, v=1048mm.s^{-1}, E =15.25e^{-4} J

INITIAL VELOCITY

The initial velocity proposed was of 1000mm.s^{-1} in order to simulate a low velocity impact but in case of material rupture the initial velocity will be changed to 500mm.s^{-1} or to 250mm.s^{-1} so that the sheet withstands the impact.

SOLUTION TIME

The selected solution time was of 0.02s so that the sphere has time to finish the interaction with the surface of the sheet. As calculated previously the estimated time that the sphere needs to impact the sheet is of about 0,015s when its initial velocity is 250mm.s^{-1} and about 0,005s when its initial velocity is 1000mm.s^{-1}.

*III.B.*6 OBTAINED RESULTS

Von Mises equivalent stress formula:

$$\sigma_{eq} = \sqrt{\sigma_x^2 + \sigma_y^2 + \sigma_z^2 - (\sigma_x\sigma_y + \sigma_x\sigma_z + \sigma_y\sigma_z)}$$

σ_x, σ_y, σ_z are the principal values. σ_{eq} should be bellow the yield stress.

Sheet of aluminium 0.3mm

Maximum displacement in the centre of the sheet (mm)	**1.906**
Maximum stress (MPa)	**254.368**

Sheet of aluminium 0.87mm

Maximum displacement in the centre of the sheet (mm)	**0.957**
Maximum stress (MPa)	**209.274**

Sheet of aluminium 1.44mm

Maximum displacement in the centre of the sheet (mm)	**0.657**
Maximum stress (MPa)	**164.955**

Sheet of GLARE 5 layers (1.44mm) 3*aluminium (0.3mm) + 2*glass fibre(0.27mm)

Maximum displacement in the centre of the sheet (mm)	**0.853**
Maximum stress (MPa)	**347.777**

Initial velocity changed to 500mm.s^{-1} due to rupture of the sheet when the initial velocity was of 1000mm.s^{-1}

Sheet of GLARE 3 layers (0.87mm) 2*aluminium (0.3mm) + 1*glass fibre(0.27mm)

Maximum displacement in the centre of the sheet (mm)	**0.617**
Maximum stress (MPa)	**121.746**

*Initial velocity changed to 250mm.s^{-1} due to rupture of the sheet when the initial velocity was of 500mm.*s^{-1}

Sheet of GLARE 3 layers (0.3mm) 2*aluminium (0.1mm) + 1*glass fibre(0.1mm)

Maximum displacement in the centre of the sheet (mm)	**0.926**
Maximum stress (MPa)	**187.37**

*Initial velocity changed to 250mm.s^{-1} due to rupture of the sheet when the initial velocity was of 500mm.*s^{-1}

*III.B.*7 ANALYSIS OF THE OBTAINED RESULTS

Sheet of aluminium 0.3mm

Von Mises stress image

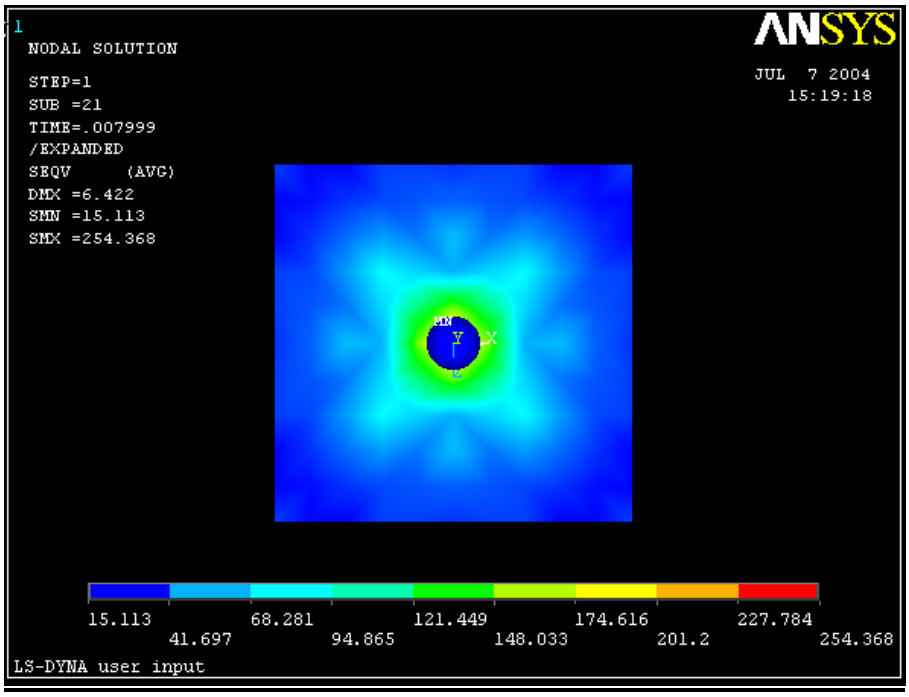

Uy deformation image

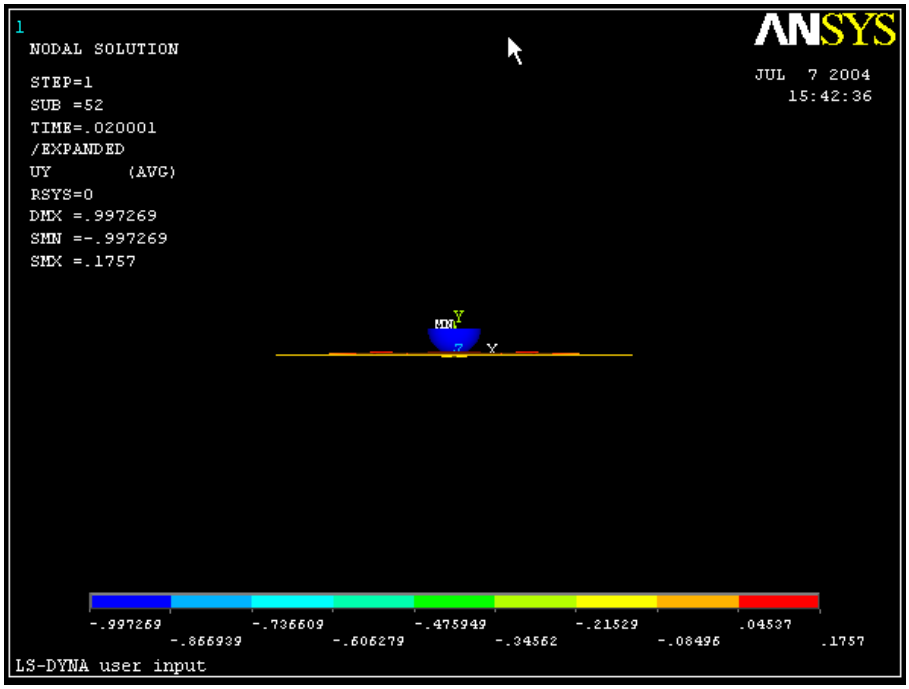

Displacement in function of distance to the centre of the sheet graphic

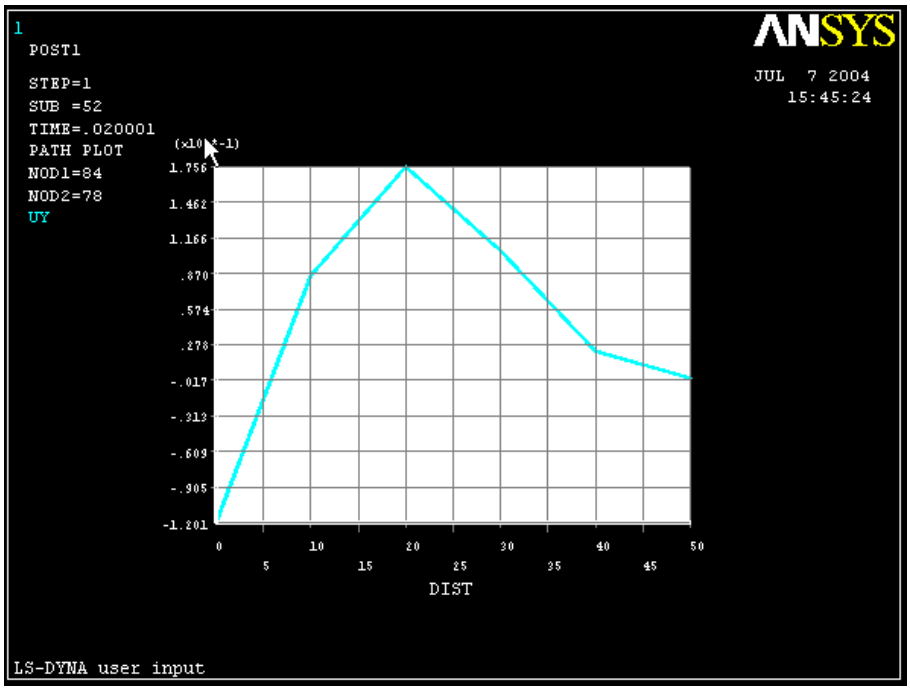

Von Mises stress of the centre point of the sheet in function of the time graphic

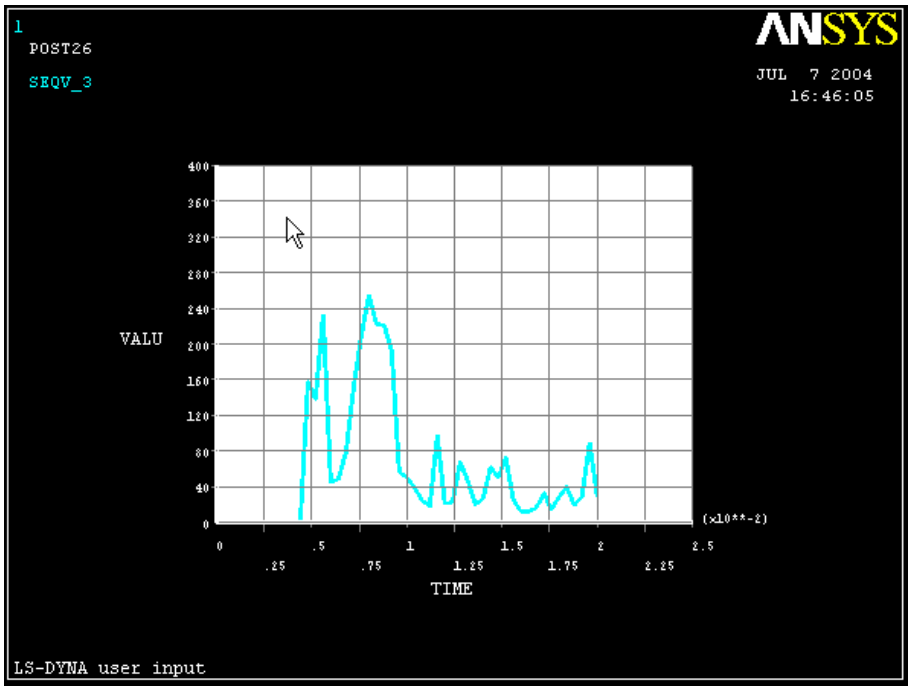

Displacement of the centre point of the sheet in function of the time graphic

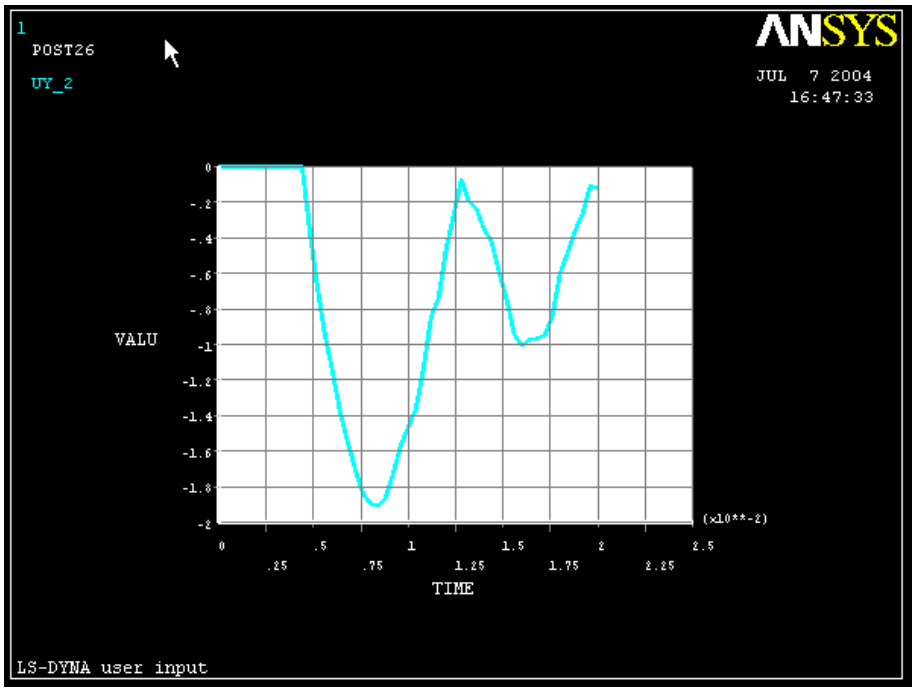

Sheet of aluminium 0.87mm

1.1 Von Mises stress image

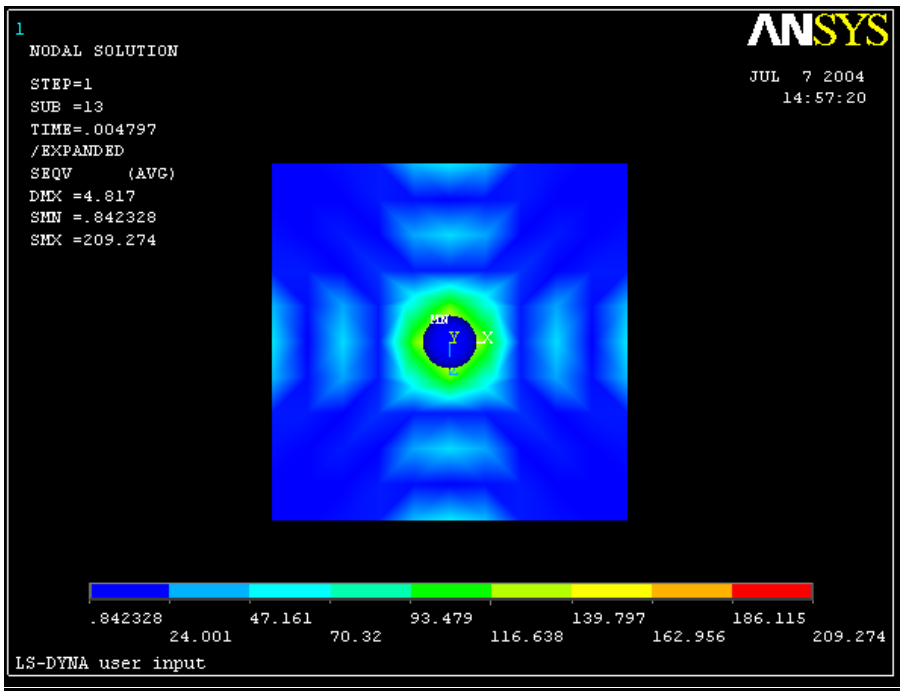

Uy deformation image

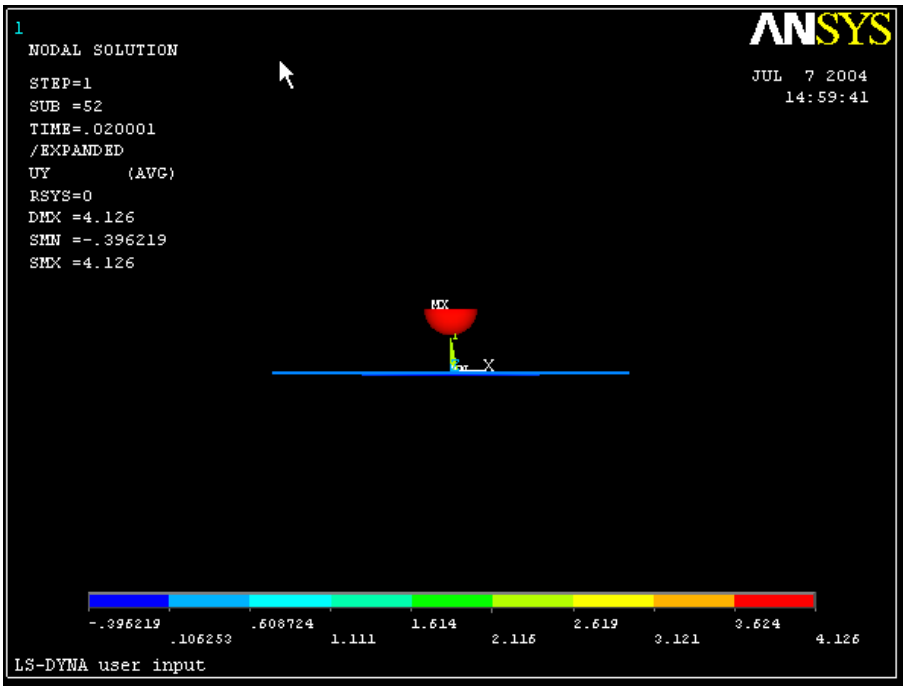

Displacement in function of distance to the centre of the sheet graphic

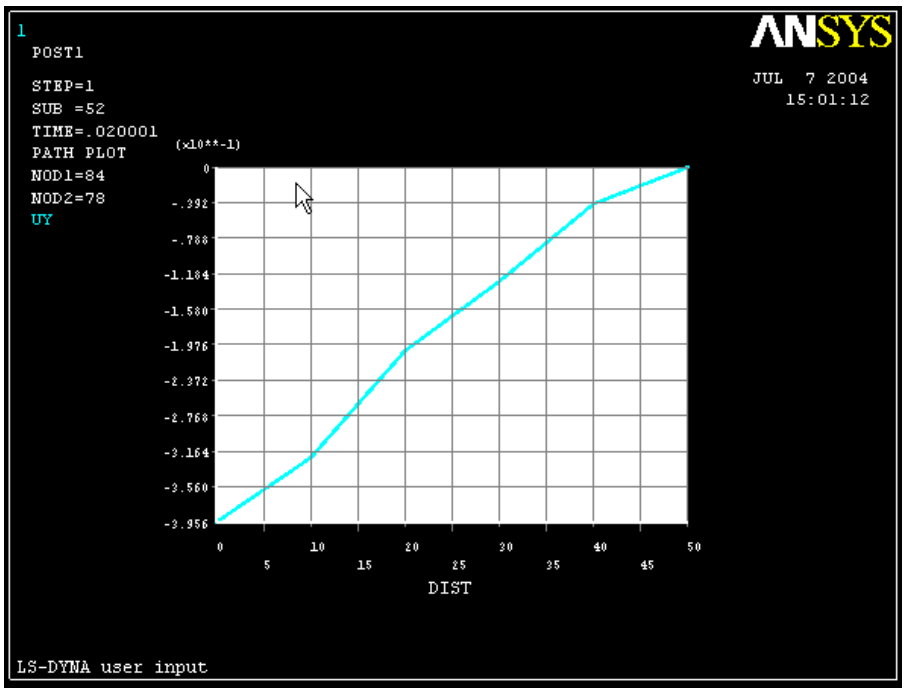

Von Mises stress of the centre point of the sheet in function of the time graphic

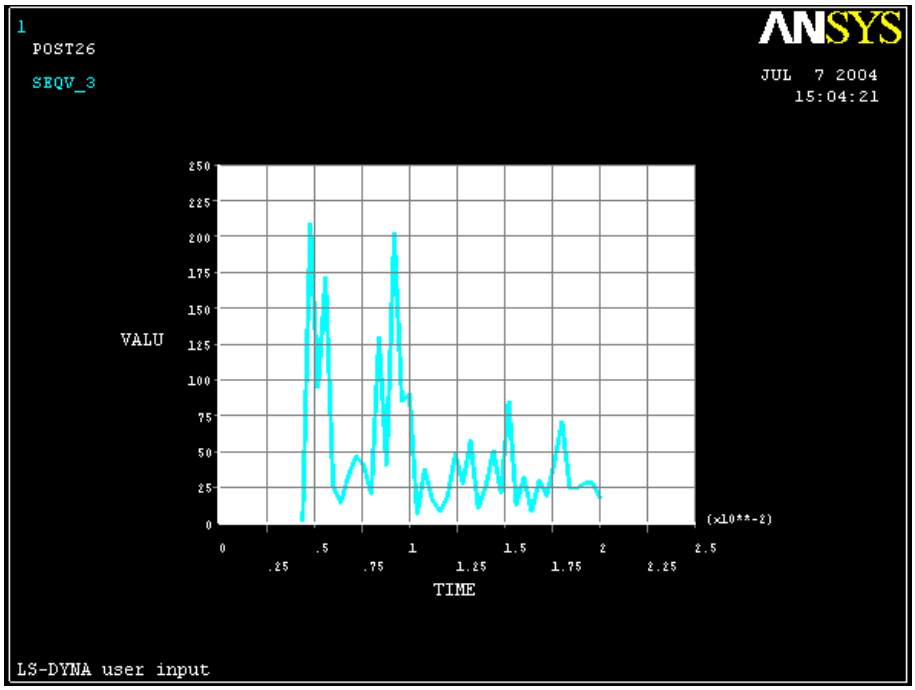

Displacement of the centre point of the sheet in function of the time graphic

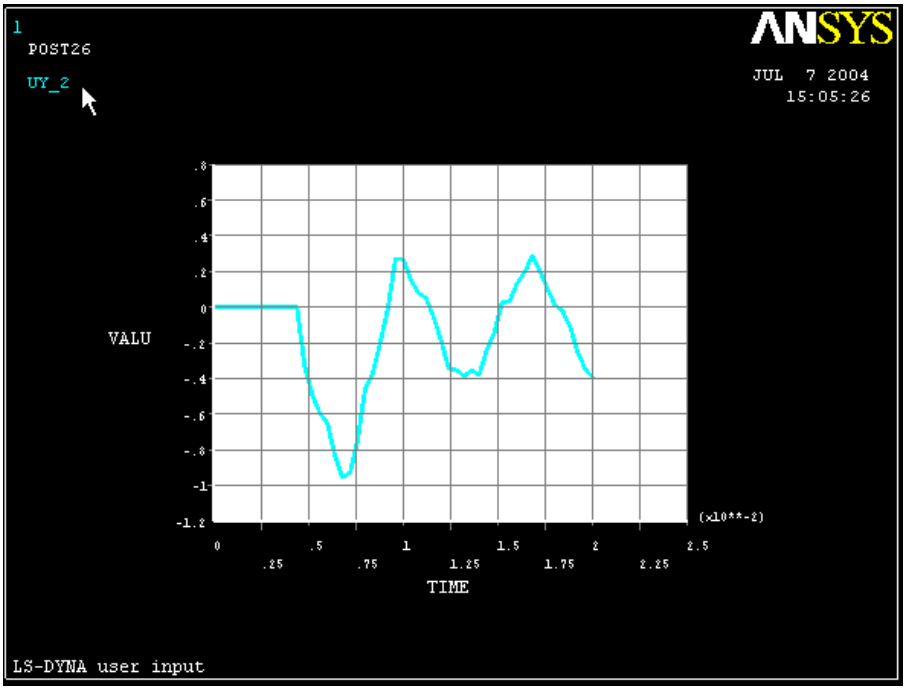

Sheet of aluminium 1.44mm

Von Mises stress image

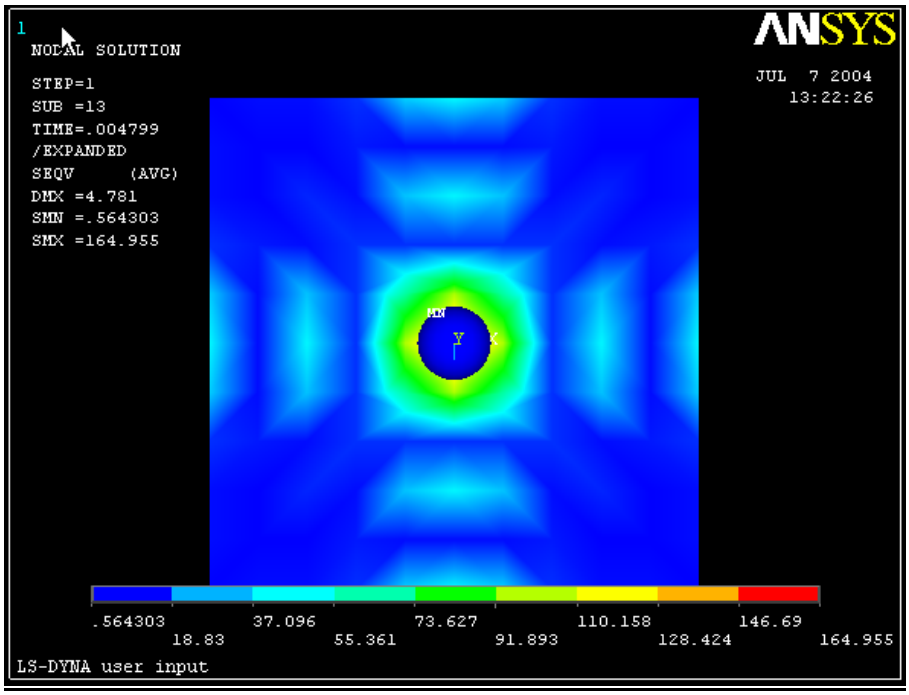

Uy deformation image

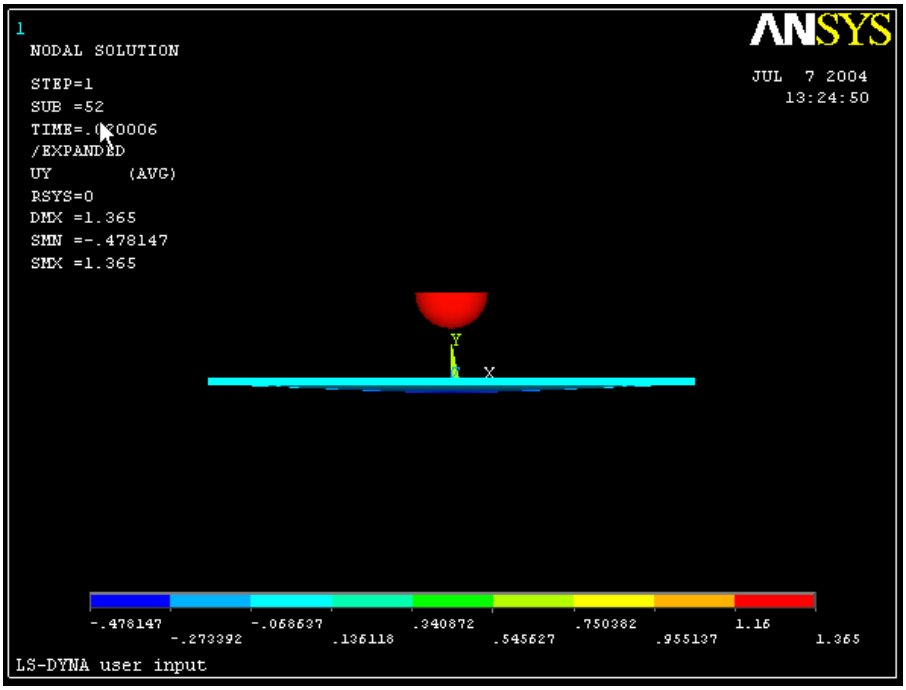

Displacement in function of distance to the centre of the sheet graphic

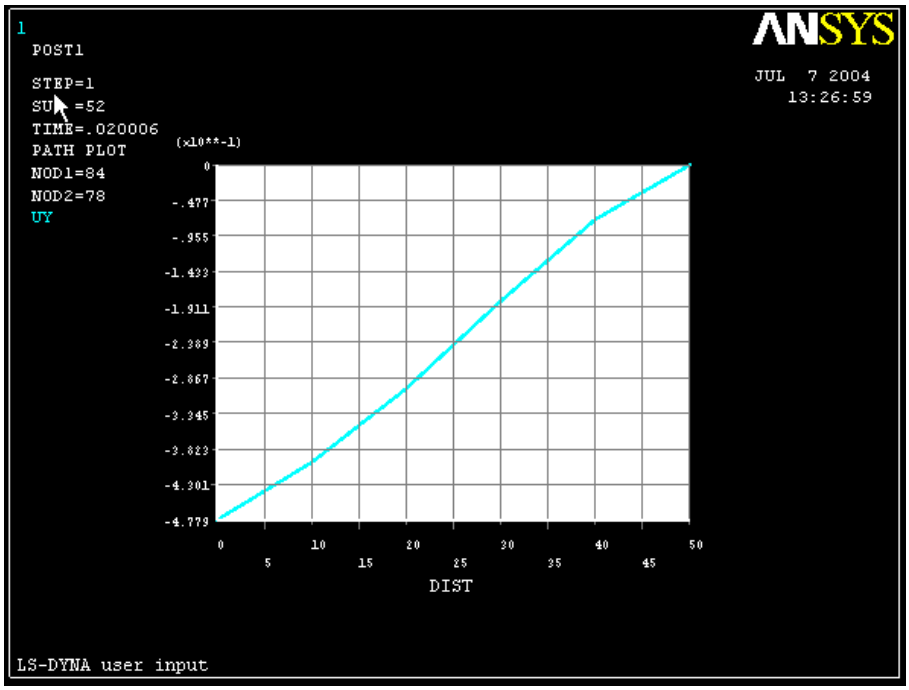

Von Mises stress of the centre point of the sheet in function of the time graphic

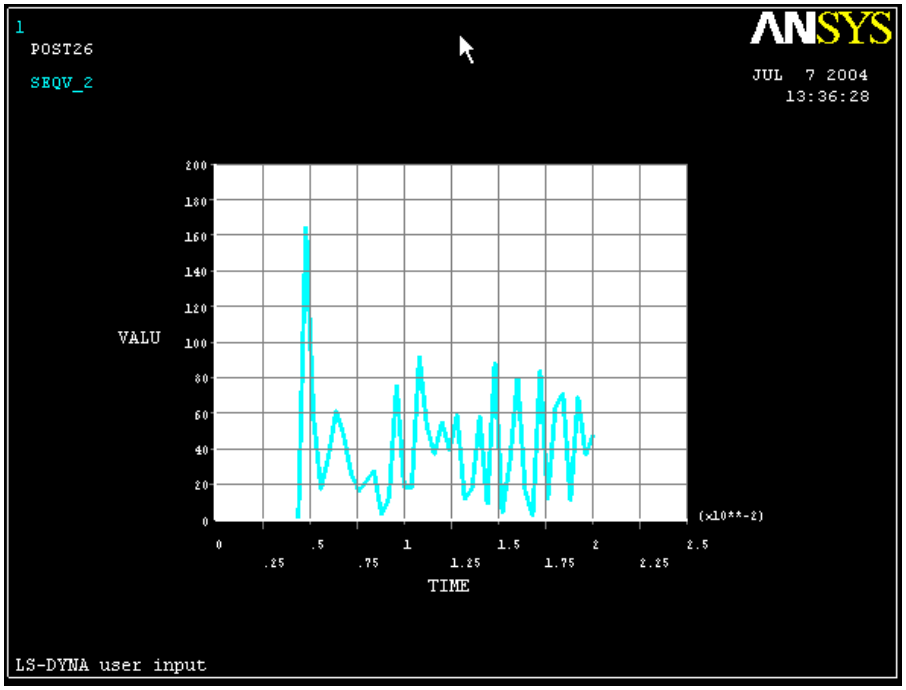

Displacement of the centre point of the sheet in function of the time graphic

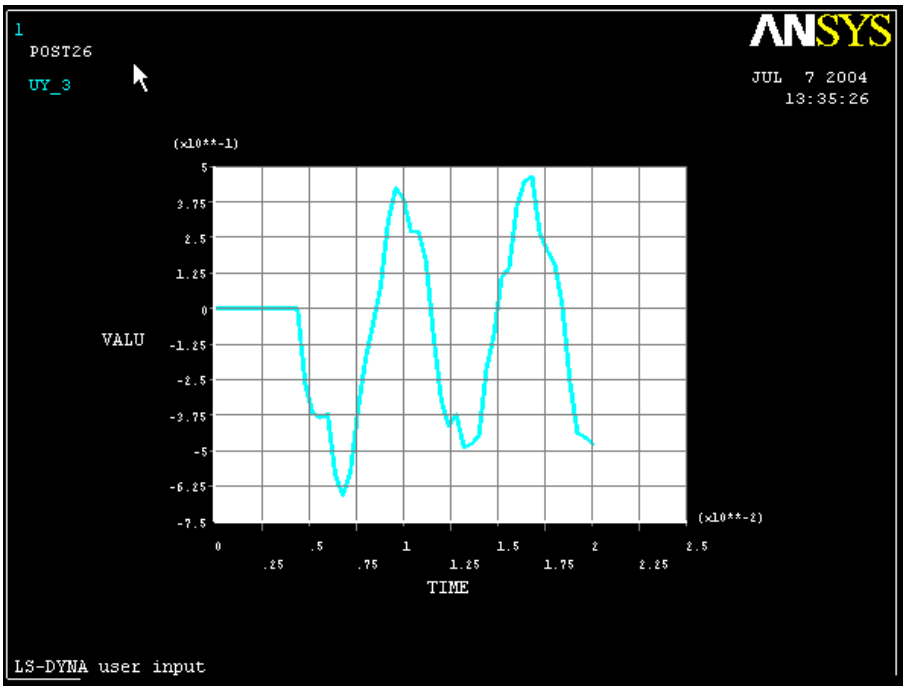

Sheet of GLARE 5 layers (1.44mm) 3*aluminium (0.3mm) + 2*glass fibre(0.27mm)

GLARE layers

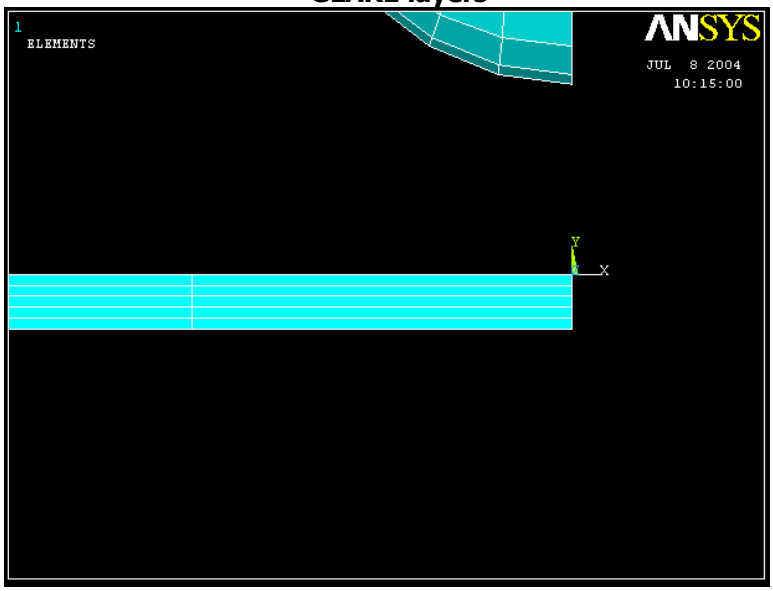

Von Mises stress image

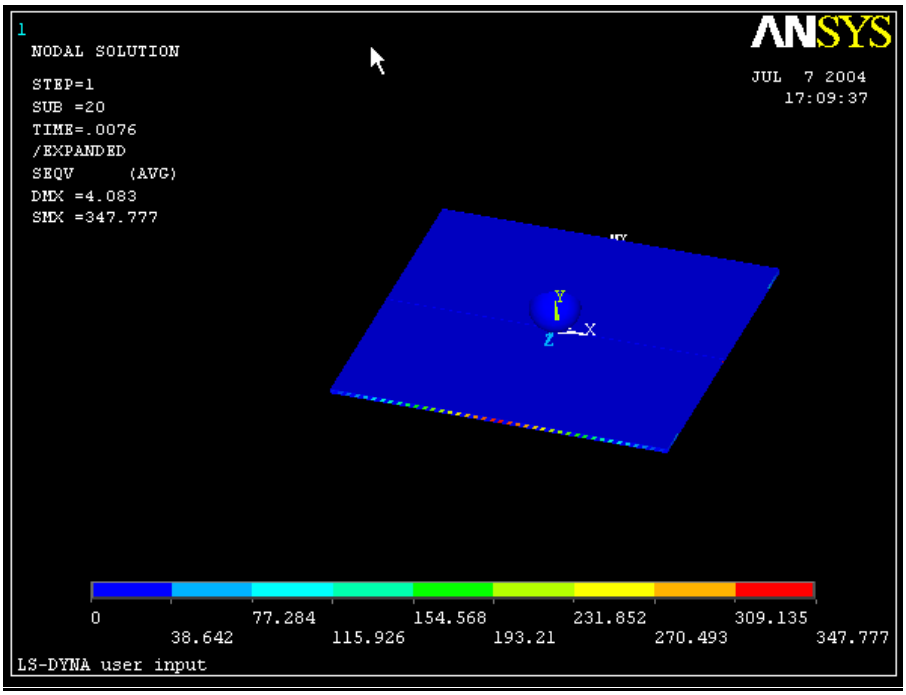

Uy deformation image

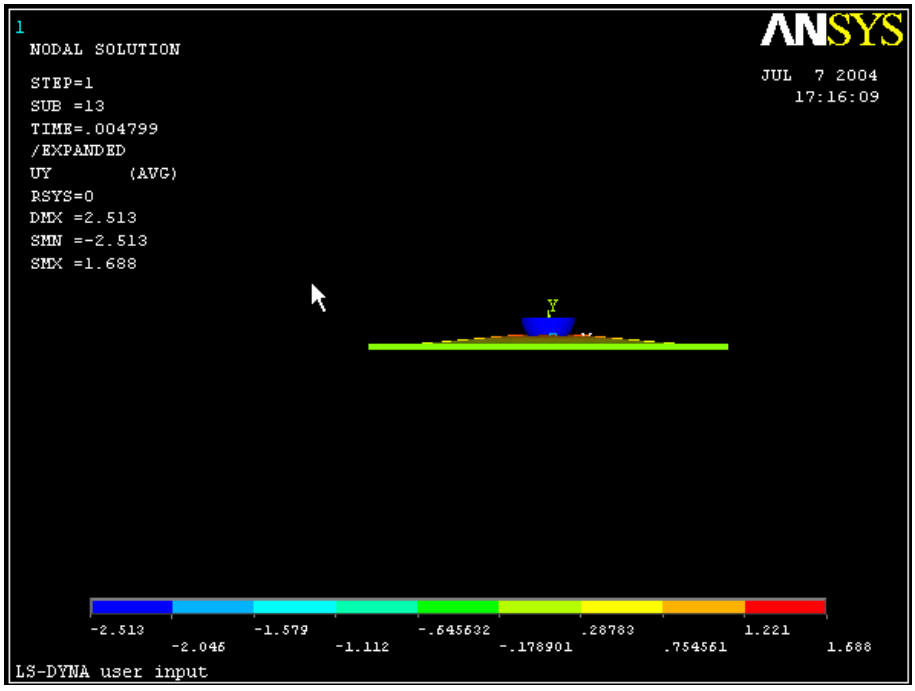

Displacement in function of distance to the centre of the sheet graphic

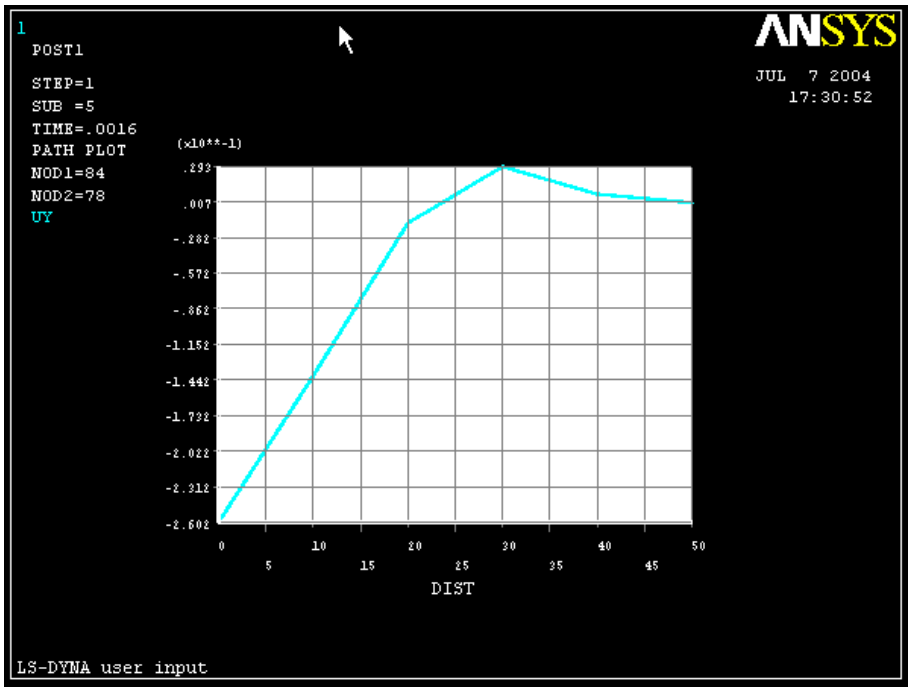

Von Mises stress of the centre point of the sheet in function of the time graphic

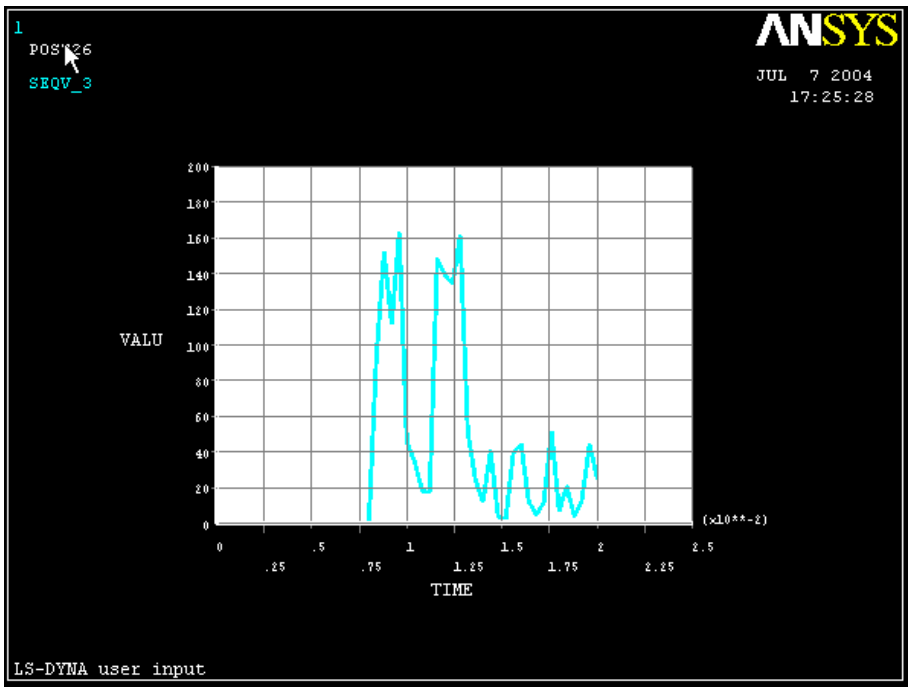

Displacement of the centre point of the sheet in function of the time graphic

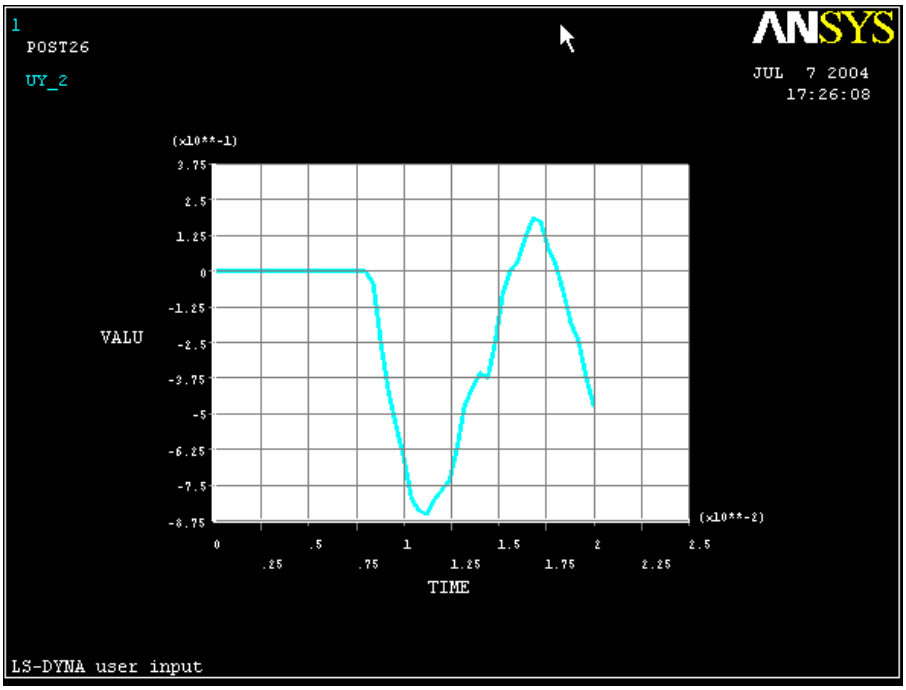

Sheet of GLARE 3 layers (0.87mm) 2*aluminium (0.3mm) + 1*glass fibre(0.27mm)

Rupture of the GLARE sheet with an initial velocity of 500mm.s^{-1} image

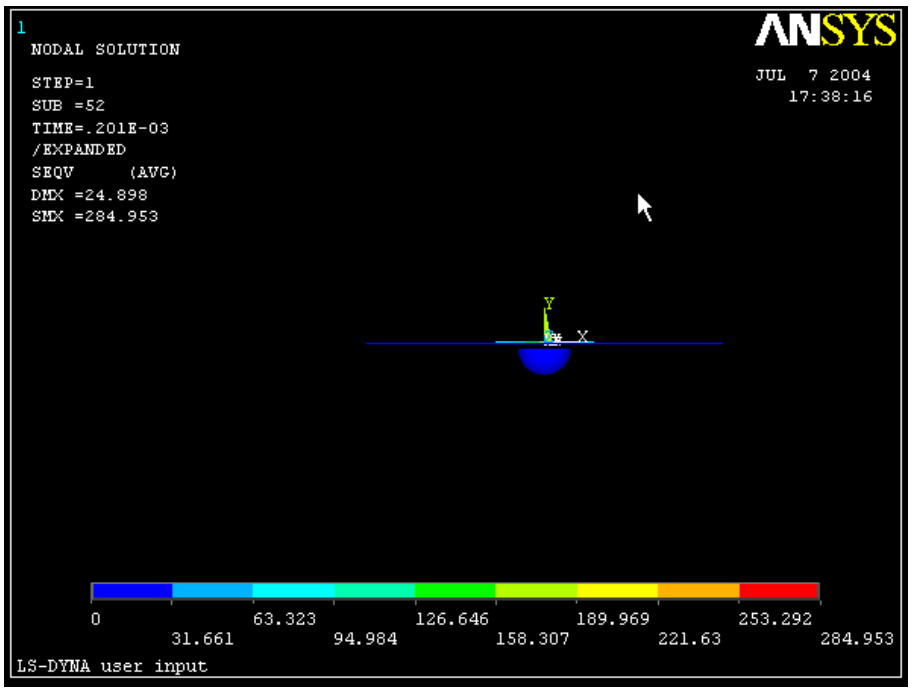

Von Mises stress image

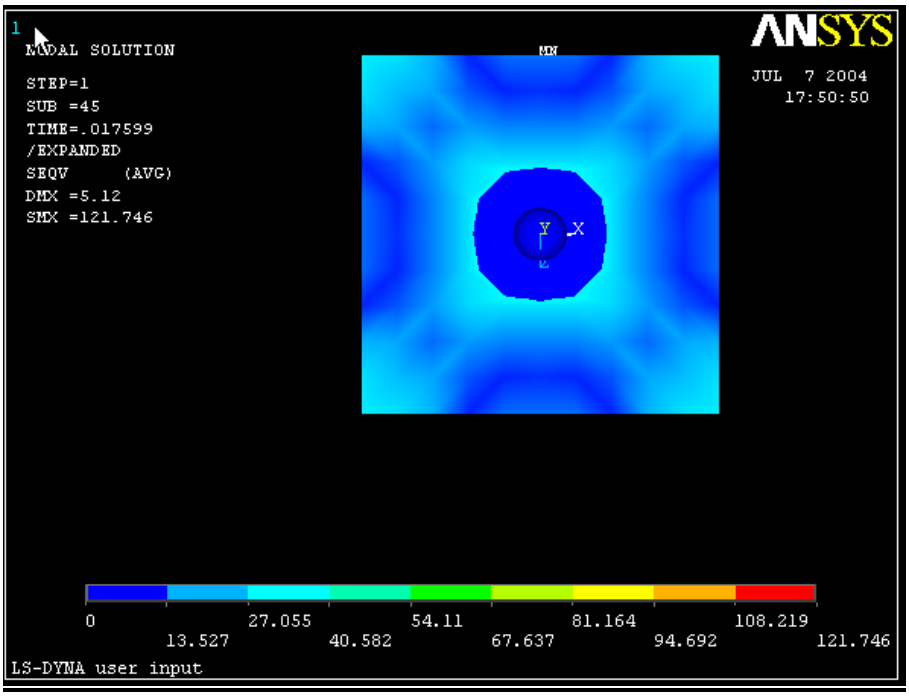

Uy deformation image

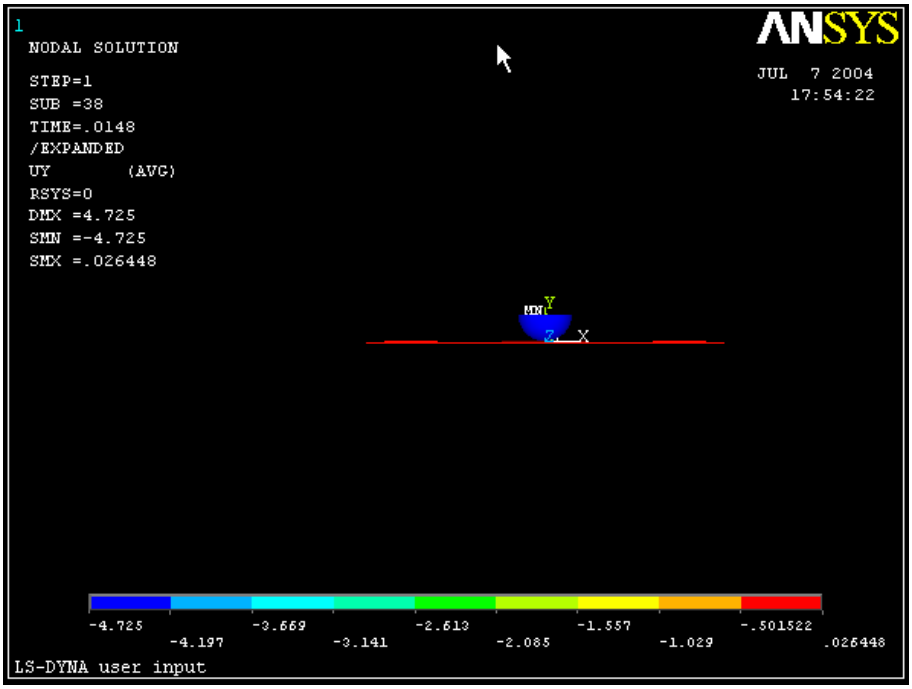

Displacement in function of distance to the centre of the sheet graphic

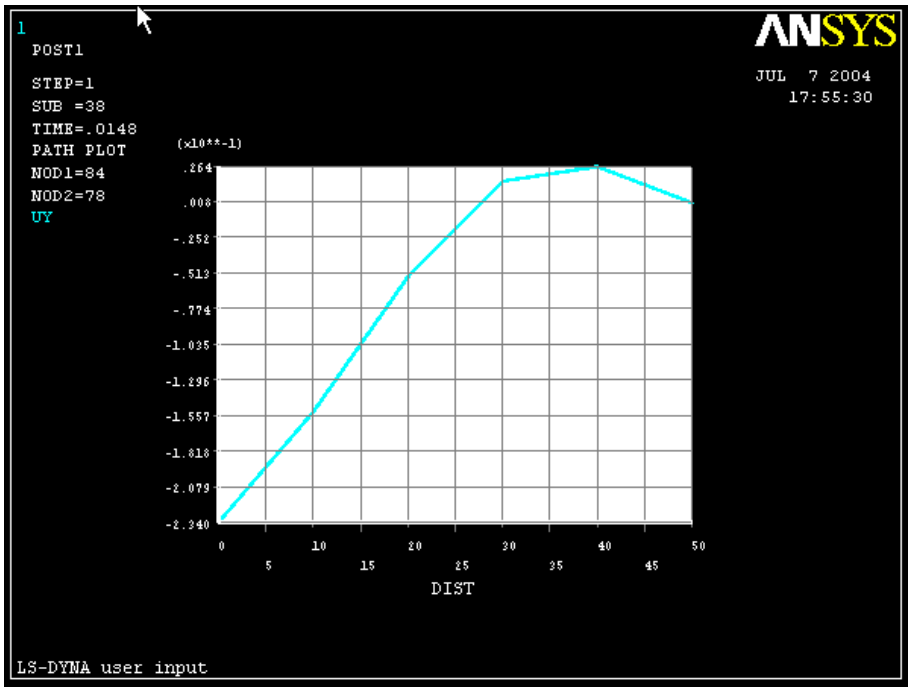

Von Mises stress of the centre point of the sheet in function of the time graphic

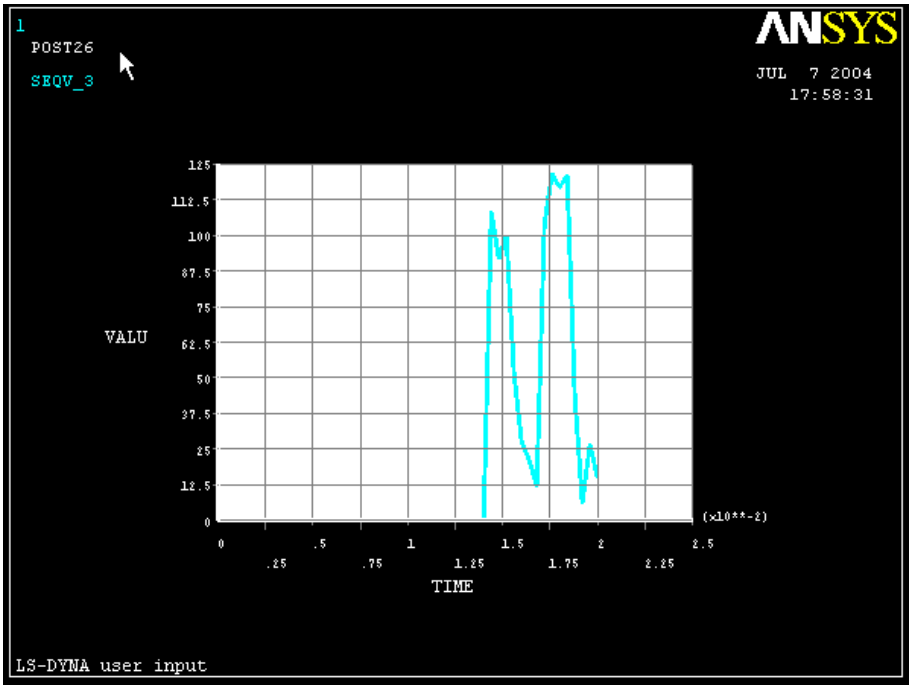

Displacement of the centre point of the sheet in function of the time graphic

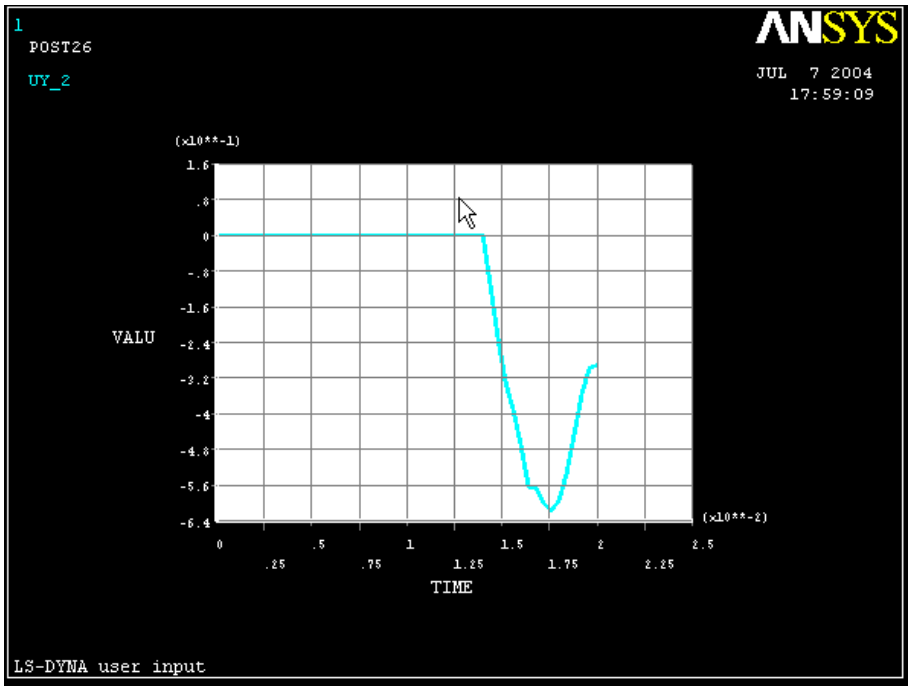

Sheet of GLARE 3 layers (0.3mm) 2*aluminium (0.1mm) + 1*glass fibre(0.1mm)

1.2 Von Mises stress image

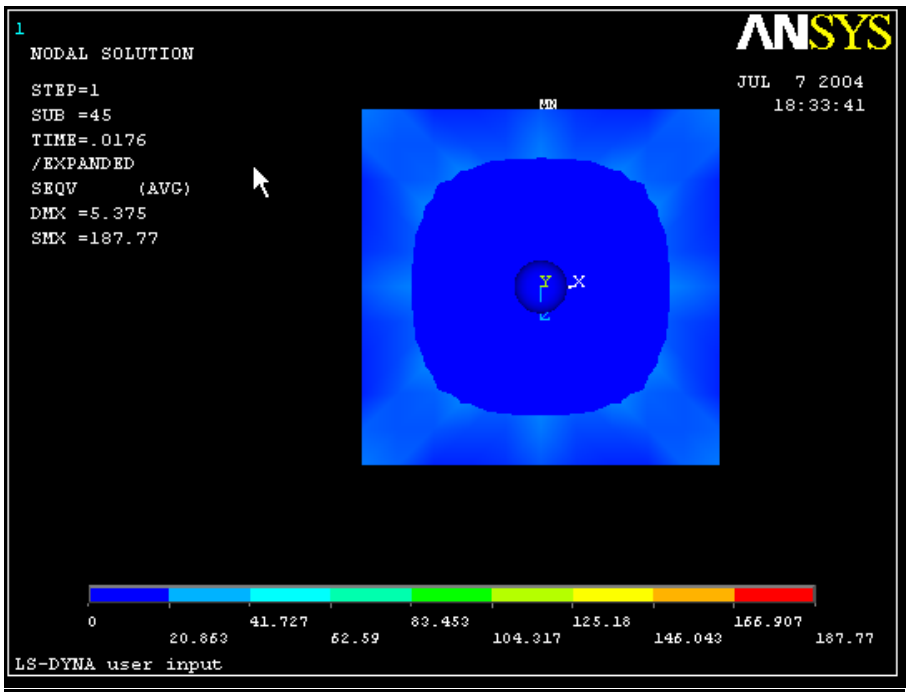

Uy deformation image

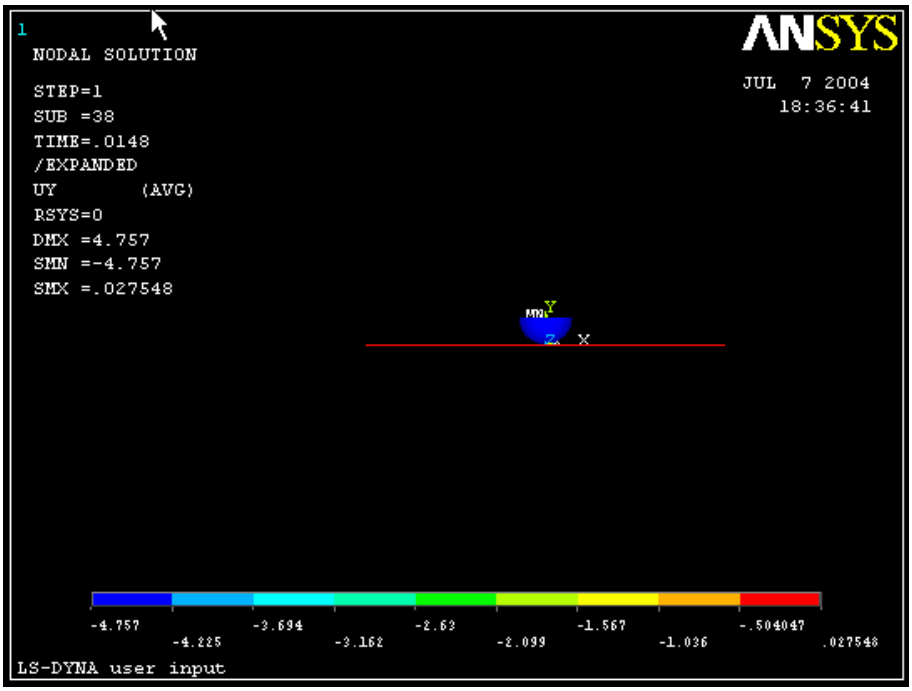

Displacement in function of distance to the centre of the sheet graphic

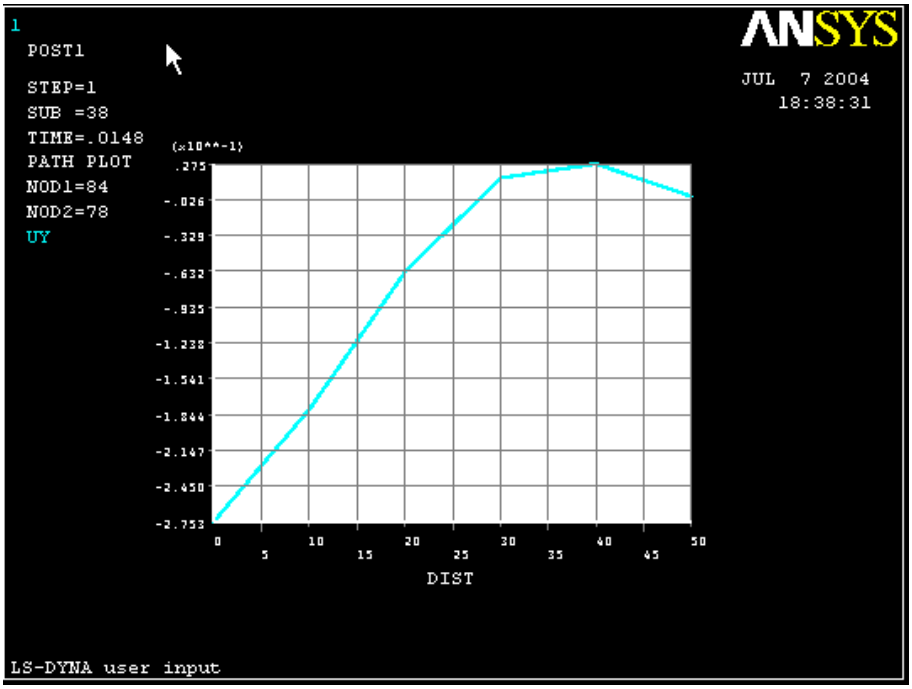

Von Mises stress of the centre point of the sheet in function of the time graphic

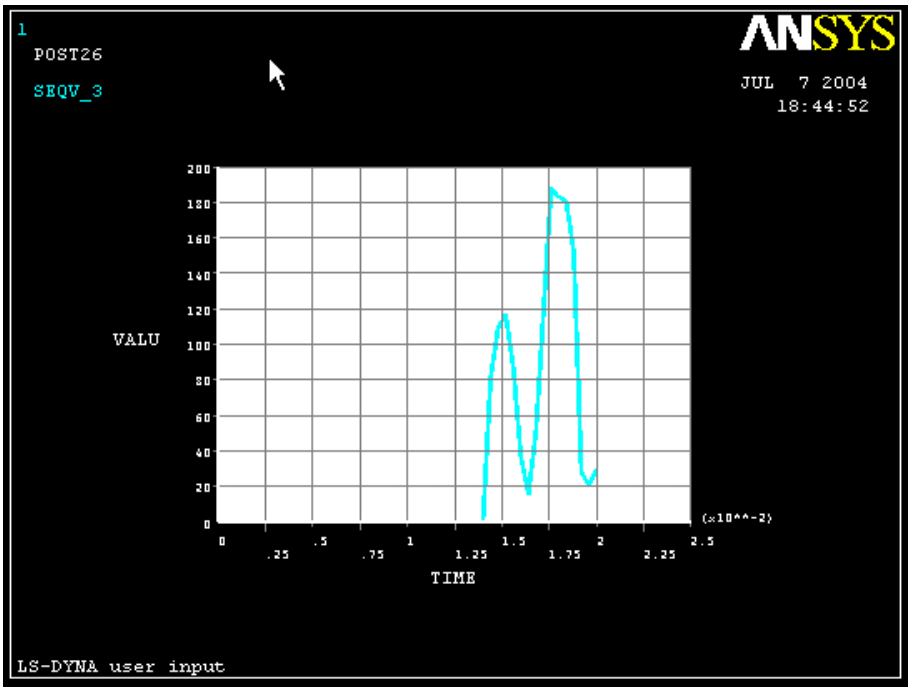

Displacement of the centre point of the sheet in function of the time graphic

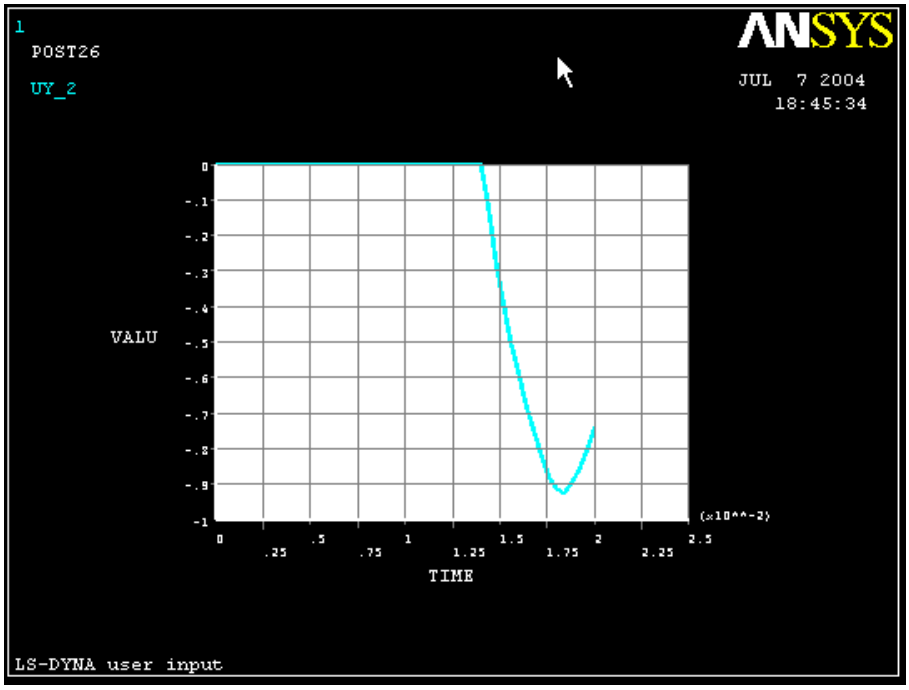

III.B.8 - **RESULTS INTERPRETATION**

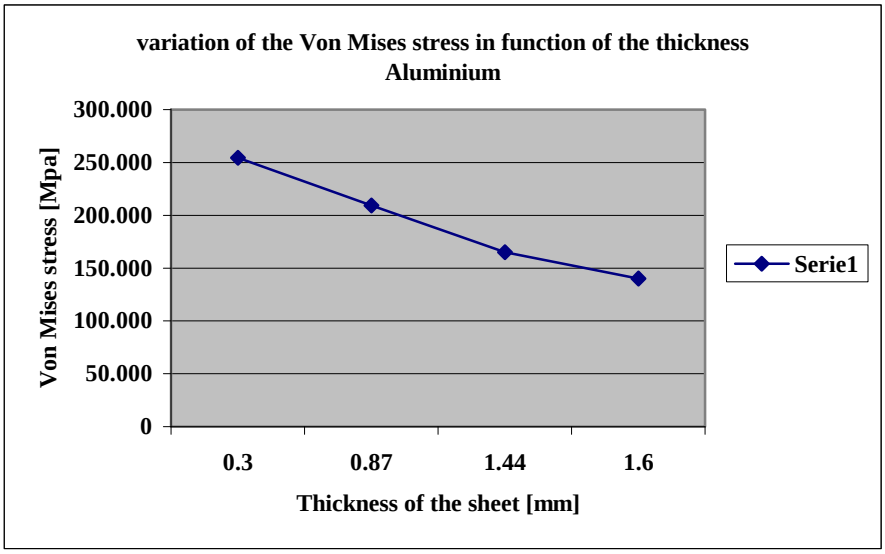

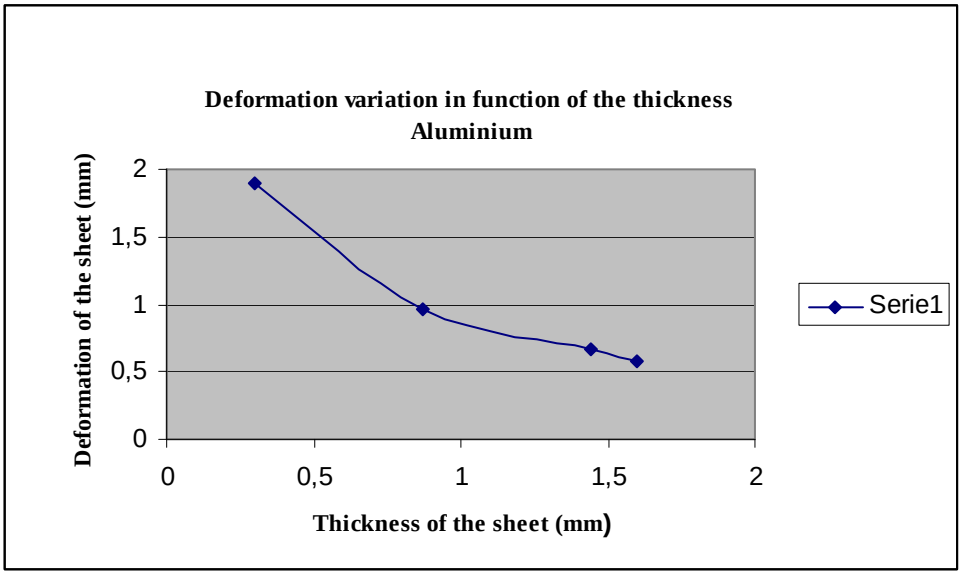

CONCLUSIONS

It can be concluded that the aluminium simulation is reasonably good, the results seem to confirm this. When we compare GLARE to aluminium it is clear that the simulated GLARE has a much inferior resistance to impact. That should not be the case, because GLARE has similar mechanical properties as aluminium. So we can conclude that the GLARE simulation does not work properly. The main problem seems to be how to define correctly the contact between layers, this seems to be more important when the solicitation increases, and when this happens the established contact between layers almost disappears, hence greatly reducing its resistance to simulated impacts, ANSYS does not seem a good software to simulate composite materials. There are ways of improving the efficiency of the simulation, but at the cost of a drastically increased calculation time. One of these ways is to divide when meshing each layer at least in five, other way is to manually input the parameters that define the contact between layers. But this is very difficult because until now no one seemed to achieve a satisfactory result, despite all the research made.

II.B.9. Bibliography

[1] Vermeeren, C.A.J.R.: The application of carbon fibres and ARALL laminates, Report LR-658, TU DELFt, 1991, 38Pg

[2] Dymacek, P., Klement, J.: Properties and Manufacturing of Steel-C/epoxy Fibre-Metal Laminates, Proceedings of Recent Research and Design Progress on Aeronautical Engineering and its Influence on education , Warsaw, Poland, 2000.

Section III.A

The first test case is the forming simulation of an automobile components

(deck lid inner body panel)

III.A.1 – Introduction

The simulation of the sheet metal forming process in this project was performed using the incremental forming simulation program AutoForm™.

AutoForm offers a fully integrated line of software modules for the design of sheet metal and hydroformed parts, and for the engineering of dies and processes for their production.

A common work environment that seamlessly integrates all the modules is provided by the *AutoForm-User Interface*. Using the different modules allows the design engineer to walk through the complete stamping simulation in one consistent environment, with maximum ease of use.

Full integration between *AutoForm-DieDesigner*, *AutoForm-OneStep*, and *AutoForm-Incremental* resolves numerical transmission issues, which saves time and allows the user to focus on stamping issues instead of numerical issues. This allows the user to simply import a CAD file and simulate the forming process step by step, from die design to an initial evaluation, then tuning and final validation.

AutoForm-DieDesigner gives the design engineer a significant flexibility to quickly test die geometry in the initial phases, *AutoForm-OneStep* enables the selection of the material properties, and finally *AutoForm-Incremental* focuses on validation part forming and quality. It's important to note that each step can be iterated many times to progressively improve quality throughout simulation process without any discontinuity.

In order to perform the necessary simulations regarding the purpose of this project only the *Incremental* and the *DieDesigner* modules were used.

AutoForm DieDesigner

Using *AutoForm-DieDesigner*, tooling engineers can design and evaluate several draw developments and choose the best one in less time than it takes to design a single draw development using traditional CAD-based tools. The software is also used to improve the accuracy of the formability assessments during product design by taking the binder and addendum into account.

AutoForm Incremental

AutoForm Incremental is the AutoForm module to simulate sheet metal forming processes (conventional deep drawing, hydromechanical deep drawing) using the finite element method in many small steps. Using AutoForm-Incremental it is possible to simulate all forming operations

beginning with the plane blank sheet and ending with the finished car body part, including springback calculation.

AutoForm Incremental is an implicit FE-program. The displacement of the nodes is calculated by a quasi-static balance. Since it is specific for sheet metal forming, the mesh and remeshing generation are automatic. The contacts and elements are formulated as a function of the typical conditions of the process, using, in order to simulate the required drawing process, two types of elements:

- Full Shell Elements
- Bending-enhanced membrane elements

Oppositely to full shell elements, Bending-enhanced membrane elements do not react to bending: the deformations are imposed by tool geometry and movement.

To calculate the stress-deformation condition a convenient correction algorithm is implemented. Thanks to this mixed formulation, trustable results are obtained with acceptable computing time.

III.A.2 **- Forming Analysis with *AutoForm-Incremental***

It is essential to have a reliable and robust simulation program for the sheet metal forming process to get trustable results when analysing a stamped part. Throughout this project, the finite element program *AutoForm-Incremental* was used.

AutoForm-Incremental is a highly specialized and optimized solver for the sheet metal forming process, which has been well established in the automotive industry during the last few years. It is proven that it meets the industrial requirements such as ease of use, high efficiency and sufficient accuracy even for complex parts.

Since the sheet metal forming process takes place at low velocity, a quasistatic implicit formulation is used.

The full implicit approach to solve the equilibrium equations

$$M^{t+\Delta t}\ddot{U} = R^{t+\Delta t} - F^{t+\Delta t} \tag{1}$$

is to use a Newton-Raphson iteration, where ***R*** is the vector of externally applied nodal forces, ***F*** is the vector of nodal point forces corresponding to the element stresses, ***M*** denotes the lump mass matrix, and ***U*** and ***Ü*** are the vectors of nodal point displacements and accelerations, respectively.

The Newton-Raphson iteration for Eq. 1 is to solve

$$M^{t+\Delta t}\ddot{U}_{(i)} + K^{t+\Delta t}_{(i-1)}\Delta U_{(i)} = R^{t+\Delta t} - F^{t+\Delta t}_{(i-1)} \tag{2}$$

until convergence measures are satisfied, where

$$U_{(i)}^{t+\Delta t} = U_{(i-1)}^{t+\Delta t} + \Delta U_{(i)} \tag{3}$$

and the initial conditions correspond to the state calculated for time ***t***.

$$U_{(0)}^{t+\Delta t} = U^t, \quad F_{(0)}^{t+\Delta t} = F^t, \quad K_{(0)}^{t+\Delta t} = K^t \tag{4}$$

In Eq. 2, ***K*** is the tangent stiffness matrix. The nonlinear iteration counter is given by the underscript (***i***).

Considering the implicit solution approach, the major computational challenge is the solution of a large sparse system of linear equations. There are two main approaches to solving the sparse linear systems from the nonlinear Newton method.

The first approach is more conservative and uses sparse direct solver technology. In the last few years algorithmic improvements alone have reduced the time for the direct solution of symmetric and unsymmetric sparse systems of linear equations by almost one or two orders of magnitude.

Remarkable progress has been made in the increase of reliability, parallelization and consistent high performance is now achieved for a wide range of computing architectures. As a result, a number of sparse direct solver packages for solving such systems are available and it is now common to solve these sparse linear systems of equations with a direct method that might have been considered as too large until recently.

Nevertheless, in large simulations with more than 300K elements, the memory requirements of direct methods as well as the time for the factorization may be too high.

Therefore, a second approach using the preconditioned Krylow subspace method is often employed to solve these systems. This iterative approach has smaller memory requirements and often smaller CPU time requirements than a direct method. However, an iterative method may not converge to the solution in some cases where a direct method is capable of finding the solution.

The sparse linear systems from sheet metal forming simulation are extremely ill-conditioned and therefore quite challenging for iterative methods. To overcome problems with ill-conditioned linear systems and to reduce the number of degrees of freedom, a special membrane element formulation is used in *AutoForm-Incremental*. Within each time step the transversal (bending) displacements and the tangential (stretching) displacements are uncoupled resulting in significantly better conditioned

systems. The *AutoForm-Incremental* method decouples these bending and stretching degrees of freedom, and the bending shape and material flow are determined separately. As a consequence of this simplification, stability problems are avoided and the condition of the system matrix is improved, so that iterative methods for the solution of the linear equations can be used. This is a reasonable simplification for the deep drawing process as the shape of the sheet is mostly defined by the tools; especially at the end of the process when the tools are closed, there are no degrees of freedom in normal direction.

Shell elements are used as well, providing results with extremely high accuracy.

An elasto-plastic material model is used. For the elastic part of deformation, Hooke's isotropic law is applied. For plastic yielding and the direction of plastic flow an anisotropical yield surface similar to Hill48 (*Appendix C*) is used. The constitutive equations are integrated numerically with the radial return method.

The stiffness of the tools which are used for the forming process is much higher than the stiffness of the sheet. For this reason it is suitable to model the tools as rigid bodies. The friction between the sheet and the tools play an important role in the drawing process. Friction is modelled by Coulomb's law with a constant friction coefficient. Values between 0.05 (good lubrication) and 0.25 (no lubrication) are typically used.

During the deep drawing process large displacements are present. This leads to the permanent change of the zones where fine-grained elements are needed. An adaptive modification of the mesh during the simulation is applied to solve this problem. In *AutoForm-Incremental*, an automatic refinement as well as an automatic coarsening is used. As refinement criteria, curvature, strain gradient, and penetration between sheet and tools are used. Using this method it is possible to handle complex industrial parts with a reasonable number of elements. A complex outer panel of a car, for example, can be modelled with approximately 200K elements.

III.A.3 **- Synthetic Description of AutoForm Process Steps**

1. Pre-Processing of Input Data

Import geometry

- Import part geometry from CAD

Part Geometry (Geometry Generator)

- Prepare
- Fillet
- Balance (Tip)
- Filling Holes (Modify Part Geometry)
- External Contour (Boundary Fill)
- Binder
- Addendum
- Modify Tools

Process Data Input (Input Generator)

- Tools
- Blank
- Lube
- Drawbeads

Material Properties / Material Selection

- True stress-True strain curve
- Normal anisotropy coefficient
- Forming limit curve

Process Description

- Process (Gravity, Closing, Drawing, Cuttings, Springback…)

Calculus Configuration

- Control data

2. Computational Analysis

3. Post-Processing of Results

Visual evaluation

Forming evaluation

- Formability
- Forming Limit Diagram (FLD)
- Wrinkling criterion
- Maximum Failure

Thickness / Strain evaluation

- Thickness
- Thinning
- Plastic strain
- Major strain
- Minor strain

Springback evaluation

- Normal displacement
- Dynamic section

The following Diagram presents the methodology used in AutoForm.

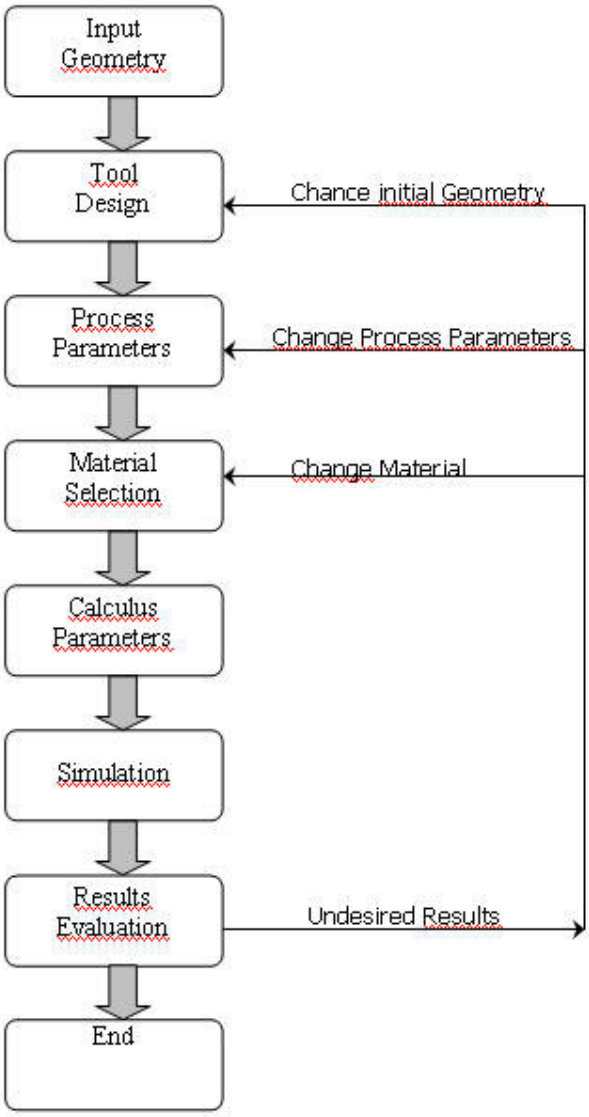

III.A.4 - Description of the Procedure in AutoForm

The *AutoForm-User Interface* is the working environment for importing and processing of geometry data. All the other AutoForm modules are started from the *AutoForm-User Interface*.

The order in which the input data is presented in this chapter is similar to the program requests. For an easier comprehension images will accompany the explanations.

III.A.4.1 - Pre-Processing of Input Data

- New Simulation File

At the beginning, a new simulation file (*.sim) has to be defined. The first input is the name of the simulation. During the generation of the input, this simulation file is filled with data, which is necessary for the simulation (geometrical data, specification of process, numerical data, etc.).

Besides the *file name*, the first inputs are the *units* and the *geometric error tolerance* (Figure 5.1).

- Import Part Geometry from CAD

The simulation is always created on the basis of a part or tool geometry. This geometry has to be available in VDAFS or IGES format. The simulation starts with the import of this CAD file (Figure III.A.1).

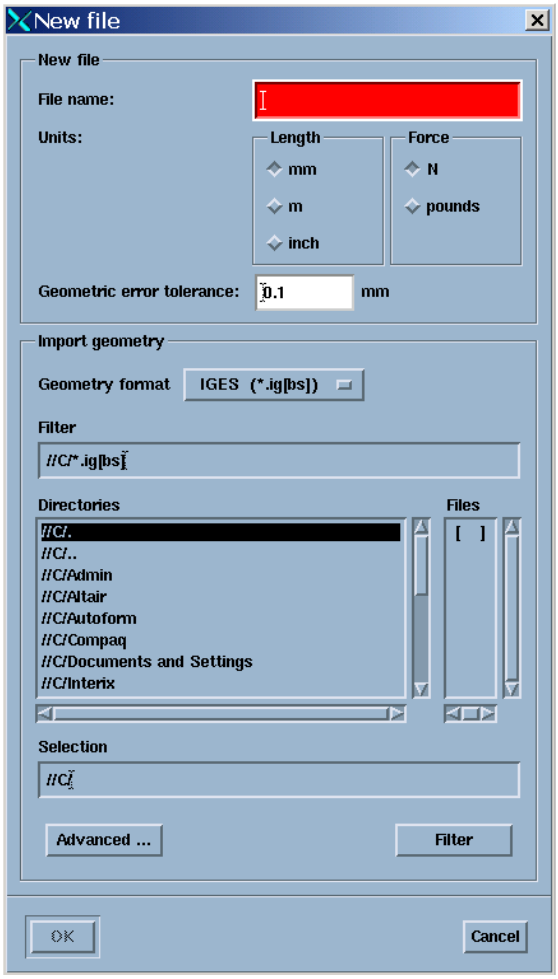

Figure III.A.1 - *Create new file and import geometry page*

The geometry import is carried out using the module **afmesh**, the integrated IGES-/VDAFS interface, which automatically meshes the part geometry. All subsequent operations are based on this mesh. Only the mesh can be visualized in AutoForm, not the original CAD data.

Basing on this imported CAD file further input is generated: Input concerning the process such as tool geometries, tool movement, information on the sheet (size, shape, material properties, thickness etc.) is defined. All this information is saved the previously mentioned simulation file (*.sim). The computed results will be added to this simulation file.

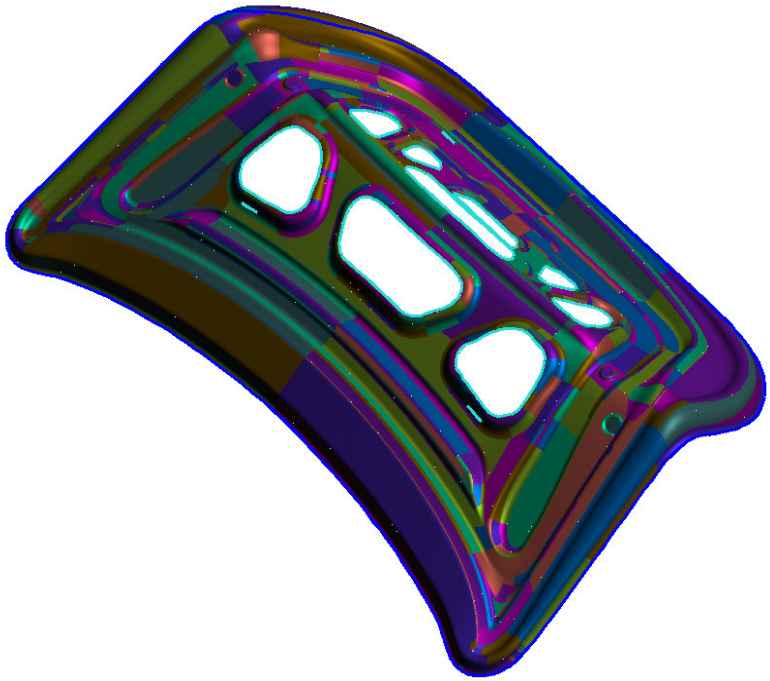

Figure III.A.2 - *The meshed geometry of a deck lid.*

The meshed geometry is immediately displayed (Figure III.A2.2) and the Geometry Generator automatically pops up (Figure III.A3.3). Now inputting geometry data is possible.

Part Geometry (Geometry Generator)

- Prepare

The imported part geometry needs to be prepared in order to serve as a reference for the die design.

In *tool setup* section it is possible to select whether the die will be the upper or the lower tool, which is the same as selecting whether deep-drawing on single action press or deep-drawing on double action press will be performed.

In *Define Objects* is possible to assign faces to the different registers:

- *Part*: Contains the CAD faces for the part, which are needed for the generation of the tool.
- *Binder*: Contains the faces of the part geometry, which are placed directly on the binder surface. (The binder surface is generated or imported on the **Binder** page later). Selected faces are then assigned to the **Binder** register.
- *Flange*: Register for CAD faces needed for subsequent operations.
- *Deleted*: Not used faces.

To generate the part boundary, which is automatically calculated, click *Generate part boundary* button.

To perform changes in the generated part boundary, the following options are available:

Outer trim – If the generated part boundary needs to be changed, it can be done using this option.

Inner trim – Undesirable geometry features (areas that are formed in flanging or restrike operations, but not in the draw die) may be eliminated using the *Inner trim* function. Holes can be created as well with this command.

If the part geometry has a symmetry plane or is built as a double part, this can be defined as well.

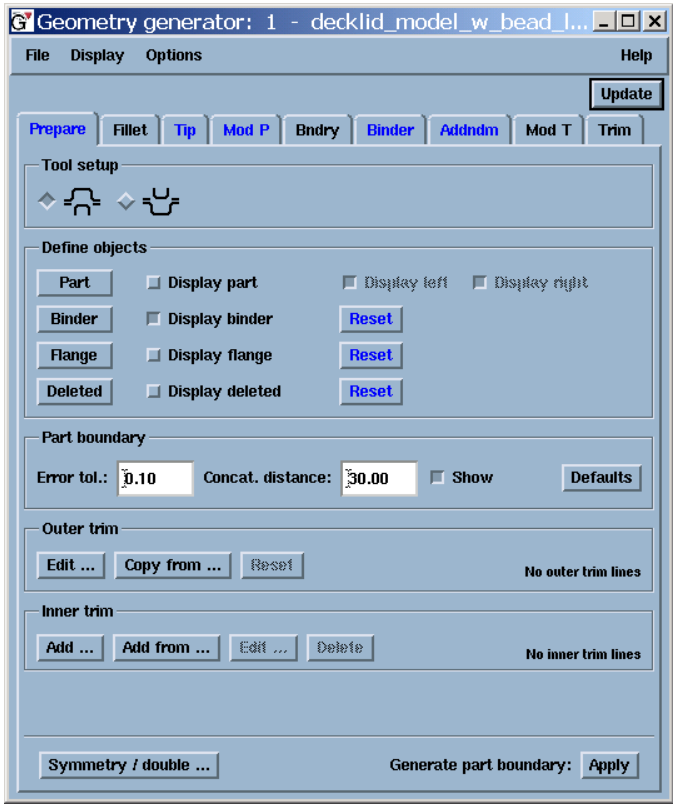

Figure III.A3 – *Prepare page (Geometry Generator)*

- Fillet

During this part preparation phase, sharp edges and filleting will be checked for eventual problems. If sharp edges are found, when clicking *OK* these edges are filleted accordingly to the value specified in *global fillet radius*.

A very common (and useful) option of morphing in this page is the modification of the radius of already existing fillets. This technology allows the user to manipulate the mesh in 3D by defining feature lines and feature nodes.

Filleting of individual edges - If it is necessary to create fillets of different radii along different edges of the part geometry, these individual edges have to be identified and fillet radius values (constant over the edge or variable) have to be specified, in addition to the global radius values. Those edges that were identified as sharp, and for which no additional fillet radius specification are made will all be filleted to the global radius value. Using the button *Add line…* at the bottom of the **Fillet** page, one can identify specific edges and to specify radius values on these edges.

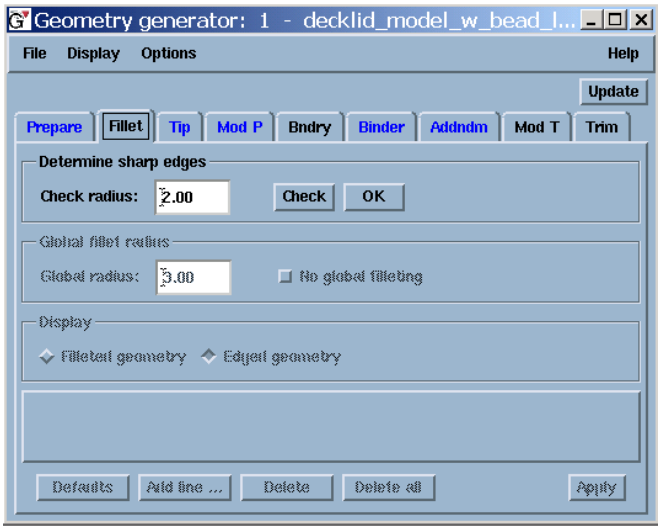

Figure III.A.4 - *Fillet page (Geometry Generator)*

- Balance (Tip): defining of the Drawing Direction

Normally, when reading a part geometry from a CAD file, this geometry is positioned in the car coordinate system (global system). However, it is possible to define a local system that can serve as a reference for the stamping direction and also has the ability to automatically detect the optimum stamping direction based on several criteria such as the **minimum draw depth**, the **minimum backdraft** or the **average normal**. In addition to the possibility to choose one out of several automatic functions, the user can (if necessary) tip the part around the x-, y- and z-axis to a more useful drawing direction. This can also be done with a local tipping centre.

The three following functions generate in the most cases a reasonably good drawing direction:

- *Average normal*: uses normal vector of geometry as drawing direction.
- *Min draw depth*: determines automatically the drawing position to minimize the drawing depth.
- *Min backdraft*: calculates a drawing direction with minimum undercuts, i.e., with minimized backdraft.

Moreover a drawing direction designed in a CAD-system can be imported and the drawing direction defined with DieDesigner can be exported to handle it within a CAD-system.

All undercuts, marginal areas and undercut free areas are calculated and displayed in different colour for the current drawing direction when the

Tip page is opened (Figure III.A.5). Undercut free areas are displayed in green (drawing angle greater than 3 degrees), marginal areas in yellow (drawing angle between 3 and 0 degrees) and undercuts in red (backdraft under 0 degrees).

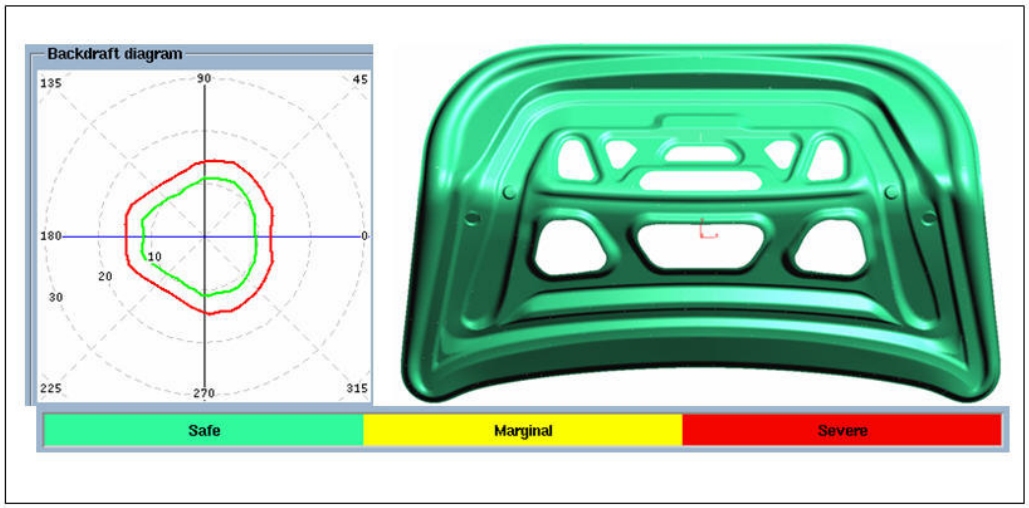

Figure III.A.5 *- Tipping of a deck lid from an automobile and the associated backdraft diagram*

Using the button *Plot* the **backdraft diagram** is activated.

Backdraft diagram – All possible undercut-free drawing direction are calculated (using **Plot**) and displayed in the diagram. The centre of the axis is the current drawing direction. The distance between the axis centre and the lines represents the backdraft-free angle to the drawing direction. The horizontal axis shows the rotation around the y-axis and the vertical axis shows the rotation around the x-axis.

This means that a rotation around the y-axis (horizontal line in the diagram) is backdraft-free as long as the rotation angle is inside the red line. The red line represents the limit angle **Severe/Marginal** and the green line the limit angle **Marginal/Safe** for the presentation of the backdrafts.

If the centre of the plot is completely within the green circle the geometry is undercut free (default: **Safe > 3º**); if the centre is between green and red circles, geometry is in marginal area (default: **Marginal: 0º ~ 3º**); if the centre is outside the red circle, geometry has undercuts (default: **Severe: ≤ 0º**).

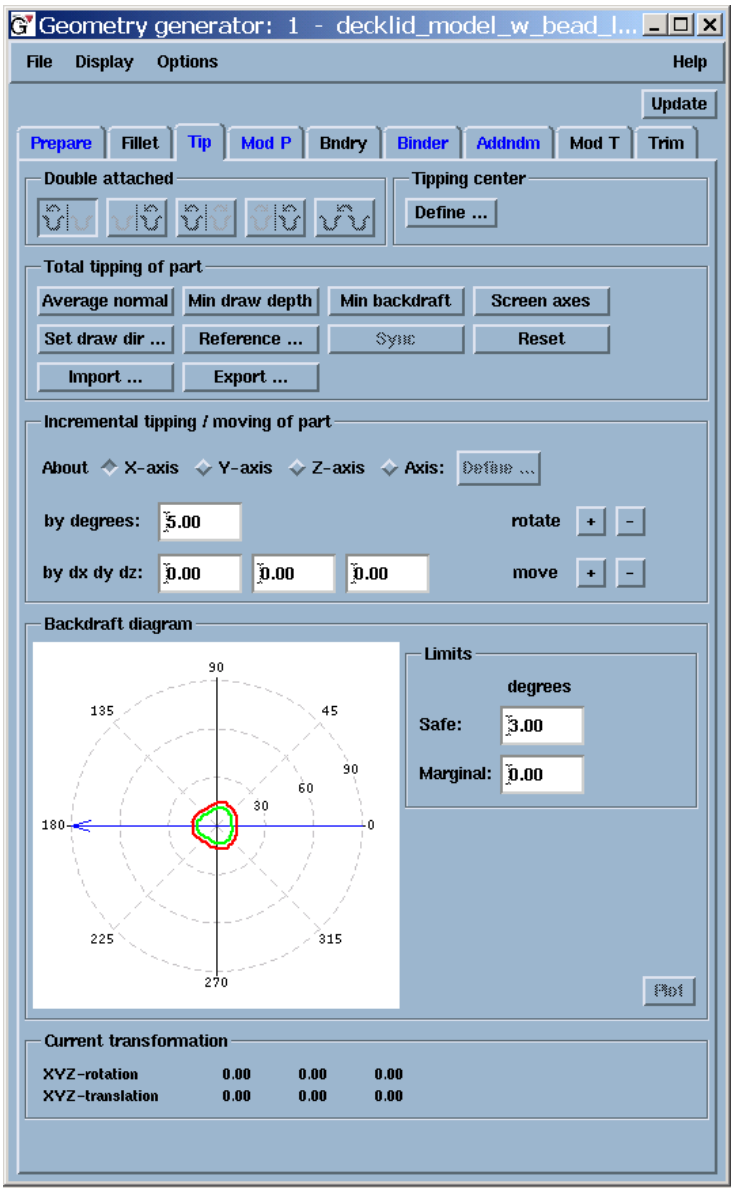

Figure III.A.6 – *Tip page (Geometry Generator)*

- Modification of Part Geometry (Mod P)

Using functionality available on this page, it is possible to modify part geometry by global overcrowning as well as by adding local detail. Further, gaps and holes can also be filled, and the filled areas can be edited / modified in this page.

Filling up holes and gaps in the part geometry:

Add hole – allows a single, specified hole to be filled, and the filled patch to be edited/modified.

All holes – allows all holes on part geometry to be filled; however, the fill patches are not modifiable.

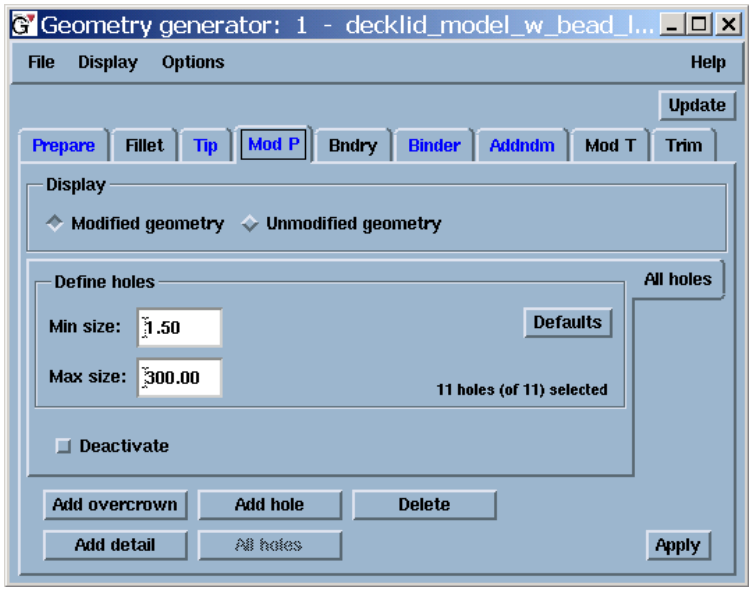

Figure III.A.7 – *Modify Part page (Geometry Generator)*

Figure III.A.8 *– Flling holes step*

- External contour (Boundary Fill)

The part boundary should be as smooth as possible. The user has the possibility to smoothen the part edge by using a so-called 'rolling cylinder' technology. The generated outer fill faces in order to do that are called boundary fill.

Filling the Part boundary – Fill areas are created automatically along the part boundary. The outer boundary fill line is determined by tangential points created by a roll cylinder moving around the part boundary and its roll radius.

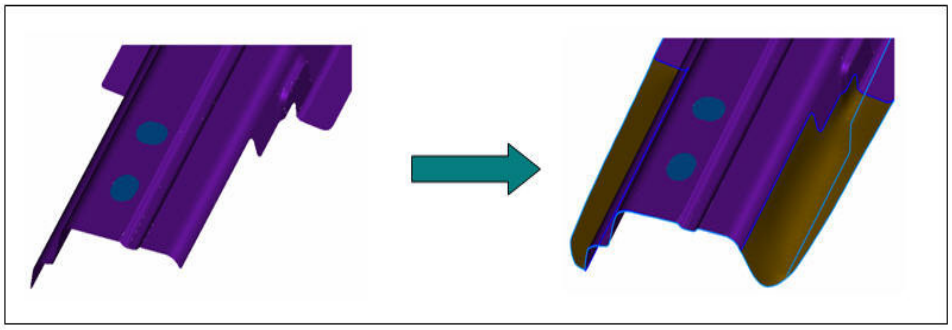

Figure III.A.9 – *Filing the part boundary*

Filling the gap between two parts - When we have two parts it's necessary to fill the gap between them before the addendum can be generated. Similar to the generation of an outer fill, the geometry between double attached pasts is filled by using the concept of roll cylinders. By selecting an appropriate roll radius the user may exert some influence on the outer edge of the fill faces (Figure III.A.10).

Modifying fill faces using Control curves - Without any effort to keep the resultant modification realistic, modifying automatically generated fill faces is possible. This procedure is typical of what the user would follow to create features such as draw bars or take up beads on the fill area between parts. Modifications are carried out by creating and using any number of control curves over the fill area; these control curves determine the shape of the modified fill faces. Control curves may be created and modified using the Curve editor.

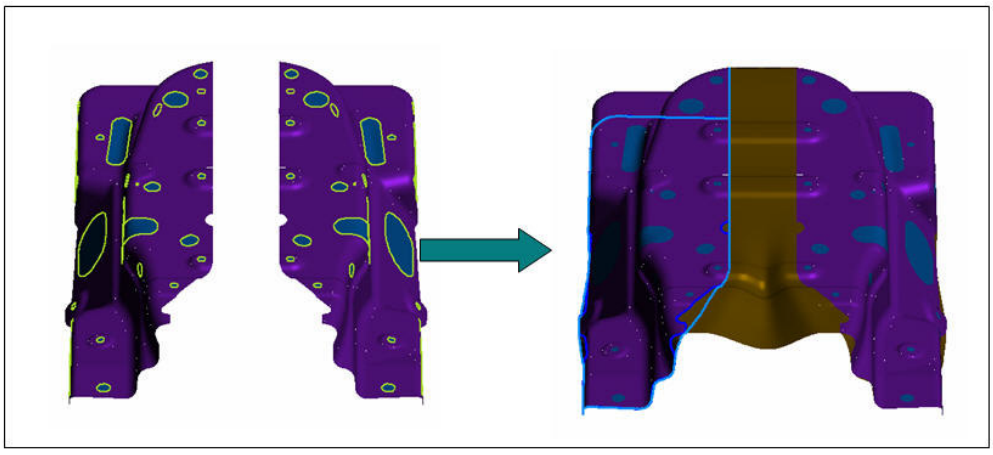

Figure III.A.10 – *Filling the gap between two parts*

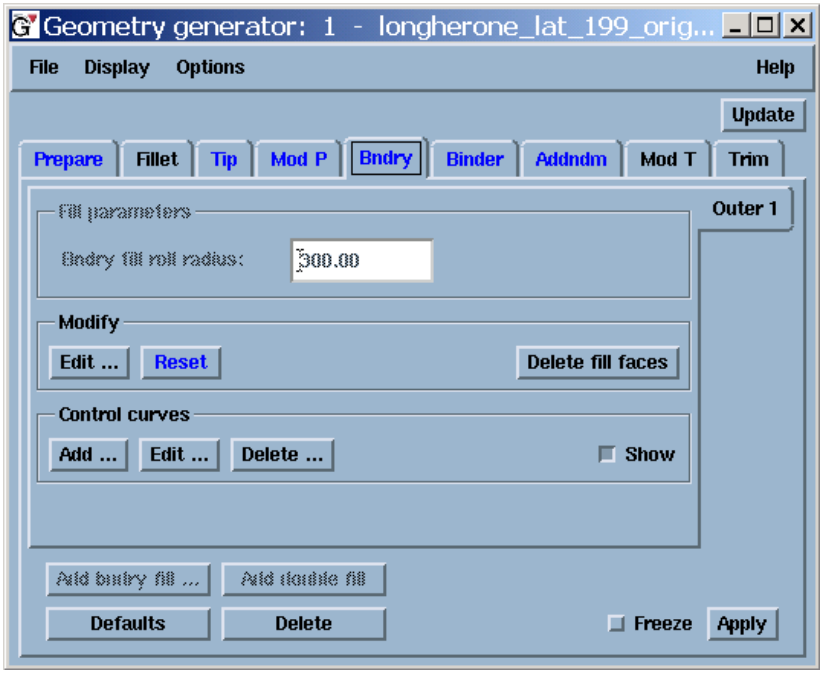

Figure III.A.11 – *Boundary Fill page (Geometry Generator)*

- Binder / Blankholder (positioning, orientation, inclination, flexibility)

Once the part geometry is prepared, the tool design can start with a first design of the binder surface. Several complete and intuitive functionalities for binder surface generation are available, i.e., the user can define the binder surface using parametric profiles and sections, using theoretical surfaces (fitting of flat, cylindrical or conical planes), or the user can import an already existing surface from a CAD file. Depending on the chosen method, the binder surface can be visualized and modified interactively in 2D and 3D simultaneously.

Next to that, there are several options in order to verify the binder definition, e.g. by checking the depth of draw (relative to the binder surface) or the developability of the surface.

Creating a binder surface with *AutoForm-DieDesigner* can be done with the module Auto-Binder, with the module Manual-Binder, or it can be imported from CAD.

The binder surface imported from CAD or generated with Auto-Binder can be optimized with the module Manual-Binder.

By changing the binder surface the existing addendum is dynamically adjusted.

- Creating the Binder surface with the module **Auto-Binder**:

The module Auto-Binder allows the creation of a first concept for the binder surface very quickly. The characteristic of the binder surface can be influenced by many adjustment parameters. Define the settings of the binder on the Auto-Binder pages (Figure III.A.12 and III.A.13). The binder surface is generated automatically. The form and position of the parts as well as a constant drawing depth is considered. The input is very often carried out with sliding bar in the window. Thus, the necessary characteristic of binder specific parameters can be more or less realized. In general the procedure is work in an iterative manner. The first concept of the Auto-Binder is generated with the default values. After this, single parameters are modified until the desired binder surface is created.

The distance from part to binder surface (= drawing depth) is displayed as coloured contours on the part geometry, in order to analyze the current binder surface for uniformity in drawing depth. Select *Uniform* to achieve a uniform drawing depth over the whole part.

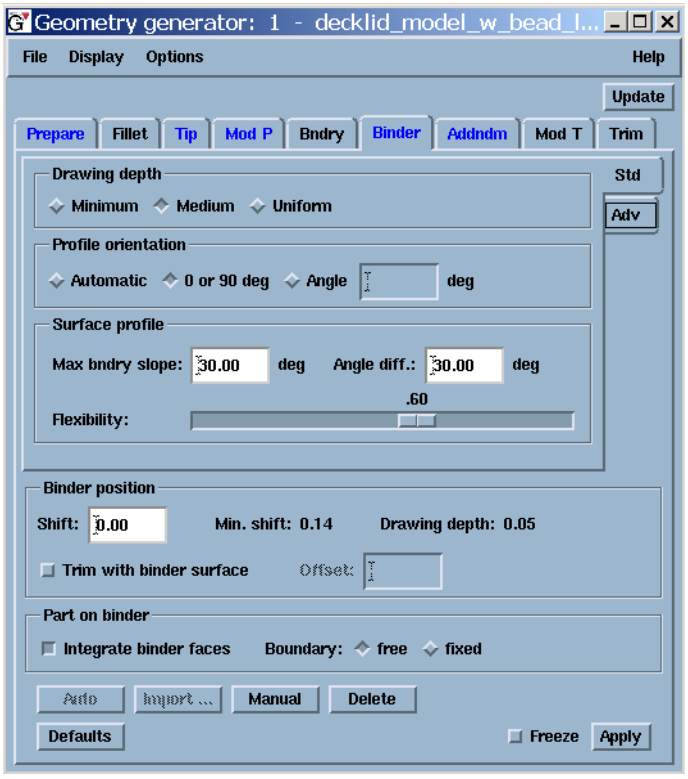

Figure III.A.12 – *Auto-Binder Standard page (Geometry Generator)*

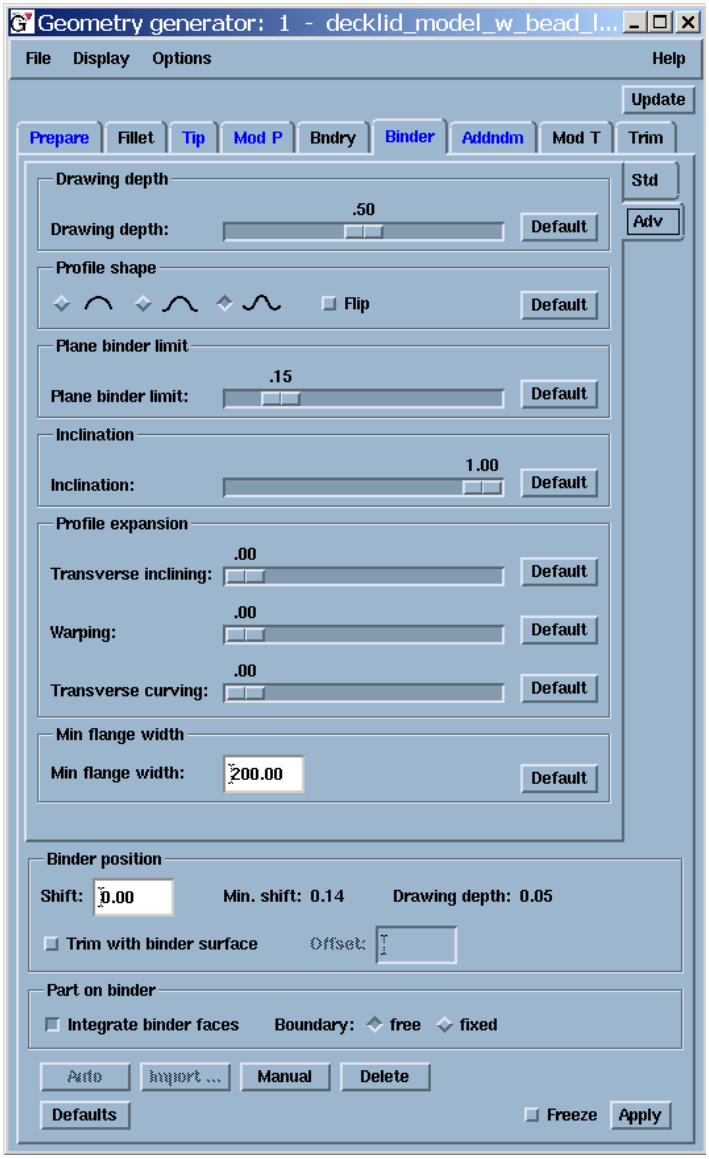

Figure III.A.13 – *Auto-Binder Advanced page (Geometry Generator)*

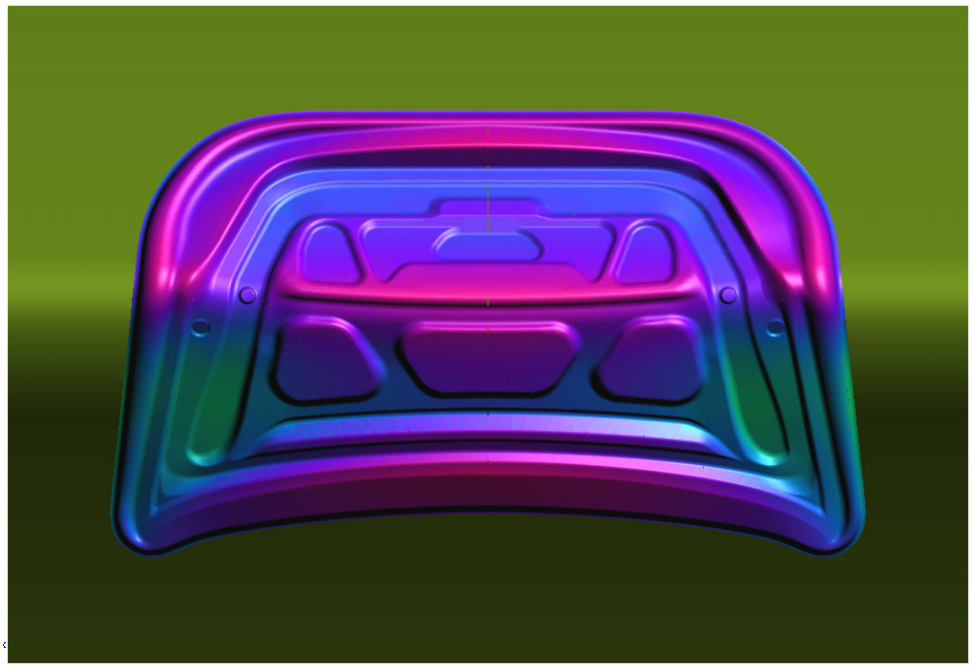

Figure III.A.14 – *Binder surface created with the module Auto-Binder*

- Modifying a binder surface with the module **Manual-Binder**:

The binder surface imported from CAD or generated with Auto-Binder can be greatly improved with the module Manual-Binder.

Binder-profiles can be added. The binder profiles are created and modified with the Curve editor. At least two crossing binder-profiles have to be generated (Figure III.A.15).

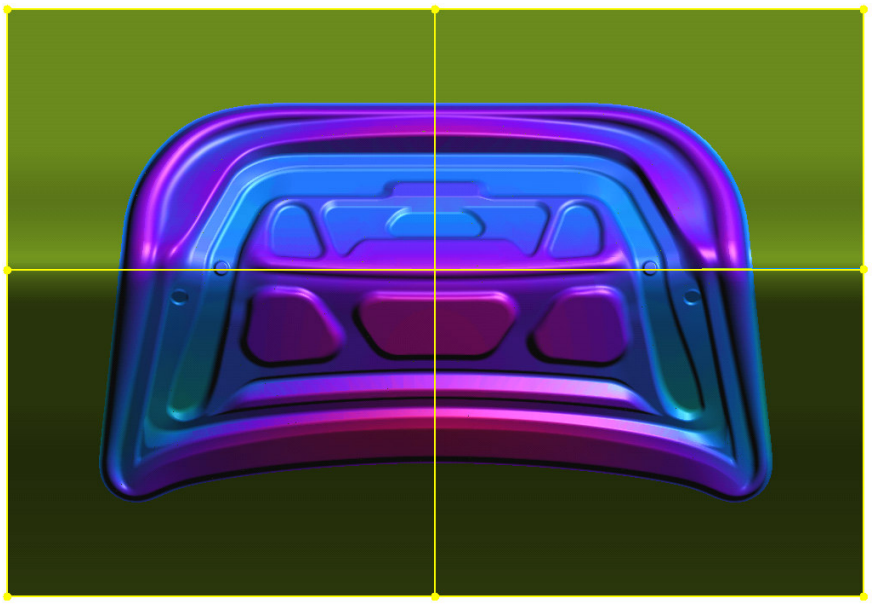

Figure III.A.15 – *Modifying a binder surface with the module Manual-Binder*

Rotating the model in the main display it is possible to see blue, green and yellow lines. These lines have the following meaning:

- Blue lines: The created binder-profiles on the binder surfaces.

- Green lines: Binder-profiles projected in z-direction on the part geometry.

- Yellow lines: The last selected (with the mouse or on the Manual-Binder page) binder-profile together with the projection lines on the part.

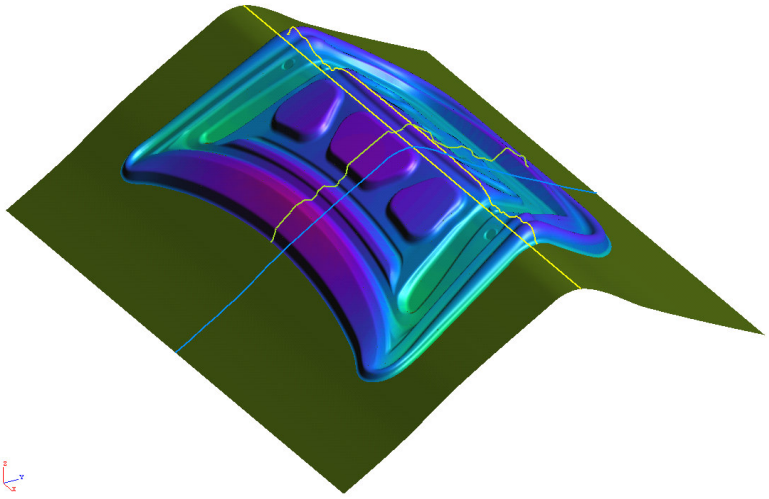

Figure III.A.16 - *Blue, green and yellow lines*

The binder surfaces generated with Auto-Binder or Manual-Binder can be exported as CAD faces in IGES or VDAFS format.

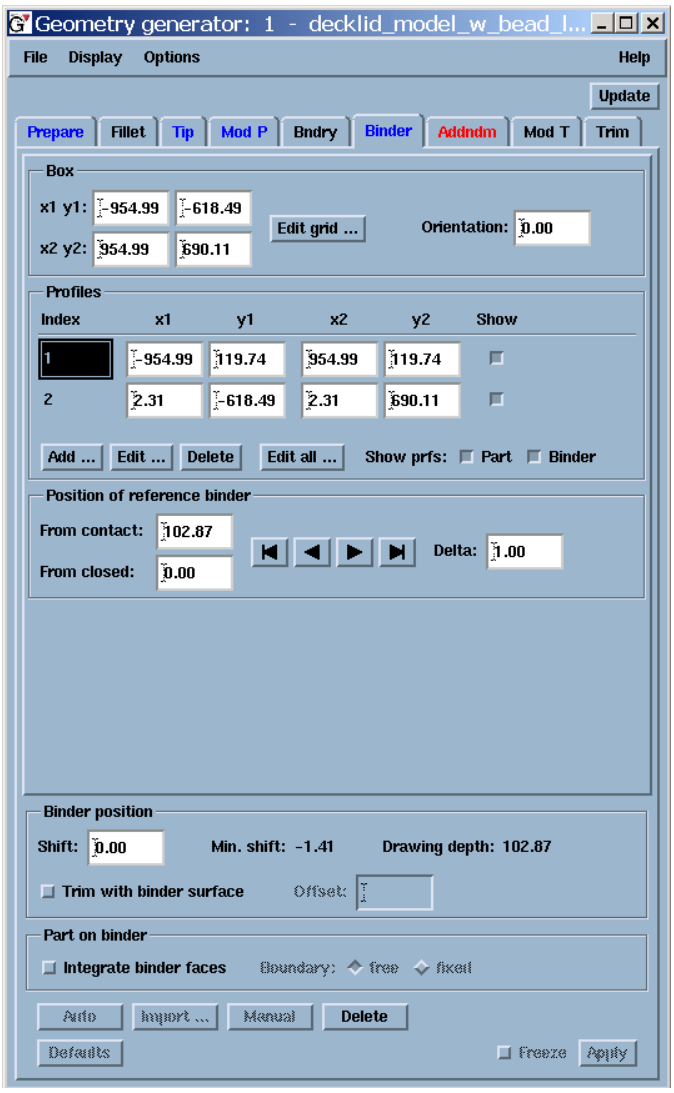

Figure III.A.17 – *Manual Binder page (Geometry Generator)*

- Addendum / Run-off surfaces

An ordinary drawing tool consists of the part geometry, the binder surface and an addendum. In forming processes, the addendum in general performs the task to make a suitable transition from the part to the binder, ensuring a good material flow. In AutoForm, the addendum is created on the basis of several profiles.

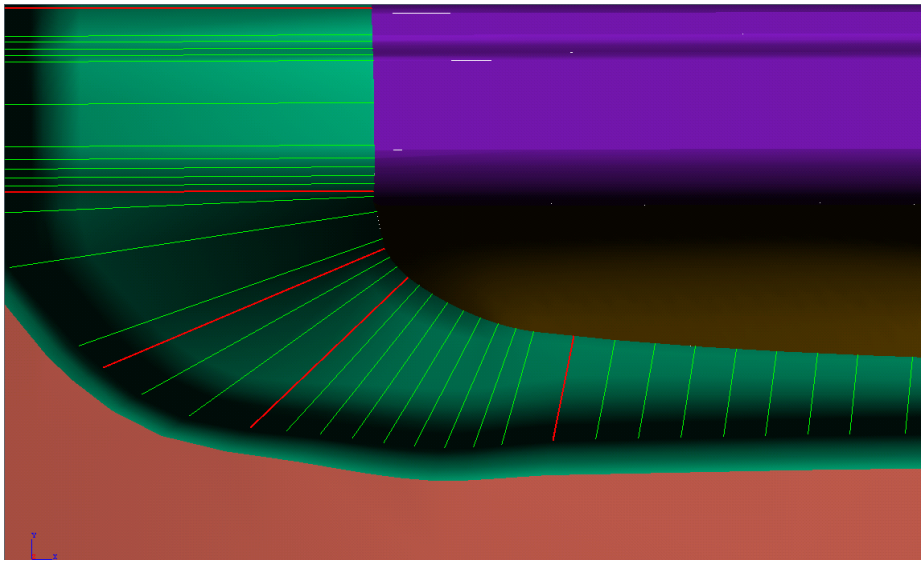

Figure 5III.A18 – *Addendum created on basis of several profiles*

Now that the binder surface is visible, the user can start building the run-off surfaces or addenda. A fully interactive method is available for this: using the drag-and-drop functionality the program lets the user decide what profile (2D section of the addendum) to select and where to position it. When the profile is attached to the part geometry, it can be further modified by changing its orientation or by extending / shortening the profile.

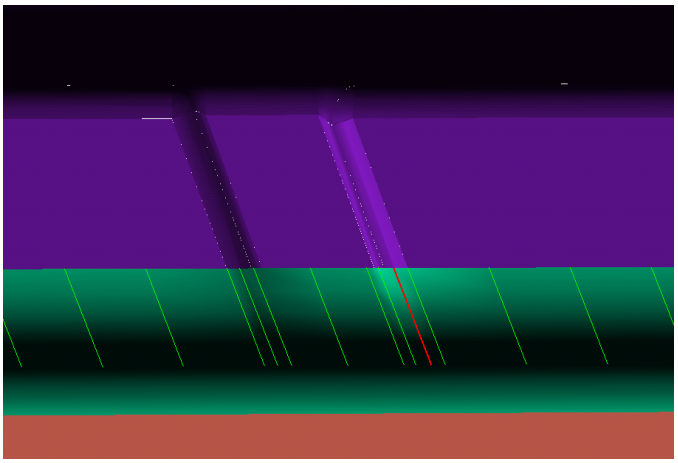

Figure III.A.19 – *One profile selected (in red) and modified (the orientation)*

Next to the 3D interaction to move and resize the profiles, one can have further control to fine-tune the run-offs: the user has the possibility to modify its geometry in 2D as well. In doing so, he will have full control over all the parameters that constructs the profile, such as angles, radii, heights, distances and tangency. By dragging and dropping the control points of the profile one can interactively modify the parameter values.

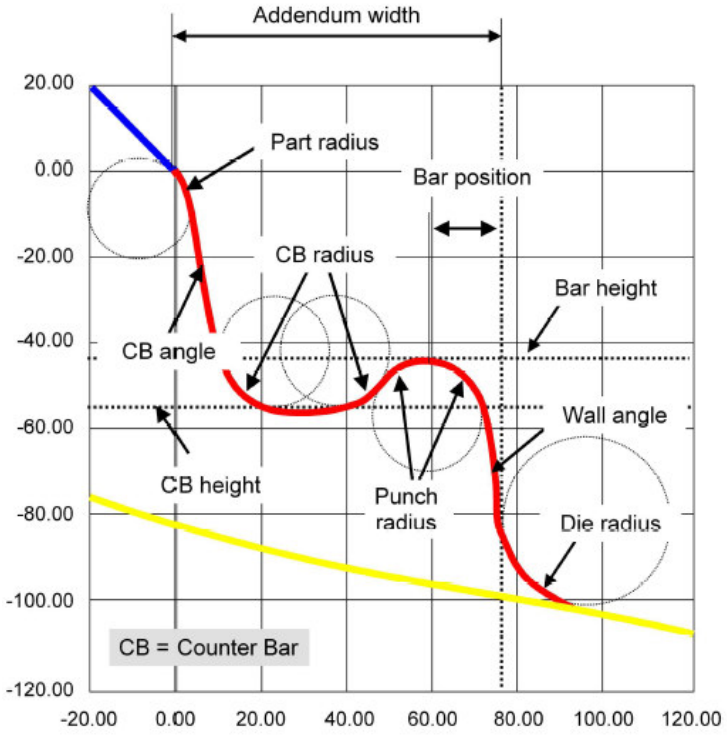

Figure III.A.20 – *All parameters that describe one profile of the addendum*

Modifications in 2D are immediately visible in 3D, thus further enhancing the interactivity. This method is especially useful in conceptual design. However, the user has full control of 2D parameters, he can lock them, impose some of them, free the others, etc. The user can also define all parameters manually.

Finally, the different profiles can be saved in the adequate database. When all profiles are defined, the user can visualize the die entry line. This line is automatically created and can be modified manually. Once the profiles and die entry line are satisfactory, the 3D surfaces can be generated in order to have a global view of the entire tool.

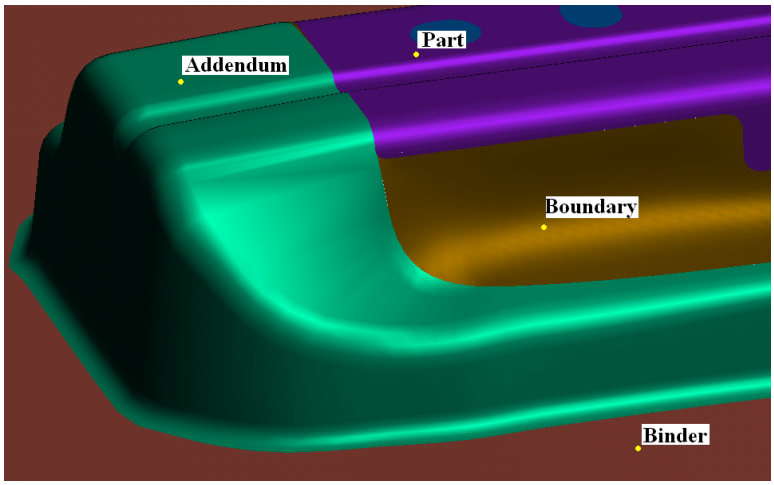

Figure III.A.21 – *Detail of an addendum in 3D*

The 3D surface information is useful for visualization purposes and early anticipation of problems such as tangency.

Brief description of the Addendum page:

The **Addendum** page contains all functions for the generation or modification of an outer or several inner addenda.

The graphic window shows the master-profile or the active individual profile together with the end sections of the part and binder geometry. All radii can be modified by picking and dragging the circle line with the mouse.

The following operations are executed clicking in the mentioned buttons:

Add addendum – generate an outer or inner addendum

Delete addendum – delete the current addendum

Add prf… - generate an user defined profile

Delete prf – delete an user defined profile

Lines… - edit the punch opening line (**PO width**), bar height line and counter bar height line (**CB height**) or import of the punch opening line

Directions… - change the profile directions

Binder… - translation of the inner binder surface (in drawing direction)

The master-profile is the reference profile for the individual profiles. The essential parameters of the addendum (bars, radii and angles) are determined by the master-profile. The heights and lengths vary for different distances between the part and the binder.

In most cases it is not possible to obtain an optimal addendum by using the master profile only. Thus the generation and modification of individual profiles is an essential part of the work.

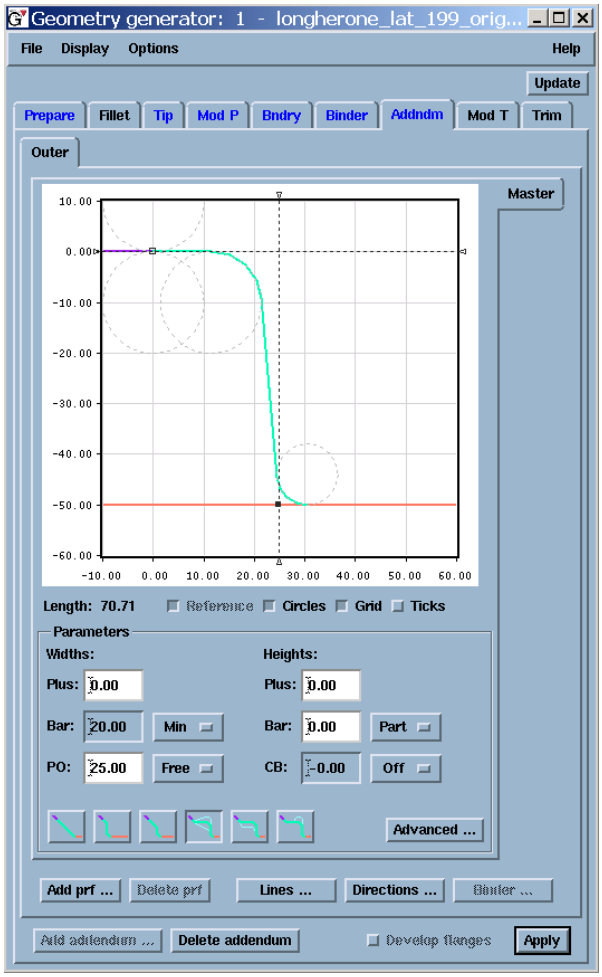

Figure III.A.22 – *Addendum page (Geometry Generator)*

- Modify Tools

To avoid (or minimize) springback problems following the forming of the part, the entire tool geometry may be overcrowned.

This page contains functionality (**Add overcrown** and **Add detail**) to modify geometry of the entire tool. This functionality is therefore basically the same as the available in the **Modify P** page.

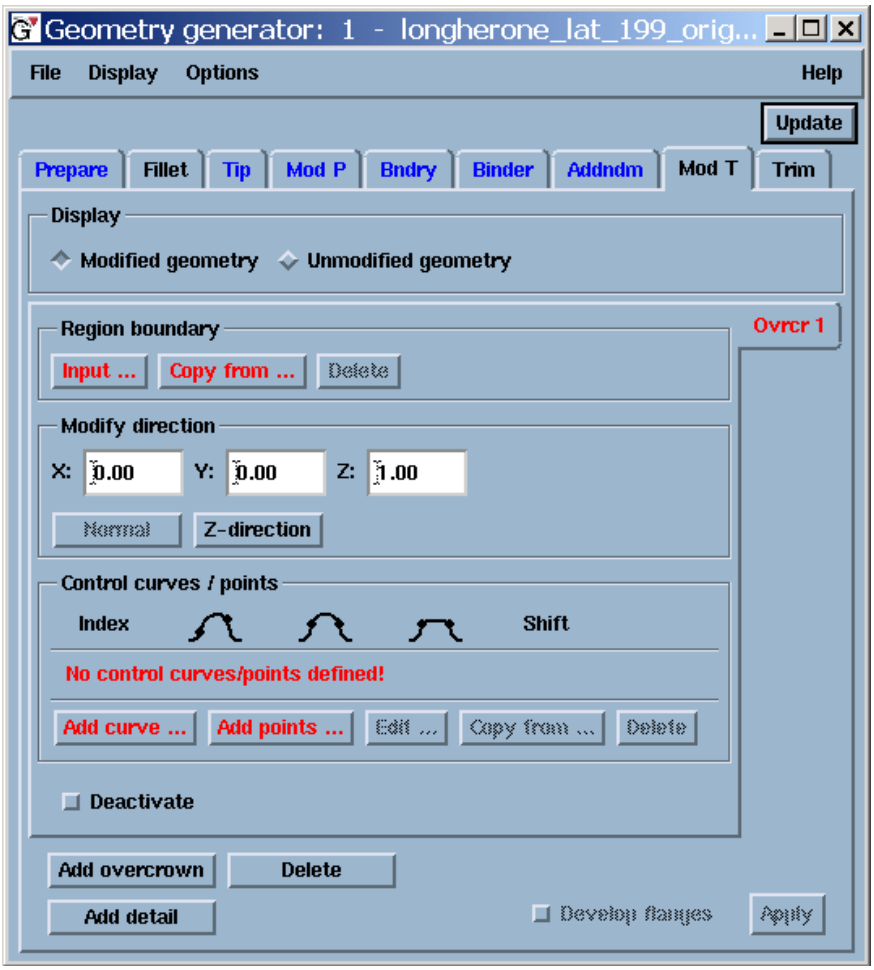

Figure III.A.23 – *Modify Tools page (Geometry Generator)*

Input Generator / Process Data Input

- Title

In this Input Generator page information about the actual simulation file is presented. The title can be changed (Figure III.A.24*)*.

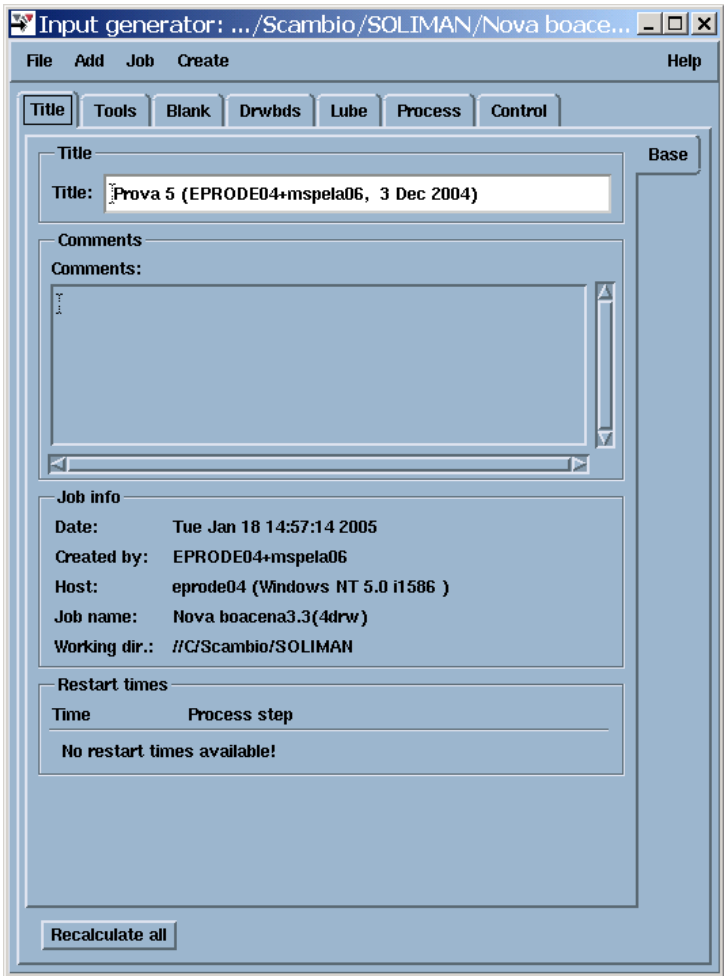

Figure III.A.24 – *Title page (Input Generator)*

- Tools configuration

A very important phase in process configuration is made in *Tools* page. In this page the initial position of the diverse tools and their movements (working direction and distance) are defined. The existing tools are configured individually as they are presented in different sub-pages. It's

important to note that in AutoForm the working direction is always defined with respect to the blank.

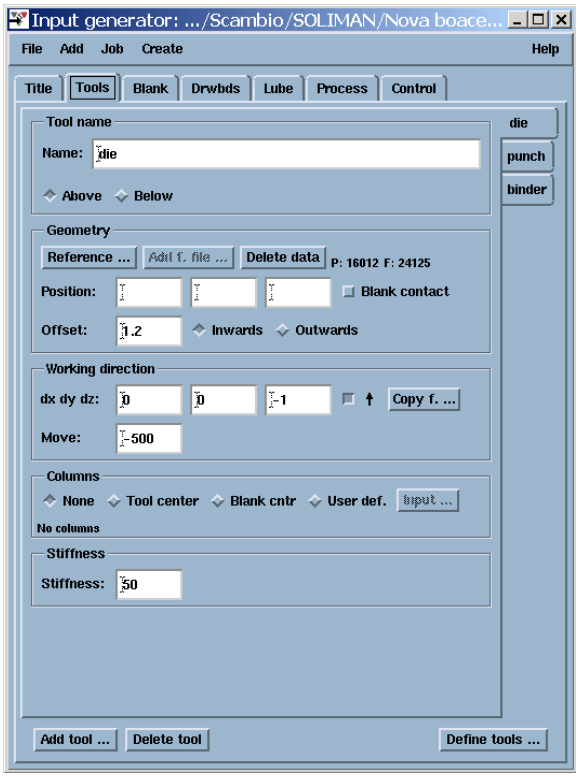

Figure III.A.25 – *Tools setup page – Die sub-page (Input Generator)*

Columns – are the input points of the force for force-controlled tools. It's recommended to use Tool Centre.

Stiffness – the tool stiffness is specified. Stiffness is the Resistance to elastic deformation.

- Blank (shape, size, material properties, thickness e positioning)

In *Blank* page (Figure III.A.26) all the input data related with the sheet metal are made: shape, dimensions, position, material properties and thickness.

In the *Outline* section the following options are possible (Figure III.A.27):

Edit: to change/edit an existing blank (convex, expand and smooth operations are possible)

Import: blank outline is imported from CAD

Rectangle: defines a rectangular blank outline
Copy from: the blank outline is copied from an existing line
Dependent: blank outline is created from an existing line. Blank outline is a reference to the base line. This means only the base line can be changed and the dependent blank outline will also change correspondingly
Arc: blank is defined as an arc segment
Delete: delete the current blank outline

Blank position – one can position the blank on binder or on the die. Insert manually the coordinates is also possible.

In *Properties* section the thickness and material of the blank are inputted. The material can be imported from AutoForm's database.

In *Symmetry–planes/welds/holes* section, add, edit and delete symmetry planes, welds and holes is possible.

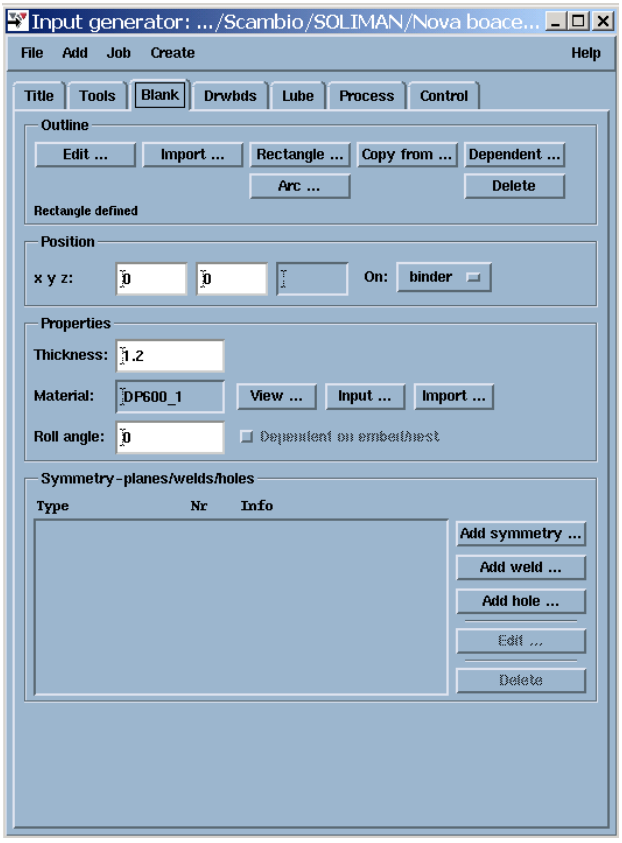

Figure III.A.26 – *Blank page (Input Generator)*

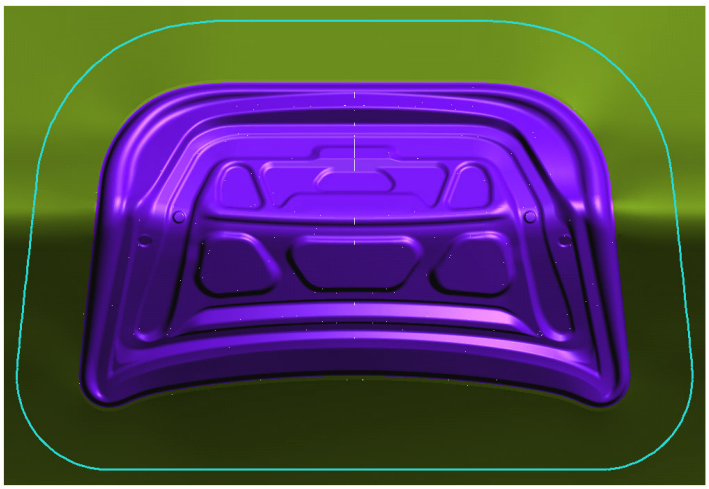

Figure III.A.27 - *Blank outline*

The material file may be selected from the extensive material library using the **Import ...** button.

Use the buttons *View* or *Preview* to display the properties of the selected material: Hardening curve, forming limit curve and r-values.

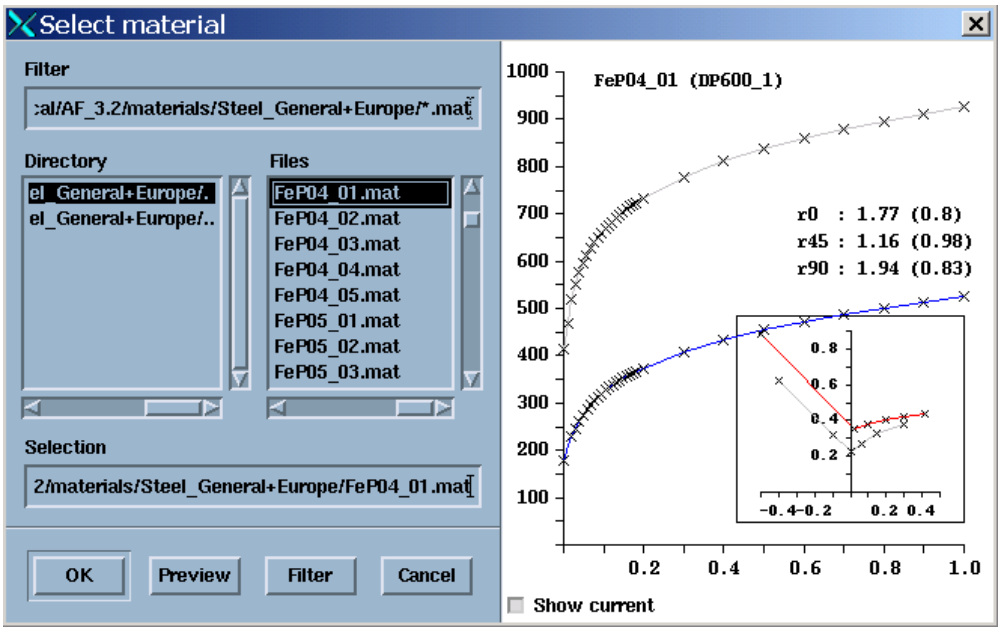

Figure III.A.28 *– The properties of two materials using Preview button*

Material Properties / Material Selection

The following information is available in AutoForm's Materials Database:

- True stress-True strain curve, with the **normal anisotropy coefficients**; and

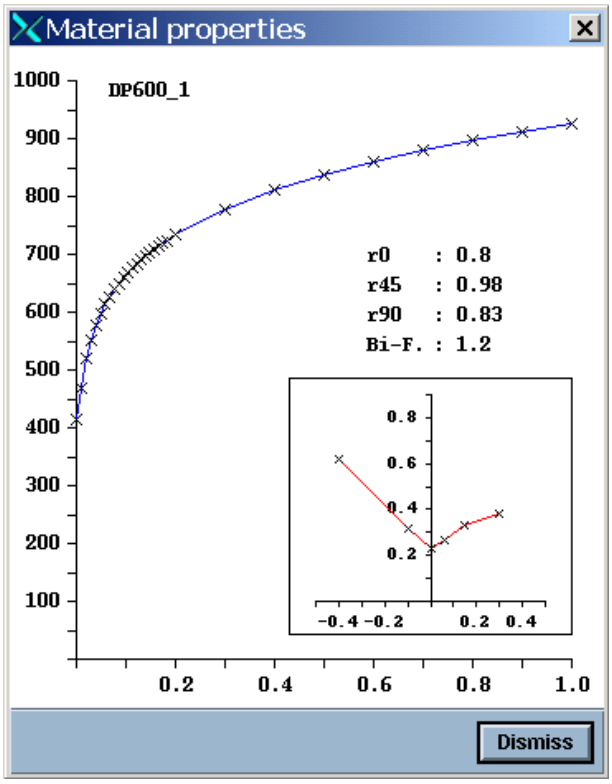

Figure III.A.29 – *Material Properties*

- the **Forming Limit Curve (FLC)** of the selected material (Figure III.A.30)

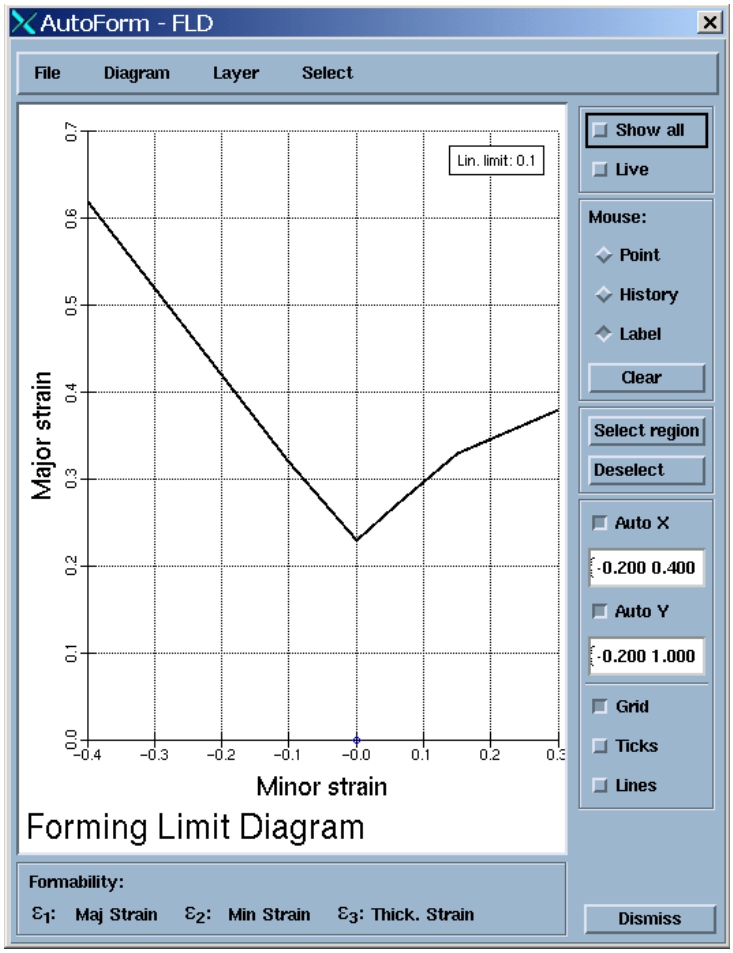

Figure III.A.30 *– Forming Limit Curve of a DP600*

- Drawbeads

The performance of the drawbead, or drawbead-like protrusions such as stepbeads or endbeads, is mainly determined by the drawbead geometry. The radii of the drawbead and the clearance between the drawbead tools can be varied, but also the shape of the cross-section. The shape of the cross-section can be semicircular, rectangular or non-symmetric, where each shape has its specific characteristics.

Drawbeads may be modelled in AutoForm using a force factor to control metal flow, without having to build the detailed drawbead geometry into the CAD model of the tool. This gives the user flexibility in using AutoForm as a tryout tool – using it to quickly compare the performance of different drawbeads regarding feasibility requirements, and to identify the best

bead configuration, based on comparisons, without having to modify tool geometry to accomplish the same. Thus, in AutoForm, drawbead is defined using only a bead centre-line and not with the real bead-profile geometry. This line specifies the position of the drawbead. Furthermore the restraining force is specified and the real profile geometry depends on it. This allows saving time as the calculations are much more faster considering this restraining force instead of the geometry of the drawbead.

AutoForm now offers a Drawbead generator for the correlation of the real profile geometry of drawbeads and drawbead force. With the Drawbead generator the real geometry of the drawbead can be specified and the force factor is automatically calculated by the program. If the force factor is known, the Drawbead generator will determine the real geometry of the drawbead.

Unfortunately the AutoForm version we used was a Beta version and the option **Drawbead Generator** was inefficient.

To define a drawbead an additional page has to be added to the Input Generator.

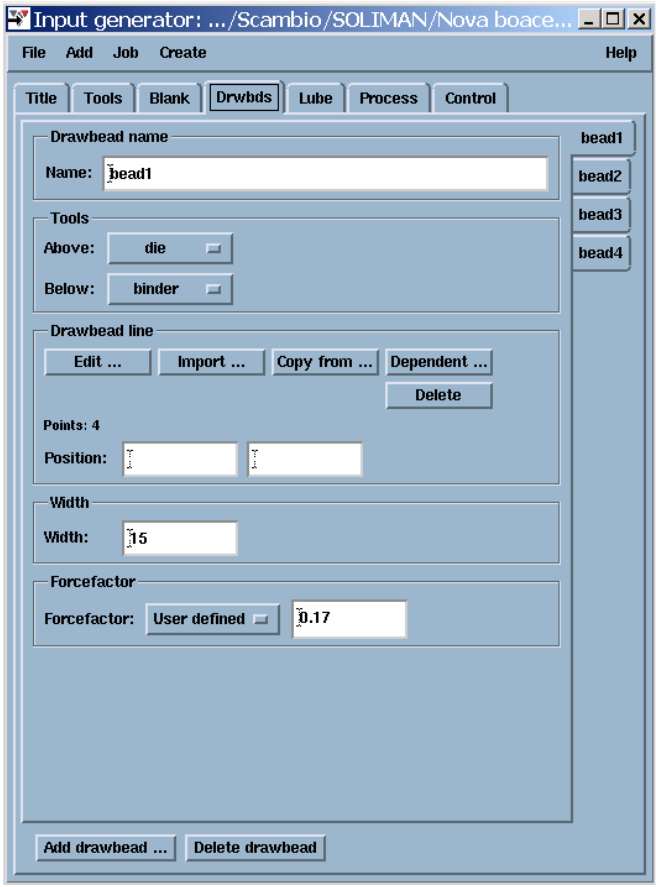

Figure III.A.31 *– Drawbeads page (Input Generator)*

Brief description of *Drawbead* page commands:

Name: Name of a drawbead can be specified.

Tools: Tools are defined; drawbead is active when these tools are closed.

Input ...: Position of drawbead line can be specified (Curve editor).

Import ...: Drawbead line is imported from CAD.

Copy from ...: Drawbead line is copied from an existing line. Base line and drawbead line are treated as different lines.

Dependent ...: Drawbead line is created from an existing line. Drawbead line is a reference to the base line. This means only the base line can be changed and the dependent drawbead line will also change correspondingly.

Position: Displacement of drawbead line in x-y plane.

Width: Width of a drawbead.

Forcefactor: Force factor of a drawbead

- Lubrication (Lube)

The friction coefficient between sheet and tools can be specified. It is recommended to use 0.15 for sheet-steel and 0.18 for aluminium. Different friction coefficients can be specified for tools above and below the sheet or for each of the sheet/tool contacts.

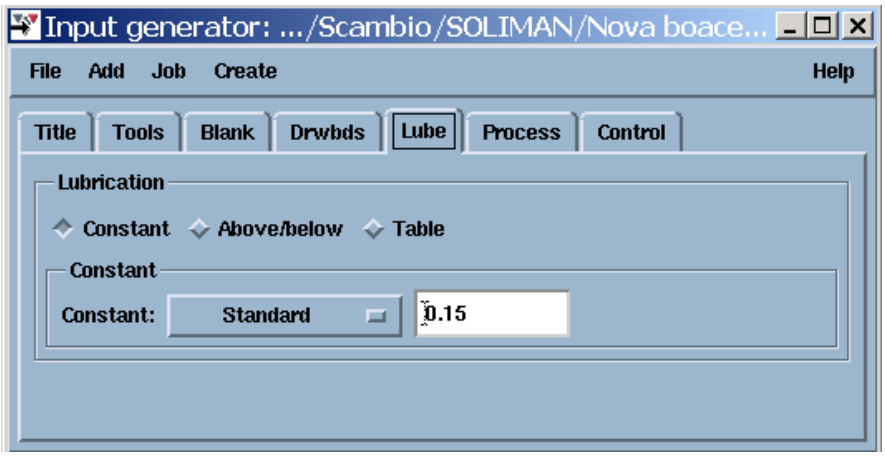

Figure III.A.32 – *Lubrication page (Input Generator)*

Process Description

- Process Steps (Gravity, Closing, Drawing, Cuttings, Springback…)

The description of the process is made in the *Process* page of the Input Generator. The various operations to be performed, their characteristics and the order in which they will be executed are defined here.

Gravity (Figure III.A.33), *Closing* (Figure III.A.34) and *Drawing* (Figure III.A.35) are always performed in a stamping simulation. Then, several other process steps may be added to the stamping process: cuttings, springback, annealing, positioning and secondary forming operations (restrike, flanging, hemming).

In the respective sub-pages, information related to each process step is inputted. The input fields are specific for each process step.

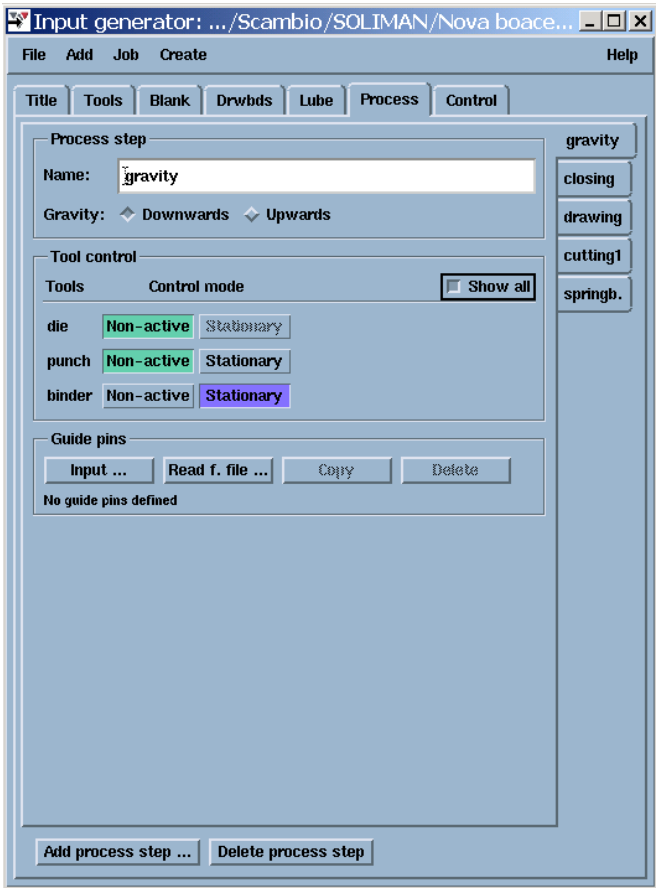

Figure III.A.33 – *Process Step page – Gravity sub-page (Input Generator)*

Closing (Binder wrap): Metal sheet is pressed between the die and binder.

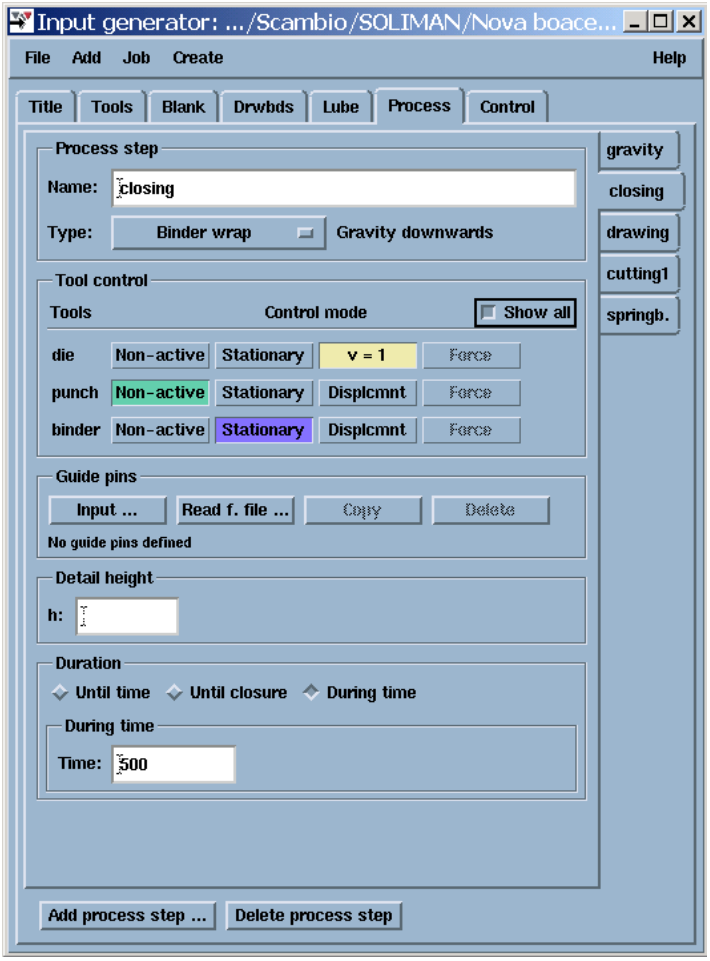

Figure III.A.34 *– Process Step page – Closing sub-page (Input Generator)*

Drawing: The metal sheet flows between the die and the punch till the end of the drawing tools movement.

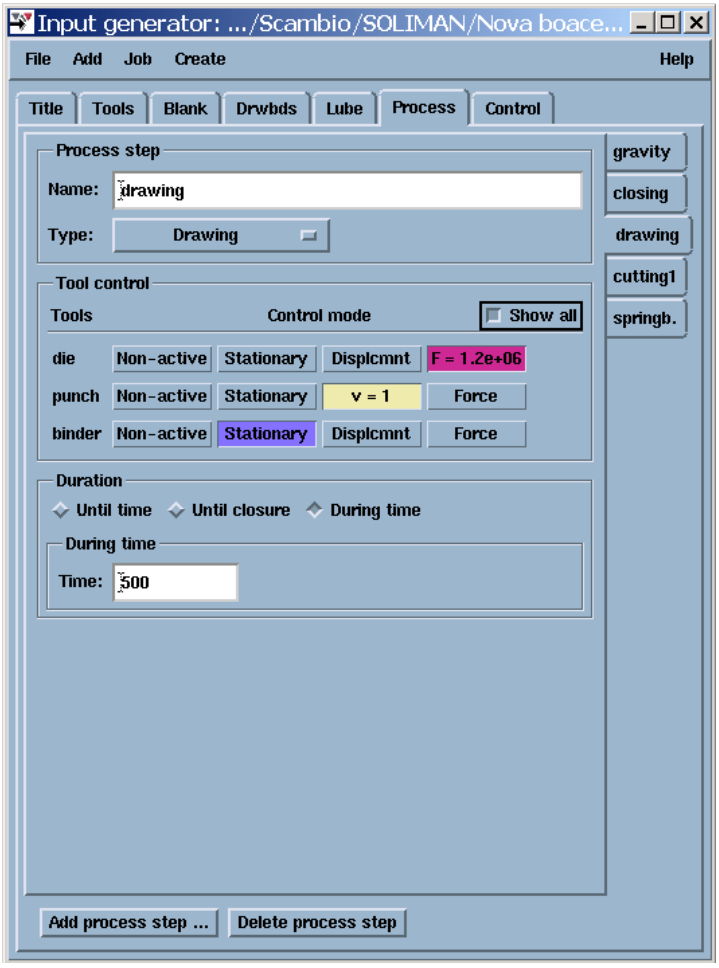

Figure III.A.35 *– Process Step page – Drawing sub-page (Input Generator)*

Definition of different cutting process types: The definition of cutting processes is always done on **Process** page of the input generator. In AutoForm different cutting types can be defined:

-relief cut

-trimming cut

-hole

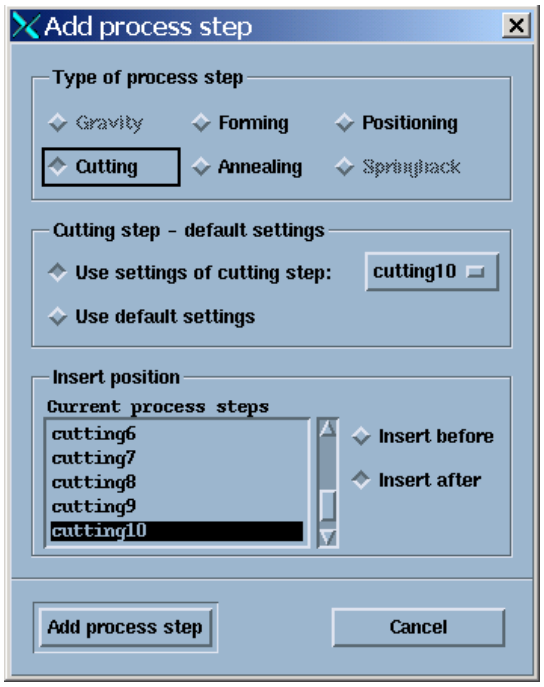

Figure III.A.36 – *Add process step dialog box*

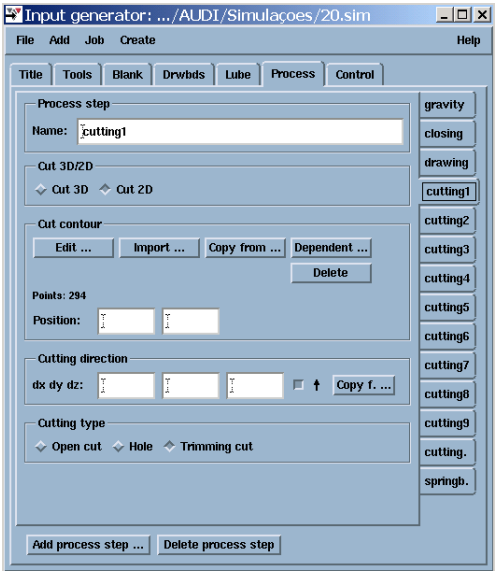

Figure III.A.37 – *Input for trimming cut (Process step page – Cutting sub-page)*

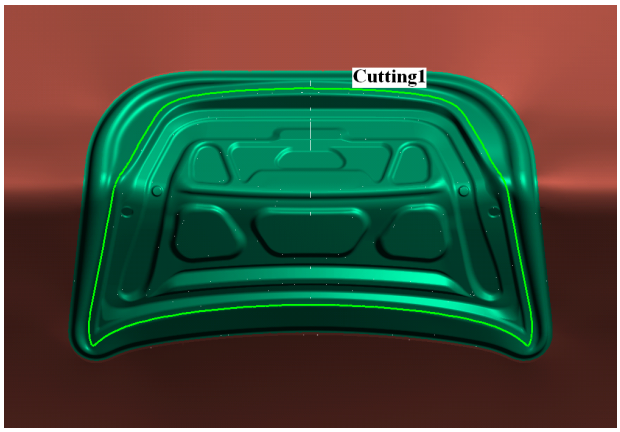

Figure III.A.38 – *Cut line for trimming cut*

Figure III.A.39 – *Cut line for hole*

Springback: A new process step must be added to simulate springback. The input page for the springback is very simple, no additional input is required.

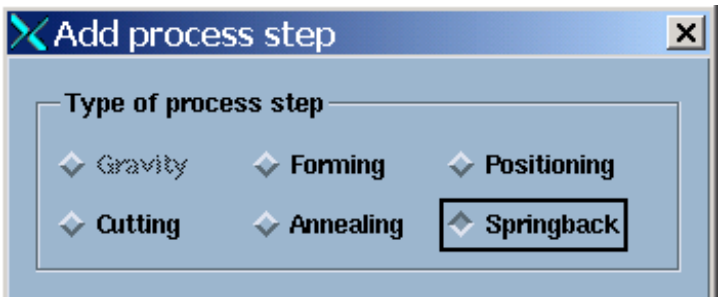

Figure III.A.40 - *Add process step: Springback*

Calculus Configuration

- Control data (Input of numerical parameters)

In this page numerical parameters concerning the calculus execution are inputted, such as the accuracy level and the number of layers used.

AutoForm calculates the stress-deformation condition in the blank's thickness subdividing it in an unpaired number of layers, so that symmetry respect to a middle plan is obtained. The larger the number of layers, the more precise the analysis, but the calculus time is therefore longer.

For sheet thickness greater than 1.5mm is recommended the selection of *ThickSheet / Springback in later restart.*

Write Restart button selects whether an additional Restart file (*.rst) should be generated during simulation. This file contains all data that is necessary to restart the simulation from a particular time. Restarts can be used to save time (e.g. for multi stage processes), as the different forming processes can be simulated one after the other. The disadvantages is the size of the *.rst file which requires greater disk space.

Taking into account the speed of AutoForm, the restart option is only useful for large parts (e.g. side panel, floor panel).

Inputs on this page may be numerical (**Main**), or may be a selection of result variables (**Rslts**):

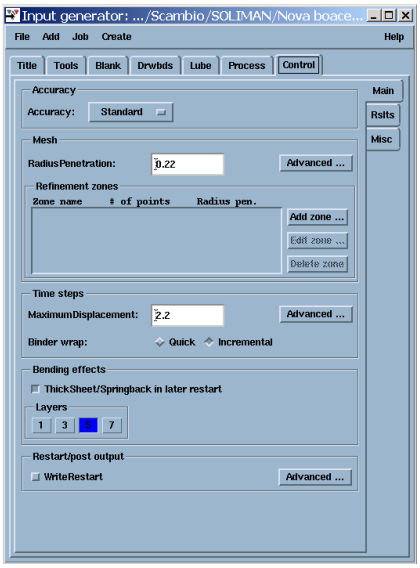

Figure III.A.41 *– Main Control Data page (Input Generator)*

Regarding the pretended results presentation, the Results division of the Control page allows its selection (Figure III.A.42).

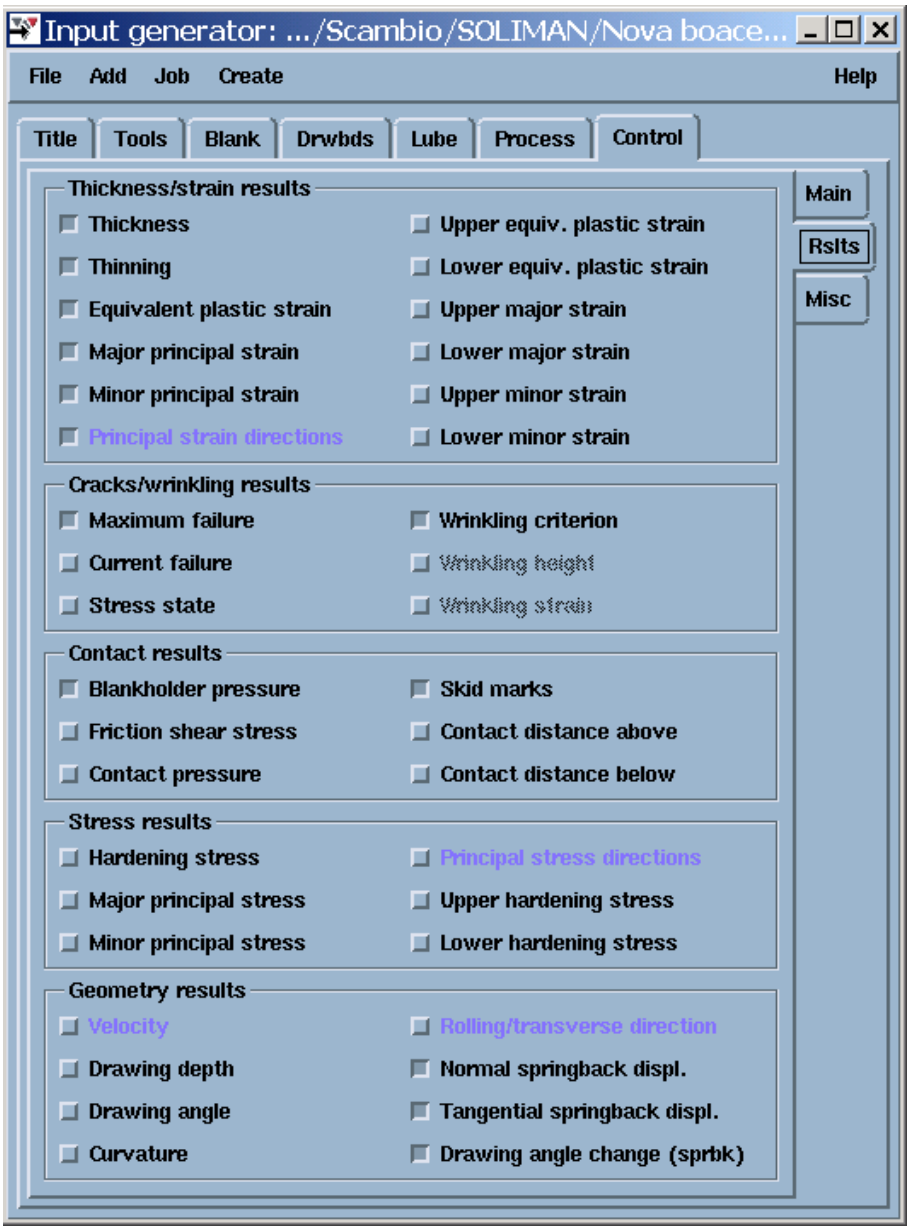

Figure III.A.42 – *Results Control Data page (Input Generator)*

III.A.4.**2 - Computational Analysis**

After the inputting of all data required, the simulation can now be executed. Selecting *Start Simulation* in the menu bar option *Run,* the *Start job* window is opened (Figure III.A.43). Clicking in *Start* button it is possible to start the computation of the simulation.

However, a previous kinematic check may be useful. Selecting *Kinematic check only* option the computer checks the tool movement only. This is completed in a few seconds. This functionality helps avoid possible errors of the tool movement or tool positioning and is recognized during the simulation. If this button is activated, only the tool movements are calculated and displayed. The blank remains undeformed.

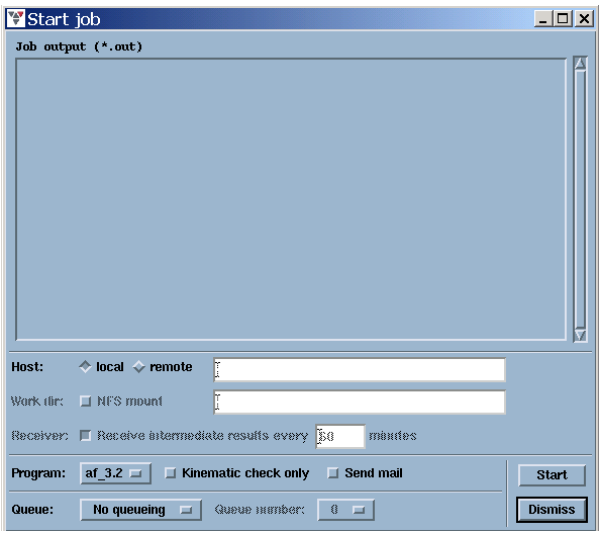

Figure III.A.43 – *Start job window: to run a simulation or a kinematic check only*

While all the information is being processed by the computer during the calculation, the process iterations are presented in an output window as shown in Figure III.A.44.

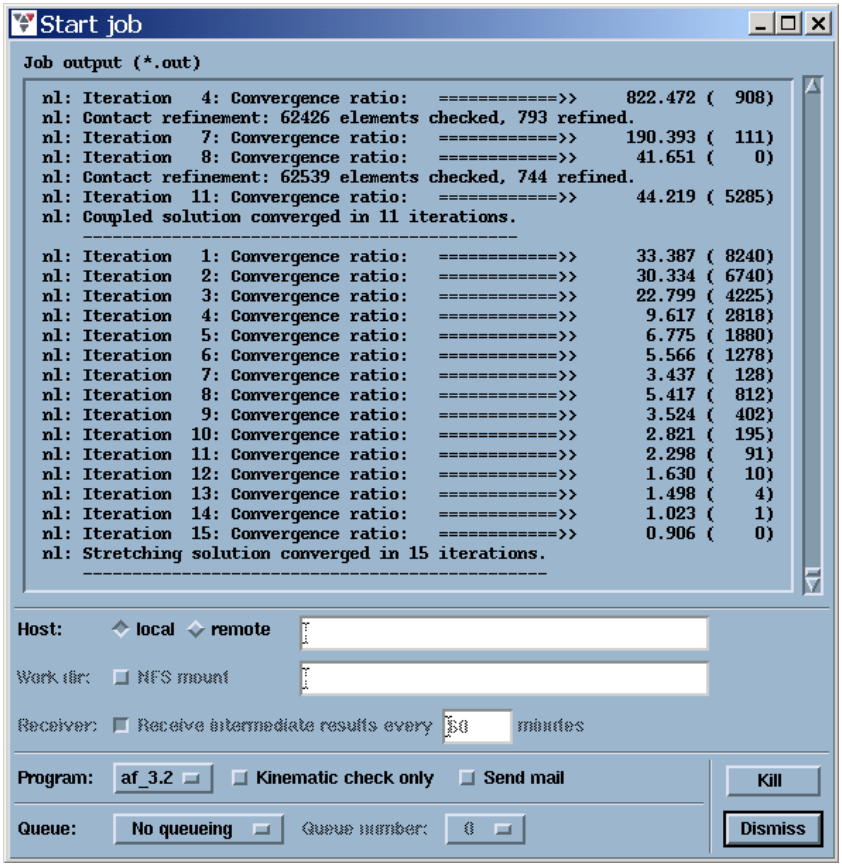

Figure III.A.44 *– Process iterations during the computation of the simulation*

III.A.4.3 - Post-Processing of Results (Analysis of Results)

After re-opening the simulation file it is possible to accompany several steps of the simulation process from plan sheet till the final stamped part, including springback effect (if selected).

This is very important since not only gives an idea of the simulation's progress but also, in case of failure, it is possible to see where did it went wrong, this way helping to understand and try to correct / improve the simulation try-out.

Colour shaded post values such as sheet thickness, cracks, strain and stress as well as process parameters such as forces are available for the evaluation of the simulation. Wrinkles are identified by inspecting the shaded representation of the model or by means of colour shaded post values. These possibilities are completed by additional special evaluation criteria such as skid/impact lines.

The punctual lecture of the diverse result parameters (thickness, thinning, normal displacement, etc.) is also possible when clicking with the

right mouse button. Display the maximum and minimum values of the current result variable is also possible.

In the following, the analysis of some important result variables will be discussed. These results can be displayed both as coloured and shaded images.

Visual evaluation

Through simple visual observation it is possible to realise coarsely if the simulation has been successfully executed or not, i.e., if the results seam satisfactory or not.

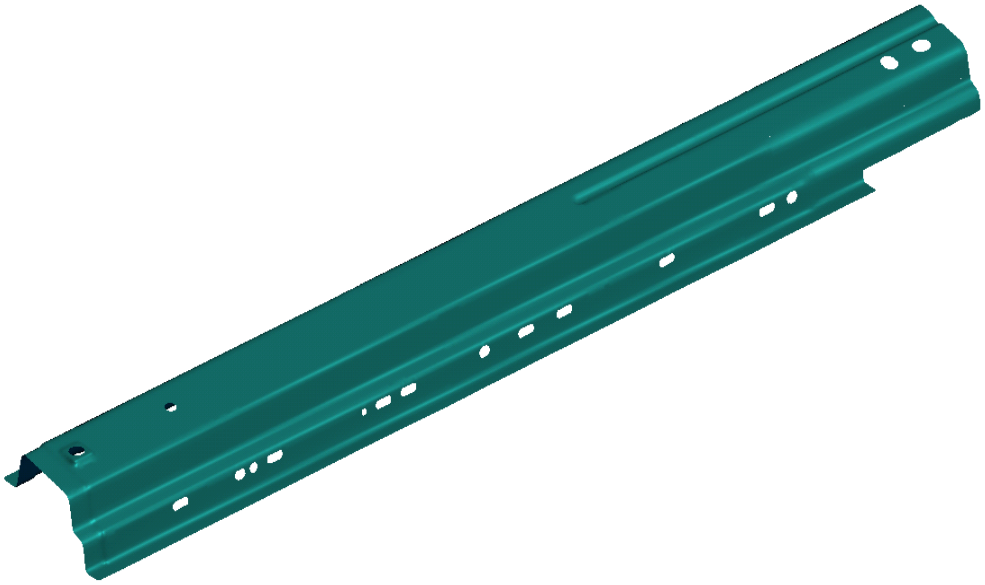

Figure III.A.45 – *Example of a component without defects*

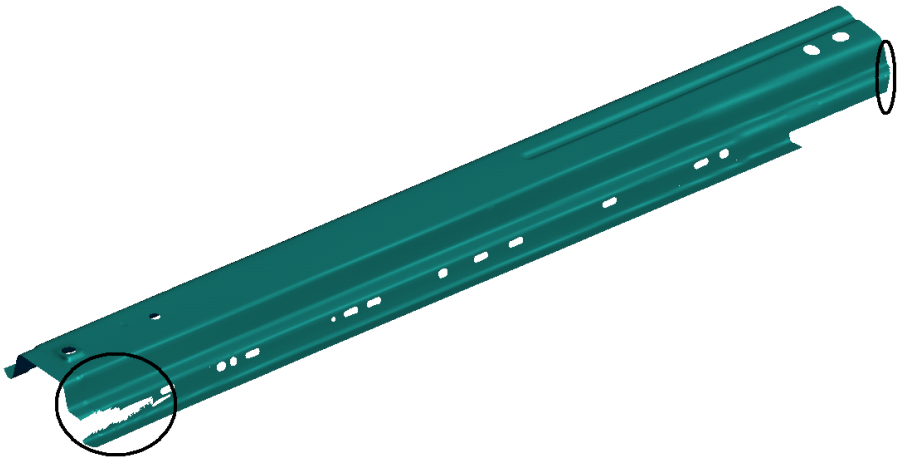

Figure III.A.46 – Example of a component with evident defects

Forming/Stamping evaluation

(formability, FLD, wrinkling criterion, failure (maximum))

Formability

The most important criteria to evaluate the forming/stamping success is the result variable *Formability*. It gives a general survey of the feasibility of the part. This result variable displays the strain state at different locations on the formed sheet (based on the Forming Limit Diagram – FLD). Different colours are used to denote the qualitative types of strain states, i.e., areas undergoing different stresses are coloured differently on the part:

- *Cracks (Red)*: Areas of cracks. These areas are above the FLC of the material used.

- *Excessive Thinning (Orange)*: In these areas, thinning is higher than the acceptable value (default value for steel is 30%)

- *Risk of Cracks (Yellow)*: These areas may crack or split. By default, this area is in between the FLC and 20% below the FLC

- *Safe (Green)*: All areas that have no formability problems, i.e., which have no defects – wrinkles, thinning or cracks.

- *Insufficient Stretching (Gray)*: Areas that have not enough strain (default 2%)

- *Wrinkling Tendency (Blue)*: Areas where wrinkles might appear. In these areas, the material has compressive stresses but no compressive strains

- *Wrinkles (Purple)*: Areas where wrinkles can be expected, depending on geometry curvature, thickness and tool contact. Material in these areas has compressive strains which mean the material becomes thicker during the forming process.

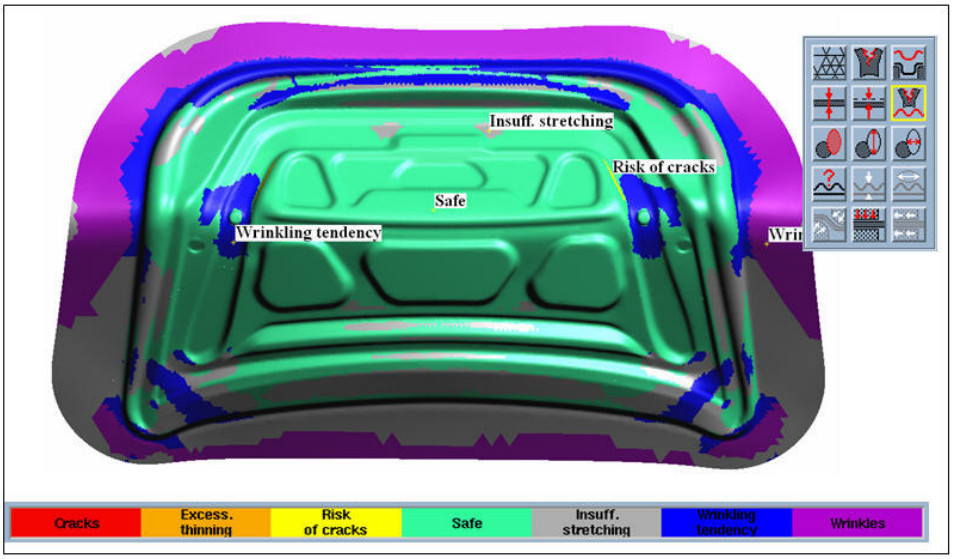

Figure III.A.47 - *Display of the result variable Formability*

The default-values of result variable *Formability* can be changed in the following menu:

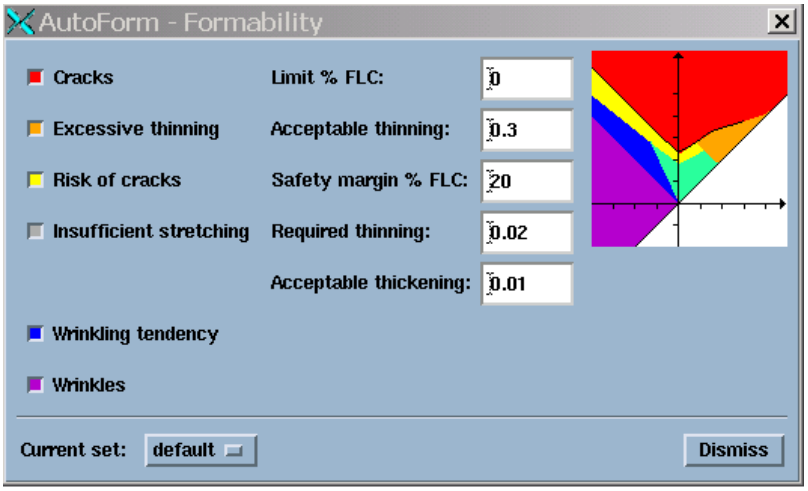

Figure III.A.48 *– Formability dialog box. The small plot shows the different strain regions/states with respect to the FLC.*

Forming Limit Diagram (FLD)

The Forming Limit Diagram (FLD) describes the failure of the sheet metal due to cracks. In the FLD the Forming Limit Curve (strain states above those failure/cracks occur) is represented as a black curve. Into this diagram, all finite elements of a simulation with the two main strain results (major and minor) are shown. So, one can judge the robustness of a reforming process also visually in this diagram.

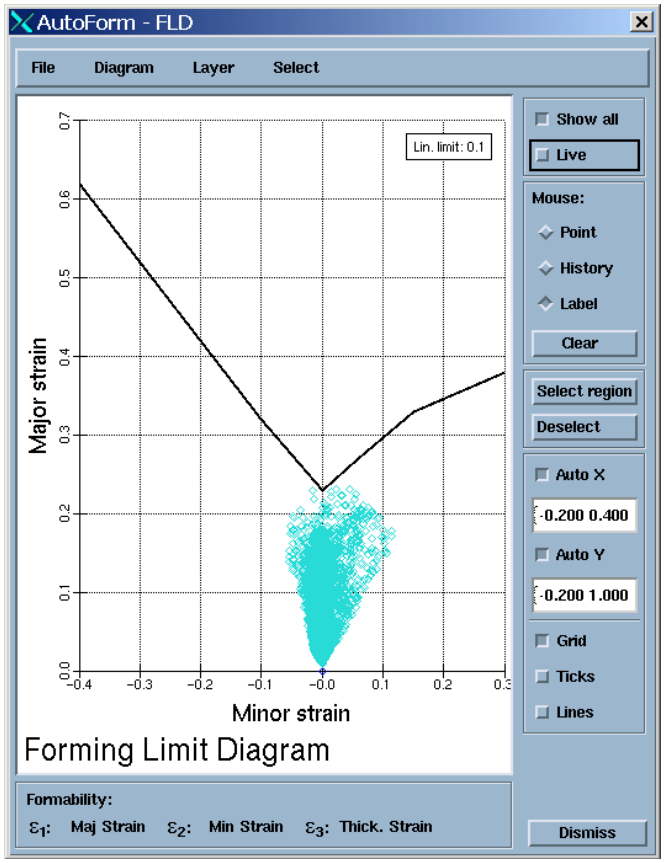

Figure III.A.49 – *Representation of all finite elements in the FLD at the end of the forming process*

By selecting *Show all* (on the top right), all the elemental strains are shown in this diagram. In the current example, all strains are situated below the border deformation curve. This indicates that the process is quite safe and robust from a formability standpoint.

It is also possible to plot the colours of the post variable *Formability* in the forming limit diagram, as shown in the following figure:

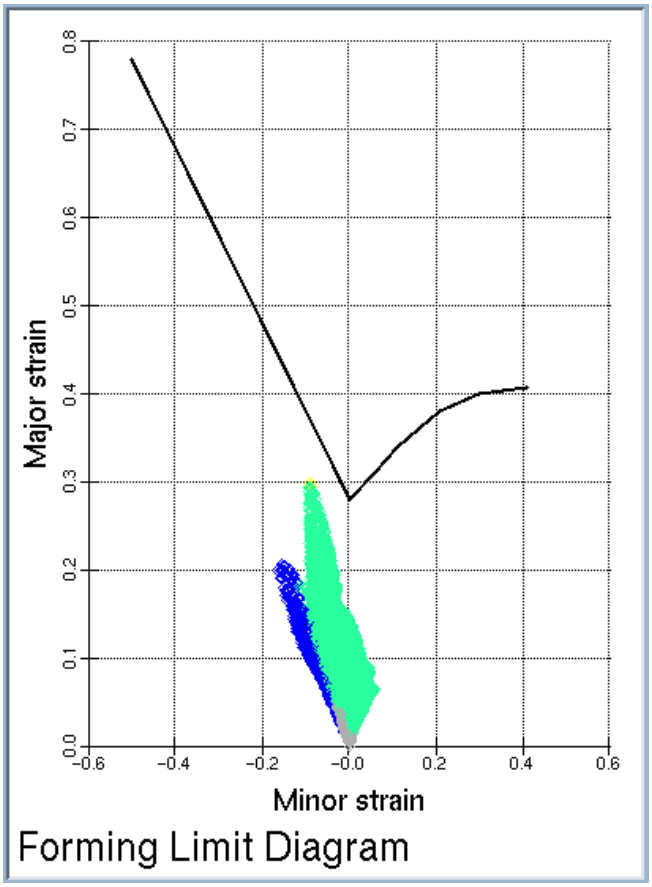

Figure III.A.50 – *Representation of all finite elements in the FLD with the colours of the post variable Formability*

Wrinkling Criterion

In order to verify if there are areas where the material has tendency to wrinkle, *Wrinkling Criterion* option should be activated (see Figure III.A.51). Thanks to the chromatic scale in the bottom it is possible to observe the areas where the metal sheet tends to become thicker and, by instability, to wrinkle.

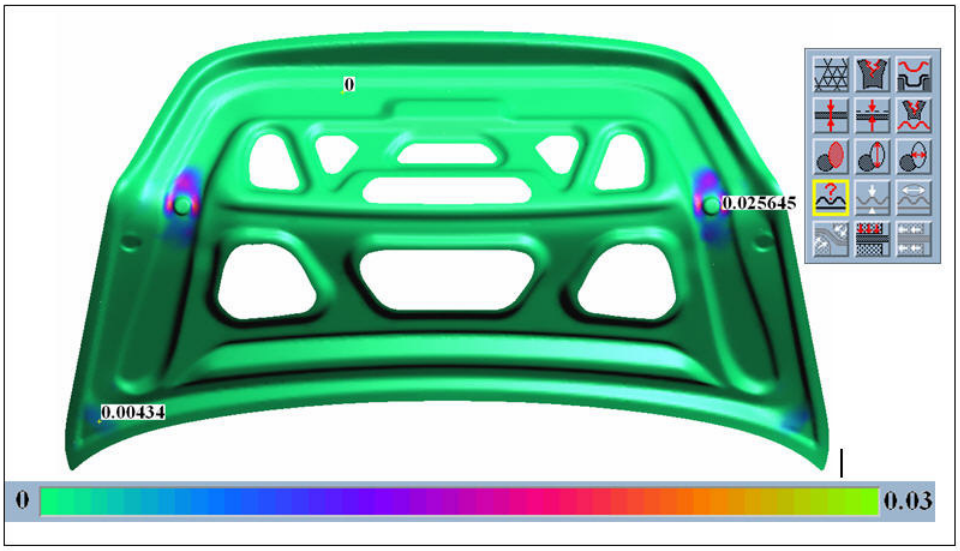

Figure III.A.51 – *Wrinkling criterion analysis of an automobile deck lid*

Thickness / Strain evaluation

(thinning, thickness, plastic strain, major strain and minor strain)

Thinning

Another result variable that is often used is the percentage thinning of the material (*Thinning*).

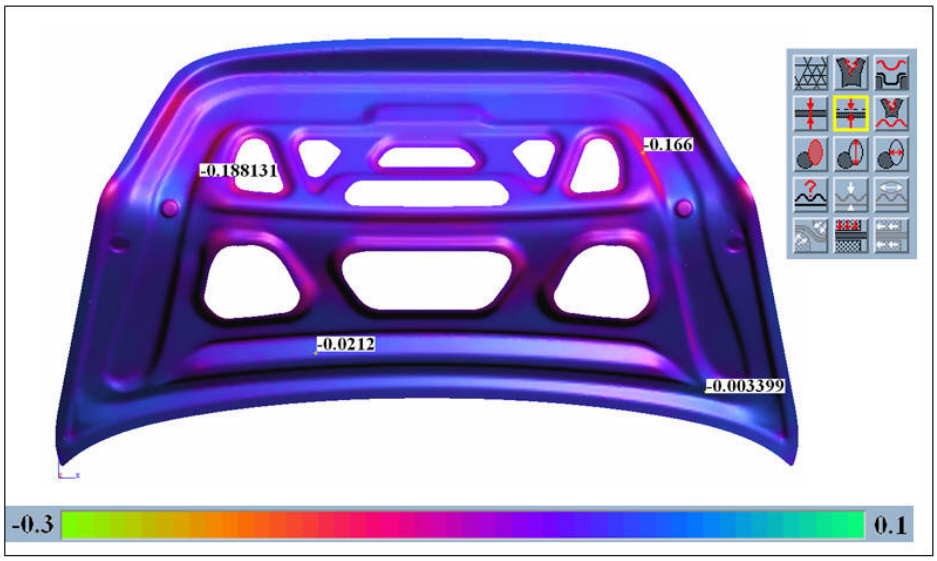

Figure III.A.52 *– Display of the result variable Thinning with min and max values in the main display*

A scale is displayed in the lower part of the main window with a range of 30% thinning (-0.3) to 10% thickening (0.1), coloured from yellow to green (depending on the use colour settings). The exact thinning level at any location on the formed sheet may be displayed by clicking at that location on the sheet (in the main display) using the right mouse button.

Thickness

The thickness of the metal sheet is displayed with this option (Figure III.A.53).

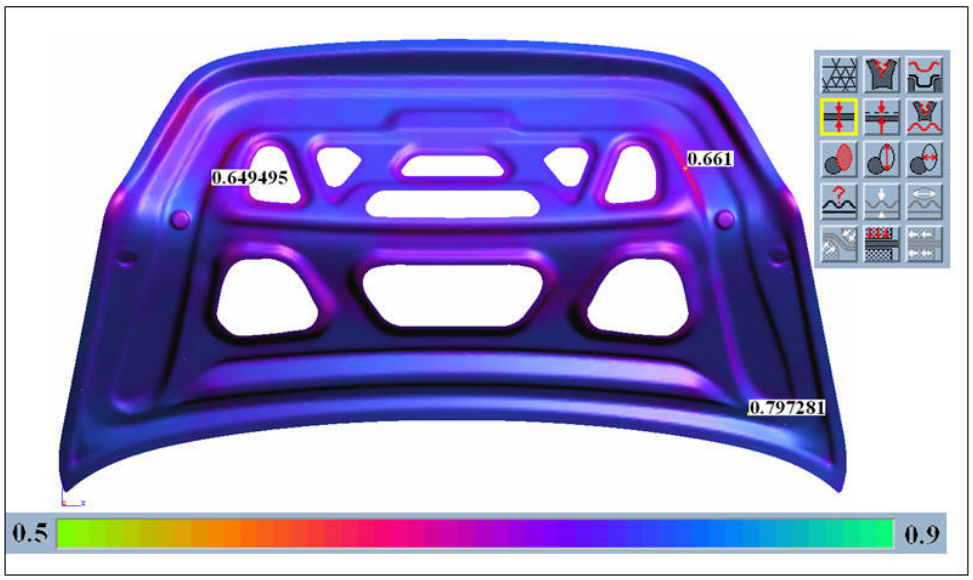

Figure III.A.53 – *Display of the result variable Thickness in the main display*

Plastic Strain

The Plastic Strain of the blank is another interesting possibility to analyse the simulation results.

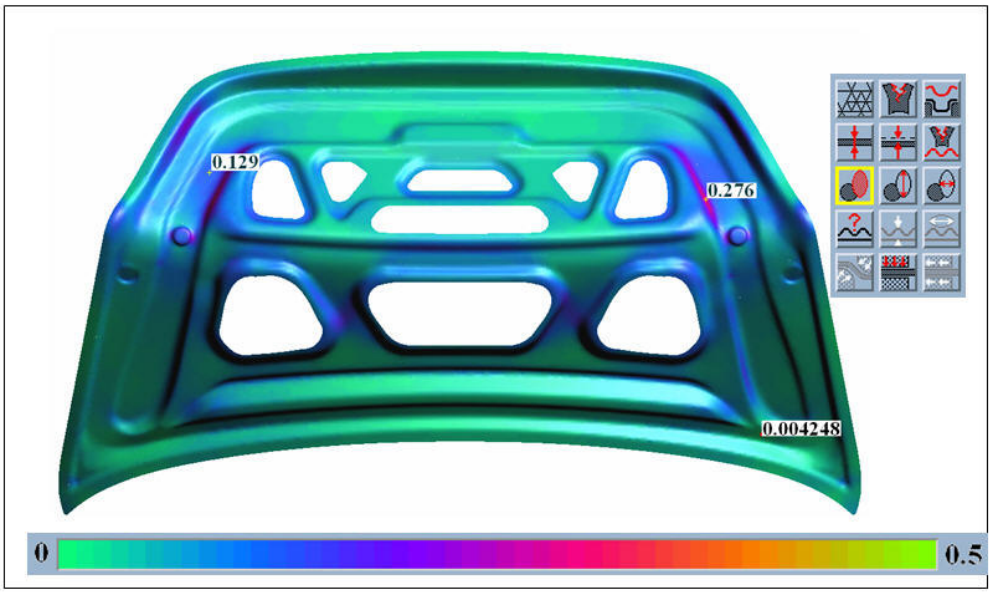

Figure III.A.54 – *Display of the result variable Plastic Strain in the main display*

Springback Evaluation

(normal displacement, dynamic section)

To analyze springback results, we need to go to the end of the simulation stage.

Normal Displacement

To display the springback results in the main display, switch on *Normal Displacement* (Figure III.A.55). With this option, due to the chromatic scale, it is possible to immediately recognize the areas more subjected to springback. However one can also analyse this phenomena punctually, by measuring quantitatively the value when clicking with the right mouse button.

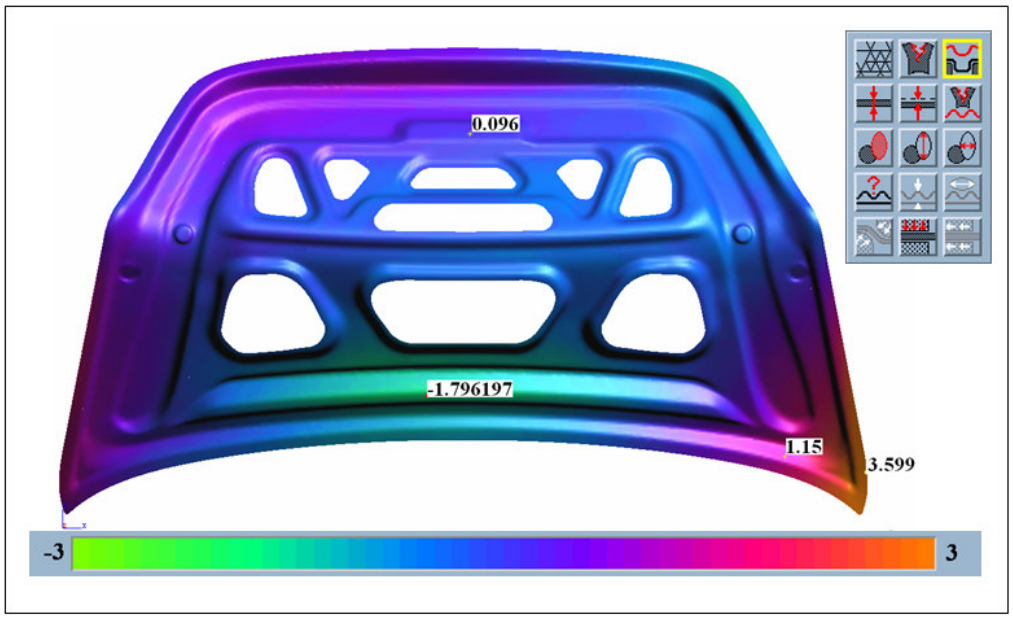

Figure III.A.55 *– Display of the result variable Normal Displacement in the main display*

Dynamic Section

AutoForm consents the analysis of sections of the simulated component (as well as the tools), and by activating the visualization of the element and the die simultaneously, to evaluate more accurately/precisely either the spacing of the walls and the angular variations. This analysis is possible with the *Dynamic Section* menu.

The option *Section* displays the selected section plane as a 2D-curve.

The option *Clipping* displays 3D geometry with the selected section plane as a clipping plane.

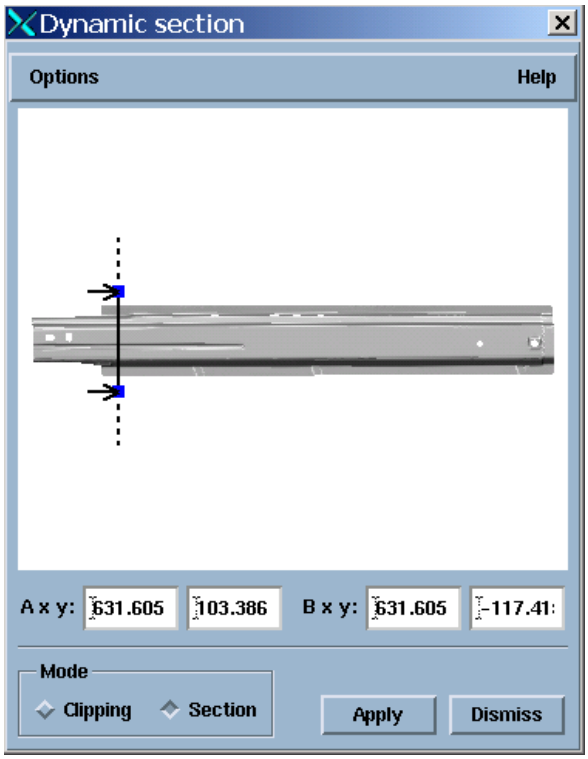

Figure III.A.56 – *Dynamic section with option Section displayed in the main display*

Pressing the button apply the 2D section is displayed in the main display (FigureIII.A.57).

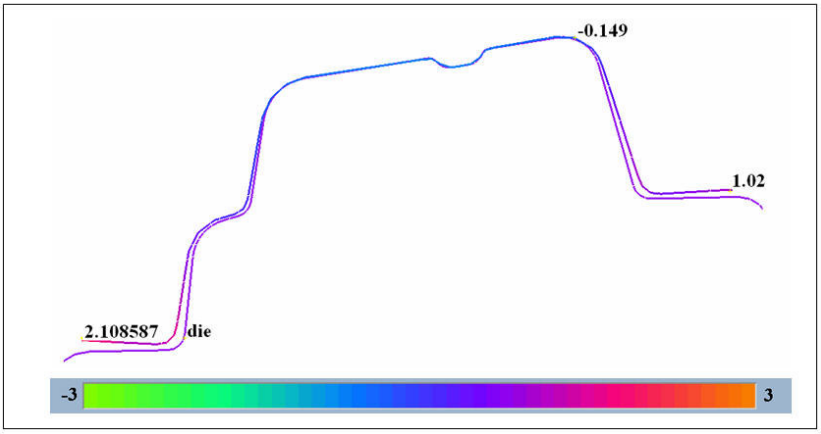

Figure III.A.57 – *Dynamic section with option Section displayed in the main display*

*III.A.*5 **Bibliography:**

[1] Schenk O and Hillmann M. Optimal design of metal forming die surfaces with evolution strategies. Journal Computers&Structures, Volume 82, Issues 20-21 , August 2004, Pages 1695-1705.

[2] www.autoform.com

[3] AutoForm Workshop Manual

[4] Kubli W and Reissner J. Optimization of Sheet-Metal Forming Process Using the Special-Purpose Program AUTOFORM. Journal of Materials Processing Technology, 50, 1995, pp. 292-305.

[5] Sester M. Implementation of the Selected Elastoplastic Models in AutoForm-Incremental. Workshop 3DS, Villetaneuse, June 2002.

Section III.B

The second test case is the forming simulation of an automobile component

(lateral longeron of Fiat Stilo)

III.B.1 – Introduction

In this chapter the results of the simulations performed in AutoForm software are exposed in detail. The components analysed are related with the automotive industry, made of advanced high strength steels and manufactured using a single action process.

The study of the first component, a lateral longeron, was divided in 3 phases before the respective analysis of results. In the first the default values of the program AutoForm were used in order to have a reference to the successive simulations. In the second the objective was to get familiar with the program, studying the influence of both the geometric and process parameters in the final results. In the third phase several simulations were performed, changing appropriate parameters seeking for the best simulation results possible.

The approach used to the second component, a deck lid inner body panel, was different, as we were quite familiarized with the program at that stage. This way, the two first study phases were unnecessary.

The main steps for the preparation of the simulation that presented more successful results for both components are described, establishing, in the longeron case, some comparisons with the parameters used in the first simulation.

The presented analysis and the obtained results have theoretical value only, as they were not validated experimentally.

The material selection is one of the most important parameters in a sheet metal forming process. Both the components are destined to the automotive industry, so the materials used to form them are AHSS due to their superior mechanical properties. However, this class of steel is more difficult to form than the conventional steels, since one of the properties of the AHSS is the higher energy absorption capacity when comparing with the conventional steels, as mentioned in the first chapter.

AutoForm is a program that allows the simulation of the complete stamping process with high accuracy, permitting afterwards several types of analysis such as the formability or the alterations caused by springback. The results may be evaluated according to the precision requested, i.e. it is possible to make a fast and global analysis visualizing the component displayed with colours corresponding to the quantitative scale of the selected result variable, or to make a more precise analysis by reading the punctual value of the selected parameter.

The principal characteristics of the computer used are: Pentium 4, CPU 2.4 GHz with 128Mb of RAM.

III.B.2 – Simulations and Results Analysis of a Longeron 199

III.B.2.1 – Component Description

The first component in analysis was a lateral longeron 199 that is part of the structure of a recent automobile manufactured by FIAT (Fiat Stilo). This component is positioned longitudinally in the lateral region, accompanying the superior part of the front doors on the right and left side. The material used to produce this part is an AHSS (DP 600), with 1.2 mm of thickness.

Through visual analysis (Figure III.B.1) it is clear that the part is not symmetric. Besides, one of the lateral areas possesses two steps and it is considerably higher, while the other only one, which unbalances the component, complicating the forming process.

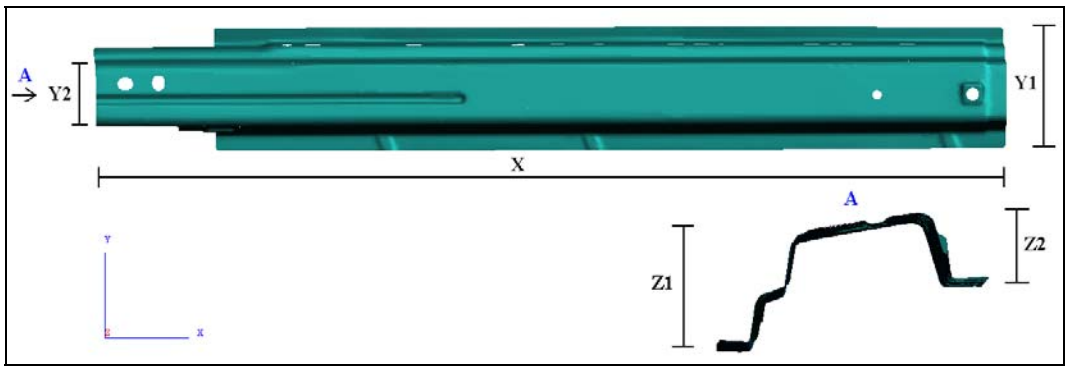

Figure III.B.1 – *Component geometry (longherone 199)*

The main measures of this component are:

X = 1145 mm

Y_1 = 147 mm

Y_2 = 80 mm

Z_1 = 64 mm

Z_2 = 31 mm

The simulations realized with this component that did not evidence critical defects were about 35 min long, while the simulations where cracks occurred could take up to 1 hour.

In the following figure (Figure III.B.2) the main mechanical characteristics of the AHSS DP600 are presented. This data is obtained from the AutoForm materials database.

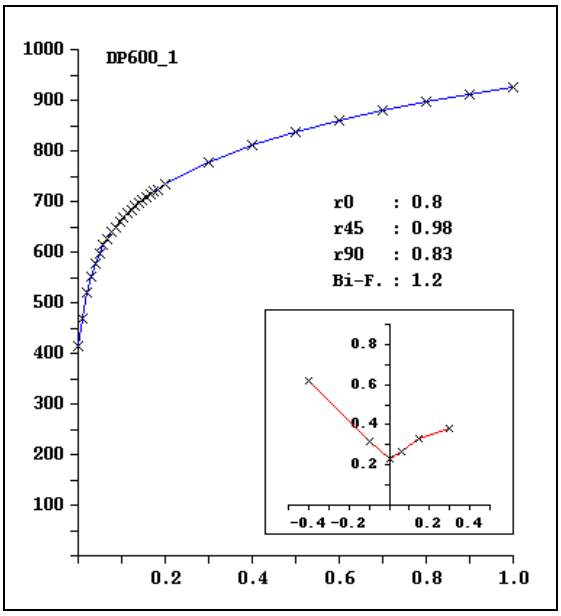

Figure III.B.2 - *Main mechanical characteristics of the AHSS DP600*

III.B.2.2 – Phases of study

- 1st Phase

To begin with the study the configurations automatically provided by AutoForm default values were used. This way a fast preparation process is possible, although the probabilities of success are quite remote.

The simulation tested is based in a single action stamping process, as presented in the Figure III.B.3.

In a first step the die moves towards the binder pressing the blank (arrow 1); in a second step these tools continue the descending movement, forming the metal sheet against the punch (arrow 2).

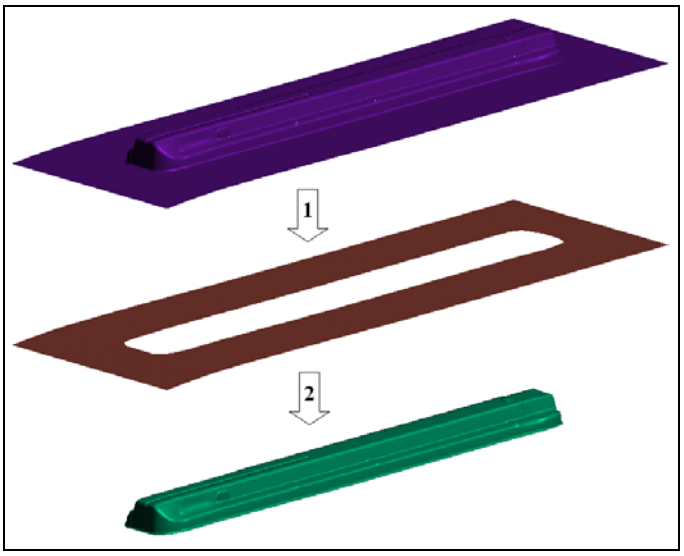

Figure II.B.3 – *Simulation process used for forming this component*

After the simulation a formability analysis was made and the results, as expected, were quite unsatisfactory (Figure III.B.4).

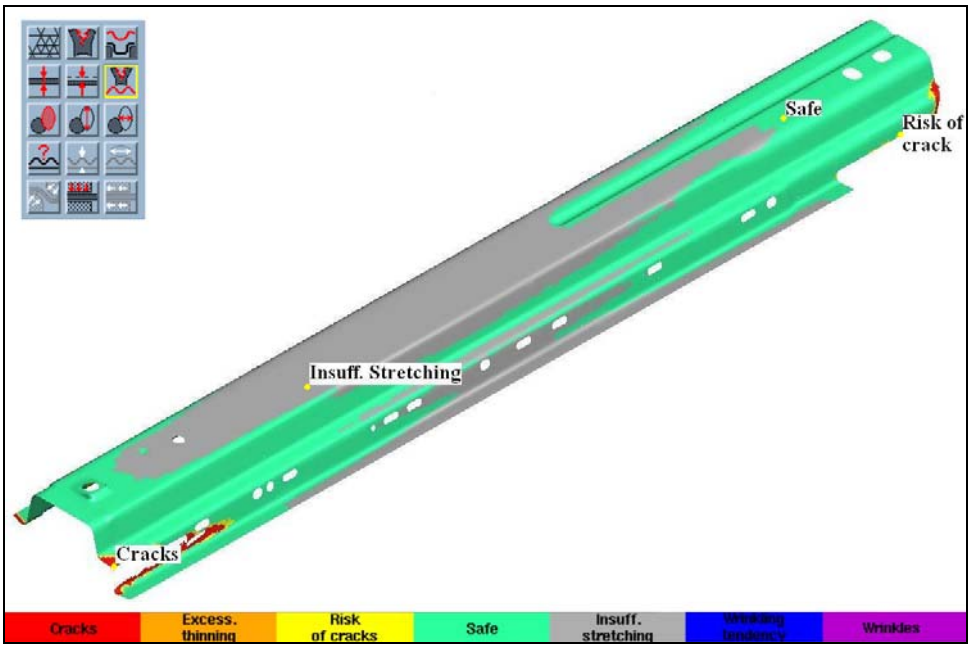

Figure III.B.4 – *Formability evaluation of the first simulation (lateral longeron 199)*

The formability analysis evidences several cracks and areas with risk of cracking in the extremities, while the top presents a large area with insufficient stretching. The FLD analysis (Figure III.B.5) confirmed what was evident through visual evaluation: several points overcame the FLC for the material used, which lead to the respective ruptures.

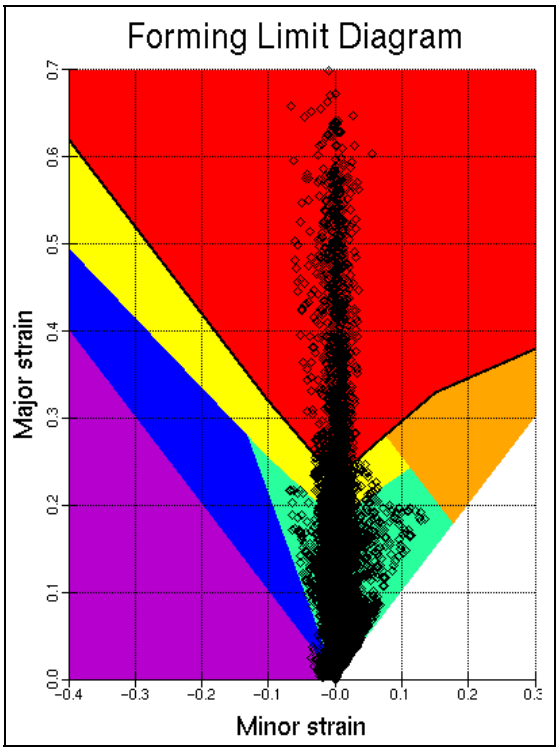

Figure 6III.B5 – *FLD of the simulation mentioned above*

The analysis of the results from the first simulation evidenced the complexity of this component regarding its forming, as there were areas with severe cracking while other areas were insufficiently stretched.

- 2nd Phase

In the second phase of the study a large number of simulations were made with the purpose of analyse the influence of the diverse parameters in the final result. This was a laborious and time-consuming stage, but extremely important and essential to familiarize with the program. An important conclusion that was achieved during the large number of experiments done was that the velocity and the distance between th

tools don't have any influence on the simulation results, contrasting with what happens in reality.

- 3rd Phase

Concluded the learning stage, the next step was the optimisation of the process, searching the best commitment between the different parameters. In this sense several alterations were made both in process parameters and tool geometries, in order to achieve the best solution. The description of the preparation phase for the most satisfactory simulation is presented in this point, as well as confronting it with the first simulation made, i.e., with the default values provided by the automatic generator of the program.

Geometry Generator

- TIP

In the beginning of the preparation phase it is necessary to define the drawing direction in the *Tip* page. When reading a part geometry from a CAD file, this geometry is positioned in the car coordinate system, which usually is not the best drawing direction, as demonstrated in this case.

The following figure (Figure III.B.6) compares the initial tip, i.e., the relative to the car coordinate system, with the one improved by the users.

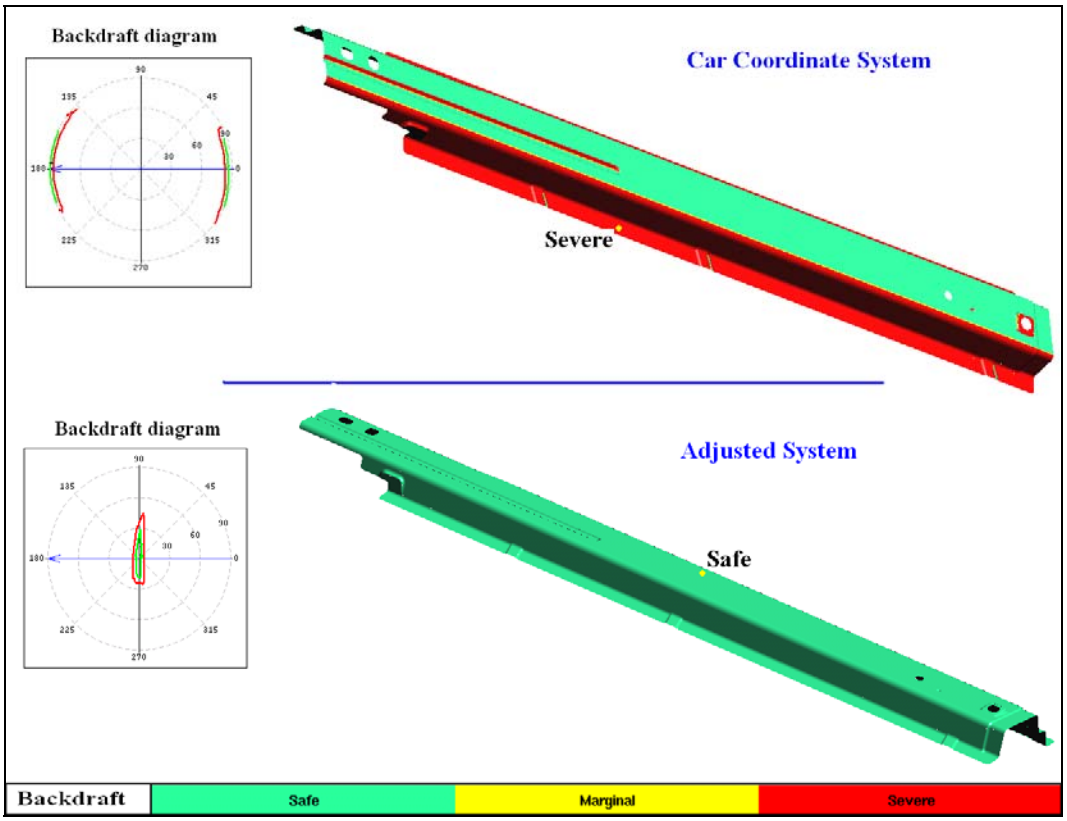

Figure III.B.6 – *Initial and adjusted drawing direction*

The improvements are quite evident, as the part had first several undercut areas and after the intervention of the user became perfectly safe for the stamping process, i.e., without undercuts.

The alteration was accomplished by the use of the command *Average normal***,** which provided a reasonable drawing direction, and then improved manually by rotating +4 degrees in relation to x-axis.

- Mod P

Then all the holes were filled using *Mod P* function, since it reduces simulation time. At the end of the drawing process this holes will be re-opened with cutting operations

- External contour (Boundary Fill)

Due to the component's geometry (Figure III.B.7 a)), the creation of a boundary fill was necessary in order to smooth the borders, making the part's contour more uniform. This way the tools will be more uniform as well, since they are built from the geometry of the part.

The automatic generation provided by AutoForm improves largely the uniformity of the part geometry (Figure III.B.7 b)). However some adjustments were made manually building the contour of the tools as smooth as possible (Figure III.B.7 c)).

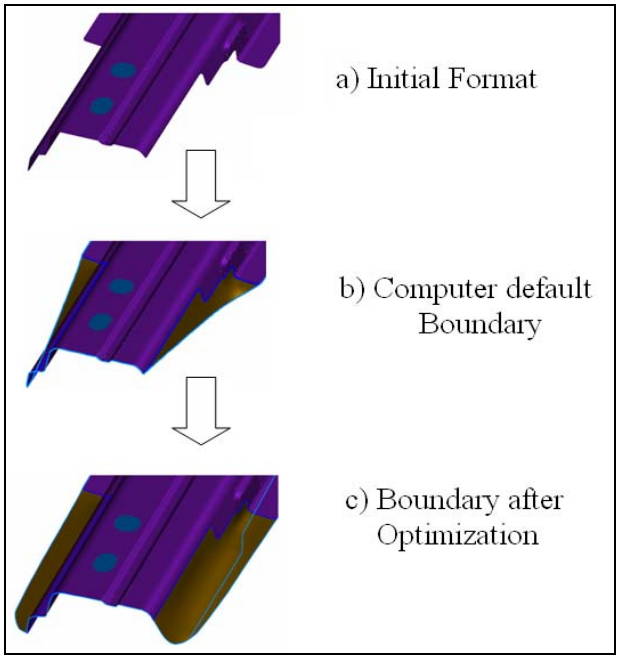

Figure III.B.7 – *Stages of the boundary modification.*

- Binder

Initially a binder automatically generated by the software was used, but the results produced were not satisfactory. Therefore, the binder generated with Auto-Binder was improved by the addition of profiles with the Manual-Binder module, in order to provide a draw depth as uniform as possible.

The following figure (Figure III.B.8) represents the comparison between the binder generated automatically and the one optimised manually. By analysing the figure, one can easily verify that the manually optimised binder has larger probabilities of success.

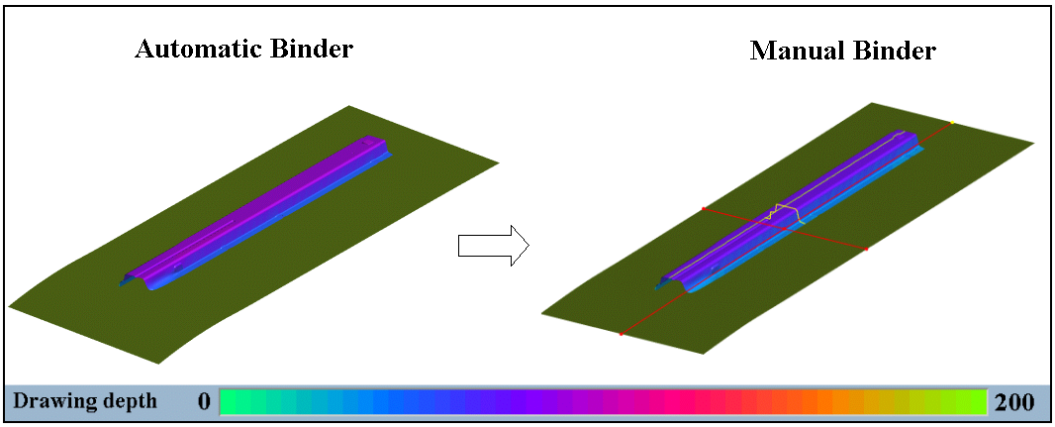

Figure III.B.8 – *Binder optimization*

- Addendum

An ordinary drawing tool consists of the part geometry, the binder surface and an addendum. In forming processes, the addendum in general performs the task to make a suitable transition from the part to the binder, ensuring a good material flow.

This was undoubtedly the parameter that suffered more changes during all the simulations performed. Initially an addendum automatically generated by the software was used (Figure III.B.9 a)), but due to its unsmooth geometry the material suffered rupture in several areas (illustrated in Figure 6.4). Afterwards the profiles (Figure 6.10) and their respective orientations were modified (Figure 6.11)) in way to create a tool with a smoother geometry, that allows an easier material flow (Figure III.B.9b)).

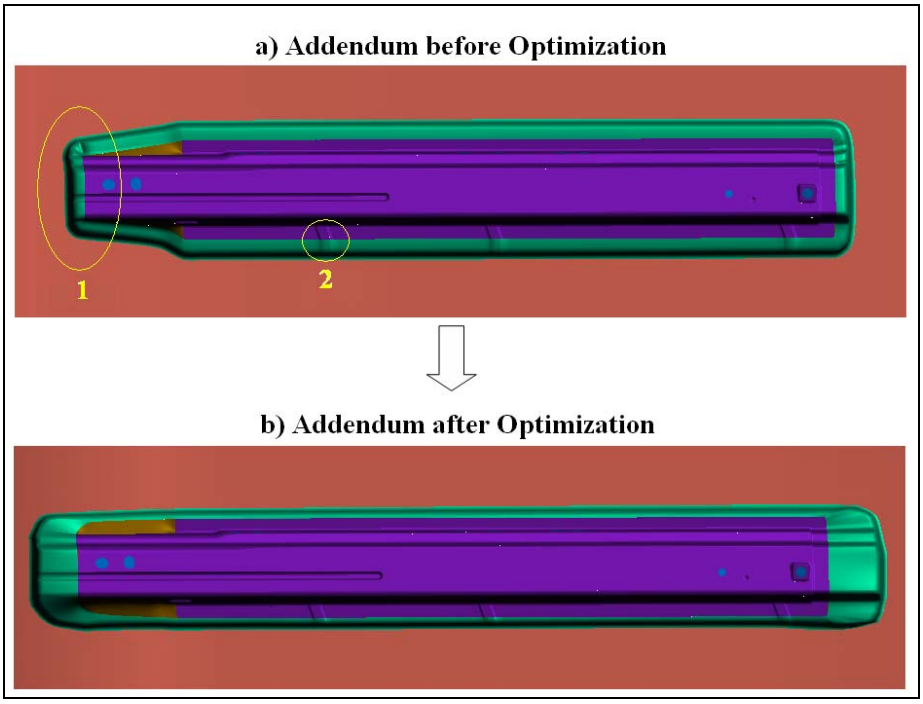

Figure III.B.9 – *Addendum optimized by the user*

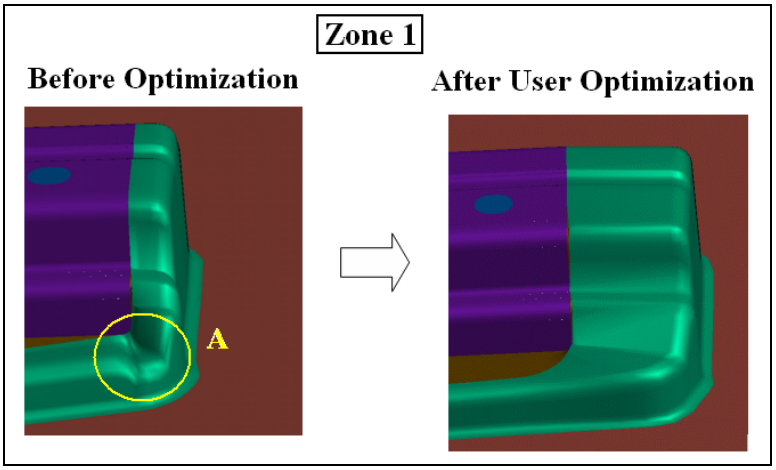

Figure III.B.10 – *Modification on the profiles of the addendum (Zone 1).*

Figure III.B.10 demonstrates the importance of changing manually the addendum. The zone 1, before optimization, had a geometry that created serious problems regarding the material flow inside the tools. Instead, the addendum manually optimised assures fine material flow, improving the final forming results

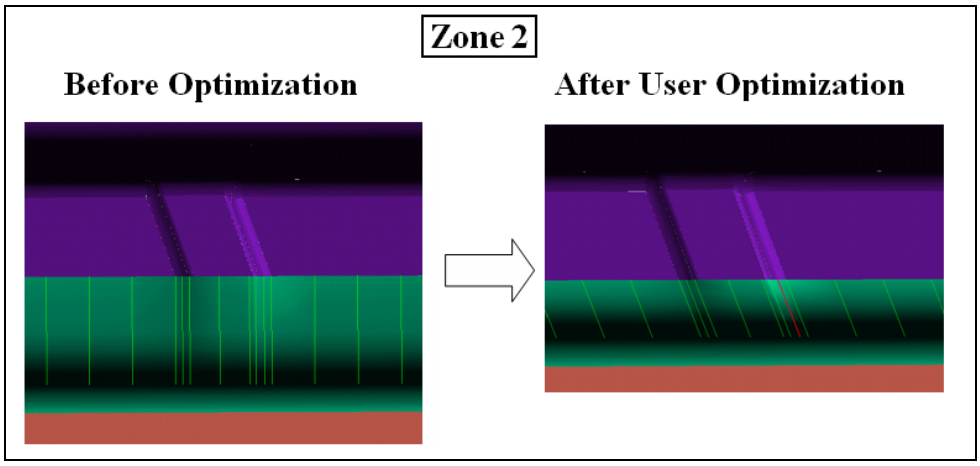

Figure III.B.11 – *Modification on the addendum profiles orientation (Zone 2)*

The figure above (Figure III.B.11) exhibits the modification of the profiles orientation in order to improve the material flow in details.

Input Generator

- Tools configuration

A very important phase in process configuration is made in *Tools* page. In this page the initial position of the diverse tools and their movements (working direction and distance) are defined.

In the second phase of the study, was concluded that both the distance and the velocities in all the stamping processes are parameters that do not influence the final result of the simulation, so the data inputted in this page was the same during the whole study. Our only concern was to input the information in order to generate a single action stamping process. The values used were:

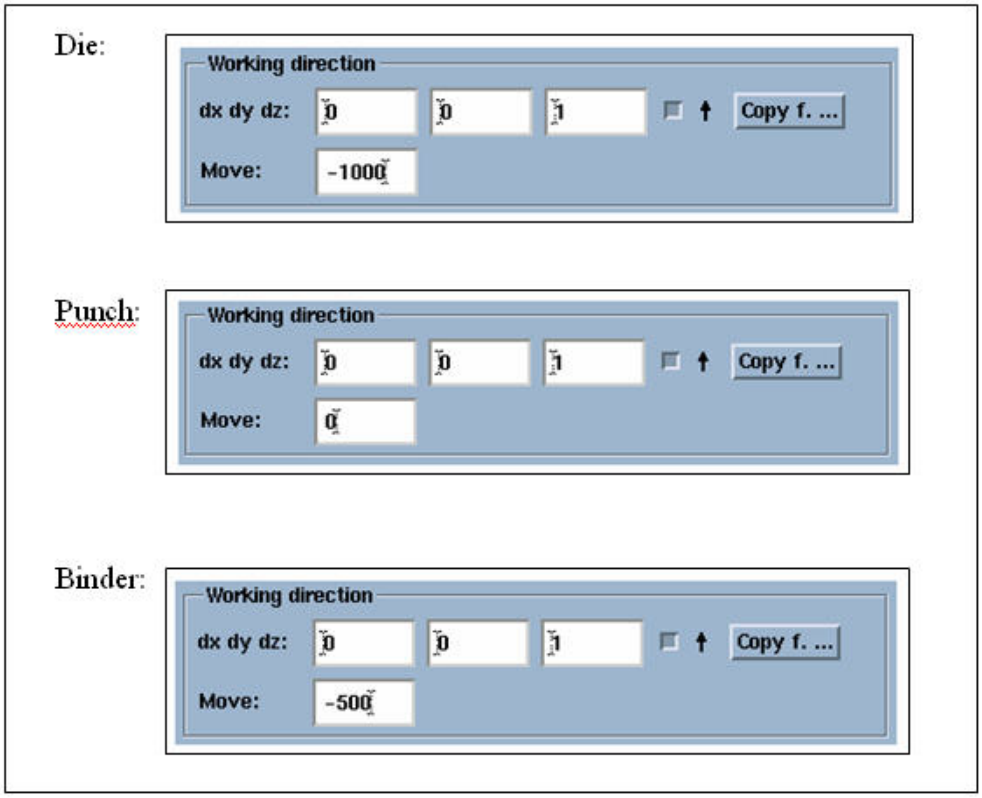

Figure III.B.12 – *Definition of the initial position of the diverse tools and their movements*

- Blank

The material of the blank used in all the simulations of this component was an AHSS, DP600, 1.2 mm thick. This parameter was not changed since FIAT has demonstrated only the interest of producing this component through the utilization of this steel, due to its mechanical properties.

The size of the blank, as well as its position, was changed several times during our study. However, the shape of the blank was always rectangular (Figure III.B.14). In the experiment where better results were obtained the measures of the sheet metal were:

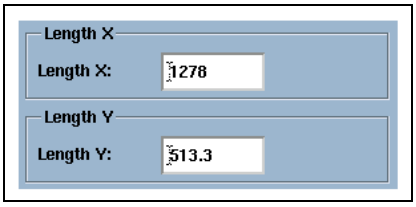

Figure III.B.13 – *Measures of the sheet metal*

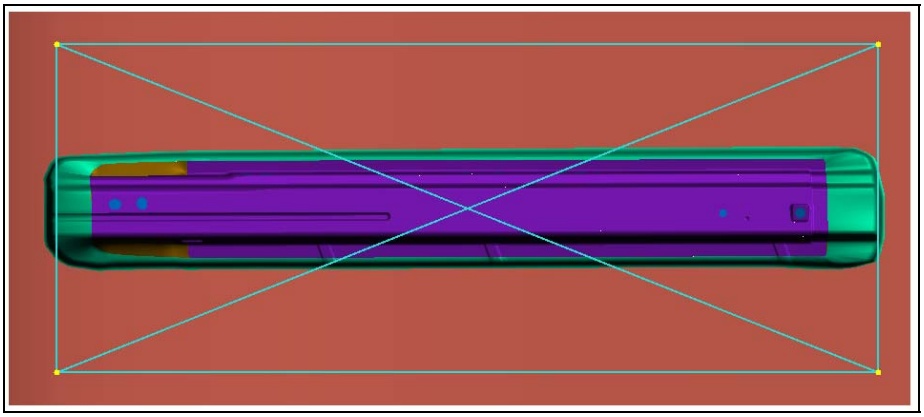

Figure III.B.14 – *Blank outline used in the simulation that presented the best results*

- Drawbeads

Drawbeads main function is to increase the restraining force to hold the blank made by the binder in specific areas *in* order to achieve a uniform stretching.

The drawbeads location and force factor are crucial parameters for the simulation results.

Initially drawbeads were not used during the simulations. Their introduction in the process occurred because the sheet was being quite stretched in the extremities of the component, while in the superior part of the component this stretching didn't happen.

A large number of simulations were made, changing the number, the force factor and the location of the drawbeads. The most satisfactory result was obtained when 4 drawbeads were used, as shown in Figure III.B.15. The force factor values used are also mentioned.

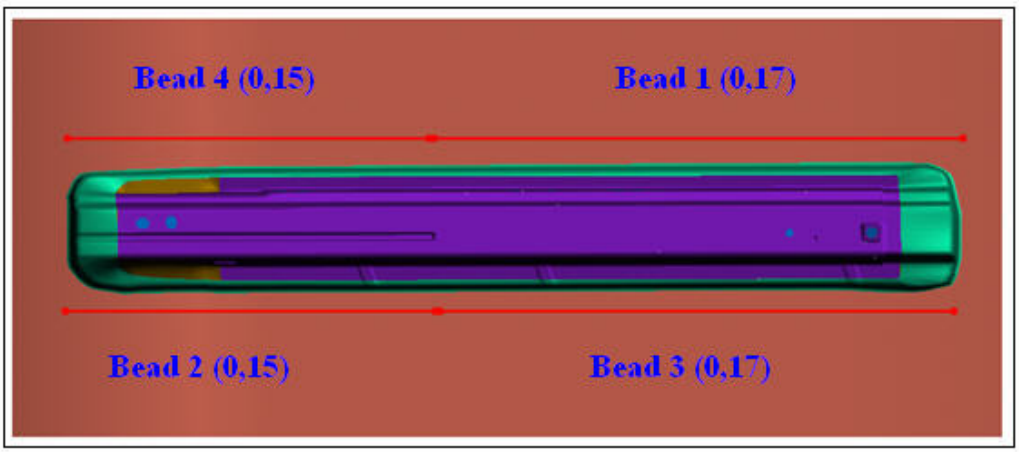

Figure III.B.15 – *Geometry, disposition and force factor of the applied drawbeads*

- Lube

The lubrication values weren't subjected to great changes, as both the FIAT *representatives* and the software manual recommended the utilization of values in the order of 0.15 for this type of steels. Though,

lubrication values between 0.09 and 0.20 were tested, without producing however very satisfactory results.

- Process

During the several simulations made to find the process with the best results in the stamping of this car body part the process steps to be performed were always the same. The only parameter that changed was the value of the force to press the blank between the die and binder. This parameter varied between 0.6e+06 and 2.0e+06 and the best result was achieved with 1.2e+06.

The process steps to be executed in order to stamp this component are: Gravity, Closing, Drawing, several Cuttings (the trimming cut to release the part from the rest of the blank and to make all the holes) and finally Springback calculation.

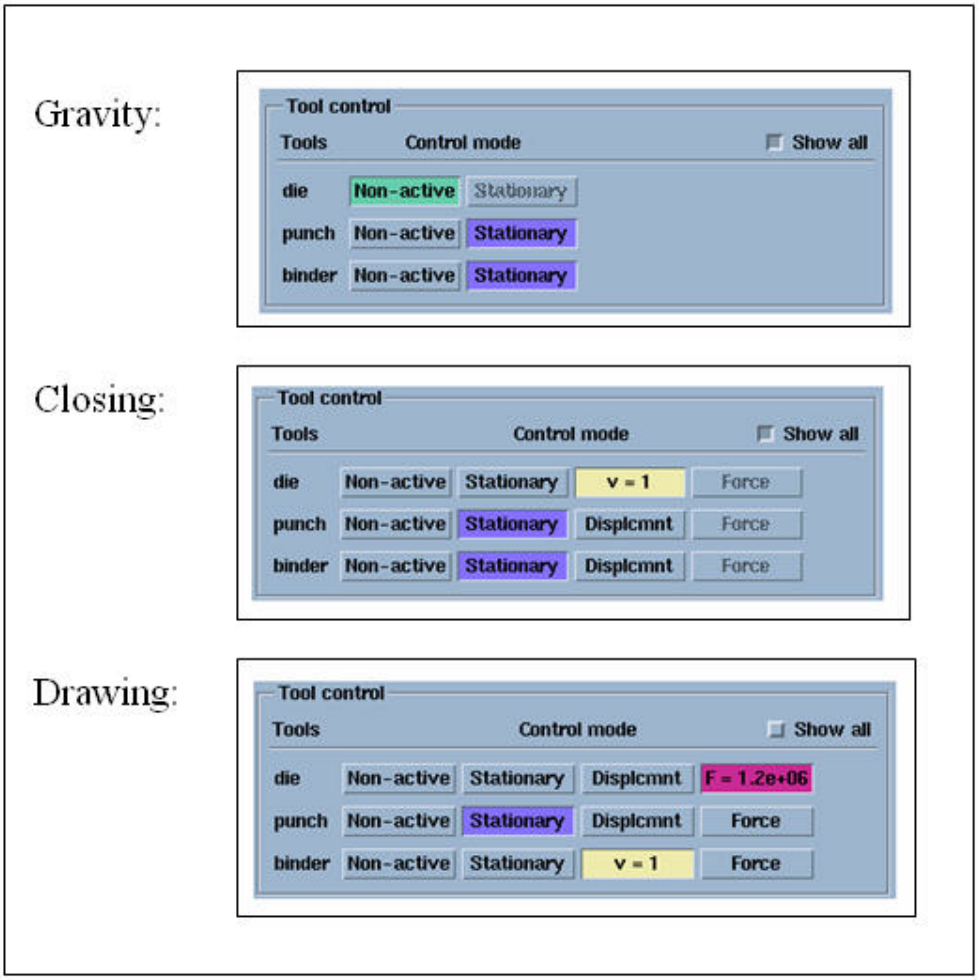

Figure III.B.16 – *Definition of the forming process steps*

III.B.2.3 **– Results Evaluation**

The simulation that provided the best results will be analyzed in detail and through several aspects. The results analysis was divided in three main fields: Forming, Thickness/Strain evaluation and Springback. Special attention was given to formability and springback analysis.

Forming Analysis

- Formability

The formability analysis provides the study regarding the component's stretching, i.e., the detection of areas excessively stretched, as well as the ones with insufficient stretching.

The following figure (Figure III.B.17) presents the formability analysis of the most successful simulation performed for this component:

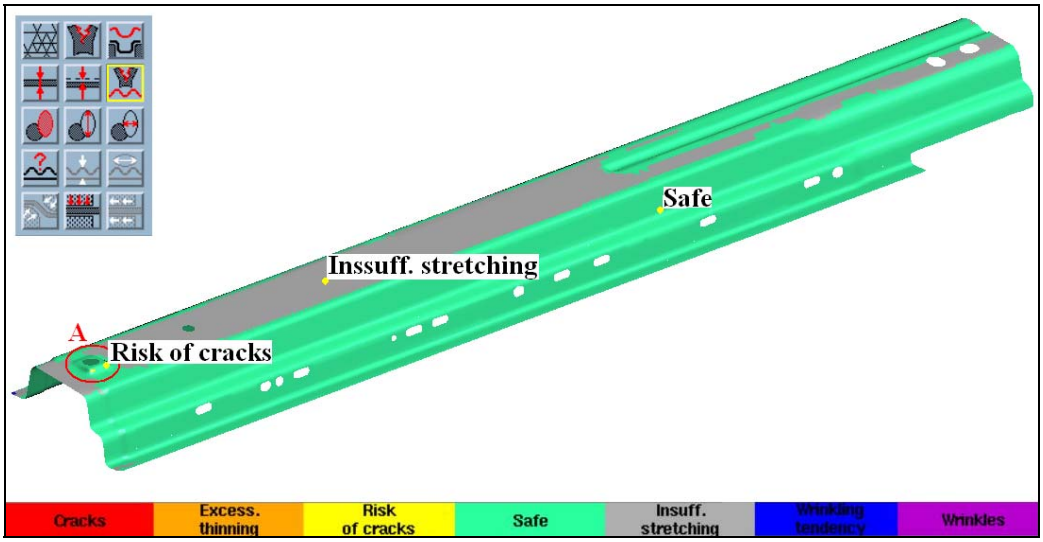

Figure III.B.17 – *Formability evaluation of the simulated component*

Since the optimal result would be 100% safe (green), the superior area of the component should be more stretched, in order to accomplish this requirement. However, to stretch the top of the component, by changing parameters such as drawbead force factors or the geometry of the addendum, the extremities are subjected to too much stretching, which cause risk of cracks or even cracks. In the best result obtained there are areas with insufficient stretching, but a component without risk zones was achieved.

The saliency *A* represented the largest challenge, once it was a sensible zone with tendency to rupture, surrounded by an area with insufficient stretching.

The FLD associated with the mentioned simulation is presented next (Figure III.B.18). In order to help the analysis the diagram is coloured

differently in areas with different strain states. These colours are equivalent to the ones displayed in the formability result variable.

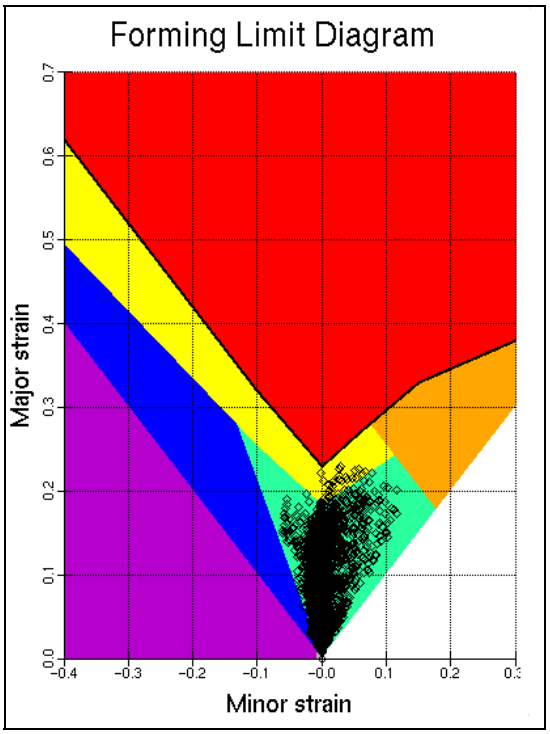

Figure III.B.18 – *Forming Limit Diagram*

Through the analysis of the diagram it is possible to see that almost all the points are located in the green (safe) area, with only a few points placed in the yellow zone (risk of cracks). This corroborates what was previously concluded with the formability analysis.

- Wrinkling Criterion

This analysis allows the verification if there are areas where the material has tendency to wrinkle.

Analysing the following figure (Figure III.B.19) one can conclude that the part doesn't have problems in this area.

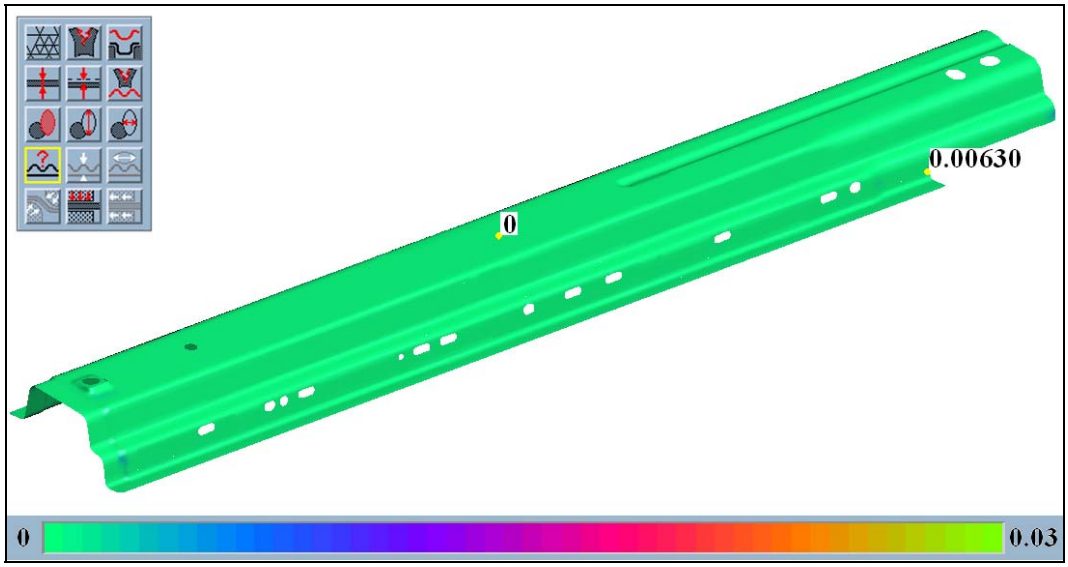

Figure III.B.19 – *Wrinkling criterion evaluation of the component*

Thickness / Strain evaluation

- Thickness

This type of analysis provides the thickness values of the part at the end of the stamping process. The thickness of the blank used was 1.2 mm, but at the end of the process the minimum thickness value in the formed part was 0.8857mm (Figure III.B.20).

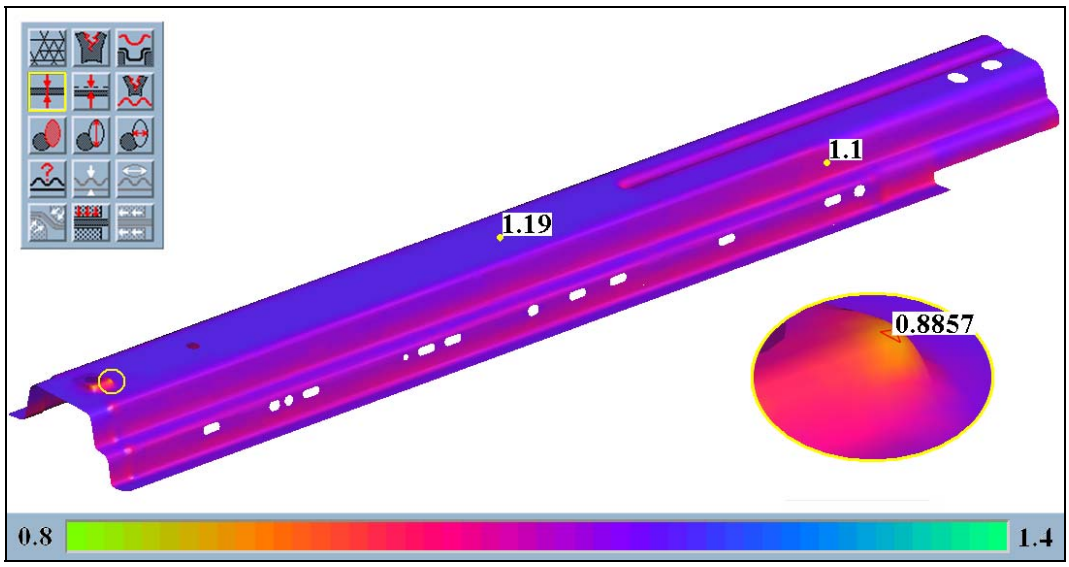

Figure III.B.20 – *Thickness evaluation with special attention to the saliency A*

The analysis of the thickness evidences once more that the critical area is essentially the saliency zoomed in the figure.

- Thinning

A very useful result variable is the percentage thinning of the material. For steels this value must be inferior to 30% (-0.3) (Poisson's coefficient), in order to accomplish a rupture free area.

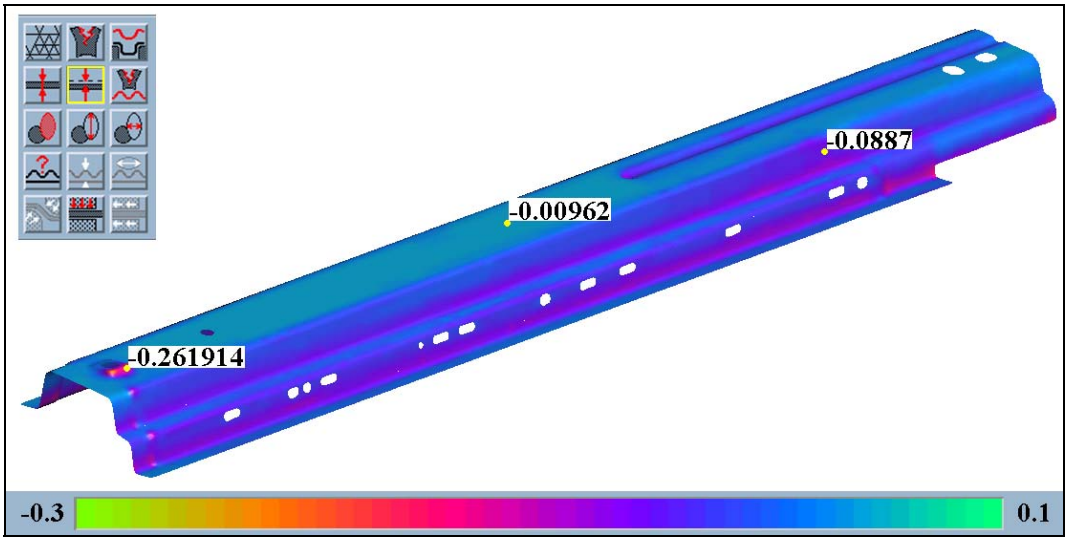

Figure III.B.21 – *Thinning evaluation of the simulated component*

The maximum and minimum points of this analysis are the same ones found in the thickness analysis, as these two result variables are directly related: the thicker the point is the smaller will be the thinning. The maximum value is reached in the critical zone (saliency A): 26% of thinning.

Springback evaluation

The springback analysis is a very important evaluation parameter in our study. This phenomenon was described and analyzed in *Chapter 3 - Springback*, and will now be evaluated in the test cases.

The following figure presents two different views of the longeron, indicating the maximum and minimum values of normal displacement. As expected, through visual analysis one can easily verify that the critical

points (the areas more subjected to springback phenomenon) are the ones located in the extremities of the wings (Figure III.B.22).

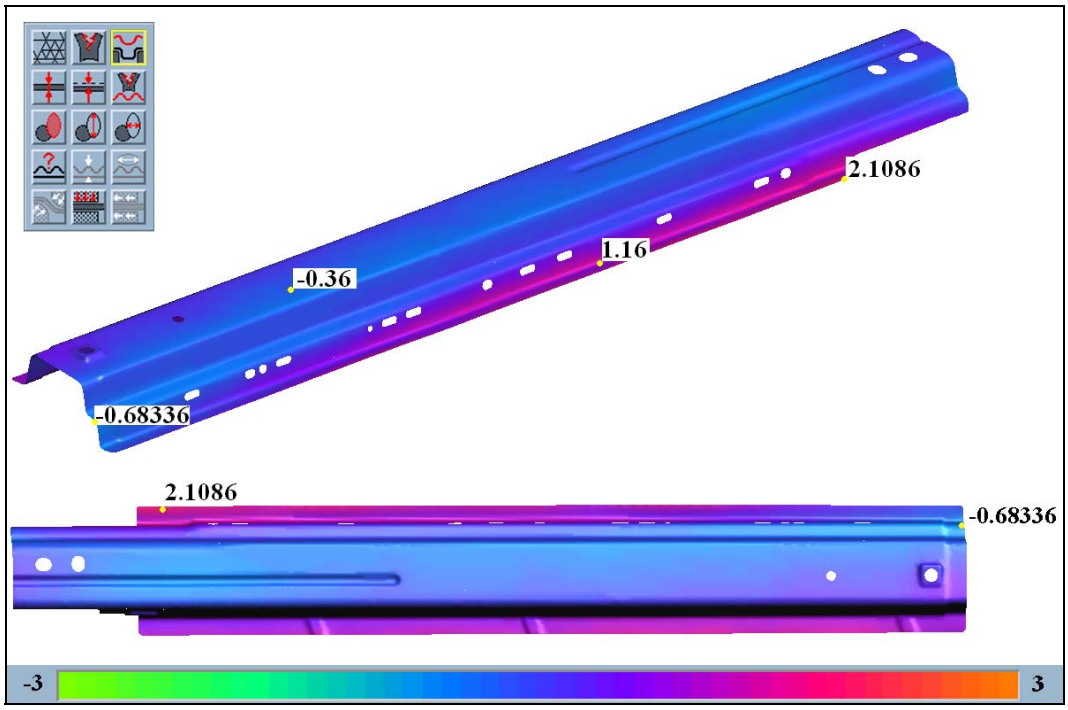

Figure 6.22 – *Springback evaluation presenting two different views*

To evaluate springback more accurately seven sections along the whole component were analysed using the function *Dynamic Section* (Figure III.B.23).

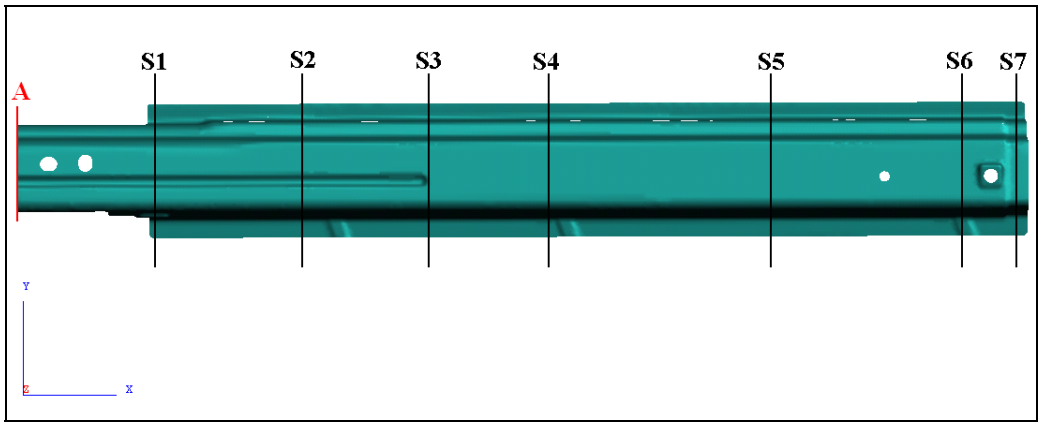

Figure III.B.23 – *Component division for a posterior springback evaluation*

Considering section A corresponding to the coordinate x = 0, the remaining sections correspond to:

S1 = 158.7 mm

S2 = 291.2 mm

S3 = 467.8 mm

S4 = 607.1 mm

S5 = 841.5 mm

S6 = 1065.7 mm

S7 = 1130.3 mm

The analysis of sections 1, 2 and 3 (Figures III.B.24, III.B.25 e III.B.26) evidence that springback in these sections is essentially from an angular change type, which as referred in chapter 3, is a consequence of the stress difference in the sheet thickness direction when a sheet metal bends and unbends over a die radius.

In the top, springback phenomenon does not occur. Instead, the opposite occurrence takes place, i.e., Spring-in. In this case the normal displacement happens in the direction outside-inside and not inside-outside.

Through the analysis of these images it is also visible that springback effect in the wings is increasing in opposite senses along x-axis.

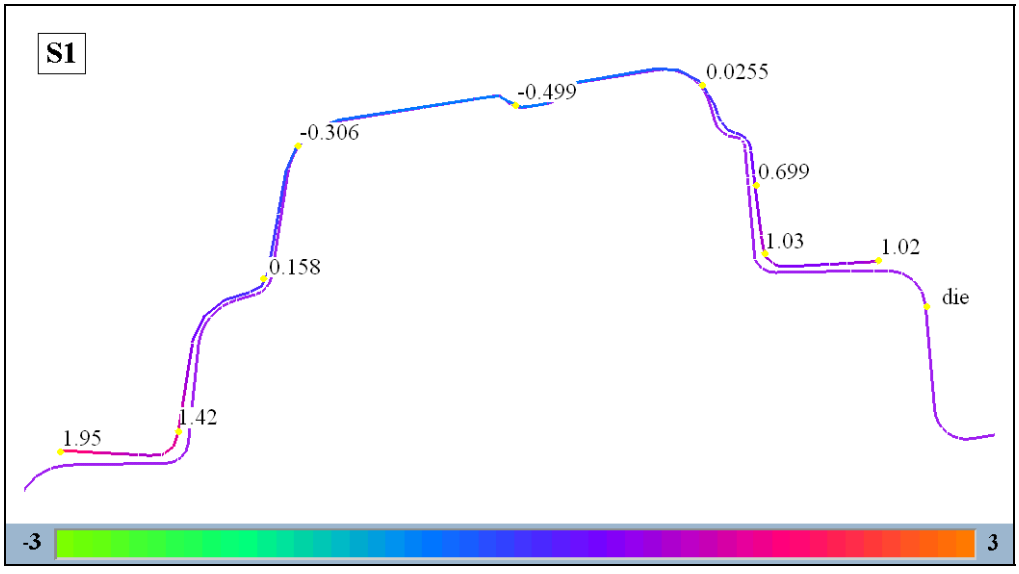

Figure III.B.24 – *Springback evaluation of section 1.*

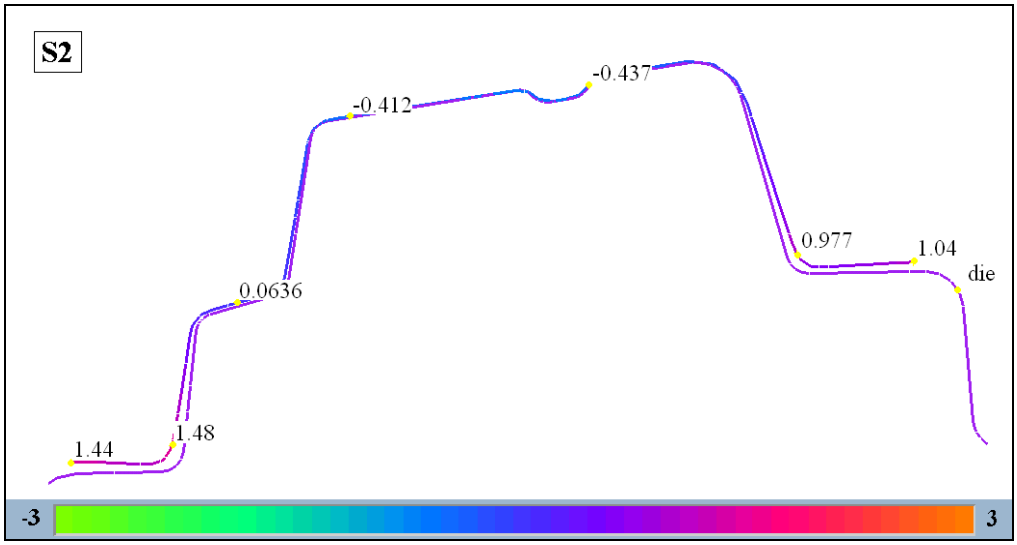

Figure III.B.25 – *Springback evaluation of section 2.*

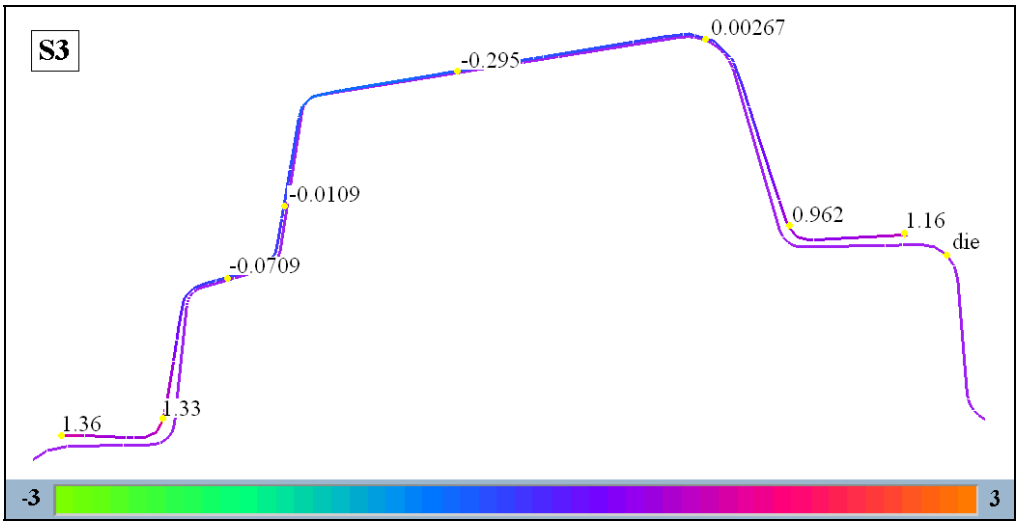

Figure III.B.26 – *Springback evaluation of section 3.*

Section III.C

The third application is the test case realized in *AutoForm 4.04 Incremental* code is a simple profile stamping simulation with angle variations in the component vertical side walls using two different Advanced High Strength Steel (AHSS) materials.

III.C.1 – Introduction

The simulation of the sheet metal forming process in this project was performed using the incremental forming simulation program AutoForm 4.04®.

The aim of the numerical simulation carried out in this chapter is to verify the stamping process and the shape of the final component for studying springback of AHSS, with a synthetic description of the process steps. The test case is the stamping simulation of three simple profiles for two different AHSS: Dual-Phase (DP 600) and Transformation-Induced Plasticity (TRIP 800).

AutoForm-Incremental is the AutoForm module to simulate sheet metal forming processes (conventional deep drawing, hydro-mechanical deep drawing) using the finite element method in many small steps. Using AutoForm-Incremental it is possible to simulate all forming operations beginning with the plane blank sheet and ending with the finished part including springback calculation.

The simulation is always created on the basis of a part or tool geometry. This geometry has to be available in VDAFS- or IGES-format. The simulation starts with the import of this CAD file.

Basing on this imported CAD file further input is generated: Input concerning the process such as tool geometries, tool movement, information on the sheet (size, shape, material proprieties, thickness etc.) is defined. All this information are saved in a simulation file (*.SIM).

III.C.2 – Methodology in AutoForm

Basically, AutoForm is a simulator of stamping processes, in figure III.C.1 are described all the steps on it utilization.

It is a 'trial and error' software where the operator prepares the stamping tools and analyzing the final results decide if it is finished or if have to make some changes to get the wanted results.

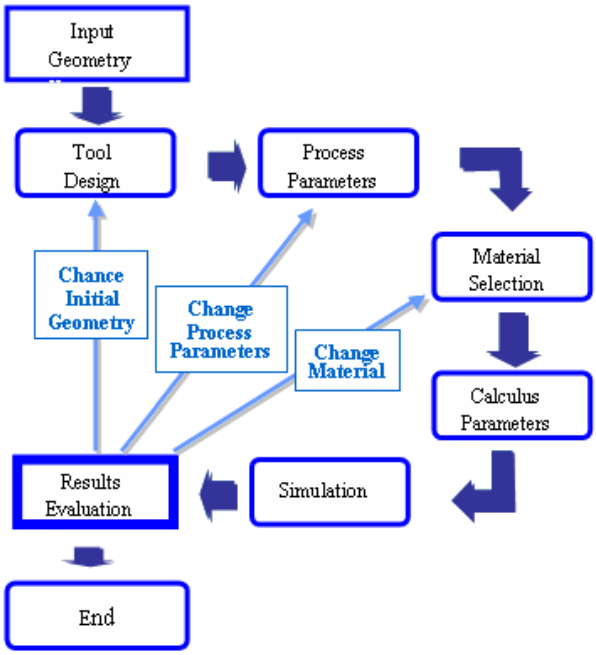

Figure III.C.1 – Methodology in AutoForm

III.C.3 **- Test Case**

The test case is the forming simulation of three simple parts with angle variations (Figure III.C.2) on the vertical walls.

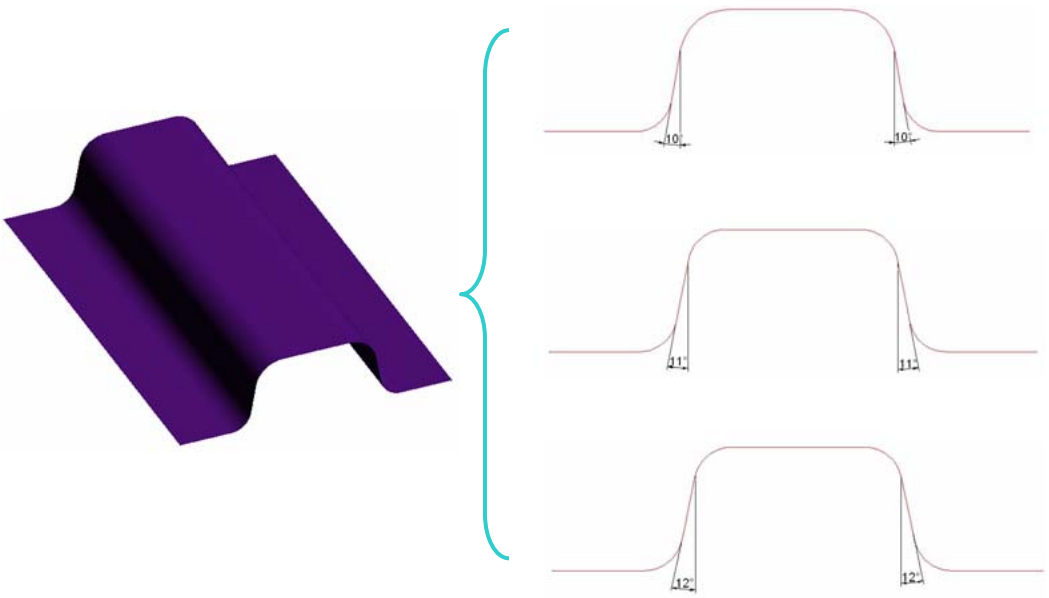

Figure III.C.2 – Test case profile for a vertical wall of 10,11 and 12°

III.C.4 **- Synthetic Description of AutoForm Process Steps**

1. Pre-Processing of Input Data

Import geometry
- Import part geometry from CAD

Part Geometry (Geometry Generator)
- Prepare
- Fillet
- Balance (Tip)
- Filling Holes (Modify Part Geometry)
- External Contour (Boundary Fill)
- Binder
- Addendum

Process Data Input (Input Generator)
- Tools
- Blank
- Lube
- Drawbeads

Material Properties / Material Selection
- True stress-True strain curve
- Normal anisotropy coefficient
- Forming limit curve

Process Description
-Process (Gravity, Closing, Drawing)
-Cutting
-Springback

Calculus Configuration
- Control data

2. Computational Analysis

3. Post-Processing of Results
Visual evaluation
Forming evaluation
-Formability (FLC)
-Forming Limit Diagram (FLD)
-Wrinkling criterion
-Maximum Failure

Thickness / Strain evaluation

-Thickness
-Thinning
-Plastic strain
-Major strain
-Minor strain

Springback evaluation

-Material displacement (X, Y, Z, □)
-Material deformation (angle change)

III.C.4.**1 - *Pre-Processing of Input Data***

- New Simulation File

At the beginning, a new simulation file (*.sim) has to be defined. The first input is the name of the simulation. During the generation of the input, this simulation file is filled with data, which is necessary for the simulation (geometrical data, specification of process, numerical data, etc.).
Besides the *file name*, the first inputs are the *units* and the *geometric error tolerance* (Figure 5.1).

- *Import Part Geometry from CAD*

The simulation is always created on the basis of a part or tool geometry. This geometry has to be available in VDAFS or IGES format. The simulation starts with the import of this CAD file. Next input is the meshing parameters (Figure III.C.3), the first accuracy parameter of simulation. With this operation the program creates a file (*.sim) that can subsequently be also open and modified.

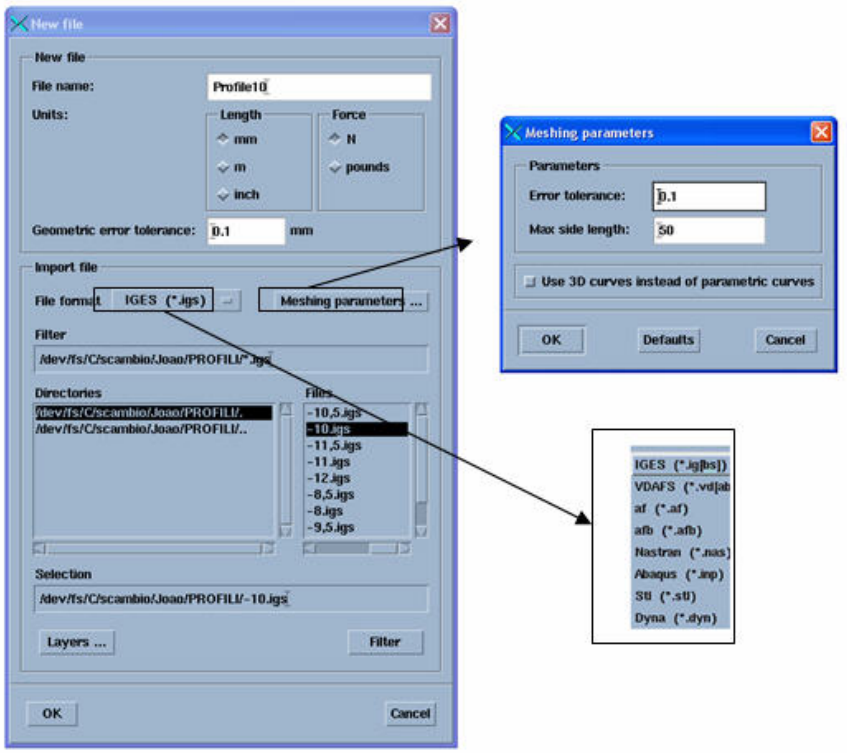

Figure III.C.3 – CAD file import

The geometry import is carried out using the module **afmesh**, the integrated IGES-/VDAFS interface, which automatically meshes the part geometry (Figure III.C.4). All subsequent operations are based on this mesh. Only the mesh can be visualized in AutoForm, not the original CAD data.
Basing on this imported CAD file further input is generated: Input concerning the process such as tool geometries, tool movement, information on the sheet (size, shape, material properties, thickness etc.) is defined.

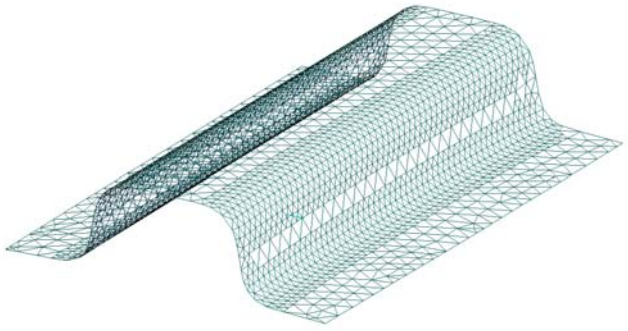

Figure III.C.4- Meshed geometry

- Part Geometry (Geometry Generator)

- Prepare

Once selected the input file begins the preparation of the model in the menu Geometry generator (Figure III.C.5).

The imported part geometry needs to be prepared in order to serve as a reference for the die design.

In *Define Objects* is possible to assign faces to the different registers:

- *Part*: Contains the CAD faces for the part, which are needed for the generation of the tool.
- *Right part*: Register for CAD faces needed for subsequent operations.
- *Deleted*: Not used faces.

To change the part boundary, which is automatically calculated, click *Default* button.

To perform changes in the generated part boundary, the following options are available:

Outer trim – If the generated part boundary needs to be changed, it can be done using this option.

Inner trim – Undesirable geometry features (areas that are formed in flanging or restrike operations, but not in the draw die) may be eliminated using the *Inner trim* function. Holes can be created as well with this command. If the part geometry has a symmetry plane or is built as a double part, this can be defined as well.

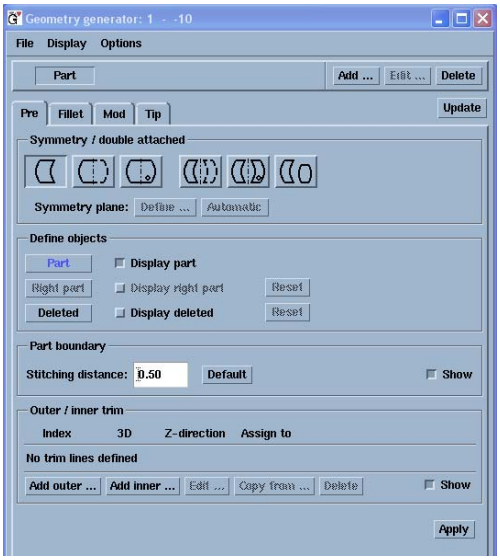

Figure III.C.5 – Preparation's window

- Fillet

During this part preparation phase, sharp edges and filleting will be checked for eventual problems. If sharp edges are found, when clicking *OK* these edges are filleted accordingly to the value specified in *global fillet radius*.

A very common (and useful) option of morphing in this page is the modification of the radius of already existing fillets. This technology allows the user to manipulate the mesh in 3D by defining feature lines and feature nodes.

Filleting of individual edges - If it is necessary to create fillets of different radius along different edges of the part geometry, these individual edges have to be identified and fillet radius values (constant over the edge or variable) have to be specified, in addition to the global radius values.

Those edges that were identified as sharp, and for which no additional fillet radius specification are made will all be filleted to the global radius value. Using the button *Add line…* at the bottom of the **Fillet** page, one can identify specific edges and to specify radius values on these edges.

- Modification of Part Geometry (Mod 1)

Using functionality available on this page, it is possible to modify part geometry by global overcrowning as well as by adding local detail. Further, gaps and holes can also be filled, and the filled areas can be edited / modified in this page.

In this case it was not used this option because the workpiece don't have holes anyway it is shown the proprieties on figure III.C.6.

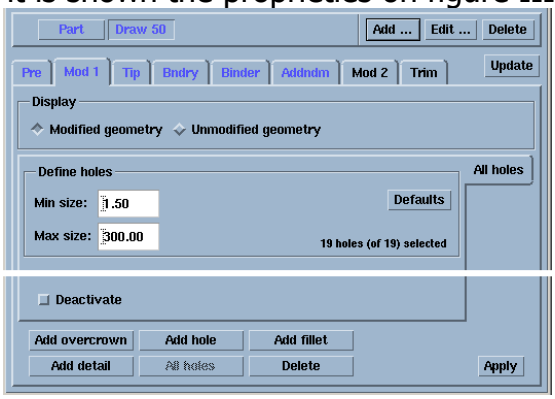

Figure III.C.6 – Mod 1 Window

Filling up holes and gaps in the part geometry:
Add hole – allows a single, specified hole to be filled, and the filled patch to be edited/modified.

All holes – allows all holes on part geometry to be filled; however, the fill patches are not modifiable.

- Balance (Tip): defining of the Drawing Direction

The balancing of the piece happens in the Tip screen of the menu Geometry generator, only a good balancing can assure the safe operation of the tools.

Normally, when reading a part geometry from a CAD file, this geometry is positioned in the car coordinate system (global system). However, it is possible to define a local system that can serve as a reference for the stamping direction and also has the ability to automatically detect the optimum stamping direction based on several criteria such as the **minimum draw depth**, the **minimum backdraft** or the **average normal**. In addition to the possibility to choose one out of several automatic functions, the user can (if necessary) tip the part around the x-, y- and z-axis to a more useful drawing direction. This can also be done with a local tipping centre.

The three following functions generate in the most cases a reasonably good drawing direction:

- *Average normal*: uses normal vector of geometry as drawing direction.
- *Min draw depth*: determines automatically the drawing position to minimize the drawing depth.
- *Min backdraft*: calculates a drawing direction with minimum undercuts, i.e., with minimized backdraft.

Moreover a drawing direction designed in a CAD-system can be imported and the drawing direction defined with DieDesigner can be exported to handle it within a CAD-system.

All undercuts, marginal areas and undercut free areas are calculated and displayed in different colour for the current drawing direction when the **Tip** page is opened (Figure III.C.7). Undercut free areas are displayed in green (drawing angle greater than 3 degrees), marginal areas in yellow (drawing angle between 3 and 0 degrees) and undercuts in red (backdraft under 0 degrees).

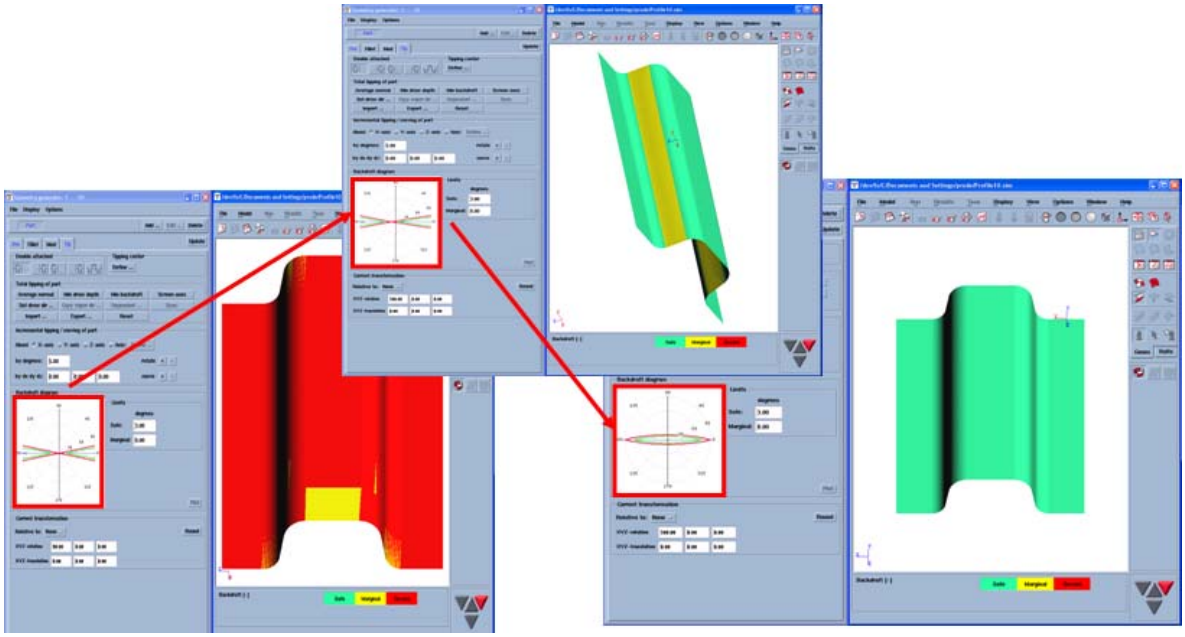

Figure III.C.7 – Balance (tip)

Using the button *Plot* the **backdraft diagram** is activated.
Backdraft diagram – All possible undercut-free drawing direction are calculated (using **Plot**) and displayed in the diagram. The centre of the axis is the current drawing direction. The distance between the axis centre and the lines represents the backdraft-free angle to the drawing direction. The horizontal axis shows the rotation around the y-axis and the vertical axis shows the rotation around the x-axis.
This means that a rotation around the y-axis (horizontal line in the diagram) is backdraft-free as long as the rotation angle is inside the red line. The red line represents the limit angle **Severe/Marginal** and the green line the limit angle **Marginal/Safe** for the presentation of the backdrafts.
If the centre of the plot is completely within the green circle the geometry is undercut free (default: **Safe > 3º**); if the centre is between green and red circles, geometry is in marginal area (default: **Marginal: 0º ~ 3º**); if the centre is outside the red circle, geometry has undercuts (default: **Severe: ≤ 0º**).

- *External Contour (Boundary Fill) :* add fill end

The part boundary should be as smooth as possible. The user has the possibility to smoothen the part edge by using a so-called 'rolling cylinder' technology. The generated outer fill faces in order to do that are called boundary fill.
Filling the Part boundary – Fill areas are created automatically along the part boundary. The outer boundary fill line is determined by tangential points

created by a roll cylinder moving around the part boundary and its roll radius.

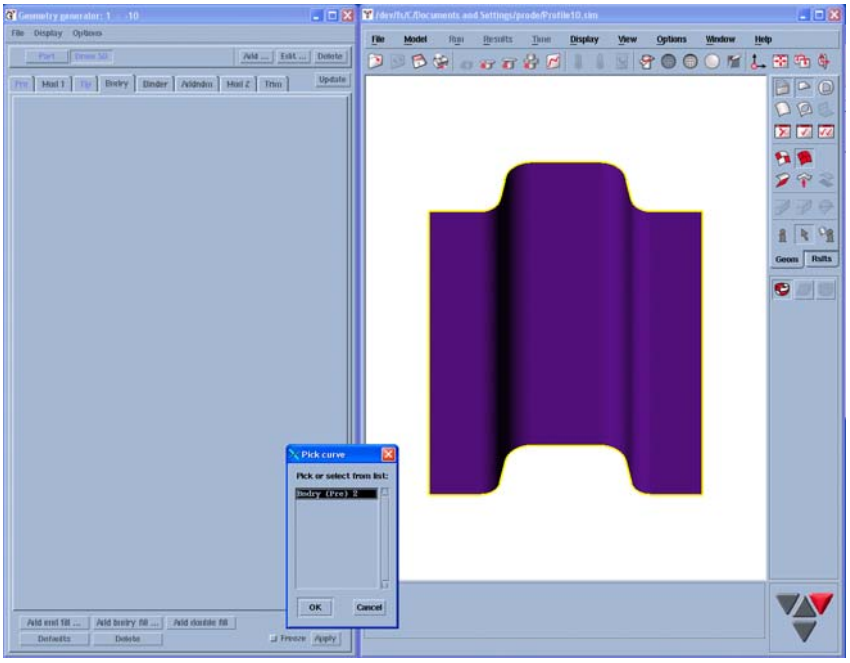

Figure III.C.8 – Boundary fill

Filling the gap between two parts - When we have two parts it's necessary to fill the gap between them before the addendum can be generated. Similar to the generation of an outer fill, the geometry between double attached pasts is filled by using the concept of roll cylinders. By selecting an appropriate roll radius the user may exert ome influence on the outer edge of the fill faces.

Modifying fill faces using Control curves - Without any effort to keep the resultant modification realistic, modifying automatically generated fill faces is possible. This procedure is typical of what the user would follow to create features such as draw bars or take up beads on the fill area between parts. Modifications are carried out by creating and using any number of control curves over the fill area; these control curves determine the shape of the modified fill faces (figure III.C.9). Curves may be created and modified using the Curve editor.

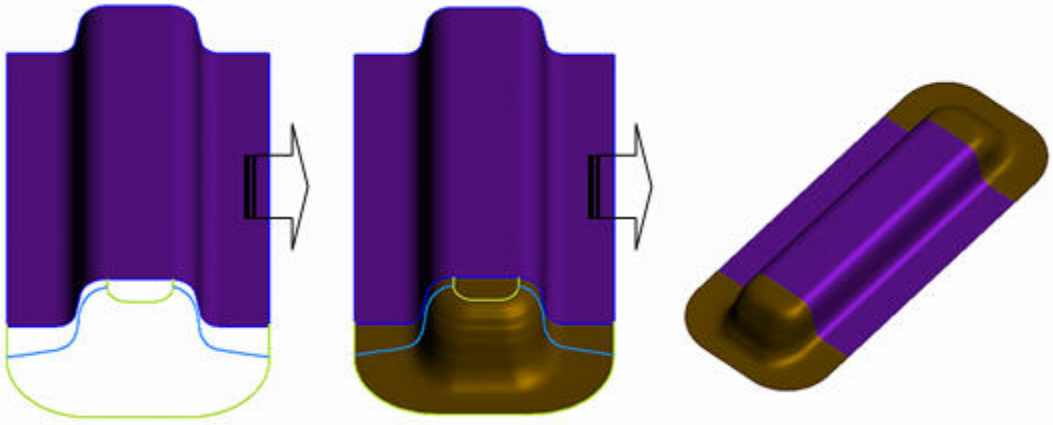

Figure III.C.9 – Modify fill faces

- *Binder / Blankholder (positioning, orientation, inclination, flexibility)*

Once the part geometry is prepared, the tool design can start with a first design of the binder surface. Several complete and intuitive functionalities for binder surface generation are available, i.e., the user can define the binder surface using parametric profiles and sections, using theoretical surfaces (fitting of flat, cylindrical or conical planes), or the user can import an already existing surface from a CAD file. Depending on the chosen method, the binder surface can be visualized and modified interactively in 2D and 3D simultaneously.

Next to that, there are several options in order to verify the binder definition, e.g. by checking the depth of draw (relative to the binder surface) or the developability of the surface.

Creating a binder surface with *AutoForm-DieDesigner* can be done with the module Auto-Binder, with the module Manual-Binder, or it can be imported from CAD.

The binder surface imported from CAD or generated with Auto-Binder can be optimized with the module Manual-Binder.

By changing the binder surface the existing addendum is dynamically adjusted.

- Creating the Binder surface with the module **Auto-Binder**:

The module Auto-Binder allows the creation of a first concept for the binder surface very quickly. The characteristic of the binder surface can be influenced by many adjustment parameters. Define the settings of the binder on the Auto-Binder pages. The binder surface is generated automatically (Figure III.C.10). The form and position of the parts as well as a constant drawing depth is considered. The input is very often carried out with sliding bar in the window. Thus, the necessary characteristic of binder specific parameters can be more or less realized. In general the procedure is work in an iterative manner. The first concept of the Auto-Binder is generated with the default values. After this, single parameters are modified until the desired binder surface is created.

The distance from part to binder surface (= drawing depth) is displayed as coloured contours on the part geometry, in order to analyze the current binder surface for uniformity in drawing depth. Select *Uniform* to achieve a uniform drawing depth over the whole part.

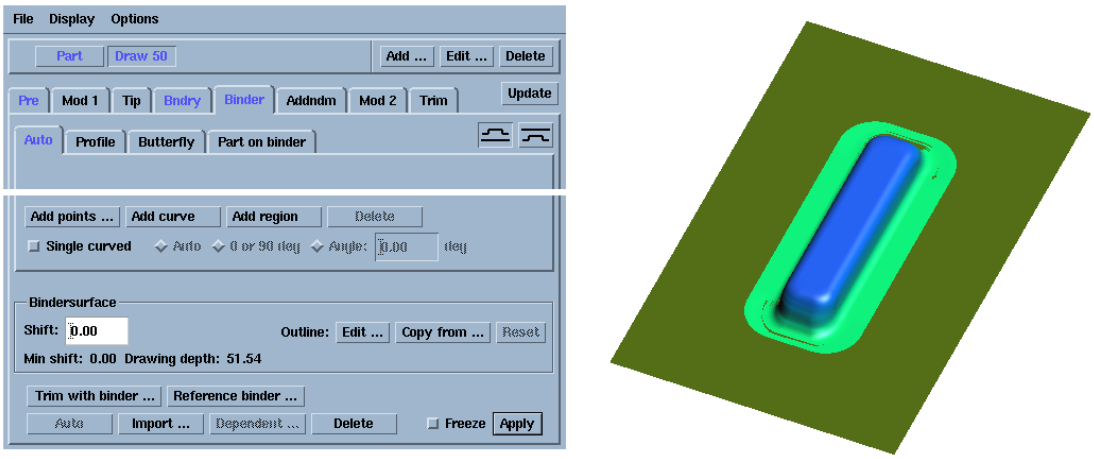

Figure III.C.10 – Auto-Binder

- Addendum

An ordinary drawing tool consists of the part geometry, the binder surface and an addendum. In forming processes, the addendum in general performs the task to make a suitable transition from the part to the binder, ensuring a good material flow. In AutoForm, the addendum is created on the basis of several profiles.

Now that the binder surface is visible, the user can start building the run-off surfaces or addenda. A fully interactive method is available for this: using the drag-and-drop functionality the program lets the user decide what profile (2D section of the addendum) to select and where to position it. When the profile is attached to the part geometry, it can be further modified by changing its orientation or by extending / shortening the profile .

Next to the 3D interaction to move and resize the profiles, one can have further control to fine-tune the run-offs: the user has the possibility to modify its geometry in 2D as well (Figure III.C.11). In doing so, he will have full control over all the parameters that constructs the profile, such as angles, radii, heights, distances and tangency. By dragging and dropping the control points of the profile one can interactively modify the parameter values.

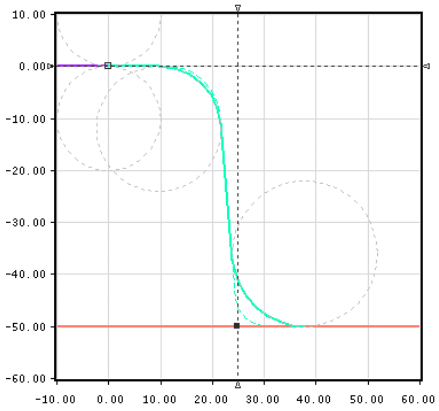

Figure III.C.11 – Addendum profile

Modifications in 2D are immediately visible in 3D, thus further enhancing the interactivity (Figure III.C.12). This method is especially useful in conceptual design. However, the user has full control of 2D parameters, he can lock them, impose some of them, free the others, etc. The user can also define all parameters manually.
Finally, the different profiles can be saved in the adequate database. When all profiles are defined, the user can visualize the die entry line. This line is automatically created and can be modified manually. Once the profiles and die entry line are satisfactory, the 3D surfaces can be generated in order to have a global view of the entire tool.

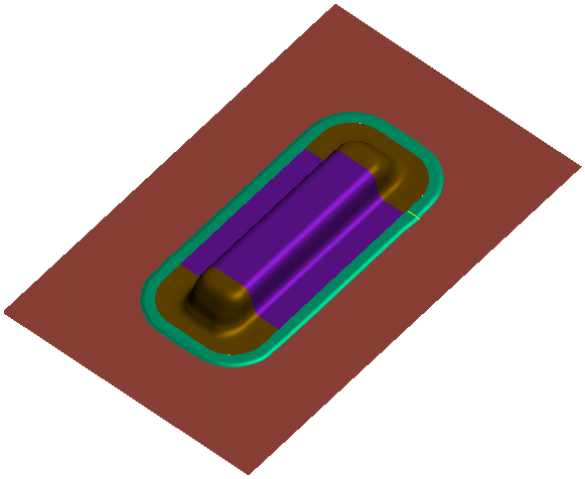

Figure III.C.12 – Modified addendum

The 3D surface information is useful for visualization purposes and early anticipation of problems such as tangency.

Brief description of the Addendum page:
The **Addendum** page contains all functions for the generation or modification of an outer or several inner addenda.
The graphic window shows the master-profile or the active individual profile together with the end sections of the part and binder geometry. All radii can be modified by picking and dragging the circle line with the mouse.
The following operations are executed clicking in the mentioned buttons:
Add addendum – generate an outer or inner addendum
Delete addendum – delete the current addendum
Add prf… - generate an user defined profile
Delete prf – delete an user defined profile
Lines… - edit the punch opening line (**PO width**), bar height line and counter bar height line (**CB height**) or import of the punch opening line
Directions… - change the profile directions

Binder… - translation of the inner binder surface (in drawing direction)

The master-profile is the reference profile for the individual profiles. The essential parameters of the addendum (bars, radii and angles) are determined by the master-profile. The heights and lengths vary for different distances between the part and the binder.
In most cases it is not possible to obtain an optimal addendum by using the master profile only. Thus the generation and modification of individual profiles is an essential part of the work.

- Process Data Input (Input Generator)

When started the process generator, the operator can choose the type of simulation to perform, in figure III.C.13 is shown the chosen parameters: incremental simulation, single action press, sheet thickness and the reference of the work geometry to the tools.

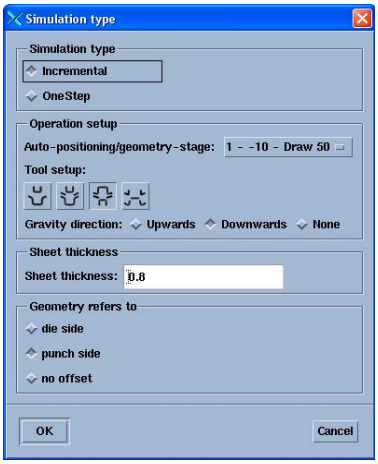

Figure III.C.13 – Simulation type

- Blank (shape, size, material properties, thickness e positioning)

In *Blank* page (Figure III.C.14) all the input data related with the sheet metal are made: shape, dimensions, position, material properties and thickness.
In the *Outline* section the following options are possible :
Edit: to change/edit an existing blank (convex, expand and smooth operations are possible)
Import: blank outline is imported from CAD
Rectangle: defines a rectangular blank outline
Copy from: the blank outline is copied from an existing line
Dependent: blank outline is created from an existing line. Blank outline is a reference to the base line. This means only the base line can be changed and the dependent blank outline will also change correspondingly
Arc: blank is defined as an arc segment

Delete: delete the current blank outline

Blank position – one can position the blank on binder or on the die. Insert manually the coordinates is also possible.
In *Properties* section the thickness and material of the blank are inputted. The material can be imported from AutoForm's database.
In *Symmetry–planes/welds/holes* section, add, edit and delete symmetry planes, welds and holes is possible.

The material file may be selected from the extensive material library using the **Import ...** button.
Use the buttons *View* or *Preview* to display the properties of the selected material: Hardening curve, forming limit curve and r-values.
In this case was used DP 600 (Figure III.C.15) and TRIP800 (Figure III.C.16).

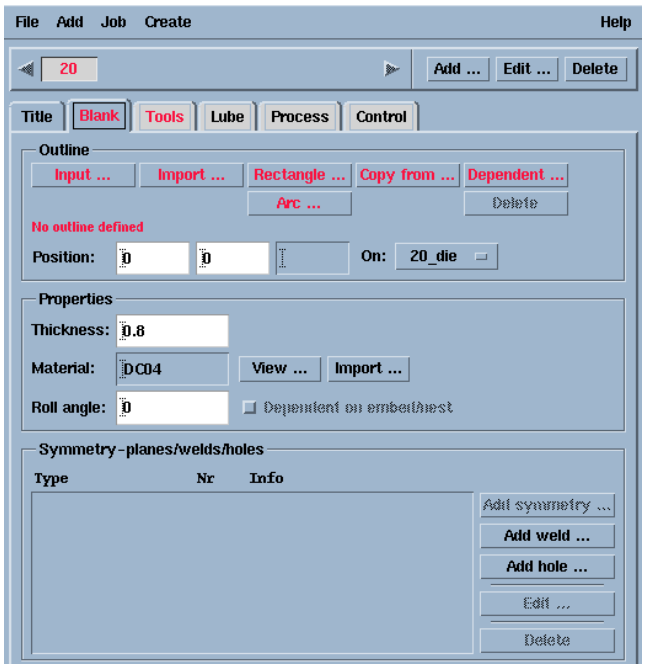

Figure III.C.14 – Blank page

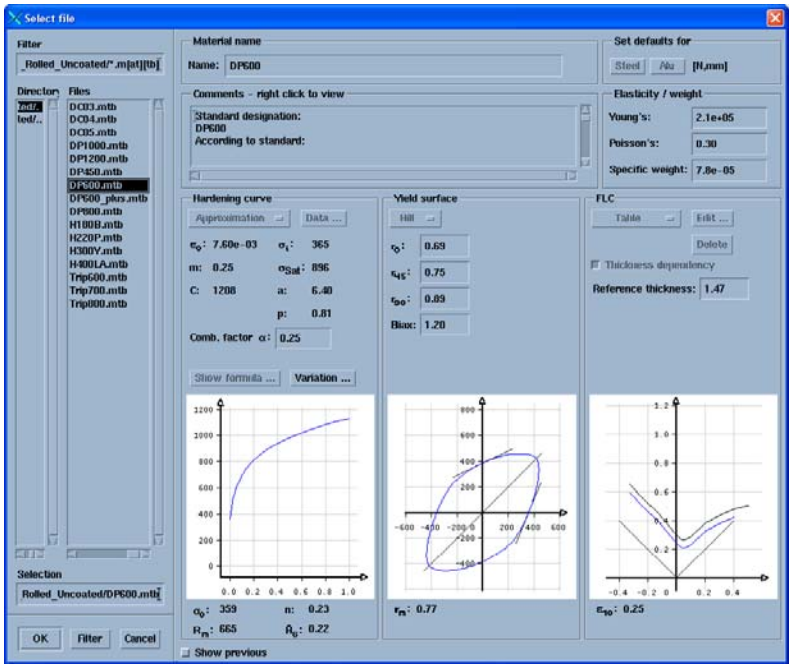

Figure III.C.15 – DP 600 properties

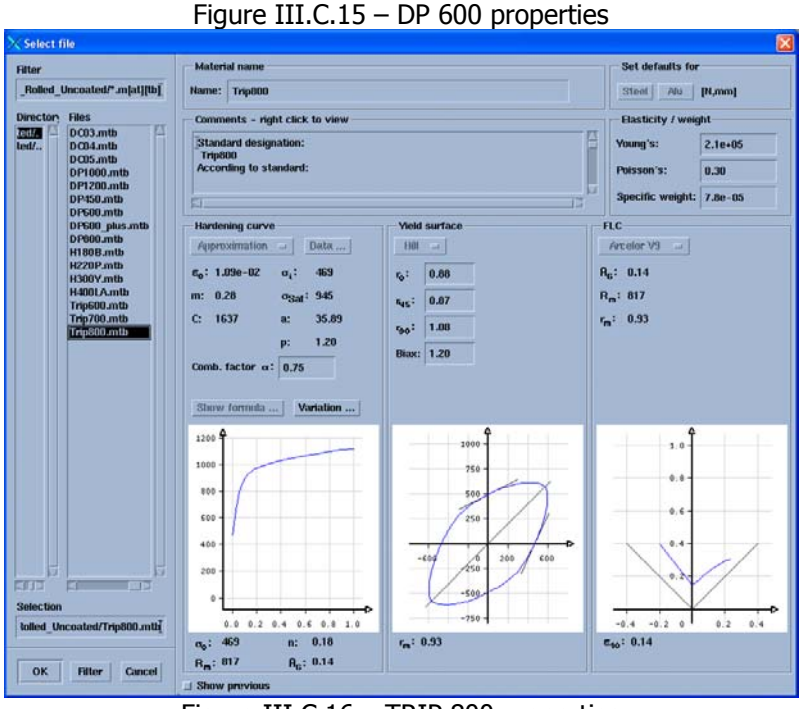

Figure III.C.16 – TRIP 800 properties

- *Tools configuration*

A very important phase in process configuration is made in *Tools* page. In this page the initial position of the diverse tools and their movements (working direction and distance) are defined. The existing tools are configured individually as they are presented in different sub-pages (Figure III.C.17 – III.C.19). It's important to note that in AutoForm the working direction is always defined with respect to the blank.

Columns – are the input points of the force for force-controlled tools. It's recommended to use Tool Centre.
Stiffness – the tool stiffness is specified. Stiffness is the Resistance to elastic deformation.

In *tool setup* section it is possible to select whether the die will be the upper or the lower tool, which is the same as selecting whether deep-drawing on single action press or deep-drawing on double action press will be performed.

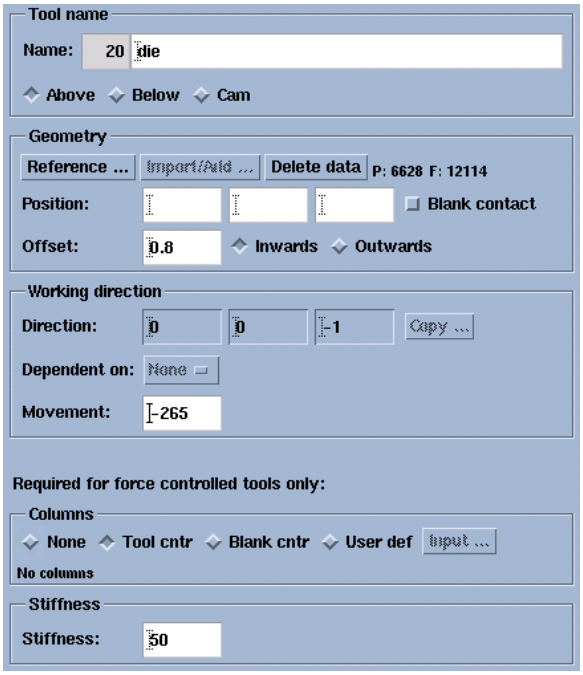

Figure III.C.17 – Die page

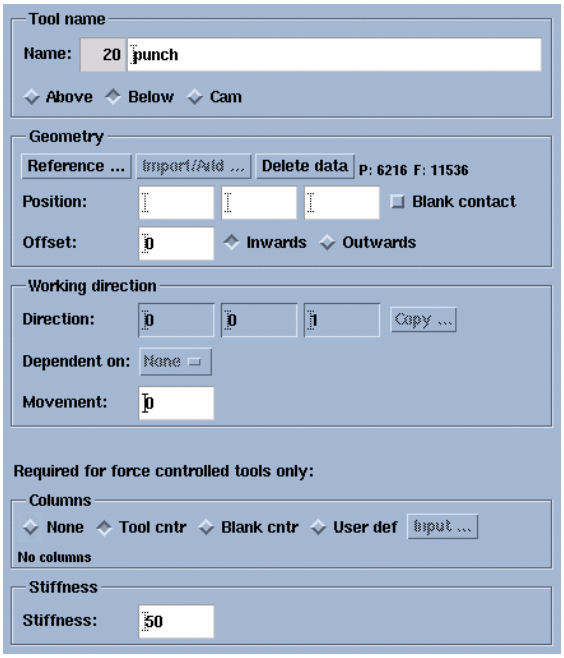

III.C.18 - Punch page

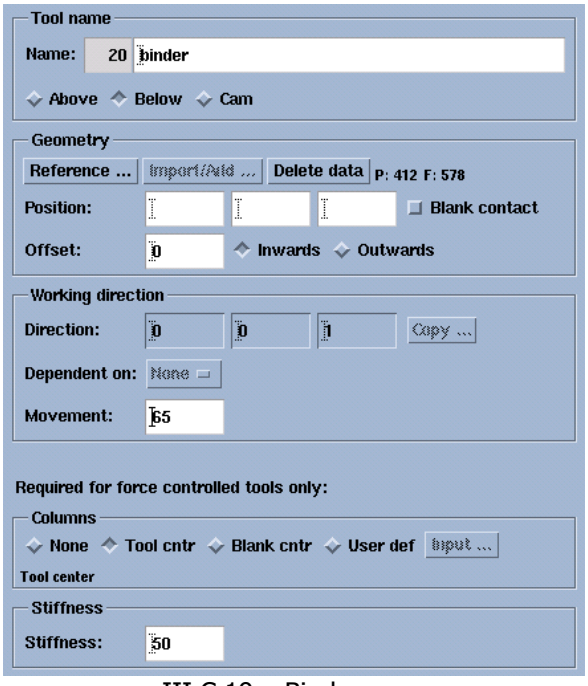

III.C.19 – Binder page

- Lube

The friction coefficient between sheet and tools can be specified (Figure III.C.20). Different friction coefficients can be specified for tools above and below the sheet or for each of the sheet/tool contacts.

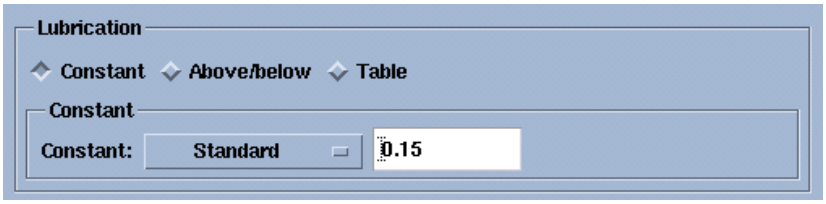

Figure III.C.20 – Lubrication page

- Process Steps (Gravity, Closing, Drawing, Cuttings, Springback…)

The description of the process is made in the *Process* page of the Input Generator. The various operations to be performed, their characteristics and the order in which they will be executed are defined here. *Gravity* (Figure III.C.21), *Closing* (Figure III.C.22) and *Drawing* (Figure III.C.23) are always performed in a stamping simulation. Then, several other process steps may be added to the stamping process: cuttings, springback, annealing, positioning and secondary forming operations (restrike, flanging, hemming).
In the respective sub-pages, information related to each process step is inputted. The input fields are specific for each process step.

Gravity: Models the initial deflection of the sheet due to gravity
Closing (Binder wrap): Metal sheet is pressed between the die and binder.
Drawing: The metal sheet flows between the die and the punch till the end of the drawing tools movement

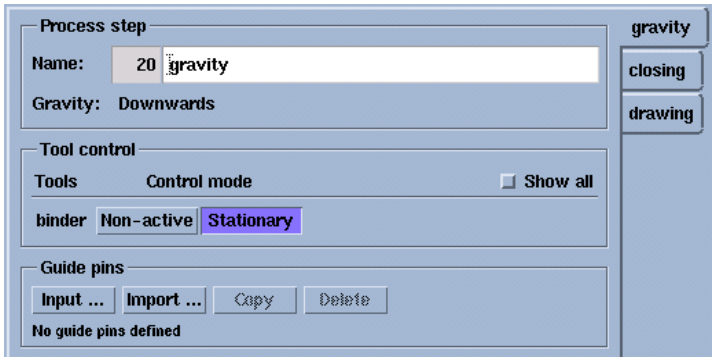

Figure III.C.21 – Gravity page

Figure III.C.22 – Closing page

.

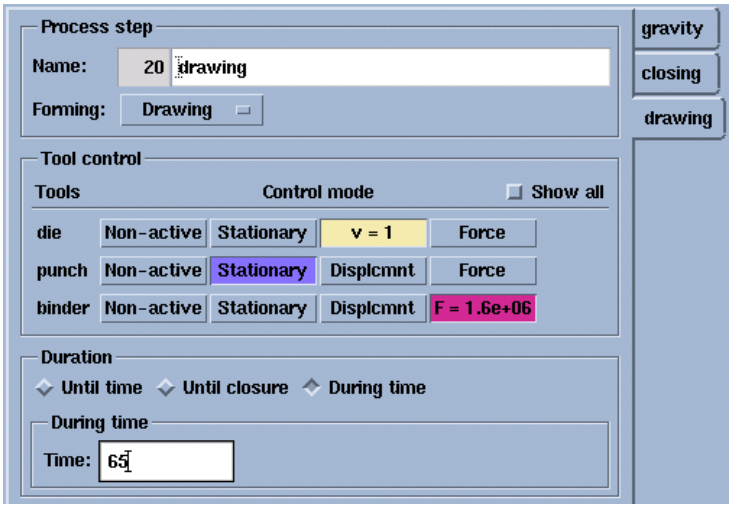

Figure III.C.23 – Drawing page

- Calculus Configuration

- Control data (Input of numerical parameters)

In this page numerical parameters concerning the calculus execution are inputted, such as the accuracy level and the number of layers used. AutoForm calculates the stress-deformation condition in the blank's thickness subdividing it in an unpaired number of layers, so that symmetry respect to a middle plan is obtained. The larger the number of layers, the more precise the analysis, but the calculus time is therefore longer.

For sheet thickness greater than 1.5mm is recommended the selection of *ThickSheet / Springback in later restart.*
Write Restart button selects whether an additional Restart file (*.rst) should be generated during simulation. This file contains all data that is necessary to restart the simulation from a particular time. Restarts can be used to save time (e.g. for multi stage processes), as the different forming processes can be simulated one after the other. The disadvantages is the size of the *.rst file which requires greater disk space.
Taking into account the speed of AutoForm, the restart option is only useful for large parts (e.g. side panel, floor panel).
Inputs on this page may be numerical (**Main**), or may be a selection of result variables (**Rslts**):

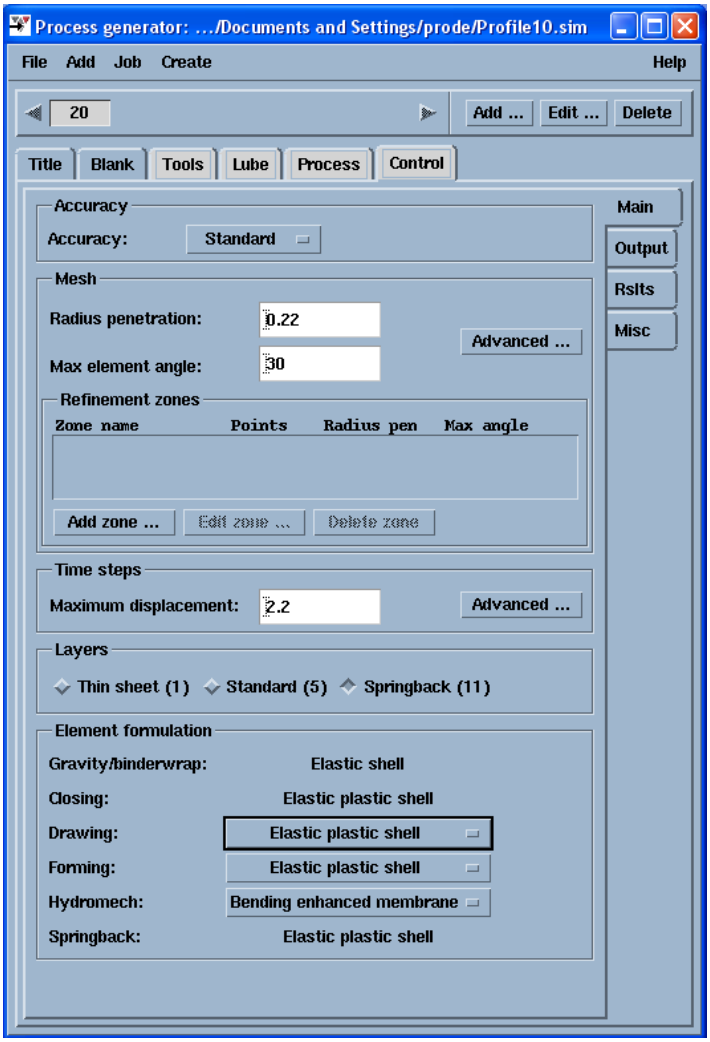

Figure III.C.24 – Control page

- Cutting

Definition of different cutting process types: The definition of cutting processes is always done on **Process** page of the input generator. In AutoForm different cutting types can be defined:

-open cut
-hole
-trimming cut

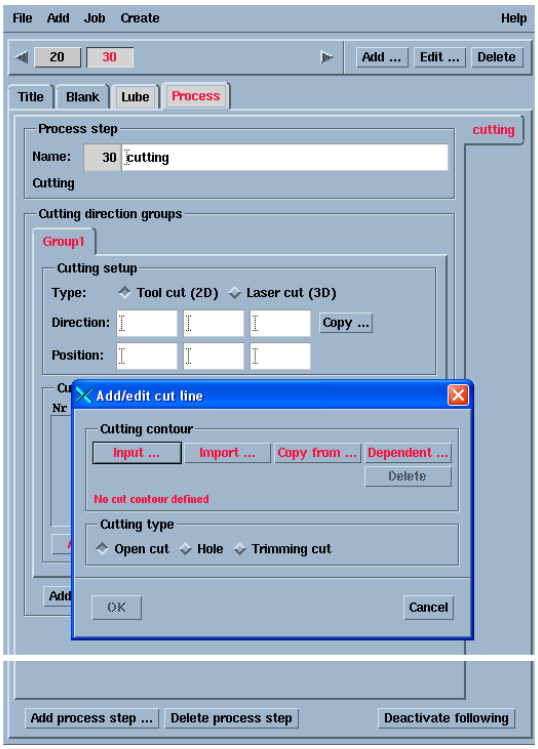

Figure III.C.25 - Cutting page

- *Springback*

Springback: A new process step must be added to simulate springback. In the input page, the geometry for the springback calculation is chosen (Figure III.C.26). Each object has to be calculated, the time of simulation depends from the quantity of objects.

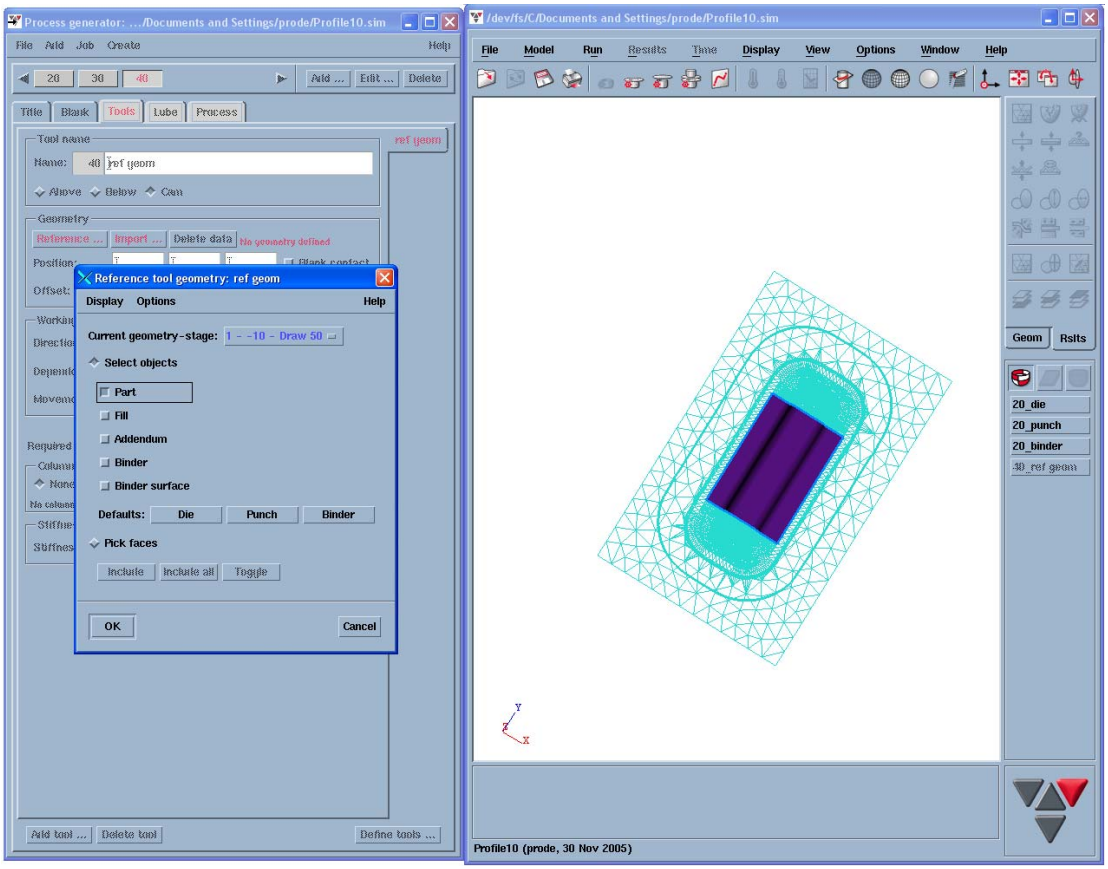

Figure III.C.26 - Springback page

III.C.*4.2 - *Computational Analysis

To perform the calculation, start is chosen simulation by the curtain menu run: The window Start simulation appears in which sets out the analysis clicking on start. Started the calculation, in this same window the file of output is visualized, that the software creates as soon as it performs the calculation. This file can always be read in the window Start simulation.

However, a previous kinematic check may be useful. Selecting *Kinematic check only* option the computer checks the tool movement only. This is completed in a few seconds (Figure III.C.27). This functionality helps avoid possible errors of the tool movement or tool positioning and is recognized during the simulation. When this option is used, only the tool movements are calculated and displayed. The blank remains not formed.

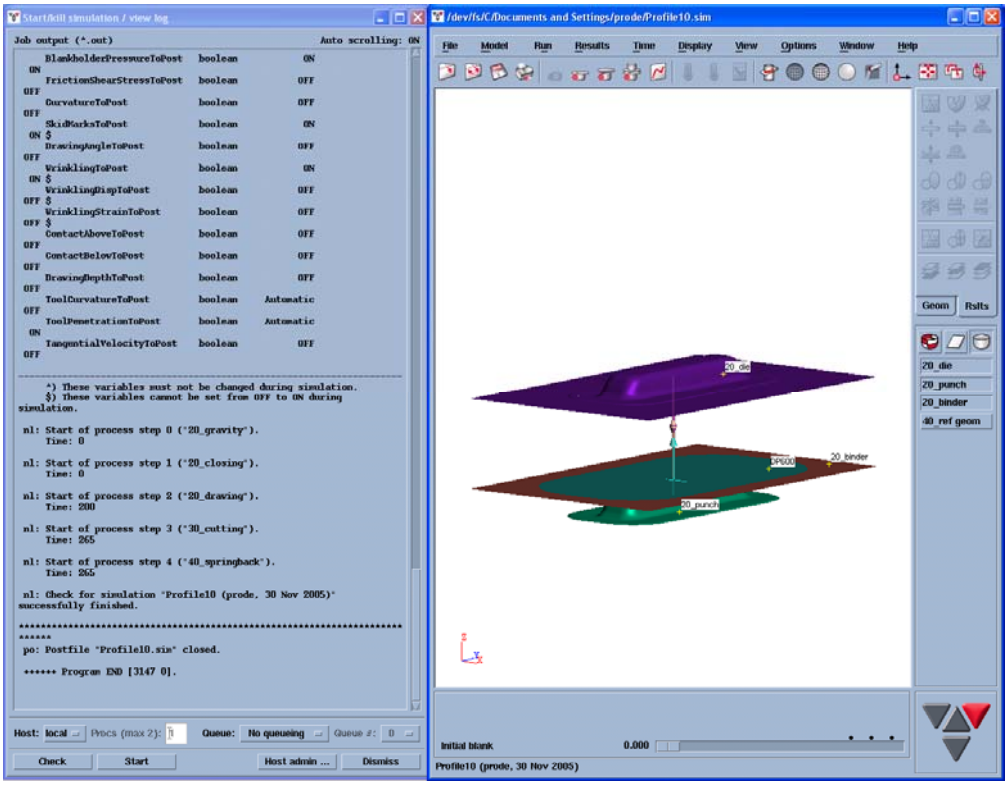

Figure III.C.27 - Start job window: to run a simulation or a kinematic check only

While all the information is being processed by the computer during the calculation, the process iterations are presented in an output window as shown in Figure III.C.28.

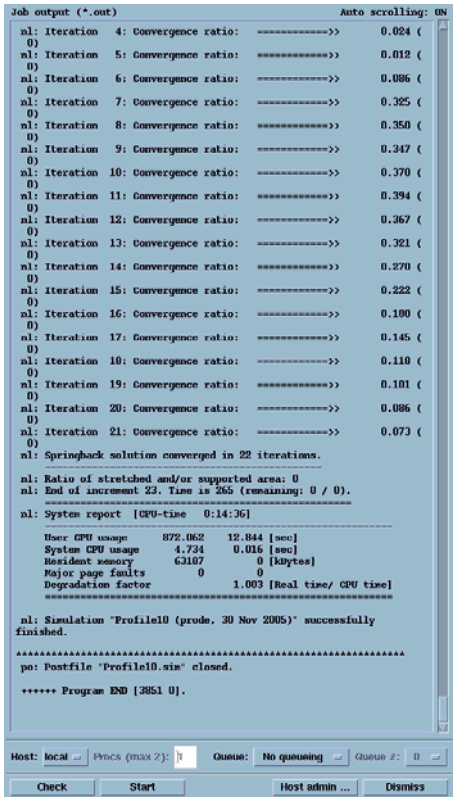

Figure III.C.28 – Start job window: finished simulation

*III.C.*4.3 *- Post-Processing of Results (Analysis of Results)*

After re-opening the simulation file it is possible to accompany several steps of the simulation process from plan sheet till the final stamped part, including springback effect (if selected).
This is very important since not only gives an idea of the simulation's progress but also, in case of failure, it is possible to see where did it went wrong, this way helping to understand and try to correct / improve the simulation try-out.
Colour shaded post values such as sheet thickness, cracks, strain and stress as well as process parameters such as forces are available for the evaluation of the simulation. Wrinkles are identified by inspecting the shaded representation of the model or by means of colour shaded post values. These possibilities are completed by additional special evaluation criteria such as skid/impact lines.
The punctual lecture of the diverse result parameters (thickness, thinning, normal displacement, etc.) is also possible when clicking with the right mouse button. Display the maximum and minimum values of the current result variable is also possible.

In the following, the analysis of some important result variables will be discussed. These results can be displayed both as coloured and shaded images.

Forming/Stamping evaluation (formability, FLD, wrinkling criterion, failure (maximum))

-Formability

The most important criteria to evaluate the forming/stamping success is the result variable *Formability*. It gives a general survey of the feasibility of the part. This result variable displays the strain state at different locations on the formed sheet (based on the Forming Limit Diagram – FLD). Different colours are used to denote the qualitative types of strain states, i.e., areas undergoing different stresses are coloured differently on the part (Figure 5.29):

- *Cracks (Red)*: Areas of cracks. These areas are above the FLC of the material used.
- *Excessive Thinning (Orange)*: In these areas, thinning is higher than the acceptable value (default value for steel is 30%)
- *Risk of Cracks (Yellow)*: These areas may crack or split. By default, this area is in between the FLC and 20% below the FLC
- *Safe (Green)*: All areas that have no formability problems, i.e., which have no defects – wrinkles, thinning or cracks.
- *Insufficient Stretching (Gray)*: Areas that have not enough strain (default 2%)
- *Wrinkling Tendency (Blue)*: Areas where wrinkles might appear. In these areas, the material has compressive stresses but no compressive strains
- *Wrinkles (Purple)*: Areas where wrinkles can be expected, depending on geometry curvature, thickness and tool contact. Material in these areas has compressive strains which mean the material becomes thicker during the forming process

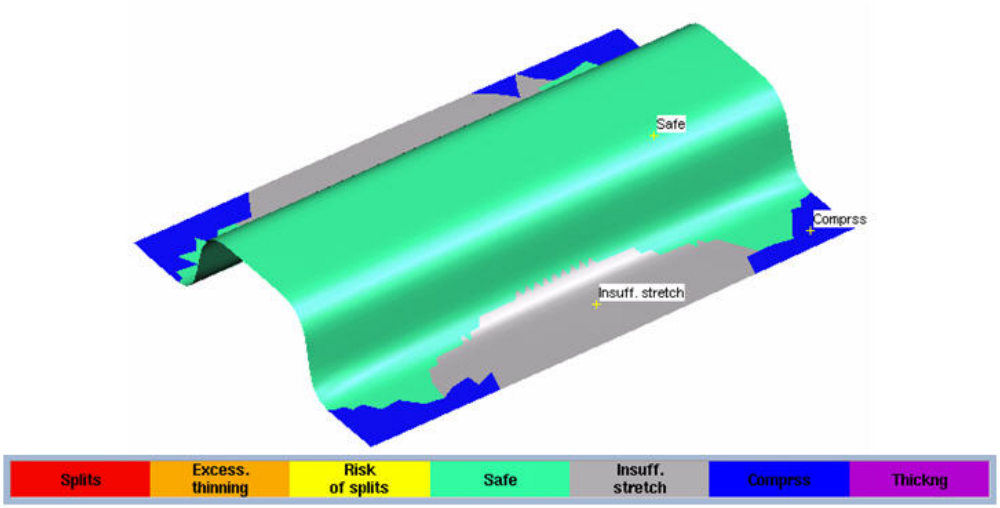

Figure III.C.29 – Formability result

-FLC parameters

The default-values of result variable *Formability* can be changed in the formability menu (Figure III.C.30).

Figure III.C.30 – Formability menu

The results of the formability didn't go however very satisfactory for such it was considered to accomplish some simulations for different force values between the binder and the die.

1. F= 1.0E+06 N
2. F= 1.5E+06 N
3. F= 2.0E+06 N
4. F= 2.5E+06 N

The best result was found for the value 3 (Figure III.C.2), however still appear zones with insufficient stretch. With the objective of finding results where the formability is in the safe area it was necessary the drawbeads application.

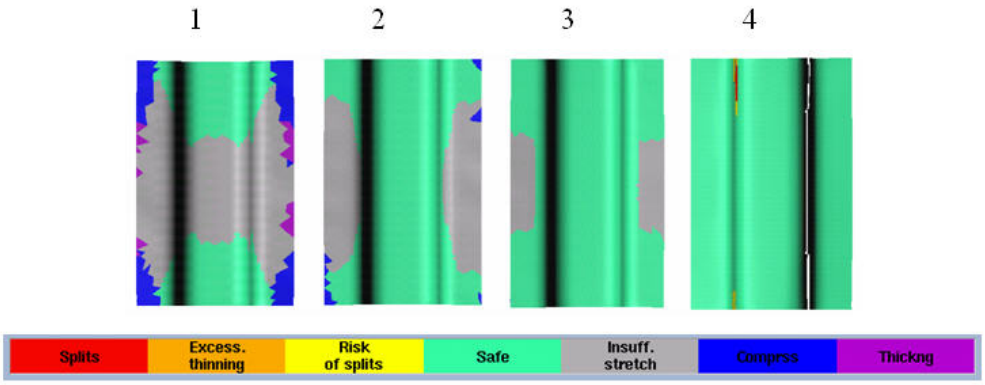

Figure III.C.31 – Formability results

-Add drawbeads

The performance of the drawbead, or drawbead-like protrusions such as stepbeads or endbeads, is mainly determined by the drawbead geometry (Figure III.C.32). The radii of the drawbead and the clearance between the drawbead tools can be varied, but also the shape of the cross-section. The shape of the cross-section can be semicircular, rectangular or non-symmetric, where each shape has its specific characteristics.

Drawbeads may be modelled in AutoForm using a force factor to control metal flow, without having to build the detailed drawbead geometry into the CAD model of the tool. This gives the user flexibility in using AutoForm as a tryout tool – using it to quickly compare the performance of different drawbeads regarding feasibility requirements, and to identify the best bead configuration, based on comparisons, without having to modify tool geometry to accomplish the same. Thus, in AutoForm, drawbead is defined using only a bead centre-line and not with the real bead-profile geometry. This line specifies the position of the drawbead. Furthermore the restraining force is specified and the real profile geometry depends on it. This allows saving time as the calculations are much more faster considering this restraining force instead of the geometry of the drawbead.

AutoForm now offers a Drawbead generator for the correlation of the real profile geometry of drawbeads and drawbead force. With the Drawbead generator the real geometry of the drawbead can be specified and the force factor is automatically calculated by the program. If the force factor is known, the Drawbead generator will determine the real geometry of the drawbead.

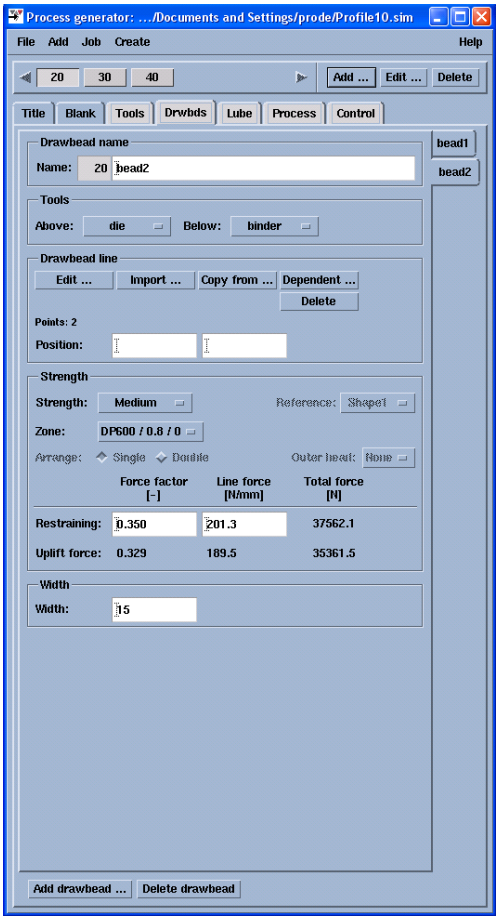

Figure III.C.32 – Drawbeads page

Brief description of *Drawbead* page commands:
Name: Name of a drawbead can be specified.
Tools: Tools are defined; drawbead is active when these tools are closed.
Input ...: Position of drawbead line can be specified (Curve editor).
Import ...: Drawbead line is imported from CAD.
Copy from ...: Drawbead line is copied from an existing line. Base line and drawbead line are treated as different lines.
Dependent ...: Drawbead line is created from an existing line. Drawbead line is a reference to the base line. This means only the base line can be changed and the dependent drawbead line will also change correspondingly.
Position: Displacement of drawbead line in x-y plane.
Width: Width of a drawbead.
Forcefactor: Force factor of a drawbead

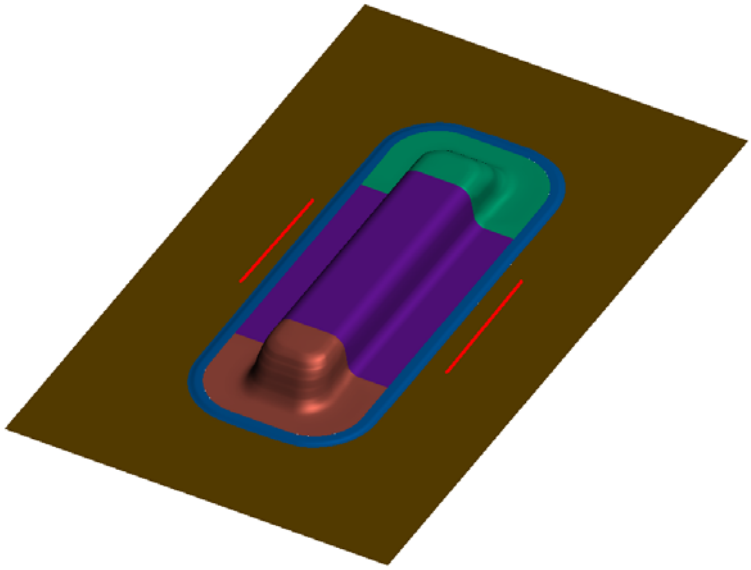

Figure III.C.33 – Drawbeads application

Was used the standard restraining forces given by the software,
Weak: 0.150
Medium: 0.350
Strong: 0.500

Combined forces between 1.5 and 2.0 and applied these straining forces was found the best formability results (Figure III.C.34) for:

Force = 1.6 e +06
Restraining force – Force factor = 0.350

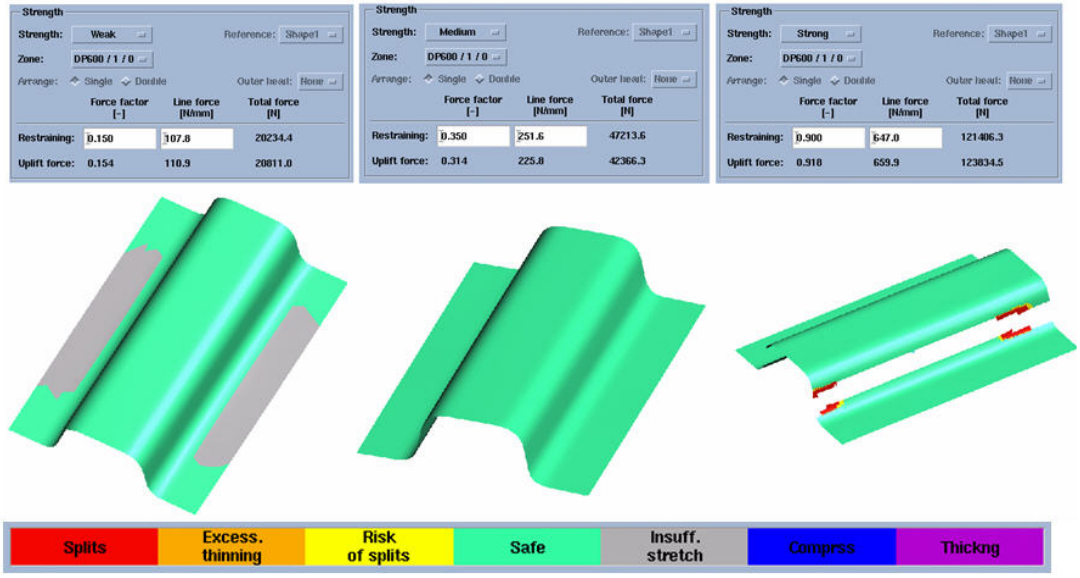

Figure III.C.34 – Formability results

-Failure

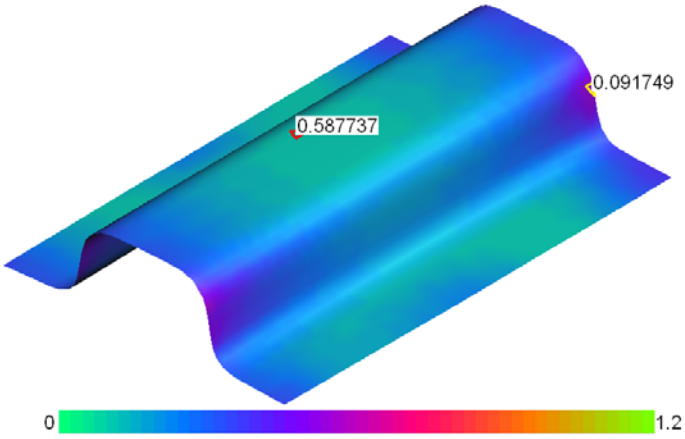

Figure III.C.35 - Display of the result variable Failure with min and max values in the main display

-Forming Limit Diagram (FLD)

The Forming Limit Diagram (FLD) describes the failure of the sheet metal due to cracks. In the FLD the Forming Limit Curve (strain states above those failure/cracks occur) is represented as a black curve. Into this diagram, all finite elements of a simulation with the two main strain results (major and minor) are shown (Figure III.C.36). So, one can judge the robustness of a reforming process also visually in this diagram.

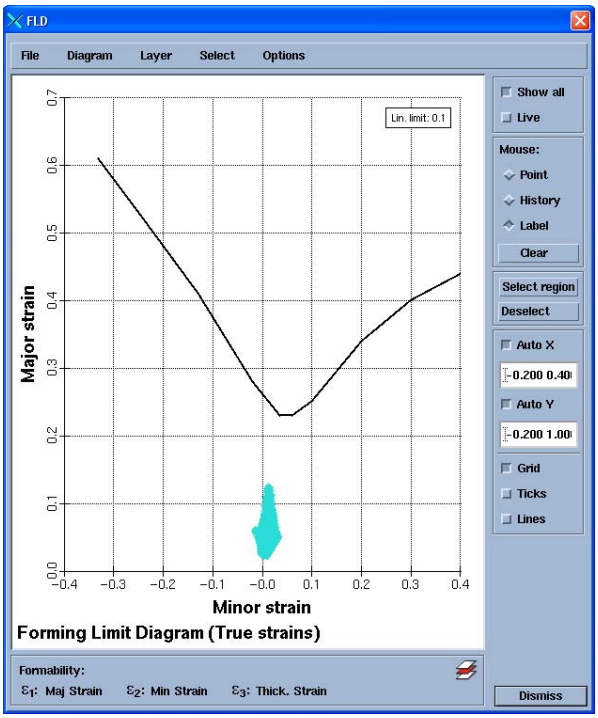

Figure 5.36 – Forming Limit Diagram (FLD)

Thickness / Strain evaluation
(thinning, thickness, plastic strain, major strain and minor strain)

-Thickness

The thickness of the metal sheet is displayed with this option (Figure III.C.37).

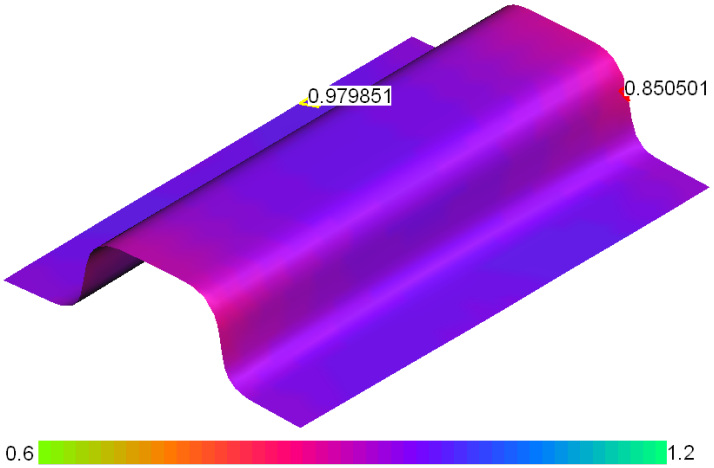

Figure III.C.37 – Display of the result variable Thickness with min and max values in the main display

-Thinning

In Figure III.C.38 another result variable that is often used is the percentage thinning of the material (Thinning).

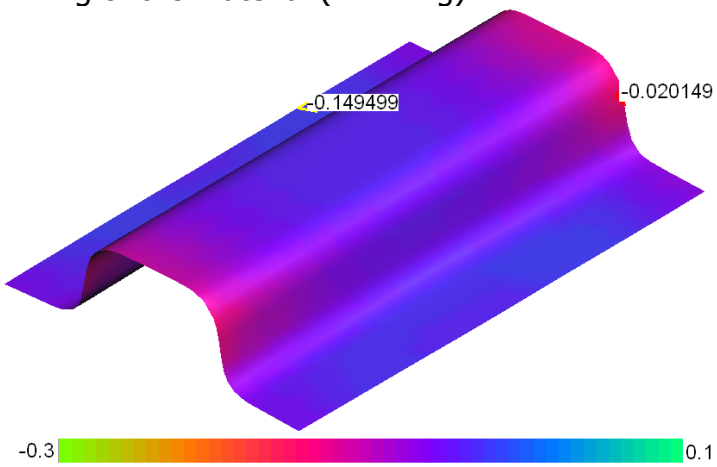

Figure 5.38 – Display of the result variable Thinning with min and max values in the main display

A scale is displayed in the lower part of the main window with a range of 30% thinning (-0.3) to 10% thickening (0.1), coloured from yellow to green (depending on the use colour settings). The exact thinning level at any

location on the formed sheet may be displayed by clicking at that location on the sheet (in the main display) using the right mouse button

-Wrinkling Criterion

In order to verify if there are areas where the material has tendency to wrinkle, *Wrinkling Criterion* option should be activated (see Figure 5.39). Thanks to the chromatic scale in the bottom it is possible to observe the areas where the metal sheet tends to become thicker and, by instability, to wrinkle.

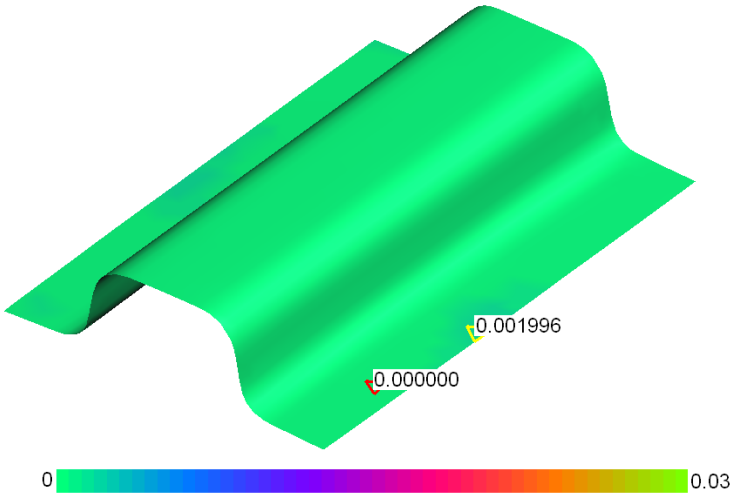

Figure III.C.39 - Display of the result variable Thinning with min and max values in the main display

-Plastic Strain (Figure III.C.49)

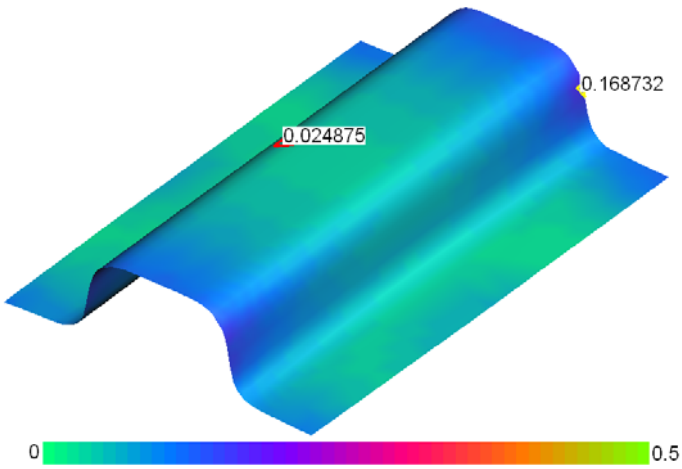

Figure III.C.49 - Display of the result variable Plastic Strain with min and max values in the main display

-Major Strain (Figure III.C.50)

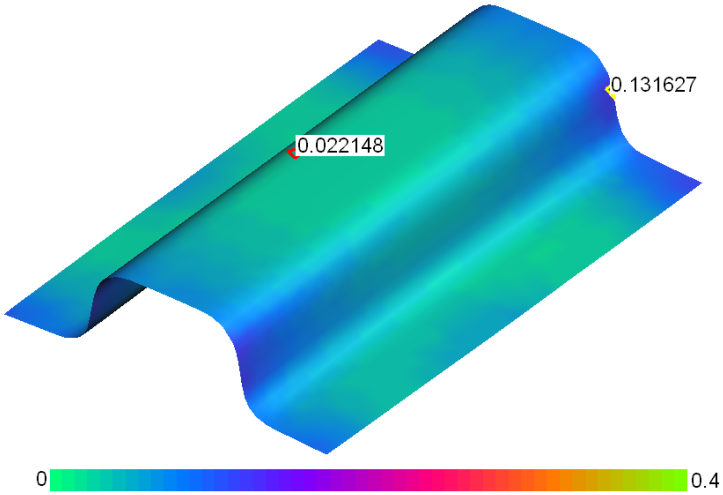

Figure III.C.50 - Display of the result variable Major Strain with min and max values in the main display

-Minor strain (Figure III.C.51)

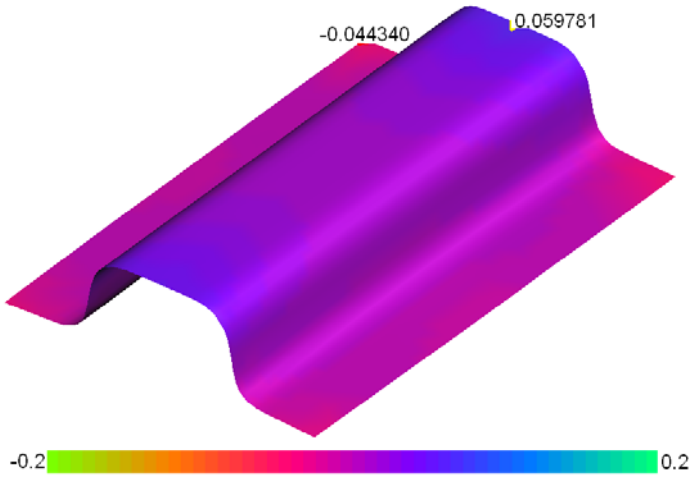

Figure III.C.51 - Display of the result variable Minor Strain with min and max values in the main display

-Springback evaluation

The program, through the command Springback of the curtain menu Results, furnishes the value of the elastic return in terms of angular variations or of moves according to the aces of reference (x, y, z) or according to the normal one to the nominal surface (Figure III.C.52).

With this option, due to the chromatic scale (Figure III.C.53 - 57), it is possible to immediately recognize the areas more subjected to springback.

However one can also analyse this phenomenon punctually, by measuring quantitatively the value when clicking with the right mouse button.

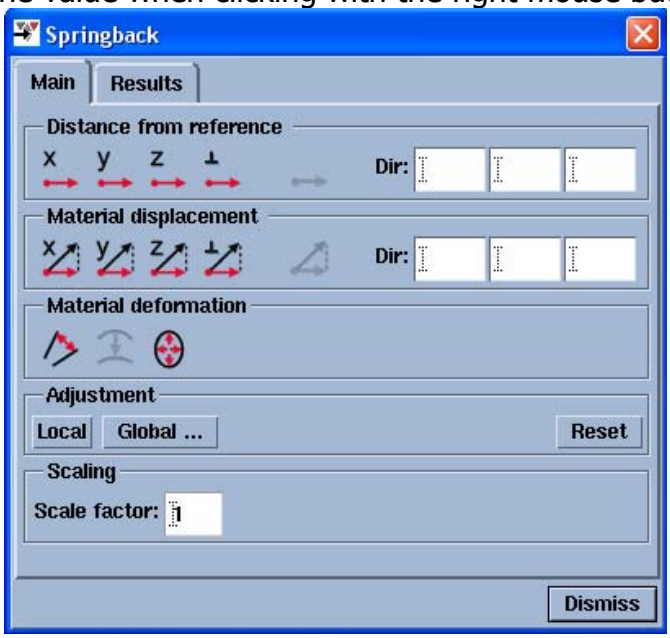

Figure III.C.52 – Springback available results

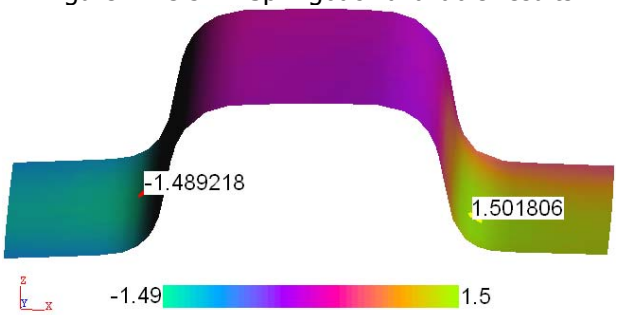

Figure III.C.53 - Material displacement in X direction with min and max values in the main display

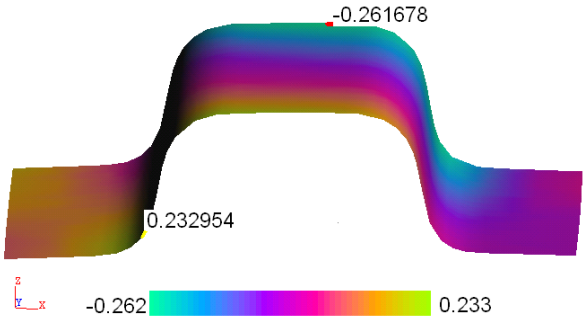

Figure III.C.54 - Material displacement in Y direction with min and max values in the main display

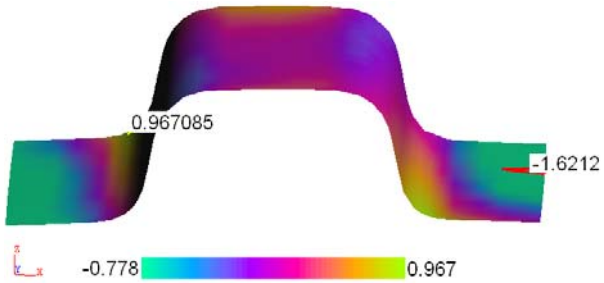

Figure III.C.55 - Material displacement in Z direction with min and max values in the main display

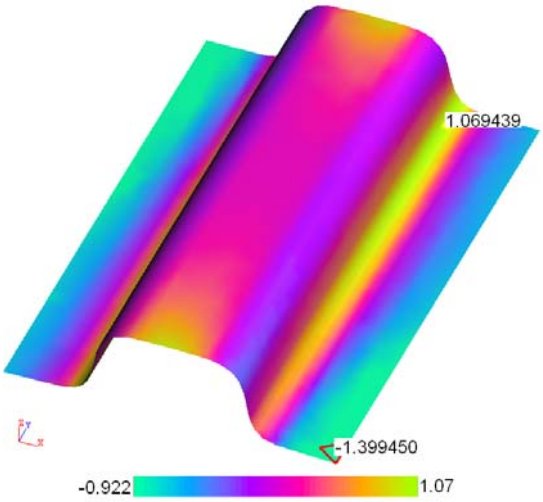

Figure III.C.56 - Material displacement in normal direction with min and max values in the main display

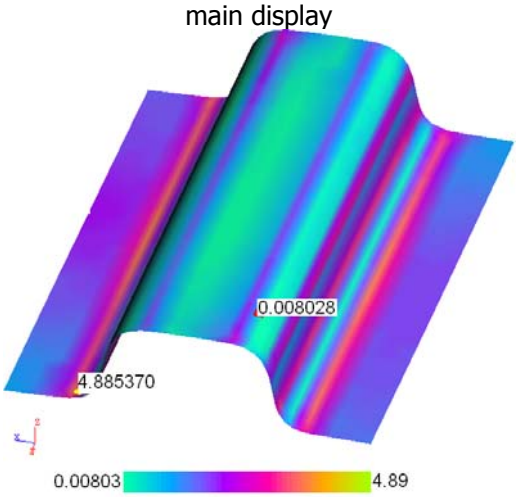

Figure III.C.57 – Angular displacement with min and max values in the main display

-Dynamic Section

AutoForm consents the analysis of sections of the simulated component (as well as the tools), by activating the visualization of the element, and the tool or the reference geometry simultaneously. This analysis is possible with the *Dynamic Section* menu (Figure III.C.58).

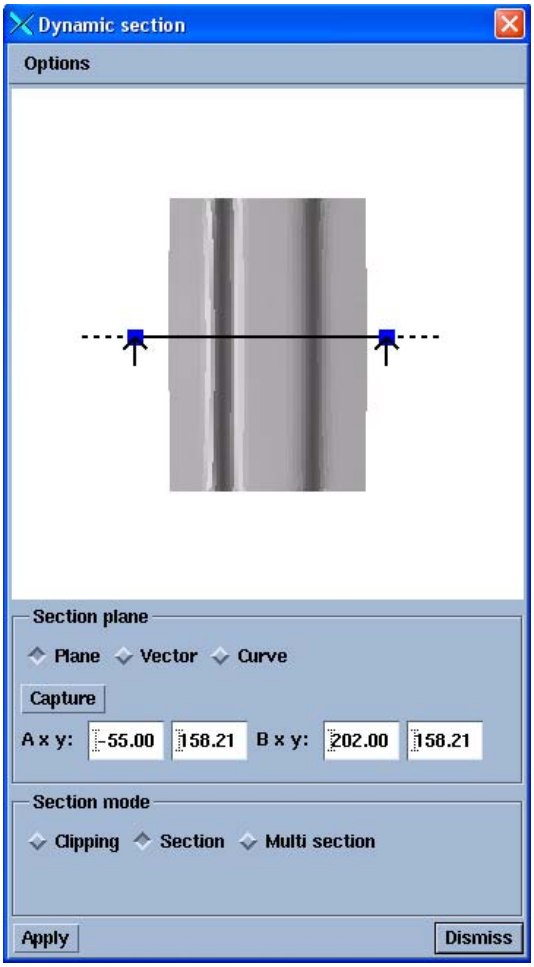

Figure III.C.58 – Dynamic section menu

The option *Section* displays the selected section plane as a 2D-curve (Figure III.C.59).
The option *Clipping* displays 3D geometry with the selected section plane as a clipping plane.
The option *Multi section displays* several sections as a 2D-curve.

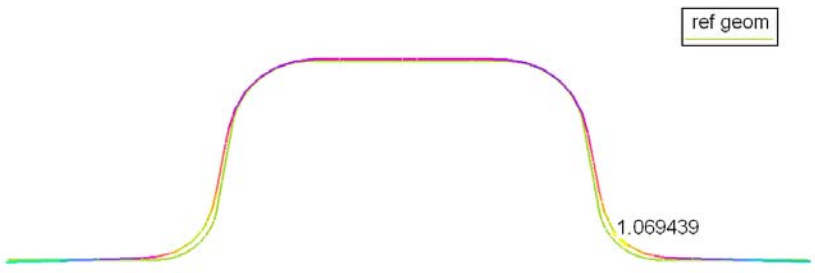

Figure III.C.59 - Maximum displacement in normal direction [mm] of profile 1 for DP600 material

The use of dynamic section is a powerful tool to evaluate more precisely the spacing of the walls (Figure III.C.60) and the angular variations.

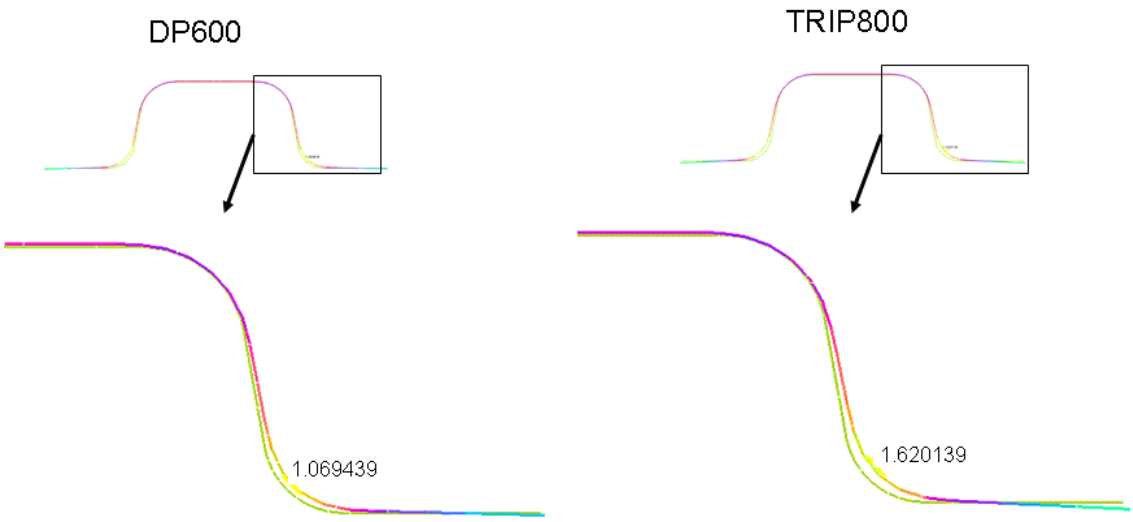

Figure III.C.60 - Comparison between maximum displacement in normal direction [mm] of DP600 and TRIP800 in profile of 10º

III.C.5 - Final Comment

The maximum springback results of test case 1 are displayed on table 5.1 where is possible to prove that for the same profile Trip 800 has bigger elastic return than DP 600 and for the same material, as larger is the angle, the springback phenomenon increases (showed in red and blue).

		DP 600	Trip 800	Difference (%)
10º	x	0,96	1,5	56,3
	y	0,2	0,23	15
	z	0,95	0,97	2,1
	normal	1,07	1,49	39,3
	[º]	4,89	5,06	3,5
11º	x	1,04	1,63	56,7
	y	0,22	0,26	18,2
	z	1,2	1,06	-11,7
	normal	1,2	1,69	40,8
	[º]	5,02	5,31	5,8
12º	x	1,02	1,79	75,5
	y	0,26	0,26	0
	z	1,29	1,18	-8,5
	normal	1,3	1,93	48,5
	[º]	5,2	5,73	10,2

Table 5.1 – Maximum springback results for material displacement and angle change

Section III.D

The fourth project, A test case was the stamping simulation of a lateral longeron for the Group Fiat. For that was considered eleven different profiles differing in angular variations realized with DP600 material.

III.D.1 – Introduction

The aim of the numerical simulation in this chapter is to verify the stamping process and the shape of the final component. To apply these final components in a real case, was considered essential the study of springback phenomenon (very influent in the welding and assembly of mobile components).

The test case was the stamping simulation of a lateral longeron for the Group Fiat. For that was considered eleven different profiles differing in angular variations realized with DP600 material.

The study was made always with base in the limits proposed by ELASIS, the Group Fiat research centre.

The conducted analyses and the achieved results have a theoretical value and they have not been validated from experimental real tests.

III.D.2 - Description of the components

The lateral longerone it is an element that belongs to the loom and it is climbed on in longitudinal position under the cabin of the vehicle (Figure III.D.1).

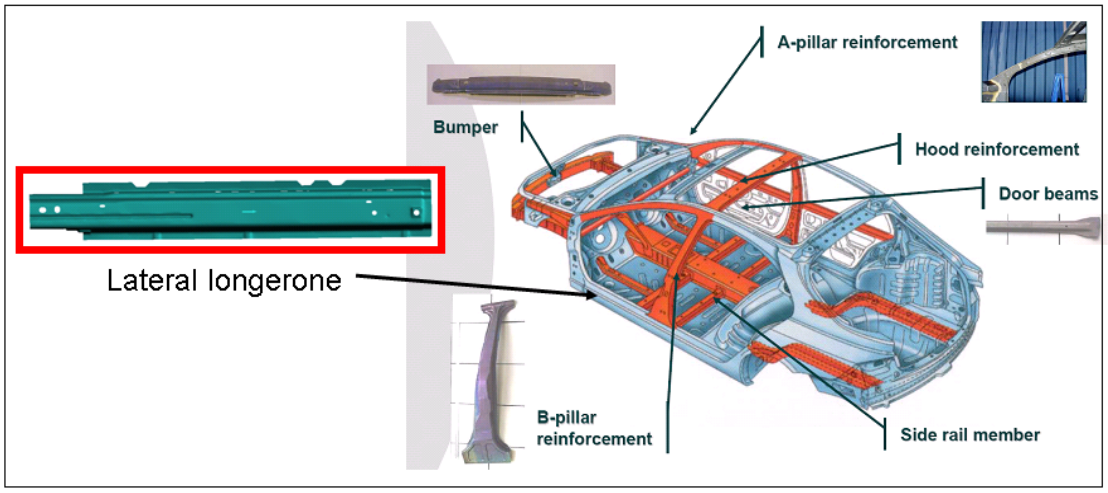

FigureIII.D.1 – Location of the lateral longerone

From the observation of the sight in plant, the component shows a predominantly longitudinal development, is not symmetrical and it has not a course completely to plane, for the presence of a bending.

For a best exposure of the results it was decided to choose one section in the component, the one that describes the bigger percentage of the all part (Figure III.D.2).

The study was based on eleven different profiles (wall's angles variation), where the measures are in [mm] and the angles in [º] (Figure III.D.3 – III.D.13).

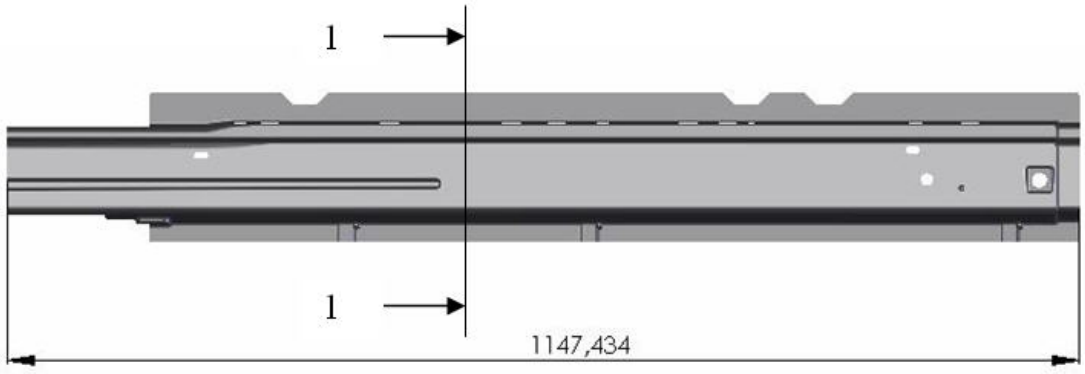

Figure III.D.2 – Chosen section to expose the results

n_l_1

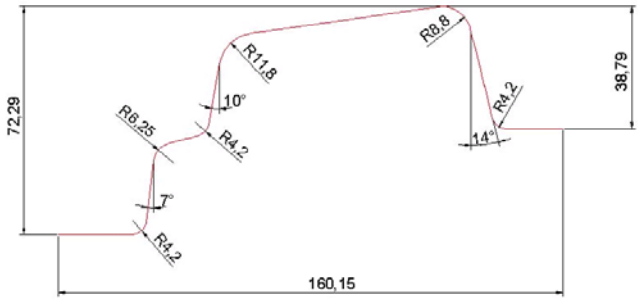

Figure III.D.3 – Section's 1-1 measures: profile 1

n_l_2

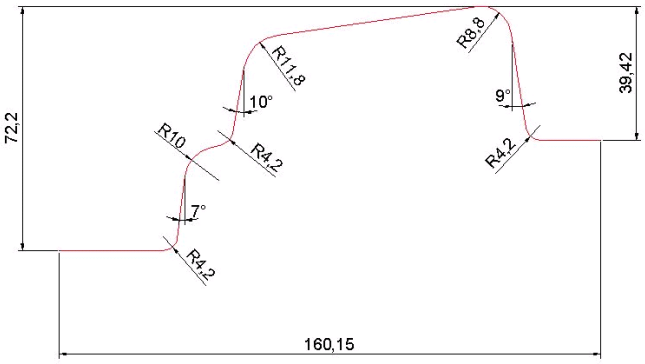

Figure III.D.4 – Section's 1-1 measures: profile 2

n_l_3

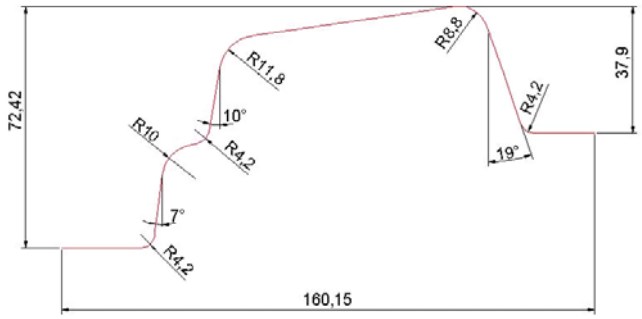

Figure III.D.5 – Section's 1-1 measures: profile 3

n_l_4

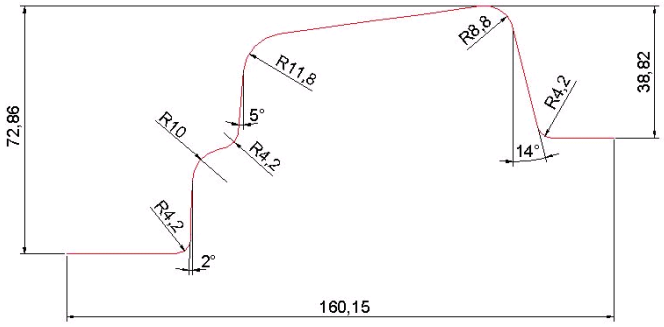

Figure III.D.6 – Section's 1-1 measures: profile 4

n_l_5

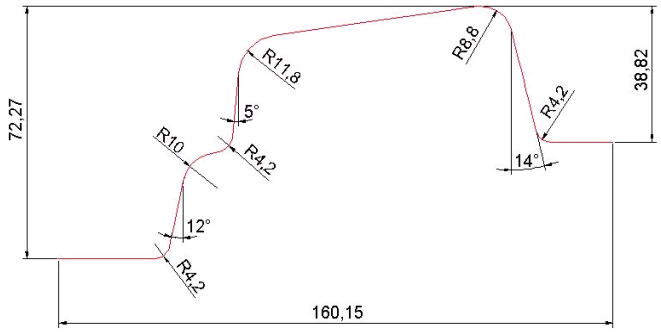

Figure III.D.7 – Section's 1-1 measures: profile 5

n_l_6

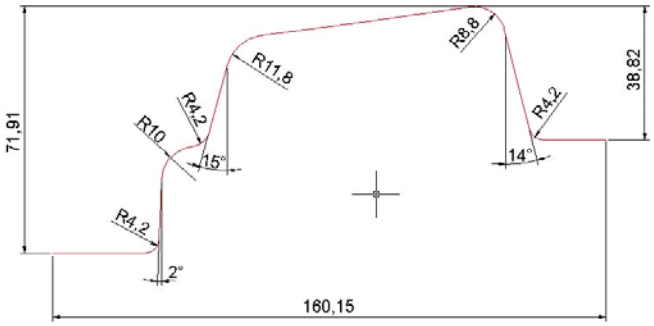

Figure III.D.8 – Section's 1-1 measures: profile 6

n_l_7

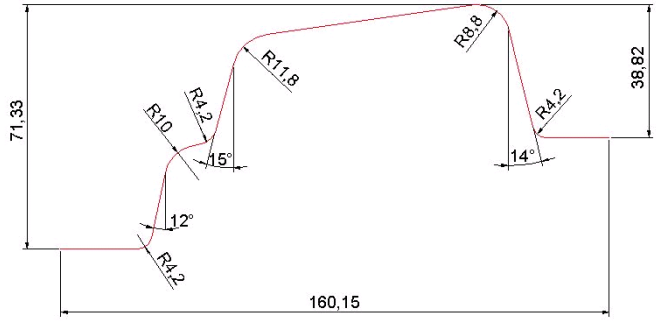

Figure III.D.9 – Section's 1-1 measures: profile 7

n_l_8

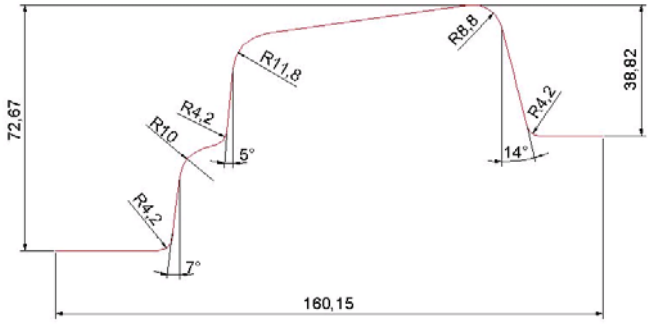

Figure III.D.10 – Section's 1-1 measures: profile 8

n_l_9

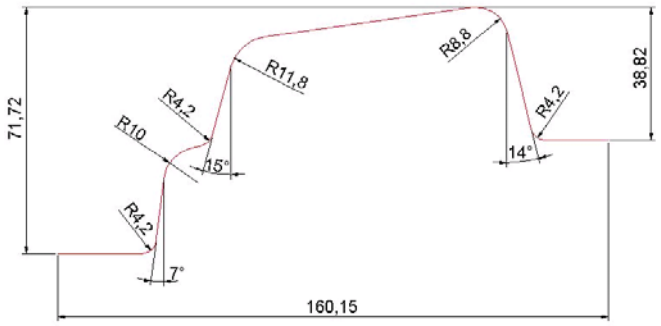

Figures III.D.11 – Section's 1-1 measures: profile 9

n_l_10

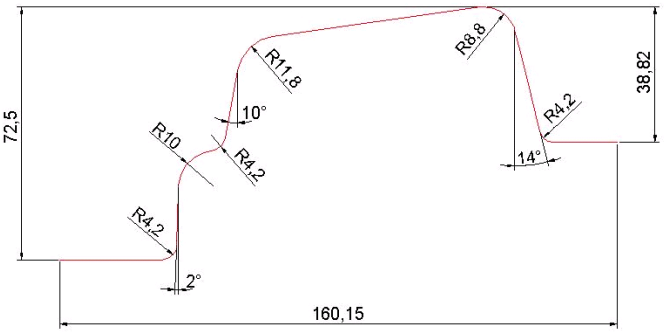

Figure III.D.12 – Section's 1-1 measures: profile 10

n_l_11

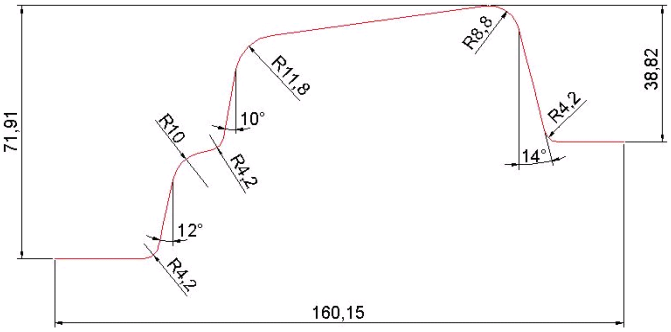

Figure III.D.13 – Section's 1-1 measures: profile 11

III.D.3 **– Limits**

The study was made obeying the limits proposed by the research centre (Table III.D.1).

		Limits	Proposed
Geometry	**Balance**		Safe: 3.00 Marginal: 0.00
Type	**Deep-Drawing**		Single Action Press
Process	**N° drawbeads**		Minimal
	Blank Tickness	Min: 1.0 mm	Minimal
	Lube	Min:0.05 Max:0.25	Maximize
Results	**Formability**	Splits Excessive Thinning Risk of Splits Safe Insufficient Stretching Compression Thickening	No presence Minimal Minimal Maximize Minimal Minimal No presence

Table III.D.1 – Proposed limits

III.D.4 – Input results

III.D.4.1 - Balance (Tip)

The balance process followed the security limits (Figure III.D.14), however it was found three profiles that couldn't be balanced, because don't have safety margins (Figure III.D.15).

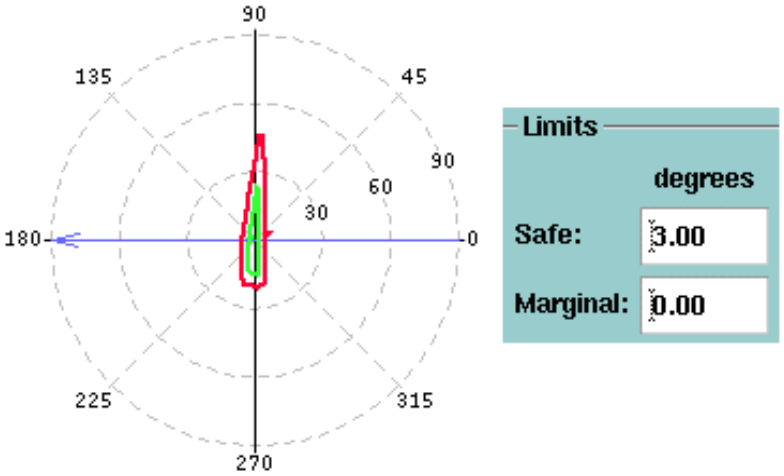

Figure III.D.14 - Security limits for balance

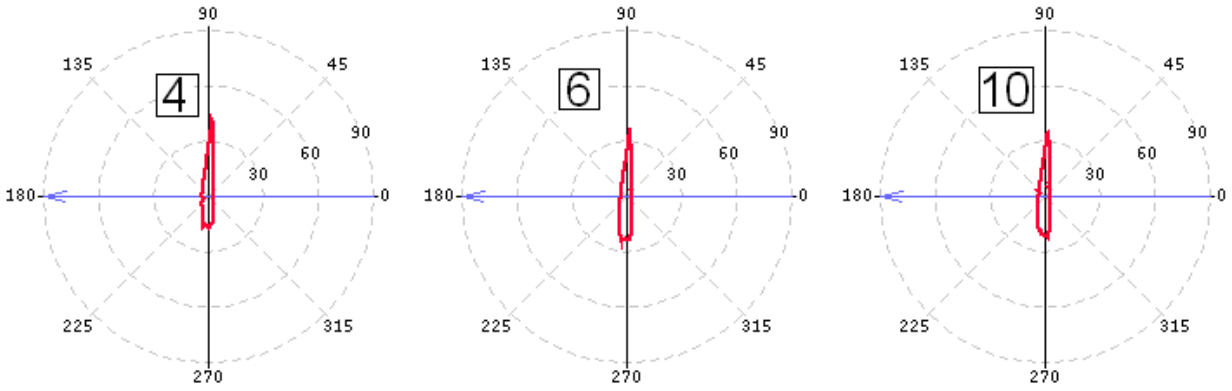

Figure III.D.15 - Backdraft diagram of profile 4, 6 and 10

III.D.4.2 - Boundary (Bndry)

Due to the unsatisfactory results given by the auto fill end it was necessary to found an optimal fill end manually. To assure a fine material in that zone it was necessary to increase the number and change the line's geometry (Figure III.D.16).

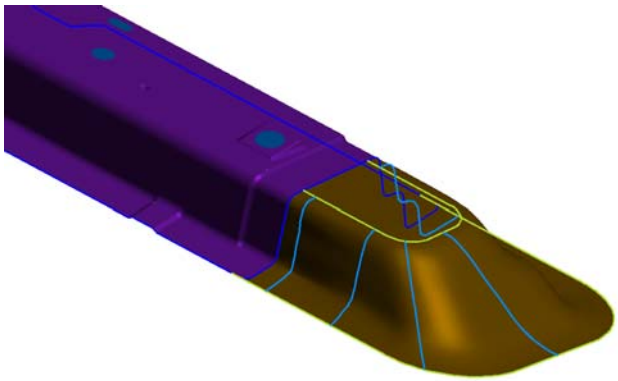

Figure III.D.16 – Changes on the profiles that constitute the end fill

III.D.4.3 - Binder

The results obtained with automatic binder were also unsatisfactory, therefore was necessary to change the geometry progressively until achieve a better solution, described in figure III.D.17.

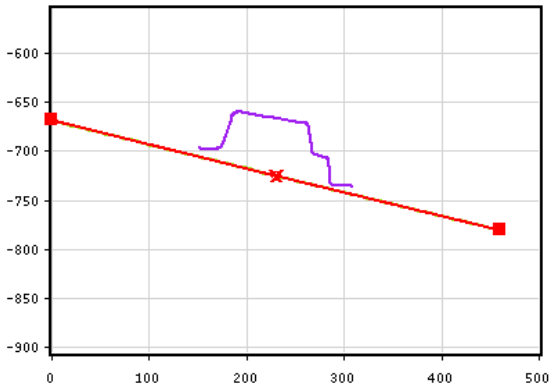

Figure III.D.17 –Final geometry of the binder

III.D.4.4 - Addendum (Addndm)

Due to unsatisfactory results by auto addendum was necessary to use the manual addendum. By changing manually the radius (r1 and r2) and the vertical inclination (α) were achieved the better results (Figure III.D.18).

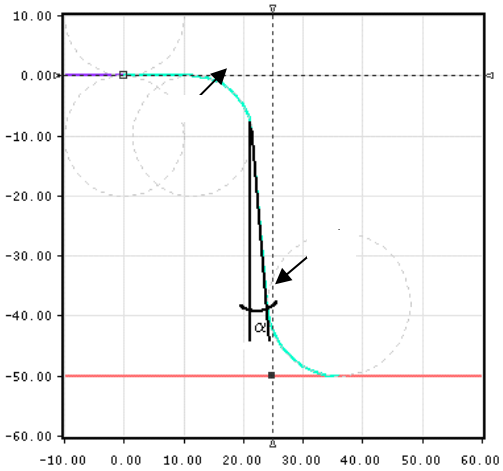

Figure III.D.18 – Final geometry of addendum

III.D.4.5 - Single action press

Single Action Process: this process is widely used, especially when surface quality is not a priority requirement. This procedure is based in a single slide (ram) movement: the punch is stationary, the die moves down in its direction pressing the metal sheet against the blankholder, and then deforms the blank with the punch. Cycle time is reduced by approximately 25% in comparison with the double action process.

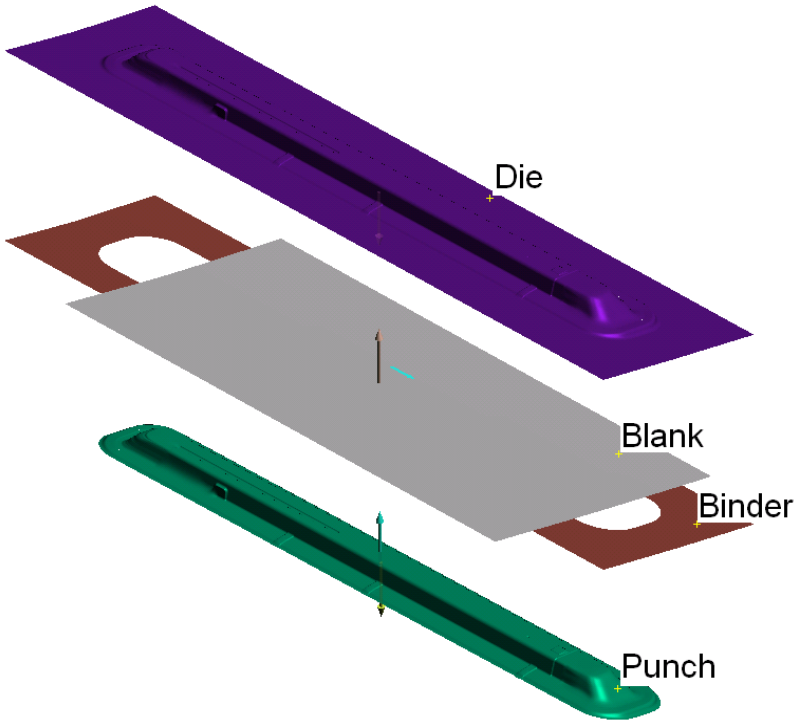

Figure III.D.19 – Single action press simulation

III.D.4.6 - Drawbeads (Drwbds)

When the workpiece is complex normally is necessary the use of drawbeads, in this case for each profile were used different number of Drawbeads, different positions and applied different restraining forces. In figure III.D.20 it is possible to see the characteristics of the drawbeads applied on the stamping simulation of profile 1.

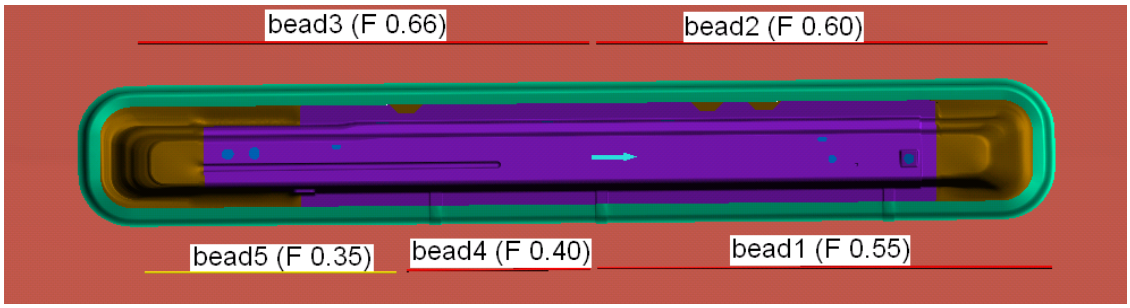

Figure III.D.20 – Characteristics of the drawbeads applied on profile1

III.D.4.7 - Blank geometry (Blank)

The blank geometry revealed being a very influent parameter on the final forming results, only by changing the length, the results become very different. In figure III.D.21 can be seen splits on formability results (red zones) when was increased the length of the blank.

The blank measures utilized on profile 1 are shown on figure III.D.22.

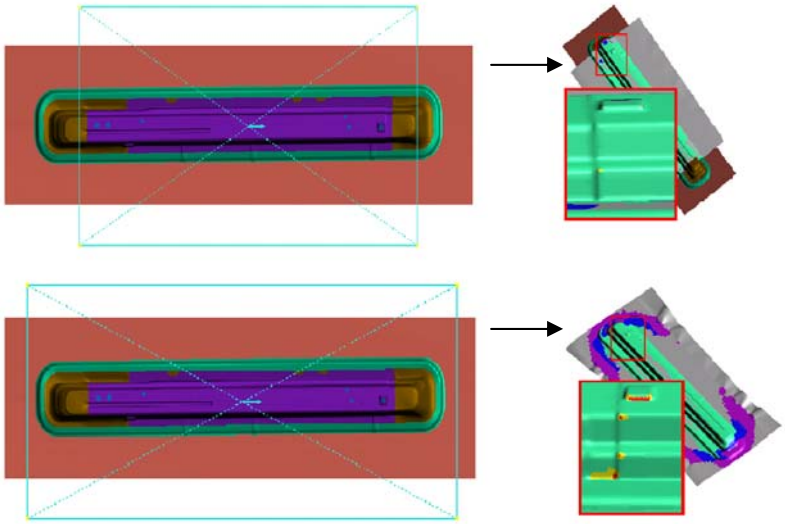

Figure III.D.21 – Formability results when was increased the length of blank

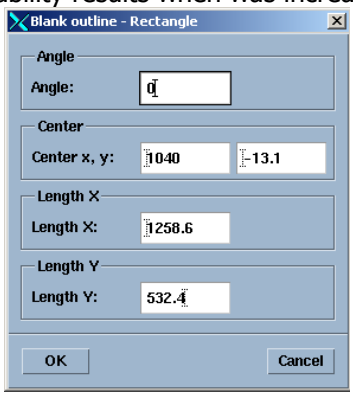

III.D.22 – Final blank measures of profile 1

III.D.4.8 - Lubrication (lube)

With the aim of improve the formability results was used special lubrication (0.05), however profile 3 has the same formability results with the value 0.1 on lubrication (Figure III.D.23).

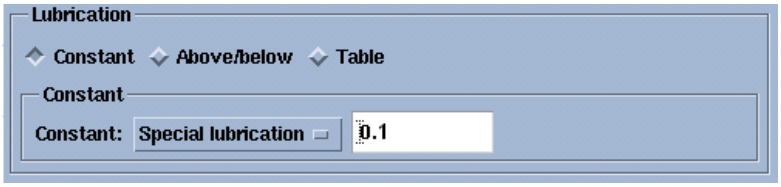

Figure III.D.23 – Lubrication value used on profile 3 forming simulation

III.D.4.9 - Process steps

After many simulations it was achieved the best force between binder and die.

The figure III.D.24 shows the parameters for single action press and the force used on profile 1 stamping (F = 5.2e+05).

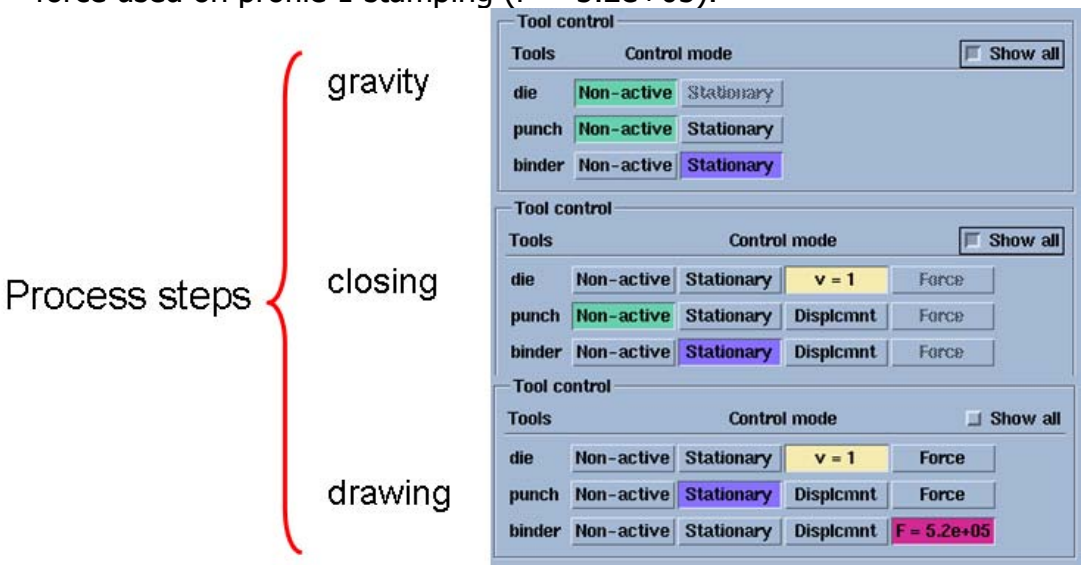

Figure III.D.24 – Process steps description

III.D.4.10 - Table of input parameters

In table III.D.2 are the parameters that where used to achieve the best final results.

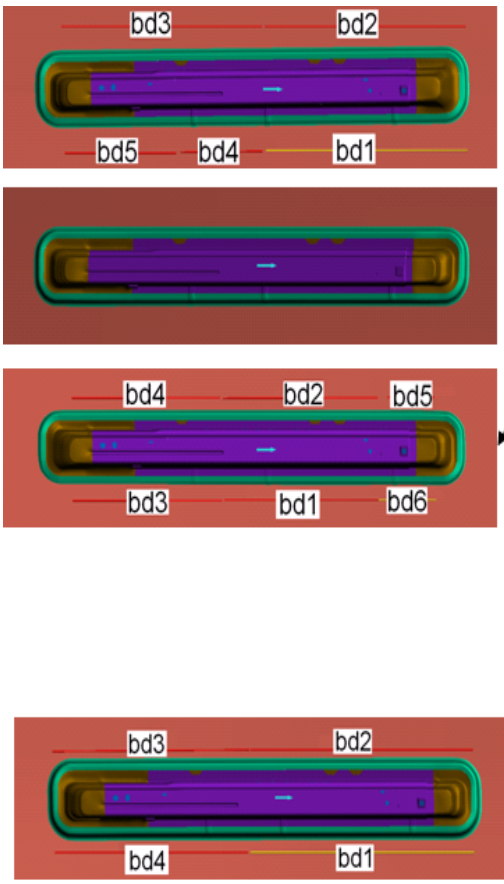

	Blank	Drawbeads	Lubrification	Force	# of simulations
		db1=0,550			
Profile1	1,6mm	db2=0,600	0,05	F=5,2e+05	200
		db3=0,660			
		db4=0,400			
		db5=0,350			
Profile2	1,6mm		0,05	F=1,0e+02	53
		db1=0,550			
Profile3	1,6mm	db2=0,500	0,1	F=2,0e+0,6	176
		db3=0,450			
		db4=0,450			
		db5=0,550			
		db6=0,550			
		db1=0,525			
Profile4	1,6mm	db2=0,600	0,05	F=5,0e+05	25
		db3=0,575			
		db4=0,350			
		db1=0,550			
Profile5	1,6mm	db2=0,600	0,05	F=7,0e+05	42
		db3=0,625			
		db4=0,350			
		db1=0,575			
Profile6	1,6mm	db2=0,550	0,05	F=5,0e+05	27
		db3=0,575			
		db4=0,400			
		db1=0,600			
Profile7	1,6mm	db2=0600	0,05	F=5,0e+05	11
		db3=0,575			
		db4=0,400			
		db1=0,550			
Profile8	1,6mm	db2=0,550	0,05	F=5,0e+0,5	19
		db3=0,450			
		db4=0,550			
		db1=0,600			
Profile9	1,6mm	db2=0,600	0,05	F=7,0e+05	67
		db3=0,500			
		db4=0,600			
		db1=0,600			
Profile10	1,6mm	db2=0,600	0,05	F=1,8e+05	46
		db3=0,675			
		db4=0,250			
		db1=0,600			
Profile11	1,6mm	db2=0,600	0,05	F=7,0e+04	5
		db3=0,600			
		db4=0,350			

Table III.D.2 – Results of Input parameters

III.D.5 - Output Results

III.D.5.1 - FLD results

The first step to analyse the formability is overview the forming limit diagrams given by the stamping simulation of the profiles, if the points are down the black curve means that the profile can be stamped without rupture. Analysing figure III.D.25 can be concluded that in profile 2 appeared some rupture zones.

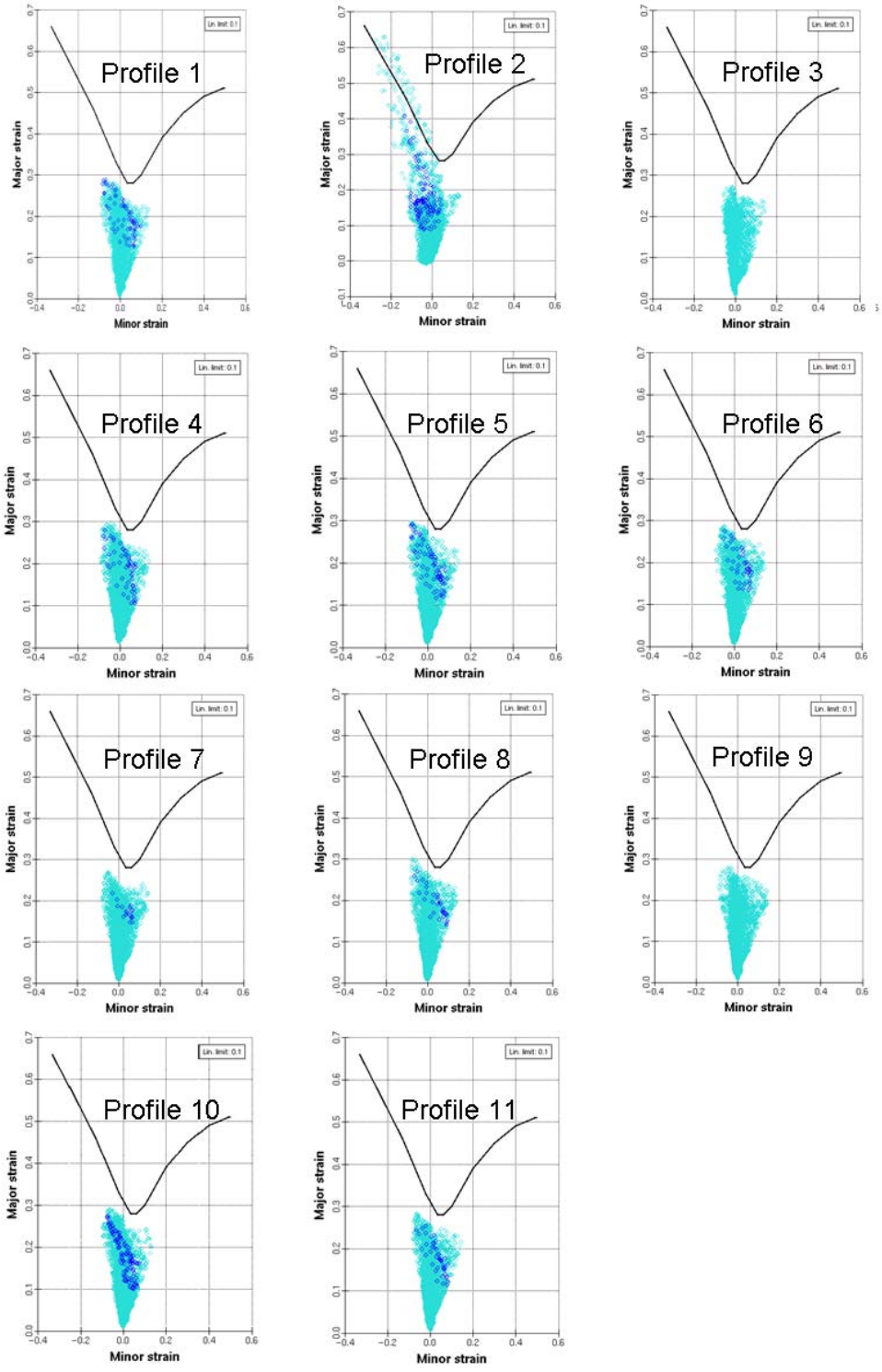

Figure III.D.25 – Forming Limit Diagrams

It was needed to restudy all the input parameters, to assure that wasn't any error made by the operator to attribute the impossibility of safe stamping to the workpiece geometry.

The profile 2 is impossible to stamp without cracks, the backdraft diagram is in the safety limits and was applied very low force between binder

and die(figure III.D.26), it is of mentioning that weren't applied any drawbeads, was used special lubrication and the geometry of the tools was similar in all cases.

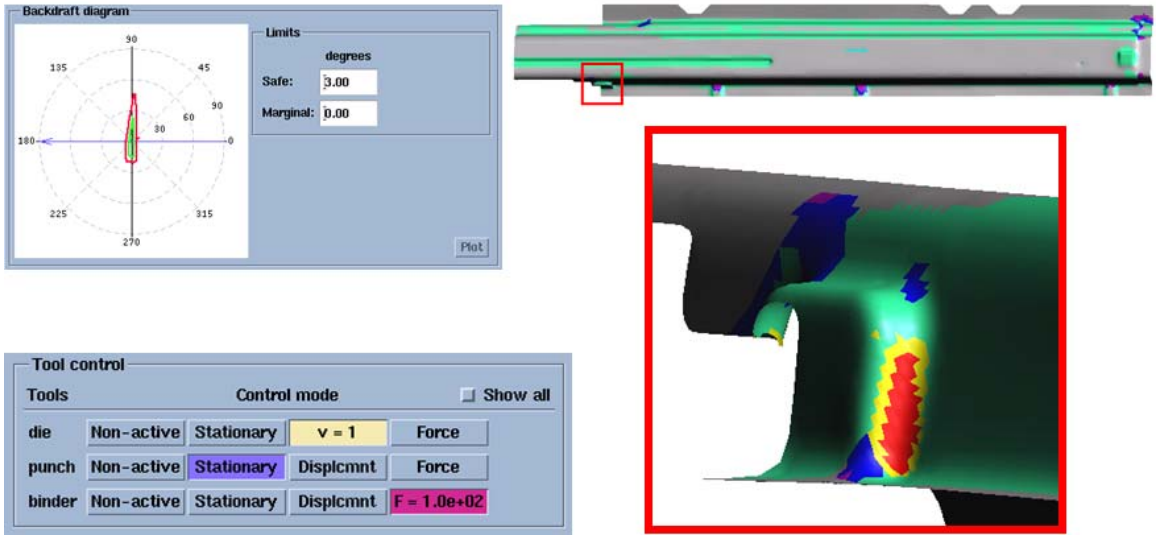

Figure III.D.26 – Forming simulation results of profile 2

III.D.5.2 - Springback results

For a best exposure of the results, it was decided to choose the same section as before (Figure III.D.27).
The objective of this choice was the improvement of precision on springback study. As it can be seen on figure III.D.28 – III.D.38 utilizing the 'dynamic section' option, it can be easily analysed the differences between the original and the final part.

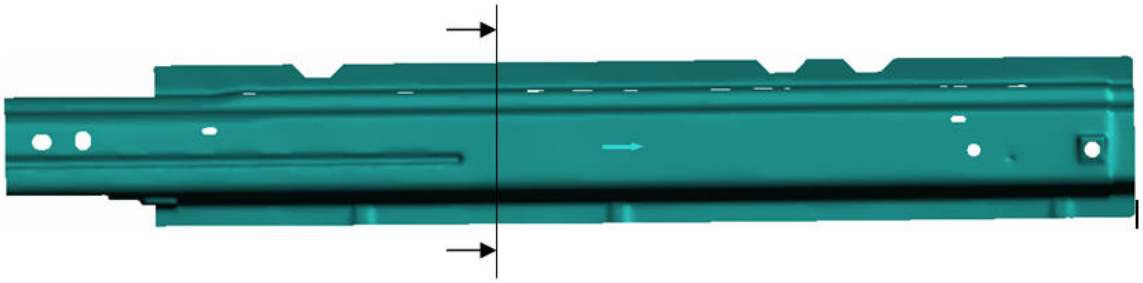

Figure III.D.27 – Chosen section for springback study

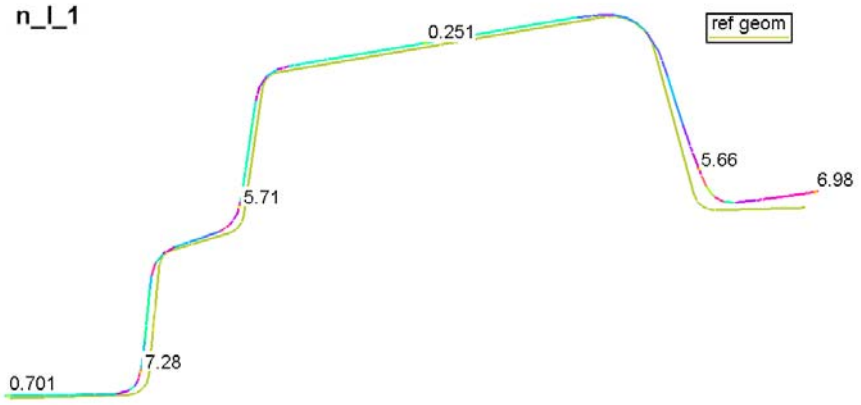

Figure III.D.28 – Profile 1's angle change

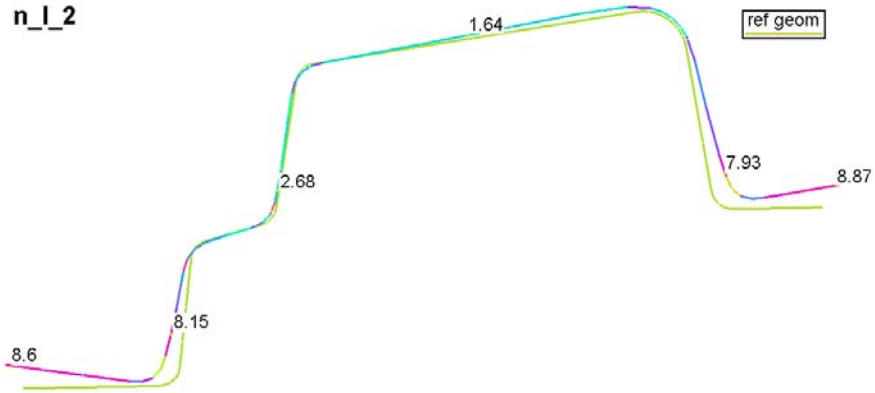

Figure III.D.29 – Profile 2's angle change

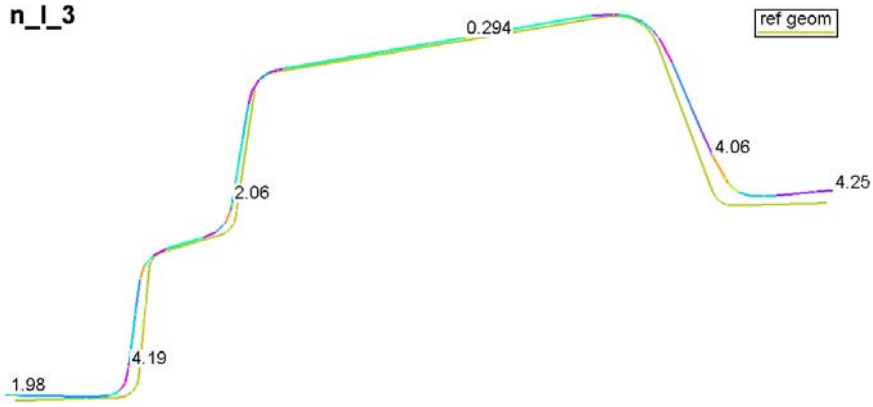

Figure III.D.30 – Profile 31's angle change

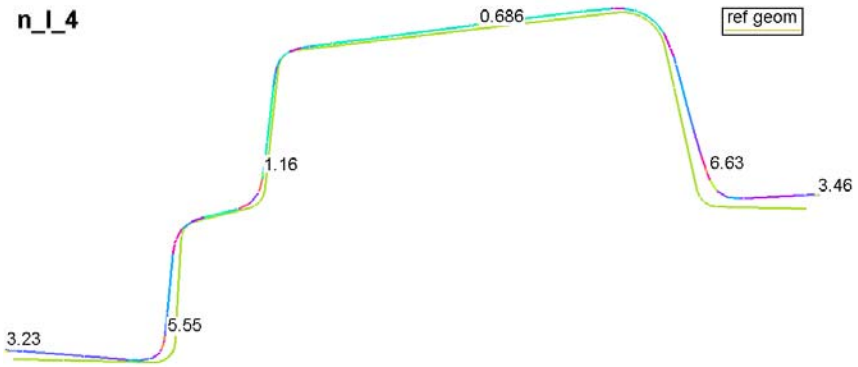

Figure III.D.31 – Profile 4's angle change

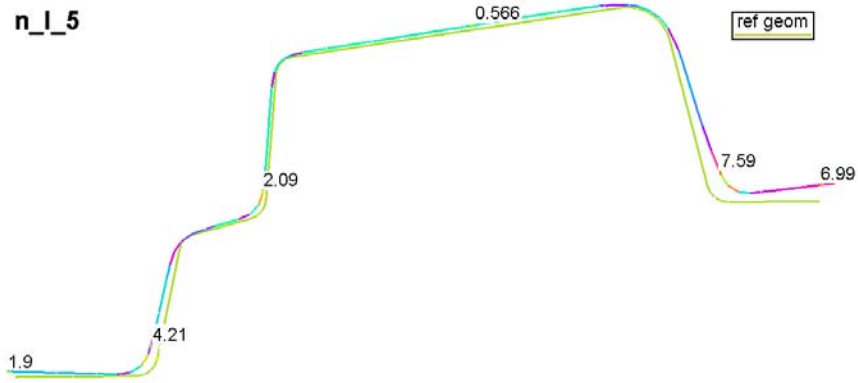

Figure III.D.32 – Profile 5's angle change

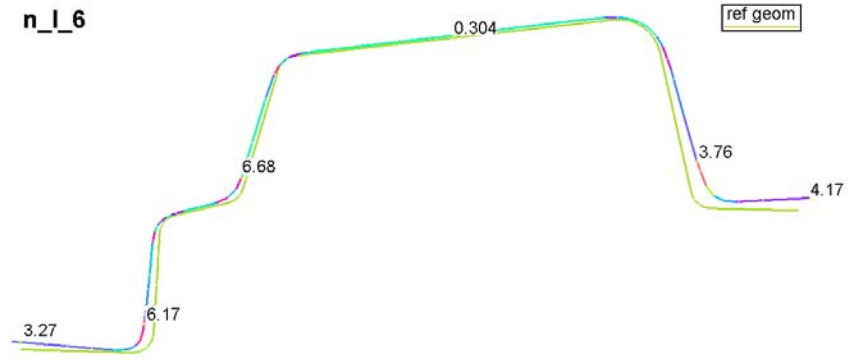

Figure III.D.33 – Profile 6's angle change

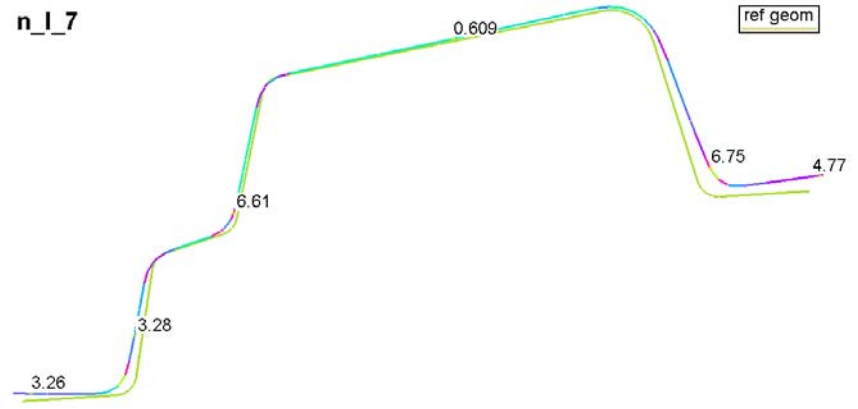

Figure III.D.34 – Profile 7's angle change

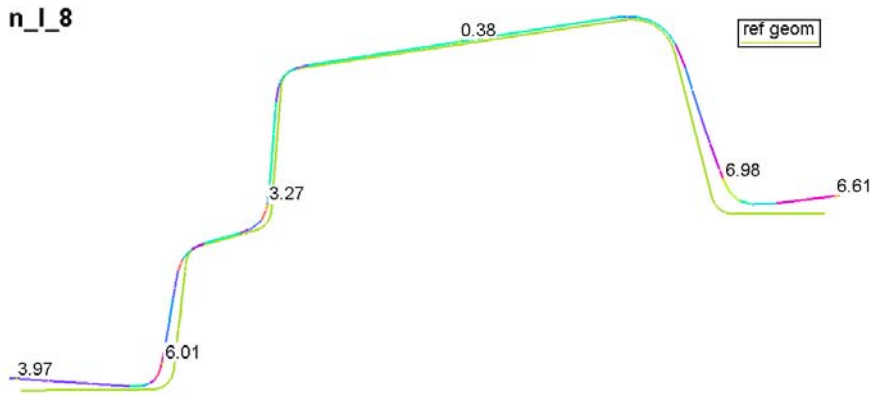

Figure III.D.35 – Profile 8's angle change

Figure III.D.36 – Profile 9's angle change

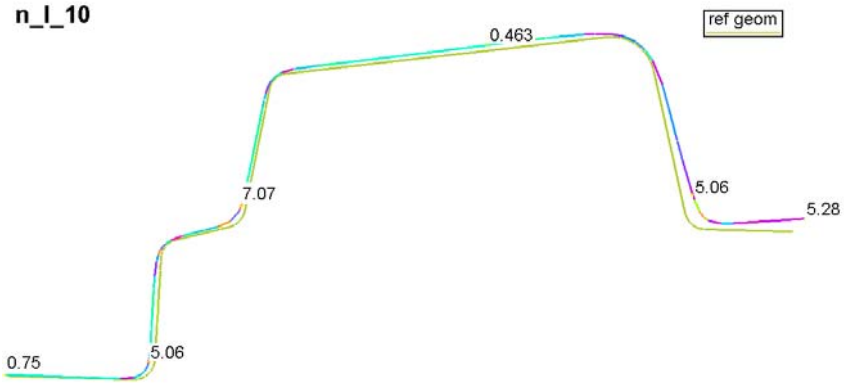

Figure III.D.37 – Profile 10's angle change

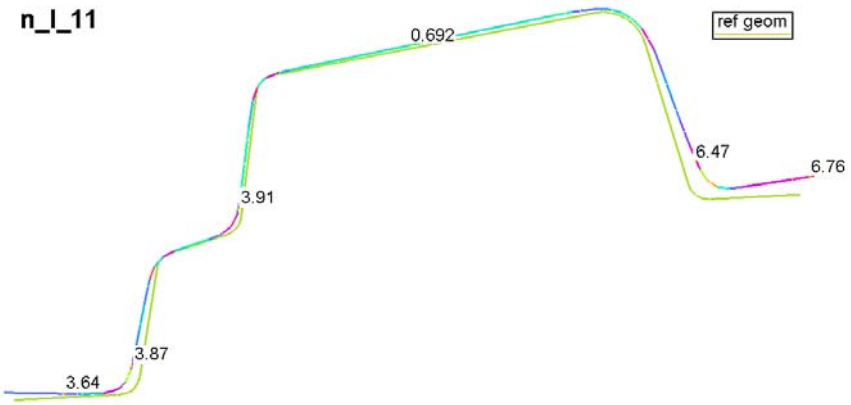

Figure III.D.38 – Profile 11's angle change

III.D.6 - Analysis of the results

III.D.6.1 - Best profile

To choose the profile with better conditions to be applied in real case was considered:

- proposed limits (table III.D.1)
- results of input parameters (table III.D.2)
- forming simulation results (table III.D.3)
    - Angular springback 'A' and 'B' – (Figure III.D.39)

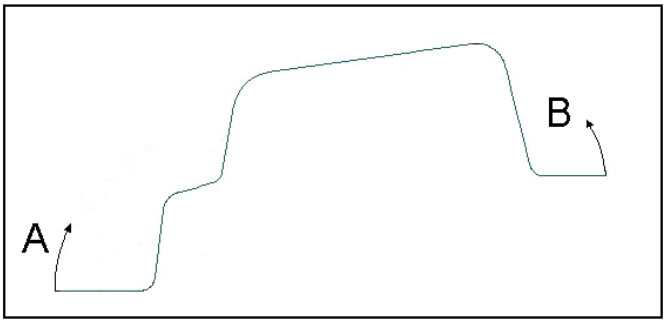

Figure III.D.39 - Angles in study

	Thinning	Wrinkling criterion	Springback[°]	A+B
Profile 1	M=-0,001 m=-0,273	M=0,013 m=0,000	A=0,70 B=6,98	7,68
Profile 2	M=-0,086 m=-0,325	M=0,200 m=0,000	A=8,60 B=8,87	17,47
Profile 3	M=-0,010 m=-0,289	M=0,004 m=0,000	A=1,98 B=4,25	6,23
Profile 4	M=-0,008 m=-0,272	M=0,010 m=0,000	A=3,23 B=3,46	6,69
Profile 5	M=-0,006 m=-0,281	M=0,012 m=0,000	A=1,90 B=6,99	8,89
Profile 6	M=-0,004 m=-0,283	M=0,010 m=0,000	A=3,27 B=4,17	7,44
Profile 7	M=-0,005 m=-0,280	M=0,009 m=0,000	A=3,26 B=4,77	8,03
Profile 8	M=0,004 m=-0,281	M=0,010 m=0,000	A=3,97 B=6,61	10,51
Profile 9	M=-0,009 m=-0,280	M=0,005 m=0,000	A=3,22 B=5,35	8,57
Profile 10	M=-0,003 m=-0,276	M=0,013 m=0,000	A=0,75 B=5,28	6,03
Profile 11	M=-0,007 m=-0,279	M=0,008 m=0,000	A=3,64 B=6,76	10,04

Table III.D.3 - Forming simulation results

- Profile 2 is impossible to stamp without splits
- Profile 4, 6 and 10 don't have safety limits for balance
- The profile with better geometry to be stamped is the profile 3

Lubrication is 0.1 and not 0.05 like the other profiles
Higher force between binder and die (2.0e+06) without splits
The thinning is less than 30% (value accepted in FLC)
Has the best wrinkling criterion
Angular springback was under 5º (good for assembly)
A=1.98º
B=4.25º
A+B=6.23º (the best obtained result)
Balance limit inside of safety limits

III.D.6.2 - Confirmation of the results

The safety limit of the FLC (Figure III.D.40) was decreased for formability's visual overview, until one profile start to be totally green.

As it can be seen in figure 6.41 the profile 3 is first one arriving totally green (100% in safe area).

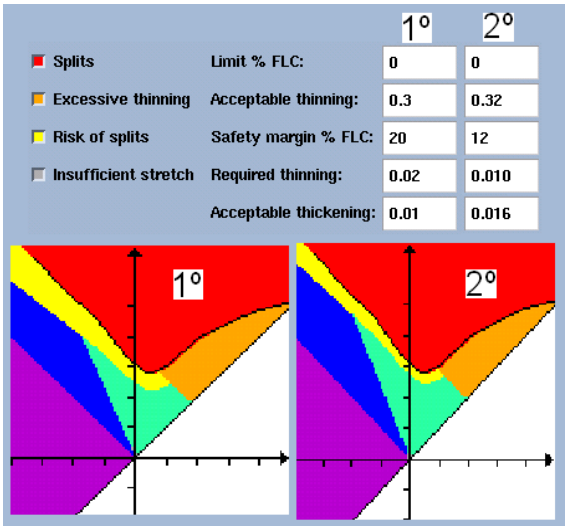

Figure III.D.40 - Changed FLC parameters

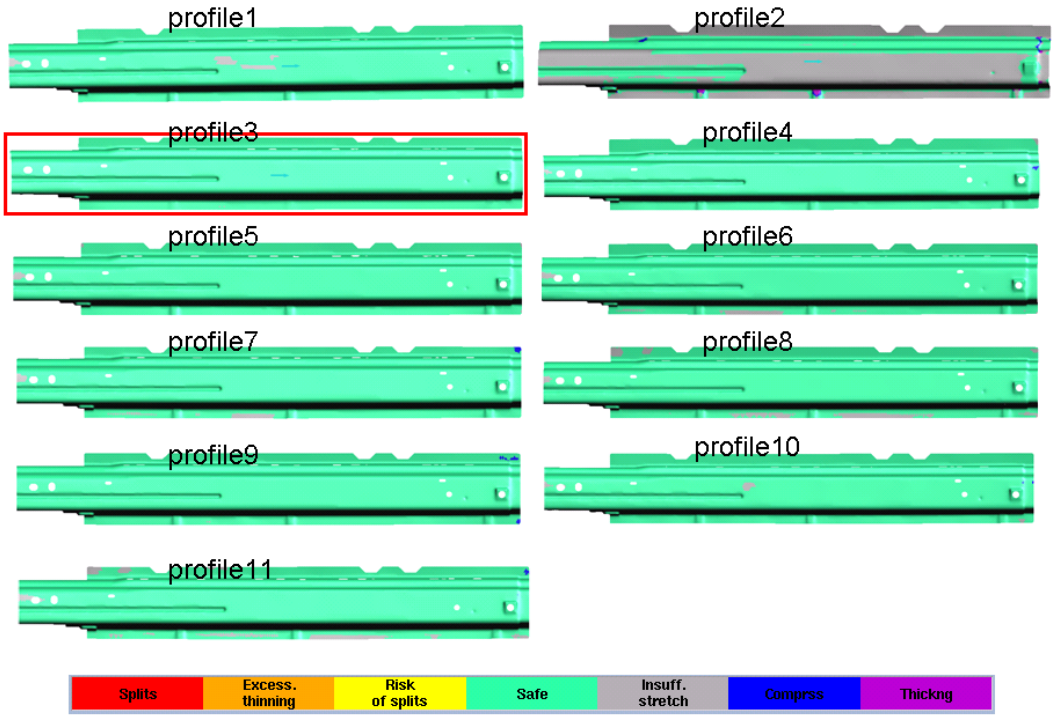

Figure III.D.41 – Formability's result for the FLC change

III.D.7 - Optimization

Found the profile with the best characteristics to stamp and the better forming simulation results, was proposed to concentrate the study on the profile 3 and try to get even better results for springback.

It was concluded along of this the work that the results of springback are related to the formability results.

The aim of this paragraph is to minimize the springback for the profile

The control parameter for discussion is the angle change, trying to find the minimal springback that could be found in the chosen section .

The objective of this related study is to stamp the workpiece closer to the rupture, forgetting the security limits, this consideration was made because the limits in the real case were imposed by the protrusions, so this study is to show that if the geometry of this protrusions could be changed without disadvantages to the real use, the springback would have for sure minor values.

Using formability background option on FLD results was found the optimal force between binder and die.

The methodology used in this case, was change only the force between binder and die, starting increase force value from 2.0e+06 until 2.6e+06, here was found rupture (Figure III.D.42) where appeared a mesh touching the formability curve.

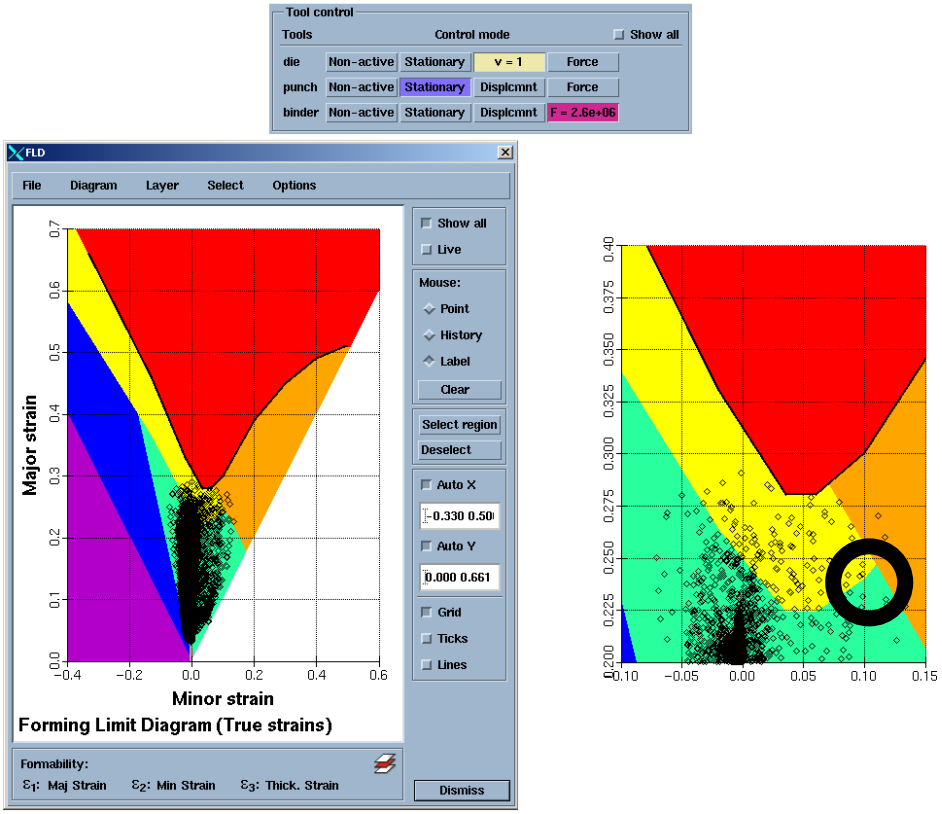

Figure III.D.42 – FLD zoom for F = 2.6e+06

It was found the best result for a force=2.5e+06, where all the meshes are down the FLC curve (Figure III.D.43).

It was concluded that the Springback (A+B=1.38+1.53) could be theoretical reduced to 2.91° without cracking of the workpiece (Figure III.D.44).

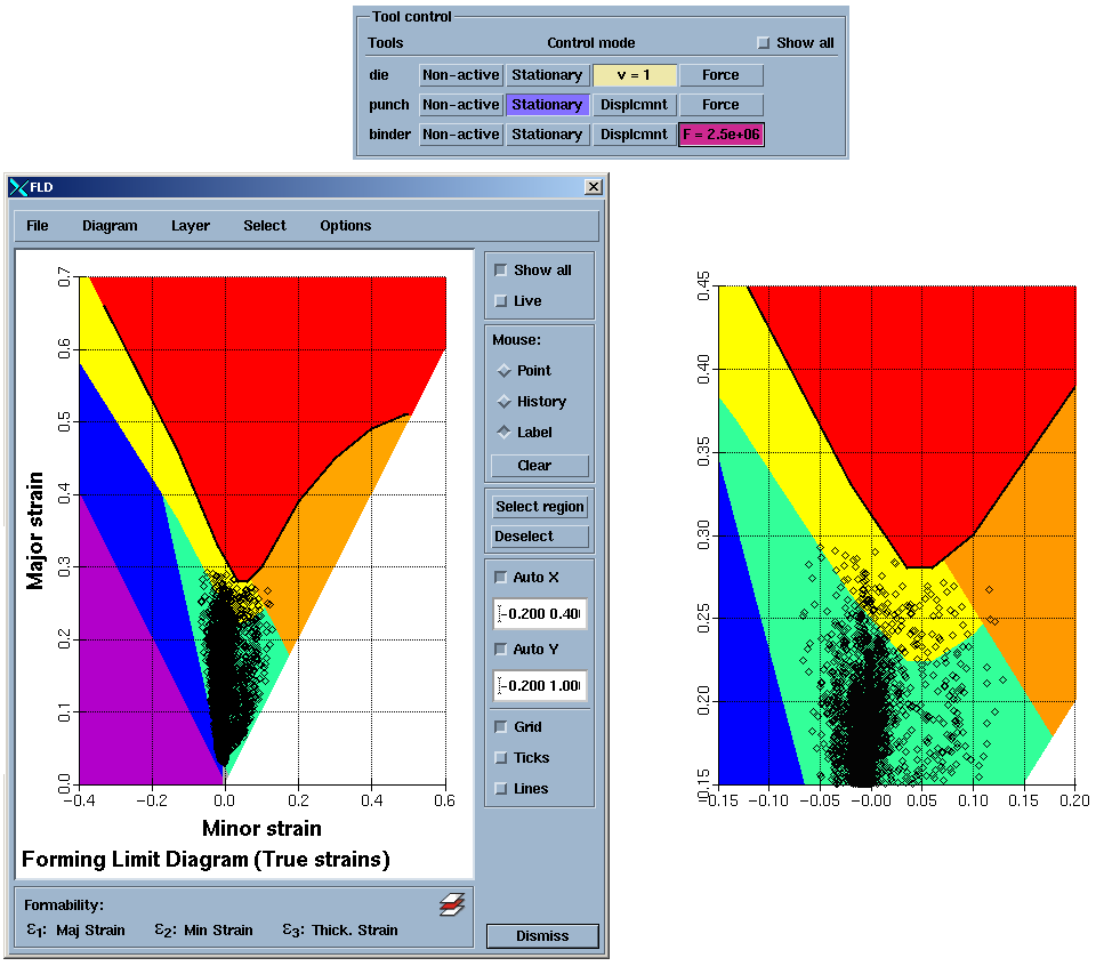

Figure III.D.43 – FLD zoom for F = 2.5e+06

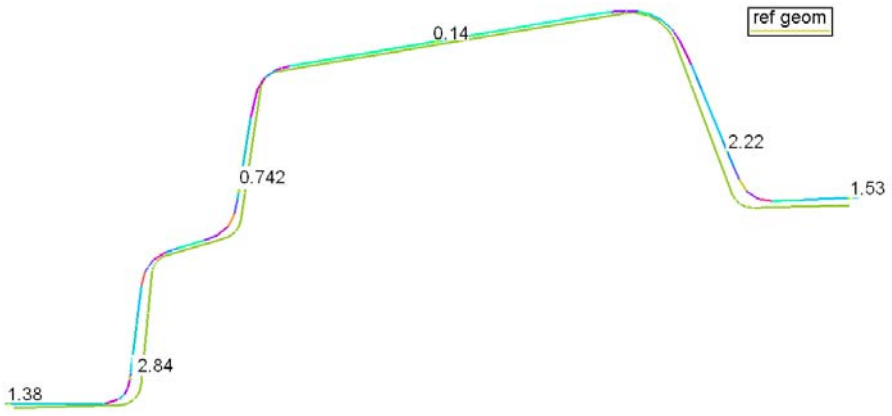

Figure III.D.44 – Optimized profile angular springback

***III.D*.8. Conclusiones**

Generales conclusiones

The application of new AHSS on car industry increases a passive safety and a static and dynamic rigidity. It also decreases the vehicle costs, structure-borne noise and interior sounds. We also have a decrease in weight, which leads to a minor consume of fuel and metal. This is not only important to the manufacture but also to the client, who will eventually buy the product. If the vehicle costs will be cheaper, then we will see an increase of sales and most important the buyer will not only save in the car but also in long term because the vehicle will also consume less fuel.

AutoForm is a powerful tool in stamping industry by reducing time to market the product. It helps to design the tools, to know the tools mechanical parameters. Reduces the trial and error steps and also has a rapid prototyping that exports CAD files, permitting quick crash and assembly tests.

AutoForm can also improve the dimensional precision by predicting the final part's shape and geometry, helps to know where are the critical points of the product and allows a springback analyses.

Springback results are very dependent of the material's formability, workpiece's geometry, press type, tool's geometry and process. Inside the tool's geometry we have the boundary geometry, binder geometry and also the addendum geometry. Inside the tool's process, firstly we have drawbeads, then blank geometry, then lubrication and last force applied between tools.

Técnicas conclusiones

1 – A uniform drawing depth offers better probabilities of success in the forming process.

2 - A more accented addendum leads to a bigger stretching of the material.

3 – Steps in certain zones of the addendum favour the local stretching of those areas.

4 – The boundary fill may be very important to the stamping process by providing a smoother connection between the part and the addendum.

5 – The higher is the force factor of the drawbeads, the more stretched will be the component in the areas influenced by their presence.

6 - In general the simulation is highly sensitive in the critical bending regions.

7 – The bigger the force factor between the die and blankholder to press the blank is, more stretched is the component.

8 – Unlevelled geometries and the existence of steps difficults the forming process.

9 – An incorrect choice of the drawing direction may disable the stamping process.

10 – The increase of stretching decreases the tendency to wrinkle.

11 – The points where the thickness values are minimum correspond to the areas where the thinning is maximum.

12 – An intense springback in the extremities of the component tend to cause the opposite phenomenon (spring-in) in the centre of the part.

FEM analysis of advanced high strength steel car body drawing process

S. Al Azraq[a], R. Teti[a], S. Ardolino[b], G. Monacelli[b]

[a] *Dept. of Materials and Production Engineering, University of Naples Federico II, Italy*
[b] *Elasis SCpA, Pomigliano d'Arco, Italy*

Abstract

Advanced High Strength Steels (AHSS) have been intensively applied to automobile components to improve crashworthiness, without increasing the body weight, under a strong pressure of the requirements for fuel consumption, durability and energy absorption. Some of the problems encountered in the forming of AHSS, due to lack of knowledge about the material behaviour, are presented and described with the purpose of showing the necessity of sheet metal simulation to save cost and time by replacing physical tryouts with virtual tryouts. The codes and elements normally used in these types of simulation programs, as well as their common approaches, are presented and evaluated. Finally, a test case of an automobile component (hood structure) was analysed using the incremental approach of the AutoForm FEM code.

1. Introduction

Automobiles play an important role in our life. This makes it necessary to incessantly try to reduce their production cost in line with the innovation of production technology. At the same time, measures are being taken toward the reduction of fuel cost and the improvement of safety so that eagerly-pursued harmony with the social and natural environment can be established. It is safe to say that thin steel sheets for automobiles have made progress in responding to the market needs. In recent years, it has become one of the most important tasks for automobiles to make the reduction in weight of auto bodies compatible with the improvement of crashworthiness, particularly with the aim of reducing CO_2 gas emissions by improving fuel consumption [1]. To satisfy these demands, a new steel grade, the Advance High Strength Steel (AHSS), has been developed, pushing the boundaries of what was previously possible with conventional steel grades.

A major negative consequence of using these new materials is the absence of knowledge about their behaviour during both the drawing process and future physical applications. Engineers turned to forming simulations in order to closely investigate and try to minimize this problem. The aim of industrial application of the simulation for drawing processes is to replace the physical tryout by the computer tryout, with the intention of time/cost reduction and quality improvement in the die design/manufacturing cycle [2].

In the past, a number of analyzing methods have been developed and applied to various forming processes. Some of these methods are the slab method, the slip-line field method, the viscoplasticity method, upper and lower bound techniques and Hills general method. These methods have been useful in qualitatively predicting forming loads, overall geometry changes of the deformed blank and material flow, and approximate optimum process conditions.

However, a more accurate determination of the effects of various process parameters in the drawing process has become possible only recently, when the finite element method (FEM) was developed for these analyses [3]. The FEM codes for sheet metal forming may be classified accordingly to their type of integration: implicit or explicit. Their main solution procedures are the dynamic explicit and the static implicit ones. The principal analysis methods used in

sheet metal forming simulation are based on shell, membrane and continuum elements.

2. Metal sheet drawing processes in the car industry

Depending on the component's complexity and quality required, the drawing process may be performed using diverse methods. The most common are: single action, double action and crash forming.

Single Action Process: this process is widely used, especially when surface quality is not a priority requirement. This procedure is based in a single slide (ram) movement: the punch is stationary, the die moves down in its direction pressing the metal sheet against the blankholder, and then deforms the blank with the punch. Cycle time is reduced by approximately 25% in comparison with the double action process.

Double action: This process is usually used to form components with large drawing widths needing large forming efforts, or uniquely because good surface quality is an important requirement. In this process type, two distinct and successive actions are performed: the blank's blocking and its posterior deformation. The first step is performed through the blankholder descending movement, pressing the blank against the die with a previously defined force factor; the second step is characterised by punch movement towards the die, deforming the blank.

Crash Forming: This drawing process type presents as principal characteristic the fact that it does not have the intervention of the binder [4]. This process may be divided into three main steps.

- descending movement of the blank towards the die;
- first deformation suffered by the blank when crashing against the die;
- the punch moves towards the blank, deforming it against the die.

3. Material requirements for sheet metal drawing

The steel industry has recently produced a number of Advanced High Strength Steels (AHSS) that are highly formable, yet possess an excellent combination of strength, durability, strain rate sensitivity and strain hardening. These characteristics may enable automotive designers to achieve both weight reduction and improved crash safety [5]. The main AHSS used in automotive industry are the Dual-Phase (DP) and the Transformation-Induced Plasticity (TRIP) steels.

3.1. Safety requirements

Many of the structural parts of a vehicle are used to protect passengers in case of crash and are expected to be strengthened most urgently in line with the intensifying safety regulations. The materials used in this kind of components should have as principal characteristic an excellent energy-absorbing capacity, as the one evidenced by AHSS.

The two key features that contribute to this high energy-absorbing property are the high work hardening (WH) rate and large bake hardening (BH) effect.

The relatively high WH rate, exhibited by AHSS steels, leads to a higher ultimate tensile strength than the one exhibited by conventional HSS of similar yield strength. This provides for a larger area under the stress-strain curve, indicating greater energy absorption when deformed in a crash event to the same degree as conventional steels. The high WH rate also allows for a better strain distribution during crash deformation, providing more stable and predictable axial crush that is crucial for maximizing energy absorption during a front or rear crash event [6].

The relatively large BH effect also increases the energy absorption of DP and TRIP steels by further increasing the area under the stress-strain curve. Conventional HSS do not exhibit a strong BH effect and do not benefit from this strengthening mechanism.

3.2. Durability requirements

An automobile component durability depends on two main factors: corrosion and fatigue resistance.

3.2.1. Corrosion

Vehicle corrosion depends on environmental causes like:

- exposure of lower body panels and under-vehicle components to road slush containing de-icing chemicals [7];
- air pollution in industrial centres, particularly where levels of sulphur dioxide [8] and chloride are high;
- dust control procedures [9] on rural roads (especially in summer);
- year-round exposure to salt-laden spray, mist, and other airborne chemicals in combination with high humidity (in coastal regions).

Most of the steels used in automotive industries, including AHSS, present good properties regarding to corrosion resistance.

3.2.2. Fatigue

Fatigue in a structural component involves complex relationships among several factors including geometry, thickness, applied loads and material endurance limit [10]. The fatigue strength of AHSS steels is higher than the one of precipitation-hardened steels or fully bainitic steels with similar yield strength for many metallurgical reasons. For example, in DP steels the dispersed fine martensite particles retard the propagation of fatigue cracks, and in TRIP steels, the transformation of retained austenite can relax the stress field and introduce a compressive stress that can also improve fatigue strength. Figure 1 represents the superior resistance to fatigue of the AHSS in comparison with conventional steels.

3.3. Environmental requirements

The most important environmental requirements to automotive industry materials are low-weight and recycling capability. However, these requirements may influence durability and safety aspects, which are extremely important as well. The automotive engineers must find the better way to balance all these requirements to obtain the best commitment solution, building a safe and durable "green" vehicle. Currently, AHSS are thought to be the best solution, since they are more resistant than conventional HSS, allowing thinner parts with equivalent or superior durability and strength, making the final product lighter, without damaging safety or environmental parameters.

3.4. AHSS disadvantages

Despite all the above advantages, AHSS present some critical drawbacks, such as:

- forming difficulties, as they present accentuated deviation shape problems (deriving from springback), making difficult the following utilisation or assembly;
- the lack of knowledge about AHSS behaviour after forming may decrease some of the part characteristics (e.g. energy absorption);
- the deterioration of press forming accuracy, due to the sheet metal high strength.

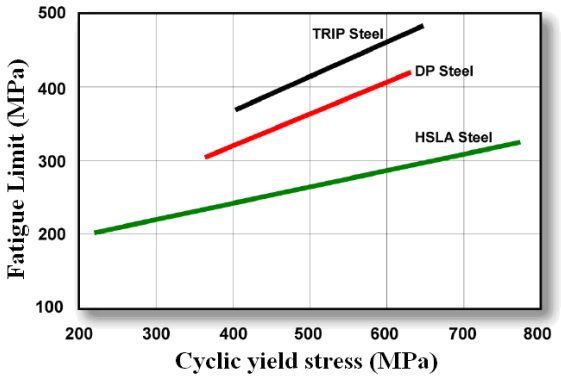

Fig. 1. AHSS fatigue limit compared to traditional steels [1].

4. FEM analysis of sheet metal drawing processes

4.1. Finite element methods (FEM)

Most analysis software employs the finite element method (FEM) where the geometry of the component to be deformed is divided or "discretised" into simplified regular shapes called "elements". There is a large range of elements available of varying complexity (or degrees of freedom) that can model different modes of deformation (and temperature fields, electromagnetic fields, etc.) [11].

4.1.1. FEM codes

The FEM codes for sheet metal drawing may be classified according to their type of integration (explicit or implicit) [12]. Explicit methods solve for equilibrium at time t by direct time integration. The explicit procedure is conditionally stable since iterative procedures are not implemented to reach equilibrium and also Δt is limited by natural time. Implicit codes solve for equilibrium at every time step $(t + \Delta t)$. Depending on the procedure chosen, each iteration requires the formation and solution of the linear system of equations.

The two main solution procedures for the simulation of drawing processes are the dynamic explicit and the static implicit procedures.

The dynamic explicit method is frequently used in simulations of drawing processes since it reduces the computational time drastically, using a diagonal mass matrix system to solve the equations of motion. For this method, the computational time depends linearly on the number of degrees of freedom (d.o.f.). However, the drawbacks of the explicit method are that small

time steps are needed and that equilibrium after each time step cannot be checked, which can result in wrong stress distributions and unrealistic product shapes. Another drawback is that springback calculations are very time consuming.

The advantage of a static implicit method is that equilibrium is checked after each time step and thus leads to more accurate results. The main drawback of this method, however, is that the computation time depends quadratically on the number of d.o.f. if a direct solver is used. Another drawback is that the stiffness matrix is often ill conditioned, which can make the method unstable and deteriorates the performance of the iterative solvers [2].

In sum, explicit codes are favoured for solving large problems although implicit codes yield more accurate results. To intensify the use of implicit codes for solving large problems, the computation time of these codes has to be decreased drastically.

4.1.2. FEM approaches (one-step vs. incremental)

The FEM numerical computation typology for drawing processes depends on the desired analysis. Nowadays sheet metal drawing processes are simulated according to one of the following approaches.

One-step method (inverse analysis)

The inverse simulation code provides for the preliminary feasibility analysis in the product (component projection) and process (preliminary drawing study phase) input phases. This method is characterized by some simplifying assumptions such as accepting a linear behaviour of deformation, ignoring contact and friction problems, etc. Using these assumptions it is possible to evaluate the drawing feasibility of the part, starting from the final deformed metal sheet configuration till the initial plane blank, in very short time, with only one step. One-Step simulation codes provide first evaluation results very rapidly (e.g. 1-5 CPU minutes for a door structure).

Incremental Method

In Incremental simulation all the process components must be taken into account: the kinematic characteristics, the blankholder and punch forces and velocities, and drawbeads force factor. This method allows for the maximum accuracy during the simulation process, but requires high hardware resources and calculation time. These codes are used to simulate the complete drawing process, providing accurate results in medium-brief time (e.g. 30-60 CPU minutes for a longeron). In order to reduce computing time, larger and (more) complex components such as body side panels should be simulated approximately, through a coarser discretisation.

The first approach is faster and consists of performing the simulation in one step only. This type of simulation only allows for the determination of the sheet final condition, while with the incremental method it is possible to know the results of intermediate steps.

4.1.3. Elements in sheet metal drawing simulation

FEM Analysis of sheet metal drawing process usually adopts one of three methods based on the membrane, shell and continuum element [13].

Membrane elements possess computational efficiency and better convergence in contact analysis than the shell or continuum elements. However, this method does not consider bending effect and has to tolerate inaccuracy in bending dominant problems.

Shell elements can capture the combination of stretching and bending as opposed to membrane elements. Use of shell elements gives more degrees of freedom to capture accurate stress distribution, including in-plane and out-of-plane deformation. The disadvantage is the notable amount of computational time and computer space for its 3D calculations with integration in the thickness direction [13].

Continuum elements are used where fully 3D theory is needed to describe the deformation process. They can handle through-thickness compressive straining whereas shell elements cannot. Its main drawback is that more elements are needed to describe the shell-type structures, so that a large system of equations must be solved [14].

4.2. AutoForm FEM code

AutoForm is an algorithm for the efficient resolution of typical automotive industry complex drawing problems.

AutoForm Incremental is the AutoForm module to simulate sheet metal forming processes (conventional drawing, hydromechanical drawing) using FEM in many small steps. It uses a highly specialized FEM quasi-static implicit code, characterized by an incremental solution procedure [15]. The AutoForm-Incremental module is the simulation approach used to perform the test case of the following section.

Using AutoForm-Incremental, it is possible to simulate all forming operations beginning with the plane blank sheet and ending with the finished car body part, including springback calculation.

AutoForm calculates the stress-strain conditions in the blank thickness, subdividing it in an unpaired number of layers, so that symmetry respect to a middle layer exists. The larger the number of layers, the more precise the analysis, but the calculation time is longer.

The stresses in the metal sheet thickness are calculated during the forming phase, using convenient elasto-plastic models. This implemented elasto-plastic model intervenes on each solution increment, each iteration, each element and in every layer.

Since AutoForm is specific for sheet metal forming, the mesh and remeshing generation are automatic. The contacts and elements are formulated as a function of the typical conditions of the process, using, in order to simulate the required drawing process, two types of elements:

- Full Shell Elements
- Bending-enhanced membrane elements

Oppositely to full shell elements, bending-enhanced membrane elements do not react to bending: the deformations are imposed by tool geometry and movement. To calculate the stress-deformation condition a convenient correction algorithm is implemented. Thanks to this mixed formulation, trustable results are obtained with acceptable computing time.

4.2.1. AutoForm process steps

AutoForm simulation process requires the definition of several tools and operations, and this input data is requested in the following order:

Import Part Geometry - When importing the part geometry, AutoForm automatically meshes the tool surfaces; all next operations are based on this mesh.

Prepare - The imported part geometry needs to be prepared to serve as a reference for the tool/die design.

Fillet - The control over sharp edges in the model and curvature radius modifications to obtain a feasible drawing geometry is possible in Fillet menu.

Part's Balance (Tip) - Part's balance is useful to eliminate undercut areas by making the local coordinate system turn around any cartesian axis in a convenient mode.

Filling Holes - Filling holes reduces simulation time; at the end of the drawing process these holes are re-opened with cutting operations.

External Contour (Boundary) - From the definition of external part (re)delimitation, the software provides a better adaptation to drawing simulation process.

Blankholder (Binder) - Binder definition is an extremely important phase of the process, because it largely affects simulation results. Binder automatic generation normally is not sufficiently optimized. However, it can be improved manually by the addition of convenient profiles. The binder surface can also be imported from CAD.

Addenda - It is possible to integrate the component to be simulated through the addition of outer forms to improve material flow's flux.

Generate simulation input - Once the geometry generator phase is complete the computing and process data input starts. The first decisions to make in the drawing process are: the simulation type (one-step or incremental) and the drawing type (single action, double action or crash forming (without binder)).

Definition of forming tools - In this section the operative parameters that will define the forming process are input. The initial position of the diverse tools and their movements (distance and working direction) are defined. The existing tools are configured individually.

Metal Sheet Configuration and Material Selection - All input data regarding sheet metal configuration and properties must be defined: shape, dimensions, positioning, material and thickness. The material properties are imported in a *material.mat* file. Besides the principal material characteristics such as Young modulus, Poisson modulus, specific weight, and yield and rupture strength, the program also provides:

- the hardening curve (stress-strain curve), where it is possible to observe the hardening effect of the material;
- the yield surface graphic, which divides the principal stress plan in two zones: an internal one corresponding to stress conditions in the elastic field and an external corresponding to stress conditions in the plastic field;
- the Forming Limit Curve (FLC) which divides the principal deformation plan in two zones: the inferior, corresponding to deformation conditions of successfully formed parts; and the superior one, corresponding to deformation conditions that lead the part to rupture;
- normal anisotropy coefficients. The metal deforms preferentially in certain planes, following flowing favourable directions.

Drawbeads - Drawbeads' principal function is to locally intensify the blankholder's effect. They avoid the creation of wrinkles and increase the material stretching (and consequently its thinning).

Lubrication (Lube) - The friction coefficient between sheet and tools can be specified.

Process description - The various operations to be performed, their characteristics and the order in which

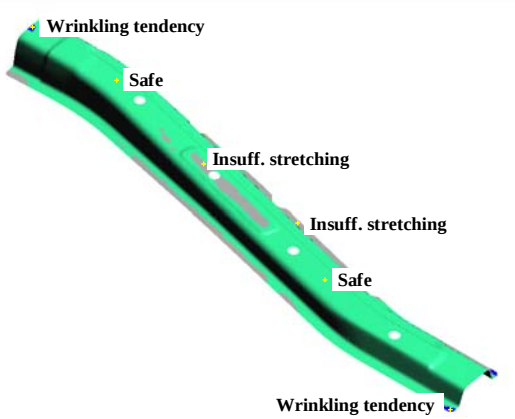

Fig. 2. Formability analysis of a deck lid inner body panel.

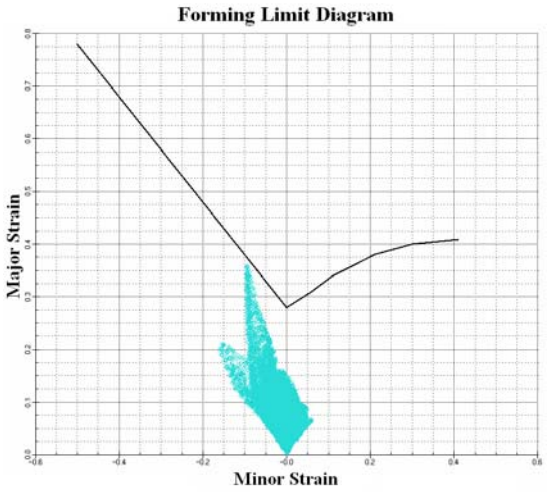

Fig. 3. FLD analysis of a deck lid inner body panel.

they are executed during simulation are defined. Gravity, Closing and Drawing are the fundamental processes performed in a forming simulation. Then, several other process steps may be added: cutting operations, annealing, springback, sheet repositioning and secondary forming operations (restrike, flanging, hemming).

The force factor between binder and die while pressing the blank affects the material flow during drawing/stretching processes. This value must be sufficient to guarantee the absence of wrinkling, but not too high to allow for the material flow during the drawing operation.

Control Parameters - Some control parameters are specified here, such as:

- the calculation accuracy level, through remeshing definition (recommended: *Fine*);
- the number of layers along sheet thickness (recommended: *Springback 11*);
- the element formulation (recommended: *elastic plastic shell*).

Computational Analysis and Results Evaluation - After inputting all data required, the simulation can now be executed. While all the information is being processed by the computer, the process iterations are presented in an output window.

Colour shaded post values such as formability, thickness, thinning, blankholder's pressure, normal displacement (to evaluate springback) and plastic strain are available for the evaluation of the simulation. The punctual lecture of the diverse result parameters (thickness, thinning, normal displacement, etc.) is also possible when clicking with the right mouse button.

5. Test case with AutoForm Incremental code

An example of a simulation realized in AutoForm for a complex deck lid inner body panel is presented as test case. An incremental simulation was performed, and the process consisted of three operations: forming, trimming and springback. The most important criteria to evaluate the drawing success are the result variables formability, thinning and normal displacement (springback).

Formability

Areas undergoing different stresses are coloured differently on the part (see Fig. 2):

- Cracks (Red): Areas of cracks. These areas are above the FLC of the specified material
- Excessive Thinning (Orange): In these areas, thinning is greater than the acceptable value (default value for steel is 30%)
- Risk of Cracks (Yellow): These areas may crack or split. By default, this area is in between the FLC and 20% below the FLC
- Safe (Green): All areas that have no formability problems
- Insufficient Stretching (Gray): Areas that have not enough strain (default 2%)
- Wrinkling Tendency (Blue): Areas where wrinkles might appear. In these areas, the material has compressive stresses but no compressive strains

- Wrinkles (Purple): Areas where wrinkles can be expected, depending on geometry curvature, thickness and tool contact. The material in these areas has compressive strains and becomes thicker during the forming process.

Another AutoForm option to analyse the formability is the Forming Limit Diagram (FLD), which describes the failure of the sheet metal due to cracks (see Fig. 3). In the FLD the Forming Limit Curve (strain states above those failure/cracks occur) is represented as a black curve. Into this diagram, all finite elements of a simulation with the two main strain results (major and minor) are shown. So, one can judge the robustness of a reforming process also visually in this diagram. In the current example, all strains are

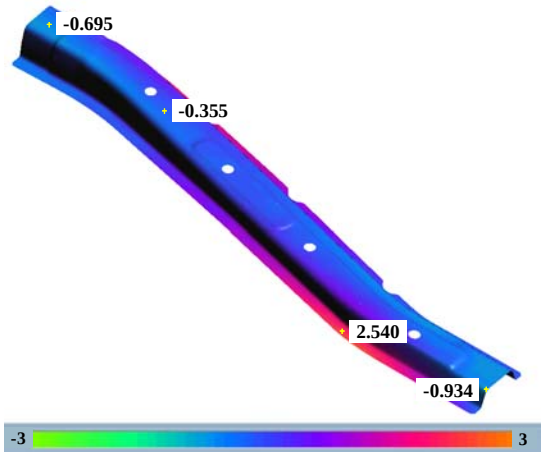

Fig. 5. Springback analysis of a deck lid inner body panel.

situated below the border deformation curve. This indicates that the process is quite safe and robust from a formability standpoint.

Thinning

Another result variable that is often used is the percentage thinning of the material *(Thinning)*, as shown in Fig. 4. A scale is displayed in the lower part of the main window with a range of 30% thinning (-0.3) to 10% thickening (0.1), coloured from yellow to green (depending on the use colour settings). The exact thinning level at any location on the formed sheet may be displayed by clicking at that location on the sheet (in the main display) using the right mouse button.

Normal displacement (springback)

To display the springback results in the main display, switch on Normal Displacement (see Fig. 5). With this option, due to the chromatic scale, it is possible to immediately recognize the areas more subjected to springback. However one can also analyse this phenomena punctually, by measuring quantitatively the value when clicking with the right mouse button.

6. Conclusions

The utilization of advanced simulation technologies (new and more powerful software system) and the AHSS implementation allows for increasing levels of product quality and a more rational employment of the materials. The introduction of this new steel grade (AHSS) in the automotive industry brought several advantages, both at environmental and performance levels, such as:

- improved safety due to the high energy absorption levels displayed by AHSS;
- reduced fuel consumption (as vehicles become lighter), consequently helping to protect the environment;
- increased vehicle durability, especially because of the steel corrosion resistance.

Nowadays, the implementation of an automobile is becoming a process where design and validation cycles are developed predominantly in a virtual environment, making it possible to quickly evaluate numerous design and processing options, in search of the best solution.

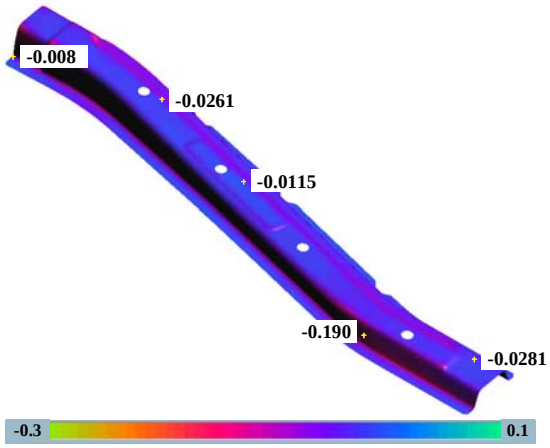

Fig. 4. Thinning analysis of a deck lid inner body panel.

These simulation programs are used to replace

experimental tryouts by virtual tryouts, saving time, money and resources. Another significant advantage of its employment is improving and making the die design process much easier, faster and efficient.

The further developments of the research will include the utilization of a neural network approach to the modeling of the behaviour of the AHSS work material under variable strain rate conditions by reconstructing the stress-strain curves from tensile test experimental data obtained using different strain rate values [16].

Acknowledgements

This research work was carried out with partial support from EC FP6 NoE on Innovative Production Machines and Systems – I*PROMS.

References

[1] Takahashi M. Development of high strength steels for automobiles. Nippon Steel Tech. Rpt. N. 88 July 2003.

[2] Makinouchi A, Teodosiu C and Nakagawa T. Advance in FEM Simulation and its Related Technologies in Sheet Metal Forming. SME – Society of Manufacturing Engineering, 1998.

[3] Boogaard A.H. Van Den, MeindersT., Huetink J. Efficient implicit finite element analysis of sheet forming processes. Int. J. Numer. Meth. Eng., 56, 2003: 1083-1107.

[4] Schenk1 O.and Selig, M. Advancing crash forming analysis capabilities through solver technology, 2nd M.T.I. Conference on Computational fluid and mechanics, June 17-21, 2003, Boston, USA.

[5] American Iron and Steel Institute & Auto/Steel Partnership, Automotive Steel Design Manual, Revision 6.1, August 2002. http://www.steel.org.

[6] International Iron Steel Institute, Advanced High Strength Steel Application Guidelines, March 2005. http://www.worldsteel.org.

[7] American Public Works Association, Vehicle Corrosion Caused by De-icing Salts, Special Report #34, September 1970. http://www.apwa.net.

[8] Baboian, R. Environmental aspects of automotive corrosion control, in Corrosion and Corrosion Control of Aluminum and Steel in Lightweight Automotive Applications, NACE Intern., Houston, TX, 1995.

[9] Dust Control, Road Maintenance Costs, Cut with Calcium Chloride, Public Works, Vol. 121, No. 6, May 1990: 83-84.

[10] Shaw, R., Zuidema, B. K. New high strength steels help automakers reach future goals for safety, affordability, fuel efficiency, and environmental responsibility SAE Paper 2001-01-3041.

[11] Miller B and Bond R. The practical use of simulation in the sheet metal forming industry. Joint paper, Confed. of British Metalforming Technical Conf. 2001

[12] Reddy, J.N. An introduction to finite element method, Mc Graw Hill, Inc., 2nd ed., 1993.

[13] Hoon Huh, Tae Hoon Choi. Modified membrane Finite element formulation for sheet metal forming analysis of planar anisotropic materials. International J. of Mechanical Sciences, 42, 1999: 1623-1643.

[14] Kawka, M., Makinouchi; A. Shell-element formulation in the static explicit FEM code for the simulation of sheet stamping. Journal of Materials Processing Technology, 50, 1995: 105-115.l

[15] Sester M. Implementation of the selected elastoplastic models in autoForm-incremental. Workshop 3DS, Villetaneuse, June 2002.

[16] Giorleo G., Teti R., Prosco U. and D'Addona D. Integration of neural network material modelling into the FEM simulation of metal cutting, 3rd CIRP Int. Sem. On Intelligent Computation in Manufacturing Engineering – ICME 2002, Ischia, 3-5 July: 335-342.

Springback prediction with FEM analysis of advanced high strength steel stamping process

S. Al Azraq, R. Teti, J. Costa

Dept. of Materials and Production Engineering, University of Naples Federico II, Naples, Italy

Abstract

tool design a very complex task. New demands have led to an increase in the use of Advanced High Strength Steel (AHSS) as work material. An increase in strength decreases the formability of the material and increases the springback behaviour. The aim of the numerical simulation carried out in this paper is to verify the stamping process and the shape of the final component for studying springback of AHSS. Finally, a test case of a simple profile stamping process was analysed using the incremental approach of the AutoForm 4.04 Incremental software code for two different AHSS materials: Dual-Phase (DP 600) and Transformation-Induced Plasticity (TRIP 800).

Keywords: Springback, Advanced High Strength Steel, Stamping, Finite Element Methods

1. Introduction

As a forming expert in one of the leading car manufacturing companies, Schacher [1] summarized the current pressure on this industry as: “In the past we introduced 3 new models every 10 years, now we introduce 10 new models every 3 years". This drastic reduction of development periods as well as the trend to reduce weight of the cars in order to reduce the fuel consumption leads especially in the car manufacturing industry to a rebuilding of the conventional design and manufacturing procedures. Sheet metal forming as an important production process (see for instance [2]) is heavily experience based and involves trial-and-error loops. These loops are repeated the more, the less the experience on the part geometry and the material is. In innovative process design procedures, however, trialand-error loops are reduced by means of modern numerical approximation analysis, which is known ironically also as virtual production. Obtaining consistent and accurate part dimensions is crucial in today’s competitive manufacturing industry. Inconsistencies in part dimensions slow new product launches, increase changeover times, create difficulties in downstream processes, require extra quality assurance efforts, and decrease customer satisfaction and loyalty for the final product. In the sheet metal forming process, a major factor preventing accurate final part dimensions is springback in the work material [3]. Springback is the geometric difference between the part in its fully loaded condition, i.e. conforming to the tooling geometry, and when the part is in its unloaded condition, i.e. free state. For a complicated 3-D part, undesirable twist is another form of springback. The uneven distribution of stress through the sheet thickness direction and across the stamping in the loaded condition relaxes during unloading, thus producing springback. Factors that affect the amount of springback include variations in both process and material parameters, such as friction conditions, tooling geometry, material properties, sheet thickness, and die temperature [4]. Because controlling all these variables in the manufacturing process is nearly impossible, springback, in turn, cannot be readily controlled. Moreover, as springback is a highly nonlinear phenomenon, numerical simulations and correcting methods become highly complex.

1.1 Forming analysis with AutoForm-Incremental

Finite element methods (FEM) simulations based on incremental approaches [5] offer a full process model that simulates the metal sheet forming stages as accurately as possible in the logical order from blankholder to final flanging. Consequently,

incremental simulations are computationally very intensive and time consuming in comparison with the corresponding one step analysis, and require tooling information to be manually inputted [6]. There are two types of incremental codes based on either 'implicit' or 'explicit' mathematical formulations. Implicit codes, such as the *AutoForm-Incremental* software code [7], typically complete the forming simulation in 1-4 hours, depending on part complexity, whereas the explicit counterparts tend to be 2-4 times slower.

In the automotive industry, FEM methods for metal forming analysis are often used, particularly explicit codes like LS-Dyna (LSTC) and Pamstamp (Easy) and implicit codes like *AutoForm-Incremental*. Explicit solvers can be used to simulate dynamic analysis and allow to evaluate large deformations (like in drawing processes), whereas implicit solvers are suitable to simulate static analysis (like the springback phenomenon). Thus, in metal forming process simulation of car body components, a final implicit static step may be used to obtain a static springback solution after the tool is removed from the die. In this way, the springback solution starts from the stressstrain state of the forming simulation without numerical dynamic oscillations [7].

In this paper, the springback phenomenon is analysed through the use of the *AutoForm 4.04 Incremental* software code by simulating a test case stamping process applied to advanced sheet metal materials of great interest for the automotive industry.

1.2 Materials

In this study two Advanced High Strength Steels (AHSS) with different hardening curves (see Fig. 1) are considered: Dual-Phase (DP 600) and Transformation-Induced Plasticity (TRIP 800).

DP steels consist of a ferritic matrix containing a hard martensitic second phase in the form of islands.

These islands create a higher initial work hardening rate plus excellent elongation. This gives DP steels much higher ultimate tensile strengths than conventional steels of similar yield strength. The microstructure of TRIP steels is retained austenite embedded in a primary matrix of ferrite. In ddition to a minimum of 5% by volume of retained austenite, hard phases such as martensite and bainite are present in varying amounts. The retained austenite is progressively converted to martensite with increasing strain, thereby increasing the work hardening rate at higher strain levels [8].

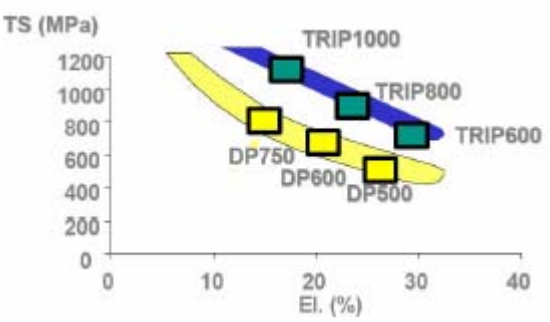

Fig. 1. Differences between Dual-Phase and Transformation-Induced Plasticity AHSS in a tensile strength (TS) vs. elongation (El) diagram.

2. Test case with AutoForm 4.04 incremental code

The test case realized in *AutoForm 4.04 Incremental* code is a simple profile stamping simulation with angle variations in the component vertical side walls using two different Advanced High Strength Steel (AHSS) materials. An incremental simulation was performed for a stamping process consisting of three stages: forming, trimming and springback. The most important criteria to evaluate the stamping process success are the following result variables: formability, thinning and springback (material displacement and angular displacement).

2.1 Input parameters

The stamping simulation was performed based on single action press. This procedure is based in a single slide (ram) movement: the punch is stationary, the die moves down in its direction pressing the metal sheet against the blankholder (binder), and then deforms the blank with the punch (Figure 4.6).

Cycle time is reduced by approximately 25% in comparison with the double action process.

In this case were applied two drawbeads (Db) to uniform the formability of the final part (see Fig. 2).

The most influent parameters on final results are described on table 1, Lubrication (Lube), Drawbeads (force factor [-] (FF), line force [N/mm](LF)) and Force apllied between binder and die (Force).

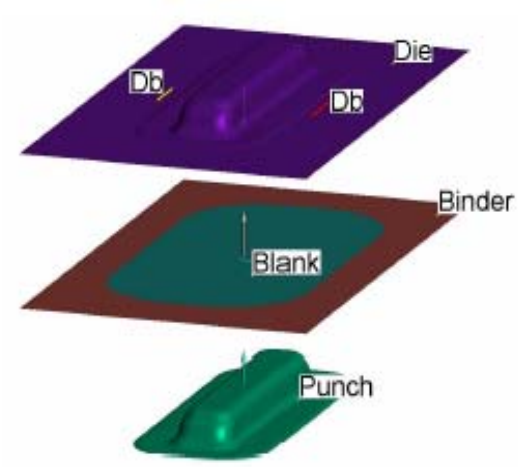

Fig. 2. Single action press tools

	Material	Blank Thickness	Lube	Drawbeads	Force
10°	DP600	0,8mm	0,15	FF - 0,450 LF - 388,2	1,80E+06
	TRIP800	0,8mm	0,15	FF - 0,530 LF - 457,2	1,90E+06
11°	DP600	0,8mm	0,15	FF - 0,450 LF - 388,2	1,60E+06
	TRIP800	0,8mm	0,15	FF - 0,530 LF - 457,2	1,90E+06
12°	DP600	0,8mm	0,15	FF - 0,350 LF - 301,9	1,80E+06
	TRIP800	0,8mm	0,15	FF - 0,620 LF - 519,3	1,80E+06

Table 1 – Input parameters

2.2 Analysis of results (colour display of result variables)

In the following, the analysis of the most important result variables will be discussed. These results can be displayed as coloured and shade images (see Fig. 3 for the results of the failure variable).

2.2.1. Formability

Formability is the ease with which a metal can be shaped through plastic deformation. Evaluation of the formability of a metal involves measurement of strength, ductility, and the amount of deformation required to cause fracture. The term workability is used interchangeably with formability; however, formability refers to the shaping of sheet metal, whereas workability refers to shaping materials by bulkforming.

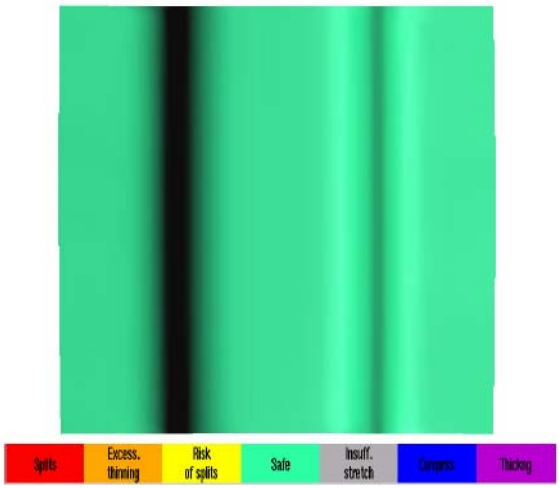

Fig. 4. Formability.

Figure 4 reports the results of the formability variable.

- Splits: Areas of cracks. These areas are above the FLC of the specified material (see Fig. 5).
- Excessive Thinning: in this area, thinning is greater than the acceptable value (default value for steel is 30%).
- Risk of splits: these areas may crack or split. By default, this area is between the FLC and 20% below the FLC.
- Safe: all areas that have no formability problems.
- Insufficient Stretch: Areas that have not enough strain (default 2%).
- Compression.
- Areas where wrinkles might appear: in these areas, the material has compressive stresses but no compressive strains.
- Thickening: Areas where wrinkles can be expected, depending on geometry curvature, thickness and tool contact; the material in these areas has compressive strains which means the material becomes thicker during the forming process (see Fig. 6).

2.2.2. Forming Limit Diagram (FLD)

The Forming Limit Diagram (FLD) provides a method for determining process limitations in sheet metal forming and is used to assess the stamping

characteristics of sheet metal materials (see Fig. 5). Usually, the Forming Limit Diagram is used in method planning, tool manufacturing and in tool shops to optimize stamping tools and their geometries. The comparison of deformations on stamped metal sheets with the FLD leads to a security estimation of the stamping process.

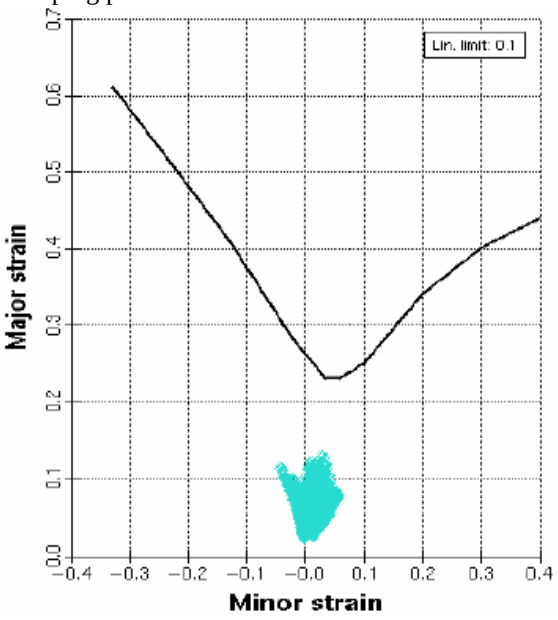

Fig. 5. Forming Limit Diagram (FLD) graphic.

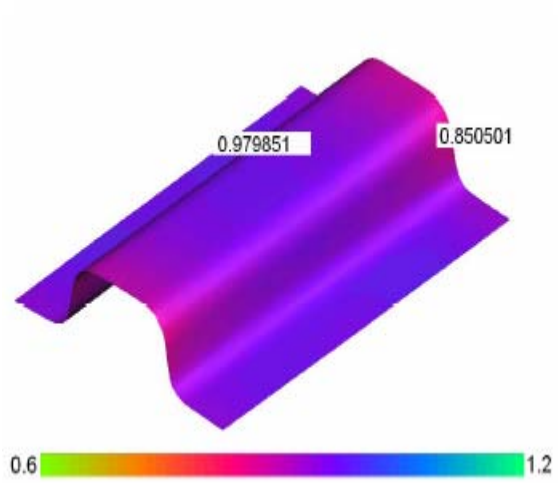

Fig. 6. Thickness.

2.2.3. Wrinkling criterion

Wrinkling is one of the major defects in stamping, especially for those parts on the outer skin panels where the final part appearance is critical. In addition, it can damage the dies and adversely affect part assembly and function. The prediction and prevention of wrinkling are, therefore, extremely important.

Naturally, wrinkling is a phenomenon of compressive instability under excessive in-plane compression. Plastic bifurcation analysis is one of the most widely used approaches to predict the onset of wrinkling.

Figure 7 reports the results for the wrinkling variable.

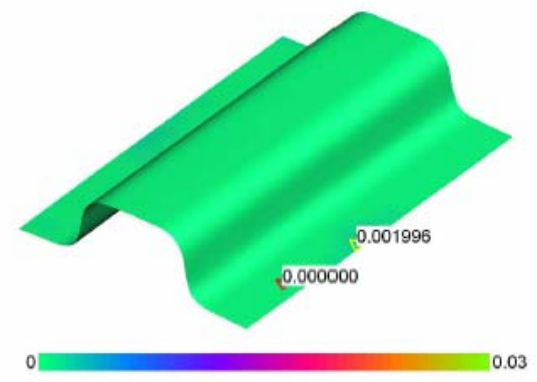

Fig. 7. Wrinkling criterion.

2.2.4 Plastic-strain ratio (revalue)

The plastic-strain is the ratio of the true width strain to the true thickness strain in a sheet tensile test. It is a formability parameter that relates to drawing; it is also known as the anisotropy factor. A high revalue indicates a material with good drawing properties.

Figure 8 reports the results of the plasticstrain variable.

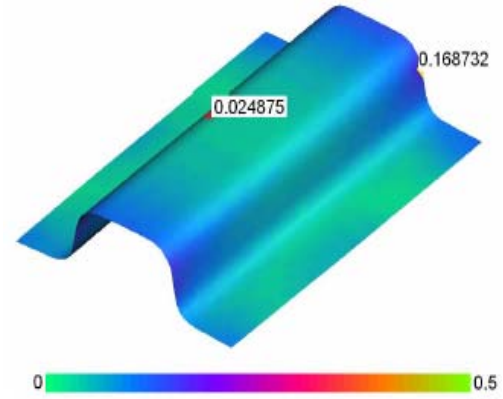

Fig. 8. Plastic-strain.

2.2.5. Springback graphic results

Figures 9-11 reports the springback variable results in graphical form.

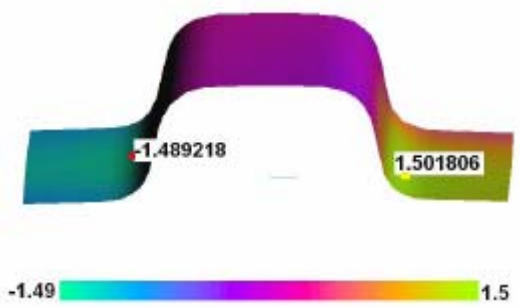

Fig. 9. Material displacement in X.

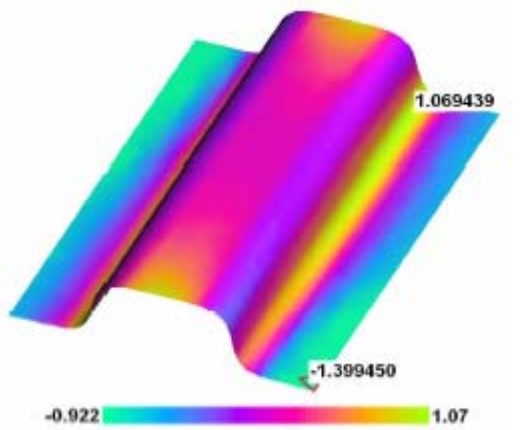

Fig. 10. Normal displacement.

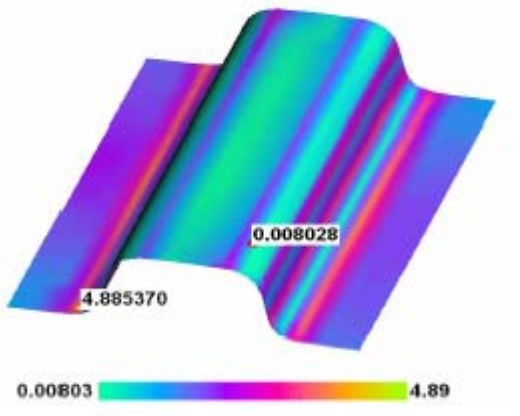

Fig. 11. Angular displacement.

2.2.5.1. Comparation between DP 600 and TRIP 800 of normal displacement in 10º profile

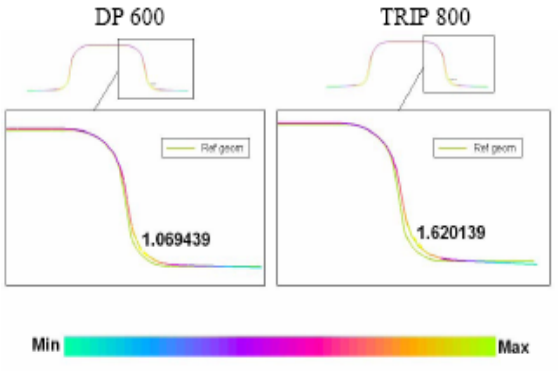

Fig. 12. Normal displacement for different AHSS.

Figure 12 reports the results of the normal displacement in 10° profile.

For the same material, the springbak increases with
the increasing of angular variation.

For the same angle profile, it can be concluded that material TRIP 800 has more displacement than material DP 600 (see Table 2).

	Displacement	DP 600	TRIP 800	Difference (%)
10°	X (mm)	0,96	1,50	56,3
	Y(mm)	0,20	0,23	15,0
	Z(mm)	0,95	0,97	2,1
	Normal(mm)	**1,07**	**1,49**	**39,3**
	Angular[°]	**4,89**	**5,06**	**3,5**
11°	X(mm)	1,04	1,63	56,7
	Y(mm)	0,22	0,26	18,2
	Z(mm)	1,20	1,06	-11,7
	Normal(mm)	**1,20**	**1,69**	**40,8**
	Angular[°]	**5,02**	**5,31**	**5,8**
12°	X(mm)	1,02	1,79	75,5
	Y(mm)	0,26	0,26	0,0
	Z(mm)	1,29	1,18	-8,5
	Normal(mm)	**1,30**	**1,93**	**48,5**
	Angular[°]	**5,20**	**5,73**	**10,2**

Displacements for DP 600 and TRIP 800.

3. Conclusion

A FEM study was carried out on springback, a great obstacle in the application of Advanced High Strength Steel sheets for the stamping of automobile parts, with focus on the mechanism of its occurrence and the techniques to counter it.

With the introduction of the examples of analyzing springback using FEM, it was shown that the analysis enables to predict the influence of material strength.

It is considered possible to decrease springback problems in actual parts in the future by the application of techniques for improving shape fixability and by FEM analysis.

It has been shown that the AutoForm software code is a powerful tool for the stamping process; it can considerably increase the product quality (production of more complicated parts, know-how accumulation for new materials, optimization by variants), reducing the time and cost of production (early checking of producibility of workpieces, reduction of development times, cheaper products, reduction of die costs).

In [9], the recent developments of modern Advanced High Strength Steel sheets were reviewed, paying special attention to their physical metallurgy.

A series of highly formable new high strength steels have been developed using sophisticated physical metallurgy and have contributed to expanding the application of high strength steel sheets, especially for production of automobile bodies and parts.

Besides further developments of new types of high strength steels with better mechanical properties, the development of proper forming and welding technology is required to expand the use of high strength steel sheets.

Therefore, a key to extending the use of high strength steel sheets for automobile parts is the cooperation of the automotive industry and steelmakers in developing materials and forming and welding technologies simultaneously. A new concept ‘early involvement and concurrent engineering’ being carried out through the joint efforts of the automotive industry and steel industry leads to expect apromising future.

References

[1] H.-D. Schacher, Entwicklungstendenzen in der Massivumformung fuer die Automobilindustrie, in: Seminarband Neuere Entwicklungen in der Massivumformung, Stuttgart, June 3-4, 1997

[2] K. Lange (Ed.), Lehrbuch der Umformtechnik. Band 3: Blechumformung, Springer, Berlin, 1975

[3] Cao, J., Liu, Z., Liu, W.K., On the structure aspect of springback in straight flanging, Symp. On Advances in Sheet Metal Forming, 1999 ASME Winter Conf.

[4] Cao, J., Kinsey, B., Solla, S., Consistent and Minimal Springback Using a Stepped Binder Force Trajectory and Neural Network Control, J. of Engineering Materials and Technology, 122 / 113, 2000

[5] H Aretz, R Luce, M Wolske, R Kop, M Goerdeler, V Marx, G Pomana and G Gottstein Integration of physically based models into FEM and application in simulation of metal forming processes Modelling Simul. Mater. Sci. Eng. 8 (2000) 881– 891

[6] Arwidson, C., Bernspång, L., Kaplan, A., Verification of numerical forming simulation of high strength steels, Int. Conf. on Innovations in Metal Forming, Brescia, Sept. 23-24, 2004

[7] AutoForm Engineering Inc. AutoForm-Incremental Reference Manual (http://www.autoform.com)

[8] International Iron Steel Institute, Advanced High Strength Steel Application Guidelines, March 2005. http://www.worldautosteel.org

[9] Al-Azraq, S., Teti, R., Ardolino, S., Monacelli, G., FEM analysis of advanced high strength steel car body drawing process, 1st IPROMS Virtual Int. Conf. on Intelligent Production Machines and Systems, 4-15 July 2005: 633-638.

Lateral Longeron Stamping through FEM Simulation Using an Incremental Approach

R. Teti[1], S. Al-Azraq[1], M. De Cosmo[2], G. Monacelli[2], M. Mattera[2]
[1] Dept. of Materials and Production Engineering, University of Naples Federico II, Italy
[2] Elasis SCpA, Pomigliano d'Arco, Italy

Abstract
Advanced High Strength Steels (AHSS) have been intensively applied to automobile components to improve crashworthiness, without increasing the car body weight. The sheet metal forming process is often influenced by springback phenomenon that represents one of the most critical problems that can occur in the car body component fabrication. The aim of the numerical simulation carried out in this paper is to verify the stamping process and the shape of the final components for studying formability and springback of AHSS. A test case of eleven different longeron configurations, obtained by angular variations in the vertical walls was examined. The stamping process was analysed through FEM simulation using an incremental approach for an AHSS material: Dual-Phase (DP 600).

Keywords:
AHSS material, Springback, Stamping, FEM simulation

1 INTRODUCTION

Each automobile component is designed to work under unique conditions. Criteria include durability, crash energy management, appearance, formability, cost, etc. Steel has the best combination of engineering capability versus material cost. Steel is formable, weldable, strong and has state-of-the-art coating that will help resist corrosion. In addition, it is cost effective and has good surface appearance.
Several new commercialized and near-commercialized advanced high-strength steels (AHSS) that exhibit high strength and enhanced formability are being offered today around the world. These steels have the potential to affect cost and weight savings while improving performance.
The increased formability allows greater part complexity, which leads to fewer individual parts (cost savings) and more manufacturing flexibility. Fewer parts mean less welding (cost and cycle-time savings) and weld flanges (mass and weight savings). Depending on design the higher strength can be translated into better fatigue and crash performance, while maintaining or even reducing thickness.
Obtaining consistent and accurate part dimensions is crucial in today's competitive manufacturing industry. Inconsistencies in part dimensions slow new product launches [1], increase changeover times, create difficulties in downstream processes, require extra quality assurance efforts and also decreases customer satisfaction and loyalty for the final product.
In the sheet metal forming process, a major factor preventing accurate final part dimensions is the springback phenomenon in the material. Springback is the geometric difference between the part in its fully loaded condition, i.e. conforming to the tooling geometry, and when the part is in its unloaded, free state.
Sheet metal forming as an important production process (see for instance [2]) is heavily experience based and involves trial-and-error loops. These loops are repeated the more, the less the experience on part geometry and material is. In the innovative process design procedure, the trial-and-error loops are reduced by means of modern numerical approximation analysis, which is named ironically also as virtual production.

1.1 Study material: Dual Phase (DP 600)

Dual phase (DP) steels consist of a ferritic matrix containing a hard martensitic second phase in the form of islands. The volume fraction of hard second phases generally increases with increased strength [3]. In some instances, hot-rolled steels requiring enhanced capability to resist stretching on a blanked edge (as typically measured by hole expansion capacity) can have a microstructure also containing significant quantities of bainite. Figure 1 shows a schematic microstructure of DP steel, which contains ferrite plus islands of martensite.
The soft ferrite phase is generally continuous, giving these steels excellent ductility. When these steels deform, strain is concentrated in the lower-strength ferrite phase surrounding the islands of martensite, creating the unique high work-hardening rate of these steels.

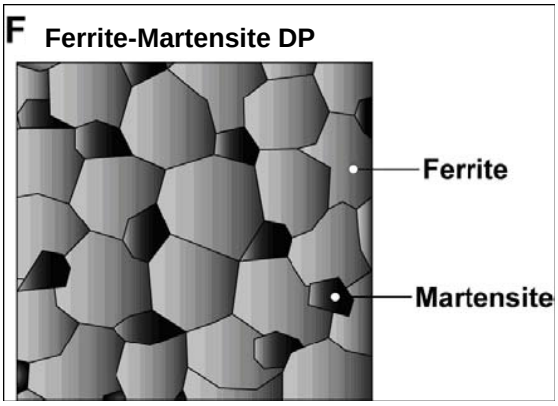

Figure 1: Schematic of DP microstructure.

The work hardening rate plus excellent elongation give DP steels much higher ultimate tensile strengths than conventional steels of similar yield strength. Figure 2 compares the quasi-static stress-strain behaviour of high strength, low-alloy (HSLA) steel to a DP steel of similar yield strength. The DP steel exhibits higher initial work hardening rate, higher ultimate tensile strength, and lower YS/TS ratio than the similar yield strength HSLA.
DP and other AHSS materials also have a bake hardening effect that is an important benefit compared to conventional steels [4]. The bake hardening effect is the increase in yield strength resulting from elevated temperature aging (created by the curing temperature of paint bake ovens) after prestraining (generated by

the work hardening due to deformation during stamping or other manufacturing process). The extent of the bake hardening effect in AHSS depends on the specific chemistry and thermal histories of the steels.

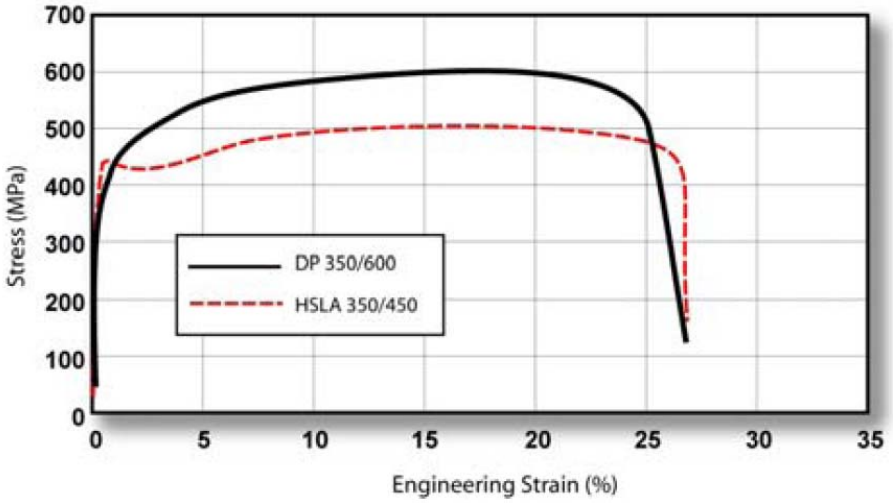

Figure 2: Comparison of quasi-static stress-strain behavior of HSLA 350/450 and DP 350/600 steels.

2 FORMING ANALYSIS WITH AUTOFORM 4.04 INCREMENTAL SOFTWARE CODE

Incremental programs offer a full process model that simulates the forming stages as accurately as possible in the logical order from blankholder closing to final flanging. Consequently, incremental simulations are computationally more intensive than the equivalent one step analysis, and require tooling information to be input [4]. There are two types of incremental codes based on either 'implicit' or 'explicit' mathematical formulations. Implicit codes such as AutoForm typically solve within 1-4 hours depending on the complexity of the part whereas explicit counterparts tend to be 2-4 times slower.

3 TEST CASE

The example of a simulation realized in AutoForm is a lateral longeron with angle variations (see Fig. 3) in the vertical walls for Dual Phase (DP 600) AHSS material. An incremental simulation was performed and the process consisted of three stages: forming, trimming and springback [5]. The most important criteria to evaluate the stamping process success are the result variables formability, thinning, wrinkling criterion and springback (angular displacement).

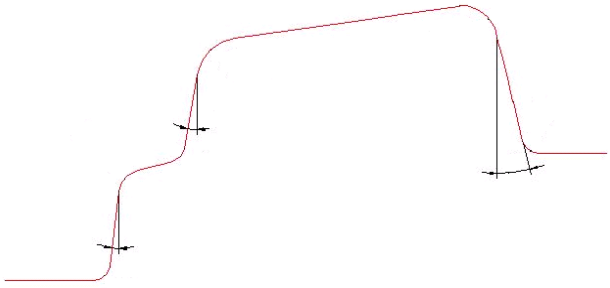

Figure 3: Location of the angles that are varied in this study.

3.1 'Input' parameters

Profile	Blank (mm)	Drawbeads medium restraining force	Lube	Force	Trials
P1	1.6	0.512	0.05	5.2e+05	200
P2	1.6	----------	0.05	1.0e+02	53
P3	1.6	0.508	0.1	2.0e+0,6	176
P4	1.6	0.512	0.05	5.0e+05	25
P5	1.6	0.531	0.05	7.0e+05	42
P6	1.6	0.525	0.05	5.0e+05	27
P7	1.6	0.543	0.05	5.0e+05	11
P8	1.6	0.525	0.05	5.0e+0,5	19
P9	1.6	0.575	0.05	7.0e+05	67
P10	1.6	0.531	0.05	1.8e+05	46
P11	1.6	0.540	0.05	7.0e+04	5

Table 1: 'Input' parameters table.

3.2 Results analysis of profile 1 (colour display of result variables)

In the following the results of formability, thinning and wrinkling criterion of profile 1 are reported.

Formability

Formability indicates the ease with which a metal can be shaped through plastic deformation. Evaluation of the formability of a metal involves measurement of strength, ductility, and the amount of deformation required to cause fracture. The term workability is used interchangeably with formability; however, formability refers to the shaping of sheet metal, while workability refers to shaping materials by bulk forming. Figure 4 reports the results of the formability variable.

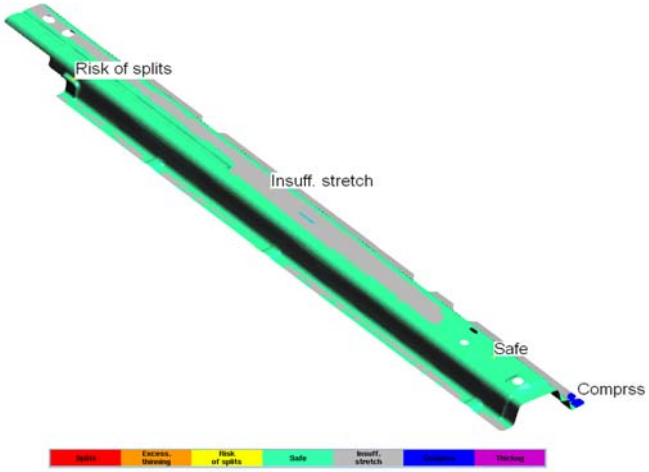

Figure 4: Formability.

- Splits: Areas of cracks. These areas are above the FLC of the specified material.
- Excessive Thinning: in this area, thinning is greater than the acceptable value (default value for steel is 30%).
- Risk of splits: these areas may crack or split. By default, this area is between the FLC and 20% below the FLC.
- Safe: all areas that have no formability problems.
- Insufficient Stretch: Areas that have not enough strain (default 2%)
- Compression
- Areas where wrinkles might appear. In these areas, the material has compressive stresses but no compressive strains
- Thickening: Areas where wrinkles can be expected, depending on geometry curvature, thickness and tool contact. Material in these areas has compressive strains meaning that the material becomes thicker during the forming process.

Forming Limit Diagram (FLD)

The Forming Limit Diagram (FLD) provides a method for determining process limitations in sheet metal forming and is used to assess the stamping characteristics of sheet metal materials (see Fig. 5).
Usually, the Forming Limit Diagram is used in method planning, tool manufacturing and in tool shops to optimize stamping tools and their geometries [6]. The comparison of deformations on stamped metal sheets with the FLD leads to a security estimation of the stamping process.

Thinning

Another result variable that is often used is the percentage thinning of the material (*Thinning*). A scale is displayed in the lower part of the main window with a range of 30% (-0.3) to 10% (0.1) thinning coloured from yellow to green (see Fig. 6).

Wrinkling criterion

Wrinkling is one of major defects in stamping, especially for those parts on the outer skin panels where the final part appearance is critical. In addition, it can damage the dies and adversely affect part assembling and function. The prediction and prevention of wrinkling are therefore extremely important.

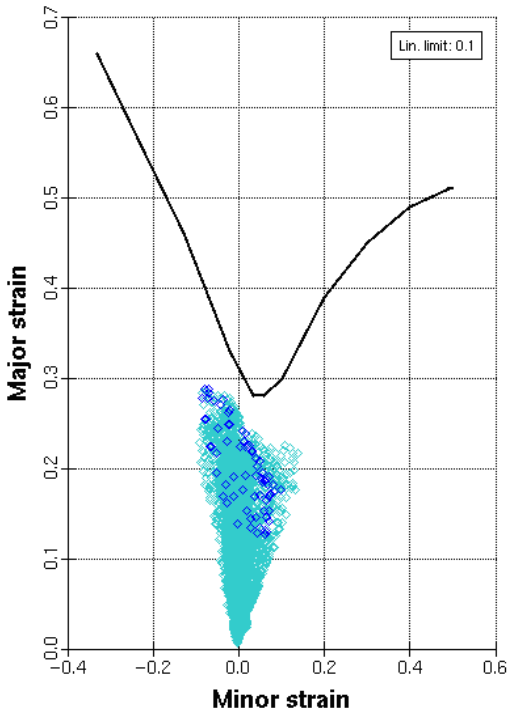

Figure 5: Forming Limit Diagram (true strains).

Naturally, wrinkling is a phenomenon of compressive instability at the presence of excessive in-plane compression. Plastic bifurcation analysis is one of the most widely used approaches to predict the onset of the wrinkling.
A scale is displayed in the lower part of the main window with a range of 0% (0) to 3% (0.03) wrinkling coloured from green to yellow (see Fig. 7).

Springback study

For the study of springback Section1 was chosen (see Fig.8) to display the results. The reference angles for the study of springback are angles A and B (see Fig.9).

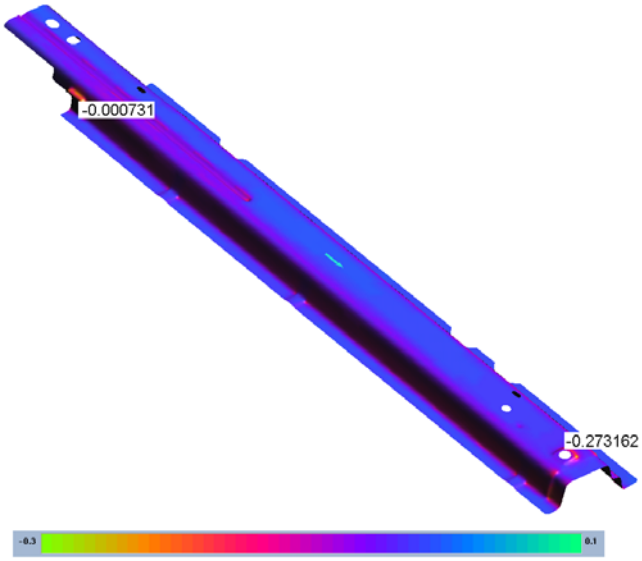

Figure 6: Thinning Display of the result variable thinning with min and max values in the main display.

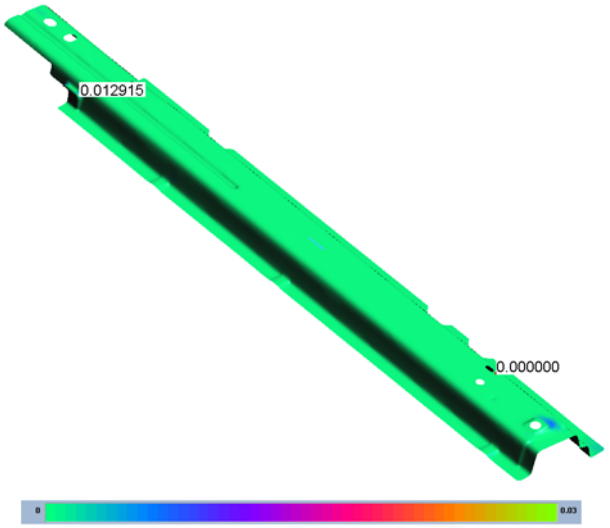

Figure 7: "Wrinkling criterion".

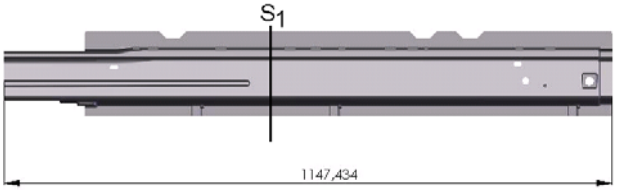

Figure 8: chosen section for the study of the springback.

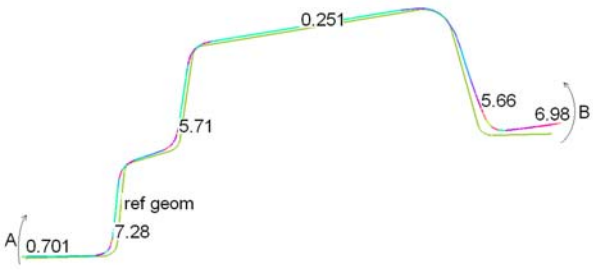

Figure 9: Reference angles for the study of springback.

4 RESULTS

4.1 Choice of the ideal profile for stamping

The stamping of profile 2 (Table 1) is not possible without splits, as it can be seen in Figure 10, this profile was stamped with a safety balance but the FLD resulted in non formable. As it can be seen in Table 1 a low binder force (F= 1.0e+02) was used and drawbeads were not used.

The stamping of profiles 4, 6 and 10 will not be considered for selection because they don't respect security limits for balance (see Fig. 11) by considering 3º for safe and 0º for marginal limits.

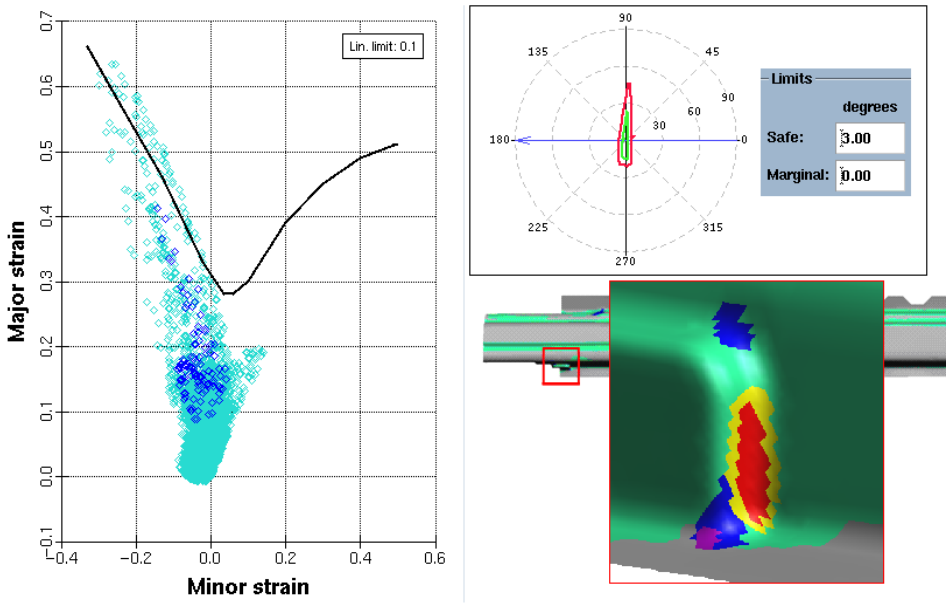

Figure 10: Simulation results of the profile2.

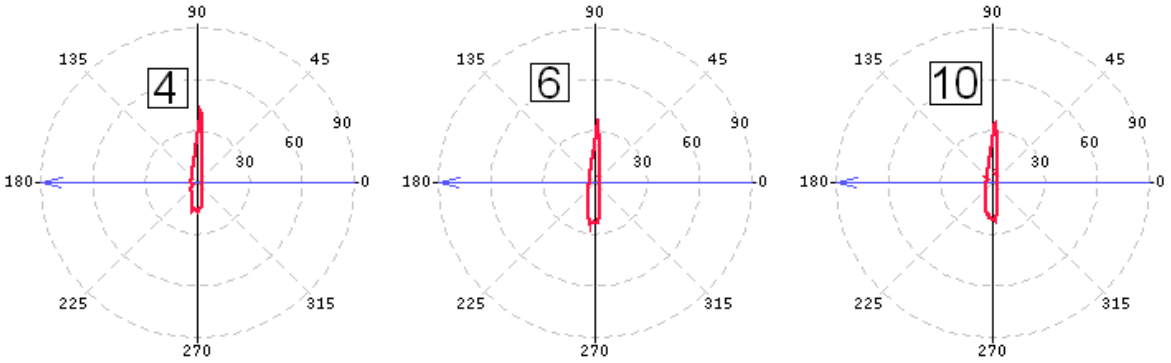

Figure 11: Backdraft diagram of profiles 4, 6 and 10.

4.2 Modifying of FLC parameters for drawing

The safety limit of the FLC (Figure 12) was decreased for formability visual overview, until one profile start to be totally green. As can be seen in Figure 13, profile 3 is first one become totally green (100% in safe area).

4.3 Final results

From analysis of Table 2, with special attention to the springback result, it was concluded that the best profile to stamp is profile 3.
Profile 2 is impossible to stamp without splits, profiles 4, 6 and 10 shouldn´t be considered because balance limit are not inside of safety limits.
The less sensitive is profile 3, because lubrication is 0.1 and not 0.05 like the other profiles, support high force between binder and die (2.0e+06) without splits and has the best formability results (is the only one that when the FLC (Fig. 12) curve was modified for the new parameters, it become totally green (Fig. 13)).
It has the best results of angular springback (A + B = 6.23° because both angles are under 5º) providing a good result for assembly (see Tab.2).
It has the best wrinkling criterion.
Its balance is inside of safety limits.

5 CONCLUSION

The application of new AHSS materials for the car industry increases the passive safety and the static and dynamic rigidity. It also decreases the vehicle costs, structure-borne noise and interior sounds. There is also a decrease in weight, leading to a minor consume of fuel and metal.
AutoForm is a powerful simulation tool in stamping industry that can reduce the time to market of the product. It helps to design the tools and to know the tools mechanical parameters.
It reduces the trial and error steps and also has a rapid prototyping that exports CAD files, permitting quick crash and assembly tests.
A FEM study was carried out on formability of AHSS and their use in automobile industry, praying special attention to the springback phenomenon, a great obstacle in the application of Advanced High Strength Steel sheets for the stamping of automobile parts, with focus on the mechanism of its occurrence and the techniques to counter it.
AutoForm can also improve the dimensional precision by predicting the final part's shape and geometry, helps to know where are the critical points of the product and allows a springback analysis
Springback results are critically dependent of the material formability, workpiece geometry, press type, tool geometry and process. Inside the tool geometry, there is the boundary geometry, binder geometry and also the addendum geometry. Inside the tool process, firstly there are the drawbeads, then the blank geometry, then the lubrication and last the force applied between tools.

6 ACKNOWLEDGMENTS

This research work was carried out at the Laboratory of Advanced Production Technology (LAPT), Dept. of Materials and Production Engineering, University of Naples Federico II, Italy, in collaboration with the FIAT Research Center ELASIS SCpA, Pomigliano d'Arco, Italy, within the EC FP6 NoEs on "Multi-Material Micro Manufacture - 4M" and "Innovative Production Machines and Systems - I*PROMS".

The Socrates/Erasmus thesis student Joao Carlos Silva Costa is gratefully acknowledged for his contribution to the development and preparation of this paper.

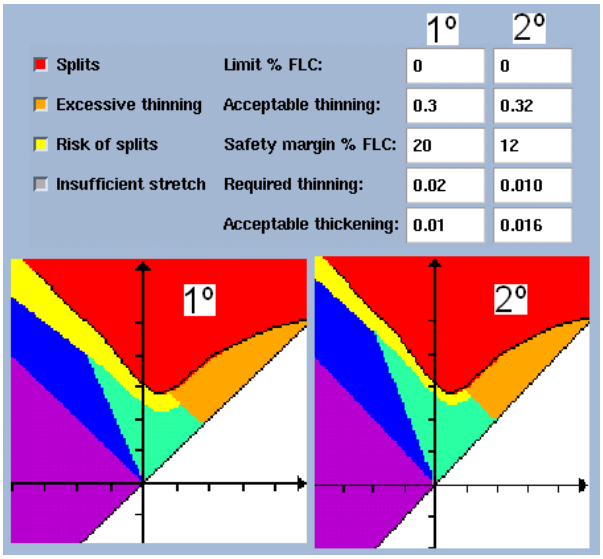

Figure 12: Modified FLC parameters.

7 REFERENCES

[1] H.-D. Schacher, Entwicklungstendenzen in der Massivumformung fuer die Automobilindustrie, in: Seminarband Neuere Entwicklungen in der Massivumformung, Stuttgart, June 3-4, 1997

[2] Cao, J., Liu, Z., Liu, W.K., On the structure aspect of springback in straight flanging, Symp. On Advances in Sheet Metal Forming, 1999 ASME Winter Conf.

[3] Journal of Engineering Materials and Technology, 122 /113, 2000

[4] International Iron Steel Institute, Advanced High Strength Steel Application Guidelines, March 2005. http://www.worldautosteel.org

[5] AutoForm Engineering Inc. AutoForm Incremental Reference Manual (http://www.autoform.com)

[6] Al-Azraq, S., Teti, R., Ardolino, S., Monacelli, G., FEM analysis of advanced high strength steel car body drawing process, 1st IPROMS Virtual Int. Conf. on Intelligent Production Machines and Systems, 4-15 July 2005: 633-638

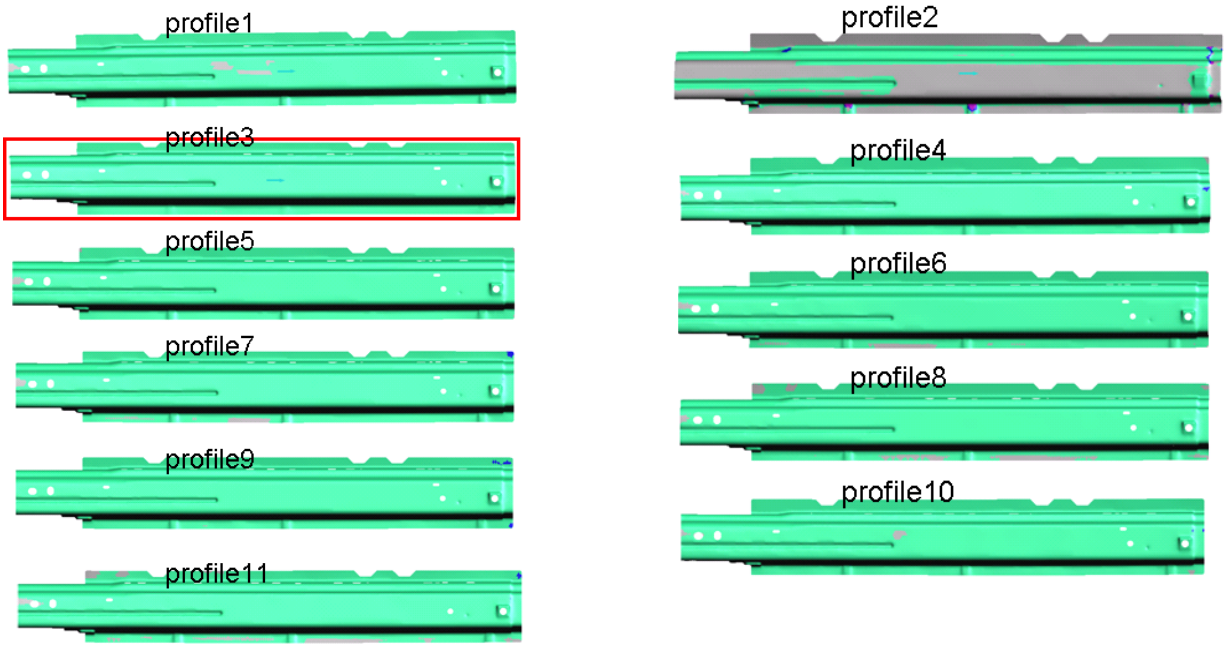

Figure 13: Formability results for new FLC parameters.

	Thinning	Wrinkling Criterion	Plastic strain	SB [°]	A+B
P1	M=-0,001 m=-0,273	M=0,013 m=0,000	M=0,494 m=0,006	A=0,70 B=6,98	7,68
P2	M=0,086 m=-0,325	M=0,200 m=0,000	M=0,685 m=0,000	A=8,60 B=8,87	17,47
P3	M=-0,010 m=0,289	M=0,004 m=0,000	M=0,402 m=0,011	A=1,98 B=4,25	6,23
P4	M=-0,008 m=-0,272	M=0,010 m=0,000	M=0,446 m=0,014	A=3,23 B=3,46	6,69
P5	M=-0,006 m=-0,281	M=0,012 m=0,000	M=0,472 m=0,012	A=1,90 B=6,99	8,89
P6	M=-0,004 m=-0,283	M=0,010 m=0,000	M=0,429 m=0,009	A=3,27 B=4,17	7,44
P7	M=-0,005 m=-0,280	M=0,009 m=0,000	M=0,383 m=0,008	A=3,26 B=4,77	8,03
P8	M=0,004 m=-0,281	M=0,010 m=0,000	M=0,423 m=0,008	A=3,97 B=6,61	10,51
P9	M=-0,009 m=-0,280	M=0,004 m=0,000	M=0,391 m=0,011	A=3,22 B=5,35	8,57
P10	M=0,003 m=-0,276	M=0,013 m=0,000	M=0,512 m=0,012	A=0,75 B=5,28	6,03
P11	M=-0,007 m=-0,279	M=0,008 m=0,000	M=0,422 m=0,008	A=3,64 B=6,76	10,04

Table 2: Output results table.

Table of Contents